Marine Research Sub-Programme
(NDP 2007–'13) Series

SeaChange
Casadh na Taoide

RESCALE: Review and Simulate Climate and Catchment Responses at Burrishoole

Project-Based Award, Technical Report

Lead Partner: Department of Geography, National University of Ireland Maynooth

NDP
National Development Plan
Transforming Ireland

Marine Institute
Foras na Mara

The Marine Institute is the national agency which has the following functions:
"to undertake, to co-ordinate, to promote and to assist in marine research and development and to provide such services related to research and development that, in the opinion of the Institute, will promote economic development and create employment and protect the marine environment" Marine Institute Act 1991.

Sea Change: A Marine Knowledge, Research & Innovation Strategy for Ireland

Sea Change—A Marine Knowledge, Research & Innovation Strategy for Ireland 2007-2013—was launched in early 2007 and was the outcome of extensive analysis and consultation with government departments, state agencies, industry and the third-level sector. It outlines a vision for the development of Ireland's marine sector and sets clear objectives aimed at achieving this vision, namely to:

1. Assist existing, and largely indigenous, marine sub-sectors to improve their overall competitiveness and engage in activity that adds value to their outputs by utilising knowledge and technology arising from research.
2. Build new research capacity and capability and utilise fundamental knowledge and technology to create new marine-related commercial opportunities and companies.
3. Inform public policy, governance and regulation by applying the knowledge derived from marine research and monitoring.
4. Increase the marine sector's competitiveness and stimulate the commercialisation of the marine resource in a manner that ensures its sustainability and protects marine biodiversity and ecosystems.
5. Strengthen the economic, social and cultural base of marine dependant regional/rural communities.

The Sea Change strategy was developed as an integral part of the government's Strategy for Science, Technology and Innovation (SSTI) and the Marine Institute as the lead implementation agency is working within SSTI policy and with government departments and agencies to deliver on the Strategy.

The Marine Institute managed Marine Research Sub-Programme, one of eight sub-programmes within the Science, Technology and Innovation (STI) Programme of the National Development Plan 2007—2013, targets funding to meet the objectives of the Sea Change strategy.

Over the lifetime of Sea Change, funding will be provided for:

- Project-Based Awards
  - o Strategic Research Projects
  - o Applied Research Projects
  - o Demonstration Projects
  - o Desk/Feasibility Studies
- Researcher Awards
  - o Strategic Research Appointments
  - o Research Capacity/Competency Building
  - o Post-Doctoral Fellowships
  - o PhD Scholarships
- Industry-Led Research Awards
  - o Company Awards
  - o Collaborative Awards
- Infrastructure Awards
  - o Infrastructure Acquisition
  - o Access to Infrastructure

Further copies of this publication can be obtained from:
Marine Institute, Rinville, Oranmore, Co. Galway, Ireland or www.marine.ie.

ISSN: 2009-3195

NDP National Development Plan Transforming Ireland

Marine Institute Foras na Mara

SeaChange Casadh na Taoide

*Marine Research Sub-Programme 2007-2013

Project-based Award

TECHNICAL REPORT: Review and Simulate Climate and Catchment Responses at Burrishoole (RESCALE)

Climate and Catchment Environment

(SS/CC/07/002(01))

Lead Partner:	Department of Geography, National University of Ireland Maynooth
Project Partners:	School of Natural Sciences, Trinity College Dublin
	Marine Institute, Furnace, Newport, Co. Mayo
Author(s):	Rowan Fealy, Norman Allott, Ciaran Broderick, Elvira de Eyto, Mary Dillane, Rachel Marie Erdil, Eleanor Jennings, Lee Hancox, Karen McCrann, Conor Murphy, Ciar O'Toole, Russell Poole, Ger Rogan, Liz Ryder, David Taylor, Ken Whelan and Jonathan White
Project Duration:	01 May 2008 to 31 January 2010

NUI MAYNOOTH
Ollscoil na hÉireann Má Nuad

TRINITY COLLEGE DUBLIN
COLÁISTE NA TRÍONÓIDE, BAILE ÁTHA CLIATH
THE UNIVERSITY OF DUBLIN

Marine Institute
Foras na Mara

Acknowledgments

This project (Grant-Aid Agreement No. SS/CC/07/002(01)) was carried out under the Sea Change strategy with the support of the Marine Institute and the Marine Research Sub-Programme of the National Development Plan (NDP) 2007–2013.

The authors are grateful to the research and support staff of the Marine Institute and in particular the staff at the Newport Facility for their help and assistance over the duration of the research. The authors would also like to thank Dr. Phil McGinnity, University College Cork, Dr. Glenn Nolan and Dr. Michael O'Toole, Marine Institute, for their input and advice. The authors would also like to extend their gratitude to Aengus Parsons and Veronica Cunningham of the Marine Institute for administrative support. The authors are grateful to Met Éireann, the Irish meteorological service, for the provision and use of their data. We also wish to thank David Livingstone, Water Resources Department, Eidgenössische Anstalt für Wasserversorgung, Abwasserreinigung und Gewässerschutz (Eawag), Switzerland, and Pam Naden, Centre for Ecology and Hydrology (CEH), United Kingdom, for their help and advice on river water temperature and dissolved organic carbon modelling, respectively, and the Centre for Water Research, University of Western Australia, for use of the DYRESM model.

Disclaimer

Project Partners

Dr Rowan Fealy
Department of Geography
NUI Maynooth
Co. Kildare

Dr Norman Allott
School of Natural Sciences
Trinity College Dublin
Dublin

Dr Ciaran Broderick
Department of Geography
NUI Maynooth
Co. Kildare

Dr Elvira de Eyto
Marine Institute
Newport
Co. Mayo

Mary Dillane
Marine Institute
Newport
Co. Mayo

Rachel Marie Erdil
School of Natural Sciences
Trinity College Dublin
Dublin

Dr Eleanor Jennings
Department of Applied Sciences
School of Health and Science
Dundalk Institute of Technology
Dundalk

Lee Hancox
Marine Institute
Newport
Co. Mayo

Karen McCrann
Department of Geography
NUI Maynooth
Co. Kildare

Dr Conor Murphy
Department of Geography
NUI Maynooth
Co. Kildare

Ciar O'Toole
Marine Institute
Newport
Co. Mayo

Dr Russell Poole
Marine Institute
Newport
Co. Mayo

Ger Rogan
Marine Institute
Newport
Co. Mayo

Liz Ryder
Marine Institute
Newport
Co. Mayo

Prof. David Taylor
School of Natural Sciences
Trinity College Dublin
Dublin

Prof. Ken Whelan*
Marine Institute
Newport
Co. Mayo
(*Current address: School of Biology & Environmental Science, UCD, Belfield, Dublin)

Jonathan White
Marine Institute
Oranmore
Co. Galway

Table of Contents

FOREWORD

Fundamental to accurate and meaningful climate change research is the availability of long-term datasets. Yet, administrations are finding the maintenance and upkeep of monitoring sites which provide fine scale climatological and environmental scientific records increasingly difficult to support. The availability of high-quality daily datasets covering three or more decades is surprisingly rare across the globe. Modelling results are greatly enhanced when using datasets in excess of 50 years duration. Very often climatological datasets are gathered remote from the monitoring of biological and chemical parameters. We're fortunate in Ireland to have available to us a monitoring station which, since the mid-1950s, has collected and collated such integrated records. We are doubly fortunate in that the monitoring facility has in place a synoptic weather station which collects synchronous meteorological data.

Today the Burrishoole site has a well-established environmental monitoring programme with developed platforms in place to continuously monitor essential climate and aquatic variables. Field monitoring is conducted on lakes, rivers and streams. The variables measured include air temperature, surface water temperature, river discharge, precipitation, air pressure, surface radiation, wind speed, wind direction and solar irradiance. The expansion of the monitoring platforms at the Burrishoole research station over various projects has amplified the site's importance and suitability for climate change research, particularly in relation to climate, land use and water interactions (Table i).

Table i: Summary of projects and installation of equipment in the Burrishoole catchment. AWQMS-automatic water quality monitoring station (lake); ARMS-automatic river monitoring station.

Summery of Burrishoole Catchment Monitoring programmes.									
Funding	EU Funding							National Funding	
	1996	1998	2000	2002	2004	2006	2008		2010
Projects	Life	Reflect	Life II		CLIME	INSIGHT	RESCALE		
							ILLUMINATE		
Equipment	AWQMS Feeagh		ARMS	Climate Change impact on Lakes			AWQMS Furnace		

The Irish Government recognised the national and international importance of the Burrishoole monitoring station in the context of its 2006 to 2013 Strategy for Science, Technology and Innovation (SSTI, 2006: 70-71)

"The Marine Institute's facilities at Oranmore and Newport, coupled with the world-class research vessels, databuoy network and the on-going oceanographic, biological and environmental survey programmes, including the Newport based indicator programme monitoring salmon migratory patterns, represent a unique asset. These, together with integrated data and information management systems, offer the opportunity to develop Ireland as a global monitoring centre for climate change assessments through the medium of marine and freshwater ecosystems (……)

The salmon research facility of the MI located in Newport, Co Mayo is a unique European research facility located adjacent to the Gulf Stream with fresh-water/sea-water facilities which monitor every salmon migrating from sea to fresh water. The resulting database with traceability over fifty years is a valuable and unique resource".

Funding provided under the Marine Institute's Sea Change Programme has facilitated the detailed integration, analysis and modelling of all of the Burrishoole data and for the first time a selection of global climate models (GCMs) have been downscaled to the catchment.

This report demonstrates that the projected changes in the climate conditions of the Burrishoole catchment, if realised, will have wide ranging implications for all aspects of the catchment system, including water temperature and quality, stream flow hydrology, soil processes, and most notably the well-being of its aquatic environment. While the projected changes in climate and their implications, outlined in this report, are specific to the Burrishoole, they are illustrative of likely changes in similar characteristic catchments along the west coast of Ireland.

Recent studies have shown that the effects of climate change on regional weather will be far more complex than simply altering temperature patterns. The results of climate change impact assessments are catchment-specific, which demand a modelling approach when major planning and policy decisions are to be made. Climate change proofing such decisions will become more critical as we move through this century and studies such as RESCALE are an essential precursor to more inclusive models, which can be applied in geographically separate areas of the country. The study has clearly shown that riverine ecosystems are particularly susceptible to climate change because they will be affected not only by shifts in water temperature but also by alterations in precipitation patterns and flow rates. In the Burrishoole catchment daily temperatures will increase by 1.7^{0}C, 1.8^{0}C, 1.7^{0}C and 2.2^{0}C for winter, spring, summer and autumn respectively by the 2080s. Our models indicate the greatest relative changes in

minimum temperature are associated with the months of September (+ 2.1°C), October (+ 3°C), November (+ 1.9°C) and February (+1.9°C).

Model simulations suggest an amplification of the seasonal flow regime for all sub-catchments in Burrishoole that is higher winter flows accompanied by lower summer flows. On a monthly basis, over the 2080s, the greatest increases in precipitation are suggested for February (+16.8 %) and January (+13 %) whilst the largest decreases are associated with the months of August (-11.7 %), June (-8.1 %) and July (-8.6 %). An increase in the incidence of extreme low flows, most notably during the summer and spring seasons, is projected. Associated with this is a suggested increase in the average number of consecutive days for which flows are equal to or below the minimum acceptable threshold. Low flow events are anticipated to become more frequent through the latter half of the century. The frequency of extreme high flows will also increase as the century progresses.

> *"Regional changes in the distribution and productivity of particular fish species are expected due to continued warming and local extinctions will occur at the edges of ranges, particularly in freshwater and diadromous species (e.g., salmon)"*
>
> (IPCC, 2007b: 275)

Such extreme changes are likely to have major impacts on the living biota of the Burrishoole catchment. Changes in climate, and in particular, temperature will affect fish at all levels of biological organization: cellular, individual, population, species, community and ecosystem, influencing physiological and ecological processes in a number of direct, indirect and complex ways. Fishes may respond directly to climate-change-related shifts in environmental processes or indirectly to other influences, such as community-level interactions with other taxa. However, the ability to adapt to the predicted changes in climate will vary between species and between habitats and there will be winners and losers. Increased temperatures are likely to favour cool-adapted and warm-adapted freshwater fishes whose distribution and reproductive success may currently be constrained by temperature rather than by cold-adapted species such as salmonids. These changes will undoubtedly prove complex and changes in food-web dynamics and physiological adaptation, for example because of climate change, may obscure or alter predicted responses.

Diadromous fish are often regarded as keystone species. They face particular uncertainties because of their utilisation of fresh, estuarine and marine waters, all of which potentially face different and complex responses to climatic change. Whatever the outcome of climate change,

it will lead to new selection pressures on fishes and indeed all organisms. The present study is limited to freshwater impacts on these stocks but diadromous fish species will integrate climate change effects on all of these aquatic areas and therefore the total impact on these fishes is very likely to be significant. Research on climate change effects on salmonids has been studied extensively by scientists working on Pacific salmon species and they have concluded that overall, changes in stock abundance can be linked to regime shifts in the climate. They conclude that population dynamics and environmental conditions can be relatively stable on decadal scales but they can abruptly shift from one state to another during a regime shift. Such regime shifts have been identified as having occurred in 1925, 1947, 1977 and 1989. The regime concept forces scientists to examine the natural processes that regulate fish abundance, particularly those processes linked to climate–ocean conditions. The impact of such regime shifts is often significant.

In assessing the full effects of climate change on diadromous species there is a need to integrate models based on the likely freshwater scenarios with those addressing their life at sea. The recently completed SALSEA programme has provided for the first time migration and distribution models for salmon during their life at sea. These show the varying migratory routes taken by salmon cohorts in different years and the effects of sea surface temperatures, wind direction and strength, salinity levels and currents on the pathways taken by these salmon in any given year. We are now in a position to track stock specific survival corridors stretching from the most remote spawning burn to the limits of the salmon's migration pathways. Modelling the environmental variables which affect the survival of diadromous fish species across both the freshwater and marine environments is fundamental to a full understanding of the impacts of climate change on the lives of these key indicator species.

Prof. Ken Whelan

Over the period from 1999 to 2011, Prof. Ken Whelan was an Executive Director in the Marine Institute. During this time he also served as the President of North Atlantic Salmon Conservation Organization (NASCO), an intergovernmental organisation which advises on all matters relating to the conservation of Atlantic salmon in the North Atlantic, and was Chairman of the International Atlantic Salmon Research Board. He is presently an Adjunct Professor in the School of Biology and Environmental Science at University College Dublin and Research Director of the Atlantic Salmon Trust.

1. Analysis of the Long Term Climate Observations in Burrishoole and Catchment Description

Karen McKrann, Rowan Fealy, Elvira DeEyto and Mary Dillane

1.1. Background

> "*warming of the climate system is unequivocal as is now evident from observations of increases in global average air and ocean temperatures*" (IPCC, 2007:5)

Based on the instrumental records, mean global surface air temperatures increased by 0.74°C ±0.18°C over the 100 year period from 1906–2005, with a doubling of the warming trend evident in the latter half of the period (IPCC, 2007) (Figure 1). However, this increase has not been uniform over the earth's surface, with mid- to high-latitude land areas in the northern hemisphere experiencing increases greater than the global average. In contrast, locations in the Pacific Ocean have exhibited little or no warming while the interior of the Antarctic Continent displayed slight cooling over the closing decades of the last century, likely associated with natural variability. From Figure 1, warming is evident between two periods in the global mean surface temperature records, between 1910 to the mid-1940s and 1970 to present, interspersed by a period of cooling between 1940 and 1970.

Seventeen of the warmest years on record (1850-2011) have occurred since 1990 and according to the Climate Research Unit (CRU) in East Anglia, 1998 remains the warmest year in the observed record (1890-2011), with a temperature of 0.55°C above the 1961-1990 mean. However, with the inclusion of additional data from stations in the Arctic, the Goddard Institute for Space Studies (NASA/GISS) found that warming in 2005 may have exceed that of 1998 (Hansen et al., 2006). More recently, 2010 tied with 2005 as being the joint warmest year on record. While natural factors, such as El Nino, are likely to have contributed to the warming experienced in 1998 and 2010, no such natural factors can be attributed to the warming experienced in 2005. According to the World Meteorological Organisation (WMO), 2011 was the tenth warmest year, in spite of the occurrence of a strong La Niña which exerts a cooling influence. Analysis of the instrumental records by CRU also indicates that while 2008 was the coolest year of the decade, it was the thirteenth warmest year in the instrumental records, which extends back to 1880. The decade 2000-2009 has now replaced the 1990s as

the warmest decade of the instrumental record. With the inclusion of more recent data, global average temperatures have increased by approximately 0.8°C since 1880 (Hansen et al., 2010).

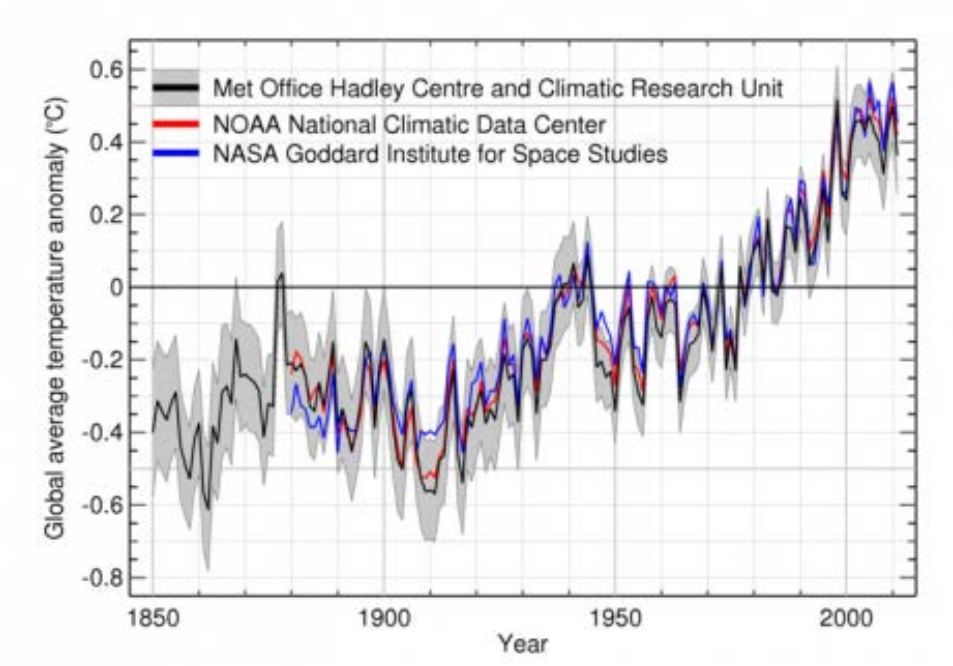

Figure 1.1: Global average temperature anomalies for the period 1850–2011 from three global temperature datasets – UK Met Office, NOAA NCDC and NASA GISS (Source: UK Met Office)

Globally, minimum air temperatures have been found to have increased more than maximum air temperatures, leading to a decrease in diurnal temperature range (DTR), albeit with significant regional variability (e.g. Alexandar et al., 2005; McElwain and Sweeney, 2007; Bartolini et al., 2008; Peralta-Hernandez et al., 2009; Rehman, 2009). Across Europe, there have been increases in both maximum and minimum air temperatures, with minimum temperatures rising more than maximum temperatures in general (e.g. Brazdil, 1996; Easterling et al., 1997; Bardossy, 2003; Klok and Klein Tank, 2009; Tecar and Cerit, 2009). These findings are consistent with the overall global trend, although some authors report the opposite, i.e. maximum temperatures rising more than minimum in Mexico (Peralta-Hernandez et al., 2009), Saudi Arabia (Rehman, 2009) and Italy (Bartolini et al., 2008). In Ireland, there has been an increase in both maximum and minimum temperatures with minimum temperatures having risen to a greater degree than maximum temperatures, although seasonally dependent, consistent with both European and global trends (Butler et al., 2007; McElwain and Sweeney, 2007).

Consistent with the changes outlined in both minimum and maximum temperatures, the occurrence of extreme events, such as heat-wave duration and the occurrence of 'hot-days'

have also increased globally, including Ireland. While indices relating to cooling, for example the number of frost days, have decreased.

Such increases in air temperature can have significant environmental impact on the freshwater environment, including phenological, physical and ecological responses (Walther et al., 2002; IPCC, 2007; Rosenzweig et al., 2008). For freshwater organisms these impacts may be further expounded by changes in water temperature. Temperature is an important physical property of rivers and streams, affecting many chemical and physical characteristics including, for example, dissolved oxygen, surface tension and chemical reaction rates (Webb, 1996; Webb et al., 2008). Water temperature also dictates the ecology of rivers and streams, with temperature regime changes affecting the entire system from microbial primary production (White et al., 1990) to plants (Anderson, 1969), invertebrates (Ward and Stanford, 1982; Hawkings et al., 1997) and fishes (Jensen, 1990; Matthews and Berg, 1997).

While the availability of published research on river water temperature has increased in recent years, there is a relative paucity of literature available on historical trends, due in part to a lack of suitable long term water temperature records (Webb, 1996; Moater and Gailhard, 2006; Webb et al., 2008). Water temperatures records that have been examined have shown increases in temperature, especially in spring (Langan et al., 2001; Moater and Gailhard, 2006). Consequently, the current research focus has been on the air/water temperature relationship in order to model future projections of increased temperature on rivers. However, increases in water temperatures, especially on major rivers, are often due to human activities such as river impoundment and diversion, catchment land-use, power-stations, canals, and urbanization with no clear link to climate change (Webb et al., 2008). The presence of lakes in undisturbed river catchments has an effect on the downstream water temperatures, due to the thermal stratification of lakes and their sensitivity to changes in air temperature. Flow also has an effect on water temperature with low-flowing or stagnant water bodies having higher temperatures than fast-flowing rivers. While increasing water temperature trends may in part be attributable to increased regional air temperatures, other factors, such as direct human activities also need to be considered particularly for more urbanised catchments.

1.2. Indicators of Climate Change

While many previous studies have employed an analysis of mean values to discern climatic trends, it is now widely recognised that an analysis of extremes is also required to fully examine trends over time (e.g. Karl and Knight, 1998; Heino et al., 1999; Haylock and Goodness, 2004; Hundecha and Bardossy, 2005; IPCC, 2007). Indices which have been used

include the number "hot-days" or "cold-nights" (e.g. Lai and Cheng, 2009), number of days with frost (Heino et al., 1999) and duration of growing season (Frich et al., 2002). Until recently, it was common practice to assess changes in climate series according to the number of days that exceeded a fixed threshold. For example, the number of "hot days" in Taiwan was defined as days when the maximum air temperature was ≥30°C which were found to have increased over the period 1897-2005 (Lai and Cheng, 2009). Nandintsetseg et al. (2007) in a similar analysis in Mongolia, reported an increase in "summer days" which they defined as days with a maximum temperature above 25°C. However, the use of such fixed-value thresholds does not facilitate comparison between regions with different climates and for this reason the use of percentile based thresholds are now considered more appropriate. For example, "cold nights" and "hot days" are calculated on the basis of the 10th and 90th percentile of minimum and maximum temperatures, respectively. The use of percentile based methods allows for the direct comparison of extreme trends between regions, such as was undertaken by Alexandar et al. (2005) who found a significant increase in warm days (daily maximum temperature greater than long-term 90th percentile) and a decrease in cold nights (daily minimum less than long-term 10th percentile) over 70% of the global landmass.

Increases in extreme warm indices and decreases in cold indices have been reported for many regions around the globe, including Central and South America (Aguilar et al., 2005), central and south Asia (Klein-Tank et al., 2006), Eastern Mediterranean (Kostopoulou and Jones, 2005), and the Caribbean (Peterson et al., 2002). In Europe, an analysis of extremes was undertaken as part of an EU Framework funded project entitled Statistical and Regional dynamical Downscaling of Extremes for European regions (STARDEX). This project examined trends in extreme weather events and developed modelling and downscaling techniques to determine likely changes in such events in the future. Among the results of the project was a key set of indices to examine trends in the mean and extremes of temperature and precipitation based on the percentile method resulting in output that is comparable across different climate regimes (STARDEX Final Report, 2005).

The study found that as well increases in maximum and minimum temperatures across Europe, there have also been increases in extreme temperature and precipitation events. A warming trend was found in Western Europe, associated with an increase in hot temperature indices, such as heat wave duration and a decrease in cold temperature indices, such as number of frost days (Hundecha and Bardossy, 2005; STARDEX Final Report, 2005). For example, in the UK, Haylock (2003) found a 0.5 days/year decrease in frost days, while in winter the hot day threshold was found to have increased by 0.04°C/year and in summer the hot day threshold

had increased by 0.06°C/year. A similar study in Ireland by McElwain and Sweeney (2007) found that frost days have decreased by 0.2 days/year in winter, heat waves increased by 0.23 days/year and cold wave duration decreased by 1.1 days/year. However, the heat wave duration and cold wave duration indices used in the study by McElwain and Sweeney (2007) were not percentile based, relying instead on a 5°C threshold deviation from the long-term mean. The appropriateness of employing fixed threshold approaches for use in maritime dominated climates, such as Western Europe, has been questioned by some authors (e.g. Bardossy, 2003). For this reason percentile-based indices are now the preferred method for calculating heat and cold wave duration indices.

Globally, changes have also been detected in precipitation with a general tendency for wetter conditions in many areas around the world (Alexander et al., 2005), including the Northern hemisphere as a whole (Zhang et al., 2007), Western Europe (Bardossy, 2003; Haylock and Goodness, 2004), regions in South America (Haylock et al., 2006), the USA (Karl and Knight, 1998), the Arctic (Min et al., 2008), Northern Taiwan (Yu et al., 2006), the UK (Osborn and Hulme, 2002; Bardossy, 2003) and Ireland (Hoppe and Keily, 1999; Keily, 1999; McElwain and Sweeney, 2007). However, many of these regions display significant variability with increased rainfall evident during winter months and decreases during summer months. For example, an increase in total precipitation was found in the United Kingdom in winter but a marked decrease was found in summer with an increase in the frequency of droughts (Osborn and Hulme, 2002). Similarly, in an analysis of precipitation data from Germany, a number of authors detected an increase in winter rainfall with decreases evident during the summer months over the period 1958-2001 (Hundecha and Bardossy, 2005) and 1851-2006 (Hansel et al., 2009).

Significant variability also exists in regional rainfall receipts. For example, opposing trends were found between north and south Taiwan; the north of the island was found to be significantly wetter and the south significantly drier (Yu et al., 2006). The eastern Mediterranean has become drier while the west has become wetter over the period 1958-2000 (Kostopoulou and Jones, 2005) and over the period 1960-2000 parts of South America have become drier and others wetter (Liebmann et al., 2004; Haylock et al., 2006).

Rainfall is highly variable with inter-annual, spatial and temporal variability making detection of total or mean changes difficult. Trends in mean annual or total annual precipitation may not reveal any significant changes but there may be changes at the extreme ends of the distribution that are not represented by the mean, such as is seen in Central America (Aguilar et al., 2005), Siberia, South Africa, North Japan and the Eastern Mediterranean (Groisman et al., 2005). It is

also possible that a change in one direction may be found in the annual mean or annual total and a change in the opposite direction is seen when extremes are examined. For example, a decrease in total annual rainfall was detected in northern India (Alexander et al., 2005), however, there was an increase in precipitation extremes related to wetter conditions, e.g. a decrease in consecutive dry days and an increase in precipitation intensity (Roy and Balling, 2004).

Changes in heavy precipitation events are likely to have a greater impact than changes in the total or mean (Aguilar et al., 2005; Groisman et al., 2005; Klein Tank et al., 2006). Analyses of extreme precipitation trends from around the globe have in general reported an increase in extremes towards wetter conditions. A number of authors have reported an increase in the contribution of extreme heavy precipitation events to annual totals in the USA (Karl and Knight, 1998) and China (Liu et al., 2005); precipitation intensity has increased in the South Pacific (Griffiths et al., 2003) and Western Mediterranean (Kostopoulou and Jones, 2005); there is more intense daily rainfall in winter in the UK and the heavy rainfall events have also increased in frequency (Osborne and Hulme, 2002). In Scotland, heavy rainfall events have also increased in frequency with 50-year events now occurring every 8 years in the east of the country (Fowler and Kilsby, 2003).

1.3. Site Details

1.3.1 Catchment Description

The Burrishoole catchment is located in the Nephin Beg mountain range near Newport, Co. Mayo (Figure 1.2). The Burrishoole catchment (9° 34' 20" W, 53° 55' 22" N; c. 89.5 km^2), located in the Western Region Basin District (WRBD) comprises seven lakes of various sizes and about 45 kilometres of interconnecting rivers and streams and (Whelan et al., 1998) (Figure 1.3). The catchment has national and international importance as an index site for salmonid monitoring. Data collected from the Burrishoole fish trapping facilities are used extensively by the International Council for the Exploration of the Seas to gauge the overall status of salmon, sea trout and eel stocks in Ireland and in the north Atlantic more generally. This is enabled by trap installations between Loughs Furnace and Feeagh that monitor all movements of fish to and from freshwater. These traps enable full censuses to be carried out on wild salmon, sea trout and eels, the stocks of which have all been declining in the last few decades (ICES, 2009a and 2009b; Poole et al., 2007).

Blanket peats are extensive in the catchment while afforestation schemes, commencing in 1951, account for 23% of land cover (Coillte pers. comm.). In addition to forestry, sheep

farming is important (Weir, 1996). Several studies have highlighted degradation of the Burrishoole catchment associated with afforestation and overgrazing (e.g., Allott et al., 2005; May et al., 2005) in the past five decades, but the impacts of this degradation on fish stocks is unknown. Possible links between climate variability and reduced numbers of Atlantic salmon in the catchment have recently been explored (McGinnity et al., 2009). Part of the catchment (the western and upper parts) has Special Area Conservation (SAC) status (Site name Owenduff/Nephin Complex; Site Code 000534).

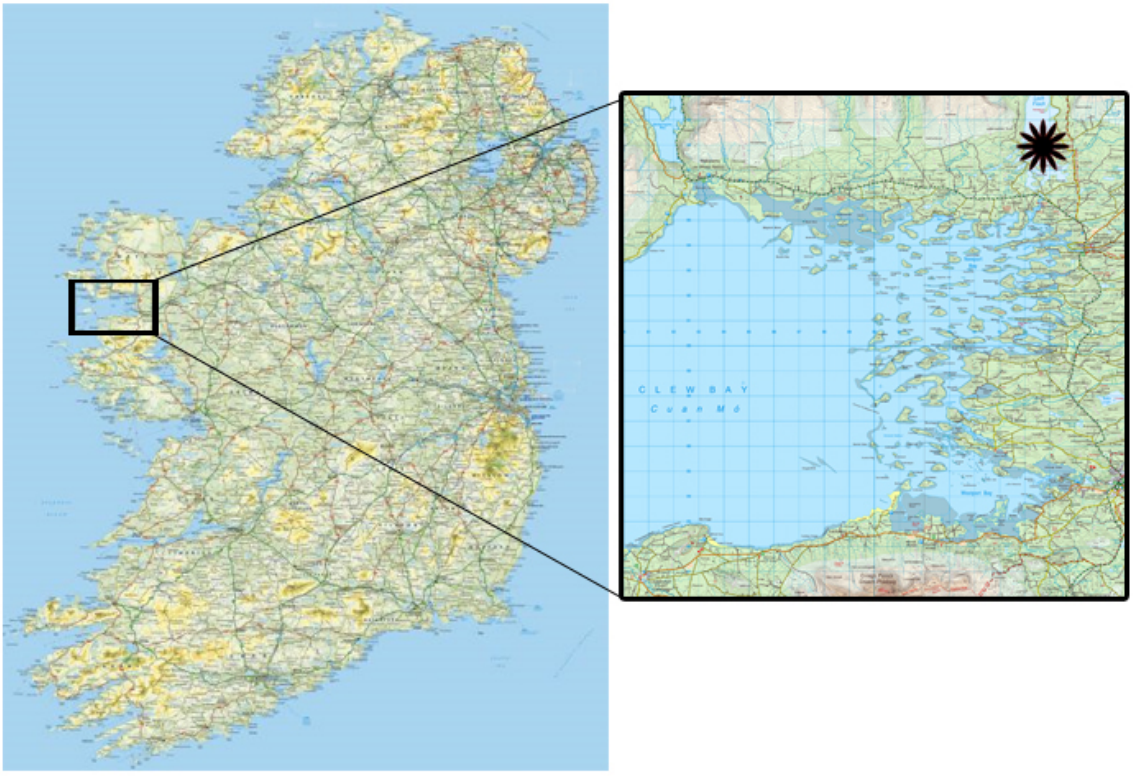

Figure 1.2: Location of Furnace near Newport, Co. Mayo on the west coast of Ireland. Site shown by asterix.

The bedrock geology of the catchment is characterised by metamorphic rocks of late Precambrian age, consisting of quartzites (44%), schists/gneiss (44%), Silurian quartzite (11%) and small areas of sandstone and limestone (1%) (Parker, 1977; Long et al., 1992; Irvine et al., 2000). The base geology on the west side of the Burrishoole catchment (Glenamong, Altahoney and Maumaratta subcatchments) is predominantly quartzite/schist, making them acidic in nature, with poor buffering capacity. On the east side of the catchment (Rough, Lodge, Goulaun and Cottage subcatchments) the geology is much more complex. While there is also quartzite/schist, it is interspersed with veins of volcanic rock, dolomite, wacke and pure schist, which means that the buffering capacity is higher as is the aquatic production. In the lower parts of the catchment, towards Clew Bay, the metamorphic rocks dip below Devonian

Old Red Sandstone and Carboniferous limestone. A terminal moraine, marking the boundary between metamorphic and sedimentary rock-types, separates Feeagh from the tidal Furnace. Deglaciation left the area blanketed with a sandstone-bearing till (the Newport till) (Kieley et al., 1974; Poole, 1994). The overlying soils are mainly poorly-drained gleys and peaty podsols, with blanket peatlands covering the mountain slopes to the north.

Land cover in the catchment comprises 64% peat bog, 23% forestry, with the remaining 13% being made up of smaller pockets of transitional woodland and scrub, natural grasslands and agricultural land (CORINE, 2000). Much of the peat bog area is commonage, and is used for sheep grazing. Vegetation cover on the blanket peats is characterised by *Molinia caerulea, Schoenus nigricans* and *Scirpus caespitosus* (O'Sullivan, 1993).

Cattle numbers in the Feeagh catchment have been consistently low since the early 1900s (< 5 per km^2), reflecting the lack of pasture and dominance of peat vegetation. Sheep numbers increased rapidly since the mid 1980s as a result of EU subsidies (Weir, 1996; O'Connor, 2000). The Central Statistics Office recorded approximately 509 sheep in the Srahmore area (roughly equivalent to the Burrishoole catchment) in the 1970s; 3,712 in the 1980s; 8,968 in the 1990s and 9,402 in the 2000s (ca. 88 km^{-2}) (CSO, 1970, 1980, 1991 and 2000). Compulsory destocking under programmes such as the Commonage Framework Plans, in combination with the introduction of Single Farm Payments, has led to a substantial decrease in the number of sheep in the west of Ireland by 2002, and recent CSO figures indicate a destocking of up to 30% for the Galway/Mayo/Roscommon area (CSO, 2008). Following consultation with landowners, the Marine Institute estimate that destocking in the Burrishoole catchment is nearer 50%. Heavy grazing, mainly by large numbers of sheep, has led to erosion of water-saturated substrates in the catchment, particularly in winter (Allot et al., 2005).

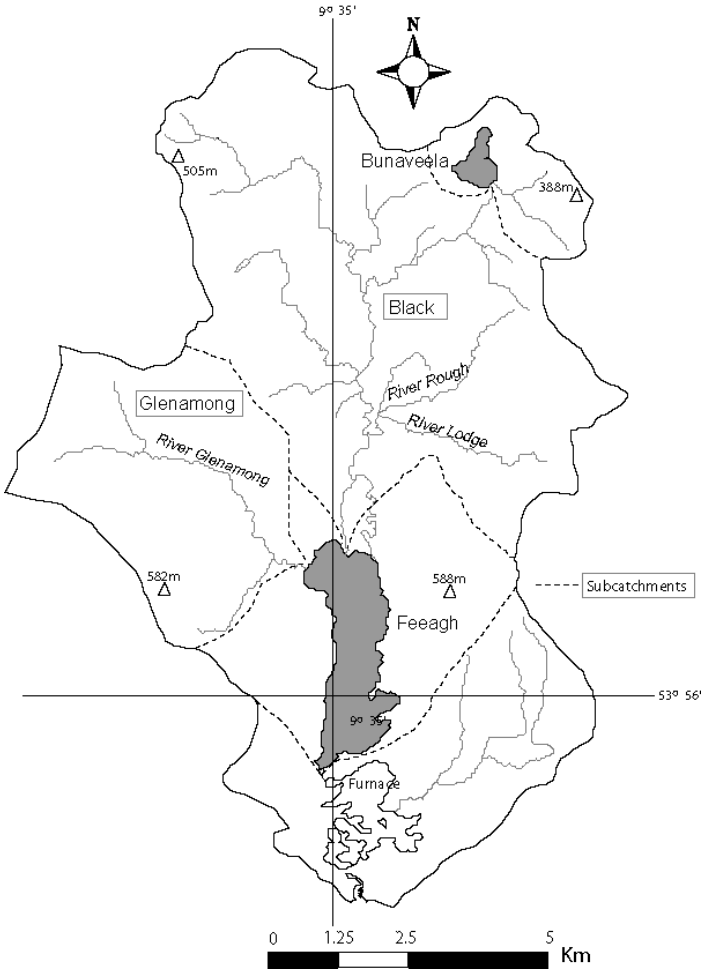

Figure 1.3: The Burrishoole catchment showing the locations of Bunaveela and Feeagh and the main subcatchment boundaries (Glenamong and Black) (Source: Dalton et al., 2010)

The human population is low and decreased from over 400 in the 1900s to 113 in the 2002 census, again reflecting regional trends (CSO, 1997). Afforestation has been the most significant change in land use over time. In total, commercial forestry accounts for about 23% of the total catchment area (FIPS database, Forest Service). Afforestation commenced in 1951 and expanded between 1960 and 1969; the main taxa are Sitka spruce (*Picea sitchensis*) (26%) and Lodgepole pine (*Pinus contorta*) (70%) (Coillte, unpublished data; Dalton et al., 2010). Clearfelling of planted trees commenced in the early 1990s: approximately 672 hectares (or c. 30% of the total plantation area) have been removed (Marine Institute, unpublished data).

As a result of geological and edaphic differences, the western and eastern subcatchments of the Burrishoole catchment are distinct. Rivers and streams on the western side are generally more acidic, with low buffering capacity (alkalinities in the order of -2.7 to 7.5 mg l^{-1} $CaCO_3$) and low aquatic production (Marine Institute, unpublished data). Those on the eastern side are nearer circumneutral with alkalinities in the order of 15-20 mg l^{-1} $CaCO_3$. Bunaveela and

Feeagh are the two largest freshwater lakes in the catchment and are part of a cascade of lakes that spans a gradient from oligotrophic headwaters to tidal transitional waters. Feeagh is an Environmental Protection Agency (EPA) typology class 4 lake (deep, >50 ha and low alkalinity) and is oligotrophic, distinctly coloured, with a pH of 6.7. Bunaveela is also an EPA typology class 4 lake and is an oligotrophic, acid-neutral, headwater lake, while Lough Feeagh is classified as 'probably not at significant risk' (category 2a) (Anon, 2005). In 2003, Lough Feeagh was classed by the EPA Ireland as a Candidate Reference Lake (CRL) indicating that the lake represented reference or non anthropogenically impacted conditions. Neither concurs with work carried out on the Burrishoole catchment over the past two decades. For example, Leira et al. (2006) provide palaeolimnological data, collected as part of the EPA/ERTDI-funded project, entitled Identification of Reference–Status for Irish Lake Typologies Using Palaeolimnological Methods and Techniques (IN-SIGHT), suggest that nutrient enrichment and slight – although not statistically significant – acidification have impacted Feeagh over the last c. 80 years. Bunaveela is too small for inclusion in the characterisation report, but the impacts of overgrazing and forestry are likely to have been significantly less than at Feeagh (where adverse impacts are evident in subcatchments).

1.3.2 Platform and Instrument Specification

Data used in this report was derived from seven main sources, including instrumented platforms and observation stations from within the catchment:

- Automatic Water Quality Monitoring Stations (AWQMS) on Lough Feeagh
- Automatic River Monitoring Systems (ARMS) on Glenamong, Srahrevagh and Black rivers
- Data logging Rain gauges
- Water level recorders
- Temperature recorders (data loggers and paper chart)
- Furnace manual weather station
- Newport Automatic Synoptic Weather Station

Automatic Water Quality Monitoring Station (AWQMS) - Lough Feeagh

The Feeagh AWQMS was developed and installed by CEH Windermere and is fitted with the equipment described in Table 1.1. Until 2009, this AWQMS had a Hydrolab Quanta positioned at 1m below the water surface, enabling temperature, conductivity, dissolved oxygen (% and mg/l) and pH of the lake to be measured. In 2009, this was replaced by a Datasonde DSX5. There is also a nephelometer and fluorometer in a fixed position 1 meter below the water column. Parameters were generally measured every 2 minutes, but in 2008 they were

measured every 5 minutes, as there were issues with battery life. An hourly average is also calculated. A weather station is also fully functional on the AWQMS measuring wind direction, wind speed, radiation, relative humidity and barometric pressure. Most of the sensors attached to the monitoring station require no routine service. Only the pH, conductivity and dissolved oxygen sensor require routine manual re-calibration every month. The station is powered by six 12v batteries which are changed once a month. Although not used in this project, a similar AWQMS was deployed in Lough Furnace in June 2008, with the additional functionality of a remotely controlled winch. This allows profiles of the water column to be conducted.

Table 1.1 Specification of Sensors on Lough Feeagh AWQMS

Equipment Name	Make	Parameters	Range	Accuracy	Resolution
DataSonde x5 (post 2009)	Hydrolab (OTT)	Temperature	-5 °C to 50°C	± 0.10°C	0.01°C
		Luminescent Dissolved Oxygen	0-20 mg/l	±0.2mg/l	0.01mg/l
		Specific Conductance	0-100 mS/cm	±1% of reading	4 Digits
		pH	0 to 14 units	± 0.01 PSS ±0.2 units	±0.01 units
Quanta (pre 2009)	Hydrolab (OTT)	Temperature	-5 °C to 50°C	± 0.15°C	0.01°C
		Dissolved Oxygen	0 to 50 mg/L	±0.2 mg/L ≤ 20 mg/l ±0.6 mg/L > 20 mg/l	0.01 mg/L
		Conductivity.	0–2000 µS/cm-1	± 1% of reading	4 Digits
		pH	2 to 14 units	± 0.01 PSS ±0.2 units	±0.01 units
Weather Station	Vector instruments A100L2-WR	Wind Speed	0 to 50m s^{-1}		
	Vector instrument W200-P-WR	Wind Direction	0 to 360°		
	Kipp and Zonen CM6B	Shortwave Radiation	0 to 2000W m-2		
	Licor Li-190-SA	Photosynthetically Active Radiation	0 to 2500µEm-1 s^{-2}		
	Macam SD-105B	Ultraviolet Radiation	_		
	Skye instruments SKH 2012	Relative Humidity	0 to 100%		
	Lab facility PT1/10 DIN four wire sensor	Air Temperature	−40°C to +60°C		
	Druck instruments (General Electric) PDCR 1830	Barometric Pressure			
Flourometer	Chelsea technologies Minitracka	Chlorophyll Fluorescence	Wavelength nm 685/30	0.03-100µg/l	0.01mg/l
Nephelometer	Chelsea technologies Minitracka	Turbidity	Wavelength nm 470/30	0.04-100FTU	0.01 FTU
PRT Chain	Lab facility PT1/10 DIN four wire sensor	Temperature			

Automatic River Monitoring Stations

There are three Automatic River Monitoring Stations (ARMS) installed in the Burrishoole catchment. The Glenamong and the Srahrevagh ARMS were installed in 2002, and the Black ARMS in 2004. All three monitoring stations share core technologies. They are all based on a Campbell Scientific data logger (Models CR23X and CR1000X) which is contacted remotely via a telemetry system (Table 1.2). The Glenamong ARMS is situated in the river, where a cage is pinned to the river bed, and all the sensors are placed within this cage. They are connected to the battery, data logger and telemetry system by cable to the river bank. The Black and Srahrevagh ARMS have all the sensors, batteries, data loggers and telemetry systems in a hut

on the river bank, and river water is pumped through a flow through system containing all the sensors.

Table 1.2 Sensors deployed in the ARMS in the Burrishoole catchment.

Model	Parameter	Make
Quanta	Temperature	OTT Hydrometery UK
	Dissolved Oxygen (Clarke cell)	
	Conductivity	
	pH	
Minitracka mk II Nephelometer	Turbidity	Chelsea Technology
CDOM (Glenamong only)	Dissolved Organic Carbon	Seapoint Sensors USA.
Pressure transducer.	Water level	Druck
CR1000x data loggers.		Campbell Scientific
Digital Transceiver Siemens TC35T GSM		Campbell Scientific

Rain gauges

There are 19 established rain gauges in the Burrishoole catchment. The rain gauges are DAVIS II tipping bucket gauges, with HOBO event loggers attached. Each gauge is set to date and time stamp every 0.2mm of rainfall and the data is downloaded approximately every 3 months.

Water level recorders

There are 13 water level recorders in full time operation in the Burrishoole catchment measuring the water level of the main streams and rivers. The majority are *Orphimedes* recorders supplied by OTT Hydrometry with an integral data logger. There is also one Thalimedes recorder operating on the Salmon Leap outflow, also supplied by OTT Hydrometery. Data from all the recorders are downloaded approximately every 2 months.

Temperature recorders

StowAway Tidbit temperature loggers are used throughout the catchment to provide stream and lake temperature every 30 minutes and are manually downloaded every four months. The tidbits are supplied by Onset Computer Corporation USA. In addition, Lough Feeagh surface water temperature was recorded continuously at the Mill Race since 1960 using a Negretti chart recorder and temperature probe. This has been replaced in recent years by a Tidbit logger.

Furnace manual weather station

The Marine Institute and Met Éireann have jointly operated a manual weather station in Furnace for almost 50 years. Variables recorded include wind speed, wind direction, cloud cover, rainfall, sunlight hours, maximum temperature, minimum temperature, humidity (using

wet and dry bulb thermometers) ground temperature and evaporation. This station is operated by Marine Institute staff.

Newport Automatic Synoptic Weather Station

In early 2005 the manual weather station was upgraded to an Automatic Synoptic Weather Station and the data is supplied to the Marine Institute by Met Éireann on a daily basis for use as a climatological station. The data is available to the public on the Marine Institute website www.marine.ie/home/publicationsdata/data/IMOS/FurnaceObs.

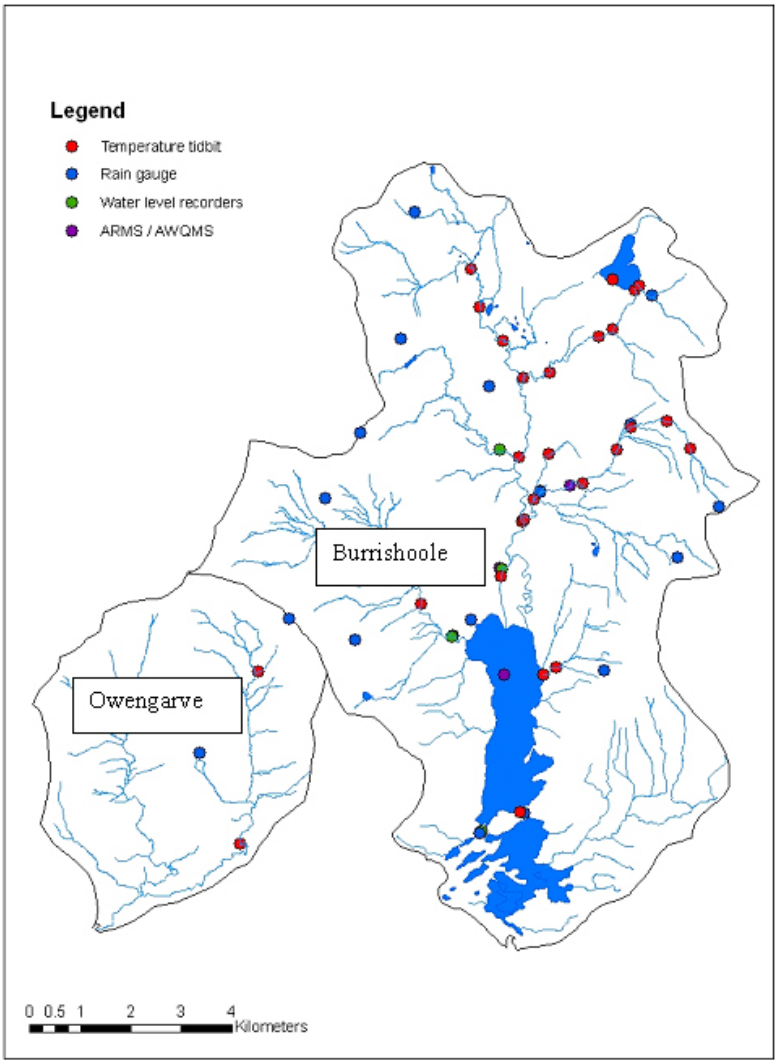

Figure 1.4 Monitoring equipment currently deployed in the Burrishoole and Owengarve catchments and maintained by the Marine Institute

1.4. Data and Methods

The Burrishoole catchment is a highly instrumented and intensively monitored catchment (Figure 1.4). Datasets available for the catchment include long-term data such as air temperature, precipitation and water temperature along with more recent high-resolution data e.g. precipitation, stream water levels, pH, dissolved oxygen, river and lake temperature. As described in section 1.3.2 a variety of equipment in used to measure these parameters. Some datasets, such as air temperature and precipitation, are long term datasets which have been measured since the late 1950s. Others are more recent and have been running for a shorter length of time, such as the ARMS which have been in operation for approximately six years (Table 1.3). The more recent datasets are high resolution with readings being taken at sub-daily or sub-hourly frequency, e.g. pH is measured every 2 minutes in three rivers. Before any analysis was undertaken, all data were quality control to ensure that all readings were accurate and were not artifacts of cleaning, maintenance or equipment malfunction. Details of procedures and techniques used can be found in the Appendices.

Table 1.3 List of data sources form the Burrishoole catchment used in the RESCALE project. Auto WS= Automatic weather station; Manual WS=Manual weather station; AWQMS=Automatic Water Quality Monitoring System; ARMS=Automatic River Monitoring System; OTT=Orphimedes water level recorder

Parameter	Equipment Type	Quantity	Year from	Year to	Duration
Air Temperature	Manual WS	1	1959	*ongoing*	50
	AWQMS	1	1996	*ongoing*	13
	Auto WS	1	2005	*ongoing*	4
Precipitation	Rain-gauge	19	2000	*ongoing*	9
	Manual WS	1	1959	*ongoing*	50
Water Temperature	Chart Recorder	1	1960	2004	44
	AWQMS	1	1996	*ongoing*	13
	ARMS	3	2001	*ongoing*	8
	Tidbit	8	2001	*ongoing*	8
Humidity	Manual WS	1	1960	*ongoing*	49
	AWQMS	1	1996	*ongoing*	13
Wind Speed	Manual WS	1	1968	*ongoing*	41
	AWQMS	1	2003	*ongoing*	6
	Auto WS	1	2005	*ongoing*	4
Wind Direction	Manual WS	1	1968	*ongoing*	41
	AWQMS	1	2003	*ongoing*	6
	Auto WS	1	2005	*ongoing*	4
Water Level	OTT's	12	2001	*ongoing*	8
pH	AWQMS	1	2003	*ongoing*	6
	ARMS	3	2003	*ongoing*	6
Dissolved Oxygen (DO)	AWQMS	1	2003	*ongoing*	6
	ARMS	3	2004	*ongoing*	5
Dissolved Organic Carbon (DOC)	ARMS	1	2004	*ongoing*	5

Water temperature has been recorded at various intervals and with a variety of equipment since records began in 1960. After investigation of the available data, it was apparent that the most consistent set of data throughout the record was water temperature readings taken at midnight. This dataset had few missing values and no significant gaps, unlike readings taken at other times of the day which were sometimes missing for several years. Midnight water temperature is an accurate representation of daily mean water temperature, albeit with negative bias (Crisp, 1990). A preliminary analysis of midnight water temperature and daily mean temperature for two years (2007-2008) was undertaken and it was found that there were no significant differences between the two datasets ($t=0.3796$, $d.f.=1460$, $p=0.704$; Figure 1.5).

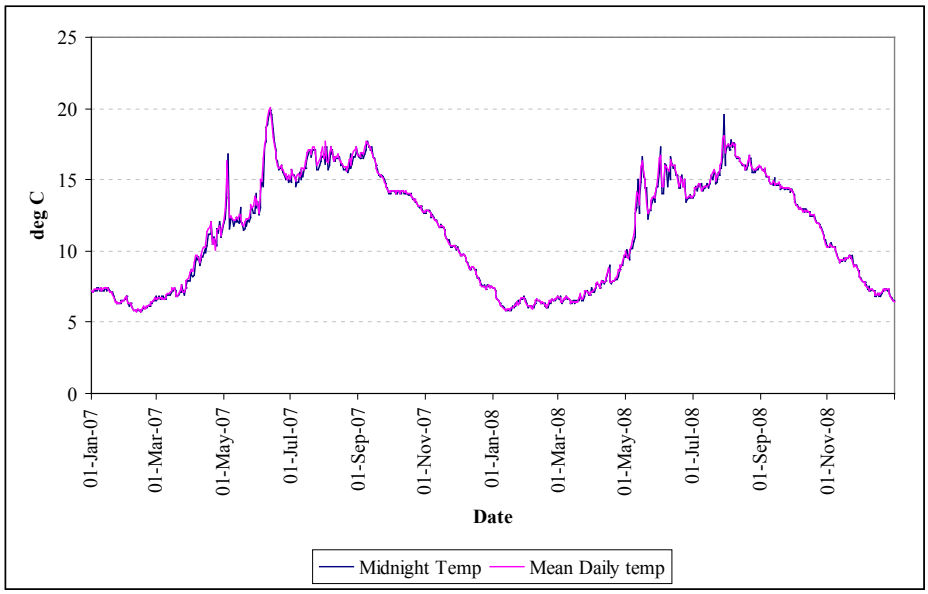

Figure 1.5 Mean daily and daily midnight water temperature for 2007-2008

It is reasonable to assume, therefore, that midnight water temperature provides a good representation of daily mean water temperature. However, daily maximum and minimum readings are not available and as indices of extremes are based on these readings an analysis of extremes could not be made. Therefore an analysis of seasonal and annual trends of mean midnight water temperature is investigated for the period 1960-2009.

All trends were calculated using STARDEX (Statistical and Regional dynamical Downscaling of Extremes for European regions) software following Hundecha and Bardossy (2005). Magnitudes and direction of trends were computed by least squares linear regression and the Kendall-tau test was used to test for statistical significance. The air temperature and precipitation indices used in this study included indices of both general trends and extremes while mean seasonal and annual water temperature changes were examined (Table 1.4).

Table 1.4 List of indices used categorised into general trends and extreme trends for air temperature, precipitation and water temperature (* indicates comparison made with McElwain and Sweeney (2007) sites for the period 1960-2005).

Code	Index	Description
	General trends	
	Air Temperature	
ATA	Air temperature anomaly	
tmax*	Mean maximum temperature	
tmin*	Mean minimum temperature	
tmean*	Mean temperature	
DTR*	Diurnal Temperature Range	
	Precipitation	
PA	Precipitation anomaly	
pmean	Mean precipitation	
	Water Temperature	
WTA	Water temperature anomaly	
wtmean	Mean water temperature	
	Extreme trends	
	Air Temperature	
tx90	tmax 90th percentile	Hot-day threshold
tn10	tmin 10th percentile	Cold day threshold
tnfd*	number days tmin < 0	Frost Days
hwd	6 consecutive days >90th percentile	Heat Wave Duration
tx90per	days > 90th percentile	Frequency at extreme high temps
tn10per	days < 10th percentile	Frequency at extreme low temps
	Precipitation	
cdd*	Consecutive dry days	Longest dry period
pfl90	% rainfall > long-term 90th percentile	Heavy rainfall proportion
pnl90*	no. events > long-term 90th percentile	Heavy rainfall days
sdii	Simple daily intensity	Average wet-day rainfall
px5d*	Greatest 5-day rainfall	Greatest 5-day rainfall
pq90	90th percentile rain-day amounts	Heavy rainfall threshold

Indices of extremes relating to air temperature calculate both the magnitude and duration of extreme events. Most indices use percentile values rather than fixed values making them transferable across a range of climate regimes (Bardossy, 2003). The exception to this is the number of frost days (tnfd) which used 0°C as a fixed threshold as this is the same regardless of climate. The Number of frost days is the count of days with a minimum temperature of less than 0°C (Bardossy, 2003). The hot day threshold (tx90) is the 90th percentile of maximum temperature i.e. the 10th hottest day per season. Cold night threshold is the 10th percentile of the minimum temperature (tn10) i.e. the 10th coldest night per season. Heat-wave duration (hwd) is an important index of extreme temperature calculated on a percentile basis not a fixed threshold. This index can therefore identify heat-waves in the cooler seasons of the year,

not just summer. It is defined as the number of consecutive days per season for which the daily maximum temperature on each day exceeds the long-term 90th percentile of that calendar day's maximum temperature calculated over a 5-day window centred on that calendar day (Hundecha and Bardossy 2005). This is a useful index as a heat-wave in winter will not have the same maximum temperatures as a summer heat-wave, but can be just as damaging to biodiversity and ecosystems (IPCC, 2007). Duration of extreme events was measured by the percentage of days where upper and lower percentile thresholds were exceeded. This indicates whether the frequency distribution is changing, with shifts towards the upper or lower extremes. The frequency that maximum temperature was above the 90th percentile (tx90per) assesses whether there were shifts in the distribution frequency to higher values i.e. high temperatures occurring more often. Conversely the frequency that minimum temperature was below the 10th percentile (tn10per) assesses for changes at the lower levels i.e. low temperatures occurring more often.

Indices relating to precipitation measure both frequency and intensity of extreme events. The frequency of extreme rainfall events was measured using three indices: consecutive dry days (cdd), heavy rainfall proportion (pfl90) and heavy rainfall days (pnl90). Consecutive dry days (cdd) is a measure of the longest dry period. An increase in this index indicates an increase in droughts. Heavy rainfall proportion is measured by the percentage rainfall that comes from events which are greater than the long term 90th percentile, i.e. the proportion of rainfall which comes from heavy events. This index measures whether there has been a change in the amount of precipitation contributed by heavy rainfall events. A heavy rainfall event is defined as those above the long-term 90th percentile. Heavy rainfall days measures the number of extreme precipitation events, i.e. those above the 90th percentile. Any change in this index reflects a change in the distribution of rainfall: an increase implies a shift to the upper end of the distribution, i.e. more heavy events and conversely for a decrease. Rainfall intensity is measured using three indices. Simple daily rainfall intensity (sdii) is the amount of rain per rain-day, or the average wet-day amount. A rain-day is defined as a day with rain of 1mm or greater. Greatest 5-day rainfall (px5d) is the greatest amount of rainfall over a five day period. Heavy rainfall threshold (pq90) is the 90th percentile of rain-day amounts. This index examines whether heavy rainfall events are getting more extreme.

General air temperature and precipitation trends at Furnace are compared to results from other sites around Ireland from McElwain and Sweeney (2007). The time period for these other Irish sites is 1960-2005 and trends for Furnace were also computed for this period for comparison. The indices that are compared are mean, maximum and minimum air

temperatures, DTR, frost days, consecutive dry days, heavy rainfall frequency and greatest 5-day rainfall.

1.5. Air Temperature Trends

1.5.1 Annual Air Temperature Anomaly for Ireland and Furnace

Annual air temperature anomalies for Furnace were calculated for the period 1960-2009. The air temperature anomaly (ATA) was calculated using the 1961-1990 average as a baseline mean, consistent with previous studies. The Irish temperature anomaly is based on McElwain and Sweeney (2007) which was calculated from an average of the annual temperature anomalies for four Irish stations: Malin Head, Birr, Valentia and Armagh over the period 1890-2005 (Figure 1.6).

The long-term Irish temperature anomaly (1890-2005) shows two significant warming periods, between 1910-1949 and 1980-2004, and a cool period between 1950-1979. The Furnace ATA followed a similar pattern to the Irish anomaly for the period 1960-2005 with no significant difference between the means for the two data sets ($t=0.461$, $p=0.65$). Both datasets also display a high degree of correlation ($r = 0.98$). The Furnace data shows greater inter-annual variability than the Irish record likely due in part to the Irish anomaly being an average of four stations. The trends for Ireland and Furnace are consistent with the global trends, but show greater inter-annual and decadal variability. Since 1988 there have been no years which were less than the baseline average at Furnace and only two years for the longer Irish record.

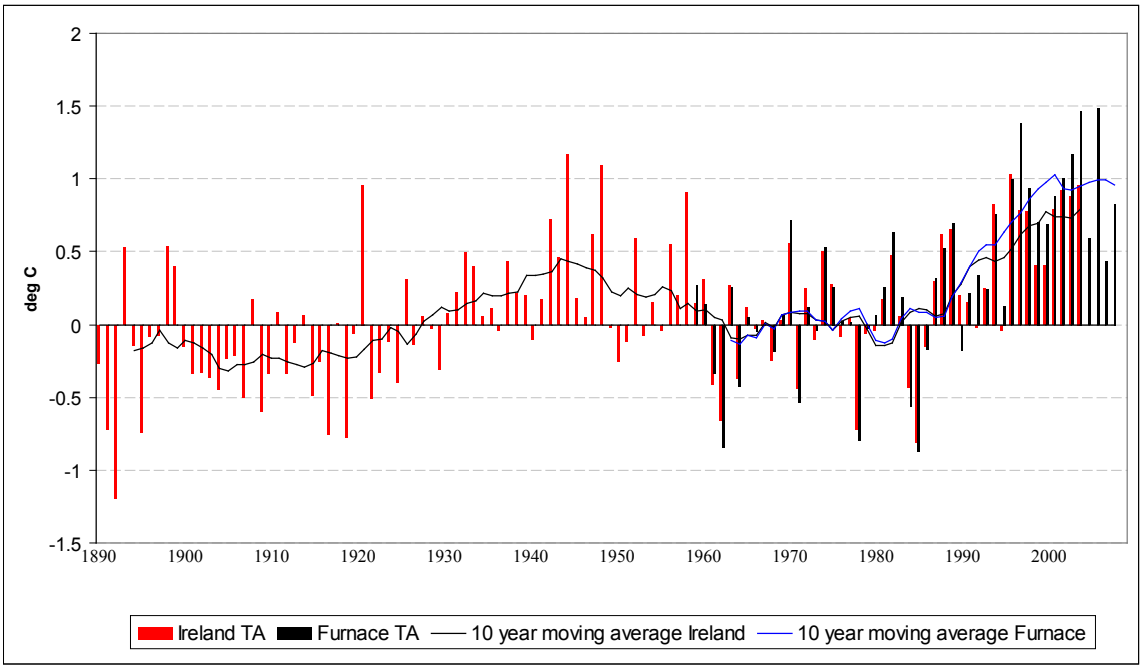

Figure 1.6 Air temperature anomalies for Furnace and Ireland (after McElwain and Sweeney, 2007) calculated with respect to the 1961-1990 reference period. The time periods are 1890-2005 for Ireland and 1960-2009 for Furnace. Bars are annual air temperature anomalies and lines are 10-year moving averages.

Trend analysis of the mean annual air temperature records, using STARDEX software, showed an increase of 0.7°C ($p<0.01$) over the period 1890-2005 for Ireland. At Furnace, a significant increase of 1.48°C ($p<0.001$) was found to have occurred over the period 1960-2009. When a comparable time period of 1960-2005 was examined it was found that mean annual air temperature rose by 0.9°C in Ireland and 1.1°C at Furnace.

1.5.2 Decadal Air Temperature Anomaly at Furnace

Mean decadal temperature anomalies for the period 1960-2009 for Furnace were also examined (Figure 1.7). Negative values in the 1960s were followed by slightly warmer values in the 1970s and 1980s. During the 1990s, the decadal air temperature anomaly was 0.59°C above the baseline mean. This anomaly was exceed by the decade covering the 2000s, when the decadal air temperature anomaly 0.93°C. However, the greatest change was found to have occurred between the 1980s and 1990s when the decadal air temperature anomaly increased by 0.55°C. Mean decadal air temperature at Furnace for the 2000s was 10.82°C which is 0.34°C higher than the 10.48°C recorded in the 1990s and 0.89°C higher than the 1980s value of 9.94°C, making the 2000-2009 period the hottest decade on record at this west of Ireland site. Such findings are consistent with those of the Goddard Institute for Space Studies (GISS) for the global records.

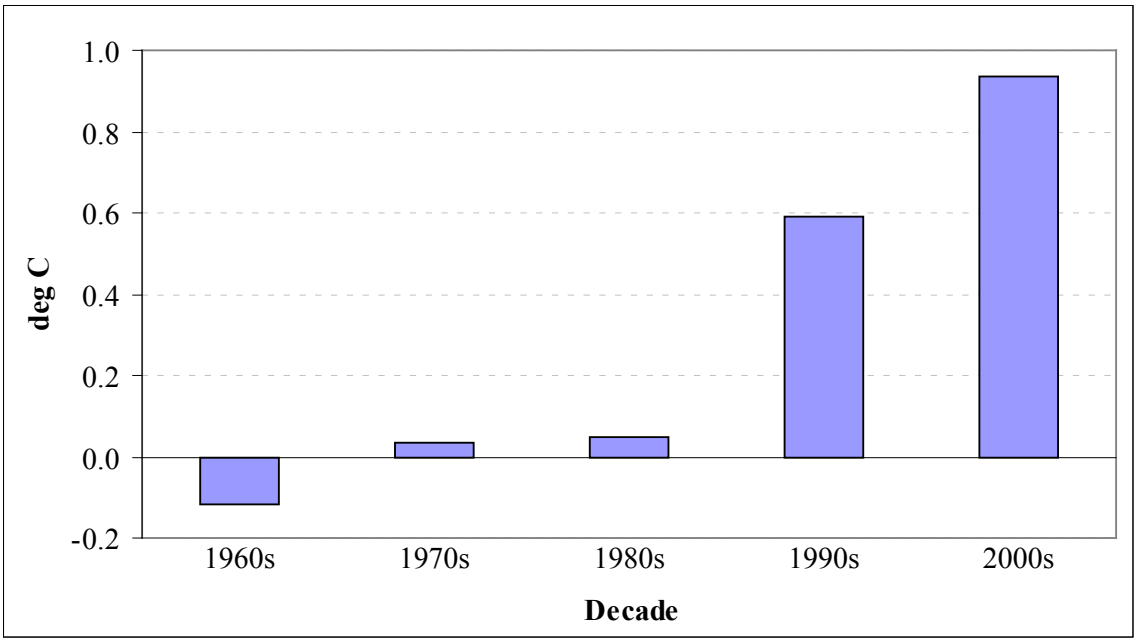

Figure 1.7 Mean decadal air temperature anomaly at Furnace for the period 1960-2009. Decades are defined as follows: 1960s (1960-1969), 1970s (1970-1979), 1980s (1980-1989), 1990s (1990-1999) and 2000s (2000-2009).

1.5.3 Mean Temperature

Trends in mean air temperature, for each season and year, for the period 1960-2009 were examined (Figure 1.8). The largest change in temperature was found in spring with an increase of 1.8°C over the period. The smallest increase was found in autumn which showed an increase in mean temperature of 1.36°C. This was followed by summer which had an increase of 1.48°C and then winter with an increase of 1.69°C. Annually, mean temperature increased by 1.48°C. All changes were significant at the 99% level (Table 1.7).

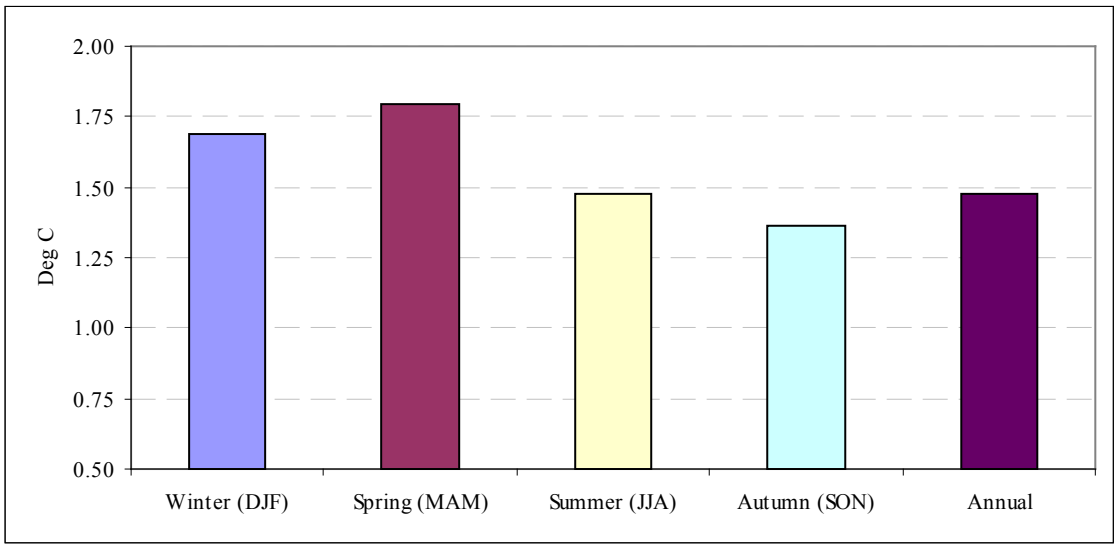

Figure 1.8 Change (°C) in mean seasonal and annual air temperatures for the period 1960–2009. Note scale

1.5.4 Maximum Temperatures

Increases in maximum temperatures were found in all seasons and annually at Furnace (Figure 1.9). The greatest change was found in spring maximum temperatures, with an increase of 1.8°C over the period 1960-2009. The increase in winter was 1.78°C, while that in summer was 1.6°C. The smallest change occurred in autumn, an increase of 1.4°C. Annually, maximum temperatures have increased by 1.57°C over the period. All changes are significant at the 99% level (Table 1.7).

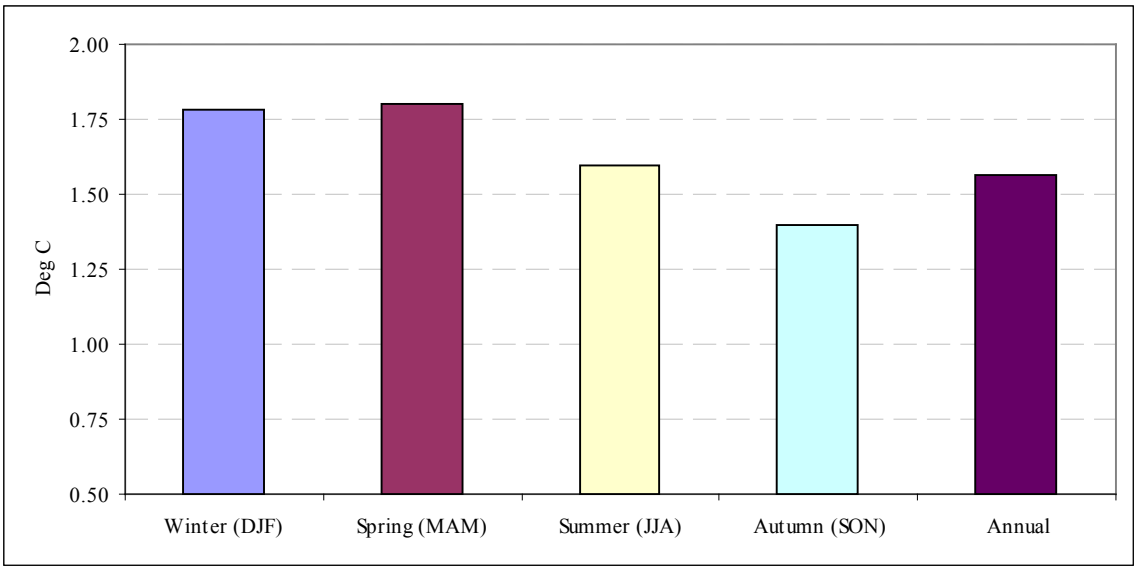

Figure 1.9 Change (°C) in maximum seasonal and annual air temperatures for the period 1960–2009. Note scale

1.5.5 Minimum Temperatures

Increases in minimum temperatures were found to have occurred in all seasons and annually. The greatest change was found in summer minimum temperatures, with an increase of 1.29°C over the period 1960-2009. The increase in winter was 1.12°C, while that in spring was 0.98°C. The smallest increase was observed in autumn 0.86°C. Annually, mean minimum temperatures increased by 0.98°C over the period 1960-2009 (Figure 1.10). All changes were significant at least at the 95% level (Table 1.5).

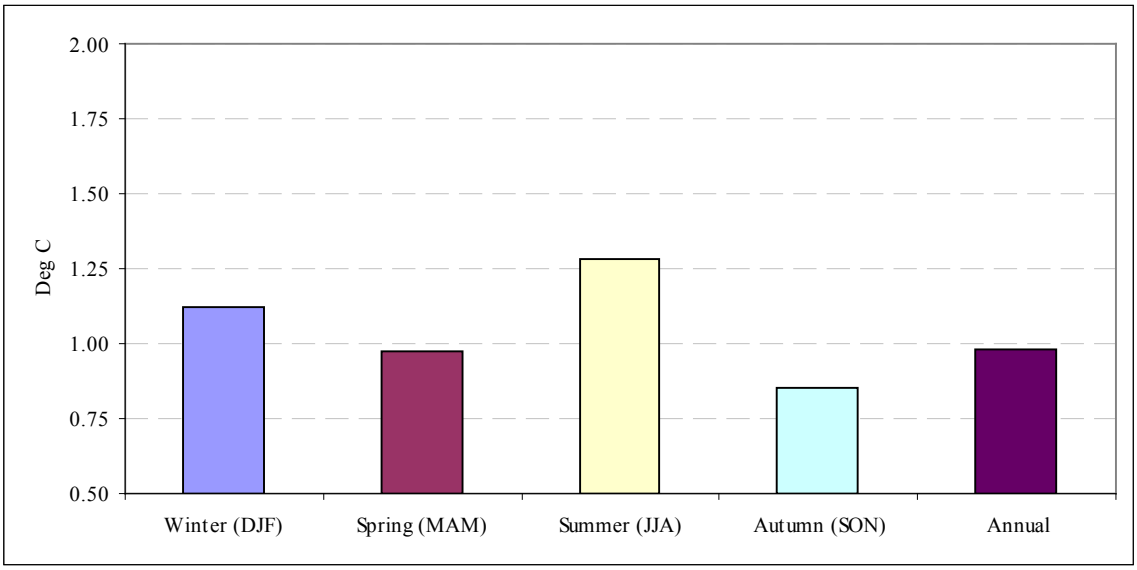

Figure 1.10 Change (°C) in minimum seasonal and annual air temperatures for the period 1960–2009. Note scale

1.5.6 Diurnal Temperature Range

Diurnal temperature range (DTR) is the difference between the daytime maximum and night-time minimum temperatures. At Furnace there has been an increase in DTR during all seasons, significant at the 95% level for winter, spring, autumn and annual (Figure 1.11; Table 1.5). There was a small non-significant increase in summer. The greatest increase in DTR at Furnace occurred in spring (0.83°C), followed by winter (0.60°C) and autumn (0.52°C). Annually DTR increased by 0.59°C at Furnace over the period 1960-2009. The increase in DTR was due to a greater increase in maximum temperatures than in minimum temperatures (Figures 1.9 and 1.10). This difference in the rate of increase was greatest in spring: maximum spring temperatures increased by 1.8°C while minimum spring temperatures only increased by 0.98°C over the period.

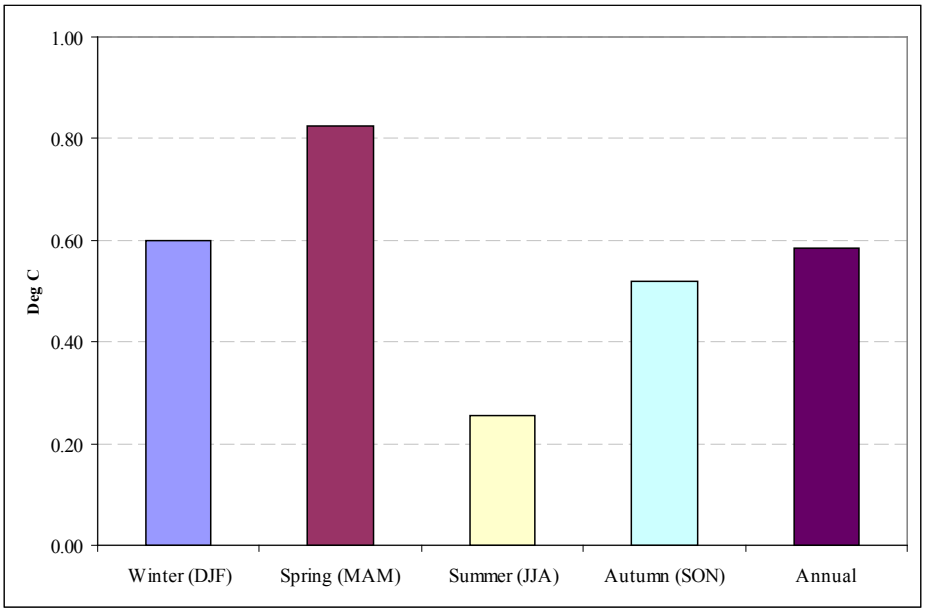

Figure 1.11 Changes (°C) in seasonal and annual diurnal temperature range (DTR) for the period 1960-2009

For the period 1960-2005 there was an increase in DTR at Furnace. This is contrary to the Irish trend for the same period which displays an overall decrease, due to minimum temperatures having risen more than maximum temperatures at the majority of sites (Table 1.7). Of the 11 other sites around Ireland the only other station which shows an increase in DTR in all seasons and annually was Phoenix Park. Rosslare and Belmullet showed an increase in annual DTR, although neither Rosslare nor Belmullet changes were significant (Table 1.8).

1.6. Analysis of Extreme Air Temperatures Indices at Furnace

1.6.1 Hot Day Threshold

Hot day threshold (tx90) increased significantly in all seasons and annually at Furnace (Figure 1.12; Table 1.5). The greatest increase was found in spring where hot day threshold increased by 2.6°C. The next greatest change was an increase of 1.73°C in summer followed by 1.27°C in both winter and autumn. Annually, the hot day threshold increased by 1.89°C over the period.

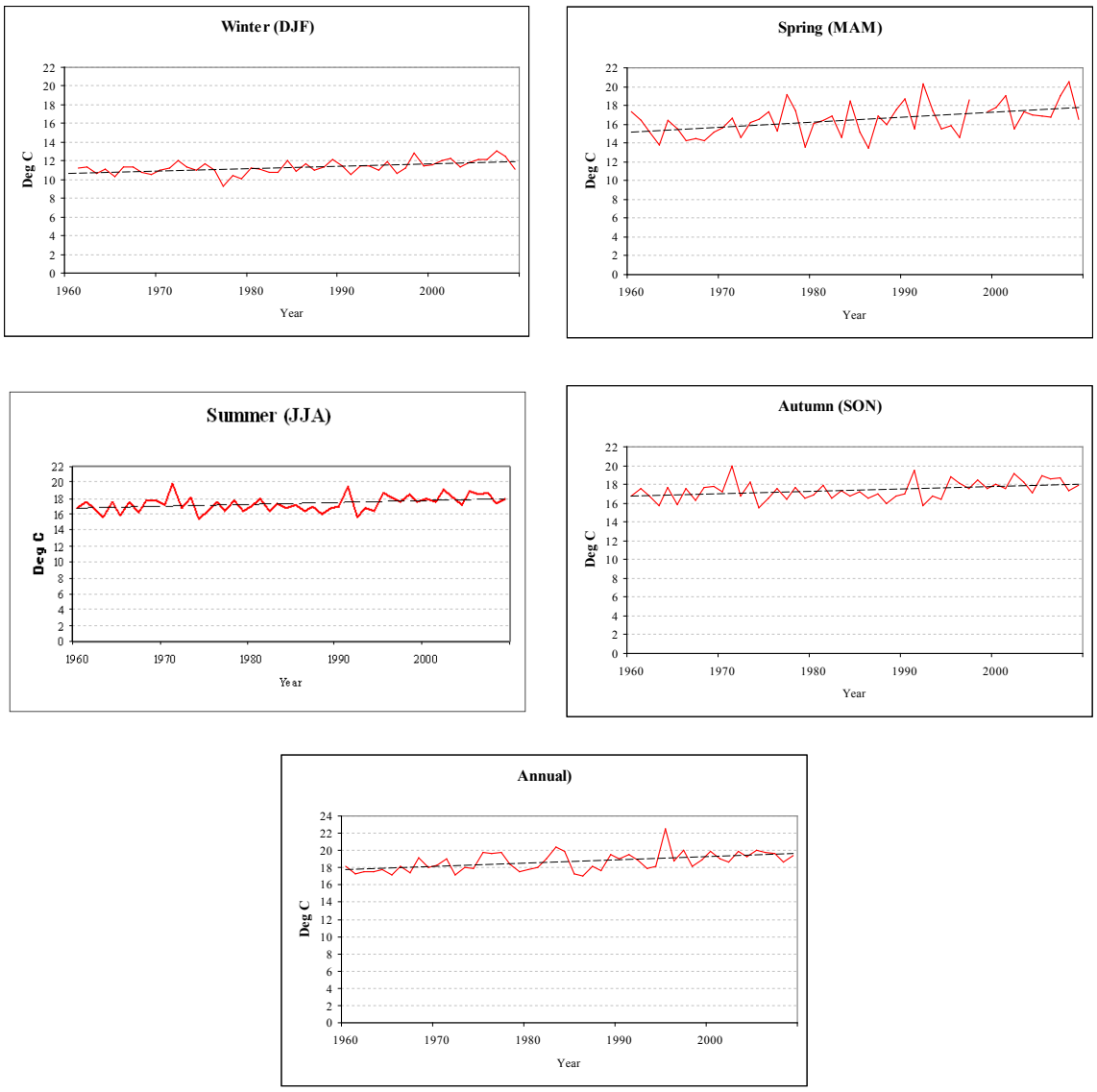

Figure 1.12 Trends in hot-day threshold (tx90) for each season and annually for the period 1960-2009. All trends are significant at 99% level except summer (JJA) which is significant at 95% level

1.6.2 Cold Day Threshold

The cold-day threshold (tn10) increased in all seasons and annually with winter, summer and annual increases showing significant trends (Figure 1.13; Table 1.5). The greatest change was found in winter where cold-day threshold increased by 1.6°C. Summer increases were

significant (0.8°C) but autumn (1.1°C) and spring (0.2°C) were non-significant. Annually the cold-day threshold increased significantly by 0.9°C over the period.

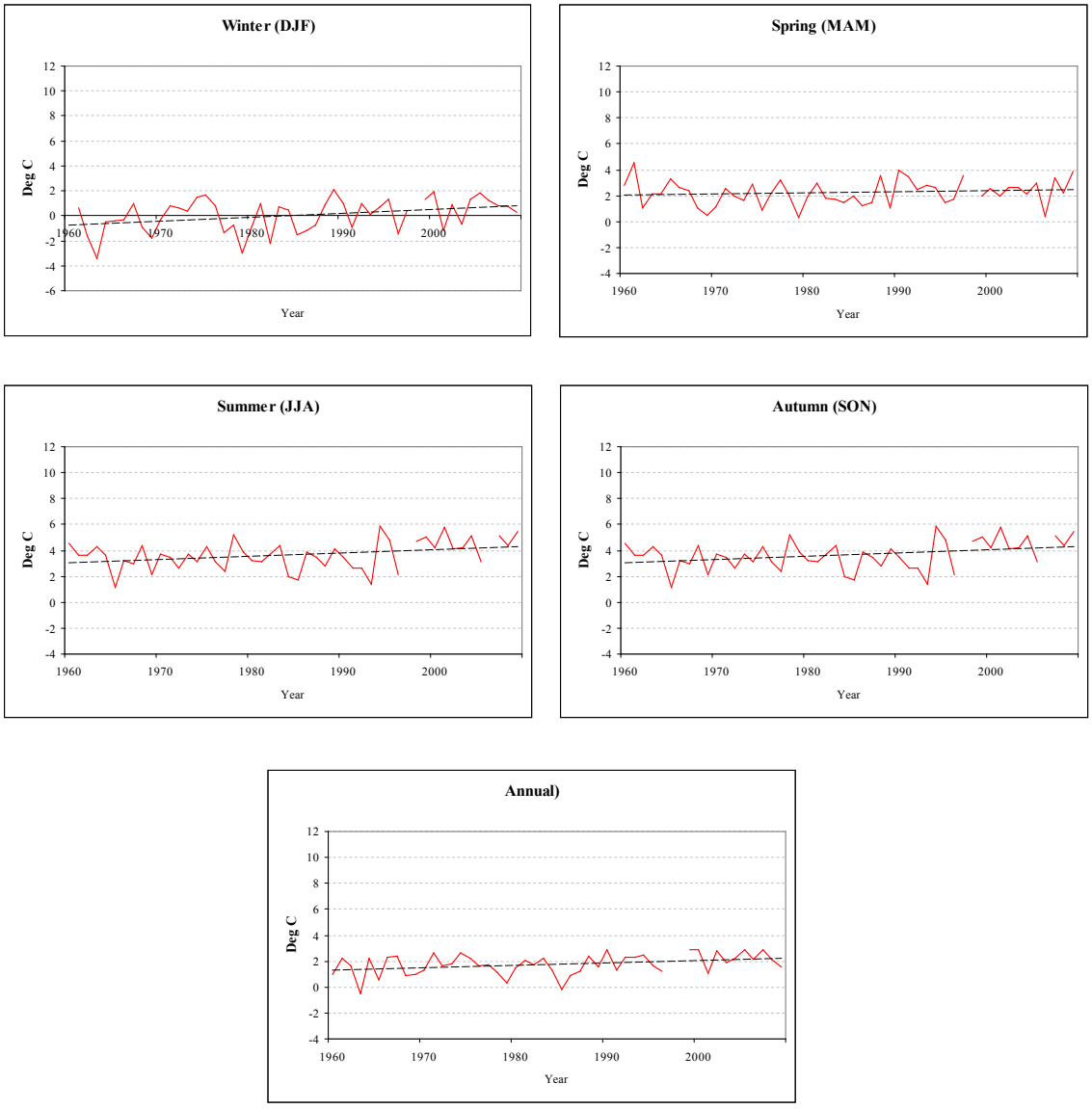

Figure 1.13 Trends in cold-day threshold (tn10) for each season and annually for the period 1960-2009. Trends in all seasons except spring (MAM) are significant at 95% level

1.6.3 Frost Days

There was a significant decrease in the number of frost days annually over the period 1960-2009 (-8.93 days; $p<0.05$; Figure 1.14; Table 1.5). This result must be assessed in the context of the maximum number of frost days recorded at Furnace. This was in 1963 when there were 41 days, with the average number of frost days over the whole period at 13 days per year. The low number of frost days reflects the mild oceanic climate of the coastal location. Similar results were found by McElwain and Sweeney (2007) for the other western and coastal sites of Valentia, Malin Head and Belmullet for the period 1960-2005.

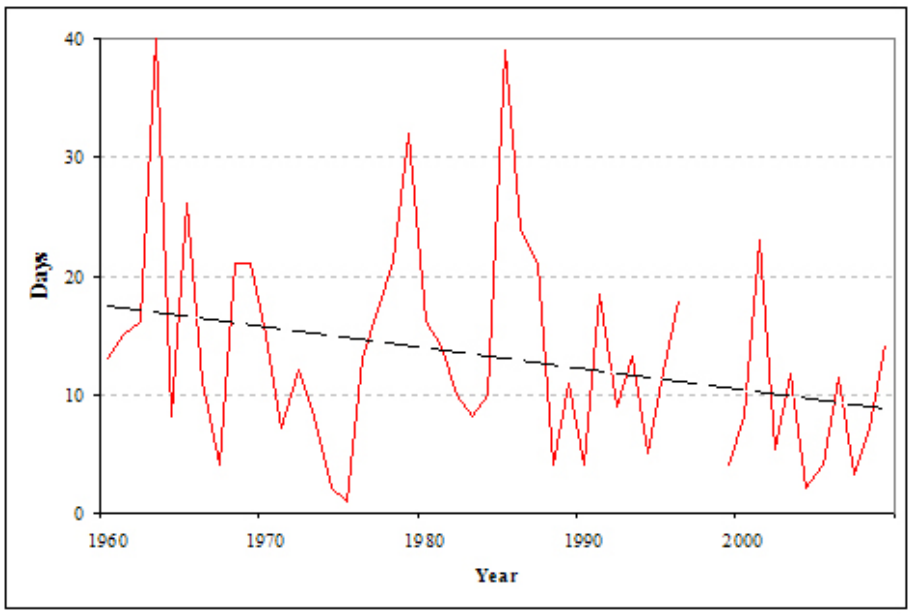

Figure 1.14 Decreasing trend in the number of frost days per year at Furnace for the period 1960-2009

1.6.4 Heat Wave Duration

Heat-wave duration increased in all seasons and annually with the increase in summer giving the only non-significant result (Figure 1.15; Table 1.5). Of the significant seasonal results, spring showed the greatest change with an increase of 4 days. This was followed by winter (3.47 days) and autumn (2.25 days). The greatest increase was found annually where heat wave duration increased by 4.6 days over the period.

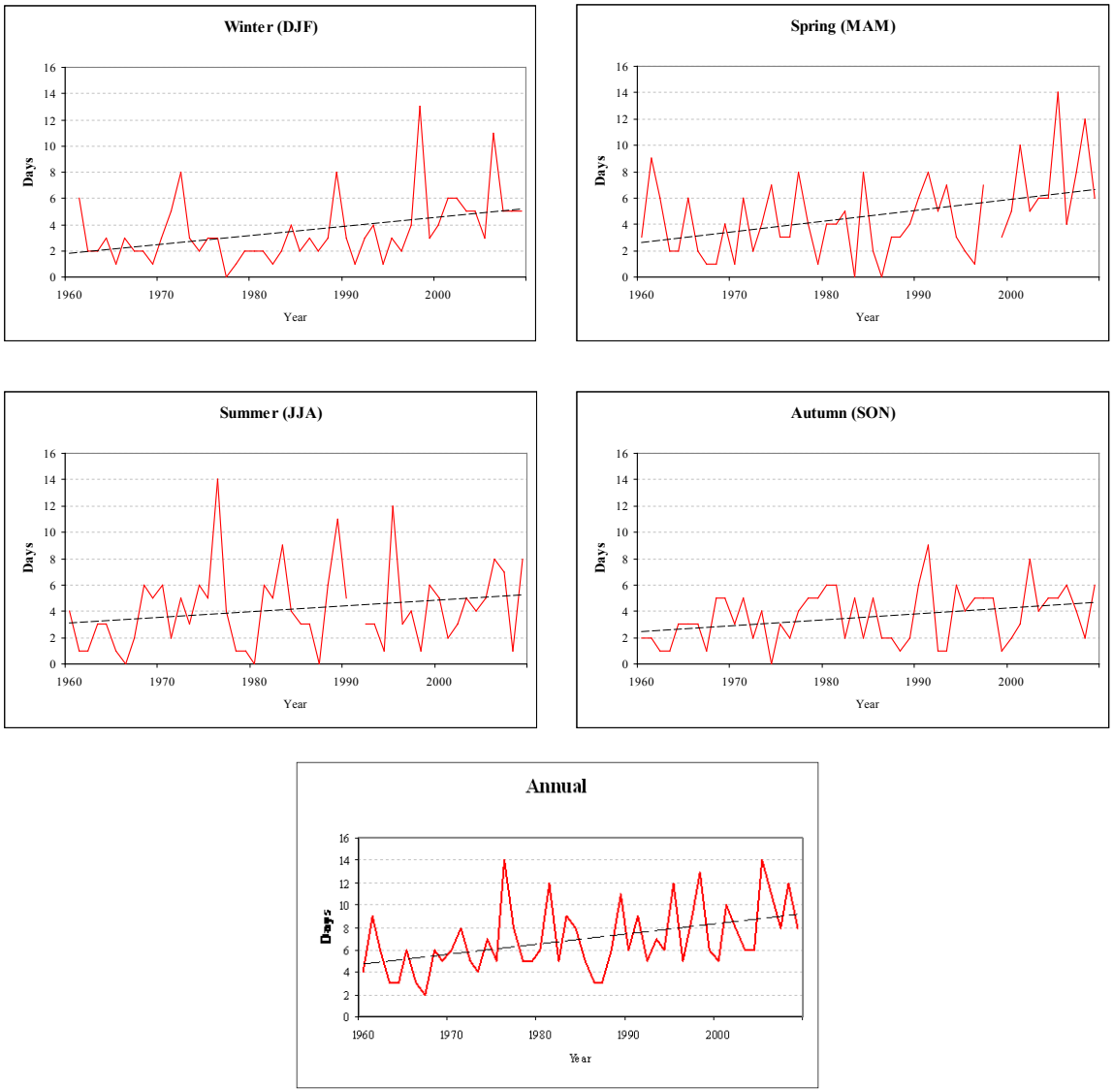

Figure 1.15 Trends in heat wave duration (hwd) at Furnace for the period 1960-2009 for each season and annually. All trends except summer (JJA) are significant.

1.6.5 Cold-wave Duration

Cold-wave duration (CWD) is the measure of the duration of percentile-based "cold snaps". There were no significant results for this index, although decreases were found in winter (-1.58 days), spring (0.09 days) and summer (-0.38 days) and increases were found for autumn (0.37 days) and annually (0.03 days). As none of these results were significant the data are not shown.

1.6.6 Frequency of Extreme Temperatures

Increases in the frequency of days with high temperature extremes (tx90per) occurred throughout each of the seasons and the year were found (Figure 1.16; Table 1.5). A high temperature extreme is defined as a day where the maximum temperature above the 90th percentile. All seasons except summer have experienced a significant increase in frequency of

extreme high temperature, with the greatest change found in spring (19.5%) closely followed by winter (17%), autumn (16%) and then annual (15%). Conversely decreases were found for low temperature extremes (tn10per) (Figure 1.18; Table 1.5). Significant decreases were found in winter (-9.5%), summer (-5.0%) and annually (-5.0%) while non-significant decreases were found in spring and autumn.

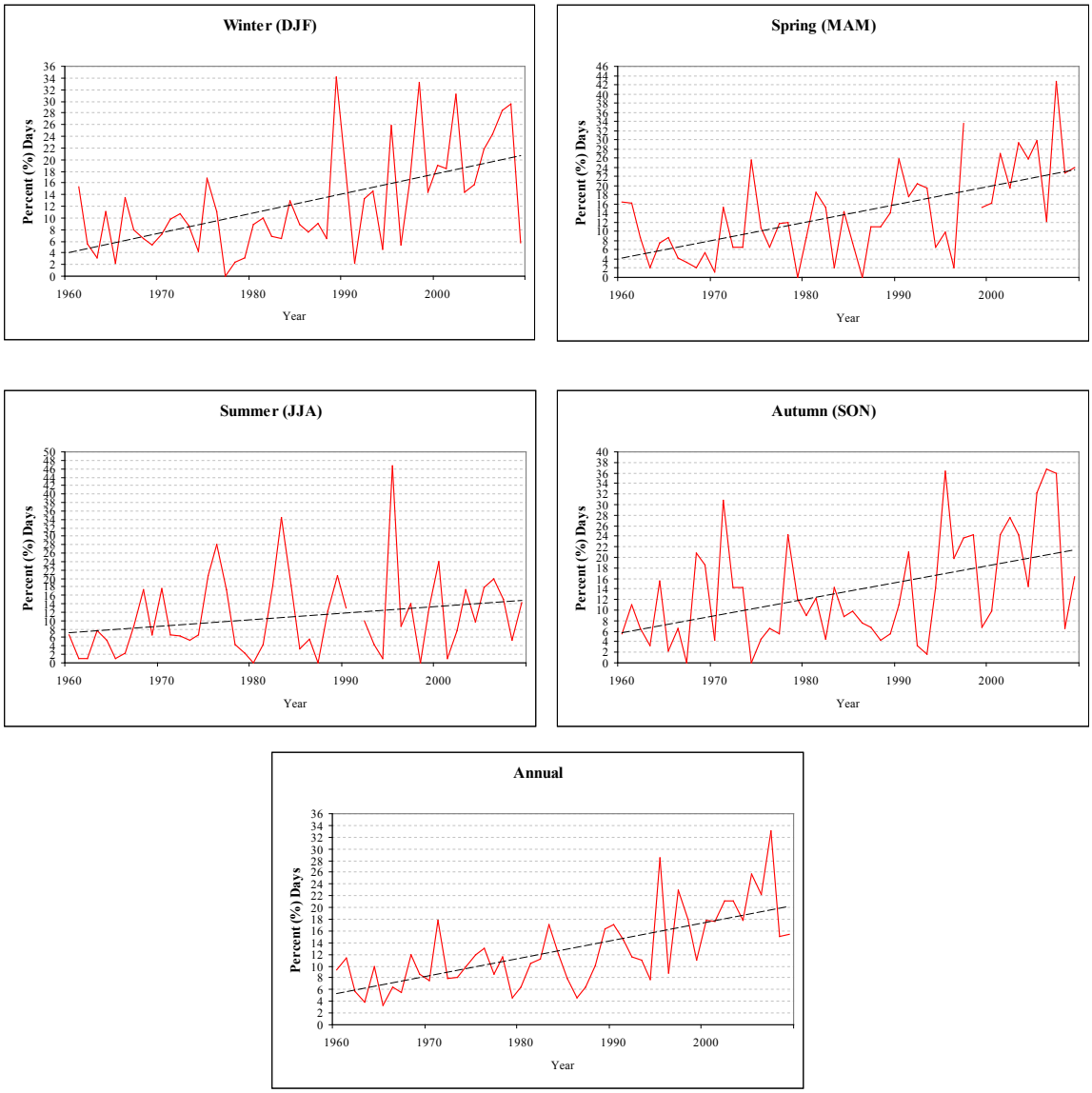

Figure 1.16 Frequency, as percentage days, in which maximum temperature is above the 90th percentile (tx90per) for each season and annually for the period 1960-2009. Significant upward trends were found for all seasons except summer (JJA).

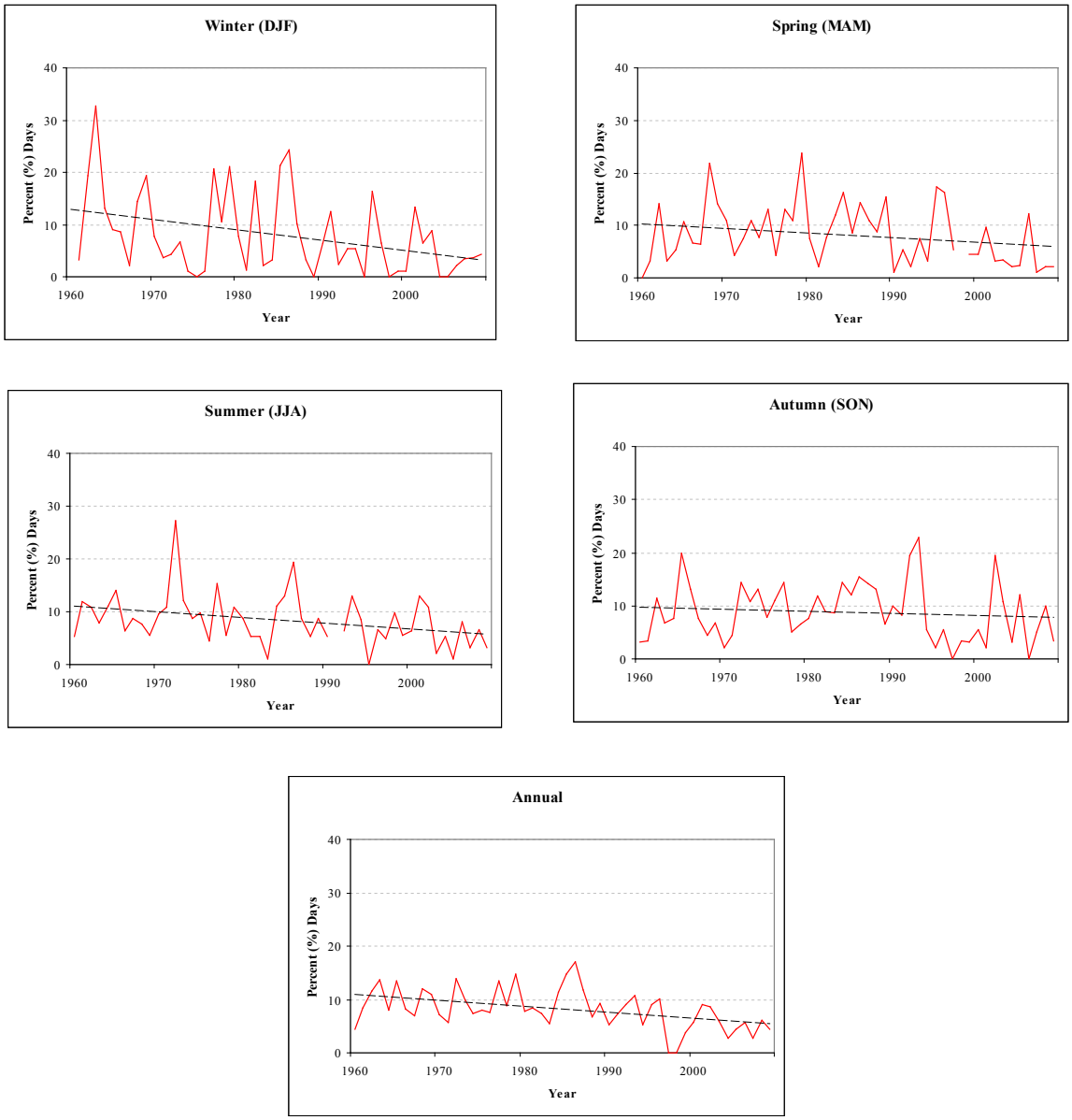

Figure 1.17 Frequency, as percentage days, in which minimum temperature is below the 10th percentile (tn90per) for each season and annually for the period 1960-2009. Significant downward trends were found in winter (DJF), summer (JJA) and annual.

Table 1.5 Summary results for extreme temperature indices. Values are change over period 1960-2009. tx90 is hot-day threshold, tn10 is cold-day threshold, tfnd is number of frost days, hwd is heat wave duration, tx90per is percentage frequency of extreme high (above 90th percentile) temperatures and tn10per is percentage frequency at extreme low (below 10th percentile) temperatures (* indicates significance at the 95% level, ** indicates significance at the 99% level).

	Mean	Max	Min	DTR	tx90	tn10	tnfd	hwd	tx90per	tn10per
	°C	°C	°C	°C	°C	°C	days	days	% days	% days
Winter (DJF)	1.7**	1.8**	1.1*	0.6*	1.3**	1.6*	-8.9	3.5**	17.0**	-9.5*
Spring (MAM)	1.8**	1.8**	1.0*	0.8*	2.6**	0.5	-1.1	4.0**	19.5**	-4.5
Summer (JJA)	1.5**	1.6**	1.3**	0.3	1.7*	0.9*	---	2.2	8.0	-5.0*
Autumn (SON)	1.4**	1.4**	0.9*	0.5*	1.3**	1.3*	---	2.2*	15.0**	-0.5
Annual	1.5**	1.6**	1.0**	0.6**	1.9**	1.0*	-8.9*	4.6**	15.0**	-5.0**

1.6.7 Temperature Variability and the North Atlantic Oscillation (NAO)

The North Atlantic Oscillation (NAO) accounts for a large proportion of climatic variability in Western Europe, especially in winter, affecting precipitation (e.g. Kiely, 1999; Murphy and Washington, 2001; Fowler and Kilsby, 2002; Gallego et al., 2005), streamflow (Kiely, 1999) and temperatures (e.g. Hurrell and van Loon, 1997; Jennings et al., 2000; Hurrell et al., 2003; Jones and Moberg, 2003; George et al., 2007). It has been shown that local changes in meteorological variables in mid-latitudes are mainly controlled by the atmospheric circulation (Parker et al., 1994; Hurrell, 1995; Hurrell and Van Loon, 1997). The NAO index is defined as the sea-level pressure differences between pressure centres located near Iceland and the Azores. In general a high winter NAO index is associated with increased winter air temperatures, high wind speeds and increased rainfall, due to a north-eastward storm track taking depressions into northern Europe, whereas a low NAO index is associated with winter tracks storms on an east-west orientation taking depressions into the Mediterranean and resulting in cooler, drier conditions for Western Europe (Hulme and Barrow, 1997). A high NAO index is associated with increased westerlies and hence precipitation in Western Europe.

Table 1.6 Correlation coefficients between monthly-NAO and monthly air temperature anomaly (* indicates significance at 0.05 level, ** indicates significance at 0.01 level).

Month	Correlation coefficients
October	0.30*
November	0.15
December	0.59**
January	0.69**
February	0.71**
March	0.40**

There was no relationship found between the seasonally averaged winter NAO and winter air temperature anomaly (r=0.1889, p=0.198). However, positive correlations were found between the monthly air temperature anomaly and monthly NAO in the winter months of October-March (Figure 1.18). Relationships were significant in all months except November (Table 1.6). The lack of correlation in the seasonal data could be due to the low monthly persistence of NAO reported by Murphy and Washington (2001).

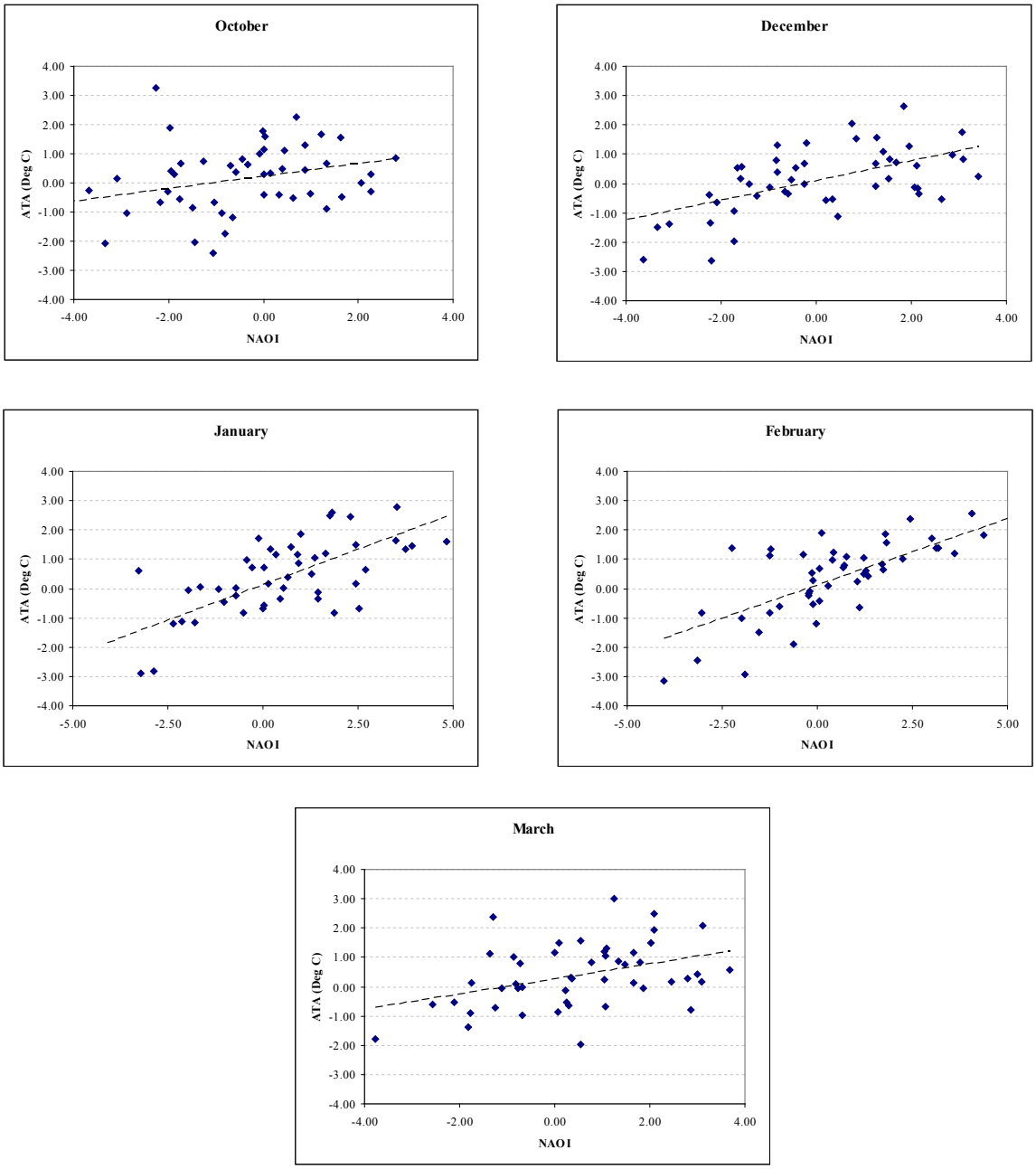

Figure 1.18 Significant monthly correlations between NAO and air temperature anomaly for the period 1960-2008

1.6.8 Summary: Extreme Temperatures

Analysis of air temperature trends at Furnace over the last 50 years indicated that there has been warming over the period. This is especially true in spring and winter, where maximum temperatures have risen by 1.8°C, minimum temperatures have risen by 1.0°C and 1.1°C respectively and mean temperatures by 1.8°C and 1.7°C respectively over the period. Maximum temperatures have increased more than minimum temperatures in all seasons and annually, resulting in increased DTR (Table 1.5).

Mean maximum and minimum temperatures increased significantly in Ireland over the period 1960-2005 (McElwain and Sweeney, 2007). For the comparable time period of 1960-2005 maximum and minimum temperatures also increased at Furnace (Table 1.7 and Table 1.8). Changes in maximum temperatures at Furnace were all greater than those reported for Ireland. However minimum temperature changes were greater for Ireland over the period than Furnace. Minimum temperatures increased more than maximum in spring, summer, autumn and annually for Ireland giving rise to an increase in Diurnal temperature range (DTR), where the opposite was found at Furnace (Table 1.7).

Table 1.7 Changes in maximum and minimum temperatures for Furnace and Ireland for the period 1960-2005. Ireland data is the all stations analysis of McElwain and Sweeney (2007). * indicates significance at 0.05 level. ** indicates significance at 0.01 level

	Furnace		Ireland	
	Max	Min	Max	Min
	°C	°C	°C	°C
Winter	1.53**	0.92*	1.37**	1.27**
Spring	1.39**	0.85*	1.16**	1.19**
Summer	1.35**	1.12**	1.07**	1.34**
Autumn	1.09**	0.63*	0.83**	0.93**
Annual	1.35**	0.85**	1.10**	1.15**

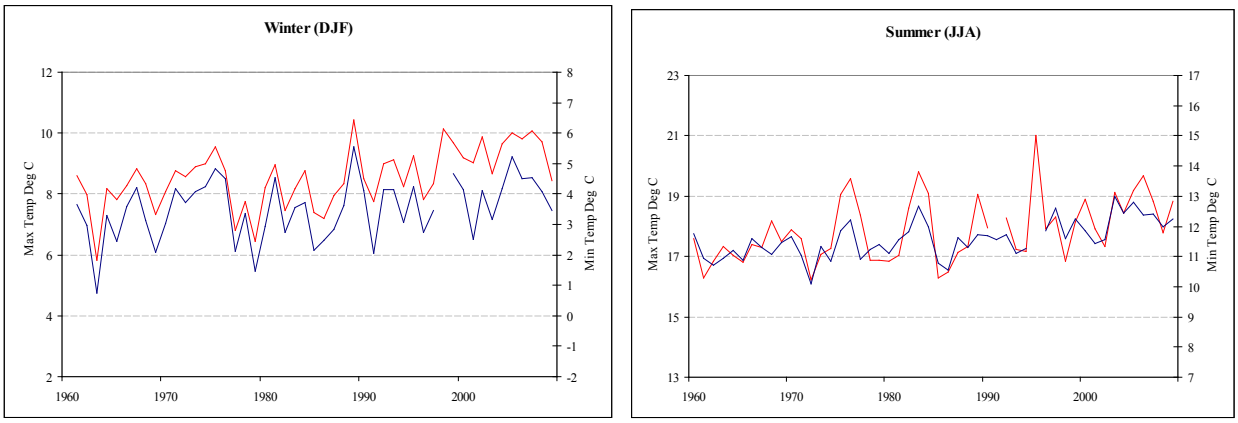

Figure 1.19 Winter (DJF) and summer (JJA) mean maximum and minimum temperatures for 1960-2009 at Furnace. Red line is mean maximum temperature and blue line is mean minimum temperature. Gaps relate to missing data due to equipment fault in late 1990s

The general upward trend in summer and winter maximum and minimum temperatures for Furnace for the period 1960-2009 was apparent from the mid-1980s, particularly in winter maximum temperature (Figure 1.19). Both maximum and minimum temperatures in winter 2009 were lower than recent years. This was due to a very cold December in Ireland. In many areas around the county it was the coldest December in almost 30 years (Met Éireann, 2009). The lowest air temperature recorded during this month was -10°C recorded at Mullingar, the coldest since 1981. Mean monthly air temperature for December was 2.3°C in some areas,

including Knock Airport, Co. Mayo. Although mean air temperature at Furnace for December was not as low as this, it was the coldest December since 1981 (4.6°C in December 2009, 3.7°C in December 1981) and the third coldest recorded since records began in 1959 (mean December air temperature for 1976 and 1981 was 3.7°C and for 1961 was 4.4°C).

Analysis of extreme temperatures also indicated a rise in temperatures and a decrease in cold-temperature related indices. This was, again, particularly apparent in spring and winter. In spring, the hot-day threshold increased significantly by 2.6°C over the period, however no significant increase in the cold-day threshold was found for this season indicating that warming in spring is confined to the upper end of the temperature distribution. In winter, hot-day threshold increased significantly by 1.3°C and cold day threshold increased significantly by 1.6°C, indicating that warming in this season is occurring at both the upper and lower ranges of the temperature distribution. This is further seen in winter by the increase in frequency of extreme high temperatures and the decrease in frequency of extreme low temperatures. In spring there was an increase in the extreme high, but not the extremes of low temperature. These changes indicate not just an upward trend, or warming in temperatures, but also a change in the frequency distribution of temperatures with warmer warm periods lasting longer as well as warmer, less frequent cold-periods. There is a strong correlation between monthly air temperature and NAO during winter. The NAO accounts for between 30%-70% of the monthly air temperature variation for the months October-March.

Table 1.8 Increases in maximum and minimum temperature over the period 1961- 2005 for 11 stations around Ireland after McElwain and Sweeney (2007) and for Furnace (* indicates significance at the 95% level, ** indicates significance at the 99% level).

1961-2005	Spring Max	Spring Min	Summer Max	Summer Min	Autumn Max	Autumn Min	Winter Max	Winter Min
Furnace	*1.39***	*0.85*	*1.35***	*1.12***	*1.09***	*0.63*	*1.53***	*0.92*
Valentia	0.68*	1.05*	0.43	1.20**	0.54	0.87*	1.17**	1.34*
Shannon	1.27**	1.58**	1.18*	1.70**	1.01*	1.28**	1.50**	1.83**
Malin	0.75*	1.18**	0.63	1.13**	0.47	0.84**	1.04*	1.20**
Belmullet	1.40**	1.21**	1.30**	1.39**	1.16**	0.80*	1.44**	1.23*
Phoenix Park	1.41**	0.88*	1.43**	0.92**	0.84*	0.41	2.52**	0.85
Clones	1.27**	1.33**	1.36**	1.63**	0.92**	1.04*	1.33**	1.41*
Rosslare	1.06**	1.28**	1.12**	1.19**	0.97**	1.02**	1.62**	1.32**
Claremorris	1.32**	1.19**	1.25**	1.49**	0.92*	0.84*	1.22**	1.32*
Kilkenny	1.40**	1.18**	1.22*	1.46**	0.95*	1.21**	1.52**	1.40**
Casement	1.05**	1.27**	0.83*	1.40**	0.55	1.15**	1.61**	1.36*
Birr	1.18**	0.95*	0.98*	1.21**	0.77*	0.77	1.44**	1.14*

1.7. Precipitation

1.7.1 Mean Precipitation

Trends in mean precipitation for each season and annually were examined for the period 1960-2009. Small non-significant upward trends were found for all seasons while a small significant increase of 0.01mm/yr in mean precipitation was found annually (p=0.023; Figure 1.20).

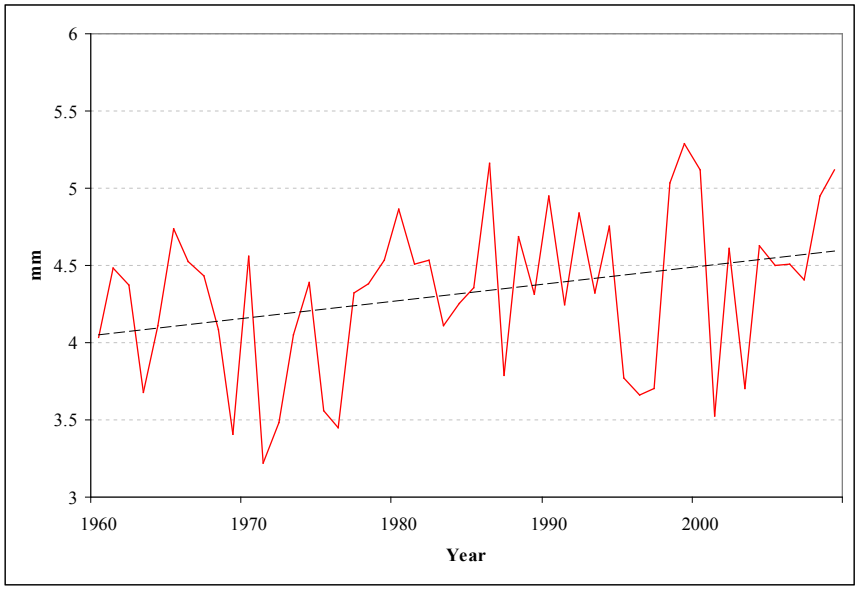

Figure 1.20 Increasing trend in annual average rainfall increase over the period 1960-2009

1.7.2 Extreme Precipitation Indices

Frequency of Extreme Precipitation

Maximum number of consecutive dry days (cdd) was examined to elucidate whether an increase in dry periods, indicative of droughts, has occurred. Although none of the results were found to be significant, increases in number of consecutive dry days were found in winter (1.85 days) and autumn (0.88 days) with a reduction in the index in spring (-1.95 days), summer (-3.33 days) and annually (-1.96 days). As these results were not significant data are not shown. These results are in line with data from 11 Irish sites which showed a general (but non-significant) increase in winter and a decrease in the in the summer (McElwain and Sweeney, 2007).

Changes in the frequency of extreme events was analysed using two indices: the percentage of total rainfall from events greater than the long-term 90th percentile (pfl90) and the number of events greater than the long-term 90th percentile of rain-days (pnl90). The first index measures the heavy rainfall proportion and the second the frequency of days with heavy rainfall.

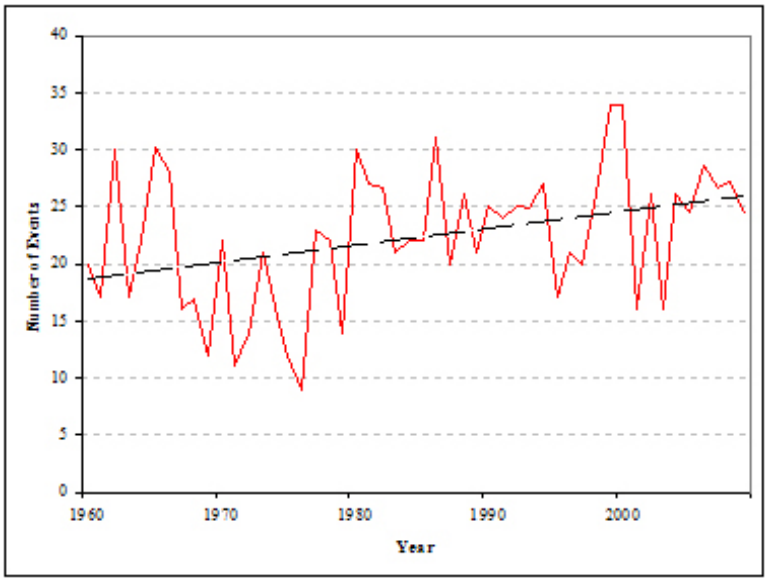

Figure 1.21 Significant increases in number of events greater than the long-term 90th percentile of rain-days in winter over the period 1960-2009

There were no significant changes in the heavy rainfall proportion (pfl90) over the period, indicating that the amount of rain falling as a result of heavy showers has not changed. However, there were significant changes in heavy rainfall frequency (pnl90) annually with an increase of 7.4 events over the period (p=0.017; Figure 1.21). This was also seen in the McElwain and Sweeney (2007) study which found increases in the north and west of Ireland with few significant results.

Precipitation Intensity

Simple daily rainfall intensity (sdii) is a measure of the amount of rain per rain-day. This index was examined in all seasons and annually. Weak upward trends were found in for all seasons and annually for this index but the results were not significant, hence data is not shown.

The greatest 5-day rainfall (px5d) showed no significant changes over the period 1960-2009. There were weak upward trends in winter and spring and weakly decreased amounts in summer, spring and annually (data not shown). This is similar to results from McElwain and Sweeney (2007) which showed an increase in winter in the north-west of the country in winter and a decrease in summer.

Rainfall intensity as measured by the 90th percentile of rain day amounts (pq90) was examined for all seasons and annually. This index measures the upper end of the rainfall distribution, i.e. extreme heavy rainfall events. Although increases were seen in all seasons, the only significant change was found annually where there was an increase of 1.19mm/day over the period (p=0.03; Figure 1.22)

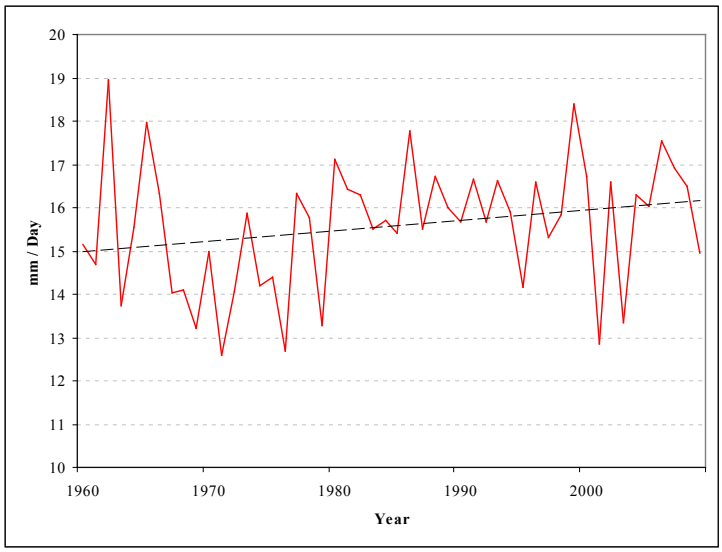

Figure 1.22 Significant increases in 90th percentile rain-day amounts annually over the period 1960-2009

1.7.3 Precipitation and the North Atlantic Oscillation (NAO)

Significant positive relationships were observed between winter NAO and precipitation anomaly (PA) in winter ($r=0.67$, $p<0.001$). The percentage precipitation variance due to the NAO in the winter season was 45%.

Table 1.5 Correlation coefficients between monthly-NAO and monthly precipitation anomaly. * indicates significance at 0.05 level. ** indicates significance at 0.01 level.

Month	Correlation coefficients
October	0.66**
November	0.71**
December	0.50**
January	0.51**
February	0.43**
March	0.69**

Positive relationships were found between monthly NAO and precipitation anomaly in the winter months October-March (Table 1.9; Figure 1.23). There was a significant positive correlation between NAO and precipitation anomaly for each of the winter months October-March. Correlation co-efficient values were highest in November, with 50% of the variance in precipitation accounted for by the NAOI. The lowest r value was found in February, which had 19% of its precipitation variance explained by the NAO.

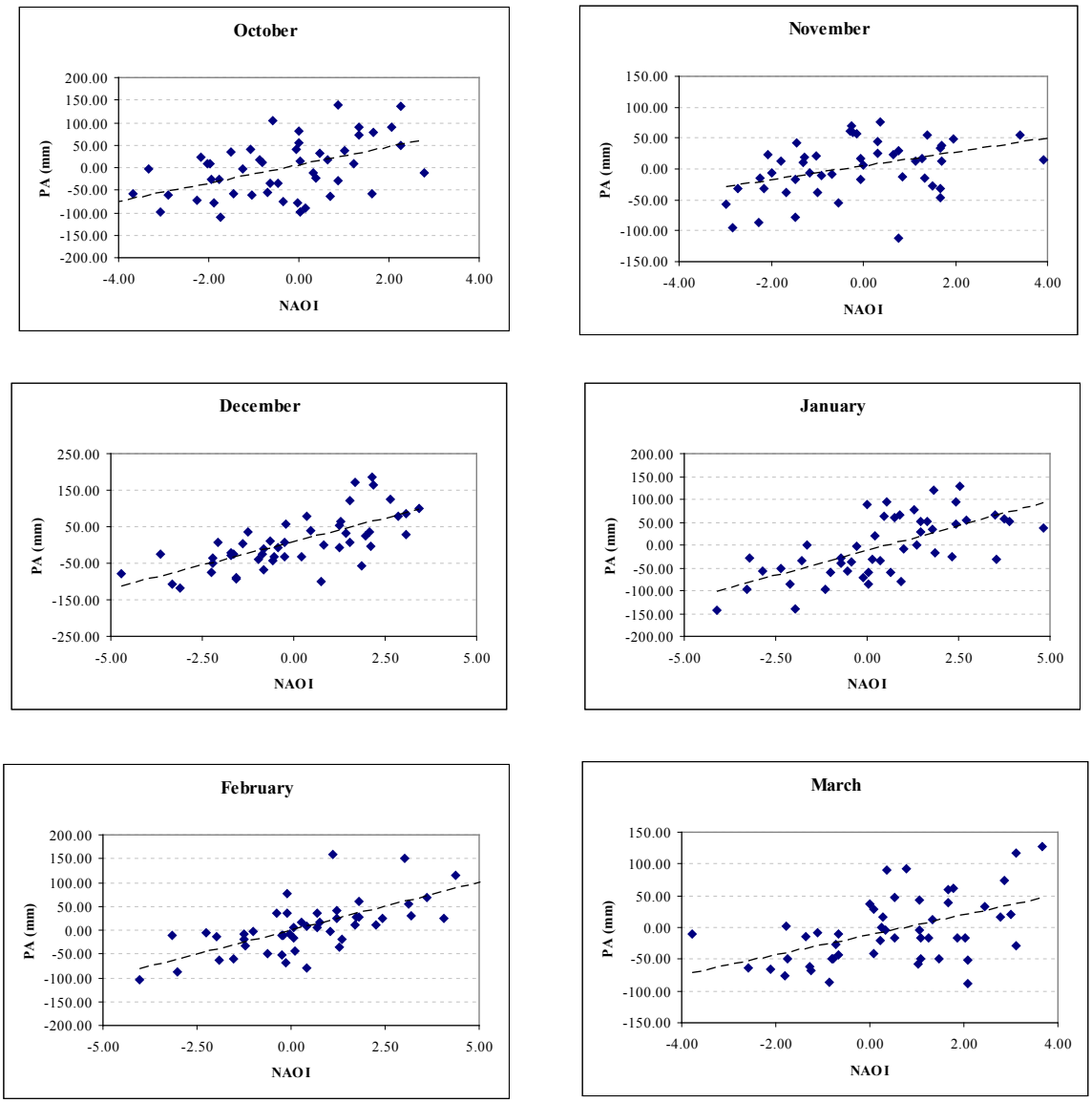

Figure 1.23 Significant monthly correlations between NAOI and precipitation anomaly

1.7.4 Summary: Precipitation

There has been an increase in the frequency and intensity of extreme precipitation in winter and annually at Furnace over the last 50 years. The frequency of heavy rainfall (90th percentile) increased. In winter there was an increase of 3.3 events over the period and annually an increase of 7.5 events. This result corroborates earlier findings that heavy rainfall frequency has increased on the west and north coasts of Ireland (McElwain and Sweeney, 2007). The intensity of heavy rainfall (90th percentile of rain day amounts) increased. In winter there was an increase of 2.5mm/day over the period and annually an increase of 1.32 mm/day. This result also agrees with previous study (McElwain and Sweeney, 2007) which found that extreme rainfall intensity has increased in the west and north of Ireland. Winter precipitation is significantly correlated with the North Atlantic Oscillation, with high NAO values resulting in increased precipitation both in the season of winter (DJF) and for each month October-March.

The r values for each month (ranging from 0.43-0.71) imply that the NAO is a significant cause of variance of precipitation in the west of Ireland during winter. Similar findings are reported by Kiely (1999) for the west of Ireland and are indicative of the strong westerly influence on precipitation in the region.

1.8. Water Temperature

1.8.1 Mean Midnight Water Temperature Trends

Water temperature anomalies were calculated using departures from the baseline 1961-1990 mean for each season and annually. The annual midnight water temperature anomaly (WTA) record displayed a cool period from the early 1960s to 1970s, followed by warmer temperatures from late 1970s-1980s. Cooling in the mid 1990s was followed by another period of overall higher temperatures until present. Four of the ten hottest years were recorded in the 1990s, three in the 2000s, two in the 1980s and one in the 1970s meaning that 70% of the ten warmest years have occurred since 1990 (Figure 1.24). A notable feature of the midnight water temperature record was the high value in 1990 which had the highest water temperature anomaly for all seasons and annually with the largest departure from the baseline mean in spring (Table 1.10).

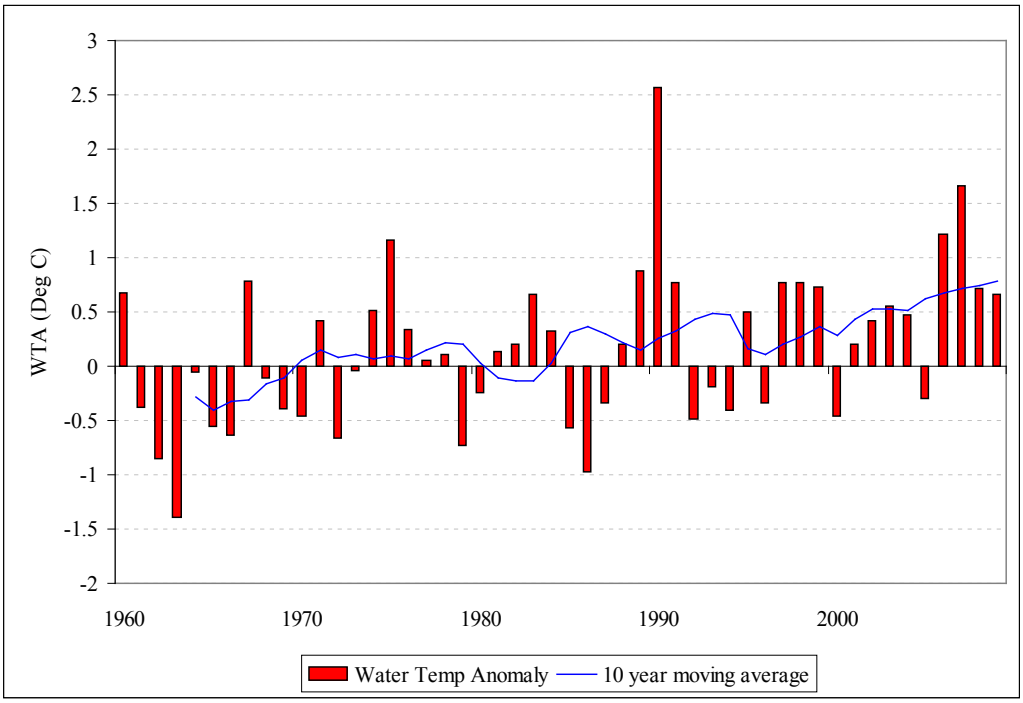

Figure 1.24 Annual water temperature anomalies for the period 1960-2009. Bars are annual WTA and line is 10 year moving average.

Trends in midnight water temperature were examined for each season and annually for the period 1960-2009. An increase in midnight water temperature was found in all seasons and annually (Figure 1.25; Figure 1.26). The largest change in midnight water temperature was seen

in winter and spring with an increase of 1.8°C and 1.79°C respectively over the period ($p<0.01$). The smallest change was seen in autumn which showed an increase of 1.13°C ($p<0.01$) and then summer with a 1.2°C increase ($p<0.01$) over the period. Annually midnight water temperature increased by 1.34°C over the period ($p<0.01$). The amount of variance accounted for by the increase in spring water temperature was 26.8%.

Table 1.10 Mean seasonal and annual water temperature (°C) and water temperature anomaly for 1990, the warmest year on record

	Water Temperature (°C)	Water Temperature Anomaly (°C) 1990
Spring	11.39	3.64
Summer	18.72	3.32
Autumn	13.81	1.90
Winter	7.58	2.19
Annual	12.48	2.35

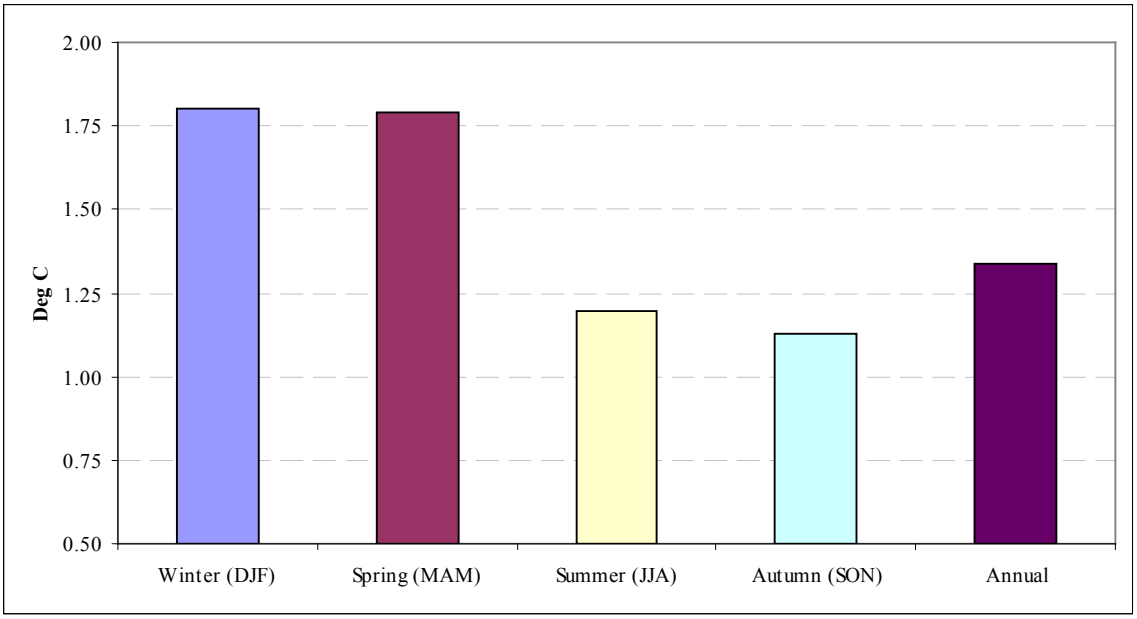

Figure 1.25 Increases in midnight water temperatures from 1960-2009 for each season and annually. All results are significant at 99% level. Note scale.

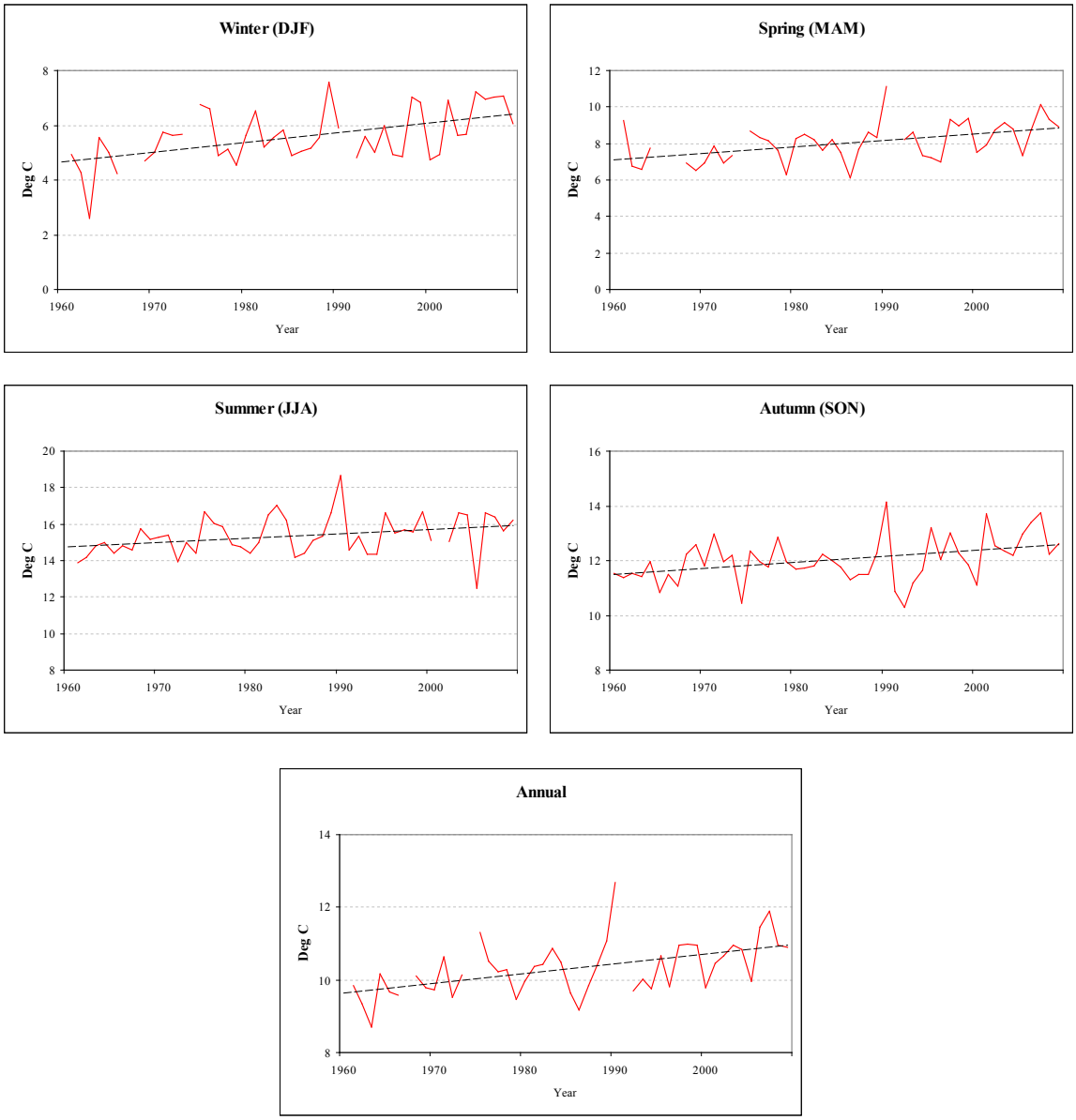

Figure 1.26 Change (°C) in mean midnight water temperature for each season and annually for the period 1960-2009. All results are significant at the 99% level.

1.8.2 Water Temperature and the North Atlantic Oscillation (NAO)

Significant positive relationships were observed between winter NAO and water temperature anomaly (WTA) in winter ($r=0.52$, $p<0.001$). The percentage water temperature variance due to the NAO in the winter season was 27%. Positive correlations were found between monthly NAO values and water temperature anomalies in the winter months of October-March, although only two of these correlations were significant (Table 1.11; Figure 1.27). There was a significant positive correlation between NAO and water temperature anomalies in January and February. The greatest r values were found in January with 20% of the variance in water temperature accounted for by the NAO during this month. The other significant result was in February, which had 11% of its water temperature variance explained by the NAOI.

Table 1.11 Correlation coefficients between monthly-NAO and monthly water temperature anomaly. * indicates significance at 0.05 level. ** indicates significance at 0.01 level.

Month	Correlation coefficients
January	0.45**
February	0.34*

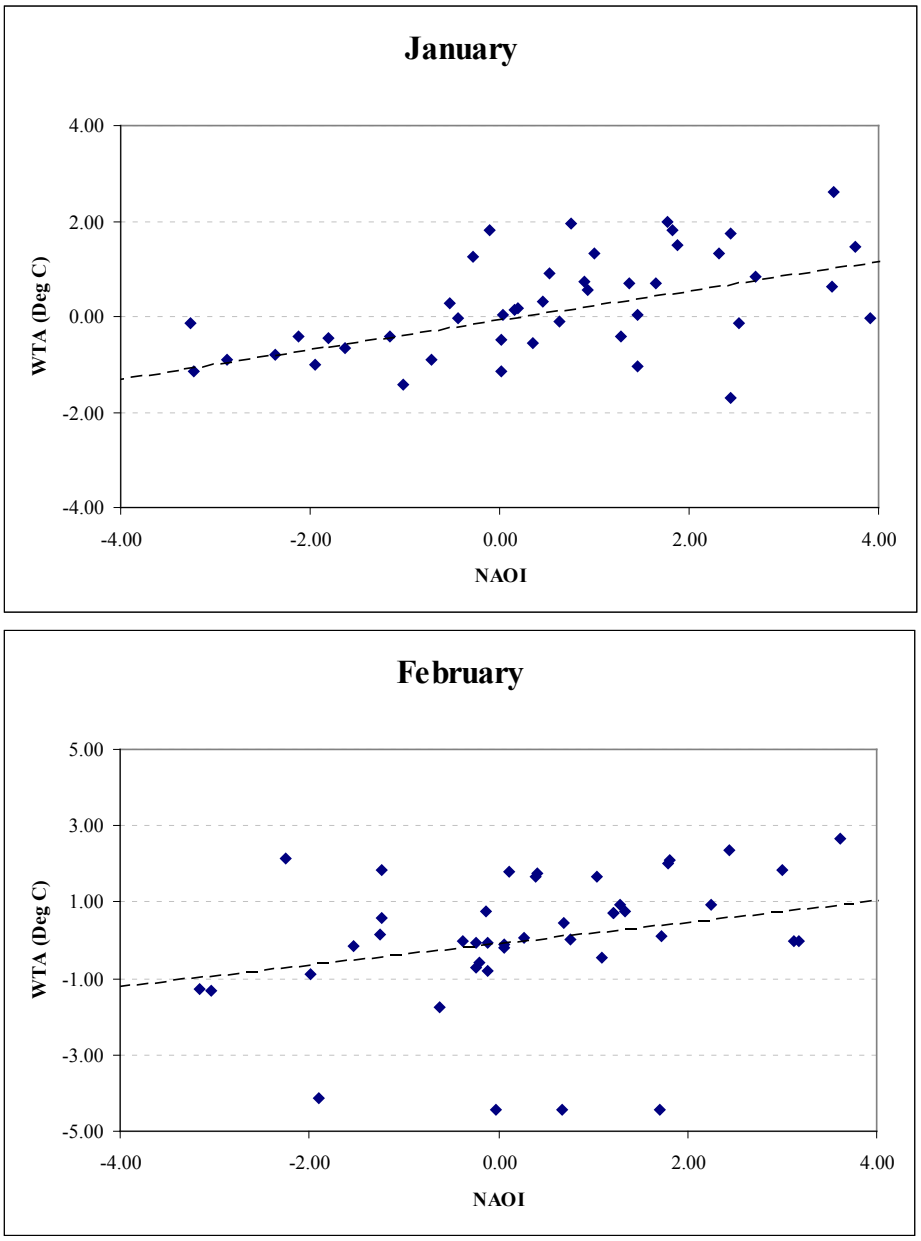

Figure 1.27 Significant monthly correlations between NAO and water temperature anomalies for the period 1960-2008

1.8.3 Summary: Water Temperature

Mean midnight water temperature has increased over the period 1960-2009 in all seasons and annually. The greatest change was found in winter (DJF) closely followed by spring (MAM) with an increase of 1.8°C and 1.79°C over the period respectively. This result is similar to other

studies of long-term water temperature records which have reported increases in water temperature, especially in spring. Water temperature in winter and in the months of January and February are significantly correlated to the NAO, with 21% of the variation in midnight water temperature in January accounted for by this large-scale circulation.

1.9. Summary

Maximum and minimum air temperatures have increased globally, with minimum temperatures increasing more than maximum in the majority of cases, albeit with regional variability (e.g. McElwain and Sweeney, 2007; Bartolini et al., 2008; Peralta-Hernandez et al., 2009; Rehman, 2009). Extreme events associated with warming, such as heat-wave duration and hot-day threshold have also increased across the globe, Europe and in Ireland, while indices relating to cooling, for example number of frost days, have decreased (Haylock, 2003; Hundecha and Bardossy, 2005; McElwain and Sweeney, 2007). There has also been a change in precipitation, with many extra-tropical regions reporting an increase in total precipitation, often due to an increase at the extreme end of the distribution (e.g. Bardossy, 2003; Haylock and Goodness, 2004; Alexander et al., 2005; Zhang et al., 2007). There have been increases in rainfall intensity and in the frequency of extreme events. However there is large regional, temporal and spatial variability and a decrease in precipitation has been found at the tropics and in some regions, such as south eastern Ireland, during the summer season (McElwain and Sweeney, 2007). A rise in water temperature has been reported, especially in spring, although direct human actions may be a contributing factor in these changes (Langan et al., 2001; Moater and Gailhard, 2006).

Due to its location on the west coast of Ireland, Furnace is largely influenced by climate variability in the Atlantic region and general long-term trends attributed to directional climate change, which have been noted both in Ireland and globally, are apparent. Air temperature at Furnace, has increased significantly over the period 1960-2009. This increase is apparent in both maximum and minimum temperatures, with maximum temperatures increasing more than minimum in all seasons and annually, particularly in winter and spring which have seen an increase in maximum temperature of 1.8°C over the period. As a result of this DTR has also increased contrary to the general Irish and global norm. The distribution frequency has also changed, with hot days now hotter and lasting longer and warmer, less frequent cold days. In essence the climate is becoming "less cold" (Alexander et al., 2005). All indices, including extreme indices, relating to warming have increased, e.g. heat wave duration, hot-day threshold, cold-day threshold and those relating to cooling have decreased, e.g. number of frost days. There has also been an increase in the frequency and intensity of extreme

precipitation in winter and annually, similar to changes found in the UK, Europe and other extra-tropical regions around the globe.

Mean midnight water temperature in the catchment has increased over the period 1960-2009 in all seasons and annually. The greatest change was found in winter (DJF) closely followed by spring (MAM) with an increase of 1.8°C and 1.79°C over the period respectively. This result is similar to other studies of long-term water temperature records which have reported increases in water temperature, especially in spring. These other studies however have often been unable to draw conclusions from the increasing trends due to the influence of local human activities on the river (Webb et al., 2008). At this site human-impact has been minimal with very few changes in the environment over the study period. Therefore, it is reasonable to suggest that the increase in water temperature in the catchment is not significantly due human-induced factors. A pan-European study of lake temperatures (Arvola et al., 2009) also reported an increase in lake water temperature in winter and summer with the most rapid increase in Ireland and the United Kingdom. Lough Feeagh, located in the Burrishoole catchment, was part of this large-scale study. It is interesting to note that no significant increase in Lough Feeagh winter water temperature was found, contrary to the present study.

Furnace is highly influenced by climate variability in the Atlantic region, in particular the North Atlantic Oscillation (NAO). Winter precipitation and water temperature are significantly correlated with the NAO, with positive phases of the NAO resulting in increased precipitation and warmer water temperatures in winter (DJF). On a monthly basis (October-March) the NAO was found to have a significant influence on air temperature and precipitation. A relationship between the NAO and water temperature was only significant for the months of January and February.

1.10. Key Findings

- Air temperatures were found to have increased significantly at Furnace over the period 1960-2009. This increase is apparent in both maximum and minimum temperatures, with maximum temperatures increasing more than minimum in all seasons and annually. Tempertaure increase is particularly evident in winter and spring which have seen an increase in maximum temperature of 1.8°C over the period of record.
- The diurnal temperature range (DTR) has also increased, contrary to global trends for this measure. However, significant regional variations can occur in the diurnal temperature range with contradictory trends apparent within regions.

- The distribution frequency of temperature was also found to have changed, with hot days now hotter and the number of consecutive hot days increasing while cold days have become less frequent and less cold.
- Indices relating to warming, e.g. heat wave duration, hot-day threshold, cold-day threshold, have increased, while those relating to cooling e.g. number of frost days have decreased.
- There has also been an increase in the frequency and intensity of annual extreme precipitation, similar to changes found in the UK, Europe and other extra-tropical regions around the globe.

1.11. References

Aguilar, E., Peterson, T.C., Ramírez-Obando, P., Frutos, R., Retana, J.A., Solera, M., Soley, J., González García, I., Araujo, R.M., Rosa Santos, A., Valle, V.E., Brunet, M., Aguilar, L., Alvarez, L., Bautista, M., Castanon, C., Herrera, L., Ruano, E., Sinay, J.J., Sanchez, E. and Hernandez Oviedo, G. (2005) 'Changes in precipitation and temperature extremes in central and northern south America, 1961-2003', *Journal of Geophysical Research*, 110 no. D23, doi: 10.1029/2005JD006119.

Alexander, L., Zhang, X., Peterson, T.C., Caesar, J., Gleason, B., Klein Tank, A., Haylock, M., Collins, D., Trewin, B., Rahimzadeh, F., Tagipoura, A., Ambenje, P., Rupa Kumar, K., Revadekar, J., Griffiths, G., Vincent, L.V., Stephenson, D., Burn, J., Aguilar, E., Brunet, M., Taylor, M., New, M., Zhai, P., Rusticucci, M., and Vazquez-Aguirre, J.L. (2005) 'Global observed changes in daily climate extremes of temperature and precipitation', *Journal of Geophysical Research*, 111, no. D05109

Allott, N., McGinnity, P. and O'Hea, B. (2005) 'Factors influencing the downstream transport of sediment in the Lough Feeagh catchment, Burrishoole, Co. Mayo, Ireland', *Freshwater Forum,* 23, 126-138.

Anderson, R. (1969) 'Temperature and rooted aquatic plants', *Chesapeake Science*, 10 (3-4), 157-164

Anon, (2005) 'Article 5 The characterisation and analysis of Ireland's river basin districts. In accordance with Section 7 (2 & 3) of the European Communities (Water Policy) Regulations 2003 (SI 722 of 2003)'. *National Summary Report (Ireland)*, Compendium of public submissions and responses.

Arvola, L., George, G., Livingstone, D.M., Järvinen, M., Blenckner, T., Dokulil, M.T., Jennings, E., Nic Aongusa, C., Nõges, P., Nõges, T. and Weyhenmeyer, G.A. (2010) 'The Impact of the Changing Climate on the Thermal Characteristics of Lakes', in *The impact of climate change on European lakes,* ed G George, *In Press*.

Bartolini, G., Morabito, M., Crisci, A., Grifoni, D., Torrigiani, T., Petralli, M., Maracchi, G. and Orlandini, S. (2008) 'Recent trends in Tuscany (Italy) summer temperature and indices of extremes', *International Journal of Climatology*, 28, pp. 1751-1760

Bardossy, A., Anagnostopoulou C., Cacciamani, C., Caspary, H., Frei, C., Goodness, C., Haylock, M., Hundecha, Y., Maheras, P., Michna, P., Pavan, V., Plaut, G., Schmidli, J., Schuepbach, E., Simonnet, E., Tolika, K. and Tomozeiu, R. (2003) *Trends in extreme daily precipitation and temperature across Europe in the 2nd half of the 20th century*, STARDEX, Climatic Research Unit, University of East Anglia, viewed 2nd June 2009, <http://www.cru.uea.ac.uk/cru/projects/stardex>.

Brazdil, R., Budikova, M., Auer, I., Bohm, R., Cegnar, T., Fasko, P., Lapin, M., Gajic-Capka, M., Zaninovic, K., Koleva, E., Niedzwiedz, T., Ustrnul, Z., Szalai, S. and Weber, R.O. (1996) 'Trends of maximum and minimum daily temperatures in central and south-eastern Europe', *International Journal of Climatology*, 16, 765-782

Brohan, P., Kennedy, J.J., Harris, I., Tett, S.F.B. and Jones, P.D. (2006) 'Uncertainty estimates in regional and global observed temperature changes: A new dataset from 1850', *Journal Geophysical Research*, 111 (D12106).

Butler, C., Garcia-Suarez, A. and Palle, E. (2007) 'Trends and cycles in long Irish Meteorological series', *Biology and Environment*, 107B (3), pp. 157-165

Crisp, D. (1990) 'Simplified methods of estimating daily mean stream water temperature', *Freshwater Biology*, 23, 457-462

CSO (Central Statistics Office) (1970) Stationary Office, Dublin

CSO (Central Statistics Office) (1980) Stationary Office, Dublin

CSO (Central Statistics Office) (1991) Stationary Office, Dublin

CSO (Central Statistics Office) (2000) *Census of Agriculture Main Results, June 2000*. Stationary Office, Dublin

Dalton, C., Jennings, E., Taylor, D., O'Dwyer, B., Murnaghan, S., Bosch, K., de Eyto, E. & Sparber, K. (2010) Past, current and future Interactions between pressures, chemicaL status and bioLogical qUality eleMents for lakes IN contrAsting catchmenTs in IrEland (ILLUMINATE). EPA/ERTDI PROJECT # 2005-W-MS-40 Draft Report 290 pp.

Easterling, D., Horton, B., Jones, P.D., Peterson, T.C., Karl, T.R., Parker, D.E., Salinger, M.J., Razuvayev, V., Plummer, N., Jamason, P. and Folland C.K. (1997) 'Maximum and minimum temperature trends for the globe', *Science*, 277 (5324), 364-367

Fowler, H. and Kilsby, C.G. (2002) 'Precipitation and the north Atlantic oscillation: A study of climatic variability in northern England', *International Journal of Climatology*, 22, 843-866

Fowler, H. and Kilsby, C.G. (2003) 'A regional frequency analysis of United Kingdom extreme rainfall from 1961 to 2000', *International Journal of Climatology*, 23, 1313-1334

Frich, P., Alexander, L.V., Della-Marta, P., Gleason, B., Haylock, M., Klein Tank, A.M.G. and Peterson, T. (2002) 'Observed coherent changes in climatic extremes during the second half of the twentieth century', *Climate Research*, 19, 193-212

Gallego, M., Garcia, J.A. and Vaquero, J.M. (2005) 'The NAO signal in daily rainfall series over the Iberian peninsula', *Climate Research*, 29, pp. 103-109

George, G., Hewitt, D., Jennings, E.J., Allott, N. and McGinnity, P. (2007) 'The impact of changes in the weather on the surface temperatures of Lake Windermere (UK) and Lough Feeagh (Ireland)', in *Water in Celtic countries: Quantity, quality and climate variability*, eds J. Lobo Ferreira and J.M.P. Viera, International Association of Hydrological Sciences Publication 310, pp. 86-93.

Goddard Institute for Space Studies (2009) 2009: Second Warmest Year on Record; End of Warmest Decade http://www.giss.nasa.gov/research/news/20100121/ Accessed on 21 January, 2010

Griffiths, G., Salinger, M.J. and Leleu, I. (2003) 'Trends in extreme daily rainfall across the south Pacific and relationship to the South Pacific Convergence Zone', *International Journal of Climatology*, 23 (8), 847-869

Groisman, P., Knight, R.W., Easterling, D.R., Karl, T.R., Hegrel, G.C. and Razuvaev, V.N. (2005) 'Trends in intense precipitation in the climate record', *Journal of Climate*, 18, 1326-1349

Hansel, S., Petzold, S. and Matschullat, J. (2009) 'Precipitation trend analysis for central eastern Germany' in *Bioclimatology and natural hazards,* eds K. Střelcová, C. Mátyás, A. Kleidon, M. Lapin, F. Matejka, M. Blaženec, J. Škvarenina and J. Holécy, Springer, Netherlands, pp. 29-38.

Hansen, J., Sato, Mki., Ruedy, R., Lo, K., Lea, D.W. and Medina-Elizade, M. (2006) 'Global temperature change', Proceedings of the National Academy of Science, 103, 14288-14293, doi:10.1073/pnas.0606291103.

Hansen, J., R. Ruedy, Sato, M.and Lo, K. (2010) 'Global surface temperature change', Reviews of Geophysics, 48, RG4004, doi:10.1029/2010RG000345.

Hawkings, C., Hogue, J.N., Decker, L.M. and Feminella, J.W. (1997) 'Channel morphology, water temperature and assemblage structure of stream insects', *Journal of the North American Benthological Society,* 16 (4), 728-749

Haylock, M. and Goodness, C.M. (2004) 'Interannual variability of European extreme winter rainfall and links with large-scale circulation', *International Journal of Climatology*, 24, 759-776

Haylock M.R., Alves L.M., Ambrizzi T., Anunciacao Y.M.T., Baez J., Barros V.R., Berlato, M.A., Bidegain, M., Coronel, G., Corradi, V., Garcia, V.J., Grimm, A.M., Karoly, D., Marengo, J.A., Marino, M.B., Moncunill, D.F., Nechet, D., Quintana, J., Rebello, E., Rusticucci, M., Santos, J.L., Trebejo, I. and Vincent, L.A. (2006) 'Trends in total and extreme south American rainfall in 1960-2000 and links with sea surface temperature', *Journal of Climate*, 19, 1490-1512

Heino, R., Brázdil, R., Førland, E., Tuomenvirta, H., Alexandersson, H., Beniston, M., Pfister, C., Rebetez, M., Rosenhagen, G., Rösner, S. and Wibig, J. (1999) 'Progress in the study of climatic extremes in northern and central Europe', *International Journal of Climatology*, 42(1), 151-181

Hoppe, H. and Keily, G. (1999) 'Precipitation over Ireland - observed change since 1940', *Physics and Chemistry of the Earth*, 24 (1-2), 91-96

Hulme, M. and Barrow, E. (1997) *Climates of the British Isles past, present and future*, Routledge, London, 454pp

Hundecha, Y. and Bardossy, A. (2005) 'Trends in daily precipitation and temperature extremes across western Germany in the second half of the 20th century', *International Journal of Climatology*, 25, 1189-1202

Hurrell, J, 1995 'Decadal trends in the North Atlantic oscillation: Regional temperatures and precipitation', *Science*, 269, 676-679

Hurrell, J. and van Loon, H. (1997) 'Decadal variations in climate associated with the North Atlantic Oscillation', *Climate Change*, 36, pp. 301-326

Hurrell, J., Kushnir, Y., Ottersen, G., Visbeck, M. (2003) 'An Overview of the North Atlantic Oscillation', in *The North Atlantic Oscillation: Climate significance and Environmental Impact,* eds J.W. Hurrell, Y. Kushnir, G. Ottersen and M. Visbeck, Geophysical Monograph Series, 134, 279pp.

ICES (2009a) *Report of the Working Group on North Atlantic Salmon (WGNAS), 30 March–8 April*, Copenhagen, Denmark. ICES CM 2009/ACOM:06. pp. 282

ICES (2009b) *Report of the 2009 Session of the Joint EIFAC/ICES Working Group on Eels (WGEEL), 7–12 September 2009*, Göteborg, Sweden. ICES CM 2009/ACOM:15. pp. 137

IPCC (2007) Contribution of working groups I, II and III to the fourth assessment report of the Intergovernmental Panel on Climate Change, IPCC, Geneva, Switzerland.

Irvine, K., Allott, N., de Eyto, E., Free, G., White, J., Caroni, R., Kennelly, C., Keaney, J., Lennon, C., Kemp, A., Barry, E., Day, S., Mills, P., O'Ríain, G., Quirke, B., Twomey, H. and Sweeney, P. (2000) *Ecological Assessment of Irish Lakes - The development of a new methodology suited to the needs of the EU Directive for Surface Waters*, Unpublished Report to EPA submitted by Department of Zoology TCD, Environmental Science Unit TDC, Natural Resources Development Centre TCD and Conservation Services.

Jennings, E., Allott, N., McGinnity, P., Poole, R., Quirke, W., Twomey, H. and George, G. (2000) 'The North Atlantic Oscillation: Effects on freshwater systems in Ireland', *Biology and Environment*, 100B (3), 149-157

Jensen, A. (1990) 'Growth of young migratory brown trout *salmo trutta* correlated with water temperature', *Journal of Animal Ecology*, 59, 603-614

Jones, P. (2009) *Global Temperature Record*, viewed 28 September 2009, <http://www.cru.uea.ac.uk/cru/info/warming/>.

Jones, P., New, M., Parker, D.E., Martin, S. and Rigor, I.G. (1999) 'Surface air temperature and its variations over the last 150 years', *Reviews of Geophysics*, 37, 173-199

Jones, P. and Moberg, A. (2003) 'Hemispheric and large-scale surface air temperature variations: An extensive revision and an update to 2001', *Journal of Climate*, 16, 206-223

Karl, T. and Knight, R.W. (1998) 'Secular trends of precipitation amount, frequency, and intensity in the united states', *Bulletin of the American Meteorological Society*, 79(2), 231-241

Kiely, G. (1999) 'Climate change in Ireland from precipitation and streamflow observations', Advances in Water Resources, 23, pp. 141-151

Kieley, J., Diamond, S., Burke, P. J. and Collins, T. (1974) 'The soil map of West Mayo', *National Soil Survey*, Soils Division, An Foras Taluntais.

Klein Tank, A.M.G., Peterson, T.C., Quadir, D.A., Dorji, S., Zou, X., Tang, H., Santhosh, K., Joshi, U.R., Jaswal, A.K., Kolli, R.K., Sikder, A.B., Deshpande, N.R., Revadekar, J.V., Yeleuova, K., Vandasheva, S., Faleyeva, M., Gomboluudev, P., Budhathoki, K.P., Hussain, A., Afzaal, M., Chandrapala, L., Anvar, H., Amanmurad, D., Asanova, V.S., Jones, P.D., New, M.G. and Spektorman, T. (2006) 'Changes in daily temperature and precipitation extremes in central and south Asia', *Journal of Geophysical Research*, 11 (D16105).

Klok, E. and Klein Tank, A.M.G. (2009) 'Updated and extended European dataset of daily climate observations', *International Journal of Climatology*, 29, 1182-1191

Kostopoulou, E. and Jones, P.D. (2005) 'Assessment of climate extremes in the eastern Mediterranean', *Meteorology and Atmospheric Physics*, 89, 69-85

Lai, L., and Cheng, W. (2009) 'Air temperature change due to human activities in Taiwan for the past century', *International Journal of Climatology*, 30(3), 432-444.

Langan, S., Johnston, L., Donaghy, M.J., Youngson, A.F., Hay, D.W. and Soulsby, C. (2001) 'Variation in river water temperatures in an upland stream over a 30-year period', *The Science of the Total Environment*, 265, 195-207

Leira, M., Jordan, P., Taylor, D., Dalton, C., Bennion, H. and Irvine, K. (2006), 'Recent histories of the main types of candidate reference lakes in Ireland: a palaeolimnological approach', *Journal of Applied Ecology*, 43, 816-827.

Liebmann, B., Vera, C.S., Carvalho, L.M.V., Camilloni, I.A., Hoerling, M.P., Allured, D., Barros, V.R., Baez, J.A. and Bidegain, M. (2004) 'An observed trend in central south American precipitation', *Journal of Climate*, 17, 4357-4367

Liu, B., Yang, D., Ye, B. and Berezovskaya, S. (2005) 'Long-term open-water season stream temperature variations and changes over Lena river basin in Siberia', *Global and Planetary Change*, 48, 96-111

Long, C. B., MacDermot, C. V., Morris, J. H., Sleeman, A. G., Tietzsch-Tyler, D., Aldwell, C. R., Daly, D., Flegg, A. M., McArdle, P. M. and Warren, W. P., (1992) *Geology of North Mayo*. Geological Survey of Ireland.

Matthews, K. and Berg, N.H. (1997) 'Rainbow trout responses to water temperature and dissolved oxygen stress in two southern California stream pools', *Journal of Fish Biology*, 50, 50-67

May, L., Place, C., O'Hea, B., Lee, M., Dillane, M. and McGinnity (2005) 'Modelling soil eroision and transport in the Burrishoole catchment, Newport, Co. Mayo, Ireland', *Freshwater Forum,* 23, 139-154.

McElwain, L. and Sweeney, J. (2007) *Key meteorological indicators of climate change in Ireland*, Johnstown Castle, Wexford, Environmental Protection Agency, 31pp.

McGinnity, P., Jennings, E., deEyto, E., Allott, N., Samuelsson, P., Rogan, G., Whelan, K., and Cross, T. (2009) 'Impact of naturally spawning captive-bred Atlantic salmon on wild populations: depressed recruitment and increased risk of climate-mediated extinction', Proceedings of the Royal Society B: Biological Sciences, 276, 3601-3610.

Met Éireann (2009) *Monthly Weather Summary*, viewed 12 January 2010, <http://www.met.ie/climate/monthly_summarys/dec09.pdf>.

Min, S., Zhang, X. and Zwiers, F. (2008) 'Human-induced Arctic moistening', *Science*, 320 (5875), 518-520

Moater, F. and Gailhard, J. (2006) 'Water temperature behaviour in the river Loire since 1976 and 1881', *C.R. Geoscience*, 338, 319-328

Murphy, S. and Washington, R. (2001) 'United Kingdom and Ireland precipitation variability and the north Atlantic sea-level pressure field', *International Journal of Climatology*, 21(8), 939-959

Nandintsetseg, B., Greene, J.S. and Goulden, C.E. (2007) 'Trends in extreme daily precipitation and temperature near Lake Hovsgol, Mongolia', *International Journal of Climatology*, 27, 341-347

O'Connor, M. (2000) 'Action Plan for Blanket Bog and Wet Heath: Technical Aspects', *Draft report to NPWS*, Dept. Environment, Heritage and Local Government, Dublin, Ireland.

Osborn, T. and Hulme, M. (2002) 'Evidence for trends in heavy rainfall events over the UK', *Philosophical Transactions*: *Mathematical, Physical and Engineering Sciences*, 360, 313-1325

O'Sullivan, A. (1993) *Site synopsis, Owenduff/Nephin complex, ASI survey*. National Parks and Wildlife service. Unpublished.

Parker, D.E., Jones, P.D., Folland, C.K. and Bevan, A. (1994) 'Interdecadal changes of surface temperature since the late nineteenth century', *Journal of Geophysical Research*, 99(D7), 14373-14399

Parker, M.M. (1977) 'Lough Furnace, County Mayo; Physical and chemical studies of an Irish saline lakes, with reference to the biology of Neomysis integer'. PhD Thesis, Trinity College Dublin, Dublin.

Peralta-Hernandez, A., Balling, R.C. and Barba-Martinez, L.R. (2009) 'Analysis of near-surface diurnal temperature variations and trends in southern Mexico', *International Journal of Climatology*, 29, 205-209

Peterson T.C., Taylor, M.J., Demeritte, R., Duncombe, D.L., Burton, S., Thompson, F., Porter, A., Mercedes, M., Villegas, E., Semexant Fils, R., Klein Tank, A., Martis, A., Warner, R., Joyette, A., Mills, W., Alexander, L. and Gleason, B. (2002) 'Recent changes in climate extremes in the Caribbean region', *Journal of Geophysical Research*, 107 (D21), doi:10.1029/2002JD002251

Poole, W.R. (1994) 'A population study of the European eel (*Anguilla anguilla* (L.)) in the Burrishoole System, Ireland, with special reference to growth and movement', *Unpublished Ph.D. thesis*, Trinity College Dublin

Poole, W. R., Dillane, M., de Eyto, E., Rogan, G., McGinnity, P., and Whelan, K. (2007) 'Characteristics of the Burrishoole Sea Trout Population: Census, Marine Survival, Enhancement and Stock-Recruitment Relationship, 1971-2003', In *Sea Trout: Biology, Conservation and Management*, ed. N.M. Graeme Harris, pp. 279-306.

Rehman, S. (2009) 'Temperature and rainfall variation over Dhahran, Saudi Arabia, (1970-2006)', *International Journal of Climatology*, 30, 445-449.

Roy, S. and Balling, J.R. (2004) 'Trends in extreme daily precipitation indices in India', *International Journal of Climatology*, 24, 475-466

Rosenzweig, C,. Karoly, D., Vicarelli, M.J., Neofotis, P., Wu, Q., Casassa, G., Menzel, A., Root, T., Estrella, N., Seguin, B., Tryjanowski, P., Liu, C., Rawlins, S. and Imeson, A. (2008) 'Attributing physical and biological impacts to anthropogenic climate change', *Nature*, 453, 353-358

Stardex Final Report (2005) *Downscaling climate extremes,* STARDEX Consortium, viewed 1st June 2009, <http://www.cru.uea.ac.uk/cru/projects/stardex>.

Tecar, L. and Cerit, O. (2009) 'Temperature trends and changes in rise, Turkey, for the period 1975 to 2007', *Clean*, 37(2), 150-159

Walther, G.R., Post, E., Convey, P., Menzel, A., Parmesan, C., Beebee, T.J.C., Fromentin, J.M., Hoegh-Guldberg, O. and Bairlein, F. (2002) 'Ecological responses to recent climate change', *Nature*, 416, 389-395

Ward, J. and Stanford, J.A. (1982) 'Thermal responses in the evolutionary ecology of aquatic insects', *Annual Review of Entomology*, 27, 97-117

Webb, B. (1996) 'Trends in stream and river temperature', *Hydrological Processes*, 10, 205-226

Webb, B., Hannah, D.M., Moore, R.D., Brown, L.E., and Nobilis, F. (2008) 'Recent advances in stream and river temperature research', *Hydrological Processes*, 22, 902-918

Weir, G. (1996) 'Sheep overgrazing in the Nephin Begs', *MSc Thesis,* Trinity College, Dublin.

Whelan, K.F., Poole, W.R., McGinnity, P., Rogan, G. and Cotter, D. (1998) 'The Burrishoole System', in: *Studies of Irish Rivers and Lakes*, ed. C. Moriarty, Marine Institute, Dublin, pp. 279.

White, P., Kalff, J., Rasmussen, J.B. and Gasol, J.M. (1990) 'The effect of temperature and algal biomass on bacterial production and specific growth rate in freshwater and marine habitats', *Microbial Ecology*, 21(2), 99-118

Yu, P., Yang, T. and Kuo, C. (2006) 'Evaluating long-term trends in annual and seasonal precipitation in Taiwan', *Water Resources Management*, 20(6), 1007-1023

Zhang, X., Zwiers, F.W., Hegerl, G.C., Lambert, F.H., Gillett, N.P., Solomon, S., Stott, P.A. and Nozawa, T. (2007) 'Detection of human influence on twentieth-century precipitation trends', *Nature*, 448, 461-466

2. Climate And Key Water Quality Parameters In The Burrishoole Catchment

Rachel Erdil, Karen McCrann, Norman Allott, David Taylor and Eleanor Jennings

2.1. Introduction

The Fourth Intergovernmental Panel on Climate Change (IPCC) assessment report showed clear evidence that terrestrial and aquatic ecosystems are being strongly affected by climate change, particularly in the form of regional temperature increases (Parry et al., 2007). It also presented strong observational evidence that climate change poses a significant threat to biodiversity, species distribution, and the functioning of ecosystems. The impact of future temperature rise and the regional effects of climate change on precipitation and catchment hydrology, however, are less certain (Parry et al., 2007). Temperature is a significant driver of ecological change in aquatic environments because of its effect on the rates of key chemical and biological processes in water, for example on respiration, photosynthesis, dissolved oxygen (DO) saturation, and metabolism (Harley et al., 2006). Average global air temperature (AT) has increased by approximately 0.74°C over the past century (1906–2005) (Parry et al., 2007), along with concurrent warming of freshwater systems (Winder and Schindler, 2004; Hari et al., 2006; Arvola et al., 2010). Similar trends have been observed in Ireland where climate-induced changes in freshwater systems are of a greater magnitude and occurring at a faster rate than has been observed in the last thousand years, according to the dendro-chronological record (Stefansson et al., 2003).

Recent studies have shown that the effects of climate change on regional weather will be far more complex than simply altering temperature patterns (Parry et al., 2007). In particular, changes in the magnitude and seasonality of precipitation are expected to have significant effects on water quality (Jennings et al., 2009; Naden et al., 2010; Whitehead et al., 2009). Although relatively few studies have considered the effects of climate change on Irish freshwaters, Burrishoole was one of two sites included in a project on climate change impacts on European lakes and catchments (Arvola et al., 2010; Jennings et al., 2010; Naden et al., 2010). The project assessed impacts of climate on dissolved organic carbon (DOC) export from the Glenamong catchment, highlighting potential increases in export rates, and also trends in lake water temperature in Lough Feeagh. Additional work on climate change impacts at Burrishoole has identified potential negative effects of higher winter temperatures on salmon survival (McGinnity et al., 2009). Increased AT will also affect the rates of the

biological and chemical processes that influence water quality (e.g. biological oxygen demand, DO saturation, DOC degradation) (Whitehead et al., 2009). Shifts in precipitation patterns may alter river flow and discharge, affecting residence times and dilution of pollutants, as well as water temperature (Arnell, 1998; Mohseni et al., 2003). Increased occurrences of extreme precipitation events could also increase the likelihood of acid pulses and DOC release through post-drought floods (Arnell, 1998; Whitehead et al., 2009).

The impacts of climate change on aquatic ecosystems are also difficult to evaluate because of confounding factors such as natural variability, physiological adaptation by organisms, and changes in food-web dynamics (Graham and Harrod, 2009). However, a large body of evidence shows that warming of freshwaters and the resulting changes in water quality have impacted on fish physiology (Fry, 1971; Stefansson et al., 2003), fish phenology (Zydlewski et al., 2005; McGinnity et al., 2009), species distributions (Friedland et al., 2003; Davidson and Hazelwood, 2005), and survival (King et al., 2007; McGinnity et al., 2009). Increased temperature affects fish at all life stages (Friedland et al., 2003), although the response varies with species and fish life stage (Elliott, 1991; Planque and Frédou, 1999). In many cases, global climate change represents an additional stress on fish populations that are already subject to human induced pressures (Allan and Flecker, 1993). This is particularly true in Ireland, where most freshwater bodies have long been affected by anthropogenic activity, such as eutrophication and deforestation (Stefansson et al., 2003; Cummins and Farrell, 2003).

Observational evidence suggests that Irish populations of both Atlantic salmon (*Salmo salar*) and brown trout (*Salmo trutta*) are already in decline (Stefansson et al., 2003; Peyronnet et al., 2007). Furthermore, using a regression model based on 37 years of population data on wild and ranched Atlantic salmon in the Burrishoole catchment, McGinnity et al. (2009) showed that, while Atlantic salmon may be able to adapt to future changes in water temperature in an ideal situation, additional stressors, for example the supplementation of populations with hatchery fish, may cause catastrophic population collapses within twenty generations.

In this chapter the influence of climate on key parameters, important for fish growth and survival, are assessed for the Burrishoole catchment. These include river water temperature (RWT), river DO levels, and river pH levels. Recent data from the catchment are also examined for the occurrence of extremes in these parameters which might be detrimental for fish. Assessment of the influence of local weather includes the relationship between AT and RWT at six sites, the impact of AT and DOC levels on river DO levels, and the relationships between low pH episodes and regional weather conditions. In addition, the degree of

coherence in RWTs across the Burrishoole catchment is assessed. A relatively high degree of coherence would indicate that a mean time series of RWT can be used to represent the variability in the individual time series when modelling RWTs. Note that the relationship between RWT and smoothed AT forms part of the modelling work included in Chapter 6.

2.2. River Water Temperature

2.2.1 Introduction

The most immediate effects of climate change on aquatic ecosystems are expected to occur as alterations in lake and river water temperatures (Hammond and Pryce, 2007). Studies have shown that both lake water temperatures (LWTs)(Livingstone and Dokulil, 2001; Livingstone et al., 2005) and RWTs (Hari et al., 2006) are highly correlated with regional air temperature. As regional air temperatures have risen over the last 100 years, so have water temperatures. The European Environment Agency has reported 1°C – 3°C increases in water temperature in major European rivers, such as the Rhine River and the Danube River (European Environment Agency, 2007). Closer to Ireland, Langan et al. (2001) found that winter and spring maximum RWTs in an upland Scottish river increased by 2°C in the last thirty years, most likely because of rising seasonal air temperature.

As temperature influences the rates of nearly all chemical and biological processes in water, RWT is a major determinant of habitat in rivers and streams (e.g. Elliott, 1984; Eaton and Scheller, 1996). Riverine ecosystems are particularly susceptible to climate change because they will be affected not only by shifts in RWT, but also by alterations in precipitation patterns. Where prolonged droughts occur, extreme RWTs may be exacerbated (Graham and Harrod, 2009). The availability of riverine habitats with a suitable range of RWTs is critical for salmonid survival because breeding, egg incubation, egg hatching, and parr development all occur in the upper reaches of river systems (Graham and Harrod, 2009). The timing of fluctuations in RWT is particularly important since the occurrence of extreme temperature events during the warmest periods of the year or during critical stages in fish development can exacerbate the deleterious effects on fish populations (Caissie et al., 2001; Morrison et al., 2002; McGinnity et al., 2009).

2.2.2 Impacts of Water Temperature on Fish Growth and Survival

There is clear observational evidence that changes in water temperature impact salmonid fish species, such as Atlantic salmon (*S. salar*) and brown trout (*S. trutta*), at all life stages through influences on phenology, growth, and metabolism. Both species exhibit distinct thermal tolerances during each life cycle stage, with the tolerances for Atlantic salmon being about 3°C

higher than the corresponding values for brown trout (Elliott, 1991). In addition, major phases of fish development, such as egg hatching, parr growth, smoltification, and migration are directly linked with specific ranges in water temperature (Table 2.1). The highest temperature limits for feeding and survival of any salmonid species have been recorded for salmon parr (Elliott, 1991; Crisp, 1996). In laboratory studies of Atlantic salmon from two northern England populations, Elliott (1991) showed that the upper mean incipient lethal level (survival over seven days) for acclimatised Atlantic salmon parr was 27.8°C $\pm$ 0.2°C and that the lower incipient level was below 0°C. The thermal tolerance range varied according to the acclimation temperature of the parr; parr which had been acclimatised in warmer water tolerated higher water temperatures at the upper extreme, but could not tolerate the coldest water at the lower extreme. However, although fish can survive at these extreme temperatures, the optimum temperature ranges for growth have been defined as 16°C – 19°C for Atlantic salmon (Peterson and Martin-Robichaud, 1989) and 13°C – 14°C for brown trout (Elliott, 1975), with the lower limit for growth occurring around 7°C – 9°C for both species (Allen, 1969).

Table 2.1 Selected thermal tolerance limits for Atlantic salmon (*S. salar*) and brown trout (*S. trutta*). This table was based on data collated by Ciar O'Toole (pers. comm.).

Parameter	*S. salar* (°C)	*S. trutta* (°C)	References
Ultimate lethal level (parr)	30 – 33	26 – 30	Elliott, 1991; 1981
Upper incipient lethal temp. (parr)	25 – 28	22 – 25	Elliott, 1991; 1981
Lower critical range (parr)	0 – 7	0 – 4	Elliott, 1994
Seek refugia (parr)	<9 and 22 – 24	<9, undefined	Gardiner, 1984; Cunjak et al., 1993
Egg hatching	2.4 – 12	1.9 – 11.2	Crisp, 1981
Feeding (parr)	7 – 22.5	4 – 19	Elliott, 1991; 1981
Optimum growth (parr)	16 – 19	13 – 14	Peterson and Martin-Robichaud, 1989; Elliott, 1975
Smolt run	5.5 – 15.5	5 – 13	Byrne et al., 2003

Fish responses to changes in temperature are complex because of their ability to adapt to higher temperatures, their susceptibility to disease, and because of confounding factors linked to temperature that alter the suitability of habitats, such as primary production, DO content of river water, and prey availability (Magnuson and Destasio, 1997; Whitehead et al., 2009). Recent studies on Atlantic salmon have also shown that changes in water temperature during key seasons can have significant effects on fish growth and survival. For example, McGinnity et al. (2009) found that higher RWTs in the first winter when eggs are incubating in gravel beds and during the second winter when fish are in the parr stage, had negative impacts on survival. Higher RWTs in the first winter may be problematic because earlier hatching in a warmer

winter is not always correlated with earlier phytoplankton or zooplankton production and therefore hatchlings may face insufficient food supply. In the case of parr survival, higher water temperatures increase fish metabolism, so juvenile fish may deplete their energy reserves before the spring food supply becomes available (McGinnity et al., 2009). Similarly, earlier and more rapid increases in RWT can lead to faster growth and earlier smoltification of juvenile salmon, but adequate food supplies may not be available in the marine environment for early smolts (Zydlewski et al., 2005). The response of aquatic ecosystems and salmonid species in particular to climate change is still unclear, but will likely differ significantly on a regional basis. Some sensitive coldwater-adapted fish, such as brown trout, may encounter RWTs close to their thermal limits, but more flexible coldwater species, such as Atlantic salmon, may not be as strongly affected or may adapt to temperature changes (Graham and Harrod, 2009).

2.2.3 Range of River Water Temperatures in the Burrishoole Catchment

River water temperature data from the Burrishoole catchment were used to assess the extent of extremes in RWTs, the relationship between AT and RWT, and coherence in RWT across the catchment. The datasets that were used were from the Black River and two of its tributaries (the Altahoney River and the Goulaun River), the Glenamong River, the Glendahurk River and the Tarsaghaun River (see map Figure 1.2). RWT has been recorded at 2-minute intervals at the Black and Glenamong, using QUANTA (OTT Hydrometry, UK) data recorders, since 2003/2004 depending on site. At the Altahoney, Goulaun, and Tarsaghaun sites, RWT has been recorded at 30-minute intervals using Stowaway TidbiTs (Onset Computer Corporation) since 2003/2004 depending on site. RWT has been recorded at the Glendahurk site at 1 hour intervals since 2003 using the same TidbiT device. Data from 5/5/2004 to 31/12/2008 were available for all these sites and were used in the analysis.

The Burrishoole catchment is located close to the Atlantic coast, and RWTs for these sites reflected this temperate, maritime climate, with mean daily RWTs rarely exceeding 20°C in summer and rarely falling below 1°C in winter (Table 2.2). There are no reports of ice cover on the catchment streams (Mary Dillane, pers. comm.). The RWT in the Glendahurk River had the highest percentage of days with mean daily RWT above 20°C, at only 1.24% of the total days in the record, while the daily mean RWT never reached 20°C in the Altahoney River. The latter site had the lowest maximum mean daily RWT (18.5°C), followed by the Goulaun (20.8°C), Glenamong (21.4°C), Tarsaghaun (21.9°C) and Black (22.5°C). The maximum value was recorded on the same date in three of the sites (18/7/06) The low maximum at the Altahoney was attributed to the location of the logger at this site, which was situated at a similar depth to others, but in a deep pool which was shaded by a rock overhang

(Mary Dillane, pers. comm). Maximum mean daily RWT for the Goulaun site was also lower than the other four sites: this site is 3.5 km downstream of a lake and therefore would also reflect fluctuations in lake water temperature which tend to be less extreme than RWT. Minimum mean daily RWT below 1◦ C were not recorded at any site.

Table 2.2 Maximum and minimum mean daily RWT (°C) for each of the six sites (Altahoney, Black, Glenamong, Glendahurk, Goulaun and Tarsaghaun). Daily mean values were calculated from higher frequency data. The table also shows the number of days, and the percentage of days, with mean RWT exceeded 20°C for each site.

	Altahoney	Black	Glenamong	Glendahurk	Goulaun	Tarsaghaun
Date	18/07/06	10/06/07	13/07/06	10/06/07	18/07/06	18/07/06
Max temperature (°C)	18.5	22.5	21.4	22.0	20.8	21.9
Date	07/02/07	07/02/07	02/02/07	04/01/08	07/02/07	08/02/07
Min temperature (°C)	2.3	2.4	1.4	2.6	2.0	1.8
No. days >20°C	0	10	8	18	4	3
% of days > 20°C	0.00%	0.73%	0.62%	1.24%	0.31%	0.21%

It should be noted here that sites where RWT is buffered, such as the Altahoney and Goulaun, may provide important refuges for fish. Many studies have demonstrated that fish seek out cold water refuges in the forms of cooler water tributaries, lateral seeps, deep pools, or cold alcoves during periods of high RWTs (Bilby, 1984; Cunjak et al., 1993; Matthews and Berg, 1997; Caissie, 2006). In small stream reaches in northeast Oregon, USA, for example, 10 – 40% of fish were observed close to thermal refuges at midday when RWTs in the same water course approached lethal levels (Ebersole et al., 2001).

Although mean daily water temperature in the rivers in the Burrishoole catchment did not exceed 23°C, the high frequency RWT readings (2, 30, and 60 minute intervals depending on site) did show more extreme maxima and minima (Table 2.3). Maximum RWTs recorded at the six sites ranged from 21.2°C to 26.8°C, while minimum values ranged from -0.7°C to 1.6°C. As with the maximum mean daily RWTs, the highest RWTs in the Altahoney, Glendahurk, and Tarsaghaun Rivers were all recorded on 18/7/06, a day when the air temperature at 9 am at the Millrace Meteorological Station exceeded 21°C.

Table 2.3 Maximum and minimum RWTs recorded in high frequency (sub-daily) data at the six sites during the monitoring record. RWT was logged every 2 minutes in the Black and Glenamong, every 30 minutes in the Altahoney, Goulaun, and Tarsaghaun, and every hour in the Glendahurk.

	Altahoney	Black	Glenamong	Glendahurk	Goulaun	Tarsaghaun
Date	18/07/06	24/08/07	11/07/06	18/07/06	11/07/05	18/07/06
Max temperature (°C)	21.2	26.5	26.8	25.3	25.5	25.5
Date	04/03/06	17/02/08	07/02/07	08/02/07	03/03/06	08/02/07
Min temperature (°C)	1.5	-0.7	0.3	1.6	0.7	0.3

RWTs over 20°C made up less than 2% of the total high frequency record at each site (Table 2.4). In the Glenamong River, the site with the highest relative number of extreme high temperature values, RWT exceeded 20°C only 1.66% of the time and exceeded 25°C in only 0.12% of all 2 minute measurements.

Seasonal mean RWT at the sites was also assessed (Figure 2.1). The Glenamong and the Glendahurk Rivers had the highest seasonal water temperatures, in spring and in summer, respectively. Those for the Altahoney site were lower than other sites in spring, summer and autumn.

Table 2.4 Percentage of RWT readings above 20°C and 25°C at each site. RWT readings were taken every 2 minutes in the Black and Glenamong, every 30 minutes in the Altahoney, Goulaun, and Tarsaghaun, and every hour in the Glendahurk.

	Altahoney	Black	Glenamong	Glendahurk	Goulaun	Tarsaghaun
Total no. of readings	51446	1045996	987322	46407	62099	46480
% of readings > 20°C	0.03%	1.41%	1.66%	1.34%	0.90%	1.30%
% of readings > 25°C	0.00%	0.20%	0.12%	0.01%	0.01%	0.02%

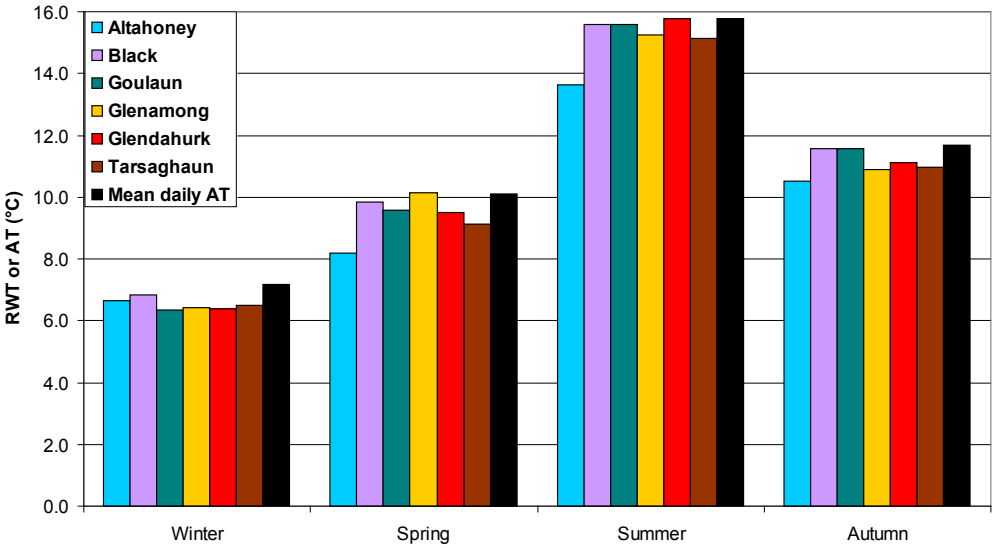

Figure 2.1 Mean daily river water temperature (RWT) (°C) for the six sites for the period 2004 – 2008 together with mean daily air temperature (AT) (°C) for each season recorded at the Millrace Meteorological Station, Burrishoole.

2.2.4 Coherence in River Water Temperature in the Burrishoole Catchment

A high degree of coherence between short-term fluctuations in both lake and river water temperatures and in regional air temperatures has been identified for sites within Europe (Livingstone and Dokulil, 2001; Livingstone et al., 2005; Livingstone and Padisak, 2007; Livingstone and Hari, 2008). This coherence indicates that air temperature fluctuations are a major determinant of short-term variability in the thermal habitats of aquatic flora and fauna (Livingstone and Hari, 2008). These studies, however, assessed coherence across relatively large areas, for example, between Alpine lakes in Switzerland and Lake Balaton in Hungary (Livingstone and Padisak, 2007), or between rivers and lakes across Switzerland (Livingstone and Hari, 2008). The latter study which assessed coherence in RWT, for example, used data from 47-92 river sites and air temperature from 40 sites (Livingstone and Hari, 2008). A high degree of correlation between RWT and AT has also been reported at a catchment scale (e.g. Langan et al., 2001). The procedures employed in Livingstone et al. (2005) and Livingstone and Hari (2008) were used in the current study to assess coherence in RWT between individual sites within the Burrishoole catchment.

Initial visual inspection of the RWT datasets suggested a relatively high level of coherence between the six sites in the catchment (Figure 2.2). As mentioned above, the logger in the Atlahoney was situated in a deep pool shaded by a rock overhang. This temperature logger recorded consistently lower RWT during summer months (light blue line, Figure 2.2).

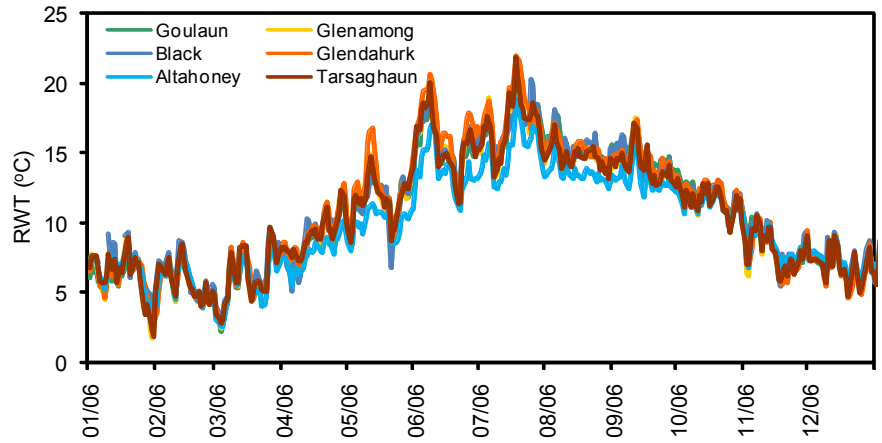

Figure 2.2 Mean daily river water temperature (RWT, °C) at the six sites in the Burrishoole catchment: 1/1/2006 to 31/12/2006.

The relationship between RWT and air temperature (AT) for the six sites was assessed using least squares linear regressions of mean daily air temperature on mean daily RWT for the calendar year 2006 (Table 2.5; Figure 2.3). The air temperature dataset used in the analysis was daily mean AT calculated as the average of daily maximum and daily minimum AT recorded at the Millrace Meteorological Station. There was a high degree of correlation between RWT and AT for all sites, with r^2 values of between 0.88 and 0.89 (Table 2.5; Figure 2.3). However, the slopes of the regression equations for the three western sites, the Glenamong, Glendahurk, and Tarsaghaun Rivers, and for the Goulaun and Black Rivers, were much steeper than that for the Altahoney River site. The latter regression line had a higher y-intercept and lower slope than the regression equations for the other rivers. Similar differences in regression characteristics have been observed in small streams heavily influenced by groundwater inflow or where other environmental factors exert stronger control on RWT than air temperature alone (Erickson and Stefan, 2000).

Table 2.5 Equations of least squares linear regression lines for the regression of mean daily RWT on mean daily air temperature data for the six sites in the Burrishoole catchment (2006).

River	Regression equation	r^2
Altahoney	y = 0.76x + 1.32	0.88
Black	y = 0.92x + 0.59	0.89
Glenamong	y = 0.93x + 0.14	0.89
Glendahurk	y = 0.99x - 0.13	0.88
Goulaun	y = 0.93x + 0.24	0.89
Tarsaghaun	y = 0.91x + 0.45	0.89

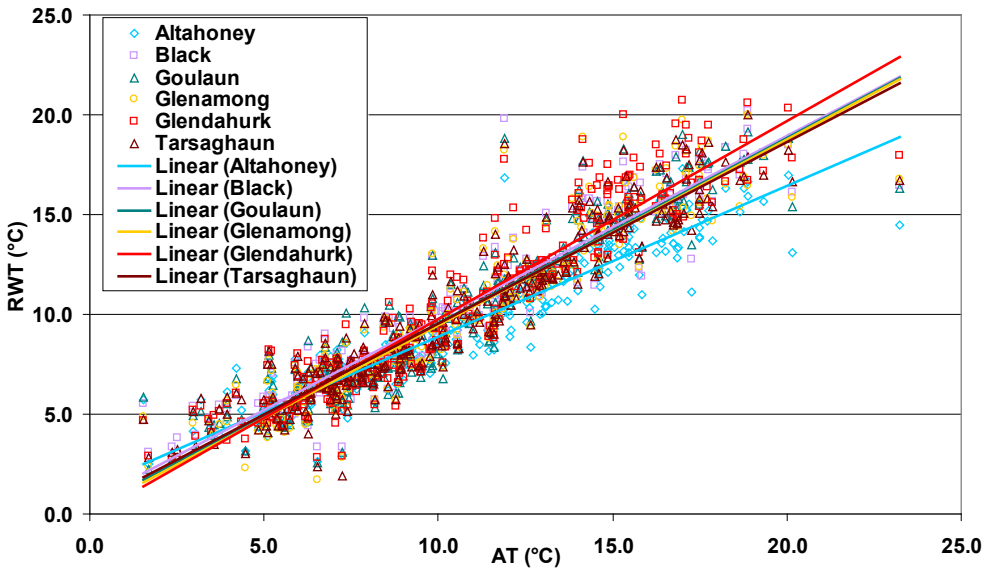

Figure 2.3 Least squares linear regression lines representing the relationship between mean daily river water temperature (RWT, °C) and mean daily air temperature (AT, °C) for the six sites in 2006.

Two years of data (1/1/2005 – 31/12/2006) from the six sites were used to quantify the degree of spatial coherence in RWT. Pairwise coefficients of determination (r^2 in percentage) were calculated for each month between the mean daily RWT for each site and the mean daily RWT calculated from data for the other five sites (referred to as the catchment mean RWT) (Livingstone et al., 2005; Livingstone and Hari, 2008). Statistical analysis was performed using DataDesk (6.0). All calculations were performed on linearly detrended time series to remove any longer-term component, the presence of which which can increase or decrease the perceived proportion of shared variance (Livingstone et al., 2005).

The proportion of variance shared pairwise between each of the detrended RWT time series and the catchment mean RWT for months between January 2005 and December 2006 ranged from 58% to 99% (Figure 2.4; Table 2.6). Mean values for months between December and March autumn were >90% in both years, while values $\leq$90% occurred more frequently between April and September (Table 2.6). This is in contrast to the values reported by Livingstone and Dokulil (2001) for Austrian alpine lakes where the lowest spatial coherence was observed in winter: this difference may reflect the fact that the streams in the Burrishoole catchment did not experience winter ice cover in this period. The sites with the highest r^2 values were the Glenamong and Tarsaghaun Rivers which both had overall mean values of 92%. The Black and Glendahurk had the lowest overall r^2 values (88%). The lower level of coherence between sites during spring and summer months may also reflect the influence of higher solar radiation levels, while differences between sites are likely to reflect local topography. The values for the Black site, for example, were lower than the upstream site in

the Black River system (Tarsaghaun): the Black logger was situated in the final, relatively flat, stretch of the river before it enters the lake, while in contrast the Tarsughaun site was in an upland stream reach with steeper topography.

Table 2.6 Pairwise coefficients of determination (r^2 in %) between mean daily RWT for each site and a catchment mean for data from the other five sites, for each month in 2005 and 2006: $r^2 \leq 90\%$ are shaded.

Month	Altahoney	Black	Gaulaun	Glenamong	Glendahurk	Tarsaghaun	Mean
Jan-05	98	91	97	98	96	98	96
Feb-05	81	95	97	98	95	97	94
Mar-05	93	*NA*	96	96	91	94	94
Apr-05	87	87	95	85	87	97	90
May-05	64	99	71	79	58	76	74
Jun-05	82	84	72	85	67	89	80
Jul-05	95	96	92	97	89	99	95
Aug-05	87	81	90	88	78	90	86
Sep-05	88	80	87	97	87	93	88
Oct-05	93	75	83	96	85	90	87
Nov-05	79	*NA*	87	81	79	91	83
Dec-05	99	99	96	99	95	97	97
Jan-06	97	83	98	98	96	94	94
Feb-06	93	91	92	98	84	94	92
Mar-06	96	94	96	96	99	97	96
Apr-06	60	65	91	88	69	80	76
May-06	90	76	92	91	88	95	89
Jun-06	76	93	93	92	94	92	90
Jul-06	92	61	95	94	85	95	87
Aug-06	74	77	75	69	86	84	77
Sep-06	92	75	76	94	75	88	83
Oct-06	95	93	90	98	81	96	92
Nov-06	92	92	90	97	91	98	93
Dec-06	98	98	93	96	99	95	96
Mean	88	86	89	92	86	92	89

The overall mean coefficient of determination (the mean proportion of shared variance) can be viewed as a general measure of the short-term coherence existing among the time-series.

Monthly mean values across the six sites ranged from 74% in May 2005 to 97% in December 2005. Mean coherence reported by Livingstone and Hari (2008) for RWTs in Switzerland for months between July and September ranged from 17% to 75% for 1997 (47 sites) and 71% to 78% for 2002 (92 sites). However, those data were for a much larger geographical area. Overall, the results for the Burrishoole catchment showed a high degree of coherence in RWT and indicated that a mean time series of RWT would represent the short-term variability in the individual time series (Livingstone and Hari, 2008).

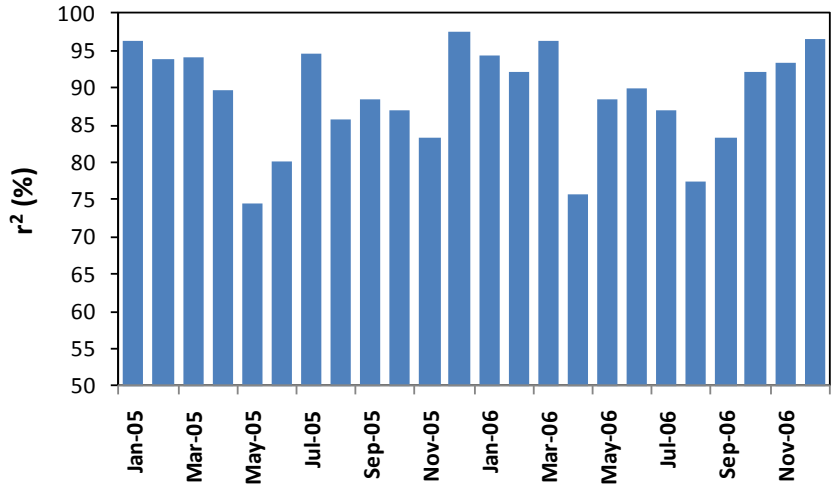

Figure 2.4 Mean coefficient of determination (r^2 in %) across the six sites, 2005 and 2006.

2.3. Dissolved Oxygen

2.3.1 Introduction

Fish in general and salmonids in particular are extremely sensitive to low dissolved oxygen (DO) concentrations (Alabaster and Gough, 1986; Crisp, 1996; Armstrong et al., 2003; Solomon and Sambrook, 2004; Youngson et al., 2004). Stream DO concentration is a function of water temperature, together with rates of in-stream primary productivity and decomposition of organic carbon. Inputs of anthropogenic carbon (e.g. silage, slurry and sewage effluents) are not considered to be a major factor in the Burrishoole catchment, however, peat soils do produce large amounts of coloured dissolved organic carbon (DOC) compounds. Decomposition of DOC can result in low oxygen levels in streams and can also decrease levels in deep lake waters i.e. below the thermocline, providing a refuge for prey species which are less sensitive to oxygen availability than fish (Wissel et al., 2003).

The solubility of oxygen is governed by atmospheric and hydrostatic pressure, turbulence, and temperature (Wetzel, 2001). The relationship with temperature is non-linear, with solubility

increasing considerably in colder water. Freshwater is considered to be saturated at 14.6 mg O_2 L^{-1} at 0°C (Wetzel, 2001). Super-saturation can also occur when the concentration exceeds the equivalent atmospheric pressure during periods of high primary productivity or high water turbulence. DO also exhibits diel variations related to CO_2 cycling that are driven by photosynthesis and respiration within the water column. This cycle is most evident during summer months, the time of peak primary productivity, and results in the lowest DO levels occurring at night (Wetzel, 2001).

2.3.2 Impacts of Dissolved Oxygen Levels on Fish Growth and Survival

The Irish salmonid water quality standards (S.I. No. 293 of 1988) state that 50% of DO measurements taken at a site must be ≥ 9 mg L^{-1}. In addition, where the DO concentration falls below 6 mg L^{-1}, the local authority must prove that there will be no harmful consequences for the salmonoid population. Alabaster and Lloyd (1982) suggested that in salmonid waters, the annual 50th percentile of DO concentrations should be at least 9 mg L^{-1}, while the annual 5th percentile could be as low as 5 mg L^{-1}. DO habitat requirements for fish vary considerably by fish species and life stage (Table 2.7) (Alabaster and Lloyd, 1982; Crisp, 1996; Louhi et al., 2008). Fish sensitivity to DO levels is also significantly affected by other water quality parameters, such as temperature (Bilby, 1984; Crisp, 1996; Matthews and Berg, 1997), flow velocity (Grieg et al., 2007), and the amount of silt in the water column (Chapman, 1988; Louhi et al., 2008). Matthews and Berg (1997), for example, observed that brown trout sought out deep groundwater-fed pools as cool refuges during hot periods, even when the oxygen content of those waters was relatively low. Greig et al. (2007) demonstrated that the mortality of salmonid eggs in redds was not dependent on the oxygen content of water alone, but also on flow velocity of water through redds. Increased mortality was observed when low flows inhibited the bulk movement of well oxygenated water past the eggs (Greig et al., 2007). Similarly, Chapman (1988) noted that the infiltration of fine sediments into river bed gravels reduced the permeability of salmonid redds and lowered the oxygen supply to developing ova, resulting in increased mortality of eggs. As a result, many researchers have defined salmonid habitat quality by ranges of DO content, rather than as absolute thresholds associated with fish mortality or specific sub-lethal effects (Crisp, 1996; Kondolf, 2000; Armstrong et al., 2003; Greig et al., 2007).

Table 2.7 Habitat requirements for salmonids as defined by dissolved oxygen (DO) concentrations.

Salmonid Life Stage	DO (mg L^{-1}) Requirement	Species	References
Early eggs	0.8	Salmon	Lindroth (1942) from Louhi et al. (2008)
Eyed eggs	2.0 - 2.5	Salmon	Marty et al. (1986), Crisp (1996)
Eggs near hatching	4.0	Salmon	Crisp (1996)
Critical level for egg survival in redds	5.0	Salmon	Greig et al. (2007)
Critical level for egg survival in redds	>83% saturation	Trout	Witzel and MacCrimmon (1983)
Hatching eggs	5.0 - 7.0	Salmon	Crisp (1996)
Hatching eggs	7.1 - 10.0	Salmon	Lindroth (1942) from Louhi et al. (2008), Hayes et al. (1951)
Alevins	2.0 - 8.0	Salmon Trout	Kondolf (2000)
Critical level for adults	3.0	Salmon Trout	USEPA (1986)
Spawning adults	5.0 (50%ile), 2.0 (5%ile)	Salmon Trout	Alabaster and Lloyd (1982)
Optimum conditions for adults	9.0 (50%ile), 5.0 (5%ile)	Salmon Trout	Alabaster and Lloyd (1982)

Oxygen deficit has been observed to impact many aspects of fish physiology and ecology, including reduced growth, premature hatching, changes in morphology, decreased reproductive success, slowed activity, and increased predation risk (Crisp, 1996; Armstrong et al., 2003; Graham and Harrod, 2009). Oxygen consumption per unit of body weight decreases as fish size increases (Crisp, 1996). Fish oxygen demands also increase as metabolic rates rise with water temperature (Pörtner, 2001). Most relatively unpolluted upland streams, like those in the Burrishoole catchment, tend to be fast flowing with high turbulence, hence have sufficient dissolved oxygen concentrations to support fish life (Sinokrot et al., 1995). Since the solubility of oxygen in water is temperature dependent, however, projected increases in stream water temperature under climate warming may be accompanied by decreases in stream DO concentrations (Graham and Harrod, 2009). Some studies have suggested that increased fish metabolism and oxygen consumption may become problematic when DO contents of surface waters are already depleted and may lead to habitat restrictions or increased fish mortality (Caissie, 2006).

2.3.3 The Impacts of Climate and Dissolved Organic Carbon on Dissolved Oxygen Levels in the Burrishoole Catchment

High frequency DO data were available from three stream sites in the Burrishoole catchment (Appendix II). However, concurrent high frequency measurements of chromophoric dissolved organic matter (CDOM) fluorescence, a proxy for DOC, were only available from the Glenamong River. While DOC data were not available between September 2005 and November 2006 (Figure 2.5), the period 1/9/2005 to 31/8/2006 had an unbroken data set for DO, RWT and flow. These data were used in a multiple linear regression approach to assess the influence of RWT, DOC, and flow on DO concentrations, with DO concentration as the dependent variable and RWT, DOC, and flow as independent variables. The time-series was split up into individual months and each variable was detrended against time to remove seasonal effects (which can increase or decrease the perceived proportion of shared variance). The coefficient of determination (r^2) was then calculated for each individual month. All data were assessed for any breach of the assumptions of regression including normality and homosedacity in the data, and serial correlation in the residuals. Daily DO concentrations for each month were also plotted against daily RWT for the calendar year 1/1/2006 to 31/12/2006.

DO concentrations exhibited a distinct seasonal cycle with levels above 12 mg DO L^{-1} for the months between October and May and lower values from June to September (Figure 2.5). This pattern was in contrast to RWTs, where highest values occurred in summer (JJA) and lowest in winter (DJF). The minimum mean daily DO concentration was recorded on the 7th June 2006 (6.9 mg DO L^{-1}). The only mean hourly DO values less than 6 mg DO L^{-1} also occurred on the night of the 6th/7th June: mean hourly values from 22.00 hours on the 6th June to 03.00 hours on the 7th June were all below 6 mg DO L^{-1}, with a minimum of 5.3 mg DO L^{-1} occurring at midnight. Concentrations of between 7 and 7.5 mg DO L^{-1} also occurred on several dates between 18th and 22th July 2006. DOC levels were lowest in winter and increased in the late summer and autumn (Figure 2.5), a pattern that has been replicated in all years since 2003 at this site.

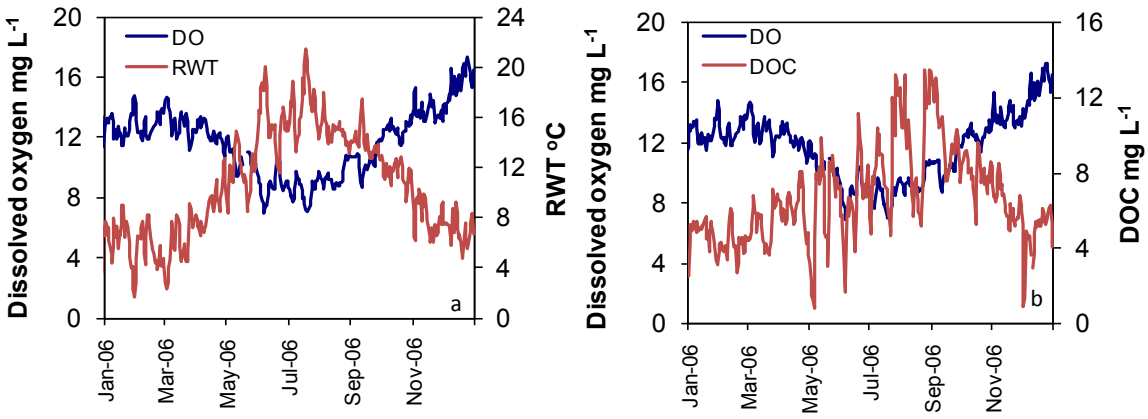

Figure 2.5 Time series of mean daily dissolved oxygen (DO) concentration (mg DO L^{-1}) in the Glenamong River, January to December 2006, with (a) mean daily river water temperature (RWT, °C), (b) mean daily dissolved organic carbon concentration (DOC, mg DOC L^{-1}).

DO concentrations in the Glenamong River were strongly dependent on RWT throughout the year (Figure 2.6; Table 2.8). The dependence of DO solubility on temperature explained between 75% and 90% of the variability in concentrations for months between September and May. This relationship reflected the negative effect of high temperatures on DO solubility (APHA, 1992). Between June and August (and for December 2005), DO was highly dependent on RWT but was also related to DOC concentrations. Although DOC contributed significantly to the regression in these months, the R^2 (adjusted) values only increased by between 5% and 8% when DOC was added to the model. DO levels were not dependent on flow levels in any month.

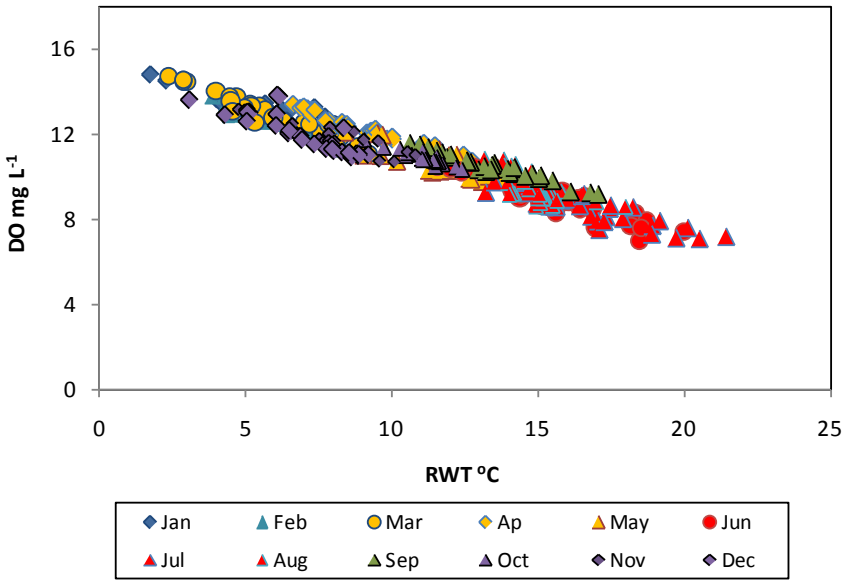

Figure 2.6 Mean daily dissolved oxygen (DO) concentration (mg L^{-1}) in the Glenamong River, plotted against river water temperature (RWT, °C) for each month, January to December 2006.

Table 2.8 Results of multiple regressions: dependent variable = mean daily DO concentration (mg L^{-1}), independent variables = mean daily RWT (°C) and mean daily DOC concentration (mg L^{-1}), Glenamong River, for each month between September 2005 to August 2006: probability levels (p) and coefficient of determination (r^2) for each month; (na = data not available, NS = not significant) (n = days in month). All data were linearly detrended to remove any seasonal component prior to analysis.

Month	RWT *p*	DOC *p*	R^2 (adj.) (%)
September	≤0.0001	na	90
October	≤0.0001	na	75
November	≤0.0001	na	78
December	≤0.0001	0.035	83
January	≤0.0001	NS	88
February	≤0.0001	NS	80
March	≤0.0001	NS	90
April	≤0.0001	NS	85
May	≤0.0001	NS	89
June	≤0.0001	0.003	85
July	≤0.0001	≤0.0001	91
August	≤0.0001	≤0.0001	91

2.4. pH and Episodic Acidification

2.4.1 Introduction

pH is a measure of the concentration of acidifying ions (e.g. H^+, hydrogen ion) in a solution. The pH scale is based on the logarithm of the reciprocal of hydrogen ion concentration in grams H^+ per litre. The lower the pH value, the higher the H^+ ion concentration. It is important to note that since the pH scale is a logarithmic scale, a drop of one pH unit at the higher (e.g. basic) end of the scale is equivalent to a much larger drop than one pH unit at the lower (acidic) end of the scale. A decrease of one unit in pH for water that is already acidic (e.g. from pH 5 to pH 4) indicates a much greater increase in acidity than, for example, the same pH drop of one pH unit in neutral waters (e.g. from pH 7 to pH 6). Stream pH in areas not affected by anthropogenic pollution is primarily a function of catchment geology and soil processes (Davies et al., 1992). The pH of surface waters is usually lower than pH 7 in areas with acid geology and acid soils (e.g. granite bedrock or upland peat soils). Streams running through areas with basic geology (e.g. limestone bedrock) will normally have a neutral (pH 7) or basic pH (above pH 7). The lowest (most acidic) pH values recorded in streams are generally c. pH 4, but these values are extreme (Table 2.9). Most of the extreme pH values that have been reported in the literature have been measured in streams draining areas of upland bog, often in catchments with non-calcareous bedrock, and with a high percentage of coniferous forest through the scavenging of H^+ ions from polluted air by coniferous trees (e.g.

Laudon et al., 2004; Monteith and Evans, 2005; Kowalik et al., 2007; Buffam et al., 2008; Ormrod and Durance, 2009).

Many of these areas have also been affected by acid deposition as a result of fossil fuel burning (Evans and Monteith, 2001; Davies et al., 2005). Maritime regions of Western Europe, in particular, have been severely affected by acidification. Large rainfall volumes have magnified anthropogenic sulphur (S) and nitrogen (N) deposition onto poorly buffered soils and surface water bodies (Ormerod and Durance, 2009). In Ireland, the impacts of acid deposition have been greatest in naturally occurring acid-sensitive waters which are chiefly located in areas with acid bedrock, and include the Burrishoole catchment (Aherne and Farrell, 2000; Allott and Brennan, 2000). Acidification of stream waters constitutes a considerable pressure on aquatic ecosystems, causing loss of species at all trophic levels, including the collapse of entire salmonid populations in severely acidified catchments (e.g. Milner and Varallo, 1990; Hesthagen et al., 1999). Salmonid fish species, such as Atlantic salmon (*S. salar*) and brown trout (*S. trutta*), are very sensitive to low pH water. Exposure to acidic waters has a wide range of effects on salmonids, from delayed hatching of eggs, decreased feeding and slowed growth of fry (Atlantic Salmon Trust, 1991); to tail deformities in adults (Campbell, 1987); migration of fish to higher-pH refugia (Baker et al., 1996); and increased mortality of all life-stages (eggs to adults) (EIFAC, 1969; Baker et al., 1996; McCartney et al., 2003; Finn, 2007; Monette and McCormick, 2008).

Acid deposition: Europe and Ireland

Anthropogenic acid deposition results from increased concentrations of sulphur dioxide (SO_2), nitrogen oxides (NO_x) and ammonia (NH_3) in the atmosphere. Both SO_2 and NO_x originate from the combustion of fossil fuels, while NH_3 is derived primarily from agricultural animal manures. These pollutants reach land as dry, wet and occult (cloud and mist) deposition. Pollutants can remain in the atmosphere for several days and may be carried thousands of kilometres from the point of emission; impacted sites may be at some distance from the pollutant source. While some of the resulting acidification of surface waters occurs through direct input, most occurs via runoff from the catchment after rain or snowmelt events (Wigington et al., 1992). In north-west Europe, frequent autumn rainstorms have been observed to produce 4 to 10 acid episodes at a given site per year. Harriman et al. (1990) observed 21 acid episodes with pH less than 5.5 (mean pH = 6.5) in a 170 day observation period in the Allt a'Mharcaidh catchment, Scotland.

The susceptibility to and extent of acidification of surface waters depends on pre-episode pH, antecedent and catchment conditions, and the hydrological flow path of acid deposition through the catchment (Wigington et al., 1992 and 1996; Lawrence, 2002). In areas with base-rich soils (e.g. calcium (Ca^{2+}) rich soils), acid deposition may be neutralized through cation-exchange reactions as it travels through catchment soils to surface waters. These reactions usually occur in the upper strata of soils, but concentrations of exchangeable calcium in mineral soils have decreased as a result of increased acid deposition since the mid-twentieth century (Lawrence, 2002). Similarly, in areas with base-poor soils, the input of these pollutants may exceed the soil buffering capacity. As a result, areas with naturally acidic soils and base-poor bedrock are particularly vulnerable to the effects of acid deposition.

Anthropogenic acidification of soils and surface waters, associated with increases in sulphur emissions from industrial sources, increased during the 20th century and peaked in the 1970s. Rates have reduced following the implementation of mitigation measures (Skjelkvåle et al., 2005), in particular the ratification of the 1979 Convention on Long-Range Transboundary Air Pollution (CLRTAP) protocol by the EU in 1981. This convention aimed to reduce emissions of acidifying compounds by 30% from 1980 levels by 1993. More recently, the UN Economic Commission for Europe (UNECE) Multi-Pollutant, Multi-Effect, or 'Gothenburg' Protocol set new targets to reduce S emissions by 63%, NO_x emissions by 41%, and NH_3 emissions by 17% by 2010 relative to 1990 levels. An early result of these protocols has been that sulphur dioxide emissions over northern Europe and the United Kingdom have declined by 50 – 65% since peak deposition in 1980 (Laudon and Bishop, 2002; Davies et al., 2005).

Ireland has few significant sources of atmospheric pollutants. One exception has been the large coal-fired power station at Moneypoint in Co. Clare on the west coast (Bowman and McGettigan 1994), although this is currently undergoing refurbishment to reduce SO_x emissions by up to 90% from current levels. There is also a potential risk of pollution from more industrialised nations such as the UK and continental Europe (Bowman and McGettigan, 1994; Allott and Brennan, 2000). Deposition from these countries mainly arises when cyclonic weather systems pass to the south of the island of Ireland, generating easterly winds across the country (Allott and Brennan, 2000). Atmospheric deposition of SO_2 and NO_x in Ireland from anthropogenic sources is low in the western part of the country, while significant in the east (Bowman and McGettigan, 1994; Aherne and Farrell, 2000). On a European scale Ireland still remains a relatively low producer (below 1000 tonnes per EMEP50-grid - Protocol on Long-term Financing of the Cooperative Programme for Monitoring and Evaluation of the Long-range Transmission of Air Pollutants in Europe) of oxidised sulphur compared to more

industrialised nations such as Poland, Germany, the UK and the Benelux countries (10-50,000 tonnes per EMEP50-grid) (Nyeri et al., 2009).

Although concentrations of atmospheric S and N have reduced in the last few decades, recovery of UK surface waters from acidification has been sporadic and inconsistent (Davies et al., 2005; Monteith et al., 2005; Ormerod and Durance, 2009\0. Kowalik et al. (2007) showed that periodic acid episodes in acid-sensitive areas of Scotland and Wales prevented the return of acid-sensitive organisms, even in streams where mean pH had increased to circumneutral levels. Conversely, across a 250,000-km^2 expanse of northern Sweden, a 65% decline in sulphur deposition between 1970 and 1990 reduced the area of chronically acidified spring floods by 75% (Laudon and Bishop, 2002). Although it was long thought that chronic acidification of streams was the most significant threat to biodiversity, it is now believed that episodic acidification, single or recurrent low-pH episodes lasting hours to several days, is a major cause of slowed recovery from acidification in both the UK and Scandinavia (Kowalik et al., 2007; Laudon, 2008) and a possible contributor to Atlantic salmon population decline (Monette and McCormick, 2008).

Acid episodes in upland areas most commonly occur during heavy precipitation and flooding events and have been linked to the flushing out of historical S and N oxides that were derived from fossil fuel burning, then deposited and stored in catchment soils; inputs of natural organic acids (e.g. humic acids) derived from degradation of peatlands; and deposition of sea-salts in maritime regions (Davies et al., 1992; Farrell et al., 1998; Evans and Monteith, 2001; Kowalik et al., 2007; Laudon, 2008; Vuorenmaa and Forsius, 2008; Ormerod and Durance, 2009). The degree to which acid deposition is modified by the vegetation, soils, and geology of a catchment is dependent upon the length of time that acidic water is in contact with the physical catchment features (e.g. buffering capacity of ion-exchange with limestone bedrock). During storm events, a large percentage of event water enters surface water bodies through overland flow or percolation into the topsoil. This rapid flow allows for only minimal soil/water contact, resulting in negligible buffering capacity, and hence "pulses" of acidity to streams (Davies et al., 1992; Wigington et al., 1996; Lawrence, 2002).

Stream pH in acid episodes has been observed to decrease very rapidly, e.g. 0.5 to 3.0 pH units within a few hours, and may be accompanied by increased levels of Aluminium (Al) leaching from the catchment soils (Farrell et al., 1998; Jarvie et al., 2001; Laudon and Bishop, 2002; Lawrence, 2002). Minimum pH values recorded in streams across Europe and North America were c. pH 3.7 – 4.0, although levels as extreme as these were not common (Table 2.9). The

lowest pH values and highest pH declines during flood events have often been observed in streams in afforested catchments draining upland peat bogs (Allott and Brennan, 2000; Likens and Buso, 2006; Buffam et al., 2008; Ormerod and Durance, 2009). In western Ireland, Allott and Brennan (2000) found that most acid episodes were associated with increases in non-marine sulphate, with organic acids contributing relatively little to the decline in pH. Organic acids did, however, form a baseline of acidity in streams, making them more prone to increased acidification. Sea-salts were rarely a major cause of pH decline during acid episodes, but contributed to base cation depletion and diminished buffering capacity of surface waters (Allott and Brennan, 2000; Kowalik et al., 2007). It has long been recognized that soils underlying coniferous forest tend to be more acid than soils under deciduous vegetation (Ovington, 1957; Federer, 1985). This discrepancy is due to a range of interactions between the trees, soils, soil-water and the atmosphere, such as increased quantity of acidic litter inputs (Alexander and Cresser, 1995), increased evapotranspitation, and accelerated nutrient uptake during tree growth leading to depletion of base cations within the soil (Federer, 1985). Soil acidification may be further accelerated in soil with low pH thus compounding the problem in areas with naturally acidic soils (Federer, 1985).

Table 2.9 Minimum pH values quoted in selected studies of episodic acidification from Ireland, the UK, Scandinavia, Russia, and North America.

Study site	Monitoring data	Catchment characteristics	Min. pH	Reference
Owenboliska, Co. Galway, Ireland	High frequency, 2 winters	Granite bedrock overlain with peat, coniferous forest	3.82 - 4.82	Allott and Brennan (2000)
UK Acid Waters Monitoring Network	22 streams/ lakes, 15 yrs	Mostly peaty upland catchments	4.6 - 6.3	Monteith and Evans (2005)
River Dee, Scotland, UK	2 week intervals 1 year	Non-calcareous bedrock Upland peatlands	5.02	Jarvie et al. (2001)
Cairn Gorm Mountain, Scotland, UK	Two sites, one winter	Upland peatlands	4.0 - 4.2	Davies et al. (1993)
Llyn Brianne catchment, Wales, UK	14 sites, weekly/monthly for 25 years	Granite bedrock, streams draining peatlands (P) and coniferous forest (F)	4.0-4.7 (P) 3.7-4.7 (F)	Ormerod and Durance (2009)
Krycklan River, Sweden	60 sites, spring/winter	Boreal, >30% peatlands in subcatchments	4.3 - 6.3	Buffam et al. (2008)
Kola Peninsula, Russia	Seven sites, four winters	Boreal catchment, peatlands, acid deposition	4.7	Moiseenko et al. (2001)
Buck Creek, Adirondack Mtns, NY, USA	storm events north Branch	Peatlands, coniferous forest	4.09 - 4.12	Lawrence (2002)
Buck Creek, Adirondack Mtns, NY, USA	storm events south Branch	Gneiss bedrock	4.61 - 4.84	Lawrence (2002)
Hubbard Brook valley, NH, USA	32 streams, spring/autumn	Acidic bedrock and soils, mixed forests	3.73	Likens and Buso (2006)

The acidity of soils under conifers can also be exacerbated by the efficiency of coniferous trees in scavenging pollutants from the atmosphere (Ahmad-Shah and Rieley, 1989; Neal et al., 1992; Allot et al., 1997; Farrell et al., 1997). In England, for example, Ahmad-Shah and Rieley (1989) observed substantially greater deposition of sulphate under Scots Pine forest than under deciduous woodland. There is also evidence that coniferous forests may scavenge pollutants during dry weather, which may be subsequently washed into surface water bodies (Allott and Brennan, 2000). In addition, high rates of evapotranspiration from coniferous forests decrease total runoff (Blackie and Newton, 1986; Johnson, 1995), which can increase the concentration of acidifying ions in runoff and exacerbate surface water acidification. A comparison of water chemistry data from fourteen sub-catchments with differing land uses in the Llyn Brianna study site in Wales found that streams draining coniferous forests had greatly lower pH when compared with peatland streams of similar water hardness in the same catchment (Ormerod and Durance, 2009). Similar results have been reported in Ireland (Bowman, 1991; Allott et al., 1997).

The critical load of acidity is defined as the upper threshold of acid deposition that will not cause chemical changes leading to long-term harmful effects on ecosystem structure and function (Nilsson and Grennfelt, 1988). Aherne and Farrell (2000) surveyed 200 Irish lakes, the majority of which were located in acid sensitive regions, and determined their critical loads of acidity. In the survey, the pH of the lakes ranged between 4.2 and 8.5 with 37% of the lakes showing a pH value lower than 5.5 (Aherne and Farrell, 2000). In 20% of the lakes with a pH below 6.0, non-marine sulphate was found to be the dominant anion and these had an average pH value of approximately 4.5 (Aherne and Farrell, 2000).

Individual reports have also highlighted the fact that some Irish waters are being impacted by acid deposition, particularly lower order streams in catchments with base-poor bedrock (Bowman, 1991; Bowman and Bracken, 1993; Allott et al. 1997; Farrell et al. 1997; Giller et al. 1997; Kelly-Quinn et al., 1997; Allott and Brennan, 2000). A detailed study on the interaction between forestry and aquatic ecology (AQUAFOR) was carried out in Ireland in the 1990s to establish whether or not forests had a negative impact on stream-water quality and fish populations through exacerbating acidity. Results were found to vary by region (Allott et al. 1997; Farrell et al. 1997; Giller et al. 1997; Kelly-Quinn et al. 1997). No clear evidence of adverse impacts of forestry on stream hydrochemistry was found in an extensive study of watercourses with varying land uses in Munster, although data were not available during periods of high flow when acid episodes may have occurred (Giller et al., 1997). In contrast, deterioration in water quality was reported from two of three sites in Counties Galway, Cork and Wicklow (Farrell et al., 1997). The third site showed no evidence of a negative impact of afforestation, which was attributed primarily to the high buffering capacity of the sandstone bedrock.

Kelly-Quinn et al. (1997) reported increased acid episodes (pH as low as 4.2) and increased levels of inorganic Al of streams in Co. Wicklow during periods of high flow, particularly in heavily afforested catchments. Many of the streams had levels of labile monomeric Al in excess of 40 $\mu g\ l^{-1}$ (the maximum concentration for salmonid waters), creating toxic conditions for both salmonids and macroinvertebrates. In the west of Ireland, Allott et al. (1997) found that stream water had lower pH and that acid episodes were longer lasting in afforested compared with catchments devoid of forests. Undesirably high levels of labile monomeric Al were associated with acid episodes in the catchments. The diversity of invertebrate species was reduced in acid forested sites and salmon eggs were found to have a lower survival rate. The study concluded that in poorly buffered catchments forestry contributed to an increase in the acid status of streams (Allott et al. 1997).

Impacts on low pH on fish growth and survival

Many acid-sensitive waters in Ireland, like the Burrishoole catchment, contain important populations of salmonids, particularly Atlantic salmon and brown trout. Due to the complexity of their life cycle, andromous salmonids are highly sensitive to changes in water quality (Atlantic Salmon Trust, 1991). Acid waters can have adverse effects on salmonids and other fish by affecting respiratory function, diminishing swimming performance, creating physical deformations, and reducing growth rate (EIFAC, 1969; Peterson et al., 1980; Campbell, 1987; Bowman and Bracken, 1993; Finn, 2007; Monette and McCormick, 2008) (Table 2.10). If the pH of surface waters is below pH 5.5, hatching of fish eggs is prevented as the necessary enzymes become inactive (Peterson et al., 1980). However, according to White (2000), salmon in Nova Scotia can withstand a lower pH level (5.0 compared to 5.5) than in those Europe (White, 2000). This was attributed to the concurrent effects in European waters of toxic Al concentrations and low pH. In Nova Scotia organic compounds bind most of the aluminium into its non-toxic form (Lacroix, 1985).

The timing of acid episodes is particularly important in terms of the deleterious effects of low-pH waters on salmonid species (Kroglund et al., 2008; Monette and McCormick, 2008). For brown trout, the most sensitive life stages are alevins and fry, whereas salmon smolts show the most heightened sensitivity to low pH waters (Rosseland and Stuatnes, 1994; Monette and McCormick, 2008). The degree of physiological disturbance to fish in acidified waters is directly related to the synergistic effects of pH and labile Al, although many studies suggest that Al, not hydrogen ions (H^+), is the principal toxicant (e.g. Poléo, 1995). For example, Atlantic salmon smolts exposed to pH 5.2 with increasing concentrations of inorganic Al ([Al]) for two days showed a loss of blood plasma ions when [Al] rose above 88 $\mu g\ L^{-1}$ and mortality at [Al] >140 $\mu g\ L^{-1}$, but showed decreased effects and mortality at pH 5.6 and no impacts at pH above 6.0 (Monette and McCormick, 2008).

Greater survival rates of brown trout have also been observed in acid waters with high Al concentrations in the presence of higher calcium concentrations (>1.0 mg Al L^{-1}) (Bowman and Bracken, 1993). Bowman and Bracken (1993) investigated the effects of low pH and increased Al on the survival rate of brown trout in two streams in Co. Wicklow. Fifteen brown trout, less than one year old, were introduced to each of two rivers. One stream (the Lugduff) was in an afforested catchment and was more acidic (pH 4.48 vs. 5.55), containing higher concentrations of labile Al (238 vs. 9 μg Al L^{-1}) and lower concentrations of calcium (1.05 vs. 2.4 μg Ca L^{-1}). The second stream (the Glenealo) was in an unafforested catchment. After

one week all fish had survived in the Glenealo while only three had survived in the Lugduff. The three remaining fish in the Lugduff were disorientated, lacked energy and lay at right angles to the flow and their gills contained an extensive coating of Al and mucus (Bowman and Bracken, 1993). The behavioural and physiological effects of acidified waters on salmonid species are caused by the disruption of fish blood chemistry and respiration by H^+ and Al ions (Atlantic Salmon Trust 1991; Monette and McCormick, 2008).

Table 2.10 Approximate ranges of pH observed to cause negative effects on Atlantic salmon (*Salmo salar*) and brown trout (*Salmo trutta*).

pH range	Effect on salmonids	References
3.0 - 4.0	Range lethal to all salmonids	EIFAC (1969) Atlantic Salmon Trust (1991)
4.0 - 4.5	Total mortality of salmonid eggs, alevins, and fry	EIFAC (1969) Atlantic Salmon Trust (1991)
< 5.0	Increased mortality of alevins	Atlantic Salmon Trust (1991)
	No nest digging by female trout	Kitamura and Ikuta (2001)
< 5.2	Triggers migration of all species to refugia.	Baker et al. (1996)
	Inability of fry to feed	Atlantic Salmon Trust (1991)
< 5.5	Prevention of egg hatching.	Peterson et al. (1980)
	Decreased abundance of salmonid smolts.	Monette and McCormick (2008)
< 6.5	Toxic effects for embryos - reduced fertilisation, lower embryonic growth	Finn (2007)
	No nest digging by female salmon	Kitamura and Ikuta (2000)
6.5 - 8.5	Maximum productivity for salmonids	Orsanco (1955) in EIFAC (1969)

Atlantic salmon are among the most sensitive of salmonid species to acid and Al exposure (Poléo, 1995; Monette and McCormick, 2008). Sensitivity to acid/Al exposure also varies between salmonid life-stages, with Atlantic salmon smolt showing greater sensitivity than parr (Monette and McCormick, 2008). Various explanations have been proposed for the discrepancy in sensitivity: loss of plasma Cl^- due to greater decline in gill NKA activity (McCormick et al., 1998), greater gill Al accumulation (Kroglund et al., 2008), and heightened stress responsiveness or morphological changes in gill structure in smolts in preparation for transition to the marine environment (Monette and McCormick, 2008). During the transformation from parr to smolt, a development necessary for seawater entry, fish develop salt secretory ability due to an increase in the number and size of gill chloride cells and gill NKA activity (McCormick et al., 1998). Monette and McCormick (2008) concluded that these

morphological changes render smolt gills more permeable, hence more vulnerable to rapid ion efflux during exposure to water with low pH and high Al concentrations.

2.4.2 Regional Weather and Low pH Events in the Burrishoole Catchment

The relationship between the occurrence of low pH episodes and regional weather patterns was assessed using data from the Glenamong River. The Lamb (1972) classification of weather types describes weather patterns across the region of the British Isles. It was originally based on subjective analysis of daily synoptic charts at 12pm but was changed to an automated system based on grid-point mean sea-level-pressure differences around Britain and Ireland (Jones et al., 1993) and was also known as the Jenkinson (Jenkinson and Collison, 1977) or Lamb-Jenkinson weather type (LJWT) classification. It has been shown that there was good agreement between the original subjective method and the automated method, although some discrepancies occur in years prior to 1960, in particular an underestimation of westerly types. These data were available up until 2008. The classification contained eight-directional types and three non-directional types which may be combined into hybrids. The directional types were defined according to the general direction of the air flow: north (N), northeast (NE), east (E), southeast (SE), south (S), southwest (SW), west (W), and north (N). The non-directional types, anti-cyclonic (A) and cyclonic (C) occurred when high or low pressures systems were dominant. The third non-directional type occurred on undefined days (U). Hybrids occurred when characteristics of both a directional type and either C or A occurred, e.g. CW type. For a detailed description of each weather type see Kelly et al., (1997). The most common LJWTs were C, A, W, N, S, NW and E (Wilby et al,. 1997). There were no major differences in the seasonal distribution of these categories but westerly conditions were more common in winter. The Lamb Catalogue has been used to investigate several meteorological variables including: regional rainfall (Sweeney, 1985; Wigley and Jones, 1987; Sweeney and O'Hare, 1992), long-term temperature variations (Sowden and Parker, 1981), lake surface temperatures (George et al., 2007), sediment yields (Wilby et al., 1997), and ozone concentration (O'Hare and Wilby, 1995).

Low pH events in rivers are often associated with floods due to heavy precipitation which causes flushing out of soil anions into river waters (Jacks et al., 1986; Hornung et al., 1990). In a previous study of the nature of acidic episodes in western Ireland, Allott and Brennan (2000) found that the Lamb-Jenkinson Weather Type (LJWT) preceding low pH events was predominantly anticyclonic (A). Of the episodes examined (n=12), 50% of events were preceded by A weather-type, 33% by cyclonic (C) weather-type, and 16% by variable weather types. The implication of these results was that preceding anticyclonic weather and associated

easterly air mass movement was causing the dry deposition of acidifying ions from Britain and Europe, which were then being flushed from catchment soils during subsequent periods of high precipitation (Allott and Brennan, 2000).

High resolution pH, water level and rain data from the Glenamong River in the Burrishoole catchment was used in the following assessment. The pH probe was calibrated on a weekly or fortnightly basis (see note in Appendix X on changes in probe type). Fifty low-pH events were defined as a drop of 1 unit or more relative to pre-event conditions and were identified through visual inspection of the 2005–2007 data record by graphing the high resolution data. All fifty low-pH episodes were associated with floods (high water levels) in the Glenamong River. Daily LJWT data were used to examine the relationship between low pH events in the river and preceding large-scale weather conditions over the period 1/1/2005-31/12/2007.

Classification of preceding conditions by Lamb-Jenkinson Weather Type

LJWT data were downloaded from the website of the Climate Research Unit of the University of east Anglia (www.cru.uea.ac.uk/cru/data/lwt.htm). The LJWT for both the day of each low-pH/flood event and for each day in the preceding 28-day period was extracted and divided into four weekly run-up periods. Week 1 (WK1) was the seven-day period immediately preceding the low pH event, week 2 (WK2) the seven-day period preceding WK1, etc. WK1 and WK2 were combined to give a 14-day run-up period (14d-RU) and all four weeks were combined to give a 28-day run-up period (28d-RU). Three methods were compared to classify each of the run-up periods as a single LJWT: the mode of the period with no ties and two or more days of the same LJWT (method A1), the mode of the period with no ties and three or more days of the same LJWT (method A2), and the most common constituent of the core seven LJWTs, i.e. A, C, E, N, NW, S, and W (method B). Method B entailed splitting each compound LJWT into its constituent parts (e.g. AW into A and W), and calculating the mode of the period with no ties.

The number of classifiable weeks was highest using method B for all run-up periods (Table 2.11). This resulted from fewer ties between equally dominant LJWTs in a period, due to the splitting of compound LJWTs into their constituent parts as mentioned previously. Methods A1 and A2 gave similar results, although on average 18% of weeks were classified differently between the two methods (Table 2.12). Both 14-day and 28-day run-up periods had identical classification using methods A1 and A2, and as such both were equally different from method B. The most complete classification (i.e. least number of unclassifiable periods) was found for

28d-RU using method B, in which 94% of periods were classified as a single dominant LJWT (Table 2.13).

Table 2.11 Percentage of weekly (WKLY), 14-day run-up (14d-RU), and 28-day run-up (28d-RU) periods with identical LJWT classification using three different methods (A1, A2, B).

	A1 = A2 = B	A1 = A2	A1 = B	A2 = B
Mean WKLY	50%	72%	60%	58%
14d-RU	58%	100%	58%	58%
28d-RU	56%	100%	56%	56%

Due to the higher sample size obtained, and the fact that most temporal variance in the Lamb-Jenkinson catalogue is accounted for by the seven basic weather types (Lamb 1972; Jones and Kelly, 1982), method B was used to classify all run-up periods as a single dominant LJWT. A similar classification scheme has also been used in other studies (e.g. Young et al., 1996).

The most common LJWT on the run-up to low pH events was anticyclonic (A). This type occurred 23% - 41% of the time, with an average of 30% (Table 2.13). A-type conditions were dominant during the longer run-up periods also i.e. 14d-RU and 28d-RU, and showed greater frequencies in weekly run-ups with 41% of 14d-RU and 45% of 28d-RU classified as A (Table 2.13). This is in agreement with earlier studies in the west of Ireland which attributed an association between low pH episodes and antecedent anticyclonic conditions to dry deposition of pollutants from eastern Ireland and Britain (Allott and Brennan, 2000) and implies that such deposition may be still occurring during periods of easterly air flow.

Table 2.12 Number and percentage of weekly, 14-day run-up (14d-RU), and 28-day run-up (28d-RU) periods classified as a single dominant LJWT by three different classification methods.

	Method	n	Percentage classified
WK1	A1	36	72%
	A2	34	68%
	B	45	90%
WK2	A1	35	70%
	A2	29	58%
	B	43	86%
WK3	A1	37	74%
	A2	23	46%
	B	39	78%
WK4	A1	34	68%
	A2	25	50%
	B	41	82%
MEAN WKLY	A1	36	71%
	A2	28	56%
	B	42	84%
14d-RU	A1	43	86%
	A2	43	86%
	B	46	92%
28-d RU	A1	42	84%
	A2	42	84%
	B	47	94%

The W weather-type was found to be a dominant component of weather in weekly run-ups. W was also the most frequent LJWT in WK3and WK4 and the second most frequent type in WK1 and WK2. The mean weekly frequency of W was 26%, second only to A. In the longer run-up periods, 14d-RU and 28d-RU, W also occurred frequently. In the 14d-RU periods both W weather type and C weather type occurred 20% of the time. This was the same as the frequency of C type for the 14d-RU period. During the 28d-RU, however, W was third most frequent at 17%, less than S type which occurred 23% of the time. Some LJWTs were poorly represented in the run-up periods to low-pH events in the Glenamong River from 2005–2007. E, N and NW weather types did not occur more than 5% of the time each during any run-up period in the record. Combined, these three LJWTs never exceeded 15% of any run-up period and sometimes were not represented (Table 2.13).

Table 2.13 Frequency of dominant LJWTs in weekly, 14day and 28day run-up periods to low-pH events.

	WK4	WK3	WK2	WK1	MEAN WKLY	14d-RU	28d-RU
A	28%	23%	40%	28%	30%	41%	45%
W	30%	28%	21%	26%	26%	20%	17%
S	15%	18%	17%	21%	18%	15%	23%
C	15%	18%	12%	16%	15%	20%	13%
E	3%	3%	5%	5%	4%	2%	0%
NW	5%	5%	5%	2%	4%	0%	0%
N	5%	5%	0%	2%	3%	2%	2%

Comparison of 2005–2007 Lamb Jenkinsen Weather Type frequencies with long-term record

The frequency distribution of run-up periods to low-pH events in the Glenamong River over 2005–2007 was compared with that of the long-term (1880-2007) LJWT record. This comparison was conducted to ascertain whether the patterns seen in the run-ups to low pH events were different from the long-term LJWT frequencies. Mean weekly, 14d-RU and 28d-RU datasets were compared to the long-term LJWT record (Figure 2.7) using the core seven LJWTs as described previously in method B. Chi-squared tests were performed to assess whether the frequency of LJWTs of run-up periods differed from the long-term LJWT record. It was found that the distribution of weather-types of each run-up period differed significantly from the expected distribution based on the long-term record (Table 2.14). The 28d-RU showed the greatest deviation from the expected values ($p<0.001$) followed by 14d-RU ($p<0.001$). The weekly run-up (7d-RU) was also significantly different from the expected values ($p=0.001$) as was the weekly mean ($p<0.019$). During run-up periods to a low pH event, A weather types were more dominant than expected from the long-term LJWT record. Conversely E, N, and NW types were under-represented during run-up periods (Figure 2.7) indicating that low pH events were preceded by predominantly A weather type.

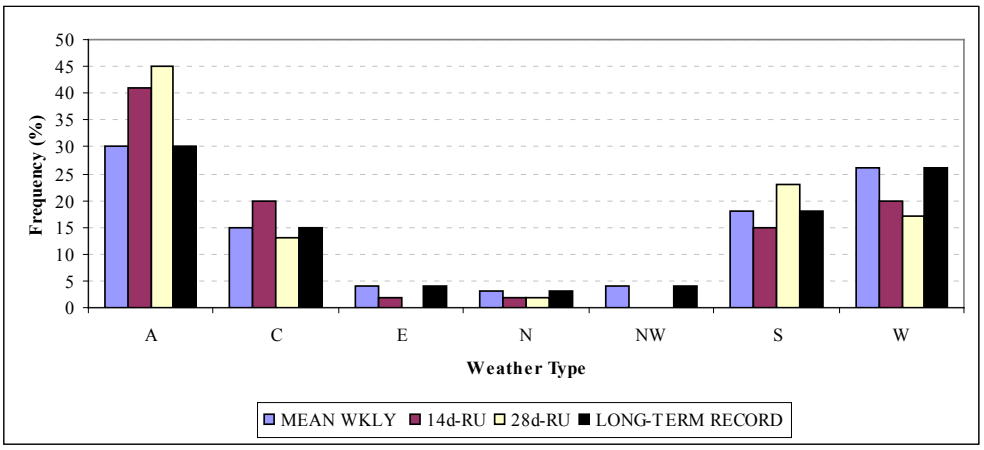

Figure 2.7 Frequency distribution of seven core LJWTs during run-up periods (mean weekly, 14d-RU and 28d-RU) to 50 low-pH events in the Glenamong River versus the long-term LJWT record 1880–2007.

Table 2.14 Chi-squared goodness of fit values and associated p-values for comparison of frequencies of LJWTs in the 2005 – 2007 record versus the long-term LJWT record 1880–2007.

	G	G(adj)	df	p
28d-RU	64.80	63.94	6	< 0.01
14d-RU	35.63	35.16	6	< 0.01
WK1	22.44	22.15	6	< 0.01
Mean WKLY	15.14	14.94	6	0.02

Lamb Jenkinsen Weather Type on low-pH event days

LJWT on the day of each of the fifty selected low-pH events in the Glenamong River over the period 2005-2007 was classified using the same method as for run-up periods. The majority of low pH events occurred on days dominated by S (31%) or W (34%) weather types (Table 2.15). This almost equal split was indicative of the dominance of southwesterly (SW) weather type on event days (Table 2.15). When compound LJWTs were not split into their constituent parts, it was found that 16 out of 29 LJWTs were represented on low-pH event days. Of these, 26% were SW-type, 14% were W-type, and 14% were C-type (Table 2.15). SW, W, and C weather types are commonly associated with precipitation in the west of Ireland (Sweeney, 1985; Wigley and Jones, 1987; Sweeney and O'Hare, 1992; Hulme and Barrow, 1997).

Table 2.15 Percentage contribution of 7 core LJWT types and 29 hybrid LJWT types (all types) to LJWT on low pH event days.

		Lamb Jenkinsen Weather Type																	
		A	ANE	ANW	ASE	ASW	AW	C	CS	CSW	CW	E	N	NW	S	SE	SW	U	W
7	No.	8	-	-	-	-	-	12	-	-	-	5	1	3	26	-	-	-	28
	Freq	10	-	-	-	-	-	14	-	-	-	6	1	4	31	-	-	-	34
	%																		
All	No.	1	1	1	2	2	2	7	1	1	2	-	-	2	5	2	13	1	7
	Freq	2	2	2	4	4	4	14	2	2	4	-	-	4	10	4	26	2	14
	%																		

2.4.3 Episodic Acidification Events in the Glenamong (October 2008 – October 2009)

In October 2008, Marine Institute staff changed pH probe types upon recommendation of the probe manufacturer and introduced new quality control procedures. These steps eliminated quality assurance issues that had been identified with some pH data collected prior to October 2008. Data from 1/10/2008 to 1/11/2009 were assessed for the occurrence of low pH events. There were thirteen days of missing data due to mechanical failure and maintenance.

An examination of the high resolution (2-minute) data from the Glenamong River showed that the lowest pH recorded between 30/10/2008 – 20/10/2009 was 3.90 and the highest was 7.04. This pH range was comparable to that observed in other upland, peat-rich catchments in Wales, Scotland, Sweden, and in the northeast USA (Lawrence, 2002; Monteith and Evans, 2005; Likens and Buso, 2006; Buffam et al., 2008; Ormerod and Durance, 2009). Allott and Brennan (2000) measured a similar range of pH in their study of twelve acid episodes in a stream draining the afforested Owenboliska catchment in western Ireland, which is also underlain by granite bedrock and peat soils. The minimum pH of 3.90 was recorded in January 2009 when the river was experiencing high flows (1.68 – 3.20 $m^3 s^{-1}$). In studies of episodic acidification, minimum pH values often coincide with or are recorded shortly after a period of maximum stormflow (Lawrence, 2002; Deyton et al., 2009). The low-pH events recorded in the Glenamong River in the period occurred both as single and multiple depressions in pH, with drops in pH ranging in magnitude from 0.50 to 2.30 pH units (Table 2.16). These drops in pH are comparable with studies of rainfall-triggered acid episodes in a study in upland peaty catchments in Sweden, where pH of streamwater declined by 1.0 – 2.4 pH units in events preceded by summer drought (Laudon and Bishop, 2002). More extreme pH depressions of c. 3 pH units were measured in Sweden and Wales following snowmelt episodes (Davies et al., 1992).

Daily mean pH was calculated for the Glenamong River for the period 30 October 2008 – 20 October 2009. The range in daily mean pH was 4.04 – 6.81, with highest frequency of pH readings falling between 6.00 and 6.50 (Figure 2.8). The daily mean pH was greater than or equal to 5.50 for 57% of the 2008 – 2009 record.

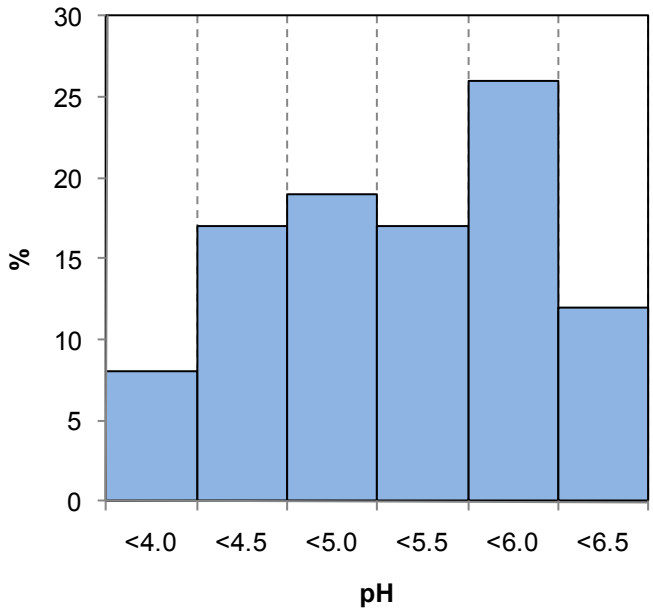

Figure 2.8 Frequency distribution of mean daily pH in the Glenamong River 20/10/2008 - 20/10/2009.

Salmonid fish are sensitive to changes in pH, with increased mortality of all life-stages found at pH levels below 5.0 (EIFAC, 1969; Atlantic Salmon Trust, 1991). Critical ranges of pH which have been reported to have negative effects on salmonid species are listed in Table 2.10. An analysis was conducted on the frequency of Glenamong River daily mean pH measurements within these thresholds for the data from 30/10/2008 – 20/10/2009 (Table 2.16). No daily mean pH values of 3.0–4.0, the range lethal to all salmonid species and life-stages, were recorded in the Glenamong River during the period. Only 17% of Glenamong daily mean pH readings fell between 4.5 and 5.0, the range where total mortality of salmonid eggs, alevins, and fry is observed (EIFAC, 1969; Atlantic Salmon Trust, 1991). More importantly, 45% of daily mean pH readings were below the threshold of pH 5.5, the level of acidity below which marked deleterious effects on salmonid fish are observed (Peterson et al., 1980; Atlantic Salmon Trust, 1991; Monette and McCormick, 2008). This suggests that fish in the Glenamong River may have been exposed to potentially harmful levels of acidity for 45% of the 2008 – 2009 record.

Table 2.16 Frequency of pH values recorded in the Glenamong River within critical thresholds for fish survival during the period 30/10/2008 – 20/10/2009.

pH range	Frequency (%)
3.0 – 4.0	0.0
4.5 – 5.0	17.5
< 5.5	44.6
> 6.0	37.9
> 6.5	11.4

Low pH events in the Glenamong River and large-scale airflow (October 2008 – October 2009)

An examination of the relationship of 2008–2009 low-pH events with LJWTs was not possible because the Climate Research Unit ceased to record LJWT data. A simple index of daily standardized sea level pressure difference between grid-points to the north (57.5°N -7.5°W) and south (50°N -7.5°W) of Ireland was calculated for the record period. This index provided an indication of air mass movement in either an easterly or westerly direction and is referred to in this study as the east-west index (EWI). Ten low-pH events were identified in the record using the method described in Section 2.4.2. Corresponding water level and precipitation data were extracted for each event and for the seven day period preceding the low-pH event (7d-RU).

Daily mean pH in the Glenamong River for the period January to October 2009 was compared with the EWI for the same period. Days classified as westerly had lower daily mean pH levels than those classified as easterly ($t=6.34$; $d.f.=278$; $p<0.01$; Figure 2.9). The association of westerly air-flow with low-pH events agrees with the analysis of the LJWT index in relation to acid episodes in 2005–2007, where W and SW conditions dominated low-pH event days.

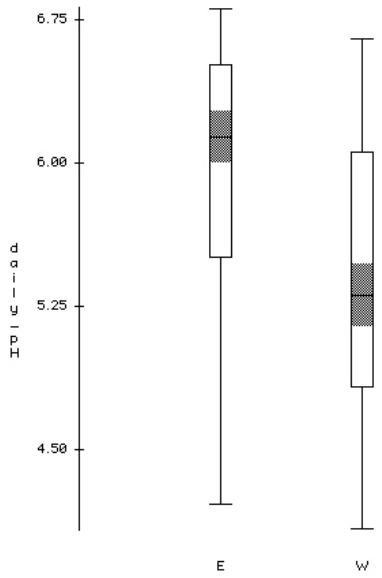

Figure 2.9 Box plot showing difference in daily mean pH for east and west type days as classified by the East West Index in the Glenamong River, where E = east and W = west.

Of the ten Glenamong low-pH events identified in the 2008 – 2009 record, six occurred as single drops in pH and four were composed of multiple decreases in pH over 1 to 2 day periods (Figure 2.10; Table 2.17). All ten episodes were associated with increased precipitation in the Burrishoole catchment and increased flow in the Glenamong River, either in the 7d-RU or on the event day. The single-depression acid episodes occurred over the course of several hours, with recovery to pre-episode pH occurring over 1.5 – 5.5 days (Table 2.17). The lowest pH recorded in a single acid event was 4.02, after a drop from 4.93 on 19/12/2008, while the largest magnitude of drop was 2.32 pH units on 22/9/09. The multiple-depression low-pH episodes were characterised by initial drops in pH followed by moderate recovery (elevation of pH), and additional depressions of pH. Individual pH depressions ranged from 0.50 – 1.60 pH units. Multiple low-pH depressions were correlated with multiple peaks in precipitation and flow, suggesting pulses of floods in the river. Recovery to pre-episode pH after the multiple-drop events was complete after 3.5 – 7 days (Table 2.17).

Table 2.17 Ten single (S) and multiple (M) low pH events in the Glenamong River from October 2008 – October 2009 with preceding (7-day run-up) and event day weather conditions (rain (mm), E-W index), extent of pH depression, and time to recovery to pre-episode pH. Seasonal abbreviations: W=DJF, S=MAM, SU=JJA, A=SON. (- indicates no data).

			7 day run-up		Event day					
No	**Date Season**	**Type**	**Rain (mm)**	**E-W index**	**Rain (mm)**	**E-W index**	**pH max**	**pH min**	**pH drop**	**Recovery to pre-episode pH (hours)**
1	04/12/08 W	S	48.6	no data	12.6	-	5.74	4.57	1.17	58
2	18/12/08 W	M	53.8	no data	11.0	-	5.16	4.66	0.50	1
	18/12/08 W	M	53.8	no data	11.0	-	4.95	4.41	0.54	19
	19/12/08 W	M	61.8	no data	13.6	-	4.93	4.02	0.91	84
3	10/02/09 S	S	16.2	E	7.2	E	5.74	4.41	1.33	65
4	07/04/09 S	M	22.2	W	21.8	W	6.31	5.06	1.25	10
	07/04/09 S	M	22.2	W	21.8	W	5.11	4.16	0.95	25
	08/04/09 S	M	43.8	W	3.0	W	5.17	4.37	0.80	171
5	15/05/09 S	M	29.0	E	7.6	E	6.59	4.98	1.61	14
	16/5/09 SU	M	20.6	E	13.0	E	6.58	5.40	1.18	85
6	16/06/09 SU	M	17.4	E	9.0	E	6.58	5.40	1.18	1
	17/06/09 SU	M	26.4	E	17.0	W	5.89	4.54	1.35	98
7	06/09/09 A	S	6.8	E	14.4	E	5.87	4.50	1.37	41
8	06/07/09 A	S	62.4	W	13.6	W	5.93	4.11	1.82	91
9	22/09/09 A	S	22.4	E-W	2.6	W	6.65	4.33	2.32	132
10	02/10/09 A	S	8.4	W	3.6	W	6.11	4.87	1.24	72

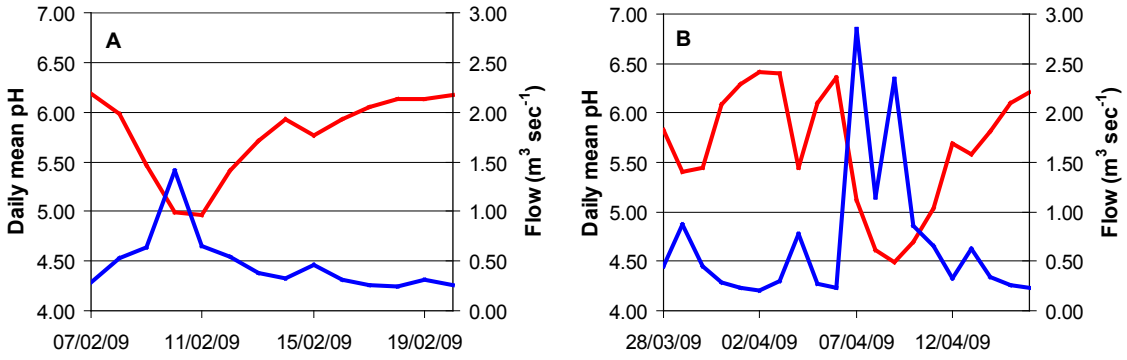

Figure 2.10 Examples of single (A) and multiple (B) pH-drop events in the Glenamong River in 2009.

2.5. Summary

River water temperatures in the Burrishoole catchment are influenced by the temperate maritime climate of the region. Previous studies have shown that salmonid fish species are negatively affected by water temperatures above 23°C and below 1°C. Maximum daily mean

RWT at six sites in the catchment exceeded 20°C on less than 1% of days. Sub-daily RWT had maxima and minima of 26.8°C and -0.7°C respectively. For the Glenamong River, a site located in the western section of the catchment and which had the highest annual mean RWT, water temperature exceeded 20°C and 25°C for only 1.66% and 0.12% respectively of all sub-daily frequency (2-minute) measurements.

Both the Altahoney and the Goulaun Rivers showed different RWT behaviour than other sites in the Burrishoole catchment. Water temperatures in the Altahoney were consistently lower than in other rivers, particularly in warm seasons, due to the location of the logger in a deep, shaded pool. Similarly, the Goulaun exhibited a more smoothed temperature record possible due to the influence of an upstream lake. Such sites are important in terms of fish growth and survival because deep pools and stream reaches with buffered RWTs have been shown to serve as cooler water refuges for fish during episodes of extreme temperatures.

There was a high degree of spatial coherence in RWT between the six sites in the Burrishoole catchment. In general coherence was high during winter months than in other seasons: mean coefficients of determination (r^2 as %) across the six sites for months between December and March autumn were >90% in both years, while values $\leq$90% occurred more frequently between April and September.

Trends in DO concentrations in the Glenamong River were assessed for the period of September 2005 – November 2006. DO concentrations showed a distinct seasonal pattern, with values above 12 mg L^{-1} between October and May and between 8 and 12 mg L^{-1} between June and September, months when temperatures and DOC levels were higher. The minimum daily mean DO value was 6.9 mg L^{-1} on 7th June 2006, while the minimum high frequency value on that date was 5.3 mg L^{-1} and was recorded at midnight. DO levels were strongly dependent on RWT throughout the year. The dependence of DO solubility on temperature alone explained between 75% and 90% of the variability between September and May. In the months between June and August 2006, DO concentrations were still highly dependent on RWT, but were also related to DOC levels. Dissolved oxygen content was not dependent on flow in any month.

Weather on the date of acid episodes and in the periods leading up to acid episodes in the Glenamong was classified by Lamb-Jenkinson weather type (LJWT). The majority of low pH events occurred on days dominated by Southerly (31%) or Westerly (34%) weather types. In contrast, the dominant LJWT type on the weekly, fortnightly, and monthly run-ups to low pH

events was Anticyclonic. This pattern was observed in 30% of weekly run-ups, in 41% of fortnightly run-ups, and 45% of monthly run-up periods. The frequency of Anticyclonic weather-type in all run-up periods was greater than expected based on the long-term LJWT record. This was in agreement with earlier studies in the west of Ireland which attributed an association between low pH episodes and antecedent anticyclonic conditions to dry deposition of pollutants from eastern Ireland and Britain. These results imply that, despite regional reductions in emissions levels, such deposition were still occurring during periods of easterly air flow.

The minimum and maximum high frequency (2-minute) pH values recorded in the Glenamong between 30/10/2008 and 20/10/ 2009 were 3.90 and 7.04 respectively. That range in pH was comparable to other upland, peaty catchments in Ireland, the UK, Sweden, and the northeast USA. Daily mean pH values ranged from 4.04 – 6.81. The daily mean pH in the Glenamong River was less than or equal to pH 5.50 for 45% of the 2008 – 2009 record. Increased mortality and other sub-lethal effects on salmonids have been observed when fish are exposed to waters with pH less than 5.50. The low pH events documented in the Glenamong River occurred both as single and multiple depressions in pH, ranging in magnitude from 0.50 to 2.30 pH units. Low pH episodes most commonly occurred on days dominated by westerly and south-westerly (precipitation-bearing) weather.

2.6. Key Findings

- The Burrishoole catchment has a temperate maritime-influenced climate where river water temperatures rarely exceed 23°C in summer and rarely fall below 1°C in winter. Daily mean RWT values within the catchment exceeded 20°C on < 1.25% of occasions. However, highest and lowest single RWTs were recorded in the Glenamong River at 26.8°C on the 7th June 2007 and in the Black River at -0.7°C on the 17th February 2008.
- There was a high degree of coherence across the catchment between RWT measured in different streams. This coherence was higher in winter with lower coherence occurring in the spring and summer.
- Dissolved oxygen (DO) concentrations in the Glenamong River over the period September 2005 – November 2006 exhibited an expected seasonal pattern, with values above 12 mg L^{-1} between October and May and between 8 and 12 mg L^{-1} between June and September when river temperatures and DOC levels were higher.
- DO levels were found to be strongly dependent on RWT throughout the year. The dependence of DO solubility on temperature alone explained between 75% and 90%

of the variability between September and May. In the months between June and August 2006, DO concentrations were still highly dependent on RWT, but were also correlated with rising DOC levels.

- The dominant weather type on the weekly, fortnightly, and monthly run-ups to low pH events was Anticyclonic (A). This result was in agreement with earlier studies in the west of Ireland which attributed an association between low pH episodes and antecedent anticyclonic conditions to dry deposition of pollutants from eastern Ireland and Britain
- No daily mean pH values of 3.0–4.0, the range lethal to all salmonid species and life-stages, were recorded in the Glenamong River during the October 2008 – October 2009 period. However, 17% of daily mean pH readings in the Glenamong River fell between pH 4.5 and pH 5.0, the range where total mortality of salmonid eggs, alevins, and fry is observed.
- A more significant 45% of daily mean pH readings were below the threshold of pH 5.5, the level of acidity below which a range of deleterious effects on salmonid fish are observed.
- Of the ten low-pH events analysed in the 2008 – 2009 record in the Glenamong River, six occurred as single drops in pH and four were composed of multiple decreases in pH over 1 to 2 day periods. All ten episodes were associated with increased precipitation in the Burrishoole catchment and increased flow in the Glenamong River.
- Recovery to pre-episode pH after the multiple-drop events was complete after 3.5 – 7 days.

2.7. References

Aherne, J. and Farrell, E.P. (eds.) (2000) '*Critical Loads and Levels. Determination and Mapping of Critical Loads for Sulphur and Nitrogen and Critical Levels for Ozone in Ireland. Final Report and Literature Review*', Johnstown Castle, Co. Wexford, Environmental Protection Agency.

Alabaster, J. S. and Gough P. J. (1986) 'The dissolved oxygen and temperature requirements of Atlantic salmon, *Salmo salar L.*, in the Thames Estuary', *Journal of Fish Biology 29,* 613–621.

Alabaster, J.S. and Lloyd, R. (eds.) (1982) '*Water Quality Criteria for Freshwater Fish*. London, Butterworths', 297pp.

Alexander, C.E. and Cresser, M.S. (1995) 'An assessment of the possible impact of expansion of native woodland cover on the chemistry of Scottish freshwaters'. *Forest Ecology and Management* 73, 1-27.

Allan, D.J. and Flecker, A.S. (1993) 'Biodiversity conservation in running waters', *BioScience* 43, 32-43.

Allott, N., Brennan, M., Cooke, D., Reynolds, J.D. and Simon, N. (1997) 'A study of the effects of stream hydrology and water quality in forested catchments on fish and invertebrates', In *AQUAFOR Report, Volume 4, Stream Chemistry, Hydrology and Biota, Galway-Mayo Region*, 157. Dublin, Ireland.

Allott, N. and Brennan, M. (2000) 'Nature and origin of acid episodes in western Ireland', *Internationale Vereinigung für Theoreische und Angewandte Limnologie* 27(4), 2471-2474.

Ahmad-Shah, A. and Rieley J.O. (1989) ,Influence of tree canopies on the quantity of water and amount of chemical elements feaching the peat surface of a basin mire in the Midlands of England', *Journal of Ecology*, 77, 357-370.

APHA. (1992) '*Standard methods for the examination of water and wastewater. 18th ed. American Public Health Association'*, Washington, DC.

Armstrong, J.D., Kemp, P.S., Kennedy, G.J.A., Ladle, M., and Milner, N.J. (2003) 'Habitat requirements of Atlantic salmon and brown trout in rivers and streams', *Fisheries Research* 62, 143-170.

Arnell, N.W. (1998) 'Climate change and water resources in Britain', *Climate Change* 39, 83-110.

Arvola, L., George, G., Livingstone, D., Jarviner, M., Dokulil, M., Jennings, E., Noges, P., Noges, T., and Weyhenmeyer, G. (2010) 'The impact of the changing climate on the thermal characteristics of lakes', In D.G. George (ed.) *The Impact of Climate Change on European Lakes*. Springer.

Atlantic Salmon Trust (1991) '*Acidification of Freshwaters: the threat and its mitigation*. Perthshire', UK, J&B Rare, 45pp.

Baker, J.P., Van Sickle, J., Carline, R.F., Baldigo, B.P., Murdoch, P.S., Bath, D.W., Kretser, W.A., Simonin, H.A., and Wigington, Jr., P.J. (1996) 'Episodic acidification of small streams in the northeastern United States: effects on fish populations', *Ecological Applications* 6(2), 422-437.

Bilby, R.E. (1984) 'Characteristics and frequency of cool-water areas in a Western Washington stream', *Journal of Freshwater Ecology* 2, 593-602.

Blackie, J.R. and Newson, M.D. (1986) 'The effects of forestry on the quantity and quality of runoff in upland Britain', In J.F.d.L.G. Solbé (ed), *Effects of land use on fresh waters: agriculture, forestry, mineral exploration, urbanisation,* Ellis Horwood Limited, UK.

Bowman, J.J. (1991) *Acid sensitive surface waters in Ireland.* Dublin, Environmental Research Unit.

Bowman, J.J. and Bracken, J.J. (1993) 'Effect of runoff from afforested and nonafforested catchments on the survival of brown trout (*Salmo trutta*) in two acid sensitive rivers in Wicklow, Ireland', *Biology and the Environment: Proceedings of the Royal Irish Academy* 93B, 143-50.

Bowman, J.J. and McGettigan, M. (1994) 'Atmospheric deposition in acid sensitive areas of Ireland – the influence of wind direction and a new coal burning electricity generation station on precipitation quality', *Water, Air, and Soil Pollution* 75(1), 159-175.

Buffam, I., Laudon, H., Seibert, J., Mörth, C-M., and Bishop, K. (2008) 'Spatial heterogeneity of the spring flood acid pulse in a boreal stream network', *Science of the Total Environment* 407, 708-722.

Byrne, C.J., Poole, W.R., Rogan, G., Dillane, M., and Whelan, K.F. (2003) 'Temporal and environmental influences on the variation in Atlantic salmon smolt migration in the Burrishoole system 1970-2000', *Journal of Fish Biology* 63, 1552-1564.

Caissie, D. (2006) 'The thermal regime of rivers: a review', *Freshwater Biology* 51, 1389-1406.

Caissie, D., El-Jabi, N., and Satish, M.G. (2001) 'Modelling of maximum daily water temperatures in a small stream using air temperatures', *Journal of Hydrology* 251, 14-28.

Campbell, R.N.B. (1987) 'Tail deformities in brown trout from acid and acidified lochs in Scotland', in Maitland, P.S., Lyle, A.A., and Campbell, R.N.B. (eds.) *Acidification and fish in Scottish lochs.* Cumbria, Institute of Terrestrial Ecology, 64-71.

Chapman, D.W. (1988) 'Critical review of variables used to define effects of fines in redds of large salmonids', *Transactions of the American Fisheries Society* 117, 1-121.

Crisp, D. T. (1981) A desk study of the relationship between temperature and hatching time for the eggs of five species of salmonid fishes. Freshwater Biology 11, 361.368. doi: 10.1111/j.1356-2427.1981.tb01267.xCrisp, D.T. (1996) 'Environmental requirements of common riverine European salmonid fish species in fresh water with particular reference to physical and chemical aspects', *Hydrobiologia* 323, 201-221.

Crisp, D.T. (2000) *Trout and Salmon: Ecology, Conservation and Rehabilitation.* Oxford, Fishing News Books.

Cummins, T. And Farrell, E.P. (2003) Biogeochemical impacts on blanket peatland streams of clearfell harvesting and reforestation I: phosphorus*', Forest Ecology and Management*, 180, 545–555.

Cunjak, R.A., Caissie D., El-Jabi, N., Hardie, P., Conlon, J.H., Pollock, T.L., Gibson, D.J., and Komadina-Douthwright, S. (1993) 'The Catamaran Brook (New Brunswick) habitat research project: biological, physical and chemical conditions (1990-1992)', *Canadian Technical Report of Fisheries and Aquatic Sciences* 1914, 1-81.

Davidson, I.C. and Hazelwood, M.S. (2005) *Effect of Climate Change on Salmon Fisheries. Science Report: W2-047/SR.*. Bristol, Environment Agency.

Davies, J.J.L., Jenkins, A., Monteith, D.T., Evans, C.D., and Cooper, D.M. (2005) 'Trends in surface water chemistry of acidified UK Freshwaters, 1988-2002', *Environmental Pollution* 137, 27-39.

Davies, T.D., Tranter, M, Wigington, Jr., P.J., Eshleman, K.N. (1992) 'Acidic episodes in surface waters in Europe', *Journal of Hydrology* 132, 25-69.

Davies, T.D., Tranter, M., Blackwood, I.L., and Abrahams, P.W. (1993) 'The character and causes of a pronounced snowmelt-induced 'acidic episode' in a stream in a Scottish subarctic catchment', *Journal of Hydrology* 146, 267-300.

Deyton, E.B., Schwartz, J.S., Robinson, R.B., Neff, K.J., Moore, S.E., and Kulp, M.A. (2009) 'Characterizing Episodic Stream Acidity During Stormflows in the Great Smoky Mountains National Park', *Water, Air, and Soil Pollution* 196, 3-18.

Eaton, J.G., and Scheller, R.M. (1996) 'Effects of climate warming on fish thermal habitat in streams of the United States', *Limnology and Oceanography* 41(5), 1109-1115.

Ebersole, J.L., Liss, W.J., and Frissell, C.A. (2001) 'Relationship between stream temperature, thermal refugia and rainbow trout *Oncorhynchus mykiss* abundance in arid-land streams in northwestern United States', *Ecology of Freshwater Fish*, 10, 1-10.

European Inland Fisheries Advisory Commission Working Part on Water Quality Criteria for European Freshwater Fish (EIFAC) (1969) 'Water quality criteria for European freshwater fish – extreme pH values and inland fisheries', *Water Research* 3, 593-611.

Elliott, J.M. (1975) 'The growth rate of brown trout (*Salmo trutta* L.) fed on maximum rations', *Journal of Animal Ecology* 44, 805-821.

Elliott, J.M. (1981) 'Some aspects of thermal stress on freshwater teleosts', in Pickering, A.D. (ed.) *Stress and Fish.* London, Academic Press.

Elliott, J.M. (1984) 'Numerical changes and population regulation in young migratory trout *Salmo trutta* in a lake district stream, 1966-83', *Journal of Animal Ecology* 53(1), 327-350.

Elliott, J.M. (1991) 'Tolerance and resistance to thermal stress in juvenile Atlantic salmon, *Salmo salar*', *Freshwater Biology* 25, 61-70.

Elliott, J.M. (1994) *Quantitative Ecology and the Brown Trout.* Oxford, Oxford University Press.

Erickson, T.R., and Stefan, H.G. (2000) 'Linear air/water temperature correlations for streams during open water periods', *Journal of Hydrologic Engineering* 5(3), 317-321.

European Environment Agency (2007) *Climate change and water adaptation issues.* Technical report No. 2/2007. Copenhagen, European Environment Agency, 9-24.

Evans, C.D. and Monteith, D.T. (2001) 'Chemical trends at lakes and streams in the UK Acid Waters Monitoring Network, 1988-2000', *Hydrology and Earth System Sciences* 5, 351-366.

Farrell, E.P., Cummins, T. and Boyle, G.M. 1997 A study of the effects of stream hydrology and water quality in forested catchments on fish and invertebrates. In *AQUAFOR Report ,Volume 1, Chemistry of Precipitation, Throughfall and Soil Water, Cork, Wicklow and Galway Regions.*, 59. Dublin, Ireland.

Farrell, E.P., Van Den Beuken, R., Boyle, G.M., Cummins, T., and Aherne, J. (1998) 'Interception of seasalt by coniferous and broadleaved woodland in a maritime environment in western Ireland', *Chemosphere* 36(4-5), 985-987.

Federer, C.A. (1985) 'The buffer capacity of forest soils in new England', *Water, Air and Soil Pollution* 26, 1573-2932.

Finn, R.N. (2007) 'The physiology and toxicology of salmonid eggs and larvae in relation to water quality criteria', *Aquatic Toxicology* 81, 337-354.

Friedland, K.D., Reddin, D.G., McMenemy, J.R., and Drinkwater, K.F. (2003) 'Multidecadal trends in North American Atlantic salmon (*Salmo salar*) stock and climate trends relevant to juvenile survival', *Canadian Journal of Fisheries and Aquatic Sciences* 60, 563-583.

Fry, F.E.J. (1971) 'The effect of environmental factors on the physiology of fish', in Hoar, W.S. and Randal, D.J. (eds.) *Fish Physiology Volume VI: Environmental Relations and Behaviour*. New York, Academic Press, 1 – 98.

Gardiner, W.R. (1984) 'Estimating population-densities of salmonids in deep-water in streams', *Journal of Fish Biology* 24(1), 41-49.

George, G., Hewitt, D., Jennings, E.J., Allott, N., McGinnity, P. (2007) 'The impact of changes in the weather on the surface temperatures of Lake Windermere (UK) and Lough Feeagh (Ireland)', in Lobo Ferreira, J. and Viera, J.M.P. (eds.) *Water in Celtic countries: Quantity, quality and climate variability*. Wallingford, Oxon., U.K., International Association of Hydrological Sciences, 86-93.

Giller, P., O'Halloran, J., Kiely, G., Evans, J., Clenaghan, C., Hernan, R., Roche, N. and Morris, P. 1997 A study of the effects of stream hydrology and water quality in forested catchments on fish and invertebrates. In *AQUAFOR Report, Volume 2, An Evaluation of the Effects of Forestry on Surface Water Quality and Ecology in Munster.*, 76. Dublin, Ireland.

Graham, C.T., Harrod, C. (2009) 'Implications of climate change for the fishes of the British Isles', *Journal of Fish Biology* 74, 1143-1205.

Grieg, S., Sear, D., and Carling, P. (2007) 'A field-based assessment of oxygen supply to incubating Atlantic salmon (*Salmo salar*) embryos', *Hydrological Processes* 21, 3087-3100.

Hammond, D. and Pryce, A.R. (2007) 'Climate change impacts and water temperature'. Environment Agency Science Report SC090017SR. 111 pp.

Hari, R.E., Livingstone, D.M., Siber, R., Burkhardt-Holm, P., and Güttinger, H. (2006) 'Consequences of climatic change for water temperature and brown trout populations in Alpine rivers and streams', *Global Change Biology* 12, 10–26.

Harley, C.D.G., Hughes, A.R., Hultgren, K.M., Miner, B.G., Sorte, C.J.B., Thornber, C.S., Rodriguez, L.F., Tomanek, L., and Williams, S.L. (2006) 'The impact of climate change in coastal marine systems', *Ecology Letters* 9, 228-241.

Harriman, R., Gillespie, E., King, D., Watt, A.W., Christie, A.E.G., Cowan, A.A. and Edwards, T. (1990) 'Short-term ionic responses as indicators of hydrological processes in the Allt a'Mharcaidh catchment, western Cairngorms, Scotland', *Journal of Hydrology* 115, 267-286.

Hayes, F.R., Wilmot, I.R., and Livingstone, D.A. (1951) 'The oxygen consumption of the salmon egg in relation to development and activity', *Journal of Experimental Zoology* 116, 377-395.

Hesthagen, T., Sevaldrud, I.H., and Berger, H.M. (1999) 'Assessment of damage to fish populations in Norwegian lakes due to acidification', *Ambio* 28, 112-117.

Hornung, M., Reynolds, B., Stevens, P.A., Hughes, S. (1990) 'Water Quality Changes from Input to Stream', in Edwards, R.W., Gee, A.S., Stoner, J.H. (eds.) *Acid Waters in Wales Monographiae Biologicae Vol. 66*. Dordrecht, Netherlands, Kluwer Academic Publishers, 223-240.

Hulme, M. and Barrow, E. (1997) *Climates of the British Isles: past, present and future*. London, Routledge, 454pp.

Jacks, G. Olofsson, E., Werme, G. (1986) 'An Acid Surge in a Well-Buffered Stream', *Ambio* 15(5), 282-285.

Jarvie, H.P., Neal, C., Smart, R., Owen, R., Fraser, D., Forbes, I., and Wade, A. (2001) 'Use of continuous water quality records for hydrograph separation and to assess short-term variability and extremes in acidity and dissolved carbon dioxide for the River Dee, Scotland', *The Science of the Total Environment* 265: 85-98.

Jenkinson, A.F. and Collison, B.P. (1977) 'An initial climatology of gales over the North Sea', *Synoptic Climatology Branch Memorandum No 62*. Bracknell, Metrological Office.

Jennings, E., Allott, N., Pierson, D., Schneiderman, E., Lenihan, D., Samuelsson, P. and Taylor, D. (2009) 'Impacts of climate change on phosphorus loading from a grassland catchment – implications for future management'. *Water Research* 43, 4316-4326.

Jennings, E., Allott, N., Arvola, L., Jarvinen, M., Moore, K., Naden, P., Nic Aongusa, C., Noges, T. and Weyhermeyer, G. (2010) 'Impacts of climate on the flux of dissolved organic carbon from catchments', In D.G. George (ed.) *The Impact of Climate Change on European Lakes.* Springer.

Johnson, R. 1998 'The forest cycle and low river flows: a review of UK and international studies', *Forest Ecology and Management* 109, 1-7.

Jones, P.D. and Kelly, P.M. (1982) 'Principal component analysis of the Lamb Classification of daily weather types: Part 1, annual frequencies', *Journal of Climatology* 2, 146-157.

Jones, P.D., Hulme, M., and Briffa, K.R. (1993) 'A comparison of Lamb Circulation Types with an objective classification derived from grid-point mean-sea-level pressure data', *International Journal of Climatology* 13, 655-663.

Kelly, P.M., Jones, P.D., Briffa, K.R. (1997) 'Classifying the winds and weather', in Hulme, M. and Barrow, E. (eds.) *Climates of the British Isles: present, past and future.* London, Routledge, London, 153-172.

Kelly-Quinn, M., Tierney, D., Coyle, S. and Bracken, J.J. (1997) 'A study of the effects of stream hydrology and water quality in forested catchments on fish and invertebrates. In *AQUAFOR Report, Volume 3, Stream Chemistry, Hydrology and Biota, Wicklow Region.*, 92. Dublin, Ireland.

King, H.R., Pankhurst, N.W., and Watts, M. (2007) 'Reproductive sensitivity to elevated water temperatures in female Atlantic salmon is heightened at certain stages of vitellogenesis', *Journal of Fish Biology* 70, 190-205.

Kitamura, S. and Ikuta, K. (2001) 'Effects of acidification on salmonid spawning behaviour', *Water, Air, and Soil Pollution* 130, 875-880.

Kondolf, G.M. (2000) 'Assessing salmonid spawning gravel quality', *Transactions of the American Fisheries Society* 129, 262-281.

Kowalik, R.A., Cooper, D.M., Evans, C.D., and Ormerod, S.J. (2007) 'Acidic episodes retard the biological recovery of upland British streams from chronic acidification', *Global Change Biology* 13, 2439-2452.

Kroglund, F., Rosseland, B.O., Teien, H.-C., Salbu, B., Kristensen, T., and Finstad, B. (2008) 'Water quality limits for Atlantic salmon (*Salmo salar* L.) exposed to short term reductions in pH and increased aluminum simulating episodes', *Hydrology and Earth System Sciences* 12, 491-507.

Lacroix, G.L. (1985) 'Survival of Eggs and Alevins of Atlantic Salmon (*Salmo salar*) in Relation to the Chemistry of Interstitial Water in Redds in Some Acidic Streams of Atlantic Canada', *Canadian Journal of Fisheries and Aquatic Sciences* 42, 292-299.

Lamb, H.H. (1972) 'British Isles weather types and a register of the daily sequence of circulation patterns', *Geophysical Memoirs (London)* 16(116), 8 pp.

Langan, S.J., Johnston, L., Donaghy, M.J., Youngson, A.F., Hay, D.W., and Soulsby, C. (2001) 'Variation in river water temperatures in an upland stream over a 30-year period', *Science of the Total Environment* 265, 195-207.

Laudon, H. and Bishop, K.H. (2002) 'The rapid and extensive recovery from episodic acidification in northern Sweden due to declines in SO_4^{2-} deposition', *Geophysical Research Letters* 29(12), doi: 10.1029/2001GL014211.

Laudon, H. (2008) 'Recovery from episodic acidification delayed by drought and high sea salt deposition', *Hydrology and Earth System Sciences* 12, 363-370.

Lawrence, G.B. (2002) 'Persistent episodic acidification of streams linked to acid rain effects on soil', *Atmospheric Environment* 36, 1589-1598.

Likens, G.E. and Buso, D.C. (2006) 'Variation in streamwater chemistry throughout the Hubbard Brook Valley', *Biogeochemistry* 78, 1-30.

Livingstone, D.M. and Dokulil, M.T. (2001) 'Eighty years of spatially coherent Austrian lake surface temperatures and their relationship to regional air temperature and the North Atlantic Oscillation', *Limnology and Oceanography* 46(5), 1220-1227.

Livingstone, D.M., Lotter, A.F., and Kettle, H. (2005) 'Altitude-dependent differences in the primary physical response of mountain lakes to climatic forcing', *Limnology and Oceanography* 50(4), 1313-1325.

Livingstone, D.M. and Hari, R.E. (2008) 'Coherence in the response of river and lake temperatures in Switzerland to short-term climatic fluctuations in summer', *Internationale Vereinigung für Theoreische und Angewandte Limnologie* 30(3), 449-454.

Louhi, P., Mäki-Petäys, A., and Erkinaro, J. (2008) 'Spawning habitat of Atlantic salmon and brown trout: general criteria and intragravel factors', *River Research and Applications* 24, 330-339.

Magnuson, J.J., and Destasio, B.T. (1997) 'Thermal niche of fishes and global warming', in Wood, C.M. and McDonald, D.G. (eds.), *Global Warming: Implications for Freshwater and Marine Fish.* Cambridge, Cambridge University Press, 377-408.

Marty, C., Beall, E., Parot, G.. (1986) 'Influence of some environmental parameters upon survival during embryonic development of atlantic salmon (*Salmo salar* L.) in an experimental stream channel'. *Int. Revue Ges. Hydrobiologia* 71, 349–361.

Matthews, K.R. and Berg, N.H. (1997) 'Rainbow trout responses to water temperature and dissolved oxygen stress in two southern California stream pools', *Journal of Fish Biology* 50, 50-67.

McCartney, A.G., Harriman, R., Watt, A.W., Moore, D.W., Taylor, E.M., Collen, P., and Keay, E.J. (2003) 'Long-term trends in pH, aluminium and dissolved organic carbon in Scottish fresh waters: implications for brown trout (*Salmo trutta*) survival', *The Science of the Total Environment* 310, 133-141.

McCormick, S.D., Hansen, L.P., Quinn, T.P., Saunders, R.L. (1998) 'Movement, migration, and smolting of Atlantic salmon (Salmo salar)', *Canadian Journal of Fisheries and Aquatic Sciences* 55, 77-92.

McGinnity, P., Jennings, E., DeEyto, E., Allot, N., Samuelsson, P., Rogan G., Whelan, K., and Cross, T. (2009) 'Impact of naturally spawning captive-bred Atlantic salmon on wild

populations: depressed recruitment and increased risk of climate-mediated extinction', *Proceedings of the Royal Society B – Biological Sciences* 276(1673), 3601-3610.

Milner, N.J. and Varallo, P.J. (1990) 'The effects of acid water on fish and fisheries in Wales', in Edwards, R.W., Stoner, J.H., and Gee, A.S. (eds.) *Acid Waters in Wales*. Dordrecht, Netherlands, Kluwer Academic.

Moiseenko T., Kudrjavzeva, L., and Rodyshkin, I. (2001) 'The Episodic Acidification of Small Streams in the Spring Flood Period of Industrial Polar Region, Russia', *Chemosphere* 42(362), 45-50.

Mohseni, O. and Stefan, H.G. (1999) 'Stream temperature/air temperature relationship: a physical interpretation', *Journal of Hydrology* 218, 128-141.

Mohseni, O., Stefan, H.G., and Eaton, J.G. (2003) 'Global warming and potential changes in fish habitat in U.S. streams', *Climatic Change* 59, 389-409.

Monette, M.Y. and McCormick, S.D. (2008) 'Impacts of short-term acid and aluminium exposure on Atlantic salmon (*Salmo salar*) physiology: A direct comparison of parr and smolts', *Aquatic Toxicology* 86, 216-226.

Monteith, D.T. and Evans, C.D. (2005) 'The United Kingdom Acid Waters Monitoring Network: a review of the first 15 years and introduction to the special issue', *Environmental Pollution* 137, 3-13.

Monteith, D.T., Hildrew, A.G., Flower, R.J., Raven, P.J., Beaumont, W.R.B., Collen, P., Kreiser, A.M., Shilland, E.M., and Winterbottom, J.H. (2005) 'Biological responses to the chemical recovery of acidified fresh waters in the UK', *Environmental Pollution* 137: 83-101.

Morrison, J., Quick, M.C., and Foreman, M.G.G. (2002) 'Climate change in the Fraser River watershed: flow and temperature projections', *Journal of Hydrology* 263, 230-244.

Naden, P., Allott, N., Arvola, L., Jarvinen, M., Jennings, E., Moore, K., Nic Aongusa, C., Pierson, D. and Schneidermen, E. (2010) Modelling the effects of climate change on dissolved organic carbon. In D.G. George (ed.) The Impact of Climate Change on European Lakes. Springer.

Neal, C., Reynolds, B., Smith, C.J., Hill, S., Neal, M., Conway, T., Ryland, G.P., Jeffrey, H., Robson, A.J., and Fisher, R. (1992) 'The impact of conifer harvesting on stream water pH, alkalinity and aluminium concentrations for the British uplands: an example for an acidic and acid sensitive catchment in mid-Wales', *The Science of the Total Environment* 126, 75-87.

Nilsson, J. and Grennfelt, P. (1988) Report from a Nordic Working Group. Nordic Council of Ministers, Milj0rapport 1986:11. 2. Nilsson, J. and Grennfelt, P. (eds). 1988. Critical-loads for sulfur and nitrogen. Report from a workshop held at Skokloster, Sweden 19-24 March 1988.

Ormerod, S.J. and Durance, I. (2009) 'Restoration and recovery from acidification in upland Welsh streams over 25 years', *Journal of Applied Ecology* 46, 164-174.

Ovington, J.D. (1957) 'Dry matter production by *Pinus sylvestris* L', *Annals Botany* 21, 287-314.

Parry, M.L., Canziani, O.F., Palutikof, J.P., Co-authors. (2007) 'Technical Summary. Climate Change 2007: Impacts, Adaptation and Vulnerability', in Parry, M.L., Canziani, O.F., Palutikof, J.P., van der Linden, P.J., and Hanson, C.E. (eds.) *Contribution of Working Group II to the Fourth Assessment Report of the Intergovernmental Panel on Climate Change*. Cambridge, Cambridge University Press, 23-78.

Peterson, R.H., and Martin-Robichaud, D.J. (1989) 'First feeding of Atlantic salmon (*Salmo salar L.*) fry as influenced by temperature regime', *Aquaculture* 78(1), 35-53.

Peterson, R.H., Daye, P.G., and Metcalfe, J.L. (1980) 'Inhibition of Atlantic salmon (Salmo salar) hatching at low pH', *Canadian Journal of Fisheries and Aquatic Sciences* 37, 770-774.

Peyronnet, A., Friedland, K.D., Maoileidigh, N.Ó., Manning, M., and Poole, W.R. (2007) 'Links between patterns of marine growth and survival of Atlantic salmon *Salmo salar*, L.', *Journal of Fish Biology* 71, 684-700.

Planque, B., Frédou, T. (1999) 'Temperature and the recruitment of Atlantic cod (*Gadus morhua*)', *Canadian Journal of Fisheries and Aquatic Sciences* 56, 2069-2077.

Poléo, A.B.S. (1995) 'Aluminium polymerization – a mechanism of acute toxicity of aqueous aluminium to fish', *Aquatic Toxicology* 31, 347-356.

Pörtner, H.O. (2001) 'Climate change and temperature-dependant biogeography: oxygen limitation of thermal tolerance in animals. *Naturwissenschaften* 88, 137-146.

Rask, M., Mannio, J., Forsius, M., Posch, M., and Vuorinen, P.J. (1995) 'How many fish populations in Finland are affected by acid precipitation?', *Environmental Biology of Fishes* 42, 51-63.

Rosseland, B.O. and Stuarnes, M. (1994) 'Physiological mechanisms for toxic effects and resistance to acidic water: an ecophysiological and ecotoxicological approach', in Steinberg, C.E.W. and Wright, R.F. (eds.) *Acidification of Freshwater Ecosystems: Implications for the Future*. New York, Wiley, 227-246.

Skjelkvåle, B.L., Stoddard, J.K., and Andersen, T. (2001) Trends in surface water acidification in Europe and North America 1989–1998, *Water Soil and Air Pollution* 130, 787-792.

S.I. No. 293/1988 (1988) *European Communities (Quality of Salmonid Waters) Regulations, 1988.* Stationary Office, Dublin,

Sinokrot, B.A., Stefan, H.G., McCormick, J.H., and Eaton, J.G. (1995) 'Modeling of climate change effects on stream temperatures and fish habitats below dams and near groundwater inputs', *Climatic Change* 30, 181-200.

Solomon, D. J. and Sambrook H. T. (2004) Effects of hot dry summers on the loss of Atlantic salmon, Salmo salar, from estuaries in South West England. *Fisheries Management and Ecology* 11, 353–363.

Sowden, P. and Parker, E. (1981) 'A study of climatic variability of daily central england temperatures in relation to the lamb synoptic types', *International Journal of Climatology* 1, 3-10.

Stefansson, S.O., McGinnity, P., Björnsson, B.T., Schreck, C.B., and McCormick, S.D. (2003) 'The importance of smolt development to salmon conservation, culture and management: perspectives from the 6th International Workshop on Salmonid Smoltification', *Aquaculture* 222, 1-14.

Sweeney, J.C. (1985) 'The changing synoptic origins of Irish precipitation', *Transactions of the Institute of British Geographers* 10(4), 467-480.

Sweeney, J.C., O'Hare, G.P. (1992) 'Geographical variations in precipitation yields and circulation types in Britain and Ireland', *Transactions of the Institute of British Geographers*. 17, 448-463.

Teien, H.C., Salbu, B., Kroglund, F., Rosseland, B.O. (2004) 'Transformation of positively charged aluminium-species in unstable mixing zones following liming', *Science of the Total Environment* 330, 217-232.

U.S. EPA (1996) *Ambient Water Quality Criteria for Dissolved Oxygen (EPA 440/5-86-003).* Washington, D.C., Environmental Protection Agency.

Vuorenmaa, J. and Forsius, M. (2008) 'Recovery of acidified Finnish lakes: trends, patterns and dependence of catchment characteristics', *Hydrology and Earth System Sciences* 12, 465-478.

Wetzel RG (2001) '*Limnology: Lake and River Ecosystems 3rd Edition',* Academic Press San Diego CA USA.

White, W. (2000) '*A review of the effectiveness and feasibility of alternate liming techniques to mitigate for acid rain effects in Nova Scotia, 25*.' Ottawa: Canadian Stock Assessment Secretariat.

Whitehead, P.G., Wilby, R.L., Battarbee, R.W., Kernan, M., and Wade, A.J. (2009) 'A review of the potential impacts of climate change on surface water quality', *Hydrological Sciences* 54(1), 101-123.

Wigington, Jr., P.J., Davies, T.D., Tranter, M., and Eshleman, K.N. (1992) 'Comparison of epiodic acidification in Canada, Europe, and the United States', *Environmental Pollution* 78, 29-35.

Wigington, P.J. Baker, J.P., DeWalle, D.R., Kretser, W.A., Murdoch, P.S., Simonin, H.A., Van Sickle, J., McDowell, M.K., Peck, D.V., and Barchet, W.R. (1996) 'Episodic acidification of

small streams in the northeastern United States: ionic controls of episodes', *Ecological Applications* 6, 389-407.

Wigley, T.M.L. and Jones, P.D. (1987) 'England and Wales precipitation: A discussion of recent changes in variability and an update to 1985', *Journal of Climatology* 7, 231-246.

Wilby, R. L., Dalgleish, H.Y. and Foster I.D.L. (1997) 'The impact of weather patterns on historic and contemporary catchment sediment yields', *Earth Surface Processes and Landforms* 22(4), 353-363.

Winder, M. and Schindler, D.E. (2004) 'Climate Change Uncouples Trophic Interactions in an Aquatic Ecosystem', *Ecology* 85(8), 2100-2106.

Wissel, B., Boeing, W.J. and Ramcharan, C.W. (2003) Effects of water color on predation regimes and zooplankton assemblages in freshwater lakes. *Limnology and Oceanography* 48, 1965-1976.

Witzel, L.D. and MacCrimmon, H.R. (1983) 'Redd-site selection by brook trout and brown trout in Southwestern Ontario streams', *Transactions of the American Fisheries Society* 112, 760-771.

Young, E.F., Bigg, G.R., Grant, A. (1996) 'A statistical study of environmental influences on bivalve recruitment in the Wash, England', *Marine Ecology Progress Series* 143, 121-129.

Youngson, A.F., Malcolm, I.A., Thorley, J.L., Bacon, P.J., Soulsby, C. (2004) 'Long-residence groundwater effects on incubating salmonid eggs: low hyporheic oxygen impairs embryo development and causes mortality', *Canadian Journal of Fisheries and Aquatic Sciences* 61, 2278-2287.

Zydlewski, G.B., Haro, A., and McCormick, S.D. (2005) 'Evidence for cumulative temperature as an initiating and terminating factor in downstream migratory behavior of Atlantic salmon (*Salmo salar*) smolts', *Canadian Journal of Fisheries and Aquatic Sciences* 62, 68-78.

3. Observed Trends in Diadromous Fish in The Burrishoole

Ciar O'Toole, Russell Poole, Mary Dillane, Ger Rogan, Elvira de Eyto, Lee Hancox and Jonathan White

3.1. Introduction

Changing climate is expected to affect fishery resources: it will present a challenge to managers to develop sustainable exploitation and management strategies (Rijnsdorp et al., 2010). With the accumulating evidence for changing climate linked to increasing concentrations of GHGs (IPCC, 2007), there is a general concern about the impact on productivity and distribution of many commercially exploited marine stocks and also the effect on the sustainability of fisheries (E.g., Rijnsdorp et al., 2010; Graham and Harrod, 2009). Fish have complicated life cycles, and each life-history stage (eggs, larvae, juveniles and adults) may have varying habitat and dietary requirements (Rijnsdorp et al., 2010). Diadromous species complicate this picture further by migrating between the sea and freshwater in order to complete their life cycle, requiring transformations in physiology often in conjunction with the maturation process. The assessment of possible impacts is further complicated by the fact that diadromous species may migrate through several climatic regions. As a result, for a full understanding of the possible effects of climate change on these species, it is important to adopt an integrated approach that includes the full life cycle and the various habitats and environments.

Worldwide, there are estimated to be roughly 250 species of diadromous fish (Nolan et al., 2009). Diadromous fish in Ireland are composed of a limited number of species because of factors such as recent glaciations and the island's northerly location. They include Atlantic salmon (*Salmo salar*), sea trout (*S. trutta*), eel (*Anguilla anguilla*), twaite and allis shad (*Alosa fallax* and *Alosa alosa*), smelt (*Osmerus eperlanus*), sea and river lamprey (*Petromyzon marinus* and *Lampetra fluviatilis*), along with flounder (*Platichtys flesus*), stickleback (*Gasterosteus aculeatus*) and some mullet species (*Family Mugilidae*). These species can be further divided into anadromous species that spend most of their lives in the sea and migrate to freshwater to breed (e.g. Atlantic salmon, sea trout and shad) and catadromous species that conversely migrate from freshwaters to the sea to breed (e.g. European eel and flounder).

Given their high sensitivity to environmental conditions and the large distances that some of these fish can cover during their migration, diadromous species are particularly vulnerable to

changes associated with climate, both in freshwater and in the marine environment (Lassalle et al., 2008). The key eco-physiological processes of the various life stages of diadromous fish in freshwater – such as hatching and survival in anadromous fish and smoltification and migration in salmonids – are controlled by a range of environmental variables, including temperature, sunlight, day length and rainfall. Other variables, such as water colour, oxygen levels, pH and water flow may also impact on these key processes by, for example, reducing light penetration or increasing drought- or flood-induced mortality.

Projected changes in rainfall and temperature associated with climate change are likely to have significant impacts on the ecology of fresh and transitional waters in Ireland. Ocean climate changes are already known to have an impact on salmon at sea, largely through the close interaction between growth and survival (Peyronnet et al., 2007). Diminishing eel populations may also be the result of changes in the ocean in conjunction with human-induced pressures (ICES, 2009). It is also expected that climate change will drive the distribution of many diadromous fish species northwards as various species respond largely to temperature and precipitation-related variables (Lassalle and Rochard, 2009). While such responses are likely to be species and catchment specific, it is largely unknown whether the observed or projected distributional shifts are caused by the relocation of spawning and feeding grounds, a change in the local survival of fish or immigration into new habitats. These species are, however, subject to a range of other pressures in addition to climatic drivers. Many of these pressures, such as exploitation, eutrophication, habitat change, fluctuating population densities and genetics (e.g. caused by stocking non-native or cultured fish) have been changing over the last number of decades in parallel with the observed changes in climate. Untangling these various drivers is part of the challenge of assessing the impacts of climate to date and of making projections for the future impact of changing climate.

3.2. Fish Census

3.2.1 Atlantic Salmon

The Burrishoole system has a run of both grilse or 1 sea-winter (1SW) and 2 sea-winter (2SW) or spring salmon. There is only a small multi-sea winter component in the Burrishoole stock, normally <10% of the total run. It has not exceeded 100 fish since the early 1960s. The numbers of Atlantic salmon recorded in the upstream traps since full trapping commenced in the 1970s have fluctuated from a high of 1,777 in 1973 to a low of 252 in 1990 (Figure 3.1). Annual escapement to freshwater is known to have been influenced by both the level of exploitation in the coastal drift net fishery and fluctuation marine survival to the coast. Following the cessation of this fishery in 2007, a marked increase in the numbers of fish

returning to the catchment was recorded in that year. However, this increase occurred only in 2007, with numbers in 2008 and 2009 falling to levels similar to those recorded prior to the cessation of drift netting. This fall in numbers would indicate a probable decrease in marine survival in line with the reported downward trend in pre-fishery abundance for the Irish stock (Peyronnet et al., 2007).

The numbers of juvenile smolts recorded in the downstream traps migrating to sea have varied from a maximum of 16,136 in 1976 to a minimum of 3,794 in 1991. It is difficult to determine an overall trend during the time-series because factors – such as ranched fish components released into the spawning stock or habitat availability and quality – have varied during the period.

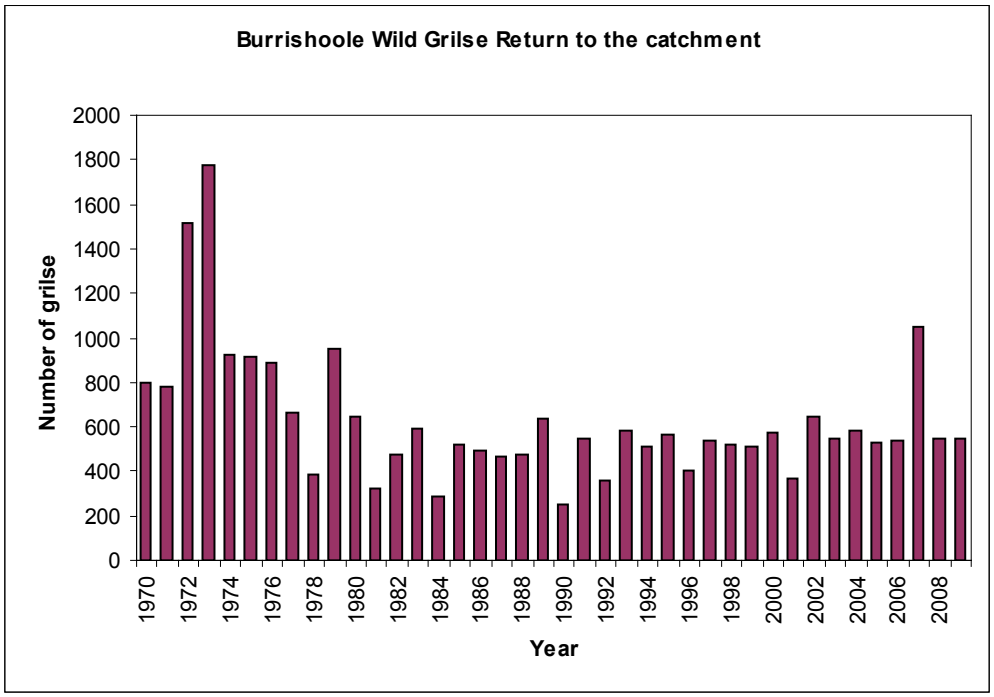

Figure 3.1: Number of returns of wild adult salmon to Burrishoole catchment (trap and fishery), 1970–2009.

3.2.2 Sea Trout

Burrishoole sea trout smolts run to sea primarily as two and three year olds, from March to June each year. Some of these fish return to fresh water in the summer following migration; in Ireland these are known as 'finnock'. A further component may not return to the natal river for at least one year and these are known as 'maidens'. Sea trout migrate back to sea after the winter, both as spawned kelts and immature fish which have over-wintered without spawning. Sea trout are often multiple spawners and there is a variation, between catchments, in smolt age and the time of first return to fresh water.

Silver smolts migrate to sea between February and June. The smolt run comprises of approximately 70% two year old smolts and 30% three year old smolts; one and four year olds are quite rare. A number of changes in the structure of the Burrishoole smolt run have been observed. From 1989 to the present, the numbers of smolts migrating dropped to below the previously recorded minimum (Table 3.1). While the average output was previously over 4000 smolts the numbers fell to an all-time low of 400 individuals in 2008. The springs of 1989 and 1990 were particularly warm and drought conditions prevailed for much of the smolt run period. It was shown that in years subsequent to a drought, the delayed smolts from the previous year tended to contribute to the older age classes. This did not occur in 1991, indicating that the drop in smolt numbers was most probably due to a reduction in spawning escapement into the system since 1987.

Table 3.1: Annual sea trout smolt numbers in Burrishoole for 1970 to 2009.

	1970-79	1980-84	1985-89	1990-94	1995-99	2000-04	2005	2006	2007	2008	2009
Number	4176	4038	4119	1531	1361	816	777	626	593	393	657

The run of adult sea trout and finnock moving upstream through the traps has ranged from 1400 to 3400 fish. These numbers, however, slumped to minimum counts of 38 in 2006 and 15 in 2005, the lowest spawning escapements ever recorded for the system. In 1987 and 1988, there was a distinct drop in the number of fish counted upstream through the traps, both finnock and adults. The catch per unit effort (CPUE) in the rod fishery and marine survival also declined significantly. The CPUE fell to an unprecedented level in 1989 and 1990 and has failed to recover to any degree in the following years. While the adult sea trout stock in Burrishoole has been declining since the mid-1970s, there was an unprecedented change from 1987, culminating in 1989 and 1990 with a complete stock collapse and a subsequent reduction in migratory juvenile recruitment.

In the Burrishoole catchment, there has been a considerable annual variation in the numbers of returning finnock (0+ sea-age adult sea trout), with returns historically varying between 11.4% and 32.4% of the smolt output, indicating that marine survival is probably affected by a number of factors (Figure 3.2a; Poole et al., 2007). The stocks of returning sea trout collapsed during the period 1989–1990, with a sudden strong reduction in marine survival to a finnock return of only 1.5% in 1989 (Poole et al., 2007). A regime shift in marine survival of 0+ sea-age trout (finnock), which began in 1987 has been detected in the Burrishoole data using Rodionov's (2005) sequential regime shift detection (Figure 3.2b). This corresponded with several factors

being negatively related to marine survival of the trout: the development of salmon farming in Clew Bay; warm winter and spring temperatures; and higher rates of sea lice on wild sea trout in Clew Bay (Tully, 1992; Gargan et al., 2003). Sea trout and salmon go through a physiologically stressful transition from freshwater to sea water and this, in conjunction with a new lice burden, can cause additional stress to the fish (Poole et al., 2000). In addition to the pressures caused by salmon farming, 1987/1988 was the year in which a significant step change was noted in air and water temperatures in Europe (e.g. Fealy and Sweeney, 2005; Hari et al., 2006) and in Ireland (Donnelly et al., 2009). This step-change was associated both with an increase in disease in trout in Switzerland (Hari et al., 2006) and increased sea lice production in western Ireland in 1987 to 1989 (Tully 1992), highlighting the problems of untangling impacts where multiple drivers are involved.

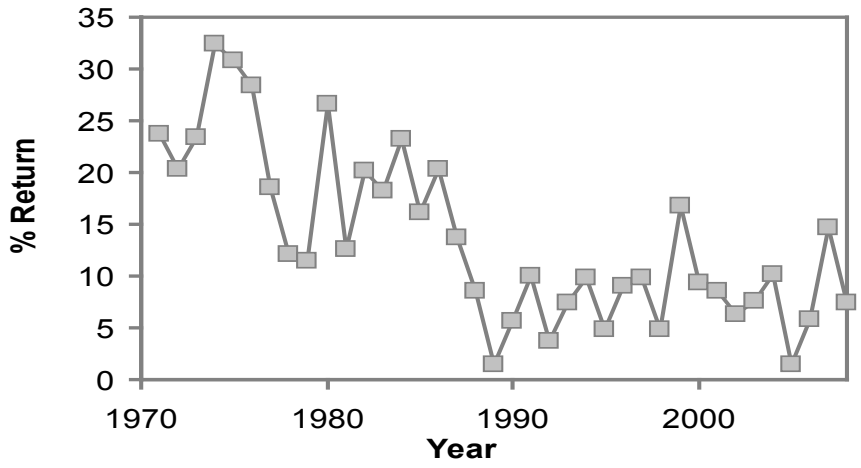

Figure 3.2: (a) Annual percentage return of sea trout smolts returning as finnock (0+ sea age) to the Burrishoole traps (updated from Poole et al., 2007.

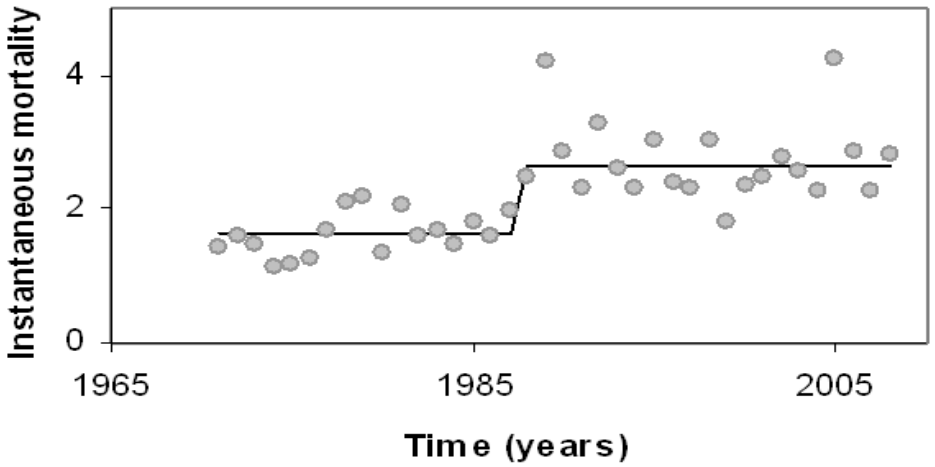

Figure 3.2: (b) Instantaneous mortality rates for finnock (circles) showing regime shift (weighted mean of regimes [black line]) before and after the 1987 step change.

3.2.3 European Eel

The silver eel migrations in Burrishoole have been studied since 1958 (Piggins, 1985; Poole et al., 1990) using the downstream fish trapping facilities. With the installation of total downstream trapping in 1970, monitoring of the complete silver eel (downstream migrating mature adults) run became possible in the Burrishoole catchment (Figure 3.3). This is the only dataset on silver eel production from a commercially unexploited system and is also the longest existing silver eel dataset in Europe (Poole et al., 1990). The migration of maturing silver eel in Burrishoole has undergone some changes over the past thirty years. Since trapping commenced in 1958 the numbers of migrants have been steadily declining and this has been most evident in the Mill Race, which is less affected by flood conditions, than in the Salmon Leap. Along with this decrease in numbers, the overall age and mean size of the eels has been increasing since the mid-1970's and the proportion of males has changed from 94% to 37.5% in 1988 and 30% average in 2008/2009 (Poole, unpublished). This increase in size and change in sex ratio may be a density dependent response to reduced recruitment and/or increased productivity in the catchment (Poole et al., 1990).

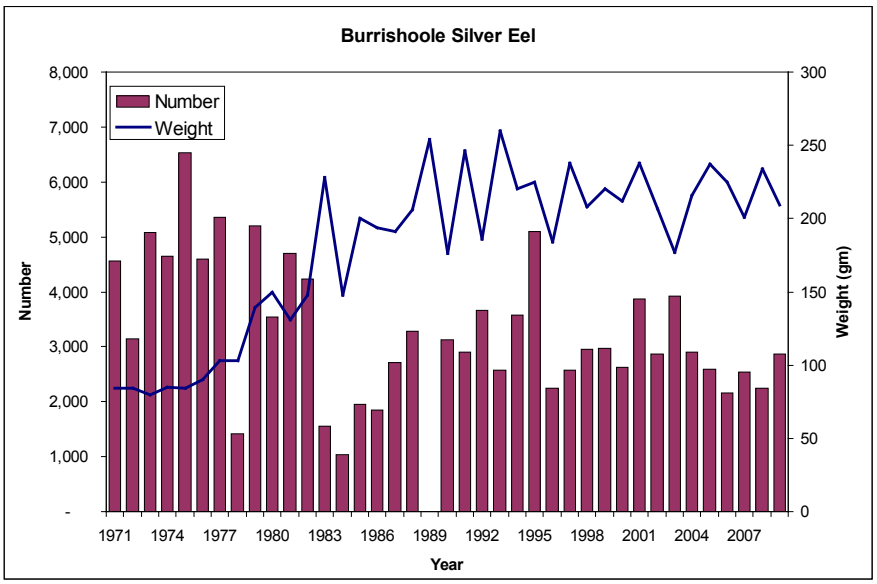

Figure 3.3: Number and average weight of migrating silver eels from Burrishoole, 1971–2009.

The silver eel migration in Burrishoole takes place mostly in September and October. The runs were usually insignificant until the first new moon in September. However, there are indications that migrations are now beginning earlier with numbers of eels moving downstream from mid-July onwards. The pattern of maximum migration in October has also been observed on the Shannon, the Corrib and the Imsa River in Norway, in contrast to that observed in North Spain where silver eels are found from September to March.

The Burrishoole eels mature at a smaller size and an older age than most of the studied European eel populations, most similar to those of L. Neagh and R. Bann, but the ages in Burrishoole are considerably older. In fact female eels as old as 57 years were recorded in the silver eel migration in 1987 and 1988.

There are no local data for the recruitment of glass eel into the Burrishoole. Anecdotal information indicates that recruitment into the catchment has fallen drastically since the early 1980s in line with other areas in Ireland and around Europe (ICES, 2009), where glass eel recruitment series demonstrated a clear decline since the early 1980s. For the different areas (Baltic, North Sea, Atlantic, Mediterranean, Britain and Ireland), levels have dropped to between 1 and 9% of 1970s' levels (ICES, 2009). Such a large-scale decrease over the large number of recruitment indices across Europe suggests that a broader meteorological or climatic change might be a contributory factor, probably in conjunction with human induced mortalities such as fisheries and hydropower turbine mortality. Such changes could also affect both the larval survival in the ocean and adult growth in the continental phase by altering the conditions needed by the species to grow and migrate.

3.3. Trends in Salmonid Smolt Run Timing in Burrishoole

3.3.1 Introduction

Migration, particularly in freshwater fish has often been regarded as an adaptive strategy to increase growth and survival which may contribute to increased abundance (Northcote, 1978). In Irish waters, salmon are obligate migrators; if they smoltify and are not able to migrate they die. There is thought to be a very short window for migration which is dependent on environmental factors such as water temperature and water level (Byrne et al., 2003). Trout are not believed to be obligate migrators. Trout (*Salmo trutta*) populations can be made up of anadromous and resident cohorts and it is accepted that, if a two year old sea trout smolt does not get to migrate downstream to the sea, it can revert and migrate in the following year as a three year old.

The term smoltification describes two different phenomena: transformation and migration. Light and temperature are both involved in the process of smoltification, it is the increase in day-length in the spring (photoperiod) acting as the synchronizer of an endogenous rhythm, which is the environmental factor most influencing the onset of par to smolt transformation (Byrne et al, 2004, Jonsson and Jonsson, 2009). Temperature can affect both the transformation and the migration. A number of studies have shown that salmonids do not commence migration until a threshold temperature has been reached (Fried *et a.l*, 1978,

Solomon, 1981), but it has been shown that temperatures above a certain threshold tend to cause a premature decrease in euryhalinity, or a detransformation in salmonids (Zaugg, 1982). There is a lack of published information in this regard relating to sea trout.

Rainfall tends to have an indirect impact on the migration process through changes in water levels; low water levels tend to inhibit or at least deter smolt migration, simply by impeding the successful passage of smolts to the sea. The effect of the spring drought of 1980 on the descent of smolts in the Burrishoole fishery is a case in point (Cross and Piggins, 1982). They suggest that due to the delayed migration of both salmon and sea trout smolts in Burrishoole caused by the drought of 1980, smolts had either passed their optimum level of adaptation for migration to seawater, or suffered physical damage in the overcrowded traps after the drought, resulting in depleted smolt runs and poor marine survival in that year.

It is thought that changes brought about by climate change may impact on the run timing of salmonid species in the Burrishoole catchment. Factors such as warmer water temperatures and more frequent droughts or floods are likely to affect the run timing of these species.

Previous work carried out in the Burrishoole catchment (STAG, 1990) looked at cumulative sea trout smolt migrations in the Burrishoole system from 1975 to 1990 and these were compared with the corresponding freshwater temperatures and rainfall levels. Sea temperatures for the past fifteen years were also plotted and their patterns noted

The STAG report (1990) found that sea trout smolt migration did not commence until freshwater temperature reached a threshold level of 9°C. Rainfall levels affected the timing of the downstream migration indirectly, through its impact on water levels. Recruitment was adversely affected by the occurrence of temperatures of 13°C or higher before sea trout smolt migration had taken place. No evidence was found to suggest that warm springs resulted in higher recruitment of sea trout smolts in the Burrishoole catchment.

3.3.2 Methods

To carry out the run timing analysis, the annual total salmon and sea trout smolt count was divided into the 5th, 50th and 95th percentiles. These divisions were picked arbitrarily to define the duration of the main period of the run and the mid-point of the smolt run. The mean duration in days and range of dates (i.e. number of days from the first of January), and the mean and range of temperatures when the 5th, 50th and 95th %tiles of the smolts were caught were calculated for each decade, and for the entire data set.

3.3.3 Results

Analysis of the results for salmon smolt run timing data shows a general tendency towards the run starting earlier. 1980 was an exception due to the severe drought experienced in the Burrishoole catchment that winter/spring. However, the trend is significant with and without the data from 1980 (Table 3.2), with the salmon run starting on average 11 days earlier in recent years when compared to data from the 1970's and 1980's (Figure 3.4). Although the changes in the timing of 50% and 95% were not significant, they have both become six and two days earlier, respectively, over the same period. A severe drought in the Burrishoole catchment in 1980 caused an exceptional delay in smolt migration. If the data from 1980 are included, a significant trend in the data ($p<0.004$) can be seen, with the salmon run starting on average 11 days (9 days excluding 1980) earlier in recent years when compared to data from the 1970s and 1980s (Figure 3.4). Although the date when 50% and 95% of salmon smolts had migrated did not show a significant trend, they were 6 and 2 days earlier, respectively, in recent years.

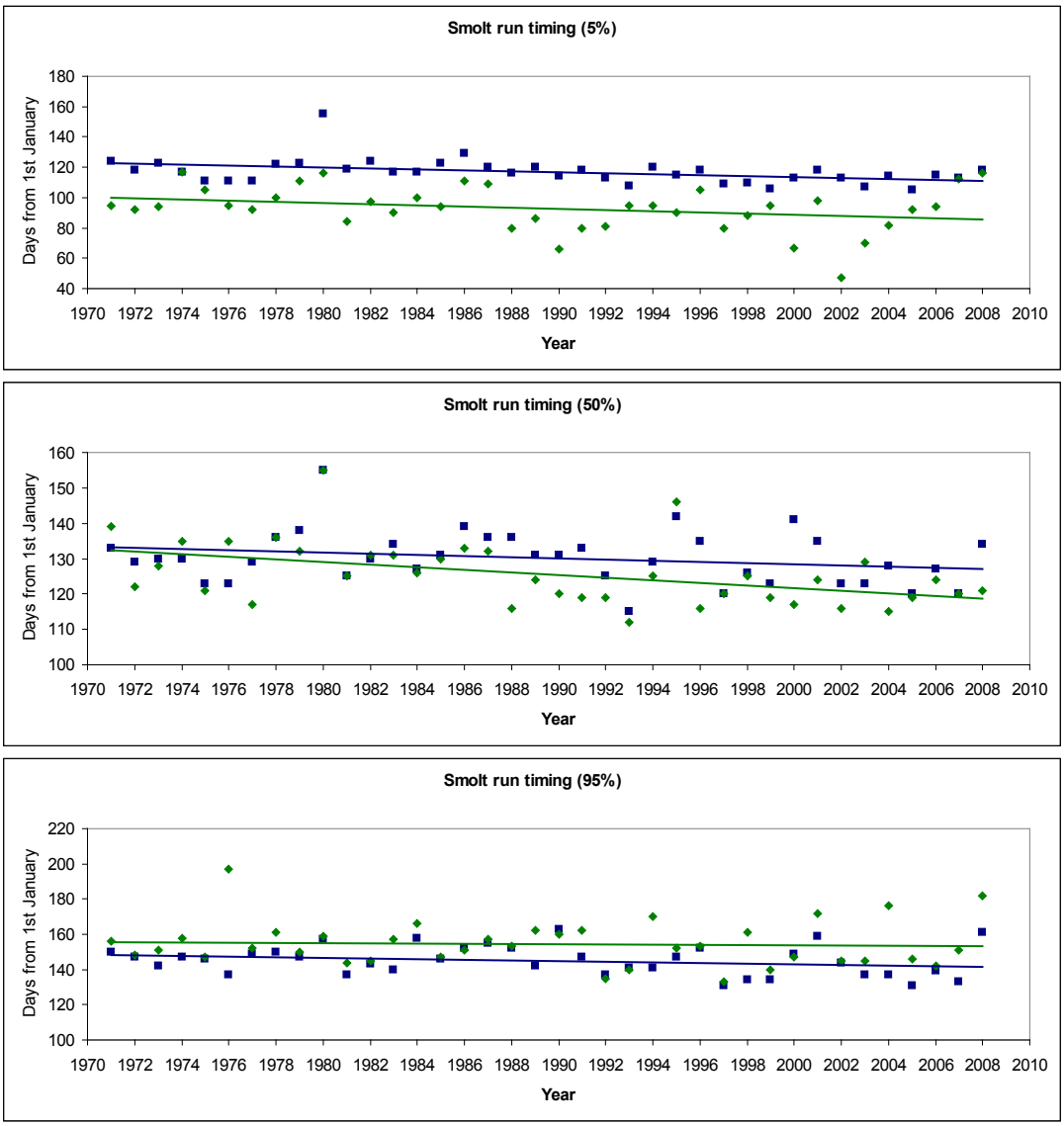

Figure 3.4: Number of days from 1 January each year for 5% (top), 50% (middle) and 95% (bottom) for the salmon (blue) and sea trout (green) smolt runs to be achieved in the Burrishoole catchment, Co. Mayo, 1971–2008.

For the sea trout smolt migration, the midpoint of the run was significantly earlier with the 50% point occurring 14 days earlier in recent years ($p<0.004$) (Table 3.2). The 5% point of the run also appears to be occurring approximately 14 days earlier, but this change was not significant ($p = 0.08$) due to the large amount of variance in the data. The 95% point of the sea trout smolt run is now 7 days earlier than it was in the 1970s.

Table 3.2: Results from regression analysis of timing of 5%, 50% and 95% of salmon and sea trout smolt runs in the Burrishoole catchment, Co. Mayo.

Salmon run	R^2	F	p
5%			
including 1980	16.80%	7.67	*0.004*
excluding 1980	21.60%	9.64	*0.01*
50%			
including 1980	5.60%	2.13	0.15
excluding 1980	3.60%	1.32	0.258
95%			
including 1980	5.60%	2.15	0.15
excluding 1980	4.50%	1.65	0.207
Sea Trout run	**R^2**	**F**	**p**
5%	8%	3.14	0.0847
50%	20.80%	9.44	*0.004*
95%	0.03%	1.02	7.5

3.3.4 Discussion on Smolt Timing

The general trend for both species is for a longer smolt run that starts earlier. However, the large amount of variability from year to year in the data means this is not an overall significant result, with only the start of the salmon smolt run and the mid-point of the sea trout smolt run being statistically significant. The earlier start time of the run is likely to be linked to warmer water temperatures during the preceding winter, although some years also see a delay in the later part of the smolt run because of droughts. Jonsson and Jonsson (2009) also observed that smolt migrations started earlier and took place over shorter time periods in mild years. There is, however, an interaction between the earlier timing due to rising temperature and the delay due to drought. The outlying point for 1980, and evidence from a similar event in 2010 when the salmon smolts migrated in a 4-day period in June, could be an indicator of what may happen if such droughts become more frequent in the future, as suggested in the Rescale report (Fealy et al., 2010; Chapter 4). Repeated higher frequency of droughts could have significant impacts on the survival of subsequent generations of salmon.

Anadromous salmonids smolt and migrate to sea primarily during spring. Byrne et al. (2004) divided factors controlling the smolt run into regulating and controlling factors. Regulating factors operate before (affecting the physiological smolting process) and controlling factors operate during the smolt run (such as those controlling speed of downstream migration).

The primary regulating factors of the smolt run are photoperiod and temperature. Day length is a timer, and increasing and decreasing photoperiods are major predictive, proximate factors which indicate the season (Wootton, 1998). Temperature affects the rate of development, and

low water temperature can limit the response of salmon parr to increased day length (McCormick et al., 2002). Also, since day length is similar on the same date each year in the same place, photoperiod does not cause variation in annual smolting times (Jonsson and Jonsson, 2009).

Other factors such as water temperature are responsible for annual variation. To smolt successfully, fish require a certain amount of heat, which can be measured in degree days (number of 'degree days' or mean temperature above a threshold (°C) for a particular day). A study by Zydlewski et al. (2005) showed that the temperature experienced over time determines the behavioural and physiological changes associated with the smolting process as well as the onset and ending of the smolt run in salmon. Smolt migrations start earlier and take place over shorter time periods in mild compared to cold years (Jonsson and Jonsson, 2009).

The main controlling factors of smolt migrations are water temperature, water flow and changes to both these factors. Some studies indicate a pervasive effect of temperature and temperature increases for the initiation of a seaward migration in salmonids (Jonsson and Rudd-Hansen, 1985, Jutila et al., 2005). Smolt migration seems not to be triggered by either a specific water temperature or a specific number of degree days but is controlled by a combination of the actual temperature and temperature increase in the water during spring (Byrne et al., 2004). In some rivers, however, the smolt migration may be triggered by water flow. A study by Carlsen et al. (2004) in the River Hals, Norway showed increasing migration of salmon smolts with increasing water flow, while sea trout smolts correlated only with temperature. The increase in salmon migrants correlated positively with the increase in water level the following day, suggesting that fish movements represent an early response to a subsequent spate. This suggests that the fishes may also sense clues other than the water flow (Jonsson and Jonsson, 2009).

In many catchments, the actual timing of the smolt run may be a complex relationship between timing of changes in water level, temperature and the ability of smolts to leave. For example, a drought in March which delays migration may have a very different impact to one in April or May, depending on temperature.

3.4. Salmonid Egg Development Times

3.4.1 Introduction

The accuracy with which salmonids return to their natal stream for spawning make it reasonable to assume that salmon and trout populations show specific adaptations regarding

spawning time that probably rely heavily on water temperature (Henderson, 1963, Jonsson and Jonsson, 2009). Up to a certain temperature, instream biological rates (such as gonadal development) should follow Van Hoff's rule that states that biological activity doubles for every 10°C increase in water temperature (Caissie, 2006).

Both wild and farmed salmon have shown evidence for strong heritability for spawning time (Lura and Saegrov, 1993). The reason for temperature dependence of spawning time is likely to be that temperature influences the duration of embryonic development (Elliott and Hurley, 1998a) and therefore hatching time (Crisp, 1981). Larval survival and development depend on the availability of appropriate food resources (Frank and Leggett, 1986), predator protection (Shepard and Cushing, 1980) and benign abiotic conditions (Elliott and Elliott, 2006). Natural selection favours commencement of external feeding at a time when the survival and growth opportunities are maximal, therefore fry survival will be lowered if emergence is either too early or too late (Jonsson and Jonsson, 2009).

Spawning time is known to vary among populations within species. Heggberget (1988) found that the day of commencement of spawning was positively correlated with mean water temperature from December through April. Spawning time was earlier in rivers where the mean winter temperature was low (<1.5°C) than in the streams with higher water temperatures.

There can also be population specific variations in spawning time e.g. some Norwegian rivers where spawning occurred later in the autumn in rivers where the winter temperature was relatively warm (2 -4°C) than cold (0-1°C), but the local variation was large probably because other factors also influence spawning time such as habitat accessibility at a particular time (Tallman and Healy, 1991). A study by Carlson and Seamons (2008) also shows that spawning time may change quickly if environmental conditions change.

Salmon and trout spawn in late autumn/winter, burying their eggs in the gravel substratum of rivers, where they hatch in spring after a certain number of degree days, depending on the species (check lit review). A study by Heggberget (1988) concluded that salmon populations revealed no local adaptation to the temperature conditions of their home rivers, but this may have been possibly due to too small a climatic variation between the study sites chosen.

There appears to be an optimal temperature for egg development, with a study by Ojanguren and Brana (2003) finding the maximum trout embryo survival occurring between 8-10°C, with

an upper thermal limit for embryonic development of between 14 and 16°C. There has been a gradual increase in river temperature in recent years and this trend is set to continue (Jonsson and Jonsson, 2009). There is expected to be a northward shift in the geographic distribution of Atlantic salmon, and higher river temperatures during gonadal development may be one of the reasons for local extinctions at the southern edge of their current range (McCarthy and Houlihan, 1997).

Emergence periods of salmonid stocks vary from year to year. Most of this variation is due to variation in water temperature, with spawning dates as a secondary factor. Spawning dates do however; have an effect on the length of emergence period (Elliott and Hurley, 1998a). There is also thought to be a trend that fish from colder rivers have higher developmental rates and require less degree-days at the same temperature (Brannon et al., 2004).

Hatching dates for salmon and sea trout ova depend on the number of degree days from spawning (510 degree days for salmon, 444 degree days for trout). When these cumulative temperatures are reached, the salmonid ova will hatch out its alevin. Warmer winters and early spring-time are therefore expected to result in earlier hatching dates for these two species, although this may be counterbalanced by later spawning times (Jonsson and Jonsson, 2009).

3.4.2 Methods

The length of time from spawning to hatching for salmonid ova is controlled by degree days, a cumulative count of temperatures over time. Salmon need 510 degree days from spawning to hatching, while trout require 444 degree days (Elliott, 1994).

Degree days are calculated by adding together the daily water temperatures of each day, starting on the day of spawning. Hatching in salmon, for example, is known to occur when 550 degree days (daily temperature x no. of days) is reached.

Estimated hatching dates were calculated by adding up the daily average temperatures from 1962-2008 (Chapter 1) from an estimates spawning state date of 15 December until the cumulative temperatures reached the total accumulated degree days needed for hatching of both salmonid species (taken from Elliott, 1994). The number of days from spawning to hatching was then plotted and a regression analysis was carried out on the data.

3.4.3 Results

Figures 3.5 and 3.6 show how the number of days required to meet these degree days has declined significantly over the previous five decades for both salmon ($p<0.0001$) and for trout ($p<0.0008$), corresponding to increasing winter water temperatures over this time period in the Burrishoole catchment (Chapter 1). The data was plotted using the 15 December of the preceding year as an arbitrary spawning start date. However, it is likely that in some years spawning occurred considerably later than this date (D. Cotter, pers. comm.). In Figure 3.5, for salmon it can be seen that five of the six years with the lowest egg development times occurred in the last decade, this rises to seven out of ten for trout (Figure 3.6).

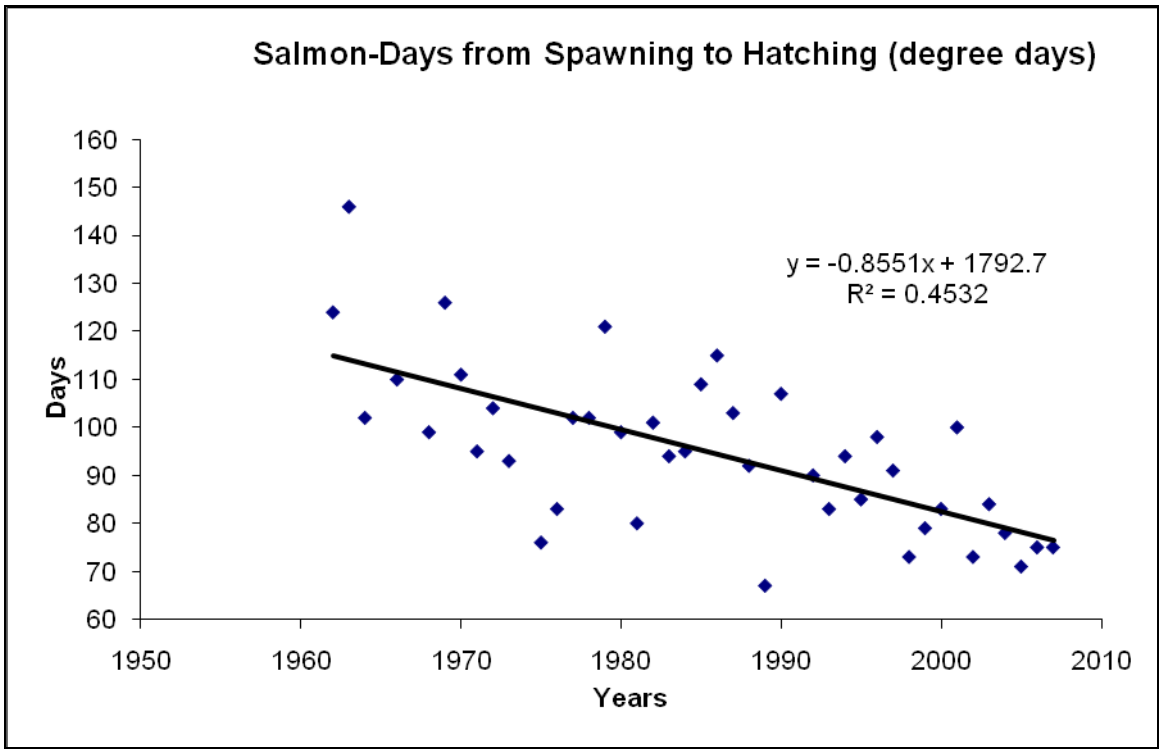

Figure 3.5: Number of days from spawning to reach the required number of degree days necessary for hatching from 1962-2008 for salmon.

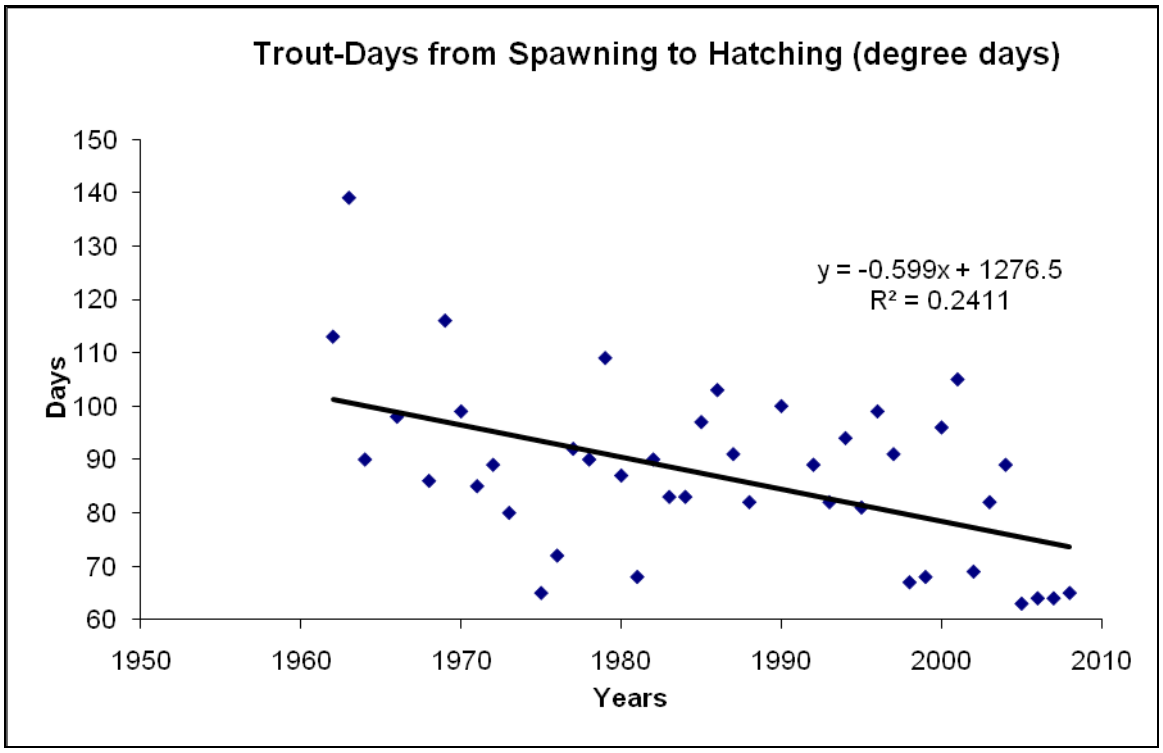

Figure 3.6: Number of days from spawning to reach the required number of degree days necessary for hatching from 1962-2008 for trout.

3.4.4 Discussion

Using the regression line on Figures 3.5 and 3.6 as an average, there has been approximately a 35 day decrease over the last five decades in terms of incubation time from spawning to hatching for salmon, and approximately a twenty five day decrease for trout. While this study shows a shortening in numbers of days required in egg development time in the wild, it does not necessarily mean that actually hatching dates have shifted to the same extent, due to possible delays in salmonid spawning in the catchment during recent years (D. Cotter, pers comm.). There appears to be an optimal temperature for egg development. A study by Ojanguren and Brana (2003) found that the maximum trout embryo survival occurring between 8-10°C, with an upper thermal limit for embryonic development of between 14-16°C. These parameters could affect successful incubation of wild salmonid eggs in the Burrishoole in future years in light of proposed water temperature increases.

One of the expected effects of climate change is an increase in frequency and intensity of extreme weather events such as droughts and floods (IPCC, 2007). There is a positive relationship between water flow and the survival of eggs and 0+ salmon, during both summer and winter (Gibson and Meyers, 1998). Extremes in flow can however affect fry survival negatively, for example, a study by Jensen and Jonsson (1999) found that years with high discharge during the alevin stage negatively affected survival in a Norwegian river. Low

discharge at the time of emergence has also been found to affect survival (Elliott, 1985). Droughts that prevent adult fish from reaching their spawning grounds may have a constraining effect on recruitment (Jonsson and Jonsson, 2009).

Gibson and Meyers (1998) found a positive relationship between temperature and survival of 0+ salmon in Canadian rivers but also noted that extreme temperatures could reduce recruitment. The negative effect of particularly high or low water temperature seems strongest during embryonic development, at hatching, just before emergence and when alevins commence external feeding (Jonsson and Jonsson, 2009).

One of the affects of high water temperature is low oxygen content in the water, with oxygen concentration declining with increasing water temperature. Oxygen deficits when accompanied by pollutants can cause egg mortality, and with low water flow, gravel interstices can be clogged by fine sediment which reduces the intra-gravel oxygen supply to eggs and alevins (Merz et al., 2004). Therefore, low flow and high temperature along with low oxygen supply and pollution can restrict salmonid recruitment. Embryos and alevins are most threatened by these abiotic factors at the southern edge of their distribution range where the water temperature is critically high (Jonsson and Jonsson, 2009) and it is not known whether these factors are critical in Burrishoole.

3.5. Growth of Atlantic Salmon

3.5.1 Introduction

Change in life histories of Atlantic salmon (*Salmo salar* L.), specifically the sea age composition has been reported for numerous populations throughout their geographic range (Garcıa de Leaniz et al., 2007; Youngson et al., 2002; Bagliniére et al., 2004; Heddell-Cowie, 2005; Quinn et al., 2006). A number of possible causes have been suggested. These include changes in the freshwater environment affecting the growth of the juveniles and therefore the age at maturity of adults (Gardner, 1976), selective exploitation of certain stock components (Gee & Milner, 1980; Consuegra et al., 2005) and climatic changes affecting the ocean environment (Friedland et al., 2003, Peyronnet et al., 2007).

This section examines the growth rate of juvenile salmon from archival scales and investigates whether increasing water temperatures in freshwater have affected the growth rates and the smolt age of migrating juvenile salmon from the Burrishoole catchment over the time period 1969-2008.

3.5.2 Methods

Fish traps

Salmon smolt samples were collected from the Salmon Leap and Mill Race downstream traps. The traps are located on the two rivers which mark the interface between saline and freshwater within the catchment. These ensure full trapping of all fish moving in and out of the catchment, allowing for a full census of juvenile and adult salmonids (Chapter 3.2.4).

Age and Growth Analysis

Samples of scales for growth analysis were collected from the Salmon Leap and Mill Race downstream traps during the annual smolt migration in all years studied (Table 3.3). All fish were measured (fork length ±1 mm) and scales taken from above the lateral line under the dorsal fin.

In the laboratory scales were mounted in water between two glass slides and then placed under a compound microscope (Olympus BX51) which was connected by camera (1.4 MP monochrome Q-cam) to a computer. Images of the scales were taken using Image Pro-plus v.6 software which was also used for increment and seasonal/annual growth measurements (Figure 3.7). The scales were interpreted independently by two individuals and ambiguous scales were discarded.

Table 3.3: showing sample sizes for years where salmon growth was determined

Year	n
1968	37
1977	53
1982	96
1984	141
1994	43
1997	100
2003	36
2004	109
2005	116
2006	125
2007	141
2008	183

Incremental growth was calculated by measuring the distance from the centre of the scale to the first annulus, and from this to the next and so on. The distances between the annuli are directly proportional to growth during the year represented by each inter-annular space.

Seasonal growth was calculated in a similar way to the annual growth by measuring the space during which rings were laid down with a wide space (summer growth) and with a narrow space (winter) between them. The boundary between fast and slow growth was most difficult to distinguish for the first year, but in subsequent years this was relatively successful. Where differentiation between the summer and winter in the first year was difficult, scales were only included in the calculations of annual growth.

The numbers of circuli laid down within each growing period were counted and were related to the actual growth of the fish calculated for that period.

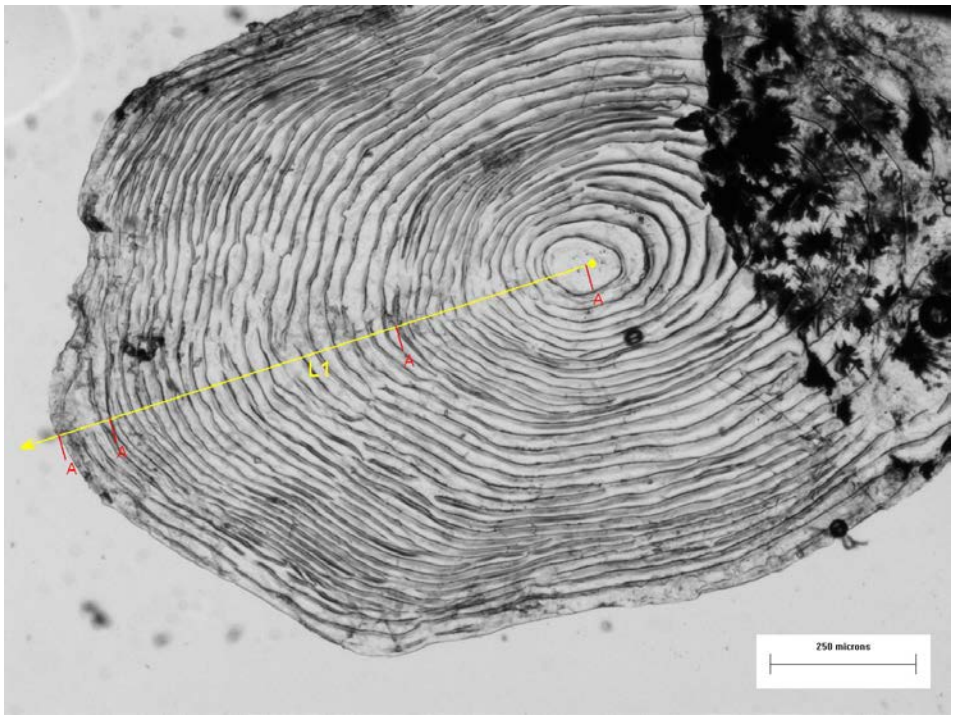

Figure 3.7: Image of a salmon smolt scale with annual markings in red.

Values for the annual incremental growth were calculated according to the formula:

$a = i \times (L/l)$ **Equation 3.1**

Where,

a = the calculated length increment

i = distance between the bands measured on scales

$l = \sum i$ for the individual

L = total length of the individual

In the measurement of scales, it is suggested (Tesch, 1968) that allowances be made for the fact that a fish does not begin to grow from 0cm but has already reached a certain finite size when the scale begins to form circuli. The initiation of growth at a finite size is known as Lee's phenomenon, and can be incorporated into incremental growth calculations (Lee, 1920). However, in our dealings with historical data and the associated literature, no allowances seem to have been made for Lee's phenomenon. Thus, in the interests of historical comparability, a less complex approach omitting any modifications was adopted.

3.5.3 Results

Significant differences in length were found between 1968 and all years sampled, with fish from 1968 being significantly smaller than all other years. After this, 1977, 1982, 84 and 2007 were significantly larger than fish from 2004 and 2008, and 2004 and 2006 were significantly smaller

than fish from 2007 (ANOVA, Table 3.4). There does not seem to be a significant trend in terms of either increasing or decreasing fish length over time.

Tables 3.5 – 3.7 shows the sample size for each age class in each year examined. It also shows the average length per age class, along with the range of lengths recorded and the percentage of the total annual sample made up by each age class. It can be seen from Table 3.7 that 2+ fish are the dominant age class (that is, fish that have spend two years in freshwater and have also shown some growth on the scale before migrating in spring as smolts). Two year old smolts form between 1.7% and 21% of the group in each year. Two year old smolts are fish that have spent two years growing in freshwater, but do not show any growth in the spring that they migrate to sea as smolts. 1+ fish make up the remainder of the sample, this portion appears to be increasing in recent years. These fish have spent one year in freshwater and show some growth on the scale before migrating as smolts. There were no examples in the study of one year old fish who did not lay down some growth in the spring before migration.
A Chi-squared analysis was carried out on the average percentages for each age class for the years 1968-1984 inclusive and 2003-2008 inclusive. This showed a significant shift in the percentage make up of the age classes over time, mainly demonstrated by the increase in the percentage make up of the 1+ age class in recent years (Chi-squared value = 10.75, DF = 2, $p \leq 0.001$).

Table 3.4: showing a one way analysis of variance looking for differences in lengths between the different years sampled for all fish sampled in each year

Source	DF	Seq SS	Adj MS	F	p
Year	11	313.81	28.53	14.6	<0.001
Error	1158	2263.17	1.95		
Total	1169	2576.98			

Table 3.5: Average lengths and ranges of the data of fish in the three different age classes for all years and percentage of each sample made up by each age class for each year.

1+				
Year	n	Av. Length (cm)	Range (cm)	%
1968	4	11.4	10.9 - 12.6	10.81
1977	2	14.1	13.1 - 15.0	3.77
1982	2	12.5	12.0 - 13.0	2.08
1984	6	12.7	10.6 - 14.6	4.26
1994	2	12.3	12.0 - 12.6	4.65
1997	3	11.7	10.3 - 12.9	3.00
2003	4	12.3	11.1 - 13.7	11.11
2004	30	12.3	10.6 - 15.8	27.52
2005	22	13.0	10.6 - 19.4	18.97
2006	17	12.6	10.8 - 14.2	13.60
2007	22	13.2	10.5 - 18.8	15.60
2008	24	12.3	10.5 - 14.5	13.11

Table 3.6: Average lengths and ranges of the data of fish in the three different age classes for all years and percentage of each sample made up by each age class for each year.

2				
Year	n	Av. Length(cm)	Range (cm)	%
1968	6	11.7	10.9 - 12.7	16.22
1977	4	15.0	14.0 - 15.9	7.55
1982	9	14.2	12.4 - 15.3	9.38
1984	21	14.8	12.8 - 16.9	14.89
1994	5	13.5	12.9 - 14.0	11.63
1997	20	14.3	10.2 - 19.2	20.00
2003	15	14.6	12.9 - 17.0	41.67
2004	10	14.9	14.0 - 17.2	9.17
2005	2	15.8	12.5 - 19.0	1.72
2006	18	14.6	12.3 - 17.0	14.40
2007	17	14.9	12.5 - 17.1	12.06
2008	39	14.0	11.4 - 17.5	21.31

Table 3.7: Average lengths and ranges of the data of fish in the three different age classes for all years and percentage of each sample made up by each age class for each year.

2+				
Year	n	Av. Length(cm)	Range (cm)	%
1968	27	11.8	10.7 - 12.9	72.97
1977	47	14.4	12.4 - 16.6	88.68
1982	85	14.4	12.4 - 19.7	88.54
1984	114	14.4	12.0 - 17.8	80.85
1994	36	14.0	11.7 - 17.5	83.72
1997	77	13.8	10.9 - 17.5	77.00
2003	17	13.7	11.9 - 16.5	47.22
2004	69	13.8	11.3 - 17.8	63.30
2005	92	14.0	10.2 - 18.2	79.31
2006	90	13.8	11.3 - 18.8	72.00
2007	102	14.5	11.2 - 18.0	72.34
2008	120	13.8	10.3 - 19.0	65.57

Annual Growth

It should be noted that plus growth does not cover a full year (mostly spring growth in these samples) so the final increment in "+" age classes does not represent a full period of annual growth. Annual growth increments were calculated for salmon smolts for all years. Table 3.8 shows average back-calculated growth for all age classes for all years, with plus growth values in italics.

One way analysis of variance could only be carried out on 2+ fish, due to low sample sizes for 1+ and 2 year old fish in some sampling years (Table 3.9). This analysis was carried out to ascertain if any change in growth rate had occurred over time in the years sampled. The data for each growth year were tested separately (Table 3.9).

Table 3.8: Average back-calculated annual growth increments (cm) for all salmon samples and all years. Plus growth is indicated by values in italic.

Age	n	Year 1	Year 2	Year 3	Age	n	Year 1	Year 2	Year 3
1968 salmon smolts N = 37					**2003 salmon smolts N = 36**				
1+	4	8.8	*2.5*		**1+**	4	9.04	*3.25*	
2	6	4.81	7.03		**2**	15	5.94	8.68	
2+	27	4.38	6.22	*1.18*	**2+**	17	4.38	7.33	*2.04*
1977 salmon smolts N = 53					**2004 salmon smolts N = 109**				
1+	2	8.93	*5.12*		**1+**	30	9.57	*2.78*	
2	4	5.86	9.12		**2**	9	7.28	7.63	
2+	47	4.99	7.41	*2*	**2+**	63	4.79	6.9	*1.91*
1982 salmon smolts N = 96					**2005 salmon smolts N = 116**				
1+	2	9.19	*3.31*		**1+**	22	10.05	*2.9*	
2	9	5.52	8.63		**2**	2	7.59	8.16	
2+	85	4.98	7.51	*1.93*	**2+**	92	4.93	7.2	*1.89*
1984 salmon smolts N = 141					**2006 salmon smolts N = 125**				
1+	6	8.71	*3.64*		**1+**	17	9.3	*3.41*	
2	19	5.78	8.9		**2**	18	5.42	9.08	
2+	113	4.63	7.59	*2.18*	**2+**	90	5.04	6.94	*1.77*
1994 salmon smolts N = 43					**2007 salmon smolts N = 141**				
1+	2	8.8	*3.5*		**1+**	22	9.13	*4.07*	
2	5	5.58	7.9		**2**	17	5.51	9.34	
2+	36	4.87	7.32	*1.86*	**2+**	102	5.14	7.4	*1.93*
1997 salmon smolts N = 100					**2008 salmon smolts N = 183**				
1+	3	9.27	*2.43*		**1+**	24	9.01	*3.33*	
2	20	5.74	8.51		**2**	39	5.2	8.76	
2+	77	5.02	8.68	*1.6*	**2+**	120	4.76	7.05	*1.93*

Table 3.9 shows the results of testing the log transformed back calculated annual growth for 2+ fish for all years. Data was found to approximate normality. There were significant differences in growth in Year 1, Year 2 and Year 3 (+ growth). The difference in Year 3 was discounted as it did not describe a full year of growth, rather the "+ growth" of the salmon smolt in the season before migration, and this can be highly variable between years.

Bonferroni pairwise comparisons were carried out on the data from Year 2 to find which annual samples were showing significant differences. Year 2 growth was significantly less in 1968 and several years (as seen in Table 11.1, Appendix IV), with 1968 being smaller. 1984 was significantly smaller than 2006 and 1997 was significantly larger than 2004 and 2006 (Table 11.1, Appendix IV). Figure 3.6 displays the cumulative growth for each age class of fish in each year. The cumulative growth without 1968 is presented in Figure 11.1 of Appendix IV.

Table 3.9: One way analysis of variance for 2+ fish

Year 1 Source	DF	Seq SS	Adj MS	F	p
Year	11	0.25	0.02	2.04	<0.022
Error	857	9.75	0.01		
Total	868	10			
Year 2 Source	**DF**	**Seq SS**	**Adj MS**	**F**	**p**
Year	11	0.38	0.03	4.36	<0.001
Error	856	6.84	0.008		
Total	867	7.22			
Year 3 (+growth) Source	**DF**	**Seq SS**	**Adj MS**	**F**	**p**
Year	11	2.08	0.19	3.85	<0.001
Error	856	41.96	0.05		
Total	867	44.04			

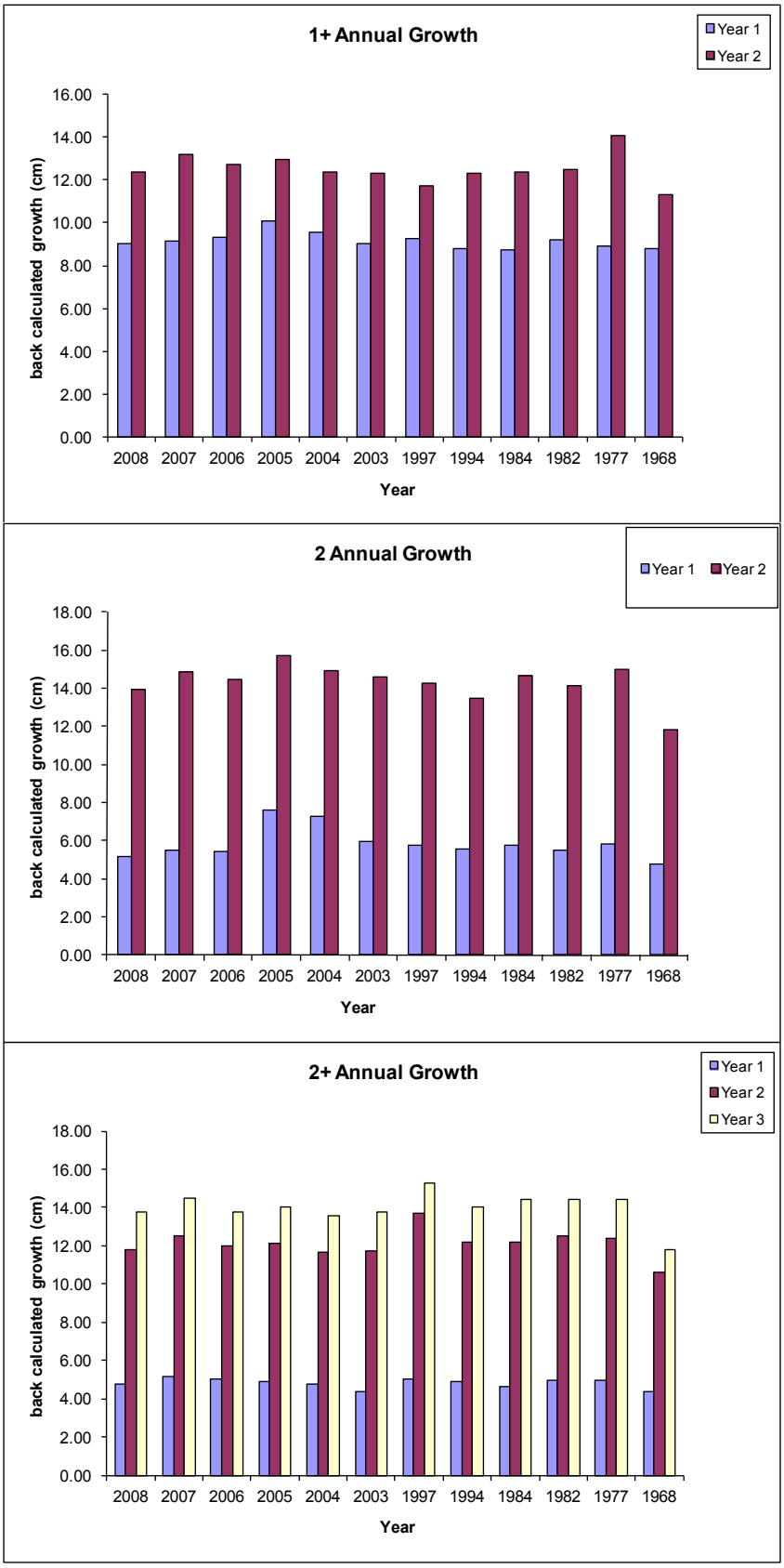

Figure 3.8: Annual growth (cumulative) for a) 1+ salmon, b) 2 salmon and c) 2+ salmon for all years. See also Figure 11.2 in Appendix IV.

Seasonal Growth

Seasonal growth was back calculated in a similar fashion to annual growth. Table 3.10 shows average growth for all age classes for all years. One way analysis of variance could only be carried out on 2+ fish, due to low sample sizes for 1+ and 2 year old fish in some sampling years (Table 3.11). This analysis was carried out to see was there any difference in growth between seasons in different annual samples.

Table 3.12 shows the results of a one-way analysis of variance on the log transformed back calculated growth for 2+ fish for all seasons (summer/winter). Data was found to approximate normality. Significant differences were found between all seasons between annual samples. Bonferroni pairwise comparisons were carried out on the data to find which years were showing significant differences (Table 11.2, Appendix IV), and in which direction (positive/negative). Summers 1 and 2 show no clear trends in the significant differences between annual samples. However, both Winter 1 and 2 indicate that the growth in 2008 was significantly larger than in all other years studied.

Due to larger sample sizes of 1+ fish for the years 2004-2008 inclusive, a one way analysis of variance was carried out on this data (Table 3.10). Data was found to be approximating normality, without transformation. The analysis was carried out to examine if growth was different in the various annual samples. Bonferroni pairwise analysis of the data found that Summer 1 growth was significantly larger in 2007 than in 2004 and 2005, even though the overall analysis was not significant. Winter 1 showed significantly less growth in all years (except 2006) when compared to 2008. Plus growth for 1+ fish was significantly smaller in 2004 and 2005 when compared with 2007. 2008 again seems to show a different pattern growth to proceeding years.

Figure 3.9 displays the seasonal growth rates for each age class of fish in each year. It also shows no clear trend in growth over time for the samples studied. There is a weak relationship of increasing growth in recent years at the end of summer 2 ($p<0.02$) and winter 2 ($p<0.06$), but if 1968 is removed from the analysis, there is no statistical relationship visible (Figure 11.1. Appendix IV).

Table 3.10: Average back-calculated seasonal growth increments (cm) for all salmon samples and all years. Plus growth is indicated by values in italics

Age	n	Summer 1	Winter 1	Summer 2	Winter 2	Summer 3
1968 salmon smolts N = 37						
1+	4	8.47	1.64	1.29		
2	6	3.47	1.14	5.40	1.69	
2+	27	3.32	1.06	4.78	1.44	1.18
1977 salmon smolts N = 53						
1+	2	6.89	2.04	5.12		
2	4	4.56	1.30	7.15	1.97	
2+	47	3.85	1.16	5.73	1.66	2.00
1982 salmon smolts N = 96						
1+	2	7.63	1.56	3.31		
2	9	4.30	1.22	6.85	1.78	
2+	85	3.74	1.24	5.91	1.61	1.93
1984 salmon smolts N = 141						
1+	6	6.98	1.69	3.97		
2	19	4.55	1.33	6.87	2.01	
2+	113	3.46	1.17	5.84	1.72	2.20
1994 salmon smolts N = 43						
1+	2	7.29	1.51	3.50		
2	5	4.42	1.16	6.33	1.57	
2+	36	3.73	1.14	5.82	1.50	1.86
1997 salmon smolts N = 100						
1+	3	7.81	1.46	2.43		
2	20	4.48	1.26	6.78	1.73	
2+	77	3.70	1.31	6.90	1.78	1.60
2003 salmon smolts N = 36						
1+	4	7.41	1.63	3.25		
2	15	4.54	1.40	7.05	1.63	
2+	17	3.17	1.21	5.80	1.53	2.04
2004 salmon smolts N = 109						
1+	30	7.90	1.66	2.78		
2	9	5.89	1.42	5.93	1.70	
2+	63	3.60	1.23	5.27	1.53	2.16
2005 salmon smolts N = 116						
1+	22	8.18	1.87	2.90		
2	2	5.52	2.07	6.07	2.09	
2+	92	3.71	1.23	5.42	1.79	1.87
2006 salmon smolts N = 125						
1+	17	7.73	1.47	3.38		
2	18	4.23	1.21	7.40	1.74	
2+	90	3.92	1.15	5.55	1.44	1.72
2007 salmon smolts N = 141						
1+	22	7.48	1.65	4.07		
2	17	4.30	1.22	7.41	1.94	
2+	102	3.96	1.17	5.87	1.55	1.93
2008 salmon smolts N = 183						
1+	24	7.71	1.31	3.32		
2	39	4.06	1.00	7.66	1.24	
2+	120	3.76	1.05	5.79	1.26	1.93

Table 3.11: One way analysis of variance for all seasons for 2+ fish from all years

Summer 1 2+ fish					
Source	**DF**	**Seq SS**	**Adj MS**	**F**	**p**
Year	11	0.48654	0.04423	3.23	<0.001
Error	861	11.7947	0.0137		
Total	872	12.28124			
Winter 1 2+ fish					
Source	**DF**	**Seq SS**	**Adj MS**	**F**	**p**
Year	11	0.756897	0.068809	8.49	<0.001
Error	861	6.97585	0.008102		
Total	872	7.732748			
Summer 2 2+ fish					
Source	**DF**	**Seq SS**	**Adj MS**	**F**	**p**
Year	11	0.51832	0.04712	3.65	<0.001
Error	861	11.1486	0.01292		
Total	872	11.66698			
Winter 2 2+ fish					
Source	**DF**	**Seq SS**	**Adj MS**	**F**	**p**
Year	11	1.72859	0.15714	18.41	<0.001
Error	861	7.36456	0.00853		
Total	872	9.09315			
Plus growth 2+ fish					
Source	**DF**	**Seq SS**	**Adj MS**	**F**	**p**
Year	11	1.72859	0.15714	18.41	<0.001
Error	861	7.36456	0.00853		
Total	872	9.09315			

Table 3.12: One way analysis of variance for 1+ fish from 2004-2008 inclusive

Summer 1					
Source	**DF**	**Seq SS**	**Adj MS**	**F**	**p**
Season	4	20.35	5.09	3.89	0.005
Error	108	141.13	1.31		
Total	112	161.48			
Winter 1					
Source	**DF**	**Seq SS**	**Adj MS**	**F**	**p**
Season	4	3.37	0.84	10.88	<0.001
Error	109	8.44	0.078		
Total	113	11.81			
Plus growth					
Source	**DF**	**Seq SS**	**Adj MS**	**F**	**p**
Season	4	24.58	6.15	4.34	0.003
Error	110	155.86	1.42		
Total	114	180.45			

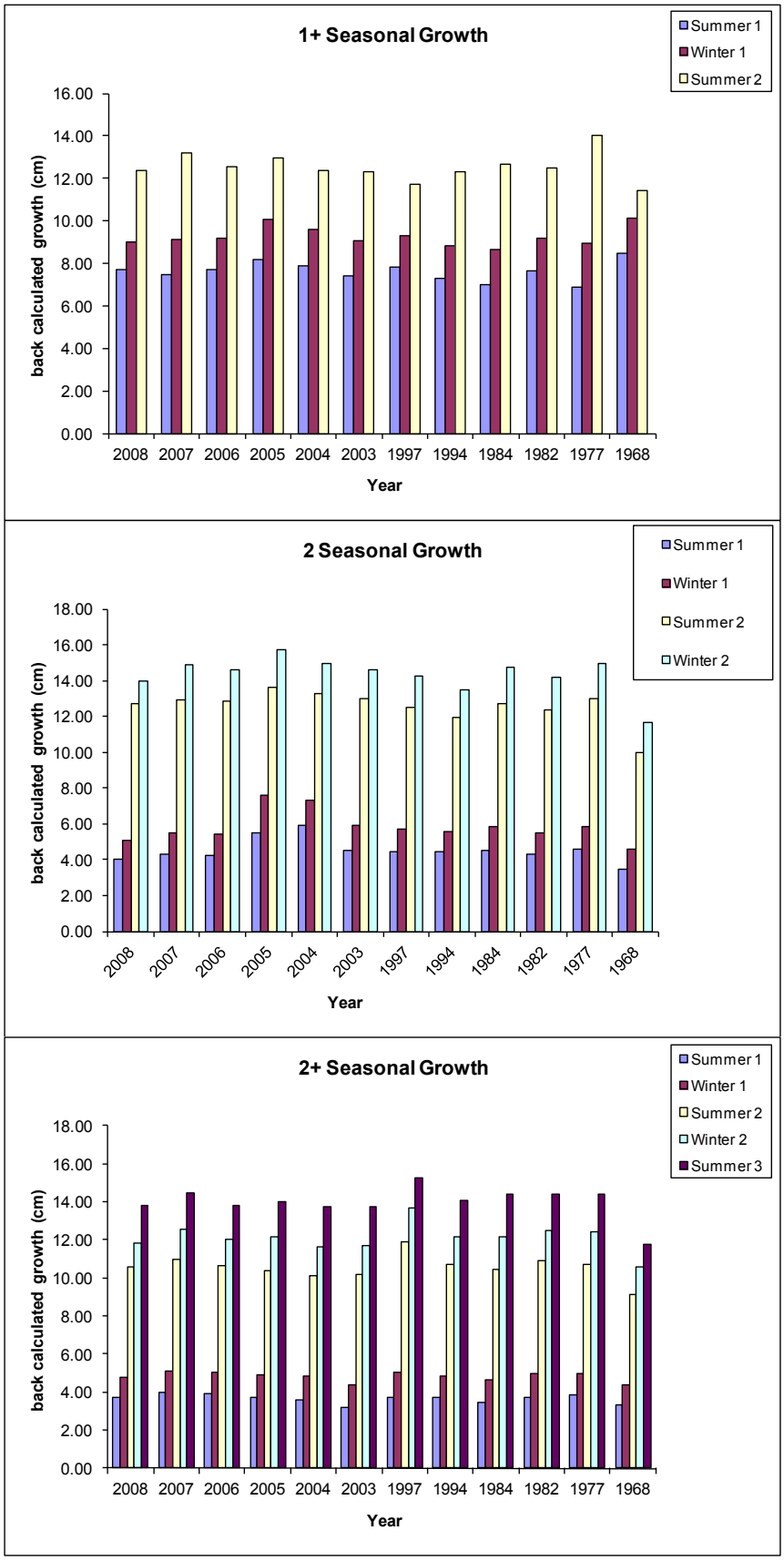

Figure 3.9: Cumulative seasonal growth for a) 1+ salmon, b) 2 salmon and c) 2+ salmon for all years. See also Figure 11.1 in Appendix IV.

Circuli count analysis

Circuli (bands laid down by fish on the scale during growth) were counted for each growth season (summer/winter) in each annual sample and averaged (Table 3.13a-c). The data shows the expected pattern of more circuli being laid down during summer (a period of high growth) when compared with winter (a period of low growth).

One-way analysis of variance on circuli counts for each season for 2+ fish (due to small sample size for some years for 1+ and 2 age fish- Table 3.14) showed significant differences in circuli counts between the different annual samples in all seasons. Table 3.13a-c indicates that the number of circuli laid down in wintertime and the second summer are lower in recent years.

Table 3.13a: Average circuli counts for all age classes in each sampling year.

1+ Year	n	S1	W1	S2	W2	Plus	Total
2008	24	24	5			4	33
2007	22	20	5			5	29
2006	17	19	5			5	28
2005	22	16	5			5	26
2004	30	19	4			4	28
2003	4	19	5			5	29
1997	3	19	5			5	29
1994	2	19	5			7	31
1984	6	19	4			5	29
1982	2	19	5			5	29
1977	2	19	4			5	29
1968	4	23	5			4	32

Table 3.13b: Average circuli counts for all age classes in each sampling year.

2 Year	n	S1	W1	S2	W2	Plus	Total
2008	39	11	5	17		5	38
2007	17	12	4	16		5	38
2006	18	12	4	18		5	40
2005	2	13	4	19		5	41
2004	9	13	4	20		5	43
2003	15	12	4	21		5	43
1997	20	12	4	20		5	41
1994	5	12	5	19		5	40
1984	19	12	4	19		5	40
1982	9	12	4	19		5	40
1977	4	15	5	15		6	40
1968	6	13	5	19		5	41

Table 3.13c: Average circuli counts for all age classes in each sampling year.

2+ Year	n	S1	W1	S2	W2	Plus	Total
2008	120	14	5	14	4	2	39
2007	102	10	4	14	4	3	34
2006	90	9	4	13	4	4	33
2005	92	11	4	13	4	5	37
2004	63	10	4	15	5	5	37
2003	17	10	4	15	5	5	37
1997	77	9	5	15	5	5	38
1994	36	9	5	16	5	4	38
1984	113	9	5	16	5	4	38
1982	85	9	5	16	5	4	38
1977	47	9	5	15	5	4	37
1968	27	9	5	16	5	4	37

Table 3.1413: One way analysis of variance for 2+ circuli counts for all seasons (summer/winter)

Summer 1 Source	DF	Seq SS	Adj MS	F	p
Season	11	1.26	0.11	6.08	<0.001
Error	856	16.11	0.02		
Total	867	17.37			
Winter 1 Source	**DF**	**Seq SS**	**Adj MS**	**F**	**p**
Season	11	0.68	0.06	7.78	<0.001
Error	856	6.76	0.01		
Total	867	7.43			
Summer 2 Source	**DF**	**Seq SS**	**Adj MS**	**F**	**p**
Season	11	0.31	0.28	2.37	0.007
Error	856	10.24	0.01		
Total	867	10.55			
Winter 2 Source	**DF**	**Seq SS**	**Adj MS**	**F**	**p**
Season	11	0.84	0.08	8.74	<0.001
Error	856	7.45	0.01		
Total	867	8.29			
Plus growth Source	**DF**	**Seq SS**	**Adj MS**	**F**	**p**
Season	11	1.05	0.1	2.56	0.003
Error	856	31.92	0.04		
Total	867	32.97			

A Bonferroni pairwise comparison was then carried out to find which years were showing significant differences (Table 11.3, Appendix IV). The Bonferroni pairwise analysis showed no clear patterns of differences, except for the 2005 and 2007 samples which showed higher numbers of circuli during Winter 2.

3.5.4 Discussion on Salmon Growth

Temperature affects metabolic processes and growth in fishes. It also influences the timing and duration of most life-history stages – from the emergence of fry from spawning gravels, to the size of parr in freshwater to the emigration of smolt to the sea (Table 3.15; Connor et al., 2002). Fish are sensitive to temperature changes both through heat exchange in the gills and by heat transfer through the body wall (Elliott, 1981). Because of the allometric relationship between the volume and the surface area of a fish, small fish are more susceptible to fluctuations in water temperature than larger ones (Elliott, 1994).

Age at smolting is influenced by parr growth and size. Fast growers tend to smolt at an earlier age and at a smaller size than more slow-growing individuals from the same populations (Strothotte et al., 2005). The effects of water temperature on smolt age and size are mediated through variations in growth rate, although smolt size may be more directly associated with water temperature (Jonsson and Jonsson, 2009). Salmon smolts growing in rivers which empty into relatively warm sea water are generally smaller than those smolts entering colder sea water. This is thought to be partly due to the fact that ionic regulation in cold sea water is easier for larger than for smaller fish (Jonsson and Jonsson, 2009). Even though growth rate is temperature dependent, there may be some confounding factors such as fish density and feeding opportunities (Jonsson and Jonsson, 2009).

An analysis was carried out on the average percentages for each age class for salmon smolts in Burrishoole for the years 1968–1984 inclusive and 2003–2008 inclusive. Smolt age showed a significant shift in the percentage make-up of the age classes over time, mainly demonstrated by the increase in the proportion of the 1+ age class in recent years from <11% to >11% compared to the 2-year-old smolts (2 and 2+ age). This increase in younger smolts may be due to increased growth rates due to higher water temperatures in recent years.

Smolt length was also assessed. Significant differences in length were found between 1968 and all other years sampled, with fish from 1968 being significantly smaller. After this, fish from 1977, 1982, 1984 and 2007 were significantly larger than fish from 2004 and 2008, and fish from 2004 and 2006 were significantly smaller than fish from 2007. However, there was no significant trend in terms of either increasing or decreasing fish length over time. The interaction between mean smolt length, smolt age and mean length at age is complex and not enough data was available in this study to fully analyse this.

In addition to the analysis on smolt age, the growth rate of juvenile salmon in Burrishoole was determined using back-calculation of increments from their scales. Scales preserve the growth history of the fish through different widths of circuli laid down, similar to annual rings used to age trees. While clear changes in growth rates within each year class of smolt were not apparent in this study there was, however, an increase in recent years in the growth rate during the second year of growth (both periods – 'summer' vs 'winter') for 2+ smolts, the dominant age class in Burrishoole. It was also clearly apparent that the winter growth in both 1-year-old and 2-year-old parr in 2008 was the fastest observed in any of the years studied.

As mentioned above, it is likely that there is an interaction between growth rate and smolt age, which means that it is unlikely that a change in growth rate would be observed in the 2 year old smolts, for example, as they would smoltify as one year olds if the growth had increased significantly.

Other studies have also observed increases in juvenile growth rate and a reduction in smolt age. Aprahamian et al. (2008) found an increase in growth rate in juvenile salmon and a concomitant decline in smolt age for salmon from the River Dee (UK) for the time period 1937–2005. On the River Dee, the increase in freshwater growth rate is likely to explain the decline in mean smolt age as the faster growing parr migrate to sea earlier (Metcalfe et al., 1989; Økland et al., 1993). This change would appear to have started in the 1980s. The study suggested that this increase in growth rate may have been related to a reduction in density-dependent processes – that is, the density of fish (i.e. less fish leads to less competition for food and faster growth) in the catchment habitat (Gibson, 1993; Jenkins et al., 1999; Imre and Boisclair, 2005; Lobón-Cervia and Mortensen, 2005). However, other studies have found no such relationship (Egglishaw and Shackley, 1977; Elliott, 1994). Temperature is known to affect the timing and the size of alevins at emergence and their subsequent growth and survival (Brett, 1979; Elliott et al., 2000). However, although the mean temperature in the Dee has increased by 0.2°C a year since the 1960s, it was unlikely that a change in emergence time alone could account for the increase in length at age (Aprahamian et al., 2008).

Lower mean smolt ages have been also been seen in other British (Davidson and Hazelwood, 2005; J. Maclean, unpublished data) and French populations of salmon (Baglinière et al., 2005). Davidson and Hazelwood (2005) reported an overall decline in the mean smolt age of both 1SW and 2SW salmon on the Severn (England) and Wye (Wales) since the 1960s. The onset of this decline also appeared in the 1980s but was less marked on the Severn. This decline in smolt age may affect reproductive success as egg size is smaller for S1 as opposed to S2 smolts

of the same sea age while early survival (egg to swim-up) may also be lower (Moffett et al., 2006). Increased marine mortality may be related to the fact that salmon smolts are migrating at a younger age and thus smaller size (Økland et al., 1993) resulting in a lower survival rate when compared to their larger conspecifics (Chadwick, 1985; Lundqvist et al., 1994). This study has indicated for the Burrishoole, that in future, in line with projected changes in temperature, the freshwater growth of juvenile salmon is likely to increase leading to younger, smaller smolts migrating to sea which may impact on marine survival. Along with the observed changes in smolt run timing and the expected increased occurrence of spring time droughts, the combination of these changes may be detrimental to the overall performance of the Burrishoole salmon stock.

Table 3.15: Critical temperatures for juvenile salmon in freshwater

Parameter	Reference	Temp °C
Feeding	Elliot (1991)	7-22.5
Seek shelter	Gardiner (1984)	<9
Egg mortality	Peterson et al. (1977)	<4
Hatching temp.	Crisp (1981)	2.4-12
Upper incipient lethal temp. (parr)	Elliot (1991)	27.8 ± 0.2
Upper critical range	Elliot (1994)	22-33
Lower critical range (parr)	Elliot (1994)	0-7
Move to cooler water (parr)	Gibson (1966)	22
Optimum growth (parr)	Dwyer and Piper (1987)	16
Smolt Run (range)	Byrne et al. (2003)	5.5-15.5

3.6 Growth of Brown Trout – Resident and Migratory

3.6.1 Introduction

In Burrishoole, trout (*S. trutta*) are a partially migratory species, with both resident and migratory forms present. The migrants move to the sea to feed, while the residents remain in freshwater. Resident individuals usually become mature at the parr stage, while the migratory individuals mature later after undergoing smoltification and a growth period in the sea. Parr maturity is linked to growth rate, and therefore indirectly related to temperature (Jonsson and Jonsson, 2009). Anadromy in trout populations also increases with increasing latitude, possibly because of improved feeding opportunities in the marine environment. This is a situation which could be influenced by future climate change (Jonsson and Jonsson, 2009).

Sea trout are plentiful in most short rivers running directly into the sea and in coastal lakes. They are essentially fish of acid waters (pH 5.5 - 6.5). In general, sea trout populations flourish where growth rates are poor and where survival in freshwater is difficult or where there is

easy access to the sea. Sea trout (*Salmo trutta* L.) is a popular angling species and in many areas have provided significant commercial fisheries. Despite their importance, little quantitative scientific research was carried out on sea trout stocks until recent serious problems in Ireland, Scotland and more recently Norway, have focused attention on the factors regulating their abundance (Whelan et al., 1993).

It has long been recognised that resident/migratory trout interactions are both subtle and complex but that the successful management and enhancement of the migratory component of the stock is dependent on a quantitative understanding of such interactions. In Ireland and Scotland many of the premier sea trout fisheries are located in lake systems, where much of the juvenile production takes place in the lakes themselves and not in the inflowing streams, which at times are little more than spawning channels. The non-availability of quantitative, non-destructive techniques with which to tackle lake systems has greatly curtailed previous efforts to estimate juvenile production or to construct even basic stock recruitment relationships. Poole et al. (2007) presented a Beverton-Holt stock recruitment model for the sea trout stock in Burrishoole and showed a relationship between the quantity of 'migratory' ova laid in the catchment and the smolt output. Previous S/R studies have mostly been from studies in relatively small isolated sections of catchments (e.g. Elliott 1985, 2007)

It is not known to what extent the propensity for marine migration amongst trout is under genetic or environmental control, although Jonsson (1982) showed genetics to be more important than environmental cues in one transplant experiment. A study by Hindar, Jonsson, Ryman & Ståhl (1991) found no genetic differentiation between resident and anadromous life-history types from the same locality with similar spawning times. However, they did demonstrate significant genetic differences between trout, regardless of life-history type, spawning in geographically separate locations and particularly when landlocked trout were included in the analysis.

3.6.2 Methods

Samples of trout scales for growth analysis were collected from trout captured by seine netting in Bunaveela L. and L. Feeagh in September 1991 and in 2007 and from downstream migrating sea trout smolts collected in the Salmon Leap trap in April and May 1992 and April and May 2008. All fish were measured (fork length ± 1 mm) and scales taken from above the lateral line under the dorsal fin. Laboratory analysis of trout scales was carried out in exactly the same manner as the method described for Atlantic salmon in the previous section (Section 3.5.2). Trout exhibiting any signs of previous spawning marks on their scales were excluded.

3.6.3 Results

Length and age

Table 3.16 shows mean length and size range for all fish studied in all years, along with a breakdown of the age classes and the sample sizes. For the Bunaveela and Feeagh samples collected in 2007, the 0+ age class is absent. This is thought to be a result of sampling bias. The lack of older fish without plus growth in the 1991 Bunaveela may be due to the date the samples were collected. The smaller sample size, to explain the lack of 4 year old or 4+ smolts in the 2007 sea trout sample, indicating these older smolts were not present in 2007 (Table 3.16).

Each age class in L. Feeagh were found to be significantly larger (in length, cm) than those in Bunaveela L. in the two years studied (1991, 2007; Table 3.17). Sea trout smolts were found to be significantly longer (in cm) in the 1992 sample than fish from the 2008 sample (Table 3.18).

Table 3.16: Lengths and ages for a) seine net captured trout in L. Feeagh in September 1991 and February and July 2007, b) seine net captured trout in Bunaveela L. in September 1991 and February and July 2007, c) trap caught sea trout smolts from April 1992 and April 2008.

Feeagh Trout 1991 N = 73				**Feeagh Trout 2007 N = 82**			
Age	**n**	**Mean Length**	**Range**	**Age**	**n**	**Mean Length**	**Range**
0+	1	7.8	7.8	**0+**	0		
1+	36	16.2	12.4-19.2	**1+**	26	14.4	10-21.2
2	0			**2**	22	17.1	15.2-19.5
2+	25	21.8	18.5-27.8	**2+**	24	17.6	14.1-23.4
3	0			**3**	4	21.0	19.2-23.4
3+	11	25.7	23.4-29.1	**3+**	6	21.0	19.5-22.9
Bunaveela Trout 1991 N = 72				**Bunaveela Trout 2007 N = 63**			
Age	**n**	**Mean Length**	**Range**	**Age**	**n**	**Mean Length**	**Range**
0+	10	8.3	6.8-11.8	**0+**	0		
1+	55	14.2	10.8-22	**1+**	4	16.1	15.2-16.4
2	0			**2**	15	17.0	15.6-19.3
2+	6	18.6	13.6-21.6	**2+**	32	16.5	14.4-22.4
3	0			**3**	1	17.3	17.3
3+	1	25.1	25.1	**3+**	10	21.2	17.3-23.8
4+	0			**4+**	1	23.6	23.6
Sea trout Smolt 1992 N = 81				**Sea Trout Smolt 2008 N = 34**			
Age	**n**	**Mean Length**	**Range**	**Age**	**n**	**Mean Length**	**Range**
2	8	21.5	18.3-26.5	**2**	6	18.9	16.5-20.8
2+	26	20.1	17-23.7	**2+**	11	19.5	15.8-22.8
3	23	22.6	17.8-26.2	**3**	11	21.6	18-25.5
3+	18	23.8	19.4-28.5	**3+**	6	21.6	19-25.7
4	4	23.9	21.5-26.6	**4**	0		
4+	2	20.7	19.9-21.5	**4+**	0		

Table 3.17: Two-way analysis of variance table for fork length between different age classes of trout in Bunaveela L. and L. Feeagh in 1991 and 2007.

Source	df	Sum of Squares	Mean Square	F-ratio	P
Age	4	3480.12	534.51	132.67	<0.001
Lake in each year	3	555.01	48.46	12.03	<0.001
Age*Lake	12	695.93	57.99	14.39	<0.001
Error	225	1120.01	4.03		
Total	236	5851.07			

Table 3.18: One-way analysis of variance table for fork length between different age classes of sea trout smolts in 1992 and 2008.

Source	df	Sum of Squares	Mean Square	F-ratio	P
Year	1	66.35	35.71	9.69	0.002
Age	2	386.98	193.49	52.51	<0.001
Error	116	427.43	3.68		
Total	119	880.76			

Table 3.19 shows the percentage of each age class within the sample for each site and year. In the 1991 survey, fish were only collected in September, and those fish which weren't clearly 0+ or 1+ based on their length were selected out for age analysis. In the 2007 survey, fish were sampled earlier in the year, resulting in fish with no visible "+ growth" for that summer. However, no size/age distinction was carried out based on length while sampling. Both sea trout samples were random subsets of the wild population passing through the Burrishoole fish traps on that year.

Table 3.19: Percentage of each sample made up by each age class.

Feeagh Trout 1991 N = 73		Feeagh Trout 2007 N = 82	
Age	**% of sample**	**Age**	**% of sample**
0+	1.4	**0+**	0.0
1+	49.3	**1+**	31.7
2	0.0	**2**	26.8
2+	34.2	**2+**	29.3
3	0.0	**3**	4.9
3+	15.1	**3+**	7.3
Bunaveela Trout 1991 N = 72		**Bunaveela Trout 2007 N = 63**	
Age	**% of sample**	**Age**	**% of sample**
0+	13.9	**0+**	0.0
1+	76.4	**1+**	6.3
2	0.0	**2**	23.8
2+	8.3	**2+**	50.8
3	0.0	**3**	1.6
3+	1.4	**3+**	15.9
4+	0.0	**4+**	1.6
Sea trout smolts 1992 N = 81		**Sea Trout smolts 2008 N = 34**	
Age	**% of sample**	**Age**	**% of sample**
2	9.9	**2**	17.6
2+	32.1	**2+**	32.4
3	28.4	**3**	32.4
3+	22.2	**3+**	17.6
4	4.9	**4**	0.0
4+	2.5	**4+**	0.0

When taking this into account, it can still be seen that the 2007 sample from Lough Feeagh contained a lower proportion of fish that are one winter old (31.7% in 2007 and 49.3%) and a significant proportion of fish in the sample that are two winters old (56.1% in 2007 compared to 34.2% in 1991) (Chi-squared, p= 0.01). Fish that are three winters old are present in the sample in similar proportions. The low numbers of 0+ fish may be due to the mesh size bias of the net used or may be due to a low rate of downstream migration of 0+ age fry into the lake.

The Bunaveela Lough sample had a similar difference between 1991 and 2007 in terms of fish that are one and two winters old, with significantly higher percentage of 2+ fish present in the 2007 sample, and a significantly higher percentage of 1+ fish in the 1991 sample (Chi squared, p = <0.001). There is also a higher proportion of 3+ fish in the 2007 sample.

The sea trout smolt sample shows no significant differences in age (Chi-squared, p = 0.547), although the 4/4+ age class was completely absent from the 2008 sample.

Annual Growth - general

It should be noted that plus growth does not cover a full year so the final increment in "+" age classes does not represent a full period of annual growth, but merely growth for the year of capture up until the point of capture. Estimated mean growth in the first year for the 0+ trout was higher than that calculated for the first year's growth in all the other, older age classes. The 1991 study selected out larger 0+ fish also, affecting results. Growth for incomplete years was excluded from the analysis. Annual growth increments were calculated for trout in both lakes (L. Feeagh and Bunaveela L.) for 1991 and 2007, and for the smolt migration in 1992 and 2008 (Table 3.20).

Table 3.20: Average back-calculated annual growth increments (cm) for all trout samples and all years

Back Calculated growth (cm)						
Age	**n**	**Y 1**	**Y2**	**Y3**	**Y4**	**Y5**
Feeagh Trout 1991 N = 73						
0+	1	7.8				
1+	36	7.76	*8.45*			
2	0					
2+	25	6.04	9.59	6.14		
3	0					
3+	11	6.71	8.98	7.01	*2.98*	
Feeagh Trout 2007 N = 82						
0+	0					
1+	26	7.82	6.63			
2	22	7.52	9.60			
2+	24	6.38	8.01	*3.19*		
3	4	5.56	7.61	7.85		
3+	6	6.68	7.76	5.27	*1.25*	
Bunaveela Trout 1991 N = 72						
0+	10	8.29				
1+	55	6.47	*8.14*			
2	0					
2+	6	6.29	11.94	*1.90*		
3	0					
3+	1	6.29	11.94	3.36	*3.51*	
4+	0					
Bunaveela Trout 2007 N = 63						
0+	0					
1+	4	8.29	*7.76*			
2	15	7.01	10.03			
2+	32	5.96	8.68	*1.82*		
3	1	3.61	6.87	6.82		
3+	10	5.59	8.12	5.96	*1.53*	
4	1	6.52	8.21	5.00	3.87	
Sea trout smolts 1992 N = 81						
2	8	9.94	11.58			
2+	26	8.05	10.22	*1.81*		
3	23	6.59	9.08	6.90		
3+	18	6.84	9.08	6.33	*1.50*	
4	4	4.97	6.79	6.98	5.17	
4+	2	5.37	6.09	4.44	3.98	*0.82*
Sea Trout smolts 2008 N = 34						
2	6	8.79	10.07			
2+	11	8.63	9.00	*1.89*		
3	11	6.90	8.84	5.85		
3+	6	6.81	7.96	5.57	*2.54*	
4	0					
4+	0					

Annual Growth – lake trout

A similar pattern of growth was observed in both lakes with the largest mean annual increments occurring in the second year, being significantly larger than growth in year one (ANOVA, Table 3.21). Mean annual growth decreased in subsequent years.

Table 3.21: One way analysis of variance showing significant differences in annual growth between both lakes in each year.

Source	df	Sum of Squares	Mean Square	F-ratio	P
Lake in each year	3	45.06	15.02	3.51	0.015
Error	554	2372.83	4.28		
Total	557	2417.88			
Source	**df**	**Sum of Squares**	**Mean Square**	**F-ratio**	**P**
Age	2	44.64	1.16	0.33	0.804
Lake in each year	3	61.84	18.14	5.16	0.006
Age*Lake	6	33.53	5.59	1.59	0.15
Error	267	938.06	3.51		
Total	278	1078.08			
Source	**df**	**Sum of Squares**	**Mean Square**	**F-ratio**	**P**
Age	1	16.95	7.8	2.55	0.58
Lake in each year	3	15.31	1.11	0.36	0.547
Age*Lake	3	22.18	22.18	2.42	0.068
Error	150	458.39	3.06		
Total	157	512.82			

There were no significant differences in the first year's growth between the 1+, 2+ or 3+ year classes in either lake from either decade. (ANOVA, Table 3.21). The Year 2 growth increments show no differences between the ages or the lakes in either year. Plus growth from 1+ fish was excluded from this analysis as it does not show a full year's growth.

Figure 3.10 and Figure 3.11 illustrate the annual back-calculated lengths of resident brown trout in L. Feeagh and Bunaveela L. in 1991 and 2007.

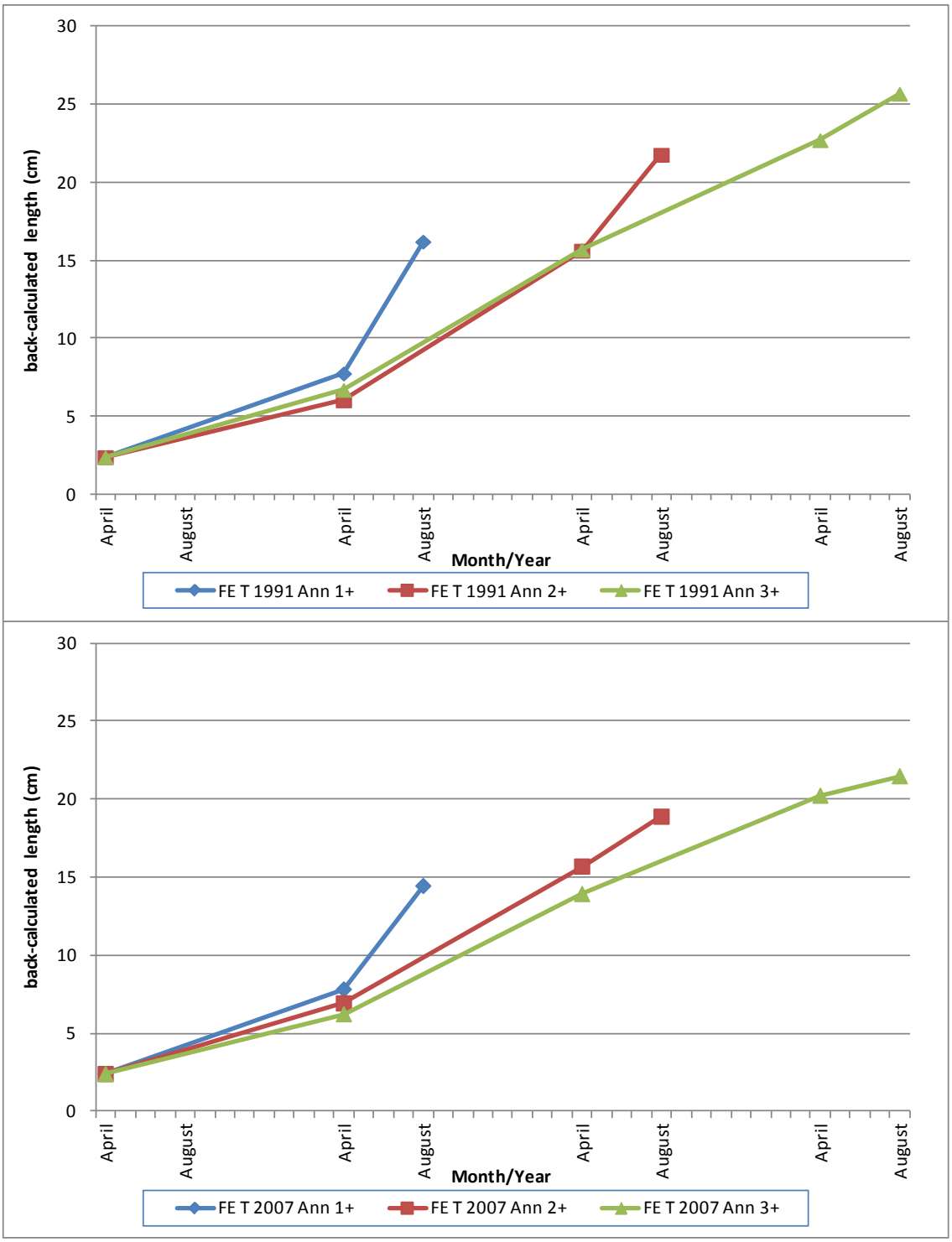

Figure 3.10: Annual and 'plus' back-calculated lengths for each age class of Feeagh resident brown trout for 1991 (top) and 2007 (bottom).

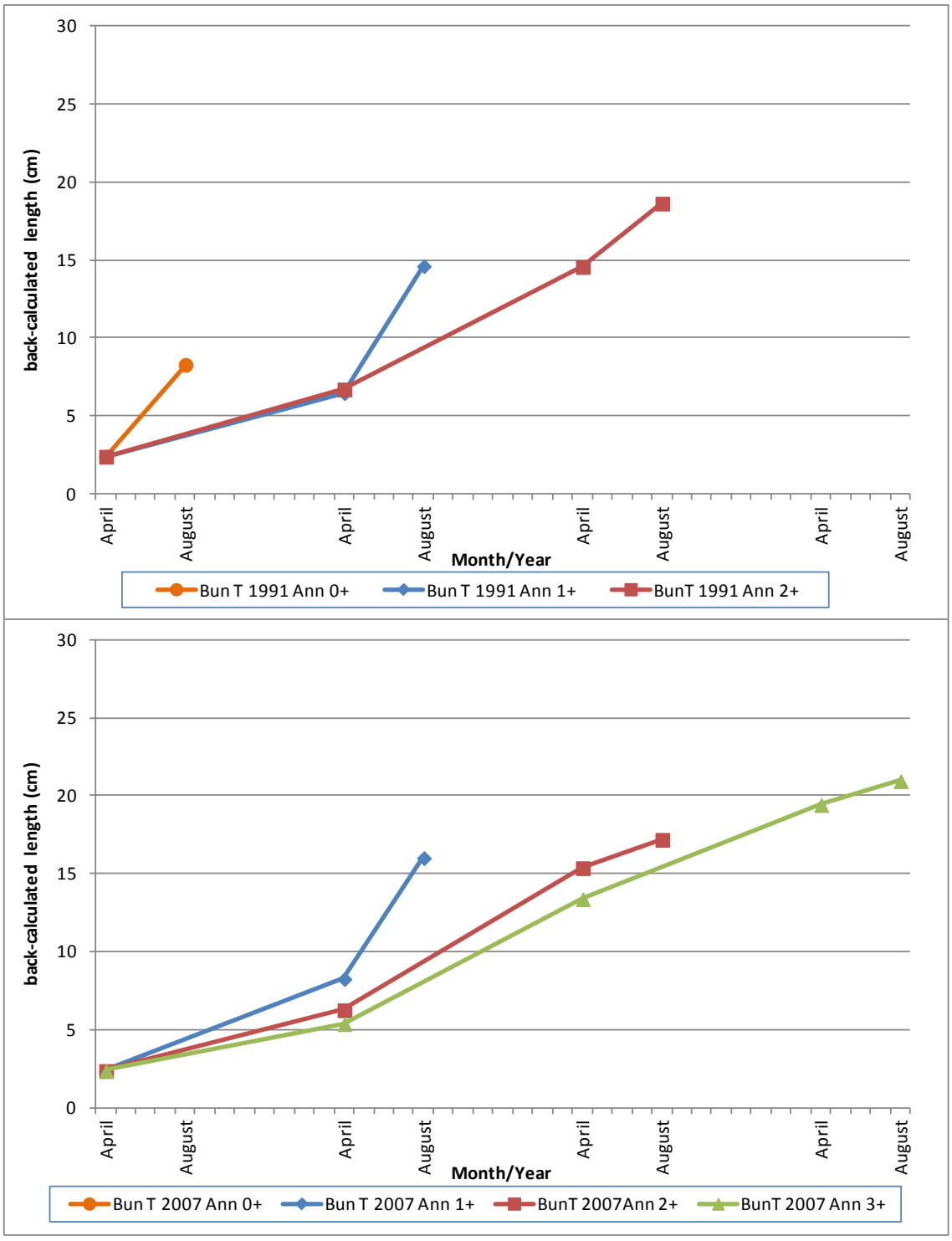

Figure 3.11: Annual and 'plus' back-calculated lengths for each age class of Bunaveela resident brown trout for 1991 (top) and 2007 (bottom).

Annual Growth – Sea Trout smolts

For sea trout smolts, the growth in Year 1 was significantly faster than growth in Year 2 (only 2+ and 3+ fish were included in this analysis, as the 4+ age class was small in the 1992 sample, and completely absent in the 2008 sample). There were no significant differences shown

between the two decades for Year 1 growth. Year 2 growth however, was found to be significantly higher in the 2008 sample when compared to 1992.

Growth was found to be significantly faster in 2+ smolts compared to 3+ smolts in both samples (Table 3.22). Figure 3.12 illustrate the annual back-calculated lengths of sea trout smolts in 1992 and 2008, the years following the trout samples taken from the lakes. Therefore, a 1+, 2+ or 3+ age class in the lake sample is the equivalent to a 2, 3 or 4 year old smolt age class in the following year.

Table 3.22: a) One way analysis of variance showing significant differences in annual growth between age classes in sea trout smolts. Two-way analysis of variance tables for b) Year One growth and c) Year Two growth.

a)	Source	df	Sum of Squares	Mean Square	F-ratio	P
	Age	2	108.72	54.36	16.42	<0.001
	Error	144	476.62	3.31		
	Total	146	585.33			
b)	**Source**	**df**	**Sum of Squares**	**Mean Square**	**F-ratio**	**P**
	Year	1	3.85	1.84	0.66	0.42
	Age	1	96.07	86.72	31.03	<0.001
	Year*Age	2	0.26	0.26	0.09	0.76
	Error	107	299.07	2.79		
	Total	110	399.25			
c)	**Source**	**df**	**Sum of Squares**	**Mean Square**	**F-ratio**	**P**
	Year	1	16.78	20.36	5.23	0.024
	Age	1	41.13	28.14	7.22	0.008
	Year*Age	2	3.34	3.34	0.86	0.357
	Error	107	416.8	3.89		
	Total	110	478.05			

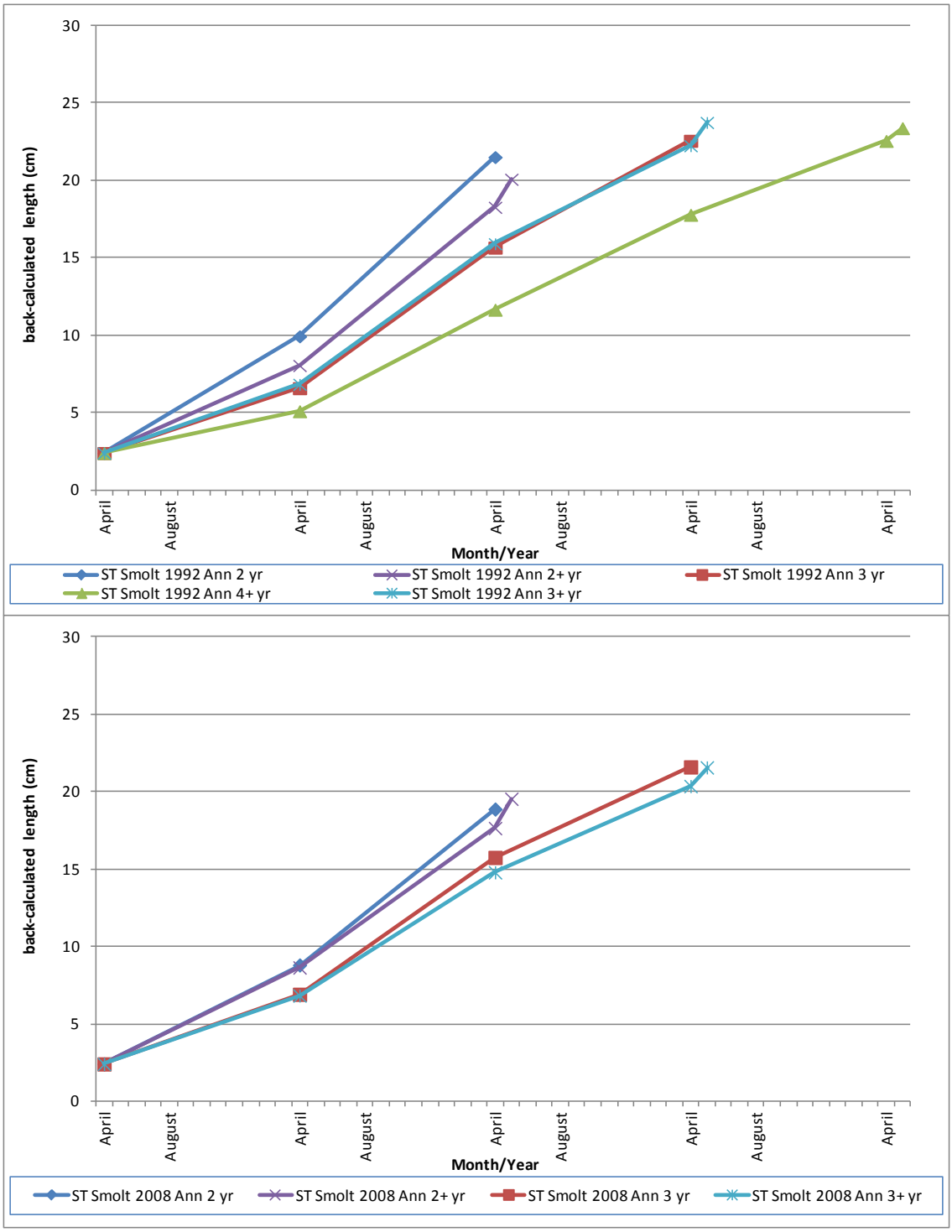

Figure 3.12: Annual and 'plus' back-calculated lengths for each age class of sea trout smolt for 1992 (top) and 2008 (bottom).

Seasonal Growth

Seasonal growth was back calculated in a similar fashion to annual growth. Growth in summer was significantly greater than in winter for all age classes in both lake trout (ANOVA $p < 0.001$) and smolts (ANOVA $p < 0.001$). Table 3.23 shows seasonal back calculated growth for all sites and years, with plus growth in italics.

Figures 3.13, 3.14 and 3.15 show average back-calculated growth curves, presented with both years for each age group, for each main age class of fish from L. Feeagh, Bunaveela L. and from the sea trout sample for each year examined. Figure 3.14 does not include a 3+ growth curve for L. Bunaveela due to only one 3+ fish in the sample.

Analysis was carried out on these growth curves using an analysis of covariance, Students t-test and unequal variance t-tests. The results of these tests are presented in Table 3.24, where the F value was found to be greater than the critical t-value, an unequal variance t-test was applied, in cases where the F-value was less than the critical t-value, a Student's t-test was used. For this analysis, fish of the same age class, both with and without "+" growth were grouped together, and the "+" portion of the growth was excluded from the analysis. Each year class, for example, referred to as 1+, 2+ etc, even though it may consist of 1 and 1+ fish, or 2 and 2+ fish.

The significant differences shown in Table 3.24 for Feeagh 3+ fish show that growth in 1991 was significantly higher when compared to 3+ growth in 2007 (Figure 3.13 bottom). For Bunaveela 1+ fish, growth in 2007 was significantly higher than growth in 1991 (Figure 3.14 top). Sea trout smolts showed no significant differences in seasonal growth rates for the two different sample years (Figure 3.15 and Table 3.24).

Figures 3.16 to 3.18 present the same data but with all the age classes presented together for each year. In Figure 3.18, smolts with plus growth (B-type) are presented separately to those without plus growth (A-type)

Table 3.23: Average back-calculated seasonal growth increments (cm) for all trout samples and all years

Back Calculated growth (cm)										
Age	**n**	**S 1**	**W 1**	**S 2**	**W 2**	**S 3**	**W 3**	**S 4**	**W 4**	**S5**
Feeagh Trout 1991 N = 73										
0+	1	*7.8*								
1+	36	6.10	1.66	*8.45*						
2	0									
2+	25	4.58	1.46	7.27	2.32	*6.14*				
3	0									
3+	11	5.18	1.53	6.67	2.31	5.05	1.97	*2.98*		
Feeagh Trout 2007 N = 82										
0+	0									
1+	26	6.16	1.65	*6.63*						
2	22	5.75	1.77	7.23	2.37					
2+	24	4.96	1.42	6.27	1.74	*3.19*				
3	4	4.17	1.39	5.42	2.19	5.66	2.20			
3+	6	5.33	1.35	5.95	1.81	3.88	1.38	*1.25*		
Bunaveela Trout 1991 N = 72										
0+	10	*8.29*								
1+	55	5.14	1.33	*8.14*						
2	0									
2+	6	4.73	1.56	9.75	2.19	*1.90*				
3	0									
3+	1	4.73	1.56	9.75	2.19	1.90	1.46	*3.51*		
4+	0									
Bunaveela Trout 2007 N = 63										
0+	0									
1+	4	6.68	1.62	*7.76*						
2	15	5.52	1.49	7.93	2.10					
2+	32	4.68	1.28	6.93	1.76	*1.82*				
3	1	2.74	0.87	5.05	1.82	4.28	2.54			
3+	10	4.34	1.25	6.31	1.81	4.42	1.54	*1.53*		
4+	1	4.69	1.82	5.87	2.33	3.36	1.64	2.49	*1.39*	
Sea Trout smolts 1992 N = 81										
2	8	7.97	1.97	8.57	3.01					
2+	26	6.38	1.68	8.44	1.78	*1.81*				
3	23	5.16	1.43	7.07	2.01	4.93	1.97			
3+	18	5.20	1.64	7.01	2.07	4.64	1.70	*1.50*		
4	4	3.96	1.00	5.23	1.56	5.33	1.64	3.39	1.78	
4+	2	4.14	1.23	4.74	1.36	3.01	1.43	2.73	1.25	*0.82*
Sea Trout smolts 2008 N = 34										
2	6	6.87	1.92	7.15	2.92					
2+	11	6.75	1.88	7.19	1.81	*1.89*				
3	11	5.35	1.54	6.49	2.35	3.96	1.89			
3+	6	5.36	1.46	5.98	1.98	3.98	1.59	*2.54*		
4	0									
4+	0									

Table 3.24: Results of growth curve analysis: analysis of covariance, Students t-test and unequal variance t-tests, where the F value was found to be greater than the critical t-value, an unequal variance t-test was applied, in cases where the F-value was less than the critical t-value, a Student's t-test was used.

Site	Age	F-value	critical t-value	t-test	df
Feeagh	1+	1.03	1.98	0.864	109
	2+	1.41	1.83	0.069	185
	3+	1.22	1.98	<0.001	124
Bunaveela	1+	6.42	2.13	0.002	15
	2+	1.14	2.04	0.675	30
Sea Trout smolts	2+	1.98	1.97	0.120	179
	3+	1.05	1.8	0.07	183

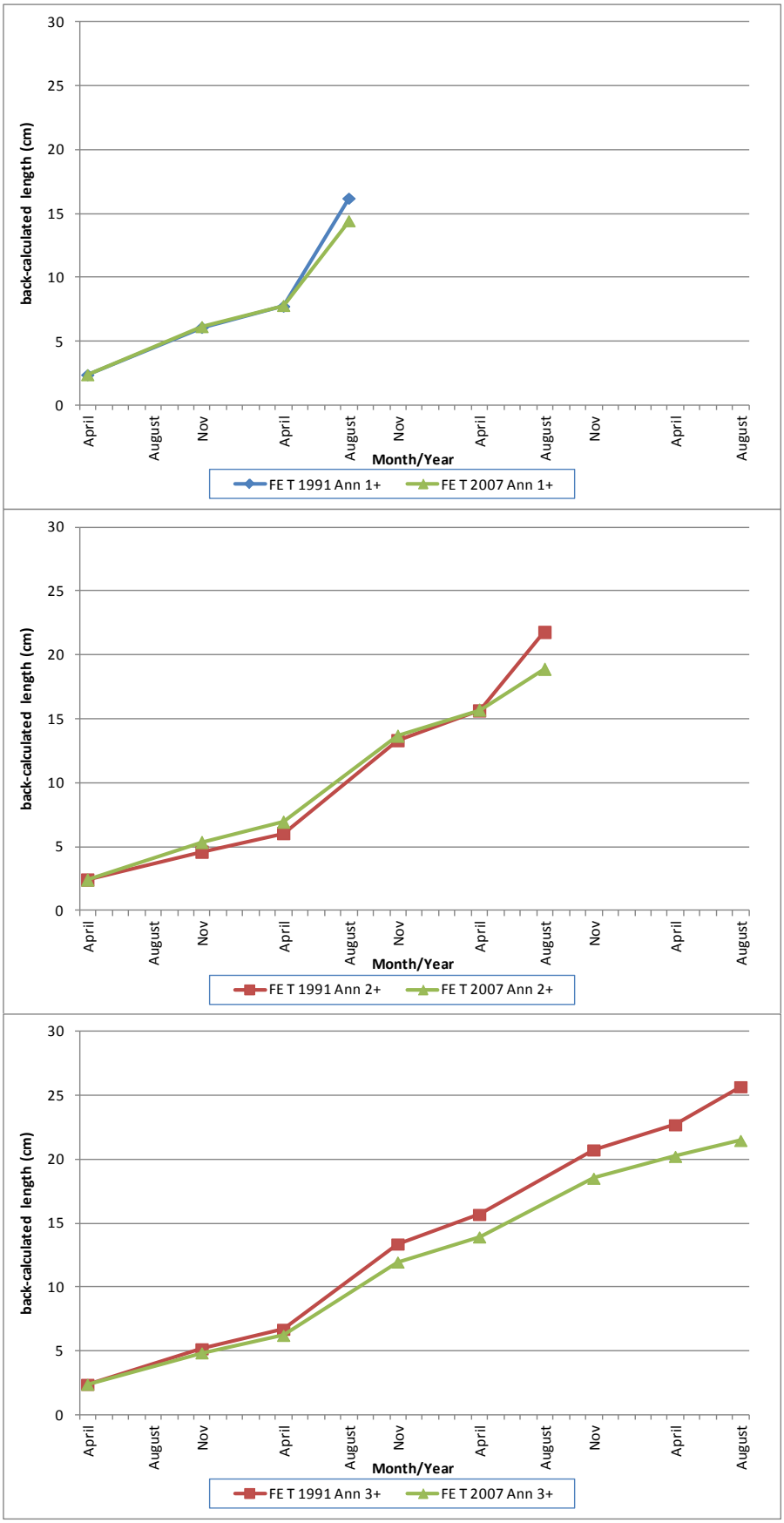

Figure 3.13: Seasonal 1+ growth (top), 2+ growth (middle) and 3+ growth (bottom) (significant changes between years-refer to Table 3.21) for fish of that age class taken from L. Feeagh in 1991 and 2007.

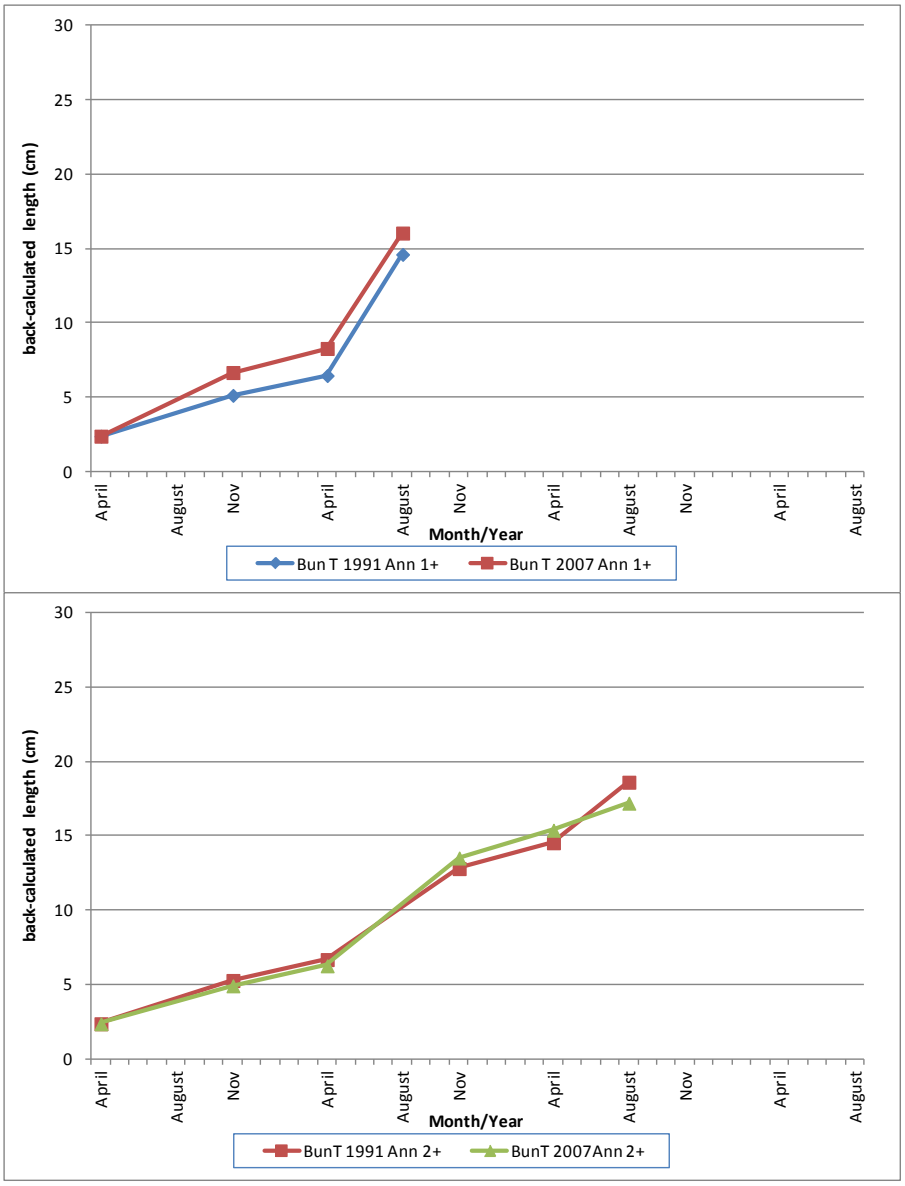

Figure 3.14: Seasonal 1+ growth (significant changes between years-refer to Table 3.21) (top), and 2+ growth (bottom) for fish of that age class taken from Bunaveela L. in 1991 and 2007.

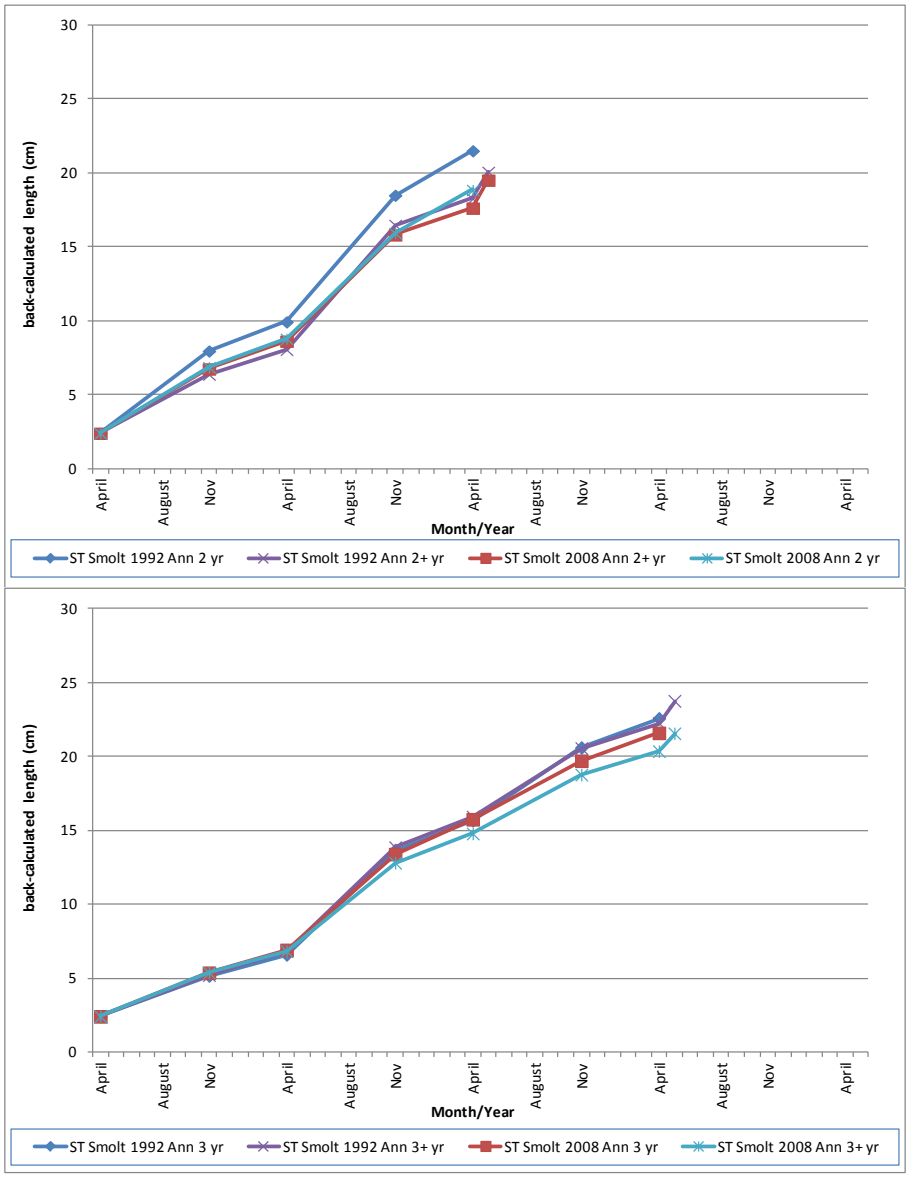

Figure 3.15: Seasonal 2+ growth (top) and 3+ growth (bottom) for sea trout smolts of that age class taken from fish traps in Burrishoole in 1992 and 2008.

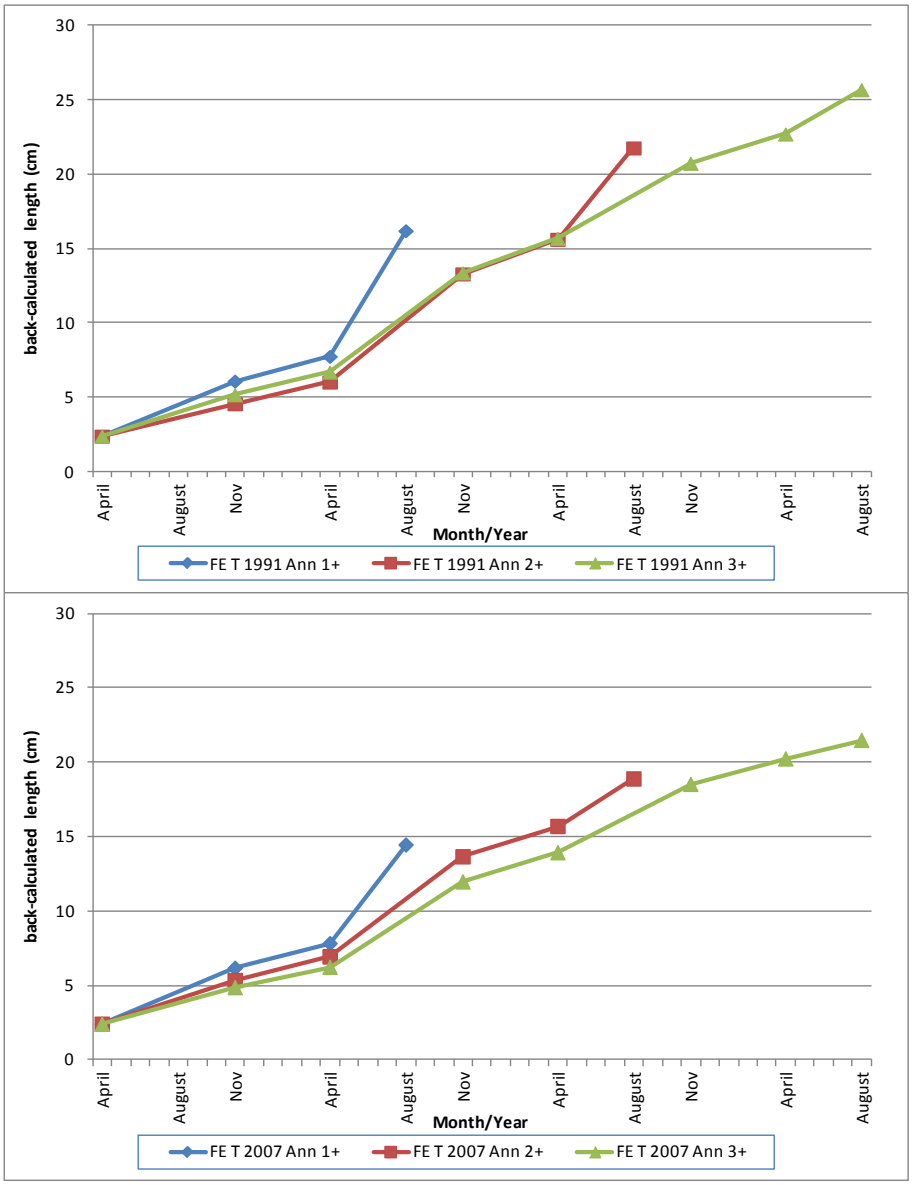

Figure 3.16: Seasonal growth for the three age classes of Feeagh trout in 1991 (top) and in 2007 (bottom).

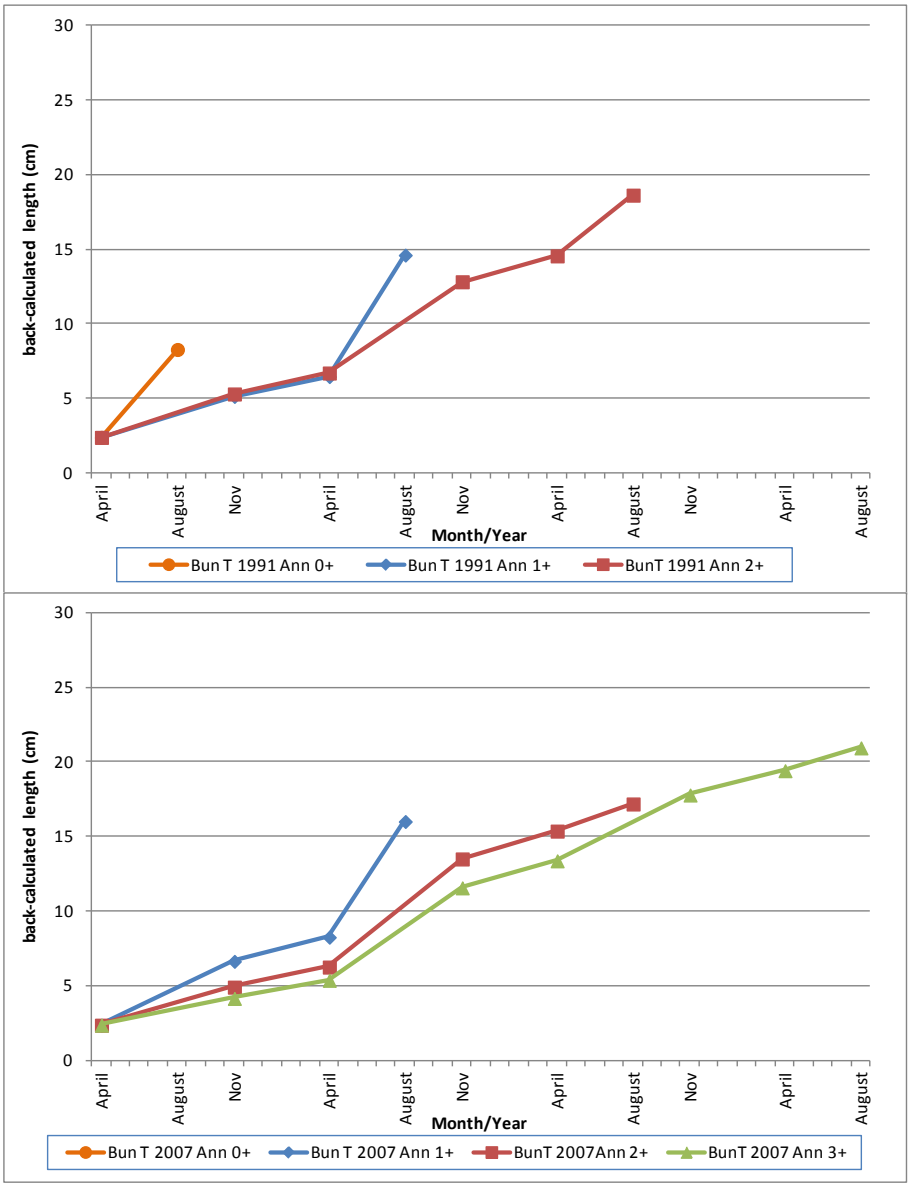

Figure 3.17 Seasonal growth for the three age classes of Bunaveela trout in 1991 (top) and, in 2007 (bottom).

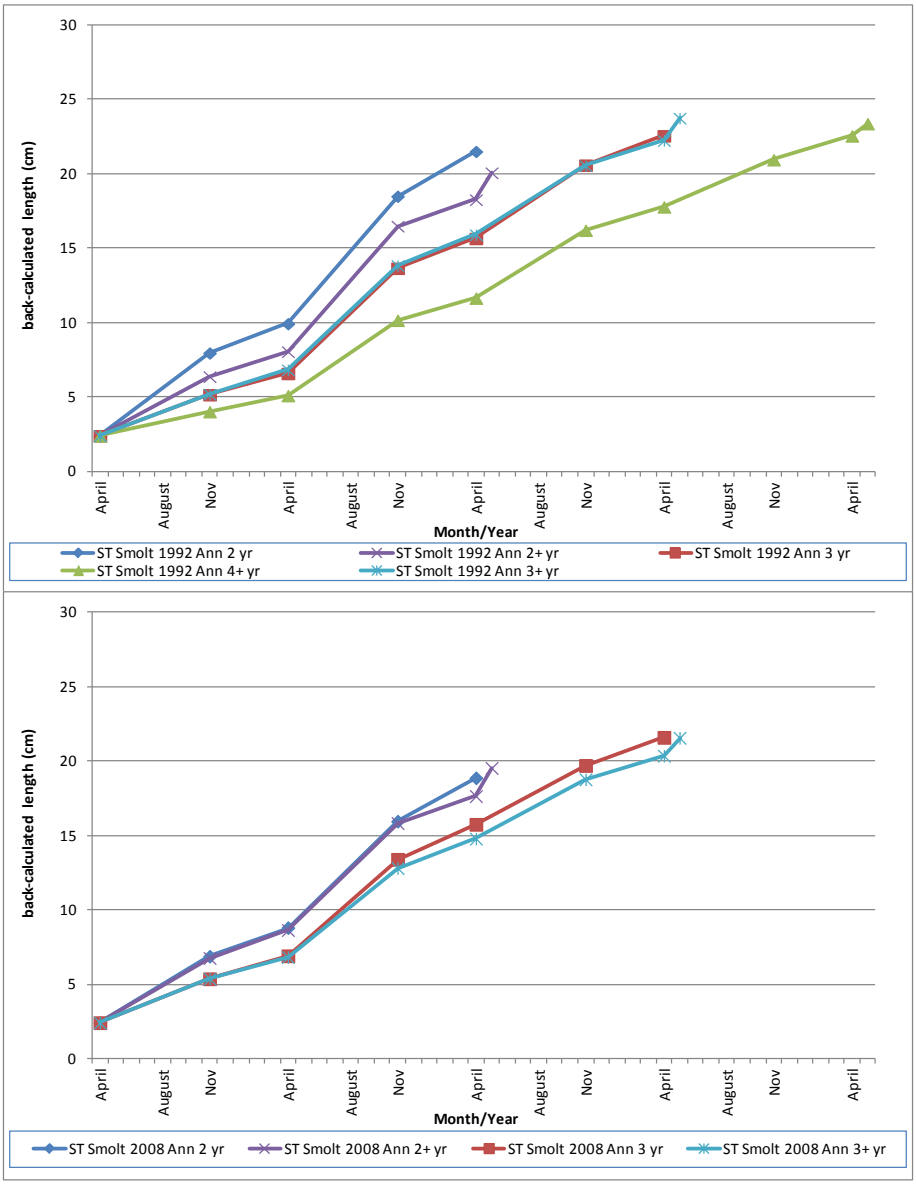

Figure 3.18: Seasonal growth for the three age classes (those with plus growth separately) of sea trout smolt in 1992 (top) and for the two age classes (those with plus growth separately) in 2008 (bottom).

Comparison between lake trout and smolt

The data from *lake trout (1991, 2007) and sea trout smolts from the following years (1992, 2008)* were examined to investigate whether differences in growth rates showed between those fish living as residents in the lakes and those that migrated as smolts. Lough Feeagh and the sea trout smolts were compared with each other (Table 3.25; Figure 3.19).

Table 3.25 shows differences in growth rates for the different seasons between resident and sea trout populations in the Burrishoole catchment. Sea trout smolts grow slightly faster than the resident trout of the same age, although this trend was not significant. 4/4+ sea trout smolts in the 1992 are one exception to this, albeit with a small sample size.

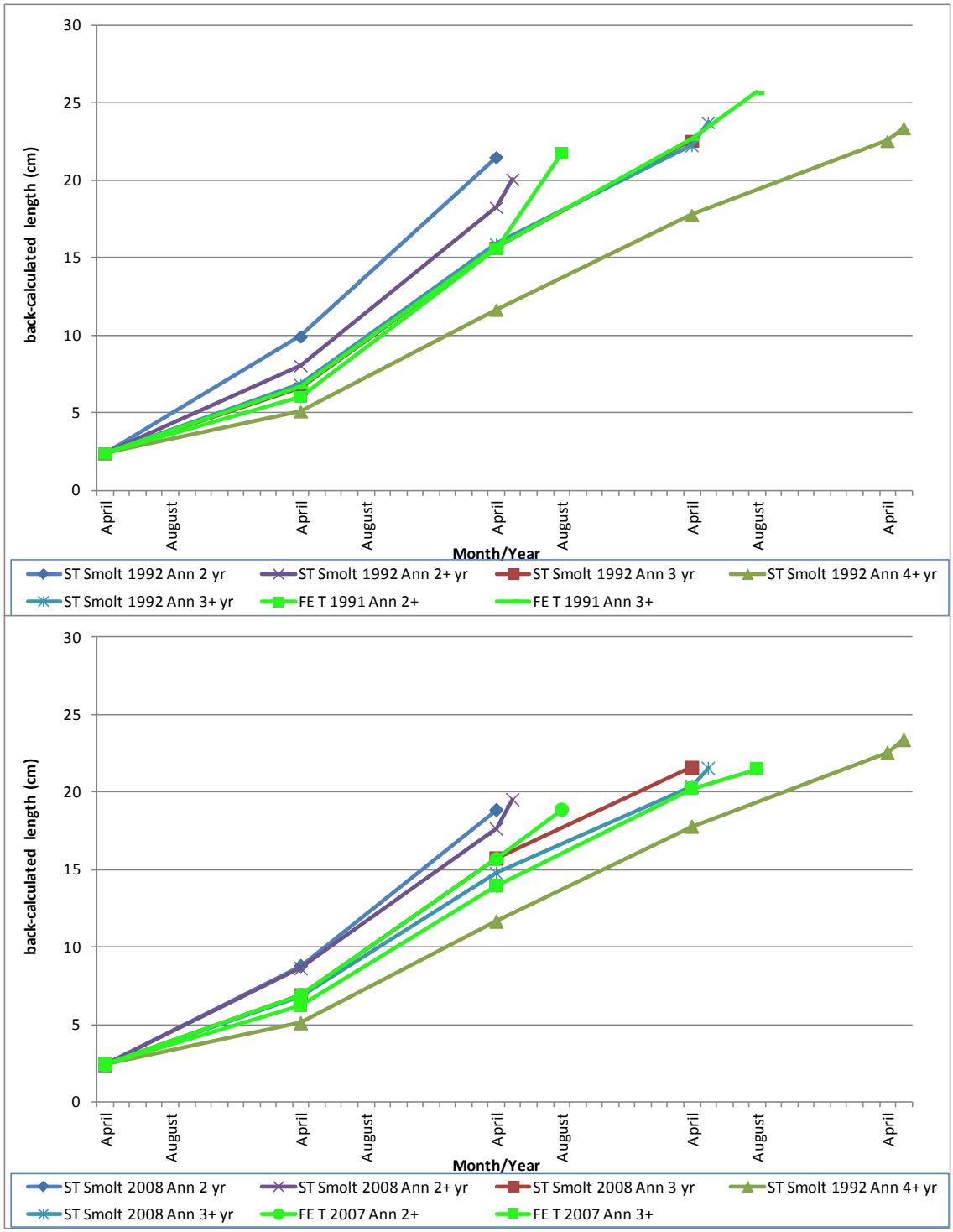

Figure 3.19: Annual and 'plus' back-calculated lengths for each age class of sea trout smolt for 1992 (top) and 2008 (bottom) and 2+ and 3+ 'resident' Feeagh trout, 1991(top) and 2007 (bottom).

Table 3.25: average seasonal growth for the different ages of brown trout in Lough Feeagh compared to seasonal growth of sea trout smolts moving through the traps in the following spring.

1991/1992	Feeagh	Smolts		Feeagh	Smolts		Feeagh	Smolts	
Age	**1+**	**2**	**2+**	**2+**	**3**	**3+**	**3+**	**4**	**4+**
n	36	8	26	25	23	18	11	4	2
S 1	6.1	7.97	6.38	4.58	5.16	5.2	5.18	3.96	4.14
W 1	1.66	1.97	1.68	1.46	1.43	1.64	1.53	1	1.23
S 2	*8.45*	8.57	8.44	7.27	7.07	7.01	6.67	5.23	4.74
W 2		3.01	1.78	2.32	2.01	2.07	2.31	1.56	1.36
S 3			*1.81*	*6.14*	4.93	4.64	5.05	5.33	3.01
W 3					1.97	1.7	1.97	1.64	1.43
S 4						*1.5*	*2.98*	3.39	2.73
W 4								1.78	1.25
S 5									*0.82*
2007/2008	**Feeagh**	**Smolts**		**Feeagh**		**Smolts**			
Age	**1+**	**2**	**2+**	**2**	**2+**	**3**	**3+**		
n	26	6	11	22	24	11	6		
S 1	6.16	6.87	6.75	5.75	4.96	5.35	5.36		
W 1	1.65	1.92	1.88	1.77	1.42	1.54	1.46		
S 2	*6.63*	7.15	7.19	7.23	6.27	6.49	5.98		
W 2		2.92	1.81	2.37	1.74	2.35	1.98		
S 3			*1.89*		*3.19*	3.96	3.98		
W 3						1.89	1.59		
S 4							*2.54*		

Circuli Counts

Circuli are the bands laid down by fish on their scales during periods of growth. Table 3.26 shows seasonal circuli counts for all seasons across all years and sites sampled. Counts for summer circuli were significantly higher for summer counts than for winter counts in all cases (ANOVA, $p = <0.001$). Similarly, growth in the second summer was significantly higher than growth in other summers (ANOVA, $p = <0.05$).

A Bonferroni pairwise analysis of data showed that the only significant differences between the same season for different groups was between Winter 2 growth which was significantly higher in the 1992 sea trout smolts than the 1991 Feeagh brown trout sample.

Table 3.26: seasonal scale circuli counts for all seasons across all years and sites sampled

	N	Mean circuli count	St dev		N	Mean circuli count	St dev
Feeagh 2007				**Feeagh 1991**			
Summer 1	82	12.8	4.4	**Summer 1**	76	12.9	4.5
Winter 1	82	5	1	**Winter 1**	76	5.1	1
Summer 2	57	14.6	3	**Summer 2**	42	15.7	3.3
Winter 2	56	5.6	1.1	**Winter 2**	38	6.2	1.5
Summer 3	10	10.4	2.6	**Summer 3**	11	10.7	2.4
Winter 3	10	4.8	1.1	**Winter 3**	11	5.5	1.3
Bunaveela 2007				**Bunaveela 1991**			
Summer 1	64	12	4.6	**Summer 1**	64	11.8	4.7
Winter 1	64	4.6	1	**Winter 1**	64	4.5	1
Summer 2	59	15.6	3.2	**Summer 2**	7	14	3.5
Winter 2	59	5.4	1.5	**Winter 2**	7	5.3	1.8
Summer 3	12	10.2	2.6	**Summer 3**			
Winter 3	12	4.6	0.8	**Winter 3**			
Sea Trout smolts 2008				**Sea Trout smolts 1992**			
Summer 1	35	13.1	4.1	**Summer 1**	86	12.5	4.4
Winter 1	35	5.3	1.4	**Winter 1**	86	4.9	1
Summer 2	35	14.4	4	**Summer 2**	86	16	3.9
Winter 2	35	6.1	1.5	**Winter 2**	86	5.5	1.3
Summer 3	17	9.3	3.7	**Summer 3**	49	10.9	2.9
Winter 3	14	4.7	1.1	**Winter 3**	45	5	1.2
Summer 4				**Summer 4**	7	8.5	1.9
Winter 4				**Winter 4**	6	4.8	1.2

3.6.4 Discussion on Trout Growth

In Burrishoole, trout are present in both resident and migratory forms. The migrants move to the sea to feed, while the residents remain in freshwater. Resident individuals usually become mature at the parr stage, while the migratory individuals mature later after undergoing smoltification and a growth period in the sea. Parr maturity is linked to growth rate, and therefore indirectly related to temperature (Jonsson and Jonsson, 2009). Anadromy in trout populations also increases with increasing latitude, possibly because of better feeding opportunities in the marine environment. This is a situation which could be influenced by future climate change (Jonsson and Jonsson, 2009).

The pattern of divided smolt migration to the sea when combined with the pattern of divided adult return to freshwater to spawn for the first time as maiden fish and then again as repeat spawners is far more robust than that of the salmon because it is better able to spread the risks to survival across a greater number of year classes and cohorts of fish. It is therefore potentially better able to withstand and recover from any short-term factors affecting survival in the river and in the sea (Harris and Milner, 2006).

There has been a significant change in the numbers of sea trout smolts migrating from the Burrishoole catchment. Sea trout smolt output has fallen from 4000+ pre-1985 to an average of ~700 in the last decade (Poole et al., 2007). This decline would have resulted in a concurrent change in fish density in the freshwater environment which could influence trout growth rate and smolt age. This makes a comparison between years and with other environmental factors difficult.

Comparison of growth of smolts and resident trout from Lough Feeagh in Burrishoole showed two and three year old smolts to be consistently larger at each age class (Poole et al., 1995; Current study). This would appear to contradict the hypothesis that smolts are largely derived from slower-growing parr unable to maintain territories and therefore undergo density-dependent downstream migration (Jonsson and Jonsson, 2009). However, Bohlin et al. (1994) also showed smolts to be longer and heavier than either mature male parr or immature parr 1 year in advance of smoltification and Elliott (1994) concluded that it is the larger, faster-growing fish in each cohort that actively migrate downstream as smolts.

The mechanisms determining the size and age at which salmonids smoltify and migrate to sea remain unresolved. For Atlantic salmon, Elson (1957) claimed that parr must attain a minimum length of 10cm by autumn in order to smoltify the following spring. Physiological studies (Wright et al., 1990; Skilbrei, 1991) provide supporting evidence that the 'decision' to smoltify is taken the previous autumn. Jonsson (1985) found growth rate, rather than absolute size, to be more effective in determining smolt age. An examination of the Burrishoole smolt data would also point towards growth rate rather than absolute size as a key factor in triggering smoltification.

Elliott (1994) recorded a slight decrease in the mean smolt age of trout from Black Brows Beck (UK) over a twenty year period. Similar trends in some Irish and Scottish populations have been attributed to increased growth due to milder winter conditions and a prolonged feeding period, and to increased abundance of prey through agricultural enrichment (Fahy, 1978; Pratten and Shearer, 1983). While the current Burrishoole study has not shown any significant increases in growth rate in trout smolts, there is an indication that smolt age may be reducing, with a higher percentage of 2/2+ smolts in the 2008 sample together with an absence of 4/4+ smolts, although this is highly variable between years (Poole et al., 2007).

It was proposed that age, length and growth rate may vary significantly from one location to another and from year to year, this result is supported by the results of this study. These

variations are affected by a number of environmental factors such as temperature, food supply and growing season (Fahy, 1985).

Age at smolting is influenced by parr growth and size. Fast growers tend to smolt at an earlier age and at a smaller size than more slow growing individuals from the same populations (Strothotte et al., 2005). The effects of water temperature on smolt age and size are mediated through variation in growth rate, although smolt size may be more directly associated with water temperature (Jonsson and Jonsson, 2009). Salmon smolts growing in rivers which empty into relatively warm sea water are generally smaller than those smolts entering colder sea water, thought to be partly due to the fact that ionic regulation in cold sea water is easier for larger than for smaller fish (Jonsson and Jonsson, 2009). Even though growth rate is temperature dependent, there may be some confounding factors such as fish density and feeding opportunities.

S. trutta are a partially migratory species, i.e. populations are split into resident and migratory individuals. The migrants move to sea to feed, while the residents remain in fresh water. Resident individuals usually become mature at the parr stage, while the migratory individuals mature later. Parr maturity is linked to growth rate, and therefore indirectly related to temperature (Jonsson and Jonsson, 2009). Anadromy in trout populations also increases with increasing latitude, possibly due to improved feeding opportunities in the marine environment as you move northwards. This is a situation which could be influenced by future climate change (Jonsson and Jonsson, 2009).

Fahy (1985a) reported that a threshold size for smoltification also exists in brown trout (*S. trutta*), but that this threshold varied among different populations. Smolt size has also been demonstrated to increase with increasing latitude (L'Abée-Lund et al. 1989). A comparative study of smolt age and size in both Atlantic salmon and brown trout was carried out by Økland et al. (1993) who concluded that smolt age and size were found to be more variable in trout than in salmon and that smolt age increased with decreased growth rate, consistent with the idea of a threshold size. In all four of the trout stocks studied (Økland et al., 1993), slow-growing, older smolts were larger at the time of migration than were fast-growing younger smolts. Therefore, as in Burrishoole, faster growing parr were undergoing smoltification earlier and at smaller sizes than slower growing parr, thus negating the threshold theory.

Elliott (1994) recorded a slight decrease in the mean smolt age of trout from Black Brows Beck. Similar trends, observed in some Irish and Scottish populations, have led to suggestions

of increased growth due to milder winter conditions and prolonged feeding period, and increased abundance of prey items through agricultural enrichment (Fahy 1978; Pratten and Shearer 1983). While this study has not shown any significant increases in growth rate, there is an indication that smolt age is reducing, with a higher percentage of 2/2+ smolts in the 2008 sample, and an absence of 4/4+ smolts.

Table 3.27 shows the critical temperatures for juvenile trout in freshwater at different stages of their life history. These temperatures are likely to be exceeded in the coming century, having a negative impact on the survival of trout in the Burrishoole catchment. However, in the shorter term, warmer winters and longer growing seasons will most likely have a positive effect on trout growth in the Burrishoole catchment. In this scenario, it would be expected that growth rates for trout would increase for all seasons, with the largest change being seen in rates of winter growth. This would be expected to have the knock-on effect of reducing the average age of sea trout smolts migrating out of the catchment.

Table 3.27: Critical temperatures for juvenile brown trout, *Salmo trutta*.

Parameter	Reference	Temperature (°C)
Feeding	Elliot (1991)	7-22.5
Seek shelter	Gardiner (1984)	<9
Hatching temp	Crisp (1981)	1.9-11.2
Egg mortality	Peterson et al. (1977)	<4
Upper incipient lethal temp.	Elliot (1994)	24.7
Upper Critical Range	Elliot (1994)	19-30
Lower Critical Range	Elliot (1994)	0-4
Smolt run range	Byrne et al. (2004)	5-13

Changes in flow regime can also impact on growth and survival of trout in the catchment when it comes to factors such as hatching, migration and feeding. There is a positive relationship between water flow and the survival of eggs and 0+ salmon, during both summer and winter (Gibson and Meyers, 1998). Extremes in flow can however affect salmonid fry survival negatively, for example, a study by Jensen and Jonsson (1999) found that years with high discharge during the alevin stage negatively affected survival in a Norwegian river. Low discharge at the time of emergence has also been found to affect survival (Elliott, 1985). Droughts that prevent adult resident sea trout from reaching their spawning grounds may have a constraining effect on recruitment (Jonsson and Jonsson, 2009).

3.7 Growth of European Eel *Anguilla anguilla*

3.7.1 Introduction

Since the 1980s, stocks of the European eel *Anguilla anguilla* (L.), have been in serious decline, with recruitment decreasing by approximately 90-95% over the past 25 years, compared to the 1970s (Dekker, 2003; ICES, 2010). Several possible causes have been suggested for this decline, including overfishing, habitat reduction, organic chemical poisoning, parasites, and larval migration failure due to ocean climate factors (Castonguay et al., 1994; ICES, 2009). All glass eel recruitment series demonstrate a clear decline since the early 1980's. For the different areas (Baltic, North Sea, Atlantic, British Isles and Mediterranean), levels have dropped to between 1 and 9% of 1970's levels (ICES, 2009). Such a large scale decrease over such a large number of recruitment indices across Europe would seem to indicate that broader meteorological or climatic change might be responsible. Such a change could also affect both the larval survival in the ocean and adult growth in freshwater by altering the conditions needed by the species to grow and migrate.

The latest scientific advice from the International Council for the Exploration of the Sea (ICES) concerning European eel was that the stock is outside safe biological limits and that current fisheries are not sustainable. ICES have recommended that a recovery plan be developed for the whole stock of European eel as a matter of urgency and that exploitation and other human activities affecting the stock be reduced to as close to zero as possible. Ireland established a National Working Group on eel management in 2006, in advance of the agreement of the Regulation (EC) No. 1100/2007 in order to begin the preparatory work required. Eel Management Plans were submitted to the European Union in June 2009 and these have been approved. Ireland has implemented its Eel Management Plan.

3.7.2 Glossary of Terms and European Eel Life Cycle

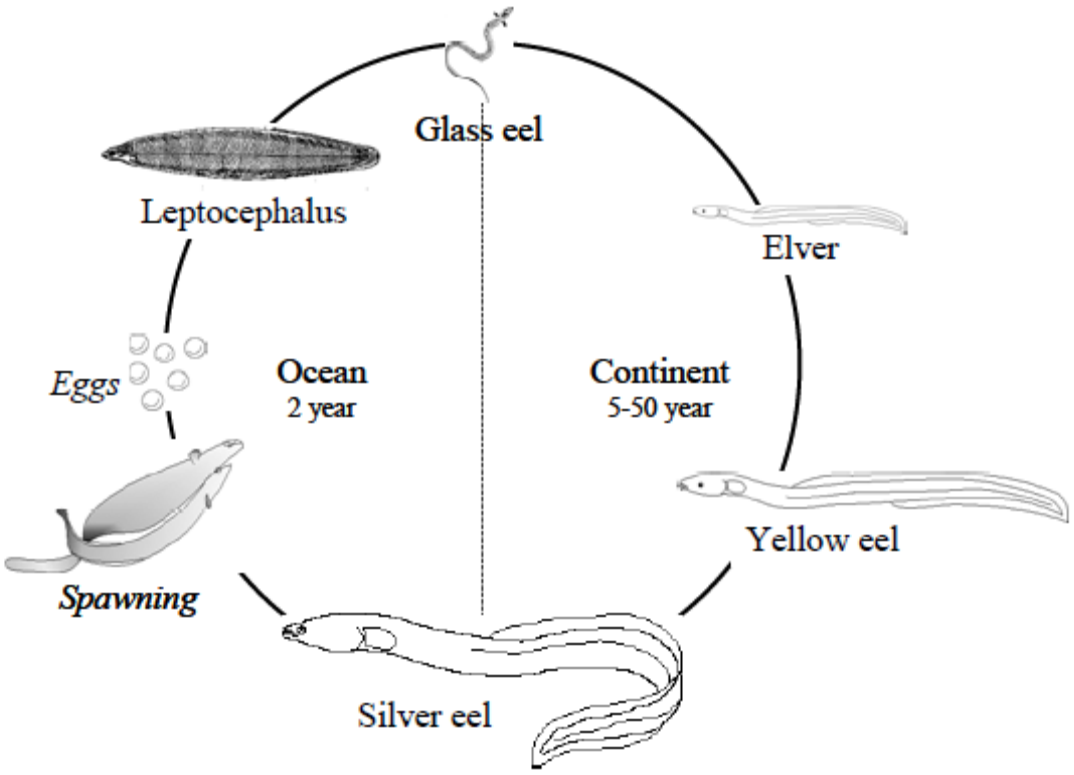

Glass eel: Young, unpigmented eel, recruiting from the sea into continental waters
Elver: Young eel, in its 1st year following recruitment from the ocean.
Bootlace: Intermediate sized eels, approx. 10–25 cm in length. These terms are most often used in relation to stocking. The exact size of the eels may vary considerably.
Yellow eel: Life stage resident in continental waters. Often defined as a sedentary phase, but migration within and between rivers, and to and from coastal waters occurs. This phase encompasses the elver and bootlace stages.
Silver eel: Migratory phase following the yellow eel phase. Eel characterized by darkened back, silvery belly with a clearly contrasting black lateral line, enlarged eyes. Downstream migration towards the sea. This phase mainly occurs in the second half of calendar years, though some are observed throughout winter and following spring.

Figure 3.20: The life cycle of the European eel, *Anguilla anguilla*, the names of the major life stages are indicated (after Dekker).

3.7.3 Methods

Yellow eels were collected by fishing using fyke nets from Lough Furnace, the most downstream tidal lough in the catchment, in 1988 and 2007. Silver eels were collected from the Salmon Leap and Mill Race fish traps during the silver eel runs of 1987, 1988 and 2007.

Otoliths were extracted following the methods described in the ICES Eel ageing manual (2009). Extracted otoliths were then prepared for ageing by cutting and burning, before being

mounted in clear silicone on a glass slide (as described in the ICES Eel ageing manual, 2009) Prepared samples were placed under a stereo microscope (Olympus SZX 12) which was connected by camera (1.4 MP monochrome Q-cam) to a computer. Images of the prepared otoliths were taken using Image Pro-plus v.6 software which was also used for annual growth measurements. Any questionable otoliths were independently aged by a second reader, as well as a random 10% of the sample, to confirm the primary reader's value.

Annual growth increments were measured by measuring from the end of a dark winter band to the end of the next winter band, along the axis of widest growth (Figure 3.21). Age and growth measurements did not include the oceanic phase of the life cycle, with ageing and growth measurement commencing from the "zero band", as defined in the ICES Eel ageing manual (2009).

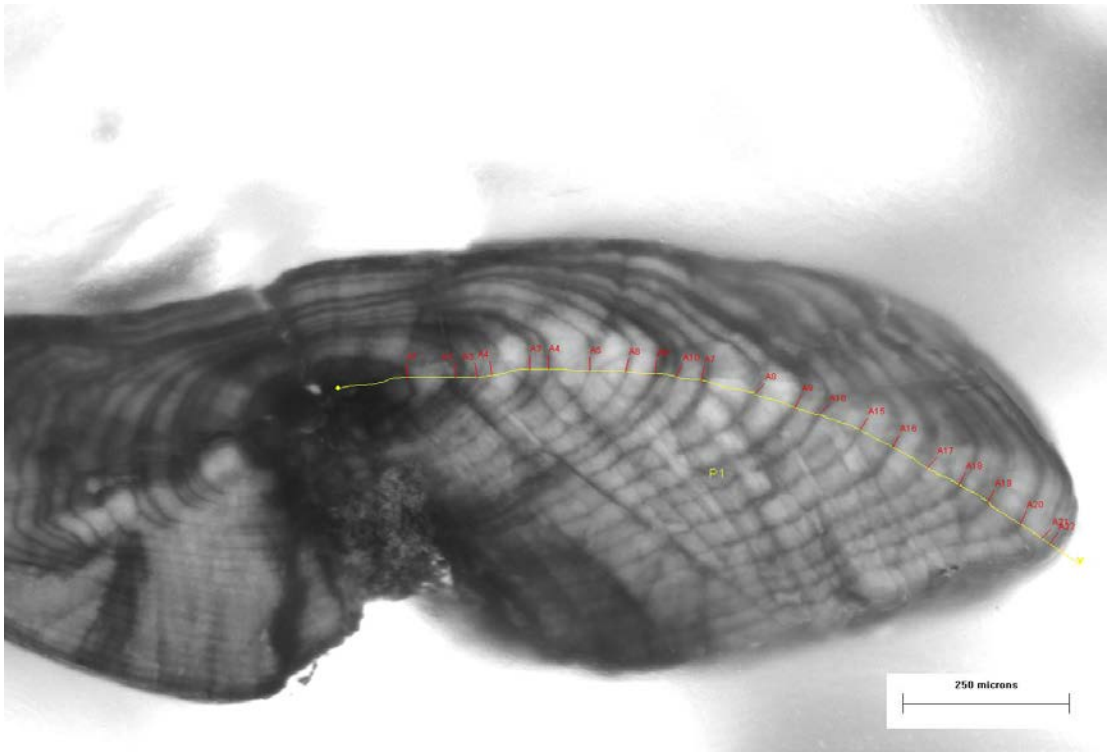

Figure 3.21: showing an image of a cracked and burnt eel otolith with annuli marked in red.

Silver eel data were split into female and male groupings for further analysis. For silver eels annual growth increments for each year were averaged, from which the average annual incremental growth was calculated according to the Dahl-Lee formula:

$a = i \times L/I$ **Equation 3.2**

Where,

a = the calculated length increment

i = distance between the bands measured on scales

I = ∑ i for the individual

L = total length of the individual

Average expected growth was calculated using the von Bertalanffy (1957) growth equation along with standard deviation:

$lt = L\infty(1-e^{-K(t-to)})$ **Equation 3.3**

Where,

lt = length at any time t

L∞= maximum size towards which the length of the fish is tending

K = a measure of the rate at which length approaches L∞

to = parameter indicating the (hypothetical) time at which the fish would have been zero size if it had always grown according to the von Bertalanffy equation

For each eel the back-calculated (Dahl-Lee) annual increment and von Bertalanffy expected growth were calculated. The first five years growth in each eel were taken and linked back to their corresponding calendar year of growth. These data were then plotted along with confidence interval against the expected average growth. All values falling outside the standard deviation around the expected growth were counted as being examples of years which showed greater or less than expected growth. These counts were then run through a Monte-Carlo simulation.

A Monte-Carlo simulation was used to accommodate possible error in ageing of the fish in their first five years. It was assumed that readings of the growth rings had a maximum error of either ± 3 calendar years. A triangular frequency distribution was placed around this error with the most likely defined as no error, and a Monte-Carlo simulation of 10,000 trials was run on the count data. The mean and standard deviations of these errors were monitored for each

year to calculate how many instances of growth above and below the standard expected growth occurred in each year.

Annual growth increments of yellow eels were calculated in a similar manner, but the yellow eel sample was not split by sex due to the uncertainty of sexing yellow eels and the length bias of the fine nets used. Owing to this standard deviation bounds around the calculated expected average growth for yellow eels were extremely wide and contained almost all individual growth. In order to allot some instances of exceptional growth, individual eel von Bertlanffy growths were compared with the average von Bertlanffy growth and standard deviations.

3.7.4 Results

The data were tested for normality and after growth back-calculations were carried out and were found to be approximating normality in all cases. Data for silver eels was then split by sex. The first five years growth were ordered chronologically and examined to see where annual growth exceeded the standard deviations expected, either in terms of reduced or greater growth for that chronological year. These results were then run through a Monte Carlo analysis to reduce the impact of any possible ageing errors (a cause for concern due to the unpredictable patterns of growth experienced with European eel and a difficulty in clearly identifying the outermost annulus on the otolith). However, by using only the first five years growth, traditionally seen as more reliable to age conclusively when compared to later, slower years of growth and because it is more likely to be comparing like with like as the eels are thought to be resident mostly in the lower reaches of the catchment during this period, and the Monte Carlo analysis, any possible ageing errors were thought to be kept to a minimum.

For female silver eels, the average length is similar in all years studied, though the average age seems to be less in the more recent sampling year. This corresponds with the indication of increasing average length at 5 years in the 2007 sample. Male silver eels also appear to be decreasing slightly in age, with varying average lengths across the years sampled. Average length at 5 years also seems to have increased in the most recent sample (2007), possibly due to one large growth measurement (Table 3.28).

Yellow eels overall seem to show more variation, possibly due to the mixture of sexes in the sample.

Table 3.28: showing sample sizes, average ages, lengths and ranges for all eels sampled.

Silver Eels	n	Average age	Age Range	Average Length (cm)	Length Range	Average Length at 5 years (cm)	Length at 5 years Range
Female							
1987	29	32	21 - 58	52.1	43.1 - 82.9	11.58	6.7 - 19.49
1988	45	33	18 - 54	52.3	42.3 - 84.3	12.57	7.35 - 24.07
2007	78	29	16 - 44	52.2	43.6 78.5	13.47	6.38 - 23.15
Male							
1987	12	23	13 - 35	39.5	34.9 - 43.4	14.96	8.94 - 21.4
1988	28	24	11 - 36	41.3	32 - 52	14.92	7.24 - 31.61
2007	59	19	8- 40	36.0	31.8 - 45.4	19.44	7.98 - 44.65
Yellow Eels	**n**	**Average Age**	**Age Range**	**Average Length (cm)**	**Length Range**	**Average Length at 5 years (cm)**	**Length at 5 years Range**
1987	24	21	15 - 38	45.45	30.1 - 86.2	13.03	8.8 - 22.9
1988	25	19	12 - 42	43.85	37.1 - 81.3	13.22	6.7 - 21.45
2007	19	16	13 - 29	37.15	30.1 - 50.8	13.5	9.06 - 19.0
2008	32	18	10 - 25	43.47	34.4 - 63.8	15.07	8.21 - 24.31

Figures 3.22 to 3.24 show the number of fish that grew more than the average amount for their particular samples (all years combined), with Figure 3.22 showing female silver eels, Figure 3.23 showing male silver eels and Figure 3.24 showing yellow eels.

Part a) for each of the figures gives the mean back-calculated growth and predicted von Bertlanffy growth curves of eels in their first 5 years for all fish. Part b) in each Figure shows mean back-calculated growth and predicted Von Bertlanffy growth curves of eels for their lifetime in freshwater. Part c) shows the mean count of predicted Dahl Lee eel size above and below 1 standard deviation unit of the von Bertlanffy predicted growth in their first 5 years. The ages of the fish were varied by ± 3 years in 10,000 Monte Carlo trials. Part d) of each Figure gives the proportion of back-calculated growth size above and below one standard deviation unit of the von Bertlanffy predicted growth in their first 5 years with ageing of fish ranged by ± 3 years in 10,000 Monte Carlo trials.

Figure 3.22d shows an increase in the proportion of female silver eels growing more than would be expected in the first five years of growth for those fish that experienced that portion of their lifestage from 1990 onwards. The line flattens out at approximately 2000 as no female silver eels were young enough to have had their first five years of growth after the year 2000.

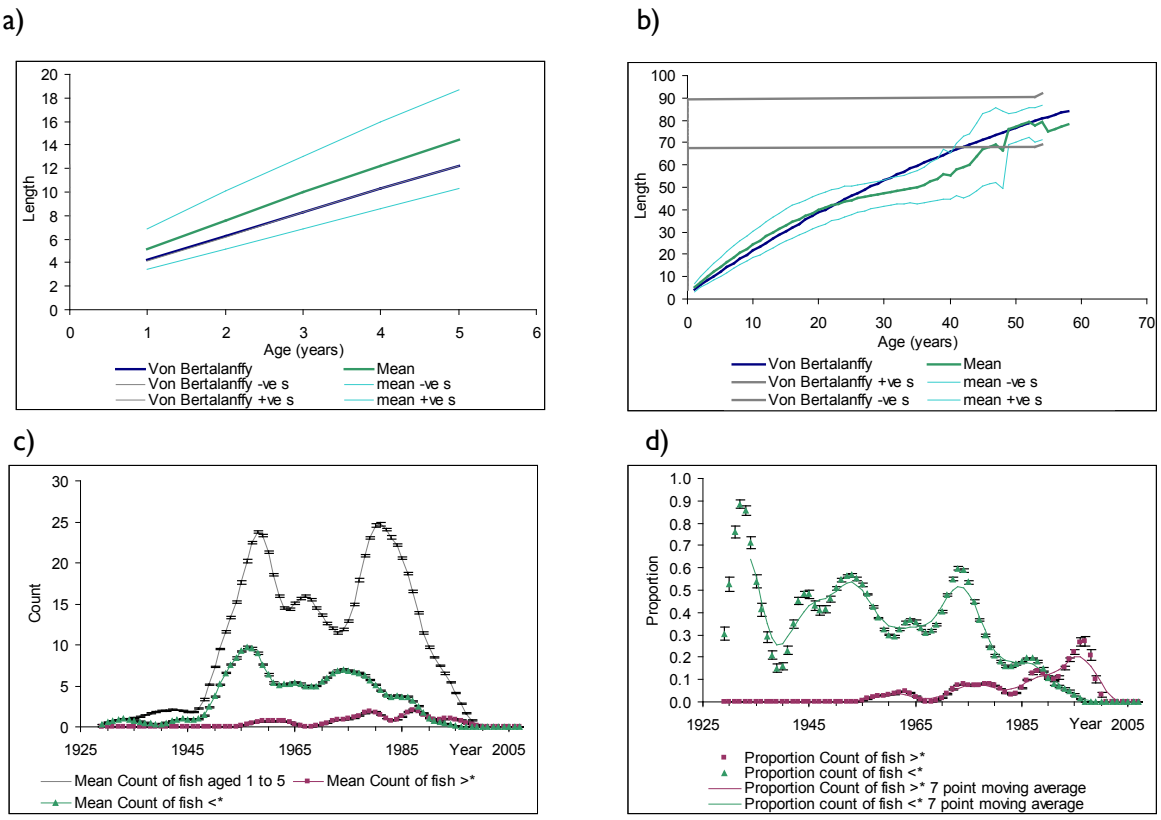

Figure 3.22: a) Mean back-calculated growth and predicted von Bertlanffy growth curves of female silver eels in their first 5 years for all fish from a sample of female silver eels captured in 1987, 1988 and 2007. n (eels) = 152, n (eel years) = 760 b) Mean Dahl lee growth and predicted Von Bertlanffy growth curves of female eels n (eels) = 152, n (eel years) = 4665, c) Mean count of female Dahl Lee eels size above and below 1 standard deviation unit of the von Bertlanffy predicted growth in their first 5 years with ageing of fish ranged by ± 3 years in 1,000 Monte Carlo trials. Errors are 95% cls. n (eels) = 152, n (eel years) = 760 d) Proportion of female Dahl Lee eels size above and below 1 standard deviation unit of the von Bertlanffy predicted growth in their first 5 years with ageing of fish ranged by ± 3 years in 1,000 Monte Carlo trials. Errors are 95% cls. n (eels) = 152, n (eel years) = 760. Notes: No over sized female fish before 1954. 1989 - 1990 switch between large and small dominance in extreme sized females.

Figure 3.23 shows a shift in the expected proportion of male eels growing outside of the expected limits. In the early 1990s there seems to be a change, with an increase in the proportion of male eels growing faster than expected in their first five years of growth. This trend seems to decline after 2005, which is similar to the flattening out seen in the female silver eel data (Figure 3.22) that is; no male silver eels were young enough to have had their first five years of growth after the year 2005 in this project.

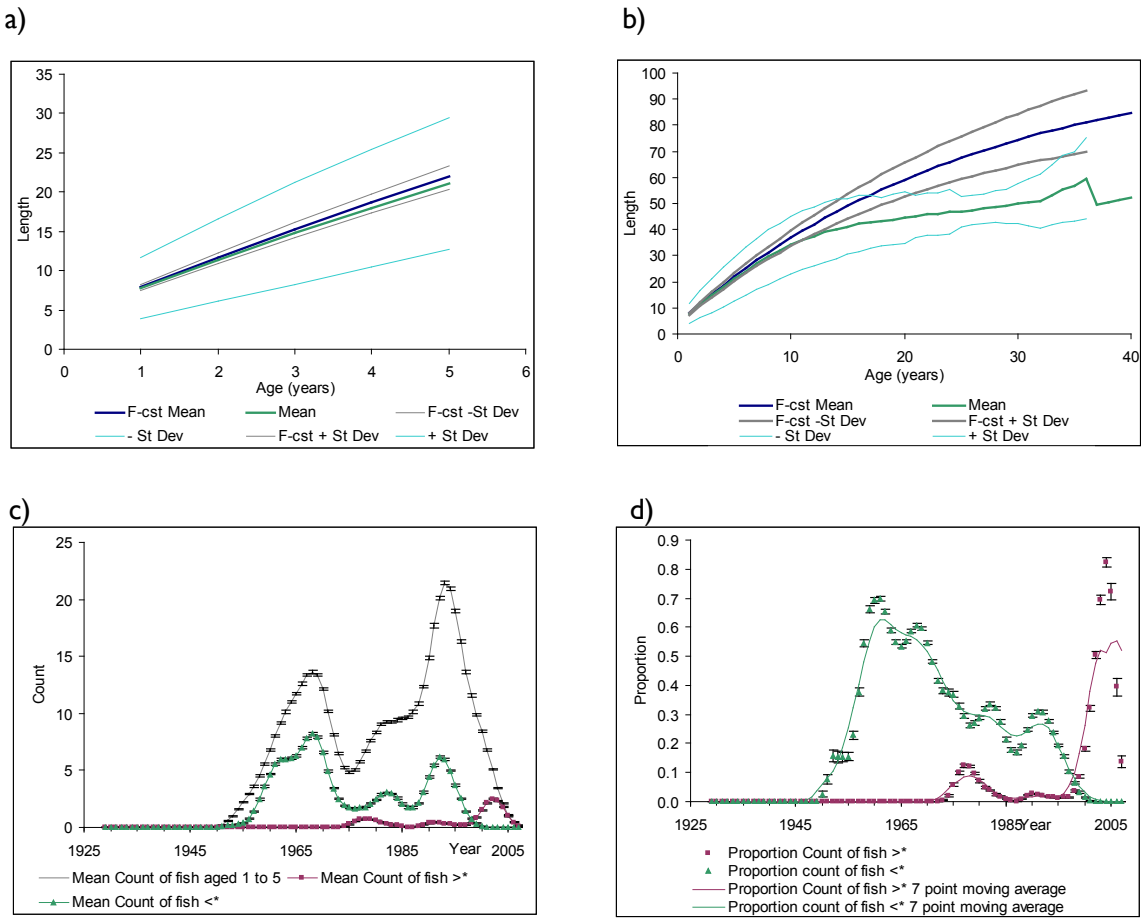

Figure 3.23: a) Mean back-calculated growth and predicted von Bertlanffy growth curves of male silver eels in their first 5 years for all fish from a sample of male silver eels captured in 1987, 1988 and 2007. n (eels) = 99, n (eel years) = 495 b) Mean Dahl lee growth and predicted von Bertlanffy growth curves of male eels n (eels) = 99, n (eel years) = 2088, c) Mean count of male Dahl Lee eels size above and below 1 standard deviation unit of the von Bertlanffy predicted growth in their first 5 years with ageing of fish ranged by ± 3 years in 1,000 Monte Carlo trials. Errors are 95% cls. n (eels) = 99, n (eel years) = 495 d) Proportion of male Dahl Lee eels size above and below 1 standard deviation unit of the von Bertlanffy predicted growth in their first 5 years with ageing of fish ranged by ± 3 years in 1,000 Monte Carlo trials. Errors are 95% cls. n (eels) = 99, n (eel years) = 495. Notes: No over sized male fish before 1973. 1998 - 1999 switches between large and small dominance in extreme sized males.

The yellow eel data in Figure 3.24 shows more variation over time (when compared to silver eel, Figures 3.22 and 3.23) in terms of the proportion of eels growing either more or less than expected in their first five years in freshwater. Figure 3.24d shows that previously in the 1960s and 1970s, the proportion of yellow eels growing faster than expected was greater than those fish growing less than expected, a trend that again occurs from approximately 1990 onwards. This dominant positive trend in the 1960s and 1970s was not as obvious in the silver eel data. The yellow eel data also shows an increase in the proportion of faster growing fish since roughly 1990, which correspond with the silver eel analysis.

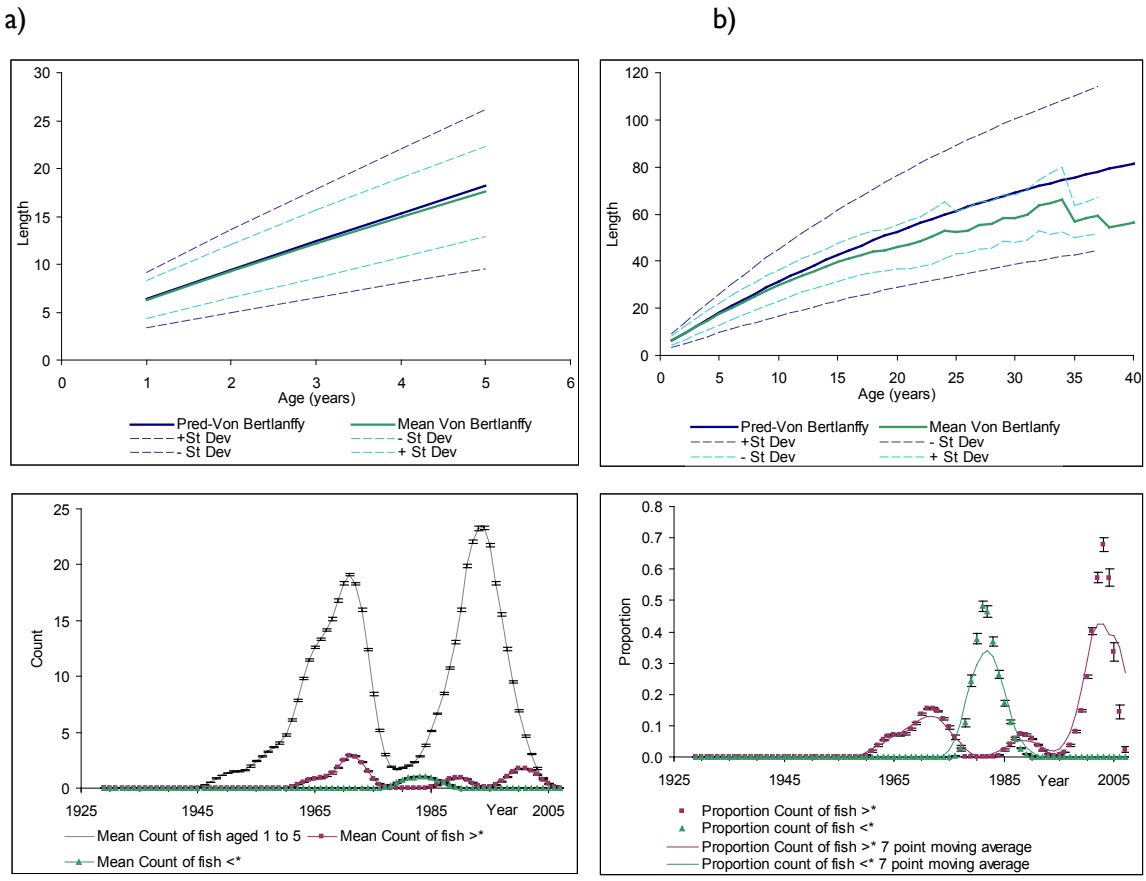

Figure 3.24: a) Mean back-calculated growth and predicted von Bertlanffy growth curves of L. Furnace yellow eels in their first 5 years for all fish from a sample of L. Furnace yellow eels captured in 1987, 1988 and 2007. n (eels) = 100, n (eel years) = 500 b) Mean Dahl lee growth and predicted von Bertlanffy growth curves of L. Furnace yellow eels n (eels) = 100, n (eel years) = 1982, c) Mean count of male Dahl Lee eels size above and below 1 standard deviation unit of the Von Bertlanffy predicted growth in their first 5 years with ageing of fish ranged by ± 3 years in 1,000 Monte Carlo trials. Errors are 95% cls. n (eels) = 100, n (eel years) = 500. Errors are 95% cls d) Proportion of male Dahl Lee eels size above and below 1 standard deviation unit of the von Bertlanffy predicted growth in their first 5 years with ageing of fish ranged by ± 3 years in 1,000 Monte Carlo trials. Errors are 95% cls. n (eels) = 100, n (eel years) = 500. Notes: All instances of Dahl-Lee expected fish lengths which were outside the expected 1 st-deviation unit were smaller than expected, this may be owing to using von Bertalanffy to predict eel growth with a mixed male-female sample. In addition, one eel was markedly larger than the others in calculating von Bertalanffy. This was corrected by using the 99th percentile length of the data set. A noted proportion of fish above the Von Bertalanffy expected in the first five years of growth occurred in two instances, the early 1970s and the early 2000s. There was one instance of a fish below the expected, in the early 1980s.

3.7.5 Discussion on Eel Growth

Burrishoole eels mature at a smaller size and an older age than most of the studied European eel populations, and are most similar to those of Lough Neagh and the Rivers Bann and Erne (Matthews et al., 2003), although the ages in Burrishoole are considerably older. In fact, female eels as old as 57 years were recorded in the silver eel migration in 1987 and 1988 (Poole and Reynolds, 1996). This is typical of the more northern latitudes in the eels' range and of nutrient-poor catchments.

According to report of the joint EIFAC/ICES Working Group on Eel (2009), eel stocks are at a historical minimum, continuing to decline and outside of safe biological limits. Recruitment is also at historically low levels and continues to decline (ICES, 2009). Several possible causes have been suggested for this decline, including overfishing, habitat reduction, organic chemical poisoning, parasites, and larval migration failure due to ocean climate factors (Castonguay et al., 1994, ICES, 2008). Such a large scale decrease over such a large number of recruitment indices across Europe would seem to indicate that broader meteorological or climatic change might be responsible. Such a change could also affect both the larval survival in the ocean and adult growth in freshwater by altering the conditions needed by the species to grow and migrate.

The effect of temperature on eel growth is well known in aquaculture (Ciccotti and Fontenelle 2001; Dosoretz and Degani 1987; Holmgren 1996), where eels are reared at optimal temperatures of between of 23-25°C. Temperature has already increased by 2°C in a century and projections of climate in Europe predict an increase of 1.4-5.8°C of the temperatures within 50 years (Houghton 2001).

The results from the current study in Burrishoole indicated that there had been an increase in the growth rate of eels in their first five years of freshwater habitation, when looking at growth from 1990 onwards compared to the average. This trend was visible in both male and female silver eels and also in sexually immature yellow eels from the tidal lough. Daverat et al. (2012) found a similar result over a longer time frame in their study. They looked at rates of growth in European eel in various catchments throughout the eel's geographic range over the past century, and found that water temperatures over 13°C were strongly correlated with growth rates. The observed changes in the Burrishoole study fit with their results and indications are that warmer water temperatures will result in faster growth rates for the Burrishoole European eel population. Table 3.29 shows the critical temperatures for the growth and survival of European eels.

Table 3.29: Critical temperatures for European eels.

Parameter	Reference	Temperature (°C)
Optimum growth	Ciccotti and Fontanelle (2001)	23-25
Upper Lethal Temp.	Sadler (1979)	38
Critical Thermal Max (fish acclimatised at 14-29°C)	Sadler (1979)	33-39
Adults enter state of Torpor	Sadler (1979)	0-3
Glass eel migration	Tesch (2003)	6-12
Elver migration	Tesch (2003)	10-25
Elver migration – Threshold Minimum temps	Tesch (2003)	9-11
Silver eel migration	Vollestad et al. (1986)	4-18

Eels are unlikely to be negatively affected by the projected changes in RWT in Burrishoole over the next century and are more likely to benefit. The results from the current study in Burrishoole, using back-calculation of growth rates from otoliths indicated that there had been an increase in the growth rate of eels in their first 5 years in freshwater based on data from 1990 onwards. It would be expected that an increases in RWT would result in a further increase. Higher winter RWT especially could have positive knock-on effects for food supply and the length of the growing season.

A comparison between the increasing water temperature trends in the Burrishoole catchment and the increased growth rates observed in yellow and silver eels in their first five years spent in freshwater seems to indicate some similarity in pattern.

An increase in growth rate is likely to have several impacts on factors – such as age and size at maturation and on the sex ratio within the catchment. Faster growth will result in eels reaching a larger size at a younger age and migrating out to sea to spawn at an earlier age than that currently observed in Burrishoole. A change in the sex ratio of eels has already been observed in the Burrishoole catchment, with the percentage of males changing from 63% in the 1970s to 32% in more recent years. One theory to explain this change is that it is linked to increased productivity in the catchment along with reduced recruitment, a situation that is likely to continue with rising water temperatures. While there are many factors affecting the survival of European eels in freshwater, it is possible that increasing water temperatures in Northern Europe will have a positive impact on the species, possibly aiding in a future recovery of the stock.

3.8 Summary

Changing climate is expected to affect fishery resources and this will present challenges to managers to develop sustainable exploitation and management strategies. Fish have complicated life cycles, and each life-history stage (eggs, larvae, juveniles and adults) may have varying habitat and dietary requirements. Diadromous species complicate this picture further by migrating between the sea and freshwater in order to complete their life cycle, requiring transformations in physiology often in conjunction with the maturation process. The assessment of possible impacts is also more complicated by the fact that diadromous species may migrate through several climatic regions. As a result, for a full understanding of the possible effects of climate change on these species, it is important to adopt an integrated approach that includes the full life cycle and the various habitats and environments.

Projected changes in rainfall and temperature associated with climate change are likely to have significant impacts on the ecology of fresh and transitional waters in Ireland. Ocean climate changes are already known to have an impact on salmon at sea, largely through the close interaction between growth and survival. Diminishing eel populations may also be the result of changes in the ocean in conjunction with human-induced pressures. It is anticipated that further changes will occur to diadromous species with shifts in distributions due to relocation of spawning and feeding grounds, a change in the local survival of fish or immigration into new habitats. These species are, however, subject to a range of other pressures in addition to climatic drivers. Many of these pressures, such as exploitation, eutrophication, habitat change, fluctuating population densities and genetics (e.g. caused by stocking non-native or cultured fish) have been changing over the last few decades in parallel with the observed changes in climate. Untangling these various drivers is part of the challenge of assessing the impacts of climate to date and of making projections for the future impact of changing climate.

The Burrishoole catchment, situated in Newport, Co. Mayo on the west coast of Ireland, has full fish-trapping facilities for counting fish migrating between the sea and freshwater and is an international index site for some diadromous species such as Atlantic salmon, sea trout and eel. It is possible to examine, in conjunction with the comprehensive environmental datasets, the growth, survival and migration patterns of these species, to look at changes that have already occurred over the last few decades and to make some projections into the future based on the downscaled climate change scenarios for the Burrishoole catchment.

This chapter examined the migrations of salmon, sea trout and eel and describes the major changes that have occurred in stock dynamics and growth rates. Changes have occurred in the

fish stocks in Burrishoole with declines in the number of adult salmon and sea trout returning to the catchment, declining salmon survival at sea, a collapse in sea trout survival between 1987 and 1989 and changes in silver eel escapement with lower numbers, higher proportions of females and larger size.

There are indications that salmon and sea trout smolt migrations are tending to commence earlier, probably linked with rising temperatures, although high variability is introduced by the interaction of temperature, rainfall and water levels. Prolonged delays to smolt runs due to spring droughts have been shown to negatively impact on salmon survival at sea.

Rising temperature is also likely to reduce egg development times for both salmon and trout. There has been approximately a 35 day decrease over the last five decades in terms of incubation time from spawning to hatching for salmon, and approximately a twenty five day decrease for trout. While this study shows a shortening in numbers of days required in egg development time in the wild, it does not necessarily mean that actually hatching dates have shifted to the same extent, due to possible delays in salmonid spawning in the catchment during recent years, possibly also temperature related. There appears to be an optimal temperature for egg development and presumably also for maturation and spawning times. These parameters could affect successful incubation of wild salmonid eggs in the Burrishoole in future years in light of proposed water temperature increases.

Studies of fish growth determined from archival fish scales (salmon & trout) and otoliths (eel) have shown a significant shift insalmon smolt age, mainly demonstrated by the increase in the proportion of the 1+ age class in recent years from <11% to >11% compared to the 2-year-old smolts (2 and 2+ age), may be due to increased growth rates due to higher water temperatures. Clear changes in growth rates within each year class of smolt were not apparent in this study. There was, however, an increase in recent years in the growth rate during the second year of growth (both periods – 'summer' vs 'winter') for 2+ smolts, the dominant age class in Burrishoole. It was also apparent that the winter growth in both 1-year-old and 2-year-old parr in 2008 was the fastest observed in any of the years studied.

In Burrishoole, trout are present in both resident and migratory forms. There has been a significant change in the numbers of sea trout smolts migrating from the Burrishoole catchment. Sea trout smolt output has fallen from 4000+ pre-1985 to an average of ~700 in the last decade. This decline would have resulted in a concurrent change in fish density in the freshwater environment which could influence trout growth rate and smolt age. This makes a

comparison between years and with other environmental factors difficult. Comparison of growth of smolts and resident trout from Lough Feeagh in Burrishoole showed two and three year old smolts to be consistently larger at each age class. Faster growing parr were also undergoing smoltification earlier and at smaller sizes than slower growing parr.

Burrishoole eels mature at a smaller size and an older age than most of the studied European eel populations, and are most similar to those of Lough Neagh and the Rivers Bann and Erne, although the ages in Burrishoole are considerably older. In fact, female eels as old as 57 years were recorded in the silver eel migration in 1987 and 1988. This is slow growth is typical of the more northern latitudes in the eels' range and of nutrient-poor catchments. The effect of temperature on eel growth is well known in aquaculture, where eels are reared at optimal temperatures of between of 23-25°C. Global temperature has already increased by 2°C in a century and projections of climate in Europe predict an increase of 1.4-5.8°C of the temperatures within 50 years (Houghton et al. 2001).

Results from the current study in Burrishoole indicated that there had been an increase in the growth rate of eels in their first five years of freshwater habitation, when looking at growth from 1990 onwards compared to the average. This trend was visible in both male and female silver eels and also in sexually immature yellow eels from the tidal lough. Eels are unlikely to be negatively affected by the projected changes in RWT in Burrishoole over the next century and are more likely to benefit. An increase in growth rate is likely to have several impacts on factors – such as age and size at maturation (and consequently lower natural mortality) and on the sex ratio within the catchment. Faster growth will result in eels reaching a larger size at a younger age and migrating out to sea to spawn at an earlier age than that currently observed in Burrishoole.

3.9 Key Findings

- A number of marked changes in the migratory fish stocks in Burrishoole have been observed over the period 1970–2009.
- Adult salmon returns fluctuated from a high of 1777 in 1973 to a low of 252 in 1990 and smolt numbers recorded migrating to sea have varied from a maximum of 16,136 in 1976 to a minimum of 3,794 in 1991.
- Following the cessation of the drift fishery in 2007, an increase in the numbers of fish returning to the catchment was recorded in that year. This increase occurred only in 2007, with numbers in 2008 and 2009 falling to levels similar to those recorded prior to the cessation of drift netting. This would indicate a probable decrease in marine survival.

- Marine survival of sea trout collapsed in the late 1980s leading to a collapse in the spawning stock and a subsequent significant reduction in smolt recruitment.
- Changes have been observed in the numbers, sex ratio and size of adult silver eels migrating from the catchment. Numbers are declining with a shift from a male dominated silver eel run to one with more than 60% females.
- The timing of smolt migrations for both salmon and sea trout appears to be changing, with a general trend towards earlier and more prolonged migration periods.
- Projected changes to rainfall patterns will impact on water flow regimes in rivers, which will affect the timing of migrations into and out of freshwater and may reduce the survival of various life history stages of salmonids.
- There has been approximately a 35 day decrease over the last five decades in terms of incubation time from spawning to hatching for salmon, and approximately a twenty five day decrease for trout. While this study shows a shortening in numbers of days required in egg development time in the wild, it does not necessarily mean that actually hatching dates have shifted to the same extent, due to possible delays in salmonid spawning in the catchment during recent years
- Salmon smolt age showed a significant shift in the percentage make-up of the age classes over time, mainly demonstrated by the increase in the proportion of the 1+ age class in recent years
- There was no obvious trend in the mean size of salmon smolts over time.
- An increase in the growth of salmon parr in their second year was observed in recent years.
- The growth of salmon both 0+ and 1+ parr in winter was fastest in 2008, probably due to the unusually warm winter temperatures.
- While the current Burrishoole study has not shown any significant increases in growth rate in trout smolts, there is an indication that smolt age may be reducing, with a higher percentage of 2/2+ smolts in the 2008 sample together with an absence of 4/4+ smolts, although this is highly variable between years.
- The critical temperatures are likely to be exceeded for trout in the coming century, having a negative impact on the growth and survival of trout in the Burrishoole catchment
- There had been an increase in the growth rate of eels in their first 5 years in freshwater based on data from 1990 onwards.
- Increases in water temperature are likely to affect eels positively through higher growth rates, survival and younger age at migration.

3.10 References

Aprahamian, M.W., Davidson, I.C., and Cove, R.J. (2008) 'Life history changes in Atlantic salmon from the River Dee, Wales'. Hydrobiologia, 602, 61–78.

Baglinière J. L., Denais L., Rivot E., Porcher J. P., Prévost E., Marchand F., and Vauclin V. (2004) Length and age structure modifications of the Atlantic salmon (*Salmo salar*) populations of Brittany and Lower Normandy from 1972 to 2002. 2004. Technical report, INRA-CSP. 24 pp.

Baglinière J. L., Marchand F., and Vauclin V. (2005) Interannual changes in recruitment of the Atlantic salmon (*Salmo salar*) population in the River Oir (Lower Normandy, France): relationships with spawners and in-stream habitat. ICES Journal of Marine Science, 62, 4, 695-707.

Brannon, E. L., Powell, M. S., Quinn, T. P. and Talbot, A. (2004) 'Population structure of Columbia River Basin Chinook salmon and steelhead trout', Reviews in Fisheries Science 12, 99.232.

Bohlin, T., Dellefors, C. and Faremoe, U. (1994) 'Probability of first sexual maturation of male parr in wild sea-run brown trout (*Salmo trutta*) depends on condition factor 1 year in advance', Canadian Journal of Fisheries and Aquatic Sciences, 51, 1920–1926.

Brett, J.R. (1979) Environmental factors and growth. In W.S. Hoar, D.J. Randall and J.R. Brett (eds.) Fish Physiology, 8. Academic Press, New York, NY, pp.599–675.

Byrne, C.J., Poole, R., Rogan, G., Dillane, M. and Whelan, K.F. (2003) 'Temporal and environmental influences on the variation in Atlantic salmon smolt migration in the Burrishoole system 1970–2000', Journal of Fish Biology, 63, 1552–1564.

Byrne, C.J., Poole, R., Dillane, M., Rogan, G. and Whelan, K.F. (2004) 'Temporal and environmental influences on the variation in sea trout (*Salmo trutta* L.) smolt migration in the Burrishoole system in the west of Ireland from 1971 to 2000', Fisheries Research, 66, 85–94.

Caissie, D. (2006) 'The thermal regime of rivers: a review', Freshwater Biology, 51, 1389–1406.

Carlsen, K. T., Berg, O. K., Finstad, B. & Heggberget, T. G. (2004) Diel periodicity and environmental influence on the smolt migration of Arctic charr, Salvelinus alpinus, Atlantic salmon, *Salmo salar*, and brown trout, *Salmo trutta*, in northern Norway. Environmental Biology of Fishes 70, 403.413.

Carlson, S. M. and Seamons, T. R. (2008) A review of quantitative genetic components of fitness in salmonids: implications for adaptation to future change. Evolutionary Applications 1, 222.238.

Castonguay, M., Hodson, P.V., Moriarty, C., Drinkwater, K.F., and Jessop, B.M. (1994) 'Is there a role of ocean environment in American and European eel decline?', Fisheries Oceanography, 3: 197–203.

Chadwick, E.M.P. (1985) 'Stock-recruitment relationship for Atlantic salmon in Newfoundland rivers'. Verhandlungen des Internationalen Verein Limnologie, 22, 2509–15.

Ciccotti, E. and Fontenelle, G. (2001) 'A review of eel aquaculture in Europe: perspectives for its sustainability', Journal of Taiwan Fisheries Research 9, 27–43.

Connor, W. P., Burge, H. L., Waitt, R. and Bjornn, T. C. (2002) 'Juvenile life history of wild fall Chinook salmon in the Snake and Clearwater Rivers', North American Journal of Fisheries Management 22, 703–712.

Consuegra,S., Verspoor,E., Knox,D. and García de Leániz,C. (2005) 'Asymmetric gene flow and the evolutionary maintence of genetic diversity in small, peripheral Atlantic salmon populations', Conservation Genetics 6: 823-842.

Crisp, D. T. (1981) 'A desk study of the relationship between temperature and hatching time for the eggs of five species of salmonid fishes', Freshwater Biology 11, 361.368. doi: 10.1111/j.1356-2427.1981.tb01267.x

Cross, T.F. and Piggins, D.J. (1982) The effect of abnormal climate conditions on the smolt run of 1980 and subsequent returns of Atlantic salmon and sea trout. ICES CM:M26:8.

Daverat, F., Beaulaton, L., Poole, R., Lambert, P., Wickstrom, H., Andersson, J., Aprahamian, M., Hizem, B., Elie, P., Yalçın-özdilek, S. and Gumus, A., (2012). 'One century of eel growth: temperature and simple habitat characteristics effects', Ecology of Freshwater Fish, (doi: 10.1111/j.1600-0633.2011.00541.x).

Davidson, I.C. and Hazelwood, M.S. (2005) Effect of Climate Change on Salmon Fisheries, Science Report. W2-047/SR. Bristol. Environment Agency, pp.47

Dekker, W., (2003) 'Did lack of spawners cause the collapse of the European eel, *Anguilla anguilla*?', Fisheries Management and Ecology, 10: 365–376.

Donnelly, A., Cooney, T., Jennings, E., Buscardo, E. and Jones, M. (2009) 'Response of birds to climatic variability; evidence from the western fringe of Europe', International Journal of Biometeorology, 53, 211–220.

Dosoretz, C.G. and G. Degani (1987) 'Effects of fat rich diet and temperature on growth and body composition of European eels (*Anguilla anguilla*)', Comparative Biochemistry and Physiology, 87A, 733–736.

Egglishaw, H.J. and Shackley, P.E. (1977) 'Growth, survival and production of juvenile salmon and trout in a Scottish stream, 1966–75', Journal of Fish Biology, 11, 647–672.

Elliott, J.M. (1981) 'Some aspects of thermal stress on freshwater teleosts'. In A.D. Pickering (ed.) Stress and Fish. London, Academic Press.

Elliott, J. M. (1985) 'Population regulation for different life-stages of migratory trout *Salmo trutta* in a Lake District stream, 1966–83', Journal of Animal Ecology 54, 617–638.

Elliott, J. M. (1994). Quantitative Ecology and the Brown Trout. Oxford Series in Ecology and Evolution. Oxford: Oxford University Press.

Elliott, J. M. and Elliott, J. A. (2006) A 35-year study of stock-recruitment relationships in a small population of sea trout: assumptions, implications and limitations for predicting targets. In Sea Trout: Biology, Conservation and Management (Harris, G. & Milner, N., eds), pp. 257.278. Oxford: Blackwell Publishing.

Elliott, J. M. and Hurley, M. A. (1998) 'An individual-based model for predicting the emergence period of sea trout fry in a Lake District stream', Journal of Fish Biology 53, 414.433. doi: 10.1111/j.1095-8649.1998.tb00990.x

Elliott J.M and Hurley, M.A. (2000) 'Daily energy intake and growth of piscivorous brown trout', Freshwater Biology, 22, 237–245.

Elson P.F. (1957) 'The importance of size in the change from parr to smolt in Atlantic salmon', Canadian Fish Culturist, 21, 1–6.

Fahy E. (1978) 'Variation in some biological characteristics of British sea trout', Journal of Fish Biology, 13, 123–138.

Fahy, E. (1985) Child of the Tides – A Sea Trout Handbook. ISBN. 0907606318.

Fealy R. and Sweeney J. (2005) 'Detection of a possible change point in atmospheric variability in the North Atlantic and its effect on Scandinavian glacier mass balance', International Journal of Climatology, 25, 1819–1833.

Fealy, R., Allott, N., Broderick, C., de Eyto, E., Dillane, M., Erdil, R.M., Jennings, E., McCrann, K., Murphy, C., O'Toole, C., Poole, R., Rogan, G., Ryder, E., Taylor, D., Whelan, K. and White, J. (2010) RESCALE: Review and Simulate Climate and Catchment Responses at Burrishoole, Final Summary Report, Marine Research Sub Programme 2007-2013, Marine Institute, Oranmore, Co. Galway, pp1-126 ISSN: 2009-3195

Frank, K. T. and Leggett, W. C. (1986) 'Effect of prey abundance and size on the growth and survival of larval fish: an experimental study employing large volume enclosures', Marine Ecology Progressive Series 34, 11.22.

Fried, S. M., McCleave, J. D., and Stred, K. A. (1976) 'Buoyancy compensation by Atlantic salmon (*Salmo salar*) smolts tagged internally with dummy telemetry transmitters', Journal of Fisheries Research Board of Canada. 33, 1377-1380.

Friedland, K.D., Reddin, D.G., McMenemy, J.R. and Drinkwater, K.F. (2003) 'Multidecadal trends in North American Atlantic salmon (*Salmo salar*) stock and climate trends relevant to juvenile survival', Canadian Journal of Fisheries and Aquatic Sciences, 60, 563–583.

Garcia de Leaniz,C.; Fleming,I.A.; Einum,S.; Verspoor,E.; Jordan,W.C.; Consuegra,S.; Aubin-Horth,N.; Lajus,D.; Letcher,B.H.; Youngson,A.F.; Webb,J.H.; Vøllestad,L.A.; Villanueva,B.; Ferguson,A.; Quinn,T.P. (2007) 'A critical review of adaptive genetic variation in Atlantic salmon:implications for conservation', Biological Reviews 82: 173-211.

Gardner, M. L. G. (1976) 'A review of factors which may influence the sea-age and maturation of Atlantic salmon *Salmo salar* L.', Journal of Fish Biology, 9: 289–327.

Gargan, P., Tully, O. and Poole, R. (2003) The relationship between sea lice infestation, sea lice production and sea trout survival in Ireland, 1992–2001. In D. Mills (ed.) Salmon at the Edge. Proceedings of the Sixth International Atlantic Salmon Symposium, July 2002. Edinburgh, UK. Chapter 10. Atlantic Salmon Trust/Atlantic Salmon Federation, pp119–135.

Gee, A. S. and Milner, N. J. (1980) 'Analysis of 70 year catch statistics for Atlantic Salmon (*Salmo salar*) in the river Wye and implications for management of stocks', Journal of Applied Ecology17, 41-57.

Gibson, R.J. (1993) 'The Atlantic salmon in fresh water: spawning, rearing and production', Reviews in Fish Biology and Fisheries, 3, 39–73.

Gibson, R. J. and Myers, R. A. (1998) 'Influence of seasonal river discharge on survival of juvenile Atlantic salmon, *Salmo salar*', Canadian Journal of Fisheries and Aquatic Sciences 45, 344–348.

Graham, C.T. and Harrod, C. (2009) 'Implications of climate change for the fishes of the British Isles', Journal of Fish Biology, 74, 1143–1205.

Harris, G.S. and Milner, N. J. (2006) Sea Trout: Biology, Conservation and Management. Proceedings of First International Sea Trout Symposium, Cardiff, July 2004. Blackwell Scientific Publications, Oxford, 499pp.

Hari, R.E., Livingstone D.M., Siber R., Burkhardt-Holm P. and Güttinger, H. (2006) 'Consequences of climatic change for water temperature and brown trout populations in Alpine rivers and streams', Global Change Biology, 12, 10–26.

Heddell-Cowie, M., (2005) 'Importance of the River Teviot to Atlantic salmon, *Salmo salar*, rod catches in the River Tweed, Scotland', Fisheries Management and Ecology 12: 137-142.

Heggberget, T. G. (1988) 'Time of spawning of Norwegian Atlantic salmon (*Salmo salar*)', Canadian Journal of Fisheries and Aquatic Sciences 45, 845.849.

Henderson, N. E. (1963) 'Influence of light and temperature on the reproductive cycle of the eastern brook trout (Salvelinus fontinalis (Mitchill))', Journal of the Fisheries Research Board of Canada 20, 859.897.

Hindar, K., Jonsson, B., Ryman, N. and Staahl, G. (1991) 'Genetic relationships among landlocked, resident and anadromous brown trout, *Salmo trutta* L.', Heredity, 66 (1), 83-91.

Holmgren, K. and Mosegaard, H. (1996) 'Implications of individual growth status on the future sex of the European eel', Journal of Fish Biology, 49, 910–925.

Houghton, J. (2001). Climate Change 2001: The Scientific Basis. IPCC.

ICES. 2008. The report of the 2008 Session of the Joint EIFAC/ICES Working Group on Eels, September 2008; *ICES CM 2008/ACOM:15.192pp* and country reports.

ICES (2009) Report of the 2009 Session of the Joint EIFAC/ICES Working Group on Eels (WGEEL), 7–12 September 2009, Göteborg, Sweden. ICES CM 2009/ACOM:15. pp. 137.

ICES. 2010. The report of the 2010 Session of the Joint EIFAC/ICES Working Group on Eels, September 2010; *ICES CM 2010/ACOM:18. 201pp* and country reports.

Imre, I. and Boisclair, D. (2005) 'Age effect on diurnal activity pattern of juvenile Atlantic salmon: parr are more nocturnal than young-of-the-year', Journal of Fish Biology, 64, 1731–1736.

IPCC (2007) Contribution of Working Group II to the Fourth Assessment Report of the Intergovernmental Panel on Climate Change, 2007M.L. Parry, O.F. Canziani, J.P. Palutikof, P.J. van der Linden and C.E. Hanson (eds)Cambridge University Press, Cambridge, United Kingdom and New York, NY, USA.

Jenkins, T.M. Jr, Diehl, S., Kratz, K.W. and Cooper, S.D. (1999) 'Effects of population density on individual growth of brown trout in streams', Ecology, 80, 941–956.

Jensen, A. J. and Johnsen, B. O. (1999) 'The functional relationship between peak spring floods and survival and growth of juvenile Atlantic salmon (Salmo salar) and brown trout (Salmo trutta)', Functional Ecology 13, 778–785. doi: 10.1046/j.1365-2435.1999.00358.x

Jonsson, B. (1985) 'Life history patterns of freshwater resident and sea-run migrant brown trout in Norway', Transactions of the American Fisheries Society 114, 182–194.

Jonsson, B. (1982) 'Diadromous and resident trout Salmo trutta: is their difference due to genetics?', Oikos 38, 297-300.

Jonsson, B. and Jonsson, N. (2009) 'A review of the likely effects of climate change on anadromous Atlantic salmon *Salmo salar* and brown trout *Salmo trutta* , with particular reference to water temperature and flow', Journal of Fish Biology, 75, 2381–2447.

Jonsson, B. and Ruud-Hansen, J. (1985) 'Water temperature as the primary influence on timing of seaward migration of Atlantic salmon (*Salmo salar*) smolts', Canadian Journal of Aquatic Science, 42, 593–595.

Jutila, E., Jokikokko, E. and Julkunen, M. (2005) 'The smolt run postsmolt survival of Atlantic salmon, *Salmo salar* L., in relation to early summer water temperatures in the northern Baltic Sea', Ecology of Freshwater Fish 14, 69–78. doi: 10.1111/j.1600-0633.2005.00079.x

L'Abee-Lund, J. H., Jonsson, B., Jensen, A. J., Sættem, L. M., Heggberget, T. G., Johnsen, B. O. and Næsje, T. F. (1989) 'Latitudinal variation in life history characteristics of sea-run migrant brown trout *Salmo trutta*', Journal of Animal Ecology 58, 525–542.

Lassalle, G., Beguer, M., Beaulaton, L. and Rochard, E. (2008) 'Diadromous fish conservation plans need to consider global warming issues: An approach using biogeographical models', Biological Conservation. 141, 1105-1118.

Lassalle, G. and Rochard, E. (2009) 'Impact of twenty-first century climate change on diadromous fish spread over Europe, North Africa and the Middle East', Global Change Biology, 15, 1072–1089.

Lee, R. M., (1920). A review of the methods of age and growth determination in fishes by means of scales. Fishery Investigations London Series 2, 4, 2: 32pp.

Lobón-Cervia, J. and Mortensen, E. (2005) 'Population size in stream-living juveniles of lake-migratory brown trout: the importance of stream discharge and temperature', Ecology of Freshwater Fish, 14, 394–401.

Lura, H. and Saegrov, H. (1993) 'Timing of spawning in cultured and wild Atlantic salmon (*Salmo salar*) and brown trout (*Salmo trutta*) in the River Vosso', Ecology of Freshwater Fish 2, 167.172. doi: 10.1111/j.1600-0633.1993.tb00099.x

Lundqvist, H., McKinnell, S., Fängstam, H. and Berglung, I. (1994) 'The effect of time, size and sex on recapture rates and yield after river releases of *Salmo salar* smolts', Aquaculture, 121, 245–257.

Matthews, M. A., Evans D. W., McClintock C. A. and Moriarty C. (2003) Age, growth, and catch-related data of yellow eel *Anguilla anguilla* (L.) from lakes of the Erne catchment, Ireland. American Fisheries Society Symposium, 2003, 207–215.

McCarthy, I. D. and Houlihan, D. F. (1997) 'The effect of temperature on protein synthesisin fish: the possible consequences for wild Atlantic salmon (*Salmo salar* L.) stocks in Europe as a result of global warming'. In Global Warming: Implications for Freshwater and Marine Fish (Wood, C. M. & McDonald, G., eds), pp. 51.77. Cambridge: Cambridge University Press.

McCormick, S.D., Shrimpton, J.M., Bjornsson, B.T. and Moriyama, S. (2002) 'Effects of an advanced temperature cycle on smolt development and endrocrinology indicate that temperature is not a zeitgeber for smelting in Atlantic salmon', Journal of Experimental Biology, 205, 3553–3560.

McGinnity, P., Jennings, E., DeEyto, E., Allot, N., Samuelsson, P., Rogan G., Whelan, K. and Cross, T. (2009) 'Impact of naturally spawning captive-bred Atlantic salmon on wild populations: depressed recruitment and increased risk of climate-mediated extinction', Proceedings of the Royal Society B – Biological Sciences, 276, 3601–3610.

Merz, J. E., Setka, J. D., Pasternack, G. B. and Wheaton, J. M. (2004) 'Predicting benefits of spawning-habitat rehabilitation to salmonid (Oncorhynchus spp.) fry production in a regulated California river', Canadian Journal of Fisheries and Aquatic Sciences 61, 1433.1446.

Metcalfe, N.B., Huntingford, F.A., Graham, W.D. and Thorpe, J.E. (1989) 'Early social status and the development of life-history strategies in Atlantic salmon', Proceedings of the Royal Society of London, Series B, 236, 7–19.

Moffett, I.J.J., Allen, M., Flanagan, C., Crozier, W.W. and Kennedy, G.J.A. (2006) 'Fecundity, egg size and early hatchery survival for wild Atlantic salmon, from the River Bush', Fisheries Management and Ecology, 13, 73–79.

Nolan, G., Gillooly, M. and Whelan, K. (eds.) (2009) Irish Ocean Climate and Ecosystem Status Report, Marine Institute, 116pp.

Northcote, T.G. (1978) Migratory strategies and production in freshwater fishes. In S.D. Gerking (ed.) Ecology of Freshwater Fish Production. Blackwell Scientific Publications, Oxford, pp. 326–359.

Økland, F., Jonsson, B., Jensen, A.J. and Hansen, L.P. (1993) 'Is there a threshold size regulating seaward migration of brown trout and Atlantic salmon?', Journal of Fish Biology, 42, 541–550. 37, 770–774.

Ojanguren, A. F. and Brana, F. (2003) 'Thermal dependence of embryonic growth and development in brown trout', Journal of Fish Biology 62, 580.590. doi: 10.1111/j.1095-8649.2003.00049.x

Peyronnet, A., Friedland, K. D., O'Maoileidigh, N., Manning, M. and Poole, R. (2007) 'Links between patterns of marine growth and survival of Atlantic salmon Salmo salar L.', Journal of Fish Biology, 71, 684–700.

Piggins, D. J. (1985) 'The silver eel runs if the Burrishoole River System: 1959–1984; numbers, weights, timing and sex ratios.' ICES/C.M. 1985/M: 5.

Poole, W. R., Matthews, M., Dillane, M. and Whelan, K. W. (1995). A Comparative Study of Migratory and Resident Juvenile Salmonid Stocks in the Burrishoole Catchment. Final Report to the Atlantic Salmon Trust.

Poole, R., Reynolds, J. and Moriarty, C. (1990) 'Observations on the Silver Eel Migrations of the Burrishoole River System, Ireland, 1959 to 1988', Int. Revue ges. Hydrobiologia, 75, 807–815.

Poole, W.R. and Reynolds, J.D. (1996) 'Growth rate and age at migration of *Anguilla anguilla*', Journal Fish Biology, 48, 633–642.

Poole, W.R., Nolan, D. and Tully, O. (2000) 'Extrapolating baseline blood cortisol levels in trout: modelling capture effects in wild sea trout *Salmo trutta* (L.) infested with *Lepeophtheirus salmonis* (Krøyer)', Aquaculture Research 31 (11); 835-841.

Poole, W.R., Dillane, M., de Eyto, E., Rogan, G., McGinnity, P. and Whelan, K. (2007) 'Characteristics of the Burrishoole Sea Trout Population: Census, Marine Survival, Enhancement and Stock-Recruitment Relationship, 1971–2003'. In N.M. Grame Harris and N. Milner (eds.) Sea Trout: Biology, Conservation and Management, Blackwell Publishing Ltd, Oxford, pp. 279–306, doi: 10.1002/9780470996027.ch19.

Pratten, D.J. and Shearer W.M. (1983) 'Sea trout of the North Eske', Fisheries Management, 14, 49–65.

Quinn, T.P., McGinnity, P. and Cross, TF. (2006) 'Long-term declines in body size and shifts in run timing of Atlantic salmon in Ireland', Journal of Fish Biology 68:1713-1730.

Rijnsdorp, A.D., Peck, M.A., Engelhard, G.H., Möllmann, C. and Pinnegar, J.J. (2010) Resolving climate impacts on fish. ICES Co-operative Research Report, 301, 372pp.

Rodionov, S. N. (2005) 'Detecting regime shifts in the mean and variance: Methods and specific examples'. In V. Velikova and N. Chipev (eds.) Large-Scale Disturbances (Regime Shifts) and Recovery in Aquatic Ecosystems: Challenges for Management Toward Sustainability. UNESCO-ROSTE/BAS Workshop on Regime Shifts, 14–16 June 2005, Varna, Bulgaria, 68–72.

Shepherd, J. G. and Cushing, D. H. (1980) 'A mechanism for density dependent survival of larval fish as the basis of a stock-recruitment relationship', Journal du Conseil international l'Exploration de la Mer 39, 160.167.

Skilbrei, O.T. (1991) 'Importance of threshold length and photoperiod for the development of bimodal lengthfrequency distribution in Atlantic salmon (*Salmo salar*)', Canadian Journal of Fisheries and Aquatic Sciences, 48, 2163–2172.

Solomon, D. J. (1981) Smolt migration in Atlantic salmon (salmo salar) and sea trout (Salmo trutta L.). In Proceedings of the Salmon and Trout Migratory Behaviour Symposium. Ed. Brennan, E. L. and Salo, E. O. University of Washington, Seattle.

STAG (1990) Declining Sea Trout Stocks in the Galway/South Mayo Region – A Scientific Appraisal. Salmon Research Agency of Ireland for the Sea Trout Action Group.

Strothotte, E., Chaput, G. J. and Rosenthal, H. (2005) 'Seasonal growth of wild Atlantic salmon juveniles and implications on age at smoltification', Journal of Fish Biology, 67, 1585–1602.

Tallman, R. F. & Healey, M. C. (1991) 'Phenotypic differentiation in seasonal ecotypes of chum salmon, Oncorhynchus keta', Canadian Journal of Fisheries and Aquatic Sciences 48, 661.671.

Tesch, F.W. (1968). Age and Growth. Chapter 5 in Methods for Assessment of Fish Production in Fresh Waters by Ricker, W. E. IBP Handbook No. 3.

Tully O. (1992) 'Predicting infestation parameters and impacts of caligid copepods in wild and cultured fish populations', Invertebrate Reproduction and Development, 22, 91–102.

United Kingdom Climate Impacts Programme (UKCIP) (2005) Future climate scenarios. URL http://www.ukcip.org.uk/ [accessed 12 February 2009]

Whelan, K.F., Galvin, P.T., Poole, W.R. and Cooke, D.J. (1993) 'Environmental factors influencing the migration and survival of sea trout (Salmo trutta L.) smolts', ICES CM 1993/M:48.

Wootton, R.J. (1998) Ecology of Teleost Fishes. 2nd edn. Dordrecht, Kuwar Academic Publishers.

Wright, P.J., Metcalfe, N.B. and Thorpe, J.E. (1990) 'Otolith and somatic growth rates in Atlantic salmon parr: evidence against coupling', Journal of Fish Biology, 36, 2421–2449.

Youngson, A. F., MacLean, J. C., and Fryer, R. J. (2002) 'Rod catch trends for early-running MSW salmon in Scottish rivers (1952-1997): divergence among stock components', ICES Journal of Marine Science, 59: 836-849.

Zaugg, W.S. (1982) 'Relationships between smolt indices and migration in controlled and natural environments'. In E.L. Brannon, E.O. Salo (eds.) Proceedings of the Salmon and Trout Migratory Behaviour Symposium. University of Washington. Seattle, Washington, pp.173–183.

Zydlewski, G.B., Haro, A. and McCormick, S.D. (2005) 'Evidence for cumulative temperature as an initiating and terminating factor in downstream migratory behavior of Atlantic salmon (Salmo salar) smolts', Canadian Journal of Fisheries and Aquatic Sciences, 62, 68–7.

4 DEVELOPING CLIMATE SCENARIOS FOR THE BURRISHOOLE

Ciaran Broderick and Rowan Fealy

4.1 Introduction

Enhanced concentrations of greenhouse gases (GHGs) in the Earth's atmosphere have contributed to changes in the global climate system. The Intergovernmental Panel on Climate Change (IPCC) Fourth Assessment Report states that, "most of the observed increase in global average temperatures since the mid-20th century is very likely due to the observed increase in anthropogenic greenhouse gas concentrations" (IPCC, 2007: 10). One of the greatest challenges facing the scientific community is to understand how the Earth's climate may change in response to further increases in atmospheric GHGs and the likely impacts any such changes may have on both human and environmental systems.

Global climate models (GCMs) currently represent the most sophisticated tools available for studying the complexities of the Earth's climate. These models are physically based, three-dimensional numerical representations of the structure and behaviour of the global climate system. GCMs account for the complex workings and interactions of various sub-systems of the Earth's climate including the atmosphere, oceans, sea ice and land-surface processes. Climate models have become a key instrument in exploring the possible evolutionary pathways of the climate system under prescribed anthropogenic forcings. Projections from GCM experiments provide a primary source of information used to carry out impacts modelling, to develop climate change adaptation strategies and to inform future policy planning.

However it is widely acknowledged that while GCMs are likely to proficient at reproducing the large-scale features and dynamics of the Earth's climate system, the coarse resolution at which they operate restricts their capacity to provide a realistic description of both the workings and condition of the system at finer spatial scales (Grotch and MacCracken, 1991; Zorita and Von Storch, 1999). This aspect of GCMs severely limits the direct use of their output in local or regional scale impact applications where higher resolution climate projections are required (Giorgi and Mearns, 1991, Wilby and Wigley 1997, Mc Guffie et al. 1999, Giorgi et al. 2001).

GCMs are currently run at a relatively coarse spatial resolution, typically of the order of 300-500 km. Operating at this scale is necessary given the constraints of currently available

computing power and the highly dynamic nature of the climate system. At this resolution the influence of important sub-grid scale features, which have a strong bearing on local climate conditions, cannot be explicitly accounted for. Considering local scale forcings in any plausible future scenario is particularly important where land–surface conditions significantly influence the characteristics of regional and local climate. This is especially true for regions which present highly heterogeneous environments such as coastal zones, regions with complex topographies and areas with diverse land types (Wilby et al., 2004). Furthermore their coarse resolution and limited physics prohibits them from resolving important climate processes which occur at a sub-grid scale level (e.g. cloud formation, evaporation, convective rainfall). Many of these processes are either omitted or approximated in the model structure using various parameterization schemes. Sub-grid scale processes strongly affect the local climate at the scales of the ecological and human environment and as such are often those with the greatest relevance to impact modellers (Zorita and von Storch, 1999).

The climate scenarios used to drive impact assessments should reflect sub-grid scale processes and capture locally specific climate details lacking in the output from GCMs. This necessitates 'downscaling' coarse resolution model output to the finer spatial scales relevant for studying the impacts of climate change. This may be to higher resolution grids or point specific locations on the Earth's surface commensurate with instrumental stations. Downscaling is based on the principle that local or regional climate is primarily determined by climate conditions on a much larger scale. Developing models which capture this relationship allows changes in key local-scale climate variables, such as temperature and precipitation, to be explored using low resolution global climate model projections.

4.2 Downscaling Methods

A number of downscaling techniques exist with which to bridge the resolution gaps between the coarse grid-scale information provided by climate models and the high resolution climate scenarios required for impacts assessments. Downscaling methods, as reviewed in Wilby and Wigley (1997), Wilby et al, (2004) and Mearns et al. (2003), are divided into four general categories: dynamical downscaling (Mearns et al., 1995), regression based methods (e.g. Hewitson and Crane, 1996; Wilby et al., 1999), weather classification approaches (e.g. Yarnal, 2001) and stochastic weather generators (Richardson, 1981; Racsko et al,. 1991; Semenov and Barrow, 1997; Bates et al., 1998).

4.2.1 Dynamical Downscaling

Dynamical downscaling involves embedding a higher resolution regional climate model (RCM) within a coarse resolution GCM with the aim of explicitly accounting for regional scale forcings (e.g. complex topographical features and heterogeneous land cover) and mesoscale climate processes not adequately captured by global models (Giorgi and Mearns, 1991; Giorgi and Mearns, 1999; Giorgi et al., 2003).

Regional models produce climate scenarios with a high spatial resolution over a specific area of interest to impact assessors. Over the bounded domain on which the model is focused the physical dynamics of the atmosphere are simulated using horizontal grids with a resolution typically of the order of 20-50 km. Information on large scale climate variables (e.g. pressure, vorticity, temperature, humidity) are provided to the regional climate model from a 'parent' global climate model. This information is processed in a physically consistent manner to produce more spatially detailed climatological simulations.

The key benefit of employing RCMs is that they operate at a much higher resolution, due to the smaller domain, and are capable of resolving important sub-grid scale processes dynamically. Thus regional models are able to realistically simulate important regional climate features such as orographic precipitation, local winds and extreme weather events. Despite their high resolution some climate processes will still occur at a sub-grid scale and must be represented parametrically. This, along with the biases inherited form the driving GCM, lead to uncertainty in regional model projections and it is recommended that multiple model scenarios are used for climate change assessments (Fowler et al., 2007). However dynamical models are computationally demanding limiting their application to multiple scenario assessments. The resolution at which RCMs operate also means their output may still require downscaling to the finer spatial scales required for impacts analysis. Where high resolution climate scenarios are required statistical methods offer a viable alternative to dynamical downscaling.

4.2.2 Statistical Downscaling

Statistical downscaling is founded on the principle that regional and local climate is conditioned by two factors: the large-scale climatic state and regional physiographic features such as topography, land-sea distribution and land use (von Storch, 1995). Based on this principle, quantitative relationships between local meteorological "predictands" or surface variable of interest and large scale atmospheric "predictors" can be developed. Once established statistical models can be then used to obtain point scale estimates of key climate variables from coarse resolution GCM projections. Predictor variables typically used for downscaling include

measures of atmospheric circulation (e.g. geopotential heights, sea level pressure, air temperature and humidity taken from different levels in the atmosphere).

A number of key assumptions are implicitly associated with statistical downscaling methods. The most fundamental of which is that the predictor-predictand relationships established under present day climate remain valid under the different forcing conditions of possible future climates. This can be tested by validating the model using an independent period from instrumental records which is representative of a climate regime 'different' to that used for fitting the model (Charles et al., 2004). Statistical downscaling also assumes that the large-scale predictors employed to derive future local scale changes are related to the underlying physical processes controlling local scale weather events and are well simulated by the driving global model. Furthermore it is assumed that the large scale predictors used adequately capture the climate change 'signal' (Hewiston and Crane, 2006; 1996). For example, downscaling which only uses circulation based predictors may fail to capture changes in atmospheric humidity under warmer climate conditions, such a model is likely to underestimate changes in key climate parameters such as precipitation. Predictor selection is therefore a critical aspect of statistical downscaling and a source of uncertainty in downscaled scenarios. Throughout the present study care has been taken to address these assumptions.

One of the weaknesses of statistical based approaches to downscaling is that they tend to underestimate the variability of local climate and consequentially may under represent the occurrence of extreme events. This primarily applies to regression based methods and certain weather classification techniques. The under prediction of variance is particularly evident when downscaling those surface variables which are to a lesser degree controlled by the large-scale atmospheric state and are instead strongly influenced by local scale forcings (e.g. precipitation, wind speed). To date a number of techniques have been employed to address this shortcoming. Variance inflation, as implemented by Karl et al. (1990), increases the variance of the downscaled series by multiplying by a suitable scaling factor. However, Von Storch (1999) criticizes this method for its assumption that all local variability can be traced back to large-scale variability. He advocates the use of an alternative method termed 'randomization' where the unrepresented variability is captured by adding white noise to the predicted series. Burger (1996) employs a more sophisticated technique based on canonical correlation analysis termed 'expanded downscaling'. A review of each of these methods is outlined in Burger and Chen (2005).

Statistical downscaling methods can be broadly categorized as follows:

i) Weather Classification Schemes - Weather classification schemes relate the occurrence of particular weather types to local and regional climate variations. Historical records of large scale surface and upper atmosphere pressure patterns are used to classify the daily circulation into discrete weather types. This can be done using an externally established system (e.g. Lamb Weather type, European Grosswetterlagan) or employ an objective classification scheme developed for downscaling purposes (e.g. Principal Components Analysis, indices of airflow, Cluster Analysis). Once a relationship is established between local climate conditions and the occurrence of each weather type, the same weather classification criteria are then applied to the output from GCMs. Future changes in the local climate can then be assessed based on projected changes in the frequency of weather types (Hay et al., 1991; Corte-Real et al., 1998; Goodess and Palutikof, 1998).

Weather typing methods have the benefit of being based on the sensible linkages between climate at the large scale and local scale. The technique can be applied to downscale a range of environmental variables and can be employed in multi–site applications. There is however a number of weaknesses associated with this method. One of the greatest problems shared by all weather classification schemes is their insensitivity to within-type variability e.g. wet circulation types which include the occurrence of dry days (Brinkmann, 2000). Also a number of assumptions are implicit when using weather classification as a downscaling tool. The most fundamental of which is that the characteristics of each weather class will remain the same under future climate conditions. The absence of other atmospheric variables from the driving data assumes that pressure patterns alone capture the main processes governing local scale weather events. For certain variables this may undermine their connection to changes in large scale atmospheric conditions, e.g. the absence of a variable representing atmospheric humidity when downscaling precipitation (Karl et al., 1990; Murphy, 2000; Beckham and Buishand, 2002). Such an approach was tested for the Burrishoole, however a clear signal between weather conditions in the catchment and each weather type was difficult to discern.

ii) Stochastic Weather Generators - Stochastic downscaling methods employ weather generators (WG) such as WGEN, LARS-WG or EARWIG, to produce multiple synthetic series of weather data conditioned on global model projections. WGs can be regarded as elaborate random number generators which replicate the statistical attributes of local climate variables but not the observed sequence of events (Wilks and Wilby, 1999). WGs firstly determine the sequence of wet and dry days, often by employing variants of Markov chain models. Secondary variables such as rainfall amounts, temperature, solar radiation and evaporation are subsequently modelled conditional on the occurrence of precipitation.

Downscaling is carried out by altering the parameters of the WG in-line with grid scale GCM simulations. Projected changes in the large scale atmospheric state are then reflected in the stochastically generated local-scale weather data (Katz, 1996; Semenov and Barrow, 1997; Wilks, 1999).

Stochastic downscaling techniques have the advantage of capturing the variability of local climate conditions allowing for a better representation of extreme events in the driving scenarios for impact models. However it has been shown that WGs which employ Markov methods tend to underestimate inter-annual variability (Semenov et al., 1998). One of the key advantages of employing stochastic methods is the ability to generate large ensembles of scenarios for use in risk assessments which may be a requirement of certain impact applications (e.g. crop modelling, water resources management). Weather generators also have the benefit of producing climate scenarios with a high temporal resolution (e.g. sub-daily rainfall data). The key drawbacks of employing stochastic methods are associated with the difficulties in modifying the model parameters. It has been found that altering the precipitation parameters can result in inconsistent changes in the secondary variables (Wilks, 1992). Related to this is the assumption that the relationship between each weather variable established under current conditions remains the same under future climates.

iii) Regression Based Methods - Regression based methods establish a statistical relationship between an observed local-scale meteorological variable (e.g. point scale precipitation) and a suite of large-scale atmospheric predictor variables (e.g. mean sea level pressure, vorticity, meridional velocity). The coarse scale output from GCMs is then used to drive this relationship, allowing changes in the corresponding local scale variable to be estimated. Although the basic methodology remains the same, specific approaches differ according to the transfer function used, predictors selected and statistical fitting procedure employed. The often complex and non-linear predictor-predictand relationships which exist have necessitated the use of a wide range of regression techniques including linear and non-linear regression (Murphy, 1999), artificial neural networks, (Crane and Hewitson, 1998), and canonical correlation analysis (von Storch et al., 1993).

Regression methods have the benefit of allowing a direct and physically meaningful connection to be made between local scale weather events and large scale atmospheric conditions. This method also has the advantage of being easy to apply, allowing for the production of multiple ensembles required for uncertainty analysis. As discussed above the key weaknesses of

regression based downscaling are related to the under prediction of variance (von Storch, 1999; Burger 1996) and the uncertainties associated with predictor selection.

4.2.3 Relative Skill of Statistical and Dynamical Downscaling

As outlined in Table 4.1 there are a number of strengths and weakness associated with both dynamical and statistical downscaling methods. Statistical downscaling is ideal when a large number of ensembles or transient climate scenarios must be generated from more than one GCM. This is an important consideration given the uncertainty associated with future climate projections and the need to address this by developing a range of local-scale scenarios. The use of dynamical models for this purpose is limited given the computational expense associated with producing multiple climate scenarios under the forcing conditions of different GCMs and emission pathways. However unlike dynamical methods statistical downscaling cannot explicitly model the physical processes which condition local-climate. Instead empirical methods aim only to quantitatively describe the relationship between large-scale atmospheric conditions and local-scale observations without any requirement to understand this relationship.

Table 4.1 Summary of the Relative Strengths and Weaknesses of Statistical and Dynamical Downscaling Techniques (adapted from Wilby and Wigley, 1997).

	Statistical Downscaling	Dynamical Downscaling
Strengths	Can derive point-scale climate information from GCM-scale output	10-50 km resolution climate information from GCM-scale output
	Computationally inexpensive	Responds to different forcing conditions in a physically consistent way
	Allows the easy production of ensembles of climate scenarios for risk/uncertainty analyses	Capable of resolving important physical processes dynamically (e.g. orographic rainfall)
	Easily transferable to other regions	Consistency with GCM
	Can be used to derive variables not available from RCMs	
Weaknesses	Dependent on the realism of GCM boundary forcing; effected by biases in driving GCM	Dependent on the realism of GCM boundary forcing
	Choice of domain size and location affects results	Choice of domain size and location affects results
	Require long and reliable observed historical data series for calibration	Requires significant computing power
	Dependent upon choice of predictors	
	Domain size, climatic region and season affects downscaling skill	
	Fundamental assumption of model stationarity is not verifiable	Limited to producing few ensembles of climate scenarios

There is a broad consensus within the downscaling community as to the skill of both dynamical and statistical methods. Each method has been shown to give comparable results when estimating surface weather variables under current climate conditions, (Kidson and Thompson 1998, Mearns et al. 1999, Murphy 1999, Hellström et al., 2001). However different downscaling approaches show a divergence between their projections of future climate at the regional scale (Cubasch et al., 1996; Wilby and Wigley, 1997; Wilby et al., 1998; Mearns et al., 1999; Murphy, 2000). Hence differences in downscaling methods are one of the key sources of uncertainty in estimates of regional-scale climate.

4.3 Sources of Uncertainty in Climate Projections

Within the scientific community there is a high degree of confidence that further anthropogenic emissions of GHGs and aerosols will continue to change the composition of the Earth's atmosphere throughout the 21st century. There is, however, less confidence about exactly how the climate will change in response to this (Dessai et al., 2007). A considerable

amount of uncertainty is associated with estimates of future climate change (Jenkins and Lowe, 2003). The divergence between future model projections applies not only to the magnitude but also to timing, spatial distribution and direction of change (e.g., some projections show more precipitation whereas others show less). These uncertainties pose major challenges for planners making decisions on mitigation and adaptation strategies.

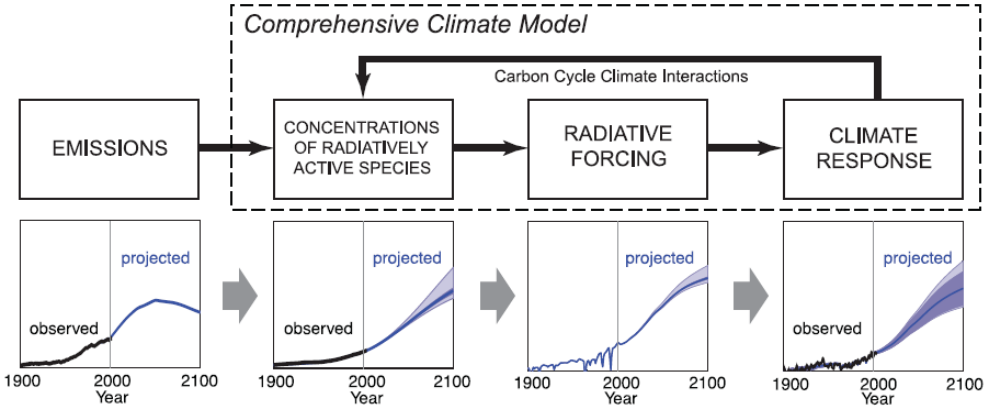

Figure 4.1 Uncertainty arises at each step in the process of developing a climate model projection. (Source: IPCC, 2007).

According to New and Hulme (2000) the uncertainties associated with climate projections are due to either "incomplete knowledge" or "unknowable knowledge". The former arises due to our limited understanding of climate system processes and their imperfect representation in climate models. Both of these factors introduce uncertainty when modelling the response of the climate system to anthropogenic forcing. However with a greater knowledge of the climate system and improvements in computing power this source of uncertainty can be redressed. Unknowable knowledge is related to the unpredictable and 'chaotic' nature of the climate system, both in the real world and in model simulations, as well as the impossibility of determining future human actions and subsequent changes in anthropogenic emissions. In order to consider uncertainties which arise due to unpredictability, different 'scenarios' or storylines are used to represent a range of possible outcomes or sequence of events which give rise to different emissions pathways. Understanding the origin of uncertainties in climate modelling and their relative significance is critical when exploring the impacts of climate change. As illustrated in Figure 4.1 uncertainty arises at each stage in the process of developing local or regional estimates of climate change. This accumulation or propagation of uncertainty has been variously described as a cascade of uncertainty (Schneider, 1983) or the uncertainty explosion (Henderson-Sellers, 1993).

4.3.1 Emission Scenarios and GHG Concentrations

To model changes in the climate system arising from anthropogenic forcings, GCMs must take account of future atmospheric concentrations of GHGs (CO_2, methane, nitrous oxide, etc.) and aerosol emissions. Based on assumptions about demographic change, economic development, technological change and energy-use the IPCC Special Report on Emission Scenarios (SRES) outlines several different storylines which plot possible directions of human development through the 21st century (Nakicenovic et al., 2000). These narratives are the basis for formulating different emission scenarios. Each of the SRES storylines of future development, of which there are 40 presented, can be related to four preliminary marker scenarios; A1, A2, B1 and B2 (Box 4.1).

The four marker scenarios outlined in Box 4.1 account for approximately 80-90% of the range of future emissions (New and Hulme, 2000). The uncertainties associated with future emission pathways stem from assumptions made about the underlying socio-economic emissions drivers and the means by which future emissions are quantified using each narrative. The uncertainty surrounding future emissions is further compounded when translating emission scenarios into atmospheric concentrations of radiatively active gases. This is in part due to an incomplete understanding about the cycle of different GHGs through the Earth system (e.g. the carbon cycle). The deficiencies in our knowledge about the sources and sinks GHGs, as well as their lifespan in the atmosphere, lead to uncertainties when modelling changes in biogeochemical cycles and atmospheric concentrations of GHGs.

Box 1. SRES Emissions Scenarios

A1. The A1 storyline and scenario family describes a future world of very rapid economic growth, global population that peaks in mid-century and declines thereafter, and the rapid introduction of new and more efficient technologies. Major underlying themes are convergence among regions, capacity building and increased cultural and social interactions, with a substantial reduction in regional differences in per capita income. The A1 scenario family develops into three groups that describe alternative directions of technological change in the energy system. The three A1 groups are distinguished by their technological emphasis: fossil intensive (A1FI), non-fossil energy sources (A1T), or a balance across all sources (A1B) (where balanced is defined as not relying too heavily on one particular energy source, on the assumption that similar improvement rates apply to all energy supply and end-use technologies).

A2. The A2 storyline and scenario family describes a very heterogeneous world. The underlying theme is self-reliance and preservation of local identities. Fertility patterns across regions converge very slowly, which results in continuously increasing population. Economic development is primarily regionally oriented and per capita economic growth and technological change more fragmented and slower than other storylines.

B1. The B1 storyline and scenario family describes a convergent world with the same global population, that peaks in mid-century and declines thereafter, as in the A1 storyline, but with rapid change in economic structures toward a service and information economy, with reductions in material intensity and the introduction of clean and resource-efficient technologies. The emphasis is on global solutions to economic, social and environmental sustainability, including improved equity, but without additional climate initiatives.

B2. The B2 storyline and scenario family describes a world in which the emphasis is on local solutions to economic, social and environmental sustainability. It is a world with continuously increasing global population, at a rate lower than A2, intermediate levels of economic development, and less rapid and more diverse technological change than in the A1 and B1 storylines. While the scenario is also oriented towards environmental protection and social equity, it focuses on local and regional levels.

Box 4.1 SRES emissions scenarios with four scenario 'families' illustrated (IPCC, 2001 after Nakicenovic et al., 2000).

4.3.2 Radiative Forcing

There are uncertainties associated with how the radiative energy budget of Earth's climate system may be altered by higher concentrations of GHGs as well as other radiative forcings including aerosols (e.g. sulphate, black carbon). Whilst the effects of increasing CO_2 concentrations is well understood and represented in climate models the influence of other GHGs and aerosols on the Earth's radiative balance are less well understood. For example it is uncertain what the dominant effect of aerosols is likely to be. This relates to both their role in cloud formation and their direct effect on the absorption and scattering of radiation. Cloud feedbacks remain the greatest contributor to uncertainty.

4.3.3 Climate System Predictability

Climate projections include predicted changes in atmospheric variables such as temperature and precipitation along with estimated changes in other components of the climate system (e.g. sea-level rise). Uncertainty arises in future projections as a consequence of the lack of scientific understanding in determining the response of the climate system to radiative forcing. Climate sensitivity is a broad measure of this response and refers to the increase in global mean surface air temperature due to a doubling of atmospheric CO2 concentrations (New and Hulme, 2000). According to the IPCC (2007), the sensitivity of the climate system is in the range of 2.0°C - 4.5°C, with a best estimate of about 3.0°C.

GCMs provide a mathematical representation of those climate processes, interactions and feedback mechanisms which are fundamental to how the climate system works. Despite their level of complexity these models remain a simplified representation of reality - based on differing conceptualizations and empirically derived assumptions about the workings and state of the climate system. Consequently when run using the same forcing scenario different climate models may produce estimates of global and regional climate change which deviate considerably. Inter-model variations regarding the climate systems response to radiative forcing is reflective of each model's respective climate sensitivity. The disagreement exhibited between GCMs is due in part to our incomplete understanding of the climate system, differing model configurations (e.g. spatial resolution as well as the approximation omission and mis-specification of important physical processes) and the 'chaotic' nature of the climate system.

According to Giorgi (2005), model configuration provides a dominant contribution to the uncertainty cascade with almost half of the overall range in the IPCC global temperature change estimates attributed to this factor alone. The resolution at which GCMs operate mean they fail to explicitly resolve sub-grid scale physical processes (e.g. cloud formation, topography) which must be represented parametrically. The approximation of important processes is one of the key sources of uncertainty in GCM simulations. The multitude of equally plausible ways in which different climate processes can be parametrically represented leads to differences in model projections. Climate change is not only a product of the direct effect of increasing GHGs but also of the interaction between different components of the climate system (e.g. atmosphere, ocean, land surface, cryosphere and biogeochemical cycles). An additional cause of intra-model variability relates to the differing representation of various climatic feedback mechanisms (e.g. water vapour/atmospheric warming, cloud formation/radiation, ice and snow albedo). Owing to the conflicting nature of different GCM responses to increased GHG concentrations the use of the output from a single model would

result in the suppression of crucial uncertainties in climate projections (Hulme and Carter, 1999) and thus could lead to inappropriate impacts planning and adaptation strategies (Wilby and Harris, 2006).

Further uncertainties are introduced due to representation of unforced internally generated climate variability. The natural variability of the climate system has the capacity to either exacerbate or mitigate the influence of both human and natural forcings. One way of addressing this uncertainty is to undertake a series of model experiments (ensembles) in which the forcing conditions remain static but the initial conditions are altered. Each model run should produce a different time series evolution but will have the same underlying trend representing the climate change 'signal'.

4.3.4 Uncertainty in the Development of High Resolution Climate Scenarios

Despite their highly complex nature GCMs currently operate a too coarse a resolution for their output to be directly applied to regional and local scale impacts analysis. This arises because GCMs can only provide a "broad-brush" interpretation of how variables, such as continental-scale temperature and rainfall patterns, might change in response to anthropogenic forcing (Diaz-Nieto and Wilby, 2005). Furthermore GCMs cannot explicitly resolve many of the important regional- and local-scale processes (e.g. convective rainfall, local winds) which are often required in the driving data for impacts studies. In order to produce scenarios of higher temporal and/or spatial resolutions than currently provided by raw GCM output some form of downscaling is required. However, as highlighted above, the limitations and underlying assumptions implicit in the process of downscaling climate scenarios introduces an additional level of uncertainty to local or regional scale estimates of climate change. Dynamically downscaled scenarios are subject to many of the same uncertainties associated with GCMs (e.g. model configuration, parameterization, resolution, climate variability), however regional models have the added complicating factor of any bias or error present in the driving GCM being propagated through to a regional level. The uncertainty introduced to statistically downscaled scenarios arises from a number of sources including the method chosen, the predictor variables employed as well as the calibration period and dataset selected. Similar to dynamical methods, statistical downscaling output is also subject to biases and errors in the parent GCM.

4.3.5 Uncertainty in Impacts Models

When attempting to model the impacts of climate change on human and environmental systems an additional source of uncertainty can be attributed to the impacts models

themselves, represented by the final step in the "cascade of uncertainty" (Figure 4.2). Not unlike climate models the limitations and assumptions associated with impacts models contribute to a level of uncertainty in their output. One of the greatest uncertainties associated with impacts analysis is the assumption that the model remains valid under future climate conditions of which it has no experience.

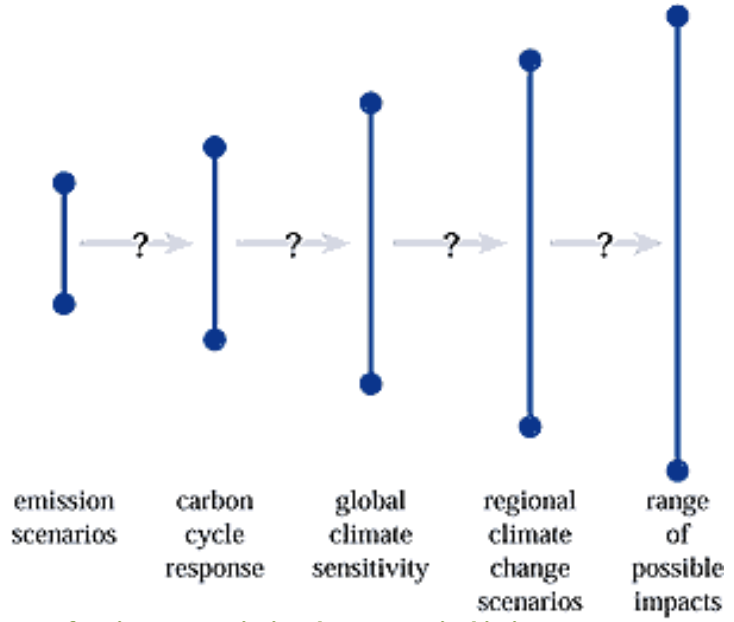

Figure 4.2 Range of major uncertainties that are typical in impact assessments showing the "uncertainty explosion". The uncertainty becomes amplified as it is propagated through from each stage in the modelling process (modified after Jones, 2000, and "cascading pyramid of uncertainties" in Schneider, 1983) (Source: IPCC, 2001).

4.3.6 Managing Uncertainty in Climate Projections

Owing to the significant issues which it creates for impact assessors as well as the implications it has for the development of robust adaptation and mitigation strategies the quantification of uncertainty has become a critical issue in the field of climate modelling and impacts analysis. Although it is common practice the over-reliance on a single realisation of future climate, typically derived using a single emissions pathway and climate model, can lead to the suppression of crucial uncertainties in estimates of climate change. Hulme and Carter (1999) go so far as to state that this practice is 'dangerous' as any subsequent policy decisions will only be founded on a partial assessment of the risk involved. Consequently employing a single prediction of future climate is an inappropriate strategy when examining the impacts of climate change and developing adequate adaptation responses (Wilby and Harris, 2006). Indeed it is now widely recognized that comprehensive impact studies must address the issue of uncertainty by considering multiple climate projections. Therefore there is an onus on climate modellers not to produce a deterministic account of climate change, but rather a range of plausible climate pathways which allow for some consideration of the uncertainties encountered at each stage in the modelling process.

By using a single scenario impacts modellers are effectively discounting the possibility of alternative outcomes which may have an equal likelihood of occurrence. Recent research has moved from using a single realisation of future climate towards embracing uncertainty by employing a range of plausible climate pathways derived from multiple GCMs and GHG emission scenarios. Producing a range of climate projections allows for some quantification of uncertainty, calculated using the probability distribution for all possible projected outcomes combined. In this study the uncertainty arising at each stage in the development of local scale climate scenarios and how they were accounted for is outlined below.

- Uncertainties due to emissions scenarios uncertainty were handled by using more than one forcing scenario (A2 and B2).
- Uncertainties due to inter-model variability were considered by using the output from more than one climate model (HadCM3, CSIROmk2 and CGCM2).
- Uncertainties due to downscaling were accounted for by using different downscaling methods.

4.4 Data and Methods

4.4.1 Data

Observed records of daily precipitation and temperature (minimum and maximum) were obtained from the Millrace climatological station located in the Burrishoole catchment. Data for the remaining meteorological variables (wind speed, relative humidity, radiation and potential evaporation) were obtained from the Belmullet synoptic station located north-west of the catchment. This station is operated by the Irish Meteorological Service Met Éireann. Although instrumental recordings are taken of these variables in the catchment, their records were either of inadequate length or insufficient quality to be used in this study. For all local-scale variables, with the exception of radiation (1981-2000) and potential evaporation (1971-2000), observed records were available for the period 1961-2000.

The observed large-scale atmospheric data required to establish the predictor-predictand relationships were obtained from the UKSDSM data archive (Wilby and Dawson, 2004). The source of this data is the National Center for Environmental Prediction (NCEP) reanalysis project (Kalnay et al. 1996). Although reanalysis data is essentially modelled data, the model is constrained by observational records from the global monitoring network and the model output is in the same gridded format as that from GCM experiments. The UKSDSM archive contains daily predictors, describing atmospheric circulation, thickness, and moisture content at the surface, 850 and500hPa, for nine regions covering the British Isles, for the period 1961–

2000. It is common practice when developing local-scale climate scenarios to take climate information from the grid box within which the study site is located. Therefore only large-scale datasets for the Irish grid box were selected for use in this study.

Future climate scenarios were generated using predictor variables for the Irish grid box supplied by four GCMs and two emission scenarios (the medium-high (A2) and medium-low (B2) Emissions of the Intergovernmental Panel on Climate Change Special Report on Emission Scenarios (IPCC SRES)) for the period 1961–2100. This data was also obtained from the UKSDSM data archive (Wilby and Dawson, 2004). The GCMs considered were: HadCM3 from the Hadley Centre for Climate Prediction and Research (Met Office, UK); CCGCM2, from the Canadian Centre for Climate Modelling and Analysis (CCCMA; Canada) and CSIRO-Mk2 from the Commonwealth Science and Industrial Research Organisation (CSIRO, Australia). All large-scale datasets, including NCEP and GCM data, were regridded to conform to the 2.5° latitude x 3.75° longitude grid corresponding to the HadCM3 GCM (Harris, 2004). To ensure the downscaled scenarios were not compromised by systematic biases in the driving GCM data, all GCM and NCEP candidate predictors were normalized with respect to their 1961-1990 climatology (after Karl et al., 1990). As carried out by Fealy and Sweeney (2007) the 1-day lead and lag of each predictor was calculated. This allows for the temporal offset between the NCEP data, averaged over the 00:00–24:00 h period, and instrumental weather records, calculated over the period 09:00–09:00 h. Employing lagged variables as predictors also allows for a temporal lag which may occur between the predictor and predictand.
The output from climate model experiments provides an inadequate basis for assessing the impacts of climate change at the scales relevant to human and environmental systems. GCMs have a spatial resolution of hundreds of kilometres whilst regional models may operate at a resolution as fine as tens of kilometres. However many impact applications and adaptation studies require the equivalent of point scale climate observations and are highly sensitive to sub-grid scale climate processes parameterized in coarse scale models. For the purposes of developing climate scenarios at the scales relevant for studying climate change in the Burrishoole catchment statistical downscaling methods were applied to the output from GCM experiments.

The assumptions implicit in statistical downscaling, along with the strengths and weaknesses associated with different downscaling techniques, are discussed above. In order to address the various components of uncertainty arising from emission scenarios, GCM structures, parameterizations and climate sensitivities the output from three GCMs, each run using two different emission scenarios, were used as the driving data for the downscaled scenarios. The

shortcomings and limitations associated with statistical downscaling represent an additional source of uncertainties in estimates of local climate change. In order to address this, and in recognition that no one optimal method exists, both Linear Regressions and Generalized Linear Models (GLMs) were employed.

4.4.2 Linear Regression

Linear regression was implemented through the use of statistical downscaling software (**S**tatistical **D**own**S**caling **M**odel-SDSM), a software package used for downscaling multiple-scenarios of surface weather variables at individual sites on a daily time-step using grid resolution NCEP re-analysis and GCM data. The model has previously been applied to a host of meteorological, hydrological and environmental assessments within a range of geographical contexts (Hassan et al., 1998; Wilby et al., 1999, 2000; Hay et al., 2000). SDSM is best described as a 'hybrid' of the stochastic weather generator and regression based downscaling methods (Wilby et al., 2002).

Multiple linear regression comprises the core deterministic component of the model and is used to establish a direct linear relationship between a set of large-scale atmospheric predictors and the point-scale variable of interest. To address the issue of underestimated variance associated with regression modelling an additional stochastic component is available in SDSM which allows the user to artificially inflate the variance of the downscaled series. Variance inflation is carried out using a pseudo-random number generator which reproduces values from a normal distribution with a mean equal to zero and a standard deviation equal to the standard error. These values are added to the deterministically derived output for each day. In this way the residual from the regression model is used to increase the variability of the downscaled series. Variance inflation is necessary given the importance of representing extreme events in the driving data for impacts models.

The weather generator element of SDSM also enables multiple synthetic series or ensembles of daily weather data to be produced using a common set of grid-scale predictors. Ensemble members differ with respect to their individual time-series evolution but possess the same overall statistical properties. Each series is considered to be an equally plausible realisation of local climate change. The degree to which each simulation differs is dependent on the relative significance of the stochastic component in the model structure. For those variables which are largely a factor of large-scale atmospheric forcing a high proportion of the variance will be accounted for by regression alone. However where grid-scale predictors only account for a fraction of the observed variance the stochastic element has a comparatively greater weighting.

This applies to variables like precipitation which display more 'noise' arising from localised factors. Stochastically generating multiple climate realizations has the advantage of allowing the range of internal variability displayed by the local climate to be somewhat represented in the downscaled ensembles.

In this study SDSM was employed to downscale climate scenarios for the following variables:

- Temperature (minimum and maximum) (°C)
- Precipitation (mm)
- Wind Speed (kt)
- Relative Humidity (%)
- Solar Radiation (Mj m^{-2})
- Potential Evapotranspiration (PET) (mm)

Where a variable did not conform to the requirements of linear regression, transformation of those variables was undertaken prior to model fitting. For each downscaled variable one hundred simulations were performed to produce one hundred synthetic series of daily values for each GCM and emission scenario.

4.4.3 Generalized Linear Model

Generalised linear models (GLM) can be thought of as a flexible generalization or expansion of the standard linear regression model. This approach to regression analysis can be used to overcome some of the limitations associated with ordinary least squares regression. Where the conventional linear model requires the response variable to be normally distributed, GLMs have the advantage of being able to model data series which follow probability distributions from the exponential family (e.g. binomial, Poisson, gamma). As a result of this, the use of GLMs avoid the need for data transformation. This is desirable given the loss of information which can occur when altering a variables distribution through rescaling.

The relationship exhibited between the response and explanatory variables may be more complex than be the simple linear form required for linear regression. GLMs can be used to overcome this allowing the non-linear relationship between the dependent variable and predictor set to be modelled. A thorough account of GLMs is given in Mc-Cullagh and Nelder (1989). GLMs have previously been used to study different climatological series (Coe and Stern, 1982; Stern and Coe, 1984; Chandler and Wheater, 1998, 2002; Yan et al., 2002) and have also been employed in the field of statistical downscaling (Abaurrea and Asín, 2005; Fealy and Sweeney, 2007). As GLMs fit probability distributions to the variable being modelled and

do not require data transformation they should provide a better representation of low frequency events. This is an important consideration given the significance of extreme events in the driving scenarios for impact models.

Given that GLMs can be used to model any variable which approximates to a distribution from the exponential family, GLMs have been used in this study to downscale scenarios for precipitation and wind speed, both of which present highly skewed distributions. Maximum likelihood estimation was used to optimize each models parameter values over the calibration period. The GLM is a fully deterministic method and as such the downscaled climate scenarios are solely the product of grid-scale forcing. Therefore for each GCM and emission scenario there is only one realisation of future climate.

4.4.4 Predictor Selection

The choice of predictor variables is a key determining factor on the character of the downscaled scenario (Winkler et al., 1997; Charles et al,. 1999) and has been shown to represent a significant source of uncertainty in estimates of local climate change (Huth, 2004). However despite the importance of this process there is little consensus within the downscaling community as to an optimum predictor set or selection process. Past studies have employed a diverse number of techniques and predictor combinations covering a range of geographical contexts and thus do not easily lend themselves to interpretations of predictor skill or applicability to different situations. As noted in previous studies selecting the most appropriate set of predictors, which are sensitive to the region and timescales for which the study is being undertaken, is a better approach than the use of a single predictor or standard predictor set (Wilby et al., 1998; Huth, 2004). Despite the differing and often subjective approaches taken to predictor selection there are a number of key points common to previous work which suggest the predictors selected should ideally:

- Be realistically simulated by climate models
- Have a strong correlation with the target variable
- Be physically related to the predictand
- Adequately capture the climate change 'signal'
- Avoid interdependence
- Capture inter-annual variability

However these criteria are frequently at odds with one another indicating that a balance must be struck when choosing an appropriate predictor set. For example it is thought that climate

models give a more realistic description of large-scale circulation variables than of surface parameters (Murphy, 1999). However many studies (e.g. Kidson & Watterson, 1995; Wilby & Wigley, 1997) have shown that downscaling models with 'circulation-only' predictors are largely insensitive to changed climate conditions, thus warranting the inclusion of additional variables which may be less well simulated by climate models.

Table 4.2. List of primary candidate predictor variables for use in the analysis from the UKSDSM data archive

Variable	Abbreviation
Mean temperature	temp
Mean sea level pressure	mslp
500 hPa geopotential height	p500
850 hPa geopotential height	p850
Near surface relative humidity	rhum
Relative humidity at 500 hPa	r500
Relative humidity at 850 hPa	r850
Near surface specific humidity	shum
Geostrophic airflow velocity	*f*
Vorticity	*z*
Zonal velocity component	*u*
Meridional velocity component	*v*
Wind direction	*th*
Wind Divergence	*zh*
Note: Italics indicate secondary airflow indices calculated from pressure fields (surface, 500 and 850 hPa).	

The process of predictor selection for this study was largely driven be the correlation shown between the candidate predictors and the target variable. Predictors were also chosen with the aim of capturing the key atmospheric mechanisms known to influence local-scale events (e.g. the inclusion of an atmospheric moisture variable when downscaling precipitation) (Table 4.2). Care was taken to avoid multicollinearity by selecting a parsimonious set of predictors which exhibited little intercorrelation. The strength of the relationship between the predictand and predictors varies both regionally and seasonally. To account for this a separate model was developed for each season for which the most appropriate set of predictors were selected. However where the downscaled climate scenario was shown to be sensitive to the selection of a particular atmospheric variable the same predictor was chosen for each season.

In addition to employing large-scale surface and atmospheric variables as predictors potential radiation and delta temperature were selected when modelling daily solar radiation and potential evaporation. This approach takes its cue from conventional weather generator

techniques which calculate incoming solar radiation using measurements of other meteorological variables (Donatelli et al. 2006; Fealy and Sweeney, 2008). The amount of solar radiation received at a given point on the Earth's surface is a function of potential radiation (i.e. the amount of radiation which that point on the Earth's surface could receive if there was no atmosphere or clouds) and some measure of atmospheric transmissivity. In this case transmissivity is related to cloud cover - for which delta temperature is taken as a proxy. Bristow and Campbell (1984) demonstrated that a relationship exists between the radiation transmitted through the atmosphere and the diurnal range in near surface air temperature.

Delta temperature is effectively a measure of temperature range and is calculated using (Bristow and Campbell, 1984):

$$\Delta T = Tmax_t \frac{(Tmin_t + Tmin_{t+1})}{2}$$ **Equation 4.1**

Where,
Tmin – minimum temperature
Tmax – maximum temperature
t - time

Tmin and Tmax represent point scale temperature at time t. A high delta temperature value is indicative of low cloud cover and a high incidence of incoming solar radiation. Conversely a low value indicates high cloud cover and a low incidence of incoming solar radiation. For the purposes of model calibration delta temperature was calculated using observed records from the Burrishoole weather station. Delta temperature for each GCM and emissions pathway was calculated using previously downscaled temperature scenarios. Potential radiation was calculated using the following formulas:

Distance from the sun:

$$dd2 = 1 + .0334 * Cos(.01721 * doy - .0552)$$

Equation 4.2

Declination:

$$dec = \arcsin\left(.39785 * Sin(4.869 + .0172 * doy + .03345 * Sin(6.224 + .0172 + doy))\right)$$

Equation 4.3

Half day length:

$$hs = \arccos(-Tan(dec) * Tan(lat))$$

Equation 4.4

Potential Radiation:

$$PotRad(day) = 117.5 * dd2 * \frac{hs * Sin(lat) * Sin(dec) + Cos(lat) * Cos(dec) * Sin(hs)}{\pi}$$

Equation 4.5

Where,
doy = Day of year
lat =latitude (radians)

Potential radiation is a function of latitude and distance from the sun; it can therefore be considered to remain constant outside changed climate conditions and thus was not altered when used to derive future scenarios. Incoming solar radiation was found to have a significant influence on potential evaporation, especially during the winter period. Therefore delta temperature and extraterrestrial radiation were also included as predictors when modelling evaporation.

4.4.5 Calibration and Validation

Downscaling using both SDSM and the GLM approach involved two steps. First a statistical relationship was established between the observed daily records for the target variable (e.g. temperature, precipitation, etc.) and a suite of grid-scale atmospheric predictors obtained from NCEP reanalysis data. These variables describe atmospheric conditions over Ireland for the 'current climate'. The dataset used for model training was selected on the basis that it included diverse conditions and was representative of future climate. The years 1990-2000 are some of the warmest in the instrumental record for the catchment and thus are taken to be more indicative of future warming conditions. For this reason, where observed records were available for the years 1961-2000, the periods 1961–1978 and 1994–2000 were selected for

model calibration. For the calibrated model to be of use in the study of future climate change it is important that the statistical relationship established over the training period is shown to remain valid for an independent period on which the model has not been exposed. For this purpose observed records for the years 1979-1993 were withheld for model validation. A separate regression model, consisting of a set of predictor variables and model parameters, were developed for each season. This removed the influence of an annual cycle, exhibited by many climatological variables, on the coefficient values and allowed for the temporal strength of different predictor sets to be accounted for. The empirical predictor-predictand relationships once established for the observed climate were then used to downscale ensembles of the same local-scale variables for future climate using the output from three GCMs and two SRES emission scenarios (A2 and B2) for the period 1961–2099.

4.5 Downscaled Variables

4.5.1 Temperature

Point scale minimum and maximum temperature scenarios for the Burrishoole catchment were developed using SDSM. Temperature is a relatively homogenous variable over large areas and a significant proportion of the variation exhibited at a local-scale is determined by the large-scale atmospheric state. Temperature also approximates to a normal distribution. Both these factors suggest that multiple-linear regression provides an ideal basis for downscaling temperature using grid-resolution GCM output. Downscaling of daily temperature was performed as a one step process using the following regression equation:

$$T_i = \gamma_0 + \sum_{j=1}^{n} \gamma_j p_{ij} + e_i$$

Equation 4.6

Where,

T denotes the daily temperature (minimum or maximum)

γ represents the model parameters

p_{ij} refers to the grid-scale atmospheric predictors, and

e_i is the model error

The model parameters were optimized over the training period using ordinary least squares. The predictors selected to derive local temperature included a number of circulation variables as well as 2 meter surface temperature. This selection avoided the use of circulation variables alone which previous studies indicate can lead to unrealistically low estimates of temperature change (Huth, 2004). The predictors selected for downscaling daily minimum and maximum temperature, along with the corresponding percentage of explained variance for the calibration and validation periods are shown in Table 4.3.

Table 4.3 Selected predictors for each season for both maximum temperature (Tmax) and minimum temperature (Tmin) and explained variance for both the calibration and independent validation period.

Season	Tmax				Tmin		
	Predictors	**Calibration (E%)**	**Validation (E%)**		**Predictors**	**Calibration (E%)**	**Validation (E%)**
DJF	temp, u, p500, zh5	72	73		temp, p500, f, zh5	67	65
MAM	temp, u5, z,v5	75	79		temp, f8, z5, v5	69	66
JJA	temp, 8u, v	65	66		temp, f8, v	50	52
SON	temp, p500, v5,u5	82	81		temp ,f8, zh, z5	74	74

Once the regression model output was obtained the stochastic component of SDSM was used to inflate the variance of the predicted series. As shown in Table 4.3, a high proportion of the variance exhibited in the observed records was accounted for by the NCEP predictors, thus within the model structure the deterministic component was dominant. Model performance was better for autumn and spring, with the lowest explained variance score achieved for the summer minimum temperature model. Figure 4.4 illustrates how well the model reproduces the monthly mean values recorded over the validation period. Table 4.4 compares the observed and modelled monthly statistics (mean, percentiles) for maximum and minimum temperature over the independent validation period. A good agreement is shown between the downscaled series and the observations from the catchment. It can be concluded that each model provided an adequate basis for downscaling GCM output. Once calibrated and validated each model was then applied to the output from the three selected GCMs. Using the weather generator component of SDSM one hundred synthetic sequences of daily minimum and maximum temperature data for the period 1961-2099 were generated.

Table 4.4 Comparison between observed and NCEP modelled monthly mean statistics (mean, percentiles) of minimum and maximum temperatures over the independent validation period of 1979-1993.

Minimum Temperature												
Observed												
	Jan	**Feb**	**Mar**	**Apr**	**May**	**Jun**	**Jul**	**Aug**	**Sep**	**Oct**	**Nov**	**Dec**
Percentile 5th	-2.2	-1.2	0	1.1	3.3	6.2	9.2	8.4	5.7	2.9	0.6	-0.5
Percentile 50th	2.9	2.9	4.2	5.4	7.8	10.3	12.3	11.9	10.2	7.6	5.2	4.1
Percentile 95th	7.7	7.8	8.5	9.1	11.9	13.7	15.2	15.5	14	12.1	9.6	9.3
Std Deviation	3.1	2.8	2.6	2.4	2.6	2.2	1.9	2.2	2.4	2.8	2.8	3
Range	17.5	15	15.2	11.3	16.5	15.1	11.1	12.6	13.3	14.7	14.4	16.8
NCEP												
	Jan	**Feb**	**Mar**	**Apr**	**May**	**Jun**	**Jul**	**Aug**	**Sep**	**Oct**	**Nov**	**Dec**
Percentile 5th	-1.8	-2.2	-0.1	1	3.5	6.9	8.7	8.5	6.3	3.2	0.7	-0.5
Percentile 50th	3.2	2.8	4.3	5.2	7.8	10.4	12.1	11.9	10.5	7.6	5.4	4.3
Percentile 95th	7.7	7.3	8.5	9.5	12.2	13.8	15.7	15.4	14.8	12	9.9	8.9
Std Deviation	2.9	2.9	2.6	2.6	2.7	2.1	2.1	2.1	2.6	2.7	2.8	2.9
Range	18	16.3	15	14.8	17	12.3	12.7	12.4	14.8	15.4	16	16.6
Maximum Temperature												
Observed												
	Jan	**Feb**	**Mar**	**Apr**	**May**	**Jun**	**Jul**	**Aug**	**Sep**	**Oct**	**Nov**	**Dec**
Percentile 5th	3.0	3.7	6.2	8.2	10.2	13	15	14.7	13.3	9.6	6.6	4.2
Percentile 50th	7.9	8.1	9.7	12.1	14.9	16.8	18.5	17.9	16.1	12.9	10.2	8.8
Percentile 95th	11.6	11.5	12.6	17	21.4	22.5	24.3	22.3	19.6	16.1	13.7	12.6
Std Deviation	2.7	2.4	1.9	2.7	3.3	2.7	2.9	2.3	2	1.9	2.1	2.6
Range	16	12.8	11.6	16.4	21.7	16.3	16.1	14.2	13.9	11.3	11.6	15.7
NCEP												
	Jan	**Feb**	**Mar**	**Apr**	**May**	**Jun**	**Jul**	**Aug**	**Sep**	**Oct**	**Nov**	**Dec**
Percentile 5th	4.0	3.2	5.5	7.0	9.3	12.2	13.9	13.5	11.9	8.6	6.4	5
Percentile 50th	8.3	7.9	9.9	11.7	14.5	16.7	18.3	17.9	15.8	12.7	10.5	9.1
Percentile 95th	12.2	11.8	14.0	16.4	19.6	21.2	23.3	22.5	19.9	16.8	14.5	13
Std Deviation	2.5	2.6	2.6	2.8	3.2	2.7	2.9	2.7	2.4	2.5	2.5	2.4
Range	15.6	14.3	15	16.6	19.5	15.8	16.6	16.2	14	13.6	14.1	13.8

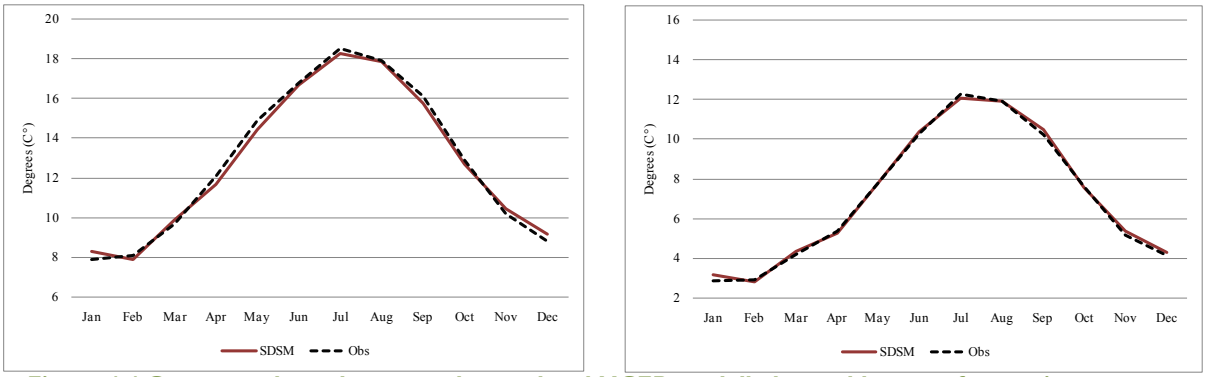

Figure 4.4 Correspondence between observed and NCEP modelled monthly mean for maximum (left) and minimum (right) temperatures over the independent validation period of 1979-1993.

4.5.2 Precipitation

Developing precipitation scenarios for the Burrishoole catchment presented a number of challenges. Firstly precipitation is an extremely heterogeneous variable over space and time and is to a large degree influenced by localised forcings not represented in large-scale atmospheric driving data due to their sub grid scale nature. Thus compared to temperature, downscaled precipitation only accounted for a small proportion of the variance observed in the catchment's precipitation regime. Precipitation also presents a highly skewed distribution resulting from the high frequency of low rainfall events and the low frequency of high rainfall events. This precludes the direct application of well established and robust statistical methods which require a normally distributed continuous response variable. The statistical distribution of precipitation also makes it difficult to represent extreme events in the downscaled series. To address these issues, and to allow for some consideration of downscaling uncertainty, both SDSM and GLMs were employed to downscale precipitation. Both methods model precipitation as a two-step process. Firstly the sequence of days on which rainfall occurs or not is determined. Subsequently the quantity of rainfall which occurs on a given 'rain day' is estimated using a second regression model. To fit the occurrence model the observed dataset was recoded into a binary sequence signifying the occurrence of a rain/dry day. To remove the influence of trace rain days from the dataset a threshold of 0.2 mm was applied.

Using the GLM approach two predictor sets were chosen to downscale precipitation. Each set was selected based on their suitability to model precipitation occurrence and amounts respectively. This is in recognition that different atmospheric processes may be responsible for firstly triggering the occurrence of rainfall and secondly for determining the intensity of a given event. For SDSM the same predictor set was used to model both occurrence and amounts. This was unavoidable as both processes are modelled using the same atmospheric variables within SDSM. For SDSM the same predictors were used as the GLM amounts model. Empirical analysis indicated that precipitation was sensitive to the selection of particular variables. For

this reason the predictors were not solely chosen on a seasonal basis but also with regard to their consistency across each season. The predictors selected for each model and season are listed in Table 4.5.

The selected predictor sets are largely consistent with previous studies being comprised of various circulation variables and some measure of atmospheric humidity. Circulation variables are frequently used to downscale precipitation as GCMs simulate these with some skill (Cavazos and Hewitson, 2005). However the use of circulation variables alone may be inappropriate as they fail to capture those key atmospheric mechanisms, based on thermodynamics and vapour content, which are conducive to local scale precipitation events (Fowler et al., 2007). Atmospheric moisture content is likely to be sensitive to warming climate conditions and as such humidity is an important predictor for capturing the climate change signal. Although humidity did not appear to be a significant predictor when evaluated under current climate conditions some measure of it was used to model precipitation. It has been shown that the inclusion of moisture variables as predictors can bring about a convergence in the projections from statistical and dynamical models (Charles et al., 1999).

Table 4.5 Selected predictors for each season for precipitation and both the linear regression (SDSM) model and GLM

Season	SDSM		GLM - Occurrence	GLM - Amounts
DJF	mslp, u8, v8, shum		mslp, u8, v8, shum	mslp, u8, v8, shum
MAM	mslp, u, v, rhum		p500, u8, zh8,shum	mslp, u, v, rhum
JJA	mslp, u, v, rhum		p500, u, zh, rhum	mslp, u, v, rhum
SON	mslp, u, v, rhum		p850, u8, zh, rhum	mslp, u, v, rhum

Linear Regression (SDSM)

Downscaling of precipitation in SDSM, as described in Wilby et al. (2002), is a two step process using the following regression equations:

$$O_i = \alpha_0 + \sum_{j=i}^{n} \alpha_j p_{ij} \qquad R_i^0.25 = \beta_0 + \sum_{j=i}^{n} \beta_j p_{ij} + e_i$$

Equation 4.7

where,

O_i and R_i represent the daily precipitation occurrence and amounts respectively,

α and β are the model parameters,

p_{ij} corresponds to a suite of atmospheric predictors, and

e_i is the model error.

The same calibration and validation periods are used to fit and test both models. Linear least squares regression was used to optimize the parameters of both models. The first regression model is used to determine the probability of rainfall occurring on a given day. If the modelled probability is greater than a given threshold then a rain day is assumed to occur. The model incorporates an additional stochastic component for generating differing sequences of wet and dry days. A random number r, ($0 \leq r \leq 1$), generated from a uniform distribution, is used to determine whether rainfall occurs on a given day. For example if the initial regression model indicates that the probability of precipitation occurrence is p = 0.65, and the random number generator returns, $r \leq 0.65$, then rainfall occurs; if $r > 0.65$ then it is a non-rain day. This stochastic component was employed when developing precipitation scenarios for the Burrishoole catchment. Once the sequencing of wet and dry days had been determined the quantity of precipitation occurring on a 'rain day' was estimated using the second regression model outlined above. The precipitation amounts model was developed using only those days in the observed series classified as a rain day (i.e. > 0.2mm). Owning to the skewed distribution which precipitation presents a fourth root transformation was applied prior to fitting the regression model. So as to give a better account of extreme events the stochastic component of SDSM was used to inflate the variance of the downscaled precipitation series. Once calibrated and validated each model was used to downscale the output from the three selected GCMs. Using the weather generator component of SDSM one hundred synthetic precipitation series for the period 1961-2099 were produced.

Generalised Linear Model (GLM)

Under the general approach of generalized linear modelling to different regression models were used. Logistic regression was firstly used to model the sequence of wet and dry days. This regression model is widely used to model the probability of a particular event occurring and can be applied where the predictand is a categorical variable. In this study logistic regression was used to model the probability of rainfall occurring on a given day conditional on the large-scale atmospheric state. The logistic regression model can be written as:

$$\log\left(\frac{P}{1-P}\right) = \theta + \sum_{j=i}^{n} \theta_j p_{ij} \qquad \textbf{Equation 4.8}$$

Where,

P is the probability of an event,

θ are the model parameters, and

p_{ij} represents the independent variables.

Logistic regression has the advantage over multiple linear regression of being more appropriate for modelling a categorical data series. Also the model output is constrained between zero and one allowing for it to be interpreted as a proper probability. Using the observed dataset a threshold probability can be determined above which a rain day is shown to occur. This threshold is taken as the conditional probability and used to delineate the occurrence of a rain/dry day from the model output.

Precipitation amounts were modelled using a GLM with a gamma distribution and log link function. This model structure was chosen as rain day precipitation amount is a positive continuous variable and presents a distribution which best approximates to the gamma distribution. A similar structure model was previously employed for modelling precipitation in Ireland by Fealy and Sweeney (2007). In this case the model relates a linear combination of the atmospheric predictors to the expected value of the response variable ($E(Y_i)$), specified as having a gamma distribution, through a logarithmic link function.

$$\log\left(E(Y_i)\right) = \emptyset + \sum_{j=i}^{n} \emptyset_j \, p_{ij}$$

Equation 4.9

Where,
E(Y) is the expected value
P is the probability of an event,
θ are the model parameters, and
p_{ij} represents the independent variables.

Table 4.6 shows the percentage explained variance for both the GLM and SDSM amounts model, it also shows the Heidke Skill Score (HSS) for the GLM occurrence model. The Heidke Skill Score is a measure of forecast skill calculated by comparing the observed binary value on a day with the 'forecast' or 'modelled' value for that day. The relatively low explained variance for wet day amounts in all seasons is consistent with previous studies and illustrates the difficulty of downscaling local precipitation scenarios using grid scale atmospheric predictors. The percentage explained variance was highest for winter. This reflects the influence of large-scale frontal weather systems on local events during this period and is in contrast to the low explained variance for summer when frontal systems are less active and localised conditions become more influential.

Table 4.6 Explained variance for the calibration (1961-1978; 1994-2000) and validation (1979-1993) models for each season for precipitation for the linear regression (SDSM) model and GLM. Due to the stochastic calculation of rain days in SDSM, no Heidke Skill Score was calculated for this model.

Season	SDSM – Rain Day Precipitation Amounts (E%)		GLM -Rain Day Precipitation Amounts (E%)		GLM - Rain Day Occurrence HSS	
	Calibration	Validation	Calibration	Validation	Calibration	Validation
DJF	32	30	30	29	60	60
MAM	26	27	24	25	67	63
JJA	19	23	19	22	61	60
SON	20	23	28	27	61	59

Figure 4.5 illustrates that SDSM better reproduced the observed variance of precipitation for each season when compared to the GLM which consistently underestimated the variance. This demonstrates the problem of capturing the observed variance using regression analysis alone and the advantages of employing the stochastic component of SDSM. Underestimating the variability has knock-on effects for representing extreme events in the downscaled series. SDSM also reproduced the 95th percentile closer to the observed when compared to the GLM which greatly underestimated it. However both were able to model the observed seasonal and inter-annual means equally well.

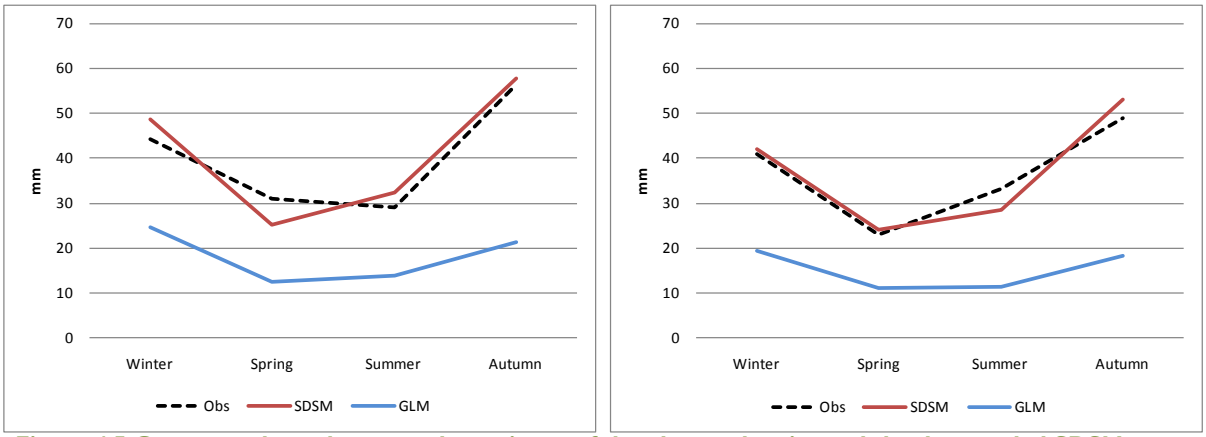

Figure 4.5 Correspondence between the variance of the observed series and the downscaled SDSM and GLM series on a seasonal basis for both the calibration (left) and validation periods (right).

As rainfall occurrence is a discrete variable the percentage of variance explained is not an appropriate statistic to measure model performance. For this the percentage of correct wet and dry day classifications is used (Wilks, 1995). The HSS score indicates that the GLM model was able to correctly classify approximately 60% of the days for both the calibration and validation periods. As precipitation occurrence was modelled using a stochastic process this measurement is not applicable to the output from SDSM. To evaluate the models predictive skill the correspondence between the percentage of modelled and observed wet days is used. These results are taken as a strong indication that each model is able to reconstruct the

catchments precipitation regime under current climate and thus are assumed to be adequate for downscaling GCM output. Both the GLM and SDSM were applied to the output from the three selected GCMs and two SRES emission scenarios (A2 and B2). The stochastic component of SDSM was used to produce one hundred synthetic sequences of daily rainfall for the period 1961-2099. As the GLM is a fully deterministic approach only one precipitation series was produced from each GCM predictor set. Table 4.7 outlines the correspondence between different statistics for the observed and downscaled series while Figure 4.6 illustrates how well both the GLM and SDSM downscaled series capture interannual variability over the validation period.

Table 4.7 Comparison between observed (obs) and modelled (SDSM; GLM) monthly mean statistics of precipitation over the independent validation period of 1979-1993.

Parameter	Model	Jan	Feb	Mar	Apr	May	Jun	Jul	Aug	Sep	Oct	Nov	Dec
mm/month	**Obs**	172.7	111.8	160.7	94.2	90.3	90.9	93.6	137.4	145.8	187.0	154.1	197.6
	SDSM	156.5	109.4	145.3	87.7	79.7	96.8	97.5	123.6	135.3	174.9	166.6	179.5
	GLM	163.1	116.0	158.6	97.8	90.1	111.2	105.1	135.8	140.3	185.9	171.7	190.7
Rain-Days (%)	**Obs**	78.2	68.5	80.4	64.7	61.5	61.7	66.9	70.3	73.1	79.4	74.0	80.4
	SDSM	73.6	65.9	76.9	63	58.2	62.5	62.8	68.9	70.8	75.3	73.6	80.1
	GLM	72.7	63.2	82.6	65.3	61.9	69.3	64.9	72.0	73.3	78.5	74.4	81.9
Std Deviation	**Obs**	6.5	5.4	6.1	5.3	5	4.7	4.9	6.3	7.2	8.4	6.8	7.6
	SDSM	6.9	6.4	5.8	4.6	4.2	5.5	5.2	6.2	6.7	8.0	7.9	7.4
	GLM	4.7	4.8	3.9	3.3	3	3.8	3.3	4.1	3.8	5.0	4.9	5.2
Percentile 95th	**Obs**	18.9	15.2	18.5	13.0	13.0	12.0	13.8	18.3	18.7	20.9	18.2	21.0
	SDSM	18.8	16.2	16.2	12.1	11.0	13.9	13.6	16.1	18.0	21.2	21.4	20.3
	GLM	13.5	12.7	12.4	9.0	8.0	9.5	9.1	11.5	11.4	14.8	14.1	14.8
Kurtosis	**Obs**	2.7	3.2	4.9	15.1	18	7.9	8.3	5.0	15.0	16.1	8.9	4.4
	SDSM	11.5	23.8	6.0	13.4	6.7	10.9	9.3	9.4	11.4	11.4	10.7	10.2
	GLM	1.7	7.1	3.3	3.3	3.1	7.1	1.0	2.4	0.9	3.7	2.2	9.9
Skewness	**Obs**	1.5	1.8	1.9	3.3	3.3	2.5	2.6	2.1	3.1	3.2	2.4	1.8
	SDSM	2.7	3.8	2.1	2.9	2.4	2.9	2.7	2.7	2.9	2.8	2.7	2.6
	GLM	1.1	2.1	1.1	1.4	1.3	1.9	0.9	1.2	0.7	1.4	1.0	2.1

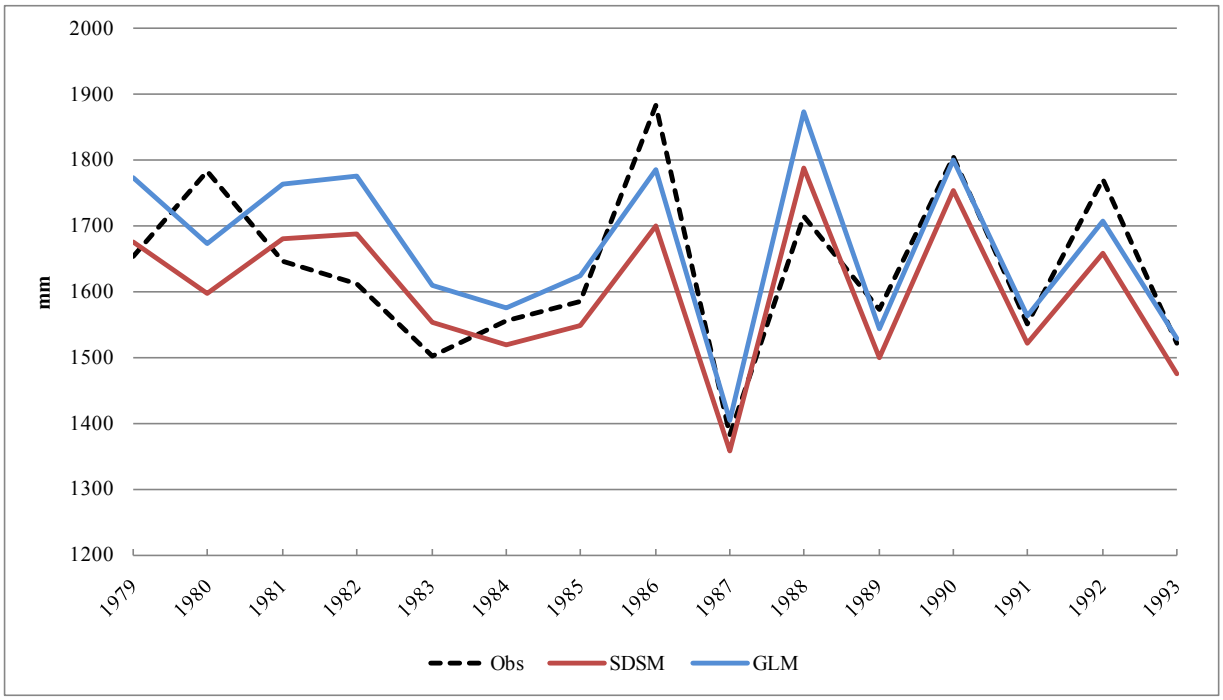

Figure 4.6 Correspondence between interannual variability for the observed and downscaled precipitation series over the 1979-1993 validation period.

4.5.3 Sub-catchment Precipitation: Quantile-Quantile Mapping

Precipitation receipts at the Millrace station, from which the downscaled models were developed, do not fully reflect rainfall conditions in upland areas. Ideally future precipitation scenarios would have been downscaled for individual catchment with the aim of capturing locally specific conditions. However, due to the short records available for upland gauging precipitation stations, scenarios were not downscaled directly to these sites. To overcome this, a quantile mapping technique was employed to construct precipitation scenarios for each sub catchment using the point-scale precipitation series downscaled to the Millrace station. This technique establishes a relationship between the magnitudes of a precipitation event observed at the Millrace station to the 'same' rainfall event observed in an upland catchment. The method has previously been employed in a downscaling context as a bias correction technique (Boe et al. 2007; Deque, 2007; Wood et al., 2004).

In this study, quantile mapping was applied on a seasonal basis using rainfall amounts only. The precipitation record from Millrace and the weighted average rainfall for each catchment, taken over the same time period, were discretized and ranked 1-99 based on their percentiles. A linear transfer function was then fitted to determine the relationship between the percentiles for each dataset. To derive the upland precipitation scenarios the formulated q-q mapping function, linking the Millrace dataset to each sub catchments average rainfall, was then applied to the point scale precipitation series downscaled to the weather station. As an example a "very high rainfall event" at Millrace of 35 mm/day would be transformed into 45 mm/day using

the q-q function in order to correspond with what observations show is a "very high rainfall event" for the given upland catchment. Figure 4.7 shows the quantile-quantile plots mapping precipitation receipts for the Millrace station onto the Glenamong sub-catchment. The mapping function derived for each catchment and season indicated that the magnitude of rainfall events recorded at Millrace were generally lower than experienced in the upland areas. This was particularly evident for low frequency events. Quantile mapping allows for some consideration of the known influence elevation has on precipitation (orographic enhancement), which is important to consider in this context given the local terrain. Other methods for translating the downscaled precipitation to upper catchments, including different regression and spatial interpolation techniques, were examined. However given the short record lengths and large number of missing daily recordings these techniques could not be employed.

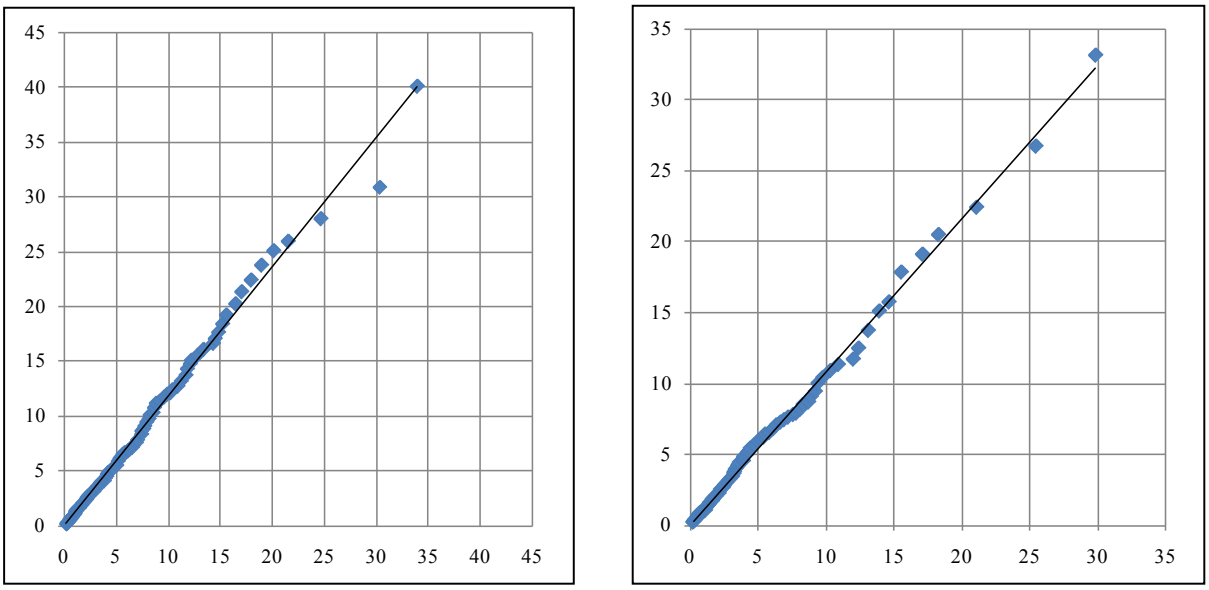

Figure 4.7 Quantile – quantile plot of precipitation recorded over the Glenamong sub-catchment (y-axis) against rainfall receipts for the Millrace climatological station (*x*-axis) for winter (left) and summer (right).

4.6 Wind Speed

Wind speed distributions are typically positively skewed and generally approximate to either a gamma or weibull distribution. To accommodate this, wind speed was modelled using a generalized linear model with a gamma distribution and log link function. SDSM was also employed to downscale wind speed. In this case, to conform to the distribution required for linear regression, a square root transformation was applied to the predictand series. Differences in the performance of both methods over the calibration and validation periods were negligible. For each season, as well as over both the training and validation periods, a

relative high proportion of the observed variance was accounted for in the downscaled series (Table 4.8).

Table 4.8 Explained variance for the calibration (1961-1978; 1994-2000) and validation (1979-1993) models for each season for wind speed for the linear regression (SDSM) model and GLM.

		SDSM		GLM	
Season	**Predictors**	**Calibration (E%)**	**Calibration (E%)**	**Calibration (E%)**	**Calibration (E%)**
DJF	zh8, mslp, f8	49	51	51	47
MAM	f8, p500, v	48	45	47	45
JJA	z, f8, v	46	41	47	42
SON	f8, zh5, z	47	47	45	45

4.7 Relative Humidity

Future scenarios for relative humidity were downscaled using SDSM only. As records of sufficient length were not available from the catchment itself, instrumental records for relative humidity were obtained from the Belmullet meteorological station operated by Met Eireann. Grid-scale relative humidity was included in the predictor set for each season. Incorporating this variable was considered to be important in order to reflect the sensible physical linkage between local and mesoscale atmospheric conditions. As they exhibited a strong correlation with local scale humidity a number of circulation variables were also included. A relatively high proportion of the variance exhibited by the observed series was captured in the downscaled dataset. The model does however appear to capture a higher proportion of the variance during the autumn when compared to the summer, which registered the lowest percent explained variance over both the calibration and validation periods.

Table 4.9 Explained variance for the calibration (1961-1978; 1994-2000) and validation (1979-1993) models for each season for wind speed for the linear regression (SDSM) model.

Relative Humidity			
Season	**Predictors**	**Calibration - (E%)**	**Validation - (E%)**
DJF	f, v, z5, rhum	31	36
MAM	v, f, z5, rhum	30	34
JJA	u, v, z5, rhum	25	23
SON	f5, z5, v, rhum	39	39

4.8 Solar Radiation and Potential Evaporation

Due to the influence which solar radiation has on evaporation rates downscaling for both variables was carried out using similar predictor sets. As described above a number of large-scale predictors, along with potential radiation and delta temperature, were employed when deriving future scenarios (Table 4.10; Table 4.11). As incoming solar radiation and evaporation approximate to a normal distribution both were downscaled using SDSM only. The instrumental records available for radiation and evaporation covered the periods 1982-2000 and 1971-2000 respectively. In order to overcome short length of the datasets available for model calibration a resampling technique, known as bootstrapping, was used to estimate each models coefficient values.

Table 4.10 Explained variance for the calibration (1981-1988; 1995-2000) and validation (1989-1994) models for each season for solar radiation for the linear regression (SDSM) model.

Solar Radiation			
Season	**Predictors**	**Calibration - (E%)**	**Validation - (E%)**
DJF	Pot Rad, Delta Temp, v ,z5 ,u8,zh	65	60
MAM	Pot Rad, Delta Temp, zh, z5, u5, rhum	65	66
JJA	Pot Rad, Delta Temp, rhum, u5, zh, z5	50	48
SON	Pot Rad, Delta Temp, zh, u8, z5	73	72

Table 4.11 Explained variance for the calibration (1971-1981) and validation (1982-1987) models for each season for potential evaporation for the linear regression (SDSM) model.

Potential Evaporation			
Season	**Predictors**	**Calibration - (E%)**	**Validation - (E%)**
DJF	Pot Rad, Delta Temp, v ,z5 ,f, rhum	64	52
MAM	Pot Rad, Delta Temp, zh, z5, u5, rhum	67	65
JJA	Pot Rad, Delta Temp, rhum, u5, zh, z5, rhum	44	45
SON	Pot Rad, Delta Temp, v, u8, z5, rhum	73	70

4.9 Projected Future Changes in Climate for the Burrishoole Catchment

To produce climate scenarios for the Burrishoole catchment grid-scale projections from three GCMs (HadCM3, CSIROmk2 and CGCM2), each run using two different emission scenarios (A2 and B2), were used as the driving data for the downscaling models described above. Each model links a suite of large-scale atmospheric predictors to local scale meteorological variables. The models have been empirically derived and independently tested using observed data representing current climate conditions. Changes in each of the downscaled variables are

considered over three future time horizons the 2020s (2010-2039), 2050s (2040-2069) and 2080s (2070-2099), with the model control period of 1961-1990 used to represent baseline conditions. Thirty years is the standard time period over which 'climate' is generally defined which allows for inter-decadal variability to be considered when determining defined changes in the system. With regard to estimated changes in temperature for the catchment each GCM is in agreement that the more carbon intensive A2 emission scenario gives rise to the greatest relative increases, with the 2080s representing the most intense period of warming. Generally, the downscaled precipitation scenarios for the catchment suggest an increase in winter rainfall amounts accompanied by a decrease in summer across all GCMs. Estimated changes in precipitation over each time horizon indicate that this trend is likely to become more acute during the latter part of the century. While differences between the individual emissions scenarios are small for all seasons, the inter-model range is large underling the importance of employing the output from multiple GCMs when developing climate scenarios.

4.10 Temperature

Climate scenarios developed for Burrishoole catchment suggest that for each season and future time horizon average temperatures are likely to be higher than reference conditions (1961-1990) with the summer and autumn months projected to experience the greatest absolute increase. Each GCM and emission scenario is in agreement that temperatures are likely to progressively increase through the 21st century with the greatest amount of warming occurring in the 2080s. Although there is a general consensus between the models in relation to temperature rise, inter model differences exist regarding the exact magnitude and time-evolution of model projected increases through the century. Significant differences between emission scenarios, i.e. the same model run using different forcing conditions, are notable from the 2050s onwards becoming most apparent over the 2080s for all models. Intra-model differences are also evident with the HadCM3 model generally producing cooler projections when compared to the CSIROmk2 and CGCM2 climate models.

4.10.1 Maximum Temperature

Table 4.12 lists the projected changes in mean maximum temperature for each future horizon on a monthly (Table 4.12a) and seasonal (Table 4.12b) basis. Based on the downscaled HadCM3 A2 scenario, average summer maximum temperatures for the 2080s are projected to be 1.9°C greater than that experienced under baseline conditions. The same downscaled temperature scenario suggests an increase in mean autumn maximum temperatures of 2.3°C. In accordance with this the downscaled output from the CSIROmk2 model, over the 2080 period, also suggests an increase in mean summer (1.6°C) and autumn (2.6°C) maximum

temperatures respectively. Similarly the temperature scenarios developed using the output from the CGCM2 model, driven using the A2 scenario, indicate an increase in average summer maximum temperatures of 2.3°C with an accompanied increase of 2.4°C for the autumn period. On a monthly basis model projections suggest that the greatest absolute increase in average max temperature is associated with November and April (CSIROmk2 A2) with increases of 2.9 and 3 degrees respectively.

Figure 4.7 displays a probability density function, constructed using the downscaled output from each GCM and emission scenario, depicting the projected change in temperature for all months. Table 4.13 catalogues the mean and standard deviation for each graph. A progressive increase in temperature through the century is suggested for each month. The spread in the range of projections is much greater for the winter months, and generally increases towards the end of the century as the divergence between the A2 and B2 emissions pathways increase.

Table 4.12a Projected changes in mean maximum temperature for each future horizon on a monthly basis.

	Jan	Feb	Mar	Apr	May	Jun	Jul	Aug	Sept	Oct	Nov	Dec
HadCM3 - A2												
2020s	0.3	0.3	0.3	0.3	0.4	0.3	0.1	0.6	0.4	0.4	0.2	-0.7
2050s	1.0	0.9	0.7	0.7	0.7	0.4	1.2	1.0	1.5	1.1	0.9	0.0
2080s	1.5	1.4	1.8	1.5	1.6	1.3	2.2	2.3	2.4	2.6	1.8	1.0
HadCM3 - B2												
2020s	0.3	0.6	0.3	0.6	0.3	0.1	0.3	0.6	0.7	0.9	0.6	-0.4
2050s	0.8	0.2	0.4	0.6	0.8	0.6	0.7	1.1	0.8	1.0	1.2	0.2
2080s	0.8	0.8	0.9	1.2	1.1	1.1	1.2	1.4	1.4	1.9	1.4	0.3
CSIROmk2 - A2												
2020s	0.5	0.5	0.9	1.3	0.6	0.6	0.6	0.6	1.0	1.1	1.3	0.9
2050s	1.2	1.2	1.5	1.7	1.5	0.9	1.2	1.5	1.8	1.8	1.9	1.5
2080s	2.2	1.8	2.6	2.9	2.0	1.5	2.2	2.4	2.8	2.7	3.0	2.5
CSIROmk2 - B2												
2020s	1.1	1.1	1.3	1.2	0.9	1.0	0.7	1.0	1.5	1.2	1.4	0.8
2050s	1.5	1.4	1.9	1.7	1.7	1.3	1.2	1.5	2.0	1.7	2.4	1.4
2080s	1.8	1.8	2.3	2.0	1.8	1.3	1.5	2.0	2.5	2.4	2.8	1.7
CGCM2 - A2												
2020s	0.6	0.5	0.9	1.0	1.1	0.9	0.9	0.9	0.8	0.6	0.5	0.8
2050s	1.3	1.2	1.8	1.6	1.7	1.5	1.9	1.7	1.8	1.8	1.8	1.4
2080s	1.4	1.4	2.0	2.2	2.3	2.2	2.5	2.2	2.5	2.5	2.3	1.8
CGCM2 - B2												
2020s	1.0	0.7	1.0	0.9	0.8	0.8	1.0	0.8	0.9	0.8	0.8	0.8
2050s	1.0	0.8	1.4	1.5	1.5	1.2	1.5	1.3	1.4	1.3	1.2	1.0
2080s	1.0	1.2	1.8	2.0	1.9	1.7	1.8	1.7	2.1	2.1	1.7	1.2

Table 4.12b Projected changes in mean maximum temperature for each future horizon on a seasonal basis.

	DJF	MAM	JJA	SON
HadCM3 - A2				
2020s	0.0	0.3	0.3	0.3
2050s	0.7	0.7	0.8	1.2
2080s	1.3	1.6	1.9	2.3
HadCM3 - B2				
2020s	0.2	0.4	0.4	0.7
2050s	0.4	0.6	0.8	1.0
2080s	0.7	1.0	1.2	1.6
CSIROmk2 - A2				
2020s	0.6	0.9	0.6	1.1
2050s	1.3	1.6	1.2	1.9
2080s	2.2	2.5	2.1	2.8
CSIROmk2 - B2				
2020s	1.0	1.1	0.9	1.4
2050s	1.4	1.8	1.3	2.1
2080s	1.8	2.0	1.6	2.6
CGCM2 - A2				
2020s	0.6	1.0	0.9	0.6
2050s	1.3	1.7	1.7	1.8
2080s	1.5	2.2	2.3	2.4
CGCM2 - B2				
2020s	0.9	0.9	0.9	0.8
2050s	1.0	1.5	1.3	1.3
2080s	1.1	1.9	1.7	2.0

Figure 4.8 illustrates the projected change in the 90th percentile for maximum temperature. This index is taken as an indicator of extreme conditions. Model projections suggest that extreme temperature events are likely to increase becoming more acute towards the end of the century. The greatest increases are associated with the autumn months with September, October and November displaying an increase of 2.7, 3 and 2.9 degrees respectively by the 2080s over the baseline period.

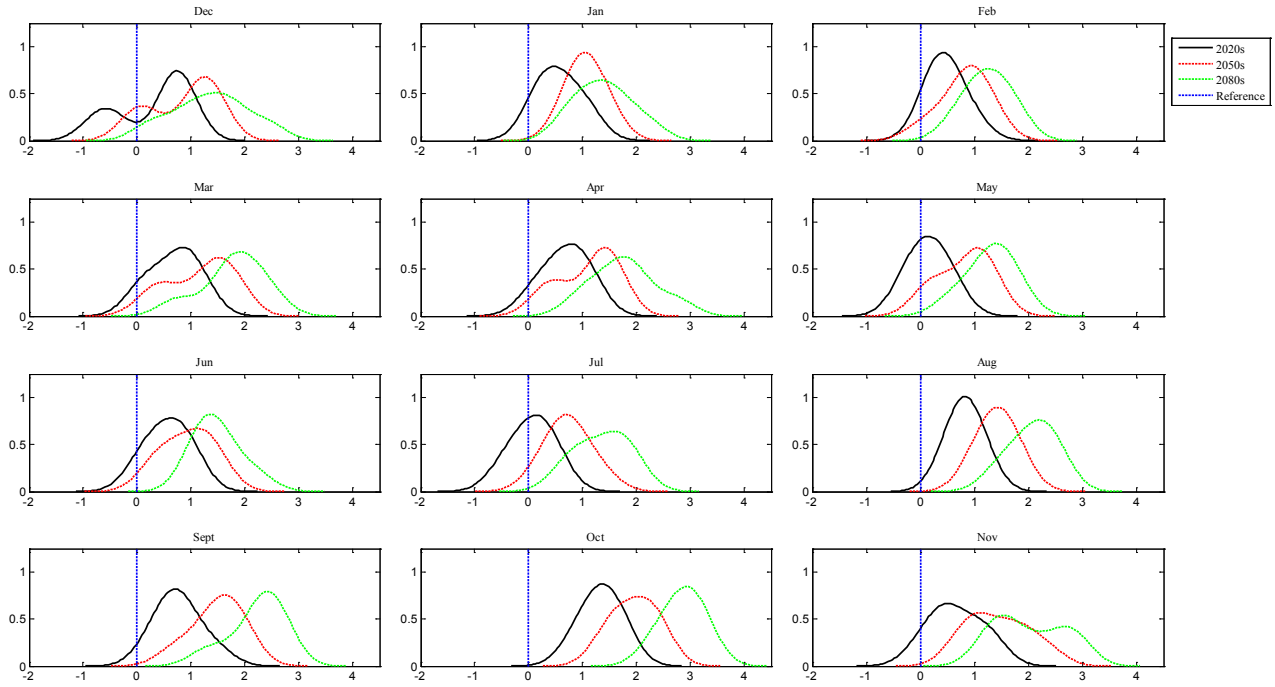

Figure 4.7 Probability density functions, constructed using the downscaled output from each GCM and emission scenario, depicting the projected change in maximum temperature for all months. The vertical line represents the baseline mean.

Table 4.13 The mean and standard deviation for maximum temperature from the PDFs in Figure 4.7.

	Dec			Jan			Feb	
	Mean	**St. Dev**		**Mean**	**St. Dev**		**Mean**	**St. Dev**
2020s	0.3	0.6		0.6	0.3		0.5	0.2
2050s	0.9	0.6		1.1	0.2		0.8	0.4
2080s	1.4	0.7		1.4	0.5		1.2	0.4
	Mar			**Apr**			**May**	
	Mean	**St. Dev**		**Mean**	**St. Dev**		**Mean**	**St. Dev**
2020s	0.7	0.4		0.7	0.4		0.1	0.3
2050s	1.2	0.6		1.1	0.5		0.8	0.4
2080s	1.8	0.5		1.8	0.6		1.3	0.4
	Jun			**Jul**			**Aug**	
	Mean	**St. Dev**		**Mean**	**St. Dev**		**Mean**	**St. Dev**
2020s	0.6	0.3		0.1	0.3		0.8	0.2
2050s	0.9	0.4		0.7	0.3		1.4	0.3
2080s	1.5	0.4		1.4	0.4		2.1	0.4
	Sep			**Oct**			**Nov**	
	Mean	**St. Dev**		**Mean**	**St. Dev**		**Mean**	**St. Dev**
2020s	0.8	0.4		1.3	0.3		0.7	0.4
2050s	1.5	0.4		2.0	0.3		1.4	0.5
2080s	2.2	0.4		2.9	0.3		2.0	0.6

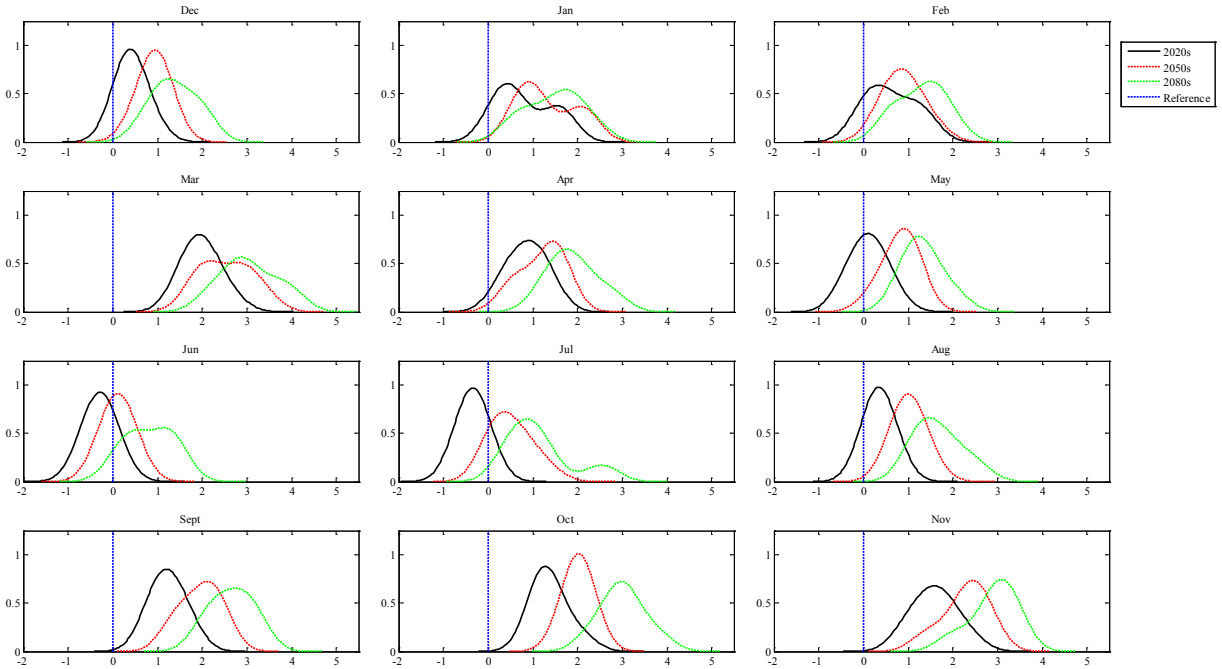

Figure 4.8 Projected changes in the 90th percentile for maximum temperature derived from all GCMs and emission scenarios. The vertical line represents the baseline statistic.

Table 4.14 Projected changes in the 90th percentile mean and standard deviation for maximum temperature.

	Dec			Jan			Feb	
	Mean	**St. Dev**		**Mean**	**St. Dev**		**Mean**	**St. Dev**
2020s	0.4	0.2		0.8	0.6		0.6	0.5
2050s	0.9	0.2		1.3	0.6		0.9	0.4
2080s	1.4	0.5		1.5	0.6		1.3	0.5
	Mar			**Apr**			**May**	
	Mean	**St. Dev**		**Mean**	**St. Dev**		**Mean**	**St. Dev**
2020s	2.0	0.4		0.9	0.4		0.1	0.3
2050s	2.5	0.5		1.2	0.4		0.8	0.3
2080s	3.1	0.6		1.9	0.5		1.3	0.4
	Jun			**Jul**			**Aug**	
	Mean	**St. Dev**		**Mean**	**St. Dev**		**Mean**	**St. Dev**
2020s	-0.3	0.3		-0.3	0.2		0.4	0.2
2050s	0.1	0.3		0.5	0.4		1.0	0.3
2080s	0.8	0.5		1.1	0.7		1.7	0.5
	Sep			**Oct**			**Nov**	
	Mean	**St. Dev**		**Mean**	**St. Dev**		**Mean**	**St. Dev**
2020s	1.2	0.3		1.4	0.3		1.6	0.5
2050s	2.0	0.4		2.0	0.2		2.3	0.5
2080s	2.7	0.4		3.0	0.5		2.9	0.5

4.10.2 Minimum Temperature

Projected changes in average minimum temperatures largely follow those exhibited by maximum temperature (Table 4.15a). However increases for other seasons are more notable. Scenarios derived using the output from the HadCM3 model, forced using the A2 scenario, indicate an increase in average autumn minimum temperatures of 2.2°C for the 2080s. Under this scenario minimum temperatures for each of the remaining seasons are projected to be 1.6°C-1.7°C greater than that experienced over the 1961-1990 baseline period. Projected changes in minimum temperature, estimated using the output from the CSIROmk2 model, suggest that the greatest warming is likely to occur during the winter, with a 2.7°C increase in average conditions by the end of the century (Table 4.15b). This increase is more extreme for winter (3.1°C), which is the greatest projected increase when compared against all other seasons and models.

Table 4.15a Projected changes in mean minimum temperature for each future horizon on a monthly basis.

	Jan	Feb	Mar	Apr	May	Jun	Jul	Aug	Sept	Oct	Nov	Dec
HadCM3 - A2												
2020s	0.4	0.4	0.1	0.3	0.5	0.4	0.0	0.3	0.4	0.4	0.1	-0.8
2050s	1.3	1.2	0.4	0.5	0.7	0.6	0.8	0.8	1.4	1.0	0.8	0.1
2080s	1.9	1.7	1.7	1.6	1.7	1.3	1.8	1.8	2.3	2.5	1.8	1.3
HadCM3 - B2												
2020s	0.4	0.7	0.1	0.6	0.5	0.3	0.2	0.3	0.7	0.9	0.6	-0.4
2050s	1.0	0.3	0.2	0.7	0.9	0.6	0.6	0.7	0.7	0.9	1.2	0.4
2080s	1.2	1.0	0.7	1.2	1.2	1.1	1.0	1.1	1.4	1.8	1.4	0.5
CSIROmk2 - A2												
2020s	0.8	0.5	0.9	1.2	0.6	0.4	0.5	0.5	0.9	1.1	1.3	1.3
2050s	1.7	1.5	1.3	1.5	1.4	0.8	1.0	1.1	1.8	1.7	1.9	2.1
2080s	3.3	2.4	2.2	2.5	1.9	1.3	1.8	2.0	2.6	2.6	2.9	3.4
CSIROmk2 - B2												
2020s	1.6	1.6	1.2	1.0	0.8	0.9	0.6	0.9	1.5	1.1	1.4	1.1
2050s	1.9	1.9	1.7	1.5	1.4	1.2	1.0	1.3	2.0	1.7	2.4	1.8
2080s	2.6	2.4	2.1	1.8	1.5	1.2	1.3	1.6	2.4	2.3	2.8	2.5
CGCM2 - A2												
2020s	0.8	0.6	0.6	0.9	0.7	0.8	0.6	0.7	0.7	0.6	0.5	0.9
2050s	1.8	1.6	1.5	1.3	1.4	1.4	1.4	1.5	1.7	1.8	1.8	1.8
2080s	1.9	1.9	1.6	1.8	1.7	1.9	1.9	2.0	2.4	2.4	2.3	2.6
CGCM2 - B2												
2020s	1.3	1.1	0.7	0.9	0.6	0.7	0.6	0.7	0.8	0.8	0.8	1.1
2050s	1.3	1.0	1.1	1.3	1.2	1.0	1.0	1.1	1.2	1.3	1.2	1.4
2080s	1.3	1.5	1.4	1.7	1.5	1.5	1.4	1.5	2.0	2.1	1.6	1.8

Table 4.15bProjected changes in mean minimum temperature for each future horizon on a seasonal basis.

	DJF	MAM	JJA	SON
HadCM3 - A2				
2020s	0.0	0.3	0.2	0.3
2050s	0.9	0.5	0.8	1.1
2080s	1.7	1.7	1.6	2.2
HadCM3 - B2				
2020s	0.3	0.4	0.3	0.7
2050s	0.6	0.6	0.6	0.9
2080s	0.9	1.0	1.1	1.5
CSIROmk2 - A2				
2020s	0.9	0.9	0.5	1.1
2050s	1.8	1.4	1.0	1.8
2080s	3.1	2.2	1.7	2.7
CSIROmk2 - B2				
2020s	1.4	1.0	0.8	1.3
2050s	1.9	1.5	1.1	2.0
2080s	2.5	1.8	1.4	2.5
CGCM2 - A2				
2020s	0.8	0.8	0.7	0.6
2050s	1.7	1.4	1.4	1.8
2080s	2.1	1.7	1.9	2.3
CGCM2 - B2				
2020s	1.2	0.7	0.7	0.8
2050s	1.2	1.2	1.1	1.2
2080s	1.6	1.5	1.5	1.9

According to the downscaled output from the CGCM2 model, minimum temperatures are projected to experience the greatest increase during the autumn with a 2.3°C increase by the 2080s. For the same horizon this model also suggests that average winter minimum temperatures will increase by 2.1°C compared to the reference period. On a monthly basis the greatest increases in minimum temperature are associated with January (3.3°C) and December (3.4°C) downscaled from the CSIROmk2 model under the A2 emissions pathway.

The combined projections for minimum temp, represented by the probability density functions in Figure 4.9, indicate a steady increase in minimum temperatures through the 21st century. Model projections suggest that September, October and November are likely to experience the greatest relative warming with increases of 2.1, 3 and 1.9◦C respectively by the 2080s. An analysis of projected changes in the 10th percentile (Figure 4.10 and Table 4.16) suggests an increase in extreme low temperatures is likely. This finding is in keeping with the general

increase in temperature exhibited for mean conditions. The greatest range in model projections with regards to the 10th percentile is exhibited over the winter months for which model projections suggest a reduction in extreme minimum temperature is possible.

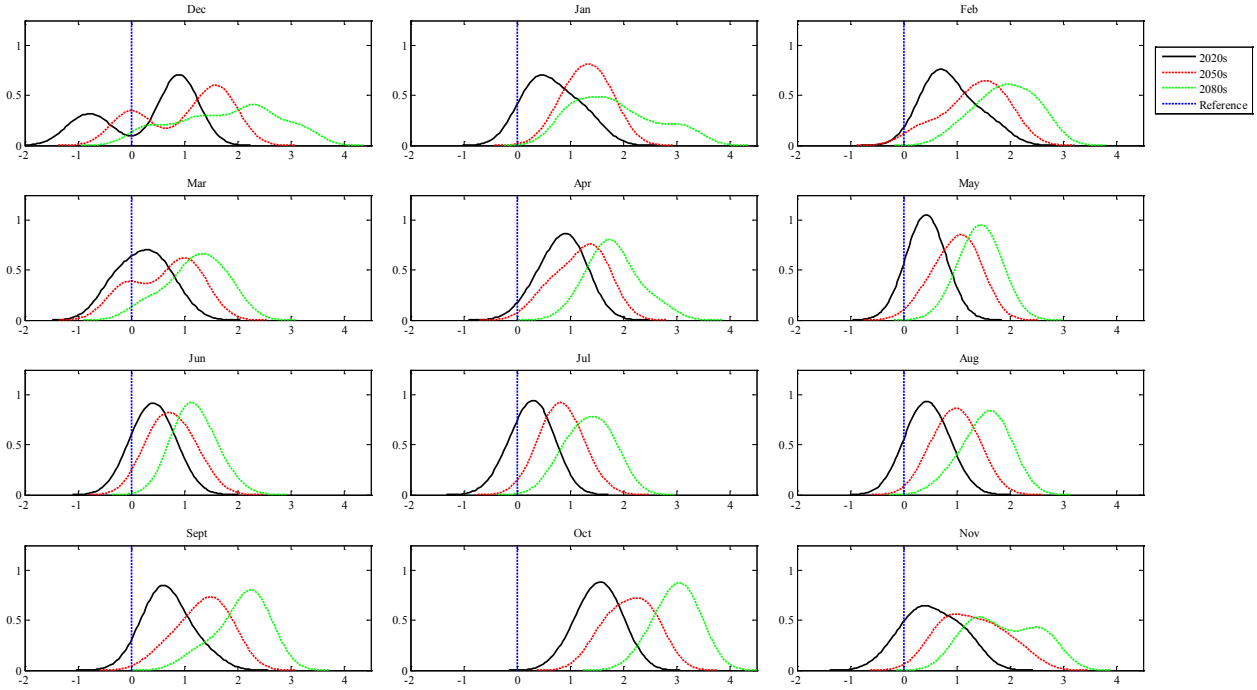

Figure 4.9 Probability density functions, constructed using the downscaled output from each GCM and emission scenario, depicting the projected change in minimum temperature for all months. The vertical line represents the baseline mean.

Table 4.16 The mean and standard deviation for mean monthly minimum temperature from the PDFs in Figure 4.9.

	Dec			Jan			Feb	
	Mean	**St. Dev**		**Mean**	**St. Dev**		**Mean**	**St. Dev**
2020s	0.3	0.8		0.7	0.4		0.9	0.4
2050s	1.0	0.8		1.3	0.3		1.3	0.5
2080s	1.8	0.9		1.8	0.7		1.9	0.5
	Mar			**Apr**			**May**	
	Mean	**St. Dev**		**Mean**	**St. Dev**		**Mean**	**St. Dev**
2020s	0.2	0.4		0.8	0.3		0.4	0.1
2050s	0.6	0.6		1.2	0.4		1.0	0.3
2080s	1.2	0.5		1.8	0.4		1.4	0.2
	Jun			**Jul**			**Aug**	
	Mean	**St. Dev**		**Mean**	**St. Dev**		**Mean**	**St. Dev**
2020s	0.4	0.2		0.3	0.2		0.4	0.2
2050s	0.8	0.3		0.8	0.3		1.0	0.3
2080s	1.2	0.3		1.4	0.3		1.5	0.3
	Sept			**Oct**			**Nov**	
	Mean	**St. Dev**		**Mean**	**St. Dev**		**Mean**	**St. Dev**
2020s	0.7	0.3		1.5	0.3		0.5	0.5
2050s	1.3	0.4		2.1	0.4		1.3	0.5
2080s	2.1	0.4		3.0	0.3		1.9	0.6

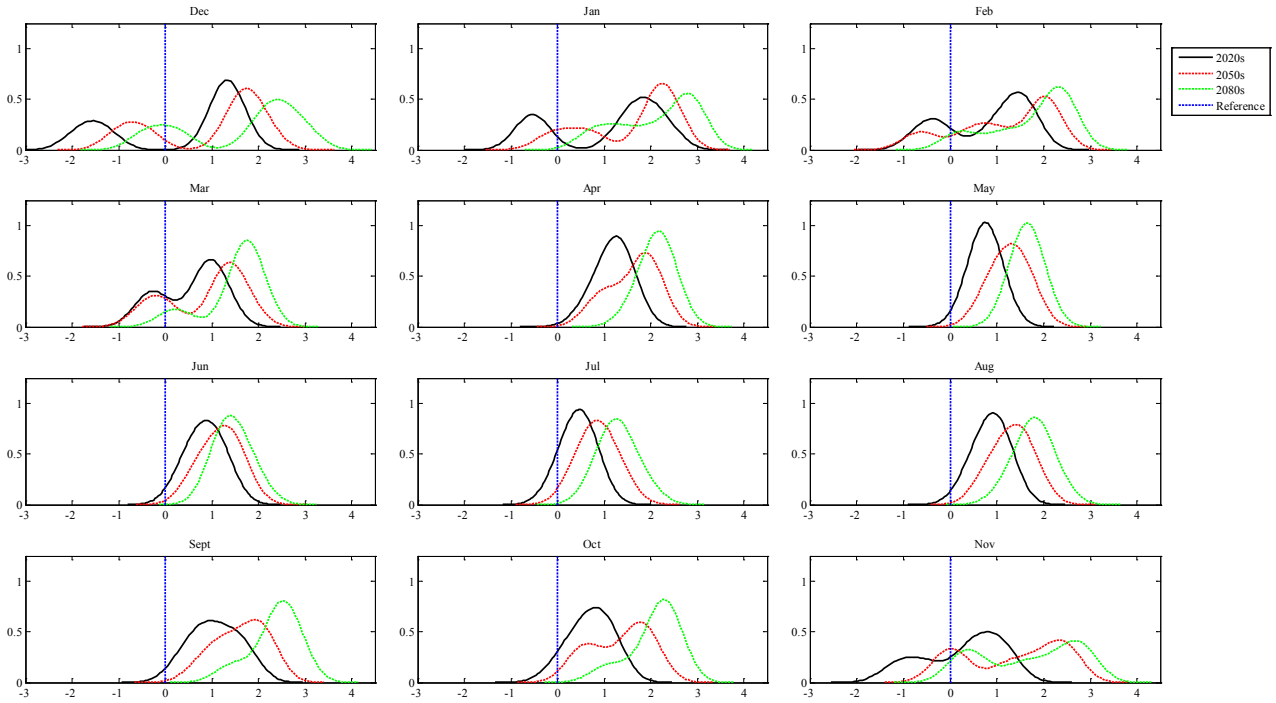

Figure 4.10 Projected changes in the 10th percentile for minimum temperature derived from all GCMs and emission scenarios. The vertical line represents the baseline statistic.

Table 4.17 Projected changes in the 90th percentile mean and standard deviation for minimum temperature.

	Dec			Jan			Feb	
	Mean	**St. Dev**		**Mean**	**St. Dev**		**Mean**	**St. Dev**
2020s	0.4	1.4		1.1	1.2		0.8	0.9
2050s	0.9	1.2		1.6	1.0		1.2	1.0
2080s	1.6	1.3		2.1	0.8		1.7	0.8
	Mar			**Apr**			**May**	
	Mean	**St. Dev**		**Mean**	**St. Dev**		**Mean**	**St. Dev**
2020s	0.6	0.6		1.2	0.3		0.8	0.2
2050s	0.9	0.8		1.6	0.5		1.3	0.3
2080s	1.5	0.6		2.1	0.2		1.6	0.2
	Jun			**Jul**			**Aug**	
	Mean	**St. Dev**		**Mean**	**St. Dev**		**Mean**	**St. Dev**
2020s	0.9	0.3		0.4	0.2		0.9	0.3
2050s	1.2	0.3		0.9	0.3		1.3	0.3
2080s	1.5	0.3		1.3	0.3		1.8	0.3
	Sept			**Oct**			**Nov**	
	Mean	**St. Dev**		**Mean**	**St. Dev**		**Mean**	**St. Dev**
2020s	1.1	0.5		0.7	0.4		0.3	0.8
2050s	1.6	0.5		1.3	0.6		1.3	1.0
2080s	2.4	0.5		2.1	0.5		1.7	1.0

4.11 Precipitation

When compared to temperature projected changes in the precipitation regime of the catchment differ to a much greater degree depending on the time horizon, climate model and emissions pathway considered (Table 4.18). There is also the added complication of the dissimilarity between each of the two downscaling techniques used to derive local-scale precipitation. There is however broad commonalities across the downscaled series. Each GCM and emission scenario suggests a reduction in summer rainfall amounts accompanied by an increase in winter, with this trend likely to become more extreme as the century progresses. The divergence between projected changes arising from emission scenario alone increases towards the end of the century. For the 2020s and in some cases the 2050s differences between the A2 and B2 emissions pathway are negligible, this applies primarily to the HadCM3 model. The 2080s exhibit the greatest difference between the A2 and B2 pathways. Significant differences also arise due to downscaling technique. This is most notable for the summer months where the GLM approach estimates greater reductions when compared to SDSM. Although both are based on regression analysis differences arise due to individual model structure and predictor selection.

From SDSM the projected changes in precipitation for the 2080s, derived using the output from the HadCM3 model driven using the A2 emission scenario, indicate an increase in mean winter precipitation amounts by 18% and a decrease in mean summer precipitation by -17% relative to the baseline period. Using the same model output a decrease of -5% in autumn rainfall is also projected to occur over the 2080s. The scenarios derived using the GLM approach, for the same GCM and emissions pathway indicate a 20% increase in winter rainfall and a much more extreme decrease of -34% in summer.

Table 4.18 Percentage change in rainfall for each future horizon on a seasonal basis downscaled using both SDSM and GLM.

	SDSM				GLM			
	Winter	Spring	Summer	Autumn	Winter	Spring	Summer	Autumn
HadCM3 - A2								
2020s	-1.5	-3.8	-2	-1.5	-0.7	-3.3	-3.8	0
2050s	3.8	-7.4	-2.8	-6.6	5.3	-5.4	-10.5	-5.9
2080s	17.3	3.7	-18	-5	20.2	1.9	-34.2	-4.5
HadCM3 - B2								
2020s	0.9	1.5	1.3	1.7	1.2	3.2	-1.8	2.9
2050s	8.2	-2.4	-9	-2.9	8.8	-3	-15.2	-2.2
2080s	9.7	4.7	-7.9	-2.9	11.1	4.4	-18.2	-2.7
CSIROmk2 - A2								
2020s	10	3.9	-7.6	1.6	10.7	1.3	-15.2	-1
2050s	13.1	1.3	-17	-4.3	14.1	-3.6	-34.3	-7
2080s	21.5	-1.3	-13.7	-4.7	22.5	-7.6	-38.4	-9
CSIROmk2 - B2								
2020s	4.7	-0.8	-1.5	-6.8	4.9	-4.3	-10	-6.6
2050s	25.4	-5.6	-3.7	-2.9	24.6	-10.4	-16.3	-3.3
2080s	14.8	-0.5	-5.4	-5.4	15.6	-3.5	-22.7	-6.7
CGCM2 - A2								
2020s	6.4	-7.7	-8.5	2.5	7.4	-9.8	-19.3	1.3
2050s	20.3	-18.1	-6.2	-4.2	19.7	-19.7	-23.1	-4.9
2080s	12.6	-27.7	-10.4	-9.9	14.7	-37.2	-36.9	-12.8
CGCM2 - B2								
2020s	2.3	2.9	0	0.6	4.4	1.5	-7.1	0.1
2050s	9.4	-13.2	-7.6	1.8	10	-14	-21	0.5
2080s	13.1	-17.8	-6.2	0.2	13.7	-21.3	-22.9	-2.2

Precipitation scenarios from SDSM, derived using the model output from CSIROmk2 under the A2 emission scenario, suggests an increase in winter rainfall amounts by 21% and a decrease of -14% in summer for the 2080s. In contrast to the HadCM3 model a reduction in precipitation of -7% for spring is projected to occur for the same horizon. The GLM derived scenarios suggests a similar increase in winter (22.5%) with a much greater decrease in summer (-38%) and autumn (-9.5%). Precipitation scenarios based on the CGCM2 climate model output, downscaled using SDSM, largely agree with those derived using climate models. Over the 2080s summer precipitation is projected to decrease by -10% whilst winter levels are expected to increase by 13%. The greatest relative reductions in precipitation are however projected to occur for the spring with an estimated -28% decrease by the 2080s. As with other scenarios a reduction in autumn precipitation amounts (-10%) is also projected to occur for this horizon. The GLM derived scenarios from the CGCM2 model are largely in-line with SDSM however the projected changes in summer (-37%) and spring (-37%) are much more severe.

The probability density functions constructed using all model projections, including those derived using both SDSM and the GLM, provide a clearer picture of changes in the catchments rainfall regime with an increase in winter accompanied by a decrease in summer evident (Figure 4.11). This enhancement in the seasonality of the precipitation regime is projected to become more pronounced as the century progresses. For a number of months, most notably April and November, little change over reference conditions is suggested.

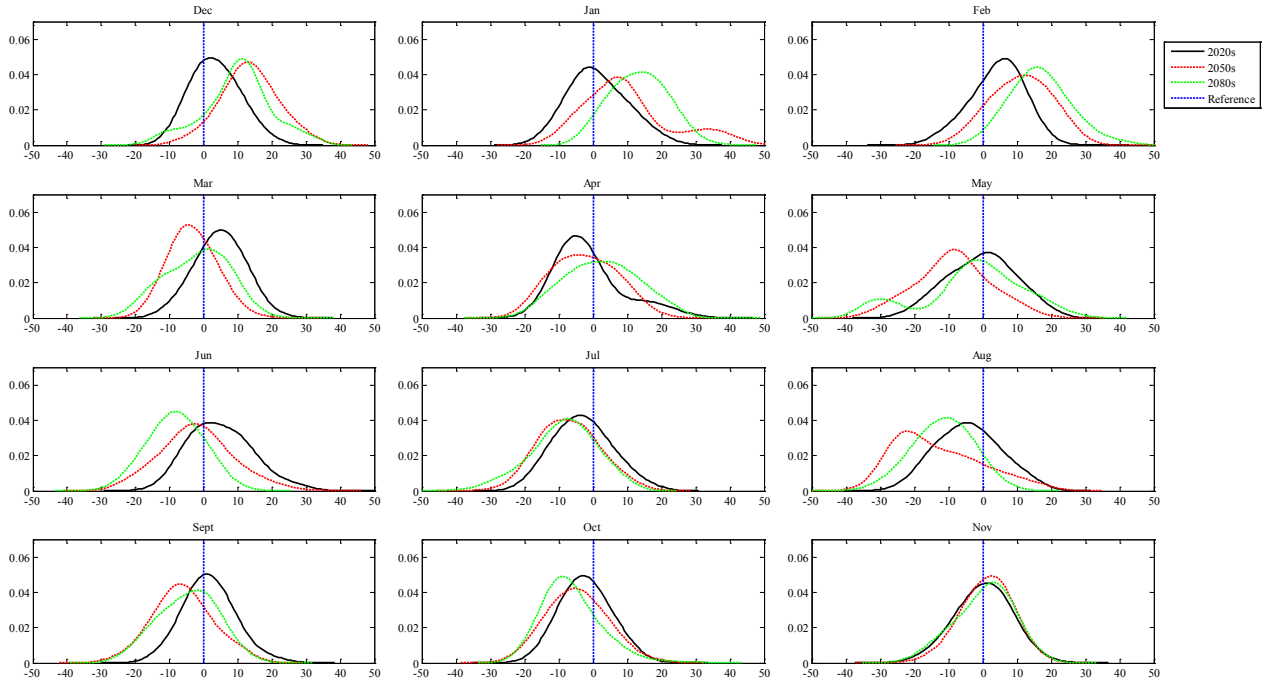

Figure 4.11 Probability density functions, constructed using the downscaled output from each GCM, emission scenario and both downscaling techniques, depicting the projected change in precipitation for all months. The vertical line represents the baseline mean.

Table 4.19 The mean and standard deviation for mean monthly precipitation from the PDFs in Figure 4.11.

	Dec			Jan			Feb	
	Mean	St. Dev		Mean	St. Dev		Mean	St. Dev
2020s	3.5	6.7		1.4	8.3		4.2	7.5
2050s	13.4	8.0		10.0	12.9		11.2	8.6
2080s	9.9	10.0		13.4	7.9		16.8	8.6
	Mar			Apr			May	
	Mean	St. Dev		Mean	St. Dev		Mean	St. Dev
2020s	4.7	6.9		-1.1	10.0		-0.3	9.8
2050s	-3.2	6.5		-2.4	9.2		-8.6	10.7
2080s	-1.9	9.0		2.6	10.7		-3.0	14.9
	Jun			Jul			Aug	
	Mean	St. Dev		Mean	St. Dev		Mean	St. Dev
2020s	5.0	9.2		-3.0	8.2		-4.2	9.2
2050s	-1.9	10.6		-7.0	8.5		-13.0	12.7
2080s	-8.1	7.8		-8.6	9.6		-11.7	8.6
	Sep			Oct			Nov	
	Mean	St. Dev		Mean	St. Dev		Mean	St. Dev
2020s	1.6	7.2		-2.2	6.9		0.1	7.9
2050s	-6.0	8.5		-4.7	8.5		1.2	7.0
2080s	-4.6	8.4		-6.3	8.3		0.4	8.1

4.12 Wind Speed

There is an absence of any distinguishable change in local wind speed for each future horizon, a detail common to the series derived from each GCM and emission scenario. This could be attributable to the absence of any thermal or moisture based variables in the downscaling predictor set. Such variables are sensitive to changes in the Earth's radiative balance and as such capture the underlying climate change 'signal'. The percent change in wind speed for each future horizon, relative to the baseline period, is displayed in Table 4.20. For this variable downscaling was carried out using both SDSM and the GLM approach. For each horizon and emission scenario deviations from the reference conditions are negligible and it is possible that the changes catalogued in Table 4.19 could be attributable to natural variability rather than an anthropogenically induced shift in local wind conditions.

Table 4.20 Percentage change in local wind speeds for each future horizon on a seasonal basis downscaled using both SDSM and GLM.

	SDSM				GLM			
	Winter	Spring	Summer	Autumn	Winter	Spring	Summer	Autumn
HadCM3 - A2								
2020s	-0.19	-1.11	0.12	0.19	0.03	-1.35	-0.14	-0.15
2050s	-0.35	-4.51	-0.37	-1.50	-0.30	-4.88	-0.36	-1.41
2080s	2.52	1.33	-3.66	0.41	3.22	0.87	-3.93	0.48
HadCM3 - B2								
2020s	-0.46	-0.71	-0.05	0.22	-0.18	-0.98	-0.09	0.09
2050s	1.97	1.51	-2.57	-0.56	2.58	1.37	-2.83	-0.62
2080s	1.03	1.34	-2.07	0.26	1.43	1.27	-2.01	0.27
CSIROmk2 - A2								
2020s	4.67	0.81	-3.21	-0.90	0.97	-0.99	-1.89	-2.04
2050s	1.86	0.35	-3.45	-0.35	5.24	-2.01	-1.72	0.98
2080s	6.62	-2.29	-3.34	-0.11	7.47	-3.44	-2.75	-0.92
CSIROmk2 - B2								
2020s	0.46	-0.87	-1.74	-2.17	5.09	0.92	-3.17	-0.98
2050s	4.67	-1.68	-1.57	0.56	2.10	0.17	-3.46	-0.78
2080s	6.61	-3.17	-2.65	-1.32	7.49	-2.37	-3.23	-0.29
CGCM2 - A2								
2020s	-1.04	1.21	-0.60	-1.43	-0.89	1.28	-0.53	-1.44
2050s	-0.73	5.30	-2.43	-0.10	-0.54	5.68	-2.58	0.05
2080s	-0.44	6.07	-1.84	0.45	-0.48	6.17	-1.81	0.46
CGCM2 - B2								
2020s	-0.17	3.57	-2.59	-0.71	0.37	3.94	-2.65	-0.49
2050s	-3.20	3.13	-1.30	-1.93	-4.58	3.26	-1.39	-1.79
2080s	-2.14	4.02	-2.59	-1.42	-2.55	4.06	-2.67	-1.38

4.13 Relative Humidity

There is a general consensus between each GCM and emission scenario that relative humidity will progressively decrease over the next century for all seasons with the greatest reductions being associated with the HadCM3 A2 scenario. The percent change in relative humidity for each future horizon, with respect to the 1961-1990 baseline period, is shown in Table 4.21. Model suggested changes in relative humidity reflect the general trend exhibited by air temperatures. This makes physical sense as a warmer air mass should in theory have a greater moisture carrying capacity and thus a lower relative humidity. Although relative humidity may decrease as a result of warmer air temperatures air masses which can hold a larger amount of moisture have potential knock-on effects for the intensity of precipitation events as well as for the stability of air masses themselves.

Table 4.21 Percentage change in relative humidity for each future horizon on a seasonal basis downscaled using SDSM.

	Winter	Spring	Summer	Autumn
HadCM3 - A2				
2020s	-0.20	-0.35	-0.32	-0.44
2050s	-0.19	-0.94	-0.63	-0.52
2080s	-0.40	-1.51	-1.44	-1.48
HadCM3 - B2				
2020s	-0.20	-0.30	-0.30	-0.20
2050s	-0.20	-0.80	-0.50	-0.50
2080s	-0.40	-1.00	-0.90	-1.00
CSIROmk2 - A2				
2020s	-0.15	0.49	0.08	0.12
2050s	-0.15	0.08	-0.13	-0.31
2080s	-0.35	0.36	0.08	-0.76
CSIROmk2 - B2				
2020s	-0.13	0.06	0.07	-0.10
2050s	0.03	0.16	-0.07	0.16
2080s	-0.66	0.06	-0.16	-0.08
CGCM2 - A2				
2020s	-0.40	-0.20	-0.50	-0.20
2050s	-0.70	-0.90	-0.60	-0.70
2080s	-0.50	-0.60	-0.80	-0.90
CGCM2 - B2				
2020s	-0.16	-0.74	-0.28	-0.18
2050s	0.27	-0.38	-0.61	-0.56
2080s	-0.22	-0.82	-0.63	-0.94

4.14 Solar Radiation and Potential Evaporation

Due to the influence which solar radiation has on controlling evaporation rates projected changes for both incoming radiation and potential evaporation are relatively similar. Table 4.22 lists the projected changes in both variables relative to baseline conditions. The downscaled scenarios suggest the greatest relative increase in both variables will be over the summer period with deviations from reference conditions for this season becoming more pronounced towards the end of the century. The greatest summer increases are suggested by the scenario downscaled from the HadCM3 model under the A2 emissions pathway. Such increases in evaporation rates are in-line with projected changes in air temperature and reductions in cloud cover suggested by a decrease in summer precipitation. Winter reductions in both variables

are indicated by the model results with the greatest decreases being associated with the CSIROmk2 GCM under the B2 emissions scenario. Such decreases during the winter period are commensurate with an increase in precipitation rates indicating greater cloud cover.

Table 4.22 Percentage change in solar radiation and potential evaporation for each future horizon on a seasonal basis downscaled using SDSM.

	Solar Radiation				Potential Evaporation			
	Winter	Spring	Summer	Autumn	Winter	Spring	Summer	Autumn
HadCM3 - A2								
2020s	0.6	0.0	1.1	1.2	-0.2	-0.1	1.2	1.6
2050s	-0.6	2.9	3.0	2.4	-0.1	2.8	3.3	3.0
2080s	-1.7	2.3	6.8	4.3	-1.1	2.0	7.6	4.7
HadCM3 - B2								
2020s	0.2	-0.1	1.8	0.2	-0.4	-0.3	1.7	0.6
2050s	-0.4	0.1	3.1	2.2	0.0	0.1	3.5	2.8
2080s	-0.1	1.0	4.3	2.5	-0.1	0.8	4.6	2.4
CSIROmk2 - A2								
2020s	0.2	0.1	1.5	-0.1	1.9	0.3	1.5	-0.1
2050s	-1.1	2.0	2.4	0.4	-0.5	1.9	2.5	0.7
2080s	-1.8	3.5	3.9	2.5	-1.5	3.5	4.0	2.5
CSIROmk2 - B2								
2020s	-2.1	0.8	2.1	-0.2	-4.6	1.1	1.8	-0.2
2050s	-4.5	1.7	3.1	-0.3	-4.0	1.9	3.0	-0.1
2080s	-2.4	3.6	4.3	0.1	-4.6	3.6	4.2	-0.2
CGCM2 - A2								
2020s	0.0	0.7	1.7	1.3	1.0	1.1	2.0	1.6
2050s	-0.2	2.7	1.8	2.1	1.3	3.1	2.2	2.3
2080s	0.2	1.6	3.7	3.0	0.7	2.3	4.3	2.9
CGCM2 - B2								
2020s	-0.9	2.1	2.3	1.3	-1.1	2.2	2.4	1.5
2050s	-2.5	1.4	1.7	2.2	0.8	1.7	2.1	2.4
2080s	-0.2	2.7	3.4	3.2	1.4	3.0	3.7	3.0

4.15 Summary

One of the greatest challenges currently facing the international community is that of an anthropogenically induced shift in the state and workings of the Earth's climate system. Changes in the composition of the atmosphere, including increases in the concentration of greenhouse gases (e.g. CO2, CH4 and N20) and aerosols (e.g. sulphates and black carbon) resulting from human activity, have the potential to fundamentally alter the global radiative balance with far-reaching and significant implications for the Earth's climate system. Model

simulations suggest that the average surface temperature of the Earth is likely to increase by 1.1 to 6.4°C by the end of the 21st century, relative to the period 1980-1990, with a best estimate of 1.8 to 4.0°C (IPCC, 2007). Such changes in temperature are indicative of the potential impact human activity may have on the climate system and alludes to the sheer scale of the problem facing humankind. Changes in climate on a global, regional and local scale will have significant societal and environmental impacts which we must attempt to mitigate and plan to adapt to.

Global climate models (GCMs) provide us with the means to study various aspects of the global climate system including its possible time evolution under prescribed anthropogenic forcings (i.e. different atmospheric concentrations of GHGs). The projections from GCM experiments represent the primary source of data used to carry out climate change impact assessments, to develop adaptation strategies and to inform future policy planning. While these models are most accurate at large spatial scales (continental, hemispheric and global), their coarse resolution (typically of the order of 300 – 500 kms) and limited physics prohibits them from resolving important sub-grid scale climate features (e.g. convective rainfall, topographic effects) meaning they fail to reproduce the workings of the climate system at the spatial scales (of the order of tens of kilometres or point scale) most relevant for studying the impacts of climate change. To properly assess the regional and local impact of climate change higher resolution climate data, which captures the nuances and details of locally specific conditions, is required. In order to overcome the resolution gap which exists between what climate modellers can provide and what impacts assessors require a range of 'downscaling' techniques have been developed. Such techniques have been applied in this study to develop high resolution climate scenarios for the Burrishoole catchment which describe changes in key meteorological variables.

To assess the potential changes in the climate conditions of the Burrishoole catchment statistical methods were employed to downscale high resolution climate scenarios using grid-scale GCM projections. In order to address the various components of uncertainty arising from emission scenarios, GCM structures, parameterizations and climate sensitivities the output from three GCMs (HadCM3, CSIROmk2 and CGCM2), each run under both the A2 (medium-high) and B2 (medium-low) SRES emission scenarios, were used as the driving data for the downscaled scenarios. The shortcomings and limitations associated with statistical downscaling represent an additional source of uncertainties in local-scale estimates of climate change. To address this, and in recognition that no one optimal method exists, both Linear Regression and Generalized Linear Models (GLMs) were employed to develop future

scenarios. Model projections were considered over three future time horizons (2020s, 2050s and 2080s) relative to the standard thirty year reference period (1961-1990).

Projected changes in the climate conditions of the Burrishoole catchment have potentially far reaching implications for all aspects of the catchment system, including water quality, streamflow hydrology, soil processes, and most notably the well-being of its aquatic environment. Future management of the catchment will need to explicitly consider the likely impacts of an anthropogenically induced shift in the catchments prevailing climate conditions with the aim of mitigating the most potentially severe impacts. A number of general conclusions can be made regarding key changes in the climate of the Burrishoole catchment.

4.16 Key Findings

- There is a general consensus between model projections that all seasons will experience an increase in both average daily minimum and maximum temperature with deviations from baseline conditions becoming more pronounced as the century progresses.
- It is intimated that changes in temperature are likely to be more acute under the A2 emissions pathway when compared to the less carbon intensive B2 scenario.
- The temperature scenarios downscaled from each GCM and emissions scenario, when collectively considered (i.e. as a probability density function shown in Figure 4.12 and catalogued in Table 4.22), indicate an increase in mean daily temperatures by the 2080s of 1.7, 1.8, 1.7 and 2.2 degrees C for winter (DJF), spring (MAM), summer (JJA) and autumn (SON) respectively.
- When considered collectively the greatest relative changes in maximum temperature are associated with the months of September (+ 2.2°C), October (+ 2.9°C) and August (+ 2°C) over the 2080s.
- When considered collectively the greatest relative changes in minimum temperature are associated with the months of September (+ 2.1°C), October (+ 3°C), November (+ 1.9°C) and February (+1.9°C) over the 2080s.
- Extreme maximum temperatures (90th percentile) are anticipated to increase as are extreme minimum temperatures (10th percentile). Both these findings are commensurate with the overall trend of increasing temperatures.
- Model simulations suggest an increasing tendency towards a more seasonal rainfall regime (i.e. higher winter and lower summer precipitation receipts) with this underlying trend becoming more pronounced as the century progresses.

- Based on the precipitation scenarios derived from each GCM and emission scenario it is likely that winter receipts will increase by 13% over the latter half of the century whilst decreases of 10% are projected for the summer over the 2080s.
- On a monthly basis, over the 2080s, the greatest increases in precipitation are suggested for February (+16.8 %) and January (+13 %) whilst the largest decreases are associated with the months of August (-11.7 %), June (-8.1 %) and July (-8.6 %).
- Model projected changes in wind speed do not present any clear indication of an alteration in prevailing conditions over that of the baseline period. It is likely that the changes suggested by the scenarios downscaled from each GCM are within the bounds of natural variability and thus cannot be attributed to an anthropogenically induced shift in local wind conditions.
- It is anticipated that relative humidity will decrease in-line with an expected increase in the moisture carrying capacity of air masses.
- The seasonal regime for receipts of solar radiation is expected to become more pronounced with increases during summer and decreases during the winter months.
- Owing to their close association projected changes in potential evaporation follow the trend exhibited by solar radiation. Thus increased losses to evaporation from the catchment system are likely over the summer months with this trend becoming more pronounced as the century progresses.

4.17 References

Abaurrea, J. and Asín, J. (2005) 'Forecasting local daily precipitation patterns in a climate change scenario', *Climate Research,* 28, 183 –197.

Bates, B.C., Charles, S.P. and Hughes, J.P. (1998) 'Stochastic downscaling of numerical climate model simulations', *Environmental Modelling and Software*, 13, 325-331.

Beckmann, B.R. and Buishand, T.A. (2002) 'Statistical downscaling relationships for precipitation in the Netherlands and north Germany', *International Journal of Climatology*, 22, 15–32.

Brinkmann, W. (2000) 'Modification of a correlation-based circulation pattern classification to reduce within-type variability of temperature and precipitation', *International Journal of Climatology*, 20, 839–852.

Bristow, K.L. and Campbell, G.S. (1984) 'On the relationship between incoming solar radiation and daily maximum and minimum temperature', *Agricultural and Forest Meteorology,* 31, 159-166.

Boe, J., Terray, L., Habets, F. and Martin, E. (2007) 'Statistical and dynamical downscaling of the Seine basin climate for hydro-meteorological studies', *International Journal of Climatology,* 27, 1643-1655.

Burger, G. (1996) 'Expanded downscaling for generating local weather scenarios', *Climate Research*, 7, 111–128.

Burger, G. and Chen, Y. (2005) 'Regression-based downscaling of spatial variability for hydrologic applications', *Journal of Hydrology*, 311, 299–317.

Cavazos, T. and Hewitson, B.C. (2005) 'Performance of NCEP variables in statistical downscaling of daily precipitation', *Climate Research*, 28, 95–107.

Charles, S.P., Bates, B.C., Whetton, P.H. and Hughes, J.P. (1999) 'Validation of downscaling models for changed climate conditions: case study of southwestern Australia', *Climate Research,* 12, 1–14.

Charles, S.P., Bates, B.C., Smith, I.N. and Hughes, J.P. (2004) 'Statistical downscaling of daily precipitation from observed and modelled atmospheric fields', *Hydrological Processes*, 18, 1373–1394.

Chandler, R.E. and Wheater, H.S. (1998) 'Climate change detection using Generalized Linear Models for rainfall – a case study from the West of Ireland I. Preliminary analysis and modelling of rainfall occurrence. Research Report No. 194, Department of Statistical Sciences, University College London.

Chandler, R.E. and Wheater, H.S. (2002) 'Analysis of rainfall variability using generalized linear models: A case study from the west of Ireland', *Water Resources Research,* 38(10), 1192.

Coe, R. and Stern, R.D. (1982) 'Fitting models to daily rainfall data', *Journal of Applied Meteorology*, 21, 1024–1031.

Corte-Real, J., Budong, Q. and Hong, X. (1998) 'Regional climate change in Portugal: precipitation variability associated with large-scale atmospheric circulation', *International Journal of Climatology*, 18(6), 619-635.

Crane, R.G. and Hewitson, B.C. (1998) 'Doubled CO2 climate change scenarios for the Susquehanna Basin: precipitation', *International Journal of Climatology*, 18, 65–76.

Cubasch, U., von Storch, H., Waszkewitz, J. and Zorita, E. (1996) 'Estimates of climate change in southern Europe using different downscaling techniques', *Climate Research*, 7, 129–149.

Deque, M. (2007) 'Frequency of precipitation and temperature extremes over France in an anthropogenic scenario: Model results and statistical correction according to observed values', *Global and Planetary Change*, 57, 16-26.

Dessai, S., O'Brien, K. and Hulme, M. (2007) 'On uncertainty and climate change', *Global Environmental Change*, 17, 1-3.

Diaz-Nieto, J. and Wilby, R.L. (2005) 'A comparison of statistical downscaling and climate change factor methods: impacts on low flows in the River Thames, United Kingdom' *Climatic Change,* 69, 245–268.

Donatelli, M., Carlini, L. and Bellocchi, G. (2006) 'A software component for estimating solar radiation', *Environmental Modelling & Software*, 21, 411-416.

Fealy, R. and Sweeney, J. (2007) 'Statistical downscaling of precipitation for a selection of sites in Ireland employing a generalised linear modelling approach', *International Journal of Climatology*, 27, 2083-2094.

Fealy, R. and Sweeney, J. (2008) 'Statistical downscaling of temperature, radiation and potential evapotranspiration to produce a multiple GCM ensemble mean for a selection of sites in Ireland', *Irish Geography*, 41(1), 1-27.

Fowler, H.J., Blenkinsop, S. and Tebaldi, C. (2007) 'Linking climate change modelling to impacts studies: recent advances in downscaling techniques for hydrological modelling', *International Journal of Climatology*, 27, 1547 -1578.

Giorgi, F. and Mearns, L.O. (1991) 'Approaches to the simulation of regional climate change: A review'. *Review of Geophysics*, 29(2), 191–216.

Giorgi, F. and Mearns, L.O. (1999) 'Introduction to special section: regional climate modeling revisited', *Journal of Geophysical Research*, 104, 6335–6352.

Giorgi, F., Jones, R., Whetton, P., von Storch, H., Fu, G., Mearns, L.O., Hewitson, B.C., Christensen, H. and Hulme, M. (2001) 'Regional climate information evaluation and projections'. In: Johnson, C.A., Houghton, J.T., Ding, Y., Griggs, D.J., Noguer, M., van der Linden, P.J., Dia, X. and Maskell, K. (eds).Climate Change 2001: The Scientific Basis. Cambridge University Press, Cambridge.

Giorgi, F. (2005) 'Climate Change Prediction', *Climatic Change*, 73(3), 1573-1480.

Goodess, C.M. and Palutikof, J.P. (1998) 'Development of daily rainfall scenarios for southeast Spain using a circulation-type approach to downscaling'. *International Journal of Climatology*, 18(10), 1051-1083.

Grotch, S.L. and MacCracken, M.C. (1991) 'The use of general circulation models to predict regional climatic change', *Journal of Climate*, 4, 286–303.

Hassan, H., Aramaki, T., Hanaki, K., Matsuo, T. and Wilby, R.L. (1998) 'Lake stratification and temperature profiles simulated using downscaled GCM output'. *Journal of Water Science and Technology,* 38, 217–226.

Hay, L.E., McCabe, G.J., Wolock, D.M. and Ayers, M.A. (1991) 'Simulation of precipitation by weather type analysis', *Water Resources Research*, 27, 493–501.

Hay, L.E., Wilby, R.L. and Leavesley, G.H. (2000) 'A comparison of delta change and downscaled GCM scenarios for three mountainous basins in the United States', *Journal of the American Water Resources Association,* 36, 387–397.

Hellström, C., Chen, D., Achberger, C. and Räisänen, J. (2001) 'Comparison of climate change scenarios for Sweden based on statistical and dynamical downscaling of monthly precipitation', *Climate Research*, 19, 45–55.

Henderson-Sellers, A. (1993) 'An Antipodean Climate of Uncertainty', *Climatic Change*, 25, 203–224.

Hewitson, B.C., and Crane, R.G., (1996) 'Climate downscaling: techniques and application', *Climate Research,* 7, 85-95.

Hewitson, B.C. and Crane, R.G. (2006) 'Consensus between GCM climate change projections with empirical downscaling: precipitation downscaling over South Africa' *International Journal of Climatology*, 26, 1315–1337.

Hulme, M. and Carter, T.R. (1999) 'Representing uncertainty in climate change scenarios and impact studies' In: Carter, T., Hulme, M. and Viner, D. eds. Representing uncertainty in climate change scenarios and impact studies, Proceedings ECLAT-2 Helsinki Workshop, 14-16 April, 1999. Norwich: Climatic Research Unit.

Huth, R. (2004) Sensitivity of Local Daily Temperature Change Estimates to the Selection of Downscaling Models and Predictors Journal of Climate, 17 640-652.

Jenkins, G. and Lowe, J. (2003) 'Handling uncertainties in the UKCIP02 scenarios of climate change', Hadley Cent. Tech. Note 44, Met Off., Exeter, U.K.

Kalnay, E., Kanamitsu, M., Kistler, R., Collins, W., Deaven, D., Gandin, L., Iredell, M., Saha, S., White, G., Woollen, J., Zhu, Y., Leetmaa, A., Reynolds, B., Chelliah, M., Ebisuzaki, W., Higgins, W., Janowiak, J., Mo, K.C., Ropelewski, C., Wang, J., Jenne, R. and Joseph, D. (1996) 'The NCEP/NCAR 40-Year Reanalysis Project', *Bulletin of the American Meteorological Society,* 77(3), 437-472.

Karl, T.R., Wang, W.C., Schlesinger, M. E., Knight, R.W. and Portman, D. (1990) 'A method of relating general circulation model simulated climate to observed local climate. Part I: seasonal statistics', *Journal of Climate*, 3, 1053–1079.

Katz, R.W. (1996) 'Use of conditional stochastic models to generate climate change scenarios', *Climactic Change*, 32(3), 237-255.

Kidson, J.W. and Thompson, C.S. (1998) 'A comparison of statistical and model-based downscaling techniques for estimating local climate variations', *Journal of Climate,* 11, 735–753.

Kidson, J.W. and Watterson, I.G. (1995) 'A synoptic climatological evaluation of the changes in the CSIRO nine-level model with doubled CO2 in the New Zealand region', *International Journal of Climatology*, 15, 1179–1194.

Mc Cullagh, P. and Nelder, J.A. (1989) *Generalized Linear Models*, Chapman and Hall London.

Mc Guffie, K., Henderson-Sellers, A., Holbrook, N., Kothavala, Z., Balachova, O. and Hoekstra, J. (1999) 'Assessing simulations of daily temperature and precipitation variability with global climate models for present and enhanced greenhouse climates', *International Journal of Climatology*, 19(1), 1-26.

Mearns, L.O., Giorgi, F., McDaniel, L. and Shields, C. (1995) 'Analysis of daily variability of precipitation in a nested regional climate model: comparison with observations and doubled CO2 results', *Global and Planetary Change*, 10, 55–78.

Mearns, L.O., Bogardi, I., Giorgi F., Matayasovsky, I., and Palecki, M. (1999) 'Comparison of climate change scenarios generated daily temperature and precipitation from regional climate model experiments and statistical downscaling', *Journal of Geophysical Research*, 104, 6603–6621.

Mearns, L.O., Giorgi, F., Whetton, P., Pabon, D., Hulme, M., and Lal, M., (2003) Guidelines for use of climate scenarios developed from Regional Climate Model experiments. Data Distribution Centre of the International Panel of Climate Change.

Murphy, J. (1999) 'An evaluation of statistical and dynamical techniques for downscaling local climate', *Journal of Climate*, 12, 2256–2284.

Murphy, J. (2000) 'Predictions of climate change over Europe using statistical and dynamical downscaling techniques', *International Journal of Climatology*, 20, 489–501.

New,M.G. and Hulme, M. (2000) 'Representing uncertainties in climate change scenarios: a Monte Carlo approach', *Integrated Assessment* , 1, 203-213.

Nakicenovic, N., Alcamo, J., Davis, G., de Vries, B., Fenhann, J., Gaffin, S., Gregory, K., Grübler, A., Jung, T.Y., Kram, T., La Rovere, E.L., Michaelis, L., Mori, S., Morita, T., Pepper, W., Pitcher, H., Price, L., Riahi, K., Roehrl, A., Rogner, H.-H., Sankovski, A., Schlesinger, M., Shukla, P., Smith, S., Swart, R., van Rooijen, S., Victor, N. and Dadi Z. (2000) IPCC Special Report on Emissions Scenarios. Cambridge University Press, Cambridge, United Kingdom.

Racsko, P., Szeidl, L. and Semenov, M. (1991) 'A serial approach to local stochastic weather models', *Ecological Modelling,* 57, 27-41.

Richardson, C. (1981) 'Stochastic simulation of daily precipitation, temperature, and solar radiation', *Water Resources Research,* 17, 182 –190.

Schneider, S. H. (1983) 'CO2, Climate and Society: A Brief Overview', in Chen, R. S., Boulding, E., and Schneider, S. H. (eds.), Social Science Research and Climate Change: In Interdisciplinary Appraisal, D. Reidel, Boston, pp. 9–15.

Semenov, M.A. and Barrow, E. (1997) 'Use of stochastic weather generator in the development of climate change scenarios', *Climatic Change,* 35, 397-414.

Semenov, M.A., Brooks, R.J., Barrow, E.M. and Richardson, C.W. (1998) 'Comparison of the WGEN and LARS-WG stochastic weather generators for diverse climates', *Climate Research*, 10, 95–107.

Stern, R.D. and Coe, R. (1984) 'A model fitting analysis of daily rainfall data (with discussion)'. *Journal of the Royal Statistical Society Series A,* 147, 1–34.

von Storch, H., Zorita, E., and Cubasch, U. (1993) 'Downscaling of global climate estimates to regional scales: An application to the Iberian rainfall in wintertime', *Journal of Climate*, 6, 1161–1171.

von Storch, H. (1995) 'Inconsistencies at the interface of climate impact studies and global climate research', *Meteorologische Zeitschrift*, 4(2), 72-80.

von Storch, H. (1999) 'On the use of 'Inflation' in Statistical Downscaling', *Journal of Climate*, 12(12), 3505-3506.

Wilby, R.L. and Wigley, T.M.L. (1997) 'Downscaling general circulation model output: a review of methods and limitations', *Progress in Physical Geography,* 21, 530–548.

Wilby, R.L., Hassan, H. and Hanaki, K. (1998) 'Statistical downscaling of hydrometeorological variables using general circulation model output', *Journal of Hydrology,* 205, 1–19.

Wilby, R.L., Hay, L.E. and Leavesley, G.H. (1999) 'A comparison of downscaled and raw GCM output: implications for climate change scenarios in the San Juan River basin, Colorado', *Journal of Hydrology,* 225, 67–91.

Wilby, R.L. and Wigley, T.M.L. (2000) 'Precipitation predictors for down scaling: observed and general circulation model relationships', *International Journal of Climatology,* 20, 641– 661.

Wilby, R.L., Hay, L.E., Gutowski, W.J., Arritt, R.W., Takle, E.S., Pan, Z., Leavesley, G.H. and Clark, M.P. (2000) 'Hydrological responses to dynamically and statistically downscaled climate model output', *Geophysical Research Letters*, 27, 1199–1202.

Wilby, R.L., Dawson, C.W. and Barrow, E.M. (2002) 'SDSM – a decision support tool for the assessment of regional climate change impacts', *Environmental Modelling & Software,* 17(2), 145–157.

Wilby, R.L. and Dawson, C.W. (2004) Using SDSM Version 3.1— A Decision Support Tool for the Assessment of Regional Climate Change Impacts. User Manual.

Wilby, R.L., Charles, S.P., Zorita, E., Timbal, B., Whetton, P. and Mearns, L.O., (2004) 'Guidelines for use of climate scenarios developed from statistical downscaling methods', Data Distribution Centre of the International Panel of Climate Change.

Wilby, R.L. and Harris, I. (2006) 'A framework for assessing uncertainties in climate change impacts: Low-flow scenarios for the River Thames, UK', *Water resources research*, Vol. 42, W02419, 10 pp.

Wilks, D.S. (1992) 'Adapting stochastic weather generation algorithms for climate change studies', *Climatic Change*, 22, 67–84.

Wilks, D.S. (1995) 'Statistical Methods in the Atmospheric Sciences', San Diego Academic Press.

Wilks, D.S. and Wilby, R.L. (1997) 'The weather generation game: A review of stochastic weather models', *Progress in Physical Geography*, 23, 329-357.

Wilks, D. S. (1999) 'Multisite downscaling of daily precipitation with a stochastic weather generator', *Climate Research*, 11, 125–136.

Winkler, J. A., Palutikof, J. P., Andresen, J. A. and Goodess C. M. (1997) 'The simulation of daily temperature time series from GCM output. Part II: Sensitivity analysis of an empirical transfer function methodology', *Journal of Climate*, 10, 2514–2532.

Wood, A., Leung, L.R., Sridhar, V. and Lettenmaier, D.P., (2004) 'Hydrologic implications of dynamical and statistical approaches to downscaling climate outputs', *Climatic Change*, 62, 189–216.

Yan, Z.W., Bate, S., Chandler, R.E., Isham, V. and Wheater, H. (2002) 'An analysis of daily maximum wind speed in northwestern Europe using generalized linear models', *Journal of Climate,* 15, 2073–2088.

Yarnal, B., Comrie A.C., Frakes, B., and Brown, D.P., (2001) 'Developments and Prospects In Synoptic Climatology', *International Journal of Climatology,* 21, 1923–1950.

Zorita, E. and H. von Storch (1999) 'The analog method - a simple statistical downscaling technique: comparison with more complicated methods', *Journal of Climate*, 12, 2474-2489.

5 CATCHMENT HYDROLOGY UNDER FUTURE CLIMATE SCENARIOS

Ciaran Broderick and Conor Murphy

5.1 Introduction

On every scale, changes in climate are likely to have significant impacts on freshwater hydrology, with increased energy resulting in an intensified hydrological cycle. Given the complex and fragile interaction between the climate system and land-surface hydrology, any changes in the primary processes of precipitation and evaporation will have considerable knock on effects for the rest of the hydrological cycle. In examining the implications of climate change for catchment hydrology in Ireland, Murphy and Charlton (2008) highlight that the potential impacts of climate change on hydrology and water resources are diverse and complex, while each catchments individual characteristics play a pivotal role in determining the hydrological response to climate change. This is in line with findings from Prudhomme and Davies (2009) who found that, for the UK, results of climate change impact assessments are catchment-specific and implies the necessity of a full modelling exercise when major planning and policy decisions are to be made. Despite results being catchment specific, a number of general conclusions can be made from the work of Murphy and Charlton (2009) in the wider Irish context;

- Reductions in streamflow are likely for the summer and autumn months in the majority of catchments, while greatest increases are suggested for winter. However, large differences exist in the magnitude of change simulated between catchments even when using the same future climate scenarios.
- The seasonality of streamflow is also likely to increase, with higher flows projected in winter and spring, while extended dry periods are suggested for summer and autumn in the majority of catchments.
- In relation to extremes the frequency of both high and low flows is likely to increase.

Such changes in freshwater hydrology are likely to have considerable implications for the distribution and abundance of key fish species where populations are influenced strongly by their habitat, which includes a range of biotic and abiotic factors that have complex interactions (Walsh and Kilsby, 2007). This is especially true for the Atlantic salmon, which is increasingly being recognised as of value, not just as a target species for fisheries but also for

conservation on grounds of biodiversity and as an indicator of environmental health (Winfield et al., 2004). In line with the importance of this species, it is now protected under the European Union Habitat Directive and is likely to be used extensively as a 'sensitive species' in the context of the European Water Framework Directive (Walsh and Kilsby, 2007).

In relation to climate change, Walsh and Kilsby (2007) highlight that changes in the flow regimes of the freshwater environment could have impacts for all life stages of Atlantic salmon; during spawning and egg deposition increases in flooding has the potential to wash out eggs laid in gravels, while decreased flows could leave redds stranded preventing the emergence of fry. The authors also highlight that wetter springs may induce earlier migration of smolts to sea, decreasing subsequent survival rates, while for juvenile salmon the increased risk of successive low flow years may have detrimental effects on salmon stocks, taking years to recover (Walsh and Kilsby. 2007).

The importance of understanding the local impacts of climate change is emphasised by Friedland et al. (2009) who highlight that during their freshwater stage salmon are locally adapted and in some contexts, an individual river stock needs to be viewed and managed as a species (Taylor, 1991). Projections of climate change over the next century suggest that temperature increases over land will exceed those expected over the surface of the oceans (Boer et al., 2000). In this context, we may look to changes in the marine environment as the forcing factor controlling stock complexity and productivity, but the changing state of conditions in fresh water may be the more important factor controlling species distribution and viability (Friedland et al., 2009). Understanding the likely impacts of climate change on catchment hydrology is critical in order to examine the sensitivity of key species and to enhance our ability to conserve and manage the viability and diversity of the species in Irish waters. This chapter examines the likely changes in the monthly flow regime and extreme hydrological events for the Burrishoole catchment.

5.2 Research Design

In order to increase the information content of simulations and fully exploit the richness of observations available, the catchment was sub-divided into constituent sub-catchments, with each being modelled independently. In line with the objective of quantifying uncertainties in future simulations of catchment hydrology, the climate scenarios developed in Chapter 4 were used as input to a suite of rainfall runoff models, trained to represent the hydrological behaviour of each catchment, for the coming century. In maintaining the priority of quantifying uncertainty in future projections the uncertainty derived from the use of different rainfall-

runoff models and the parameter uncertainties that emerge in applying the models were quantified. Three future time periods, of thirty years duration, were employed for the analysis of future changes in catchment hydrology; the 2020s (2010-39), the 2050s (2040-69) and the 2080s (2070-99). Changes in the monthly flow regime, the frequency and duration of low flow events and the frequency of flood events for each future period were calculated relative to the simulated control (or reference) period of 1961-1990. Natural variability in the hydrological regime of each sub-catchment was also quantified to assess the significance of future changes driven by climate change.

5.3 Catchments and Datasets

5.3.1 Catchments Modelled

This study was undertaken on five sub-catchments which comprise part of the greater Burrishoole catchment system (84 km2). In addition, the Glendahurk, a much smaller catchment system which borders the Burrishoole catchment to the west, was also considered. Figure 5.1 outlines the catchments modelled and their key characteristics. The Burrishoole catchment itself lies in a North-South direction at the Northeast corner of Clew Bay where it drains into the Atlantic. The catchment is located at the heart of the Nephin Beg Mountain.

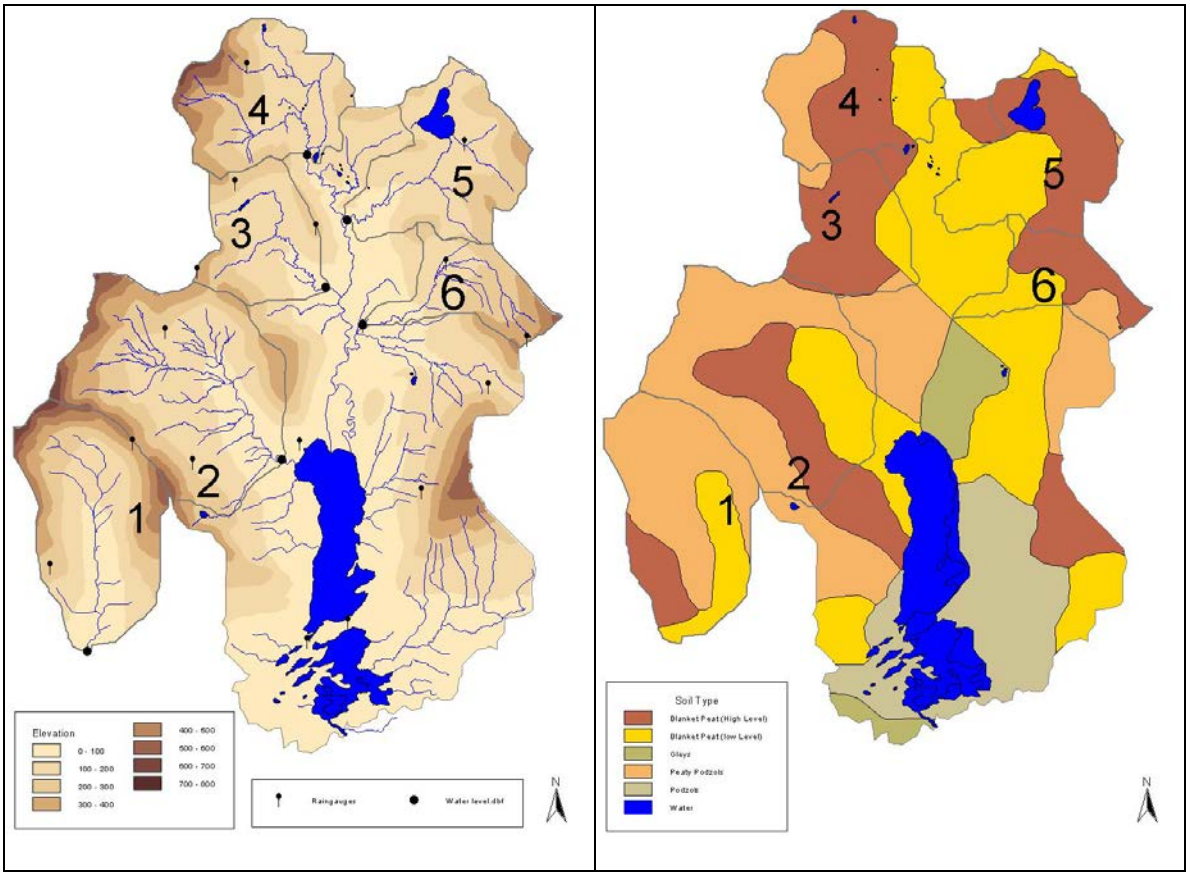

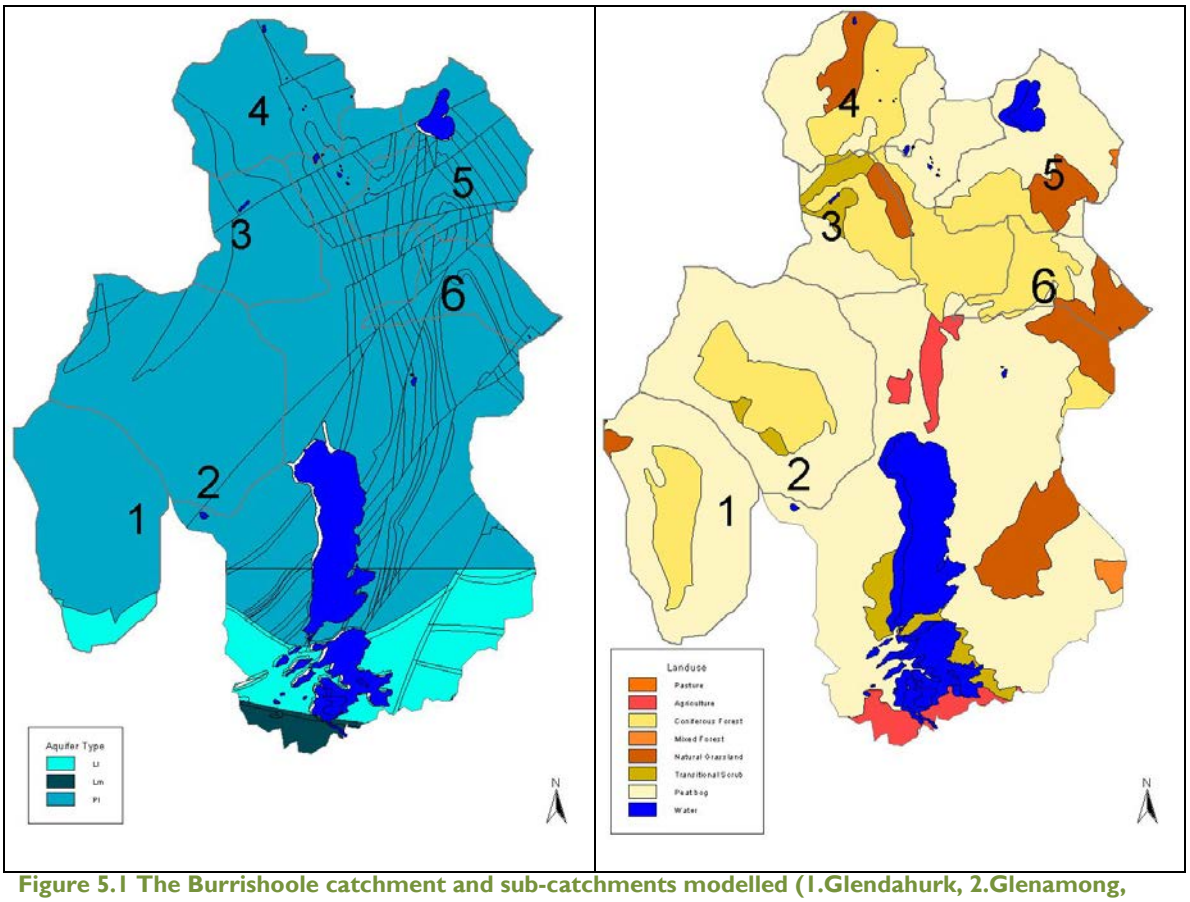

Figure 5.1 The Burrishoole catchment and sub-catchments modelled (1.Glendahurk, 2.Glenamong, 3.Maumaratta, 4.Altahoney, 5.Goulan, 6.Srahrevagh). Maps represent catchment elevation and the location of river level and precipitation gauges (top left), soil type (top right), aquifer type (bottom left) and landuse (bottom right).

Range and takes on an amphitheatre like shape with steep slopes to the north, west and east delineating the drainage boundary. The surrounding terrain is complex being characterised by localised valleys, steeply sloping mountain ranges and rapid changes in elevation. The altitudinal range for the catchment spans 700 metres, from 10m at the outlet point to 710m at the highest peak on the contributing upland areas. The Burrishoole system includes three main lakes, the brackish Lough Furnace (1.41 km2) as well as Loughs Feeagh (4.1 km2) and Bunaveela (0.54 km2), both of which are freshwater lakes. Lough Furnace and Lough Feeagh are situated in the lower part of the Burrishoole valley whilst Bunaveela is located in the upper reaches of the Goulan sub-catchment. The catchment system has a dense drainage network comprised of at least 70 km of rivers and streams (Poole, 1994).

The five main constituent sub-catchments of the Burrishoole system were selected for analysis in this study. Included were the Glenamong, Maurmatta and Altahoney located in the west and north-west parts of the catchment. Also selected were the Goulan and Srahrevagh sub-catchments situated in the north-eastern and eastern parts of the catchment. Each of these catchment systems, either directly or through the drainage network, feed into the two lakes situated on the valley floor. The additional catchment considered (Glendahurk) lies adjacent to

the Glenamong sub-catchment and is a completely independent system, forming a tributary of the Owengarve River which flows directly into Clew Bay.

Each catchment displays relatively similar properties in terms of their land cover, soil type, groundwater capacity and morphometric attributes (e.g. basin slope, area and shape). Of each catchment considered the Glenamong, with an area of 17.2 km2, is the largest followed by the Glendahurk (12.42 km2). The smallest catchment is the Srahrevagh which has an area of just 4.9 km2. Coniferous forests (20-45% coverage) and blanket peat bogs (40-60%) are the dominant land cover across each catchment system with small areas of natural grassland (10-20%) and transitional scrubland present (Corine, 2003). The entire area is underlain by unproductive bedrock and consequently each catchment has a relatively poor groundwater storage and transmissive capacity (GSI, 2003). The overlying soils mainly consist of blanket peat and peaty podzols (Gardiner and Radford, 1980). Peat is overwhelmingly dominant in all catchments, especially in those situated in the upper reaches of Burrishoole including the Altahoney (80% coverage), Goulan (100%) and Srahrevagh (90%) sub-catchments. The Glenamong (70%) and Glendahurk (75%) are also notable for a high proportion of blanket peat coverage. Tables 5.1 - 5.4 describe the physical attributes of each catchment including percent landuse (Table 5.1), aquifer (Table 5.2) and soil type coverage (Table 5.3) along with their respective geometric properties (Table 5.4).

Table 5.1 Percent coverage of Corine classified landuse in each sub catchment modelled.

Corine Land Cover Classification							
Code	**Classification**	**Catchment**					
		Glendahurk	**Glenamong**	**Maurmatta**	**Altahoney**	**Goulan**	**Srahrevagh**
312	Coniferous Forest	40	30	40	45	20	45
412	Blanket Bog	60	60	40	35	60	45
321	Natural Grassland		10	10	20	20	10
324	Transitional woodland scrub			10			

Table 5.2 Percent coverage of aquifer category in each sub catchment modelled.

Aquifer Classification							
Code	**Classification**	**Catchment**					
		Glendahurk	**Glenamong**	**Maurmatta**	**Altahoney**	**Goulan**	**Srahrevagh**
PL	Poor aquifer, generally unproductive except in local zones	90	100	100	100	100	100
Ll	Locally important, generally moderatively productive in local zones	10					

Table 5.3 Percent coverage of soil type in each sub catchment modelled.

Soil Type						
Classification	**Catchment**					
	Glendahurk	**Glenamong**	**Maurmatta**	**Altahoney**	**Goulan**	**Srahrevagh**
Blanket Peat	75	70	90	80	100	90
Peaty Podzols	25	30	10	20		10

Table 5.4 Geometric characteristics of each sub catchment modelled.

Geometric Properties						
Attribute	**Catchment**					
	Glendahurk	**Glenamong**	**Maumaratta**	**Altahoney**	**Goulan**	**Srahrevagh**
Area (km2)	12.4	17.1	6.4	9.2	9.6	4.9
Min Elevation (m)	47	12	54	94	59	23
Max Elevation (m)	710	708	383	626	389	550
Slope (°)	14	12	10	13	8.8	9

All of the selected catchments have a flow regime which is highly responsive to rainfall and exhibit behavior which is typically associated with runoff dominated systems. This is related to the geometric properties of each catchments drainage basin (e.g. steep slope, small area), and the low storage capacity of the underlying geology. Both these factors contribute to each catchments inability to attenuate the rapid movement of water through the catchment system or dampen the streamflow response to high precipitation events. The low contribution of baseflow to catchment discharge, especially during drier summer months, underlines the deficiency in groundwater capacity across all catchments. Streamflow records for two of the selected catchments showed that they had completely dried up on at least one occasion after a sustained period without rainfall. The presence of blanket peatland plays a significant role in shaping the hydrology of each catchment. It has been shown that well developed macropores and pipes which exist in the peat matrix provide an effective conduit for rapid subsurface flow. Peat covered hillslopes give rise to optimum conditions for overland flow during a storm event. Both these factors contribute to the flashy nature of storm runoff from peat dominated catchments such as those included in this study (Holden and Burt, 2003).

5.3.2 Observed Datasets

Historical records of streamflow and precipitation were taken from instrumental stations located at various points across the study area. River levels are recorded at the outlet for each catchment on a 15 minute interval time step. Average daily volumetric flow values were derived from recorded water levels using a rating curve calculated for each gauging point. Observed streamflow datasets were of varying lengths and quality with some displaying

evidence of disruption subsequent to extreme events. Table 5.5 provides some details of the streamflow records for each catchment.

Table 5.5 Data statistics for river flow record at each gauging point

Catchment	Record Start Date	Record End Date	Data (days)	Missing n (%)	Mean Daily (m3/sec)	Std. Dev (m3/sec)	95 % ile (m3/sec)
Glenamong	Jun-02	Aug-09	2398	10.1	0.928	1.172	3.258
Maumaratta	Jun-02	Aug-09	2392	10.3	0.460	0.662	1.492
Altahoney	May-02	Aug-09	2546	3.7	0.597	0.890	2.342
Srahrevagh	Jun-02	Aug-09	2419	9.3	0.320	1.848	1.032
Goulan	Apr-03	May-06	1096	5.3	0.337	0.384	1.108
Glendahurk	Jun-02	Aug-09	2125	20.4	0.183	0.290	0.714

An extensive upland rain gauge network traverses the study region with multiple gauging stations being located in each catchment. Precipitation datasets used in this study were obtained from each of these recording points. Historical records of daily precipitation were also obtained from the Millrace climatological station located close to the outlet of the Burrishoole catchment. The observed rainfall series for this station is considerably longer (1961- 2009) than those provided by the more recently established gauging points in the upper reaches of the catchment.

Owing to the complexity of the local terrain (e.g. elevation, slope, aspect) the precipitation regime varies considerably across the catchment system. For each catchment considered a weighted average rainfall series, derived using precipitation records from gauges located close to or within each catchment boundary, were employed during model development. This allowed the spatial distribution of rainfall across each catchment to be considered and addressed the problematic issue of missing values in individual datasets. Only those rainfall records which exhibited a high correlation with streamflow for a given catchment were selected. For calculation of the averaged time-series, each of the individual rainfall records considered were weighted according to the correlation they had with streamflow. Observed records for potential evaporation were obtained from the Belmullet synoptic station located north-west of the catchment. This station is operated by the Irish meteorological service Met Eireann. Table 5.6 provides statistics for the precipitation records available for use in this study.

Table 5.6 Data statistics for precipitation record at each gauging point

Precipitation Gauging Station	Record Date Start	Data (days)	Missing n (%)	Mean (mm/day)	Median (mm/day)	Std. Dev (mm/day)	95 % ile (mm/day)
Glenamong 1	May-02	1510	43.4	4.8	2.2	7.6	18.2
Glenamong 2	May-02	2397	10.2	5.4	3.0	7.7	20.4
Glenamong 3	May-02	2535	5.0	5.1	2.0	7.7	20.4
Glenamong 4	Jul-03	1925	14.4	6.5	2.6	9.4	24.7
Maumaratta	May-02	2083	21.9	5.2	2.2	7.3	20.8
Altahoney	May-02	1903	28.7	6.3	2.2	10.4	25.2
Srahrevagh 1	May-02	2505	6.1	4.4	1.6	6.9	18.8
Srahrevagh 2	May-02	2224	16.6	4.0	1.8	5.6	15.4
Srahrevagh 3	May-02	2233	16.3	4.8	1.8	7.0	19.3
Goulan	May-02	2492	6.6	5.1	2.0	7.6	20.1
Namaroon	Jan-04	1848	10.5	6.6	3.2	8.7	24.3
Glendahurk	Jun-03	1676	26.5	4.9	2.2	6.6	17.4
Millrace	Jan-61	17696	0.4	4.3	1.8	6.2	16.6

5.3.3 Future Climate Scenarios

To examine the impacts of climate change on each catchment's hydrological regime point scale estimates of precipitation and potential evaporation, for the full period 1961-2099, were derived from large-scale GCM output using statistical downscaling techniques as discussed in Chapter 4. In order to address the various factors which contribute to uncertainty in climate projections (e.g. emission scenarios, GCM structure, parameterisations and climate sensitivities) the output from three GCMs, each run using two different SRES emission scenarios (the medium-high (A2) and medium-low (B2)) were used as the input data for the downscaled series. The GCMs considered included: HadCM3 from the Hadley Centre for Climate Prediction and Research (Met Office, UK); CCGCM2, from the Canadian Centre for Climate Modelling and Analysis (CCCMA; Canada) and CSIRO-Mk2 from the Commonwealth Science and Industrial Research Organisation (CSIRO, Australia). The limitations associated with statistical downscaling represent an additional source of uncertainty in estimates of local climate change. To address this both Generalised Linear Models (GLMs) and a statistical downscaling software package (SDSM) were used to develop climate scenarios for the catchment.

The GLM approach was used only to downscale precipitation whilst SDSM was employed to produce downscaled scenarios for both precipitation and potential evaporation (PE). The GLM is a fully deterministic method and as such only one downscaled rainfall series was produced from each GCM and emission scenario. SDSM is also a regression based downscaling method;

however it incorporates an additional stochastic component which allows multiple synthetic series or realisations of future weather data to be produced using a common GCM predictor set. Each individual realisation exhibits a different time-series evolution but has the same overall statistical properties. The integration of this weather generator type module allows new temporal sequences of extreme events to be generated for future climate assessment (Diaz Nieto and Wilby, 2005) and represents an attempt to capture the 'chaotic' nature, or natural variability, of local weather conditions in the predicted series. Using SDSM an ensemble of one hundred individual sequences of daily precipitation and evaporation data for the period 1961-2099 were generated using grid-scale climate projections from each of the aforementioned GCMs. In order to assess the impacts of projected climate change on the river flow regime of each sub catchment each ensemble member, along with the deterministic scenario derived from the GLM, were used as input data for hydrological models.

5.4 Estimation of Natural Climate Variability for Baseline Conditions

Natural climate variability refers to natural fluctuations within the climate system that occur across a range of time scales from daily to multi-decadal and spatially from the regional to global scale. While a number of authors have related changes in climate variability to changes in observed records, very few have compared the effect of natural multi-decadal climate variability with human induced climate change over the coming century. Arnell (2003) conducted such as assessment for simulated changes in river flows in the UK by using climate projections from the HadCM2 model assuming no change in greenhouse gas concentrations and concluded that even by the 2050s streamflow in some seasons will be well within the range of multi-decadal climate variability, especially in groundwater dominated catchments. Furthermore, when the effects of anthropogenic climate change and natural variability are combined, the range of possible future changes increases substantially (Arnell, 2003). More recently, Prudhomme and Davies (2009) estimated natural climate variability by running a hydrological model with rainfall and PE series resampled, using block resampling from observations. Results derived by Prudhomme and Davies (2009) found that only half of the changes projected are significant within the estimated natural variability of the observed flow regime.

In estimating natural variability for the catchments modelled, a procedure similar to that of Prudhomme and Davies (2009) was employed. Given the short length of observed records in the catchments, NCEP reanalysis data was used to estimate the ranges of natural variability using an ensemble of 100 synthetic precipitation series. Each series generated was long enough

to span the period 1961-1990 as this represents the standard baseline used in climate impact assessments. The scenarios derived from grid-scale NCEP data were downscaled to the Millrace station. In order to translate this downscaled dataset to each study catchment Quantile mapping was applied. The translated NCEP dataset for each catchment was then used to calculate the natural variability of their flow regime under 'current' climate conditions. Quantile mapping is discussed below in section 5.5.

To construct each synthetic series the NCEP precipitation data was split on a seasonal basis into four sub-series (winter, spring summer and autumn). Each sub-series consisted of a sequence of 'blocks' representing observed daily values for a three month period (e.g. DJF). Resampling was carried out on a seasonal rather than monthly basis in order to preserve the annual precipitation cycle and avoid any unrealistic alteration in the catchments water budget. Individual series were generated by selecting at random one block from each of the four seasonal sub-series, respecting their sequential order (e.g. a spring block is selected after a winter block). Each seasonal block was selected independently from the preceding one to ensure that two consecutive blocks were not selected from the same year in which they were recorded. Once sampled the data was returned to the sampling pool which allowed the same block to be sampled repeatedly. This ensured that low frequency events could be represented in the same synthetic series multiple times. A rainfall runoff model (HYSIM) was used to simulate the runoff generated by each resampled member. Observed potential evaporation at Belmullet for the period 1961-1990 was used in each model run. This input variable was not resampled as it displays a strong annual cycle and exhibits little interannual variability. The combined output from all models and ensemble members provides some measure of natural variability under reference climate conditions.

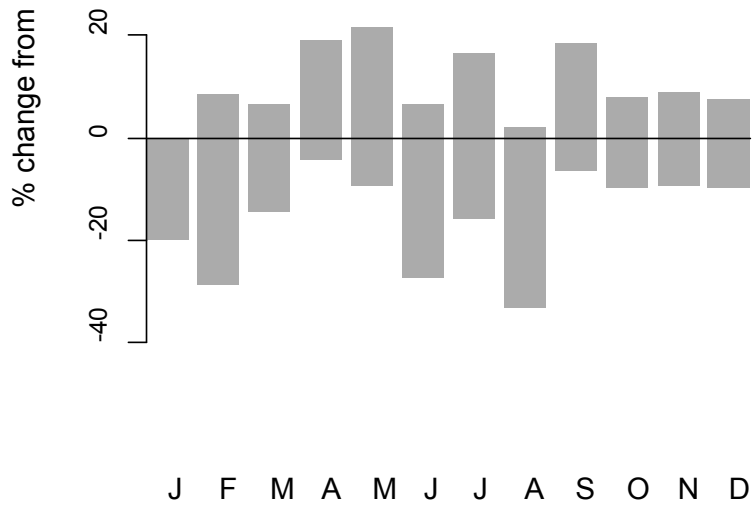

Figure 5.2 Natural variability bounds for the Glenamong catchment constructed through resampling of NCEP data.

Ranges for natural variability for the Glenamong catchment are shown in Figure 5.2. For most months the estimated ranges of natural variability are within plus or minus 20 percent of the 1961-1990 monthly averages. The largest bounds are evident for February, June and August, in excess of 30 percent deviation from the long term mean. Such a large range of natural variability in the flow regime is representative of the flashy response of the catchment and are consistent with ranges derived for UK catchments by Prudhomme and Davies (2009).

The natural variability ranges produced for each catchment were employed to assess the significance of future changes in the monthly flow regime for each future time period. Future changes due to climate change are only defined as significant if at least 75% of all ensemble member simulations are outside of the 90% confidence interval of the natural variability range of the reference period 1961-1990. Future changes within the range of natural variability of the baseline climate cannot be attributed to anthropogenic climate change. This is line with the approach advanced by Prudhomme and Davies (2009), who highlight that adopting the threshold of 75% is a practical choice that can be compared to 68% of values that fall within plus or minus one standard deviation around the mean and 16% of values below or above one standard deviation from the mean for a normal distribution.

5.5 Quantile Mapping of Climate Scenarios

When developing the hydrological model for each catchment, model simulations which used weighted average rainfall as their input data displayed far superior efficiency scores when compared to model runs which employed the observed precipitation record from the Millrace climatological station. This is due to the localised nature of the rainfall regime across the study area - which is to a large extent driven by the complex terrain and the strong influence of topographical features (e.g. elevation, slope, aspect). Thus, precipitation receipts at the Millrace station do not fully reflect the spatial variability of rainfall across upland areas. Ideally future precipitation scenarios would have been downscaled for each individual catchment with the aim of capturing locally specific conditions. However, due to the short records available for upland gauging points, precipitation scenarios could not be downscaled directly to these sites. Instead it was only possible to downscale rainfall scenarios to the Millrace station, for which records of the required length were available to develop downscaling models. To overcome this, quantile mapping was used to construct precipitation scenarios for each sub catchment using the point-scale precipitation datasets downscaled to the Millrace station outlined in Chapter 4.

5.6 Hydrological Modelling

5.6.1 Uncertainty in Hydrological Models

In order to translate future climate scenarios into hydrological simulations different hydrological modelling approaches were employed. Conceptual rainfall-runoff (CRR) models have been the most widely used for climate impact assessment (Cunnane and Regan, 1994; Arnell and Reynard, 1996; Sefton and Boorman, 1997; Pilling and Jones, 1999; Arnell, 2003; Charlton and Moore, 2003; Wilby, 2005; Murphy et al., 2006; Murphy and Charlton 2008; Steel Dunne et al., 2008; Prudhomme and Davies 2009). Central to the use of CRR models in climate impact assessment is their ability to characterise the catchment system as a simplified agglomeration of stores representing catchment processes, enabling such models to be applied to a wide variety of catchments in different climates. CRR models also tend to contain a small number of parameters, many of which can be measured from physical reality, while the lumped nature of such models only require parameter values on a catchment or sub-catchment scale. Consequently, simple model structures, non-linear representations of the hydrological system as well as the ability to simulate the movement and storage of water in soils have led to the widespread use of CRR models in climate impact assessment. Despite their wide application CRR models are associated with considerable uncertainty due to their simplified structure and varying degrees of complexity. Broadly speaking there are three principal sources of uncertainty in hydrological models; errors associated with input data and data for calibration, imperfection in the model structure and uncertainty in model parameters (Jin et al., 2009).

Due to their conceptual nature CRR models only reflect a particular interpretation or simplification of the hydrological system, with for example, different system processes and components being omitted, added or given a different weighting in the model structure. As a consequence not all models are the same and although they may provide an adequate representation of the system over the observed fitting period, under the same future climate forcing scenario their projections may diverge significantly. Refsgaard et al. (2006) state that although model structure is one of the key sources of uncertainty in model projections it is frequently neglected and no generic methodology exists with which to address it. They highlight the use of a scenario based approach where a number of alternative conceptual models are considered. For each of these, the model input and parameter uncertainties are considered, following from this the differences between model simulations can then be used as a measure of the uncertainty attributable to model structure. This multi-model approach has previously been applied in a flood forecasting context. Butts et al. (1993) used 10 different models to assess the uncertainty in flood projections arising from model structure. Their study suggested that exploring an ensemble of model structures provides a valuable method with

which to address this aspect of model uncertainty. Marshall et al. (2007) reiterate this point stating that the uncertainty arising from model structure requires developing alternatives, where the output from multiple models are combined to produce an ensemble of model simulations, the range of which provides some estimate of model structure uncertainty. The strategy of applying several alternative models, or at least the same model with a different internal set-up or architecture, is already common practice in climate modelling. Uhlenbrook et al. (1993) previously assessed the uncertainties arising from different model structures in the context of the HBV CRR model. Their study demonstrated that it is possible to obtain good efficiency scores using model structures which represent both sensible and incorrect conceptualisations of a given catchment system. This alludes to the compensatory role parameter estimates can play in concealing a poor representation of the true system in the model structure.

Addressing model uncertainty is an important aspect of climate impacts assessment and in the context of this study was considered by employing two different modelling strategies. The first employed HYSIM, a CRR model which has previously been used in the field of climate impacts analysis. The second modelling strategy implemented was based on the use of Artificial Neural Networks (ANNs). To assess model uncertainty previous studies have used the results from several different hydrological models to produce a range of equally plausible streamflow projections. The level of agreement exhibited between different models provides some indication of model uncertainty. In this study the two selected modelling techniques were firstly applied to a single catchment to determine the magnitude of inter-model uncertainty and following from this, whether the application of both models to each of the remaining catchments was necessary. The Glenamong catchment was selected as the study catchment for this analysis. To assess the relative skill of each method under observed conditions both were used to simulate streamflow for the same validation and calibration periods. In addition the agreement shown between the future simulations from each model under the same climate forcing scenario were examined.

A second key source of uncertainty associated with CRR models is that due to limitations associated with the definition of model parameters, with such models commonly associated with issues of parameter stability, parameter identifiability and equifinality, each of which gives rise to uncertainty in model output. Wilby (2006) shows that uncertainty in future flow changes due to equifinality is comparable in magnitude to the uncertainty in emissions scenario. In this study the uncertainty associated with parameter identifiability is addressed using the

Generalized Likelihood Uncertainty Estimation (GLUE) procedure. This is discussed below in the context of the CRR model employed.

5.6.2 HYSIM: a Conceptual Rainfall- Runoff Model

HYSIM (Manley, 1993) is a lumped CRR model, which uses rainfall and potential evaporation data to simulate river flow using parameters for hydrology and hydraulics that define the river basin and channels in a realistic way. HYSIM was chosen for use in this study for a number of reasons, firstly many of its parameters are physically based. Of the 17 parameters which must be set in the model most are relatable to readily measurable basin characteristics. Such a model is likely to perform well under climactic conditions more extreme than those on which it has been calibrated. The lumped nature of HYSIM was also commensurate with the relatively homogenous conditions across each catchment (e.g. soil type, geology). Furthermore the model was shown to perform well in the presence of complicating factors such the presence of peatlands and the 'flashy' nature of the selected catchments.

The model is built around two sub-routines; the first of these simulates catchment hydrology while the second simulates channel hydraulics. A complete overview of the parameters included in the model and the linkages between stores are given in Figure 5.3 below. In relation to the hydrology routine seven natural stores are represented. These include snow storage (not implemented), interception storage, from which evaporation takes place at the potential rate, the upper soil horizon, the lower soil horizon, transitional groundwater, groundwater and minor channel storage. Interception storage represents the storage of moisture by the vegetation canopy. Evaporation accounts for losses from this store. Any moisture in excess of storage, determined by vegetation type, is passed on to the upper soil horizon. The upper soil horizon represents the moisture held in the upper (A) horizon or topsoil and has a finite storage capacity equal to the depth of the A horizon multiplied by its porosity. A limit on the rate at which moisture can enter the upper soil store is applied based on its potential infiltration rate. Losses are met by evaporation, interflow and percolation to the lower soil horizon. Evaporation is controlled by the forces of capillary suction, while interflow is a function of the effective horizontal permeability of the soil layer. The lower soil horizon represents moisture below the upper horizon but still within the rooting depth of vegetation. Again evaporation and interflow account for losses from this store as well as percolation to groundwater.

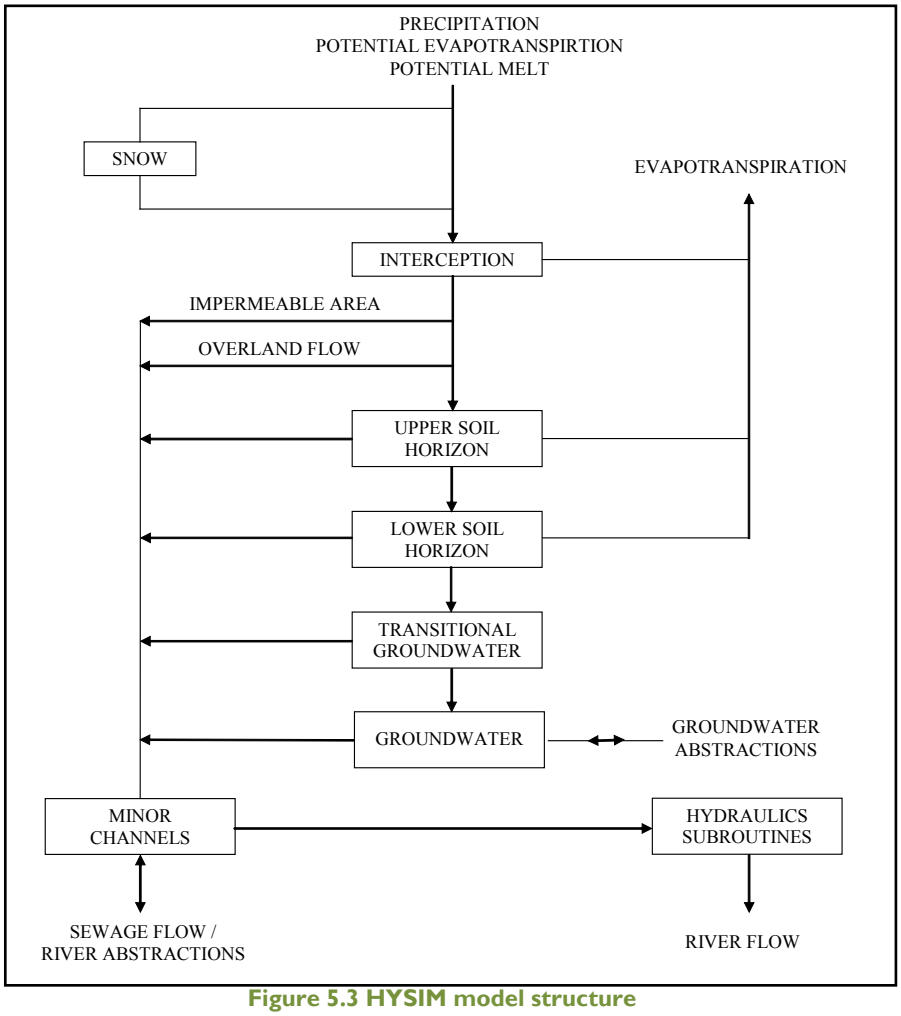

Figure 5.3 HYSIM model structure

The transitional groundwater store is an infinite linear reservoir, which serves to represent the first stage of groundwater storage. This store has greatest importance in catchments with permeable geologies where many of the fissures and fractures holding moisture may interact with the stream channel rather than with deeper groundwater. Losses from this store are controlled by a discharge coefficient and by the proportion of the moisture leaving storage that enters the river channel. Groundwater is also represented as an infinite linear reservoir. The final conceptual store represented by HYSIM is minor channel storage. This component represents the routing of flows in minor streams and ditches.

One of the defining features of CRR models is that a number of their parameters are not physically measurable and must be calibrated using some form of manual or automatic optimization procedure. Model calibration involves iteratively altering the models effective parameter values with the aim of minimising deviations between model simulations and observed streamflow from the selected catchment. These parameters represent important physical processes in the catchments hydrology but the requirement for them to be optimised

in order to fit the model may result in parameter estimates which bear no semblance to their true value in the field.

Many CRR models incorporate an optimisation algorithm which searches the n-dimensional parameter space for global optimum set of parameter values defined using some measure of model efficiency. For the purposes of model calibration HYSIM employs the Rosenbrock algorithm in conjunction with a number of objective functions. While in theory an optimum parameter set may exist, finding this point presents difficulties given the complexities of the response surface as well as the limitations of search algorithms and the differing efficiency criteria of objective functions. Sorooshian and Gupta (1995) highlight a number of difficulties associated with the parameter response surface which are common to CRR models. These include the presence of several major regions of attraction into which the search algorithm may converge and the existence of multiple local optima on the response surface. Furthermore where parameters exhibit varying degrees of sensitivity a great deal of interaction and compensation may be evident. The problems associated with determining a global optimum parameter set gives rise to uncertainties in model simulations.

The idea that one optimum model or parameter set exists has been challenged by the concept of 'equifinality' (Beven, 2007); that multiple parameter sets can be found, perhaps in very different regions of the response surface, all of which provide equally good performance scores (Duan et al., 1992; Freer et al., 1996). The concept also applies to different model structures. Essentially the theory suggests that there may be many representations of a catchment, consisting of numerous combinations of model structures and parameter values, which are equally valid in terms of their ability to provide acceptable simulations of the observed streamflow series. Conversely it has been shown that different parameter sets, all of which give comparable results during calibration, may yield significantly different results under forcing conditions on which the model has not been trained (Harlin and Kung, 1992). This demonstrates the uncertainty associated with model projections which arise from parameter uncertainty.

5.6.3 Artificial Neural Networks

This empirical approach to rainfall-runoff modelling is based solely on the inputs (precipitation and past discharge measurements) and outputs (current or future discharge) of a catchment system without any consideration given to the physical properties of the catchment itself. Essentially the catchment is treated as a 'black box' system, without any explicit consideration given to the internal processes and storage components which control how streamflow is

generated from rainfall. Despite omitting any representation of the internal physics of the catchment system, the ability of ANNs to model complex and highly dynamic non-linear systems mean they have gained popularity in the field of hydrological modelling. Given the responsive nature of each study catchment, underlined by the high correlation shown between daily rainfall and streamflow records, neural networks were thought to provide an adequate means of modelling the rainfall-runoff relationship.

The collective behaviour of an ANN, like the biological neural system on which it is based, demonstrates the ability to learn, recall and generalise from training patterns and experienced data. Neural networks are organised as layers of parallel processing nodes called neurons which are the basic elements of the network and make up its underlying structure. The set of neurons in each layer are connected via a series of weighting functions to all the neurons in the proceeding layer. The action of each neuron is to calculate a response based on the weighted sum of its inputs using a predetermined activation function. In order to learn the relationship between the input and target variables the network must undergo a training process. During this the connection weights are iteratively adjusted until the predicted network output best matches the observed system output. At this point the network is said to have learned the relationship between the input and output training datasets. The exact nature of the relationship cannot be extracted from the neural network but is rather contained in the optimised weighting values and connections between nodes. In this context ANNs can be considered as the 'ultimate black box model' (Minns and Hall, 1996). Two types of neural networks, a feedforward (static) network and a dynamic network, were assessed to determine their suitability for this study. The former is determined solely by the input-output pattern and has no feedback elements or time delays. Conversely using dynamic networks the model output depends not only on the current input but also on the previous inputs, outputs, or states of the network. Using dynamic networks allows information on antecedent conditions in the catchment, relating to both precipitation and flow levels, to be incorporated in the model. This is an important consideration given the significant influence preceding conditions can have on high flow and flooding events.

5.6.4 Training and Validating Models

HYSIM training and validation

Parameters within HYSIM can be divided into two categories; the physically based parameters and process or free parameters. The physical parameters for each study catchment were derived using GIS (Geographical Information System) mapping software. The use of GIS ensures that the information required by the model is objectively defined and grounded in

physically reality - thereby reducing the uncertainty associated with parameter estimates. The first task was the delineation of each catchment boundary using the Environmental Protections Agency's (EPA) Digital Elevation Model (DEM) (Smith, 2005). Digital terrain analysis tools specifically for the purposes of deriving watershed characteristics are available to supplement basic GIS tools and were employed in this study. Soil hydrological properties for each catchment were derived from the General Soil Map of Ireland (Gardiner and Radford, 1980). The soil association for each catchment was subsequently determined using information from the soils map. The dominant soil texture was calculated by establishing the percentage sand, silt and clay in each soil association with the derived texture being used to calculate the models soil parameters. So that the hydrological significance of different soils was given proper consideration in the model the proportions of each soil as well as its location within the catchment were taken into account when setting the parameter values. Vegetation parameters were obtained using the CORINE land-cover (Coordination of Information on the Environment) dataset (O'Sullivan, 1994). Owing to the lumped nature of the model the land-use type shown to be dominant in each catchment were used to define the land-use parameters. Finally the groundwater parameters were derived using an analysis of flow records and an examination of the underlying groundwater properties for each catchment taken from the Aquifer Map of Ireland (GSI, 2003).

In contrast, the process parameters are derived by minimising the difference between observed and simulated flows using a local search technique. To address parameter uncertainty and to negate the problems associated with determining a single optimum parameter set, the Generalised Likelihood Uncertainty Estimation (GLUE) procedure, a methodology based on the equifinality of parameter sets, was implemented in this study (Beven and Binley, 1992). GLUE is a well established method for uncertainty analysis and has been widely applied in the field of hydrological modelling (e.g. Beven and Binley, 1992; Beven, 1993; Freer, 1999; Cameron et al., 1999; Blazkova and Beven, 2002; Montanari, 2005, 2007).

The underlying principle of the GLUE procedure is that many 'behavioural' parameter sets exist and consequently it is only possible to assign a likelihood value to each one indicating whether it can adequately replicate the system and provide an acceptable or behavioural simulation of the observed flow (Beven and Binley, 1992). This method facilitates the assessment of parameter uncertainty by allowing probability bounds or confidence limits to be constructed based on the distribution of the combined model projections derived from each plausible parameter set. This approach to model calibration also has the advantage of allowing

the interaction between parameters to be implicitly accounted for as whole parameter sets are varied rather than varying individual parameters.

The GLUE procedure has the five main steps (Beven and Binley, 1992):

1. The definition of a likelihood measure, chosen on the basis of an objective function to determine model performance
2. The definition of a prior distribution for each parameter
3. Parameter sets are sampled from the defined prior distributions using sampling techniques such as Monte Carlo Random Sampling and Latin Hypercube Sampling
4. Each parameter set is classified as behavioural or non-behavioural through assessing whether it performs above or below a specified threshold
5. Predictive model runs generate results from each of the parameter sets that yield acceptable calibration simulations. These combined simulations are in turn used to determine the weighted mean discharge and simulation probability bounds (Melching, 1995)

For this study the GLUE procedure was employed as part of the modelling strategy for each catchment. Before the procedure was implemented a sensitivity analysis was firstly undertaken. Essentially this type of analysis is used to determine the sensitivity of the model output to changes in a given parameter. The results from this highlighted those parameters which had the greatest influence on the model response and as such warranted inclusion in the GLUE procedure. By drawing attention to those parameters which are poorly identified in the model structure the sensitivity analysis allows for a more efficient and effective calibration process.

For the purposes of this study a regional sensitivity analysis (RSA) was employed (e.g. Hornberger and Spear, 1981; Young, 1983; Beck, 1987). This method provides a measure of the absolute sensitivity of the model parameters and gives some indication of the level of interaction between them. The technique employs a Monte Carlo simulation procedure to run the model with randomly generated parameter sets. Visual inspection of the resulting 2-D dotty plots was used to determine the most sensitive parameters. Those which were well defined in the model structure produced the best efficiency scores within a narrow parameter range, for those which were relatively insensitive good simulations were produced using values sampled right across the parameter space. Based on the results of the sensitivity analysis the models four process parameters, as well as the parameters representing groundwater recession and the pore size distribution index, were selected for inclusion in the GLUE

procedure. Table 5.7 lists the parameters selected and their initial ranges for Monte Carlo sampling.

Table 5.7 HYSIM parameters included in GLUE analysis and initial parameter bounds sampled

Parameter	Minimum Value	Maximum Value
Saturated Permeability at the Horizon Boundary	1	250
Saturated Permeability at the Base of the Lower Horizon	1	250
Interflow Run-off from the Upper Horizon at Saturation	1	250
Interflow Run-off from the Lower Horizon at Saturation	1	250
Groundwater Recession	0.05	0.99
Pore Size Distribution Index (PSDI)	500	6000

The likelihood measure adopted for all catchments was the Nash Sutcliffe efficiency criterion:

$$1 - \frac{\sum(R_i - S_i)^2}{\sum(R_i - \bar{R}_i)^2}$$

Equation 5.1

where,

R represents recorded streamflow,

S is simulated streamflow, and

$\bar{R}$ is the mean of the recorded flows.

Based on this, parameter sets which attained a score above 0.7 over the calibration and validation period were considered to be behavioural. For the purposes of generating random parameter sets, the ranges used to delineate the sampling space had to be specified. This process was informed using a sensitivity analysis and empirical testing of possible parameter bounds. Care was taken to ensure that an adequate region of the parameter space was considered where behavioural sets were shown to exist. Using a Monte Carlo random sampling strategy 10,000 parameters sets were generated from a uniform distribution within the given ranges for each parameter. HYSIM was run using each randomly generated parameter set over the calibration period. Due to the differing lengths of observed precipitation and streamflow data which were available different calibration and validation periods were selected for each catchment (Table 5.8). All those parameters which met the required efficiency score over the calibration period were retained. In order to validate these parameter sets a blind simulation was conducted on each set for the validation period. The 20 best performing behavioural parameter sets over this period were considered to provide equally plausible representations of the catchment and used in the climate impact analysis presented in the following sections.

Table 5.8 Calibration and validation periods for each catchment and the max and min efficiency scores obtained

Catchment	Calibration	Max	Mean	Validation	Max	Mean
Altahoney	10/2002 - 6/2007	0.74	0.73	07/2007 - 07/2009	0.75	0.73
Goulan	10/2002 - 5/2007	0.76	0.72	06/2005 - 05/2006	0.76	0.72
Srahrevagh	10/2002 - 7/2007	0.75	0.72	09/2007 - 08/2009	0.71	0.70
Glendahurk	06/2003 - 3/2007	0.72	0.71	04/2007 - 07/2009	0.72	0.72
Glenamong	07/2002 - 3/2007	0.84	0.78	04/2007 - 04/2009	0.78	0.71
Maumaratta	07/2002 - 3/2007	0.66	0.64	04/2007 - 04/2009	0.65	0.62

ANN Training and Validation

In the present study a two-layer feed-forward network, comprised of a hidden layer with ten nodes and an output layer with single node, was used to predict catchment discharge on a daily time step taking precipitation and PE as the model inputs. The tan-sigmoid function was used as the hidden nodes activation function whilst a linear function was applied to the output node. A trial and error method was used to select the optimum number of hidden nodes. The network was trained over the calibration period (Table 5.8) using the scaled conjugate gradient backpropagation algorithm.

The use of dynamic networks is an attempt to capture the dynamic nature of the hydrological system and has the advantage of allowing 'memory' to be built into the model. To determine an optimum model structure a number of different dynamic networks were tested. This included networks with various time delays on their input and feedback connections. The use of delayed inputs allows rainfall at both current and previous time intervals to be considered as contributors to catchment discharge. Preliminary work by Hall and Minn (1993) indicated that the number of antecedent rainfall ordinates required was broadly related to the lag time of the drainage area, reflecting the time differential in the routing of precipitation from different areas of the catchment to its outlet point. Incorporating a feedback mechanism (i.e. the use of an output variable as a model input) in the model structure allows river levels from the preceding days to be considered when determining catchment discharge on a given day. Past studies have used runoff from previous time steps as one of the inputs to the model in order to represent conditions in the catchment (e.g. soil moisture). This may be important given the role catchment conditions play in determining runoff behaviour. The common underlying structure used for each dynamic network, including the number of layers and activation functions used, followed that outlined for the feed-forward network. In addition the same training algorithm was used.

Table 5.9 outlines the various dynamic network configurations considered. Also listed is the percent explained variance (R^2) for each model, including the feed-forward network and CRR model, for the calibration and validation periods. Int represents model input (precipitation and PE) at time t and Qt represents catchment discharge at time t.

Table 5.9 Comparison of performance of each modelling approach for the calibration and validation period in the Glenamong catchment. Model performance is evaluated using percent explained variance (R^2)

Modelling Approach	Calibration (E %)	Validation (E %)
HYSIM	85	81
Feed-Forward (Int)	76	71
Dynamic Network Configuration		
Int and Int-1	82	80
Int, Int-1 and Int-2	82	80
Int, Int-1 and Qt-1	86	82
Int, Int-1, Qt-1, Qt-2 and Qt-3	85	81
Int, Int-1, Int-2, Qt-1 and Qt-2	88	83

Both the dynamic neural networks and CRR model were shown to account for a higher proportion of the variance exhibited in the observed series when compared to the feedforward network. This model was also shown to vastly underestimate high flow events. The performance of each model suggests that the use of rainfall inputs alone is insufficient and that those networks which included some feedback or input delay mechanisms provided a better representation of the system. This is in-line with findings from previous studies (Minns and Hall, 1996; Campolo et al., 1999; Rajurkar, 2004).

There was little variation in the performance of different dynamic network configurations. However increasingly complex model structures, which considered greater time lags, did perform worse than those models which took account of antecedent rainfall and flow ordinates from two to three days pervious. This indicates that the catchment has a short memory i.e. the influence of a rainfall event on the catchments hydrology lasts only for a day or two. The comparable performance of HYSIM and the neural networks suggests that an empirical approach was adequate for modelling the relationship between rainfall and catchment runoff. To assess model uncertainty, HYSIM and the final dynamic neural network listed in Table 5.9 were both used to simulate streamflow using the same climate scenario. Both models produced very similar results under future climate forcing.

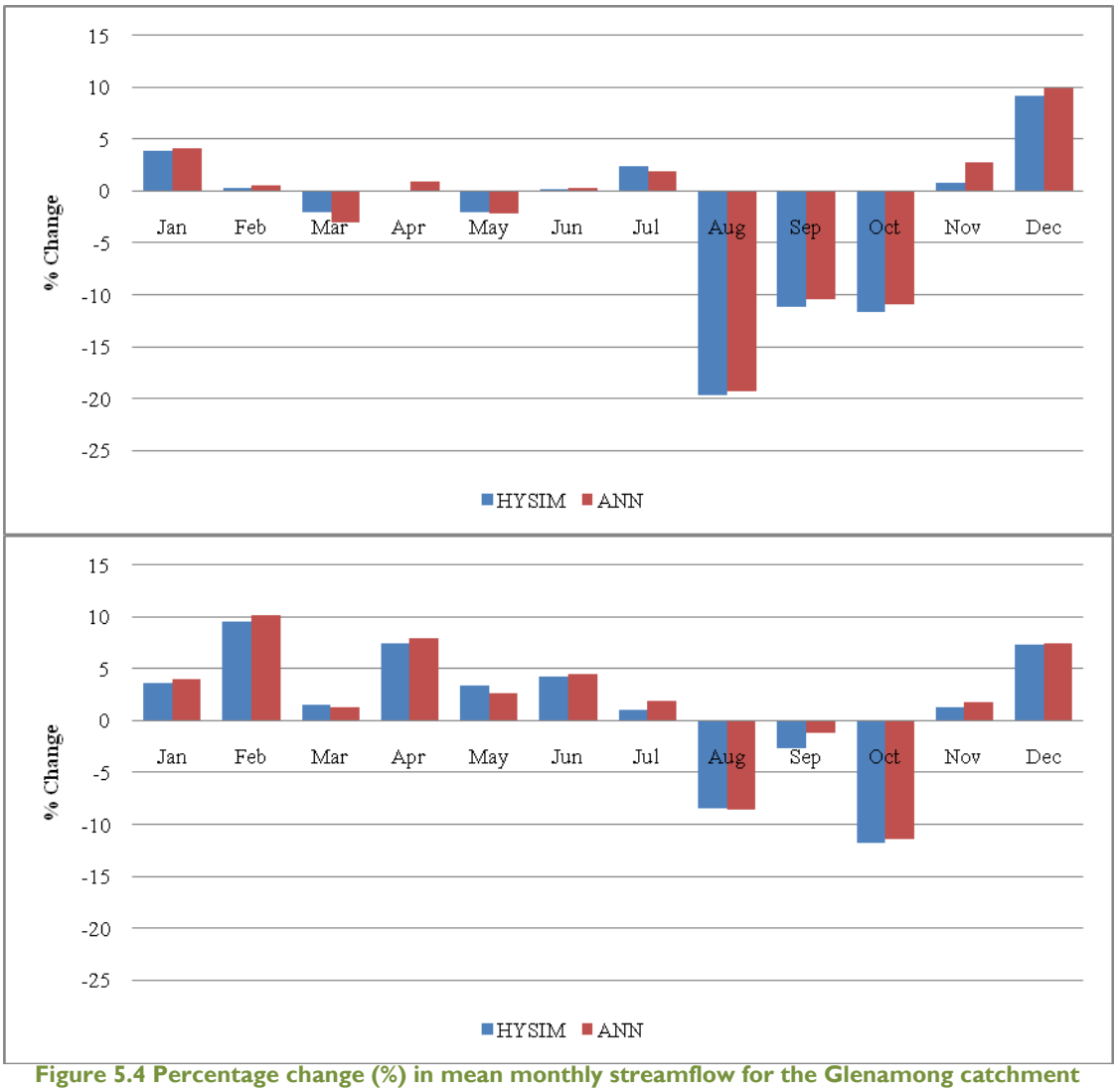

Figure 5.4 Percentage change (%) in mean monthly streamflow for the Glenamong catchment simulated using HYSIM and ANN for the 2050s (top) and 2080s (bottom). Both models are run using data from the HadCM3 GCM under the B2 emissions scenario.

Figure 5.4 illustrates the monthly percent change in mean streamflow, as simulated by the selected neural network and HYSIM, using climate projections downscaled from the HadCM3 GCM. Given the agreement shown between each models simulated changes in the Glenamong flow regime it was assumed that the uncertainty associated with the final streamflow projections arising due to model choice would be negligible. Consequently only HYSIM was employed to model future streamflow for the remaining catchments. This model was selected over the ANNs as it allows for the hydrological dynamics of the catchment to be explicitly represented in the model structure.

5.7 Extreme Value Analysis

In order to examine changes in frequency of flooding in each of the catchments modelled, an extreme value analysis was conducted to assess how the frequency of selected flood events for the control period are likely to change for each future time period. In total six flood events

were chosen; the flood expected every 2, 5 10, 15, 20 and 50 years. Therefore flood events ranging from fairly frequent (2-year) to moderately infrequent (50-year) are analysed. Due to the limited years of data more extreme return periods were not included. One of the key assumptions of flood frequency analysis is that the return period of a flood peak of a given magnitude is stationary with time (Cameron et al., 2000). However, a number of studies (Arnell and Reynard, 1996; Hulme and Jenkins, 1998) have demonstrated the variability of climate characteristics, with such variability having implications for statistical methods used in flood frequency analysis. Consequently assumptions regarding the stationarity of the flood series are made. In dealing with non-stationarity in the flood series Prudhomme et al. (2003) contend that it is possible to assume stationarity around the time period of interest (i.e. the thirty year periods represented by the 2020s, the 2050s and 2080s). Under this assumption, standard probability methodologies remain valid and are thus considered representative of the flood regime of the time horizon considered (Prudhomme et al., 2003). Similar assumptions are made in this work.

For each realisation of future streamflow the maximum annual flood series was extracted for each future time period. Therefore, in each of the catchments a 30 year maximum annual flood (MAF) series was extracted for each simulation for the control period (1961-1990), 2020s, 2050s and 2080s. Having extracted the flood series an extreme value distribution was fitted to each series using the methods described in the Flood Estimation Handbook (FEH) (Robson and Reed, 1999).

The distribution employed for the analysis was the Generalised Logistic (GL) distribution, a three parameter distribution defined by:

$$Q(F) = \xi + \frac{\alpha}{\kappa}\left[1 - \left(\frac{1-F}{F}\right)^{\kappa}\right] \qquad \textbf{Equation 5.2}$$

where,

ξ is the location parameter,
α is the scale parameter,
κ is the shape parameter, and
F is the non-exceedance probability.

The range of possible values for the GL distribution is:

$$-\infty < Q \leq \xi + \frac{\alpha}{\kappa} \qquad \text{if } \kappa > 0$$

$$\xi + \frac{\alpha}{\kappa} \leq Q < \infty \qquad \text{if } \kappa < 0$$

Therefore the GL distribution is bounded above for κ>0 and bounded below for κ<0 (Robson and Reed, 1999). Using the FEH methodology, the GL growth curve is obtained by substituting $x = Q/\xi$ into the equation for the GL distribution and rearranging to give:

$$x(F) = 1 + \frac{\beta}{\kappa}\left[1 - \left(\frac{1-F}{F}\right)^{\kappa}\right] \qquad \textbf{Equation 5.3}$$

where

$$\beta = \alpha / \xi$$

(Robson and Reed, 1999)

The growth curve can also be written in terms of the return period T:

$$x_T = 1 + \frac{\beta}{\kappa}\left[1 - (T-1)^{-\kappa}\right] \qquad \textbf{Equation 5.4}$$

The growth curve is also bounded above for κ>0. The parameters of the GL growth curve are calculated by fitting the distribution to observed data. There are a number of different techniques that can be used for this purpose, including the method of moments, Maximum Likelihood Estimation and the L-moment approach. In this work the latter is employed to fit the GL distribution to the MAF series of each simulation. Hosking and Wallis (1997) highlight some of the benefits of the method of L-moments over alternative methods of distribution fitting. For example, L-moments are more suited to flood analysis than ordinary moments due to the skewness of the flood series, while the method of L-moments has been shown to be more reliable than maximum likelihood estimation in situations were only small or medium sized samples are available, as is the case here with 30 years of data in each MAF series. In order to fit a distribution to a flood series, sample L-moments are calculated from the flood data using unbiased probability weighted moment estimators (Landwehr et al., 1979).

The frequency of flows associated with each return period during the control period was assessed for each future time period. Robson and Reed (1999) highlight that for the GL distribution the return period for a flow of a certain magnitude is given by:

$$T = 1 + \left[1 - \frac{\kappa}{\alpha}(Q - \xi)\right]^{\frac{-1}{\kappa}} \qquad \textbf{Equation 5.5}$$

Therefore in each catchment for each future time period new return periods are derived for the flow attributed to the 2, 5, 10, 15, 20 and 50 year floods under the control period. Results for each catchment are detailed below.

5.8 Future Hydrological Impacts of Climate Change

Future streamflow for each of the six catchments selected was modelled using meteorological data for the period 1961-2099 downscaled from three GCMs (HadCM3, CSIROmk2 and CGCM2) each run using two different emission scenarios (A2 and B2). Employing multiple GCMs, emission scenarios and downscaling methods allows the uncertainties associated with local scale estimates of climate change to be accounted for in streamflow projections. The incorporation of the stochastic element in SDSM downscaling allows an element of natural variability to be included in future simulations. HYSIM was employed to simulate catchment discharge on a daily time step using precipitation and potential evaporation as model input.

For future runs the hydrological model is used with parameter sets fitted on observed data, with the assumption that catchment parameter sets are not dependent on climate, i.e. that the processes involved in the physical transformation of precipitation into streamflow are independent from climate. The majority of climate change impact assessments are based on this assumption (Booij, 2005; Wilby, 2005; Fowler and Kilsby, 2007; Prudhomme and Davies, 2009). Giving weight to this assumption, Neil et al. (2003) highlight that there is no evidence that non-stationarity in climate would incur parameter instability. In order to account for parameter uncertainty 20 parameter sets, each of which were shown to provide an equally plausible model of the catchment system under observed conditions, were employed when simulating streamflow under the forcing conditions of future climate scenarios. Thus, in total over 12,000 simulations were produced for each catchment, sampling across the uncertainty range in employed GCMs, emission scenarios, downscaling technique and hydrological model uncertainty.

Projected changes in streamflow for each study catchment are considered for three future time horizons the 2020s (2010-2039), 2050s (2040-2069) and 2080s (2070-2099), with the period 1961-1990 used to represent baseline or reference conditions. For each catchment changes in the monthly flow regime and for high and low flow events were considered. Changes in the monthly flow regime for each catchment are presented using box plots. The whiskers represent the 95% confidence intervals of projected changes, also presented are the 75th and 25th percentiles and the mean (middle line). Changes in the monthly flow regime are presented relative to the natural variability for the current climate.

5.9 Uncertainty in Future Hydrological Simulations

As a first component of the analysis a comparison of the sources of uncertainty considered was carried out for the Glenamong catchment. By far the largest component of uncertainty is derived from the use of different GCMs. Figure 5.5 shows the changes in the monthly flow regime for the Glenamong catchment for each of the GCMs considered, all other sources of uncertainty were held constant (i.e. one emissions scenario (A2), one downscaling technique (SDSM) and one parameter set). Evident is the fact that there is a good deal of deviation in relative changes between climate models in relation to both the timing and magnitude of changes in the monthly flow regime. Of particular note are the large reductions in spring flow simulated by CGCM2 climate model, particularly by the 2080s. The HadCM3 model tends to be the driest model with the largest decreases in flow associated with the 2080s. The disparities between models emphasise the importance of including multiple GCMs in impact assessment in order to increase the robustness to uncertainty of policy making in adapting to climate change.

In relation to the uncertainty in future flows derived from greenhouse gas emissions, Figure 5.6 depicts the results for the Glenamong catchment. In assessing the contribution from this source of uncertainty only the emissions scenario was varied between both sets of simulations. Obvious from the results is that the A2 scenario simulates greater increases in winter flows and greater reductions for summer and autumn flows than the more optimistic B2 emissions scenario. Divergence between the scenarios is greatest after the middle of the century and largest by the 2080s. For the B2 scenario no changes in the flow regime are significant outside of natural variability, even by the 2080s. While the uncertainty between emissions scenario is important, it is not as large as the uncertainty derived from the use of different GCMs.

A final source of uncertainty analysed here is that derived from parametric sources in the HYSIM model due to issues non-identifiability of an optimum parameter set. Within this experiment only the behavioural parameter sets were varied. Of interest is the range of changes characterised by the box plots (Figure 5.7). For the winter months the range of uncertainty is small with greatest uncertainties evident for spring and summer months. There is also an increase in uncertainty from the 2020s to the 2080s. However, in comparison to GCM uncertainty, parameter uncertainty from HYSIM is small, but can be as large as emissions scenario uncertainty during summer months. This is consistent with the findings of Wilby and Harris (2006).

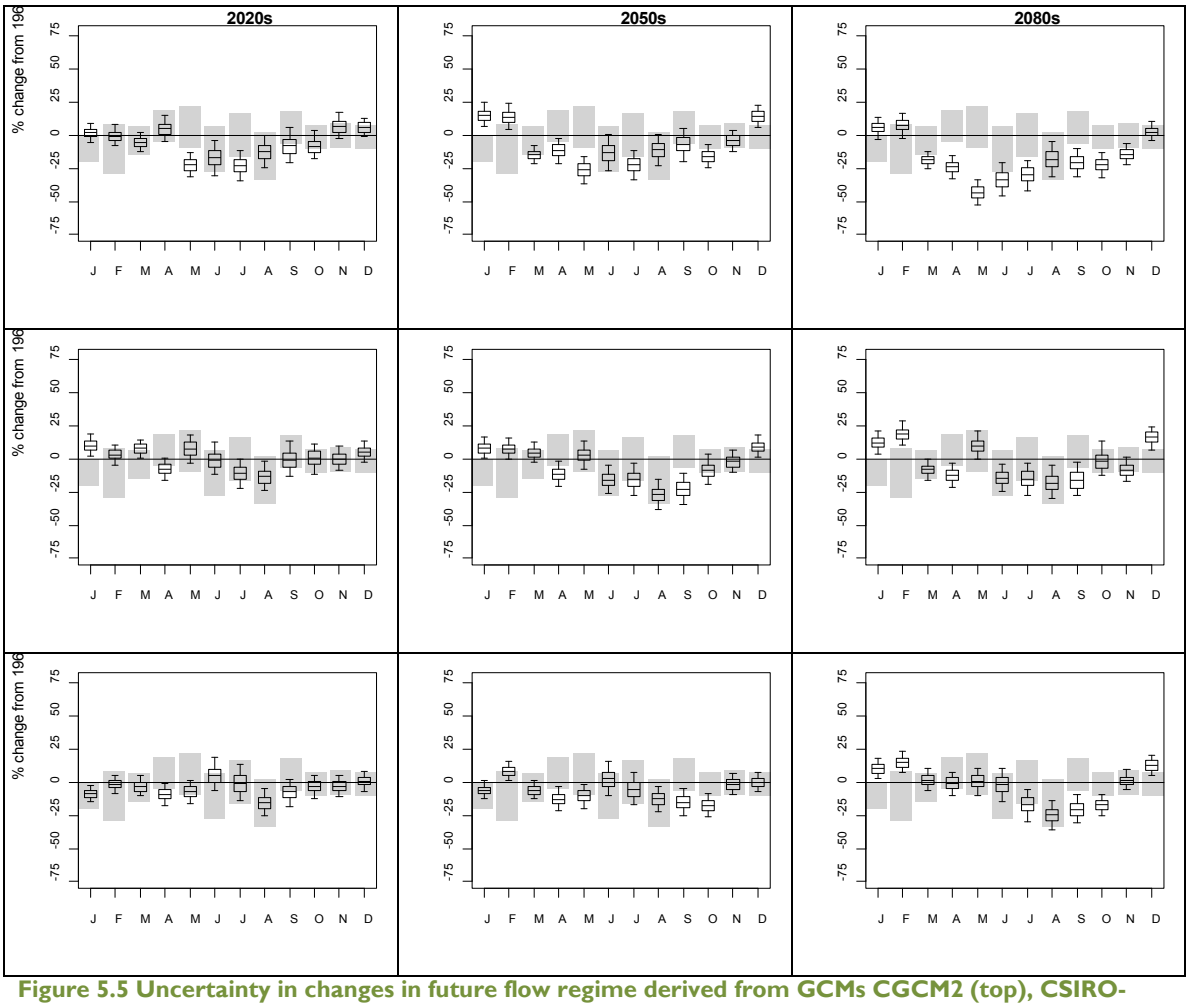

Figure 5.5 Uncertainty in changes in future flow regime derived from GCMs CGCM2 (top), CSIRO-Mk2 (middle) and HadCM3 (bottom).

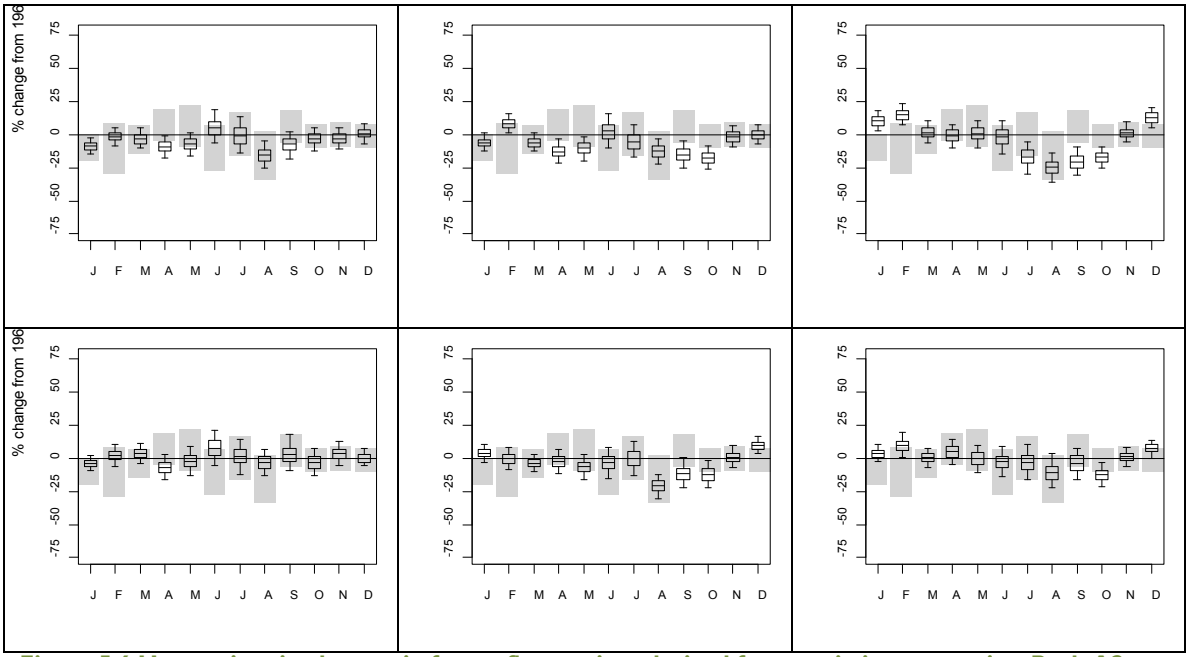

Figure 5.6 Uncertainty in changes in future flow regime derived from emissions scenarios. Both A2 (top) and B2 (bottom) are run using HadCM3.

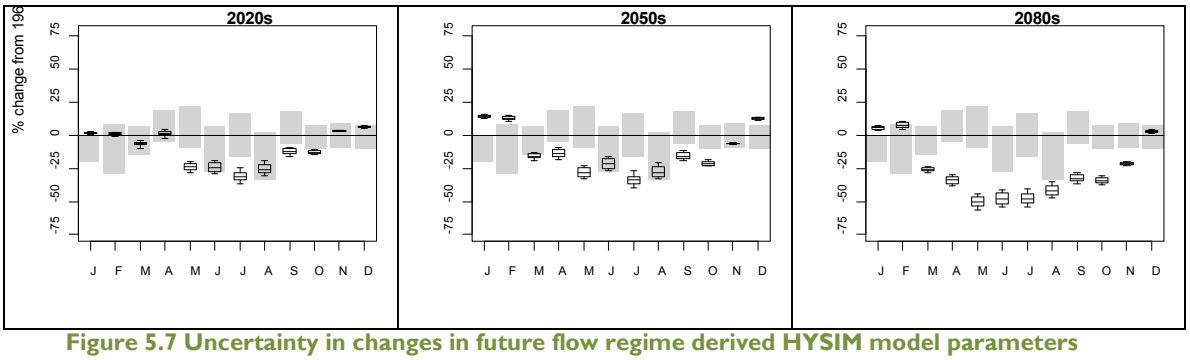

Figure 5.7 Uncertainty in changes in future flow regime derived HYSIM model parameters

5.10 Simulated Changes in Hydrology

5.10.1 Glendahurk Catchment

Changes in the monthly flow regime for the Glendahurk catchment are outlined in Figure 5.8. Evident is that fact that no clear signal of change is evident for the 2020s with results for each month spanning a sign change. Further, no changes are significant outside of natural variability for the control period. By the 2050s, while uncertainty ranges are still large there is clear evidence of a shift towards increased seasonality of flows with wetter winter and drier summers. Changes for May are significant outside natural variability, while the majority of runs show decreases in monthly flows from March through to October. By the 2080s the increased seasonality is further developed with significant increases in flow simulated for December and January of up to 25%, while significant decreases are suggested for June and October. For the remaining months the climate change signal is not deemed to be significant outside of natural variability.

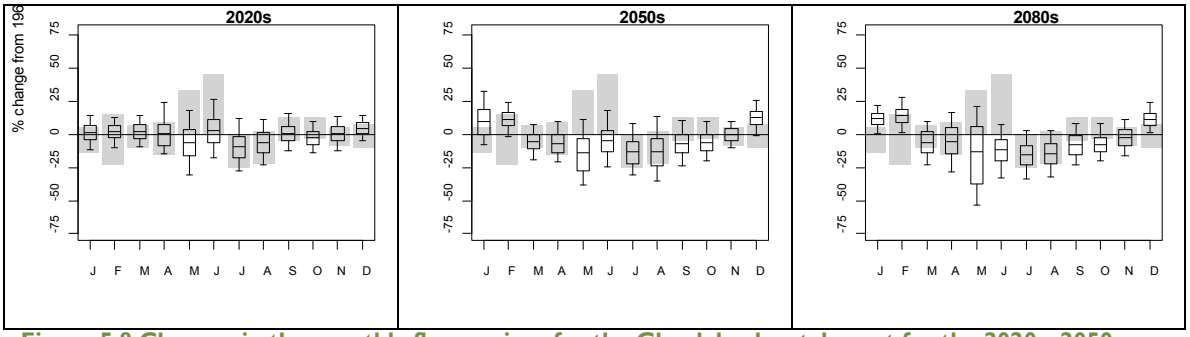

Figure 5.8 Changes in the monthly flow regime for the Glendahurk catchment for the 2020s, 2050s and 2080s relative to the control period 1961-90.

Changes in the full range of flow conditions were assessed by analysing changes in the flow percentiles for each future time period relative to the control period 1961-1990. Of particular interest are changes at the extremes of the flow distribution; represented as Q05, the flow exceeded only five percent of the time and representative of high flow conditions and Q95, the flow exceeded 95% of the time and representative of low flow conditions. Overall an increase

in high flows is likely, particularly by the end of the century; while a decrease in low flows are suggested for the majority of model runs. Changes in the tails of the flow distribution for the Glendahurk are further investigated below in Figure 5.9.

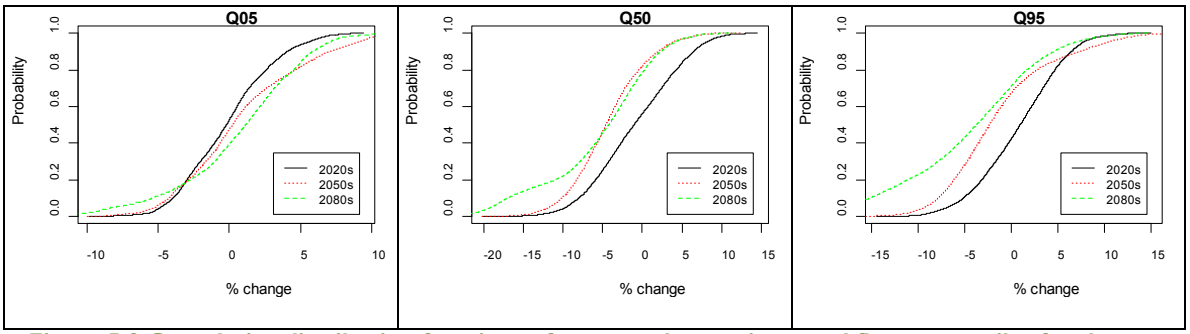

Figure 5.9 Cumulative distribution functions of percent changes in annual flow percentiles for the Glendahurk catchment.

Changes in the frequency of low flow events are presented in Figure 5.10. The flow threshold used to characterise low flow events is the Q95 for the relative season during the control period. To assess changes in the frequency, a count of the number of days in the year/season when flows fall below this threshold is conducted for each future time period. Results are presented as a change in the number of days relative to the control period 1961-1990. From the results obtained for the Glendahurk catchment an increase in the frequency of low flow events is suggested for each future time period with increases of 9.75, 11.2 and 30.12 days simulated for the 2020s, 2050s and 2080s respectively. Uncertainty ranges are large, particularly for the 2080s with changes ranging from a reduction of almost thirty days per year to an increase of up to 90 days a year. On a seasonal basis summer and autumn show the greatest increase in frequency of low flow days with uncertainty bounds again spanning a sign change. From all simulations a mean increase of approximately thirteen days is suggested for the summer by the end of the century.

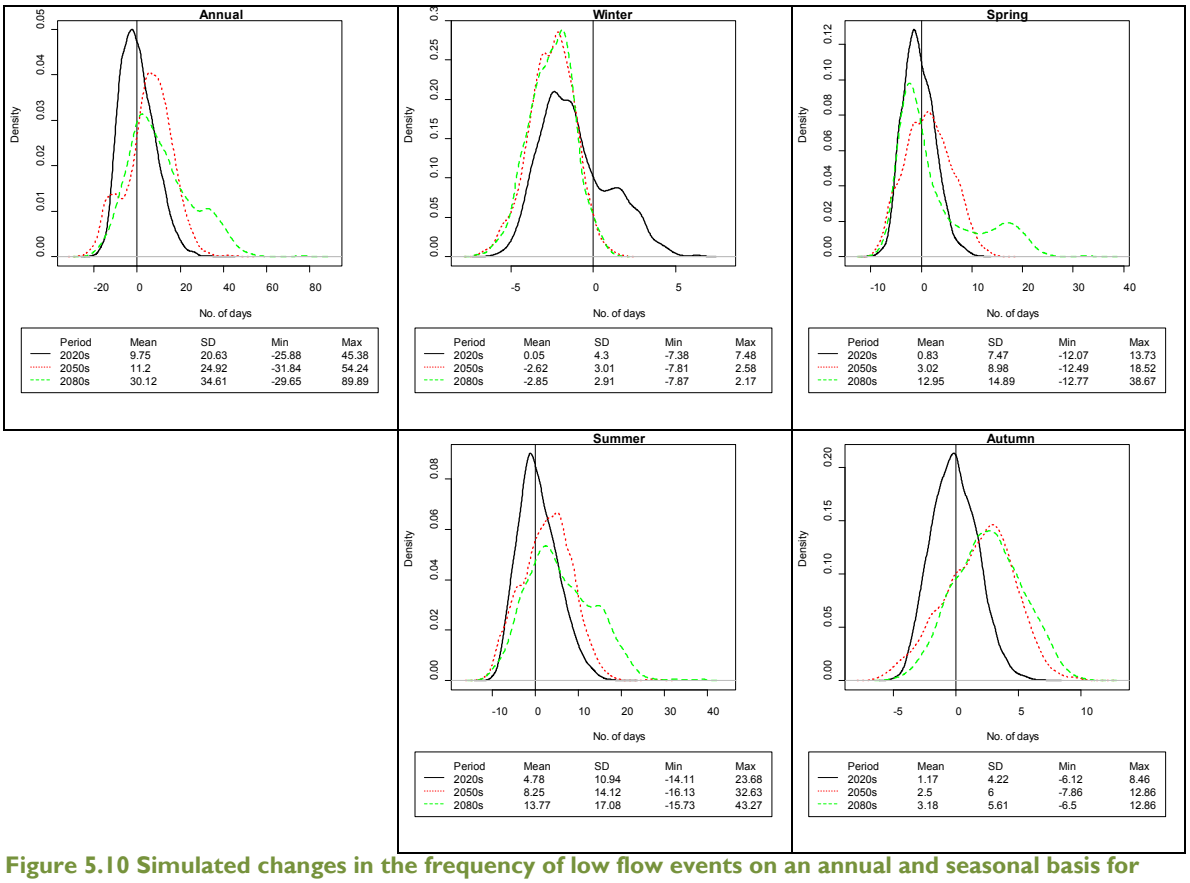

Figure 5.10 Simulated changes in the frequency of low flow events on an annual and seasonal basis for each future time period in the Glendahurk catchment

Figure 5.11 depicts the simulated changes in the duration of low flow events for the Glendahurk catchment. Calculation of the duration of low flow events was based on assessing the difference, for each future time period, in the cumulative number of days for which flows were below Q95 for the baseline period. On an annual basis a slight reduction in the duration of low flow events is evident for the 2020s, however for the end of the century an average increase in the duration of low flow events of approximately three days is suggested. The greatest increases in the duration of low flow conditions are shown for spring and summer, with the latter showing an increase of almost five days in the average duration of low flow conditions.

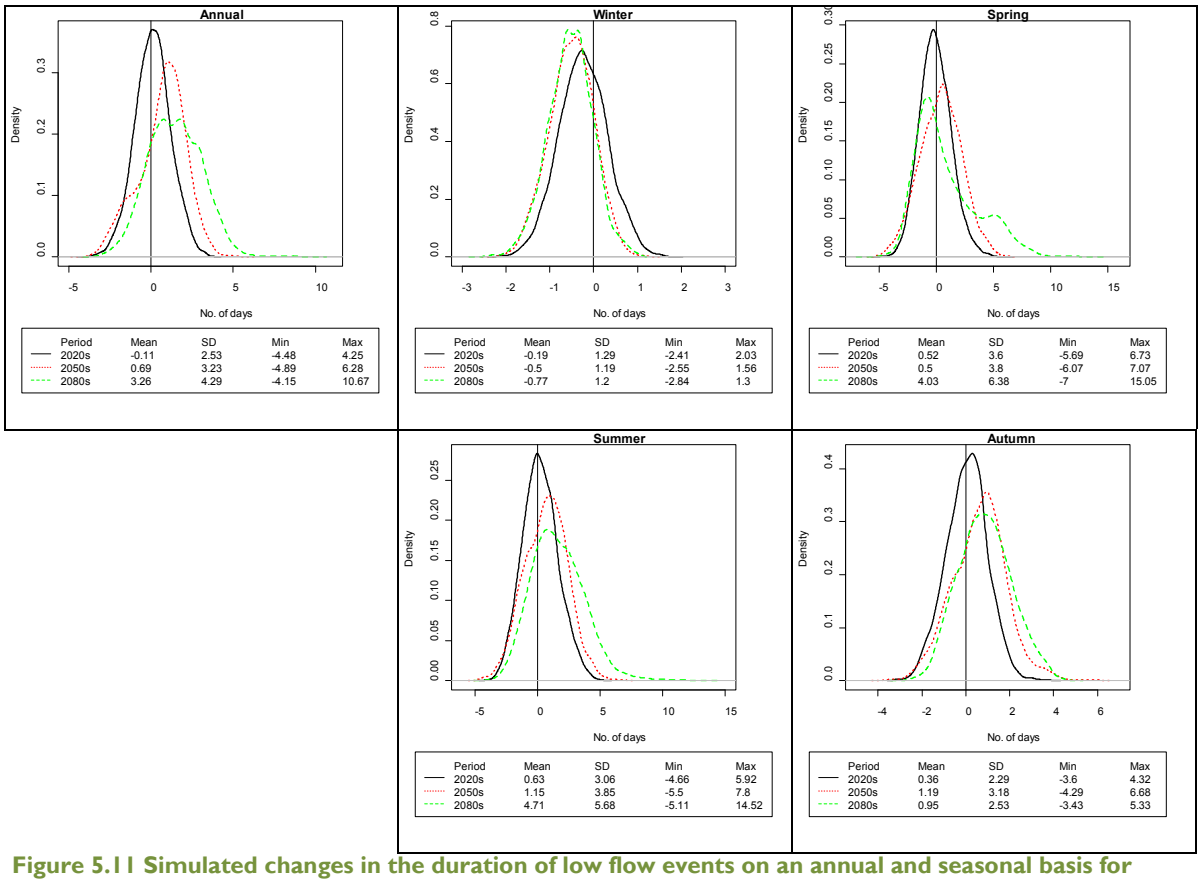

Figure 5.11 Simulated changes in the duration of low flow events on an annual and seasonal basis for each future time period in the Glendahurk catchment

In relation to the frequency of flood events Table 5.10 shows the changes in the frequency of selected flood events for each future time period. Particular emphasis is given to the uncertainty in future frequencies derived from each of the GCMs and emission scenarios employed. For each future time period the greatest increases in frequency are derived from the CGCM2 model which shows a consistent increase in frequency for all flood events for each time period. On the other hand a reduced frequency of occurrence of the selected flood events is suggest by the CSIRO A2 and B2 runs and Hadley A2 runs for the 2020s and 2050s. However, by the end of the century all runs with the exception of CSIRO B2 suggest and increase in the frequency of selected flood events. In the most extreme case (CGCM2 A2) the current flood with a return period of 50 years is likely to occur once every ~9 years.

Table 5.10 Changes in the frequency of selected flood recurrence intervals from the control period for each future time period for the Glendahurk catchment.

2020s	CGCM2-A2	CGCM2-B2	CSIRO-A2	CSIRO-B2	HADCM3-A2	HADCM3-B2
t2	1.95	2.87	1.69	2.405	1.05	1.78
t5	3.76	4.99	4.42	7.79	17.05	4.45
t10	6.1	7.02	10.05	17.35	73.26	9.02
t15	8.07	8.5	16.87	26.91	138.25	13.45
t20	9.7	9.61	24.19	36.82	204.59	18.04
t50	17.67	14.37	81.91	96.27	588.55	44.52
2050s	**CGCM2-A2**	**CGCM2-B2**	**CSIRO-A2**	**CSIRO-B2**	**HADCM3-A2**	**HADCM3-B2**
t2	1.65	2.74	2.01	1.53	2.02	2.17
t5	2.67	5.0	6.7	3.16	6.14	6.11
t10	3.95	6.02	15.23	5.85	15.2	12.97
t15	5.03	6.54	24.48	8.47	26.21	19.75
t20	5.92	6.85	33.51	11.15	38.78	26.86
t50	10.37	7.85	92.59	27.04	143.3	69.21
2080s	**CGCM2-A2**	**CGCM2-B2**	**CSIRO-A2**	**CSIRO-B2**	**HADCM3-A2**	**HADCM3-B2**
t2	2.37	2.4	1.53	1.79	1.39	1.59
t5	3.61	3.99	3.43	4.61	2.68	2.86
t10	4.79	5.47	7.49	10.03	4.54	4.17
t15	5.61	6.53	12.68	15.92	6.16	5.11
t20	6.23	7.31	18.43	22.42	7.62	5.91
t50	8.74	10.6	70.53	67.61	14.94	9.01

5.10.2 Glenamong Catchment

Projected changes in the mean monthly flow regime for the Glenamong catchment are depicted in Figure 5.12. For the 2020s there is no clear indication of any significant changes in monthly streamflow outside the bounds of natural variability for reference climate conditions. A similar picture is produced from model simulations for the 2050s. However the seasonality of the discharge regime does begin to become more pronounced with significant changes in streamflow being registered for the months of January and April. By the 2080s changes in local climate conditions, i.e. drier summers and wetter winters, become more apparent in the projected flow regime. Increases in January, February and December are deemed to be significant whilst decreases in catchment discharge are significant for September and October. For the remaining months model simulations are not considered to be significant outside natural variability.

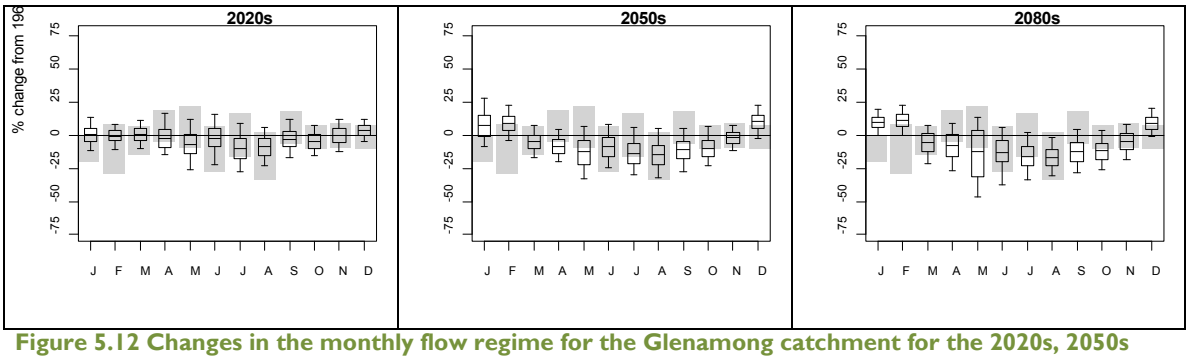

Figure 5.12 Changes in the monthly flow regime for the Glenamong catchment for the 2020s, 2050s and 2080s relative to the control period 1961-90

Model projected changes in the full range of flow conditions for the Glenamong catchment are assessed by examining changes in the annual flow percentiles for each future time horizon relative to the baseline period. Of particular interest are changes at the extremes of the flow distribution considered here using Q05 and Q95 flow percentiles. The cumulative distribution functions presented in Figure 5.13 depict the projected changes in each flow percentile. Model results suggest that an increase in high flows (Q05) is likely becoming more pronounced as the century progresses. A decrease in low flows (Q95) is also suggested, again with the trend becoming more acute towards the end of the century.

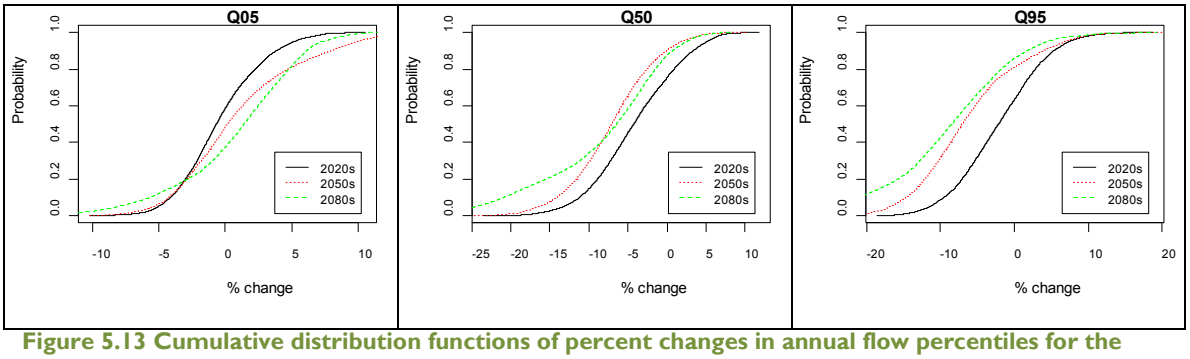

Figure 5.13 Cumulative distribution functions of percent changes in annual flow percentiles for the Glenamong catchment.

Changes in the frequency of low flow events are presented in Figure 5.14. From the results obtained for the Glenamong catchment an increase in the frequency of low flow events is suggested for each future time horizon - with increases of 15.2, 14 and 40.5 days projected for the 2020s, 2050s and 2080s accordingly. On a seasonal basis the greatest increase in the number of low flow days is projected to occur for the summer (18.27) over the 2080s horizon. Uncertainty ranges are also largest for this season, particularly for the 2080s, with model projections ranging from a reduction of almost sixteen days per annum to an increase of up to 52 days. The spring also exhibits a notable increase in low flow days for the same horizon (13.43) with uncertainty bounds again spanning a sign change (-14.63 to +41.5).

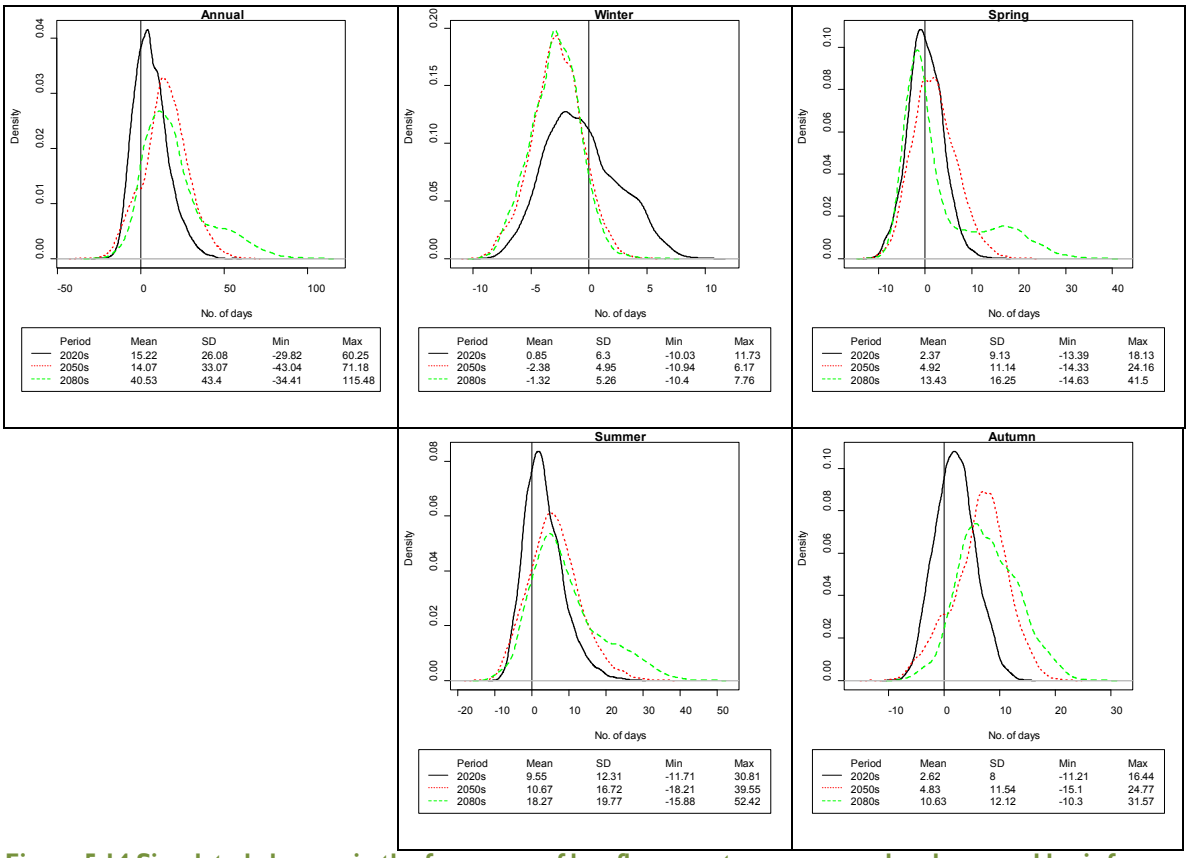

Figure 5.14 Simulated changes in the frequency of low flow events on an annual and seasonal basis for each future time period in the Glenamong catchment

Figure 5.15 displays the model projected changes in the duration of low flow events for the Glenamong catchment. On an annual basis an increase in the duration of low flow events is evident for each future time period with increases of 1.57, 2.26 and 2.89 days for the 2020s, 2050s and 2080s respectively. The greatest increases in the duration of low flow conditions are shown for spring and summer, with the latter showing an increase of over six days by the end of the century. The uncertainty bounds are also largest for these seasons with a standard deviation of 7.07 and 6 in the statistical distribution of model projections for the 2080s.

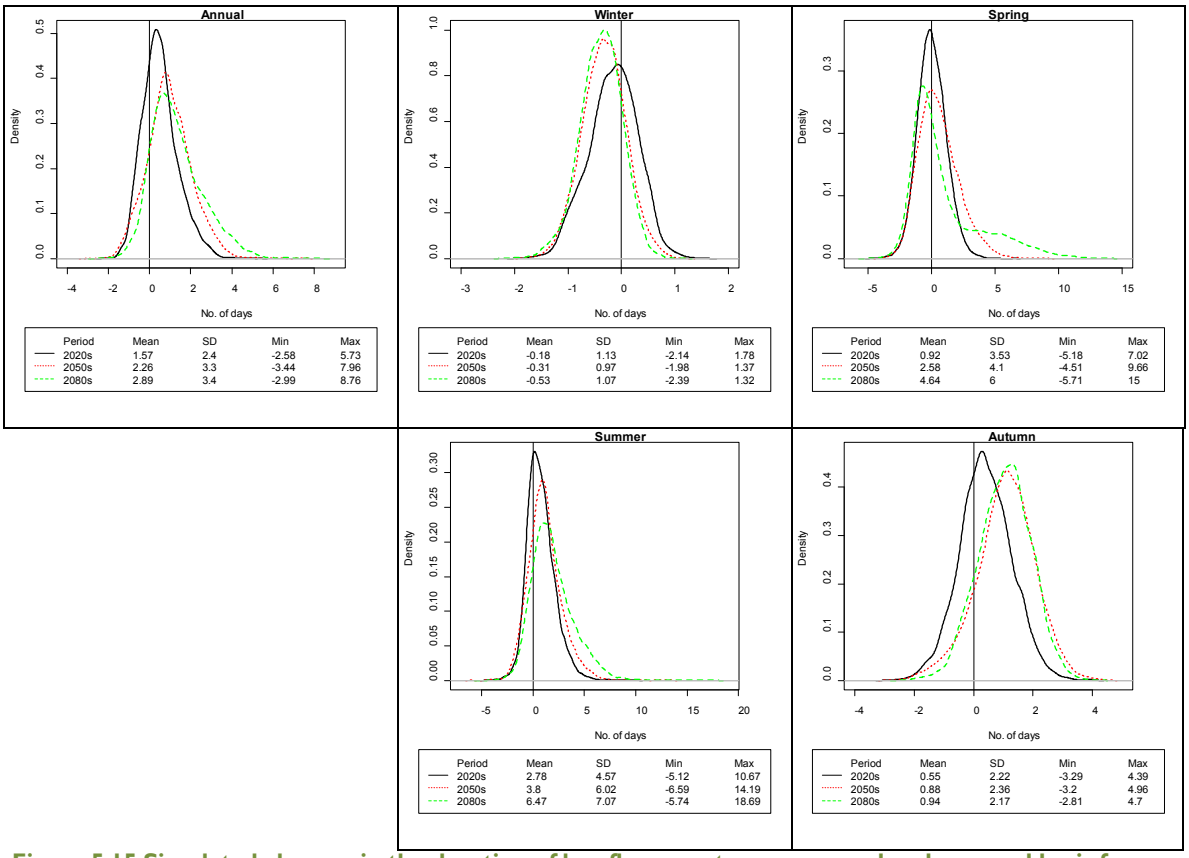

Figure 5.15 Simulated changes in the duration of low flow events on an annual and seasonal basis for each future time period in the Glenamong catchment.

Table 5.11 displays the model simulated changes in the return period for selected flood events. For each horizon the greatest increases in the frequency of flooding events are derived from the CGCM2 model, which exhibits a consistent decrease in the return period for each event over the three future horizons. Conversely a reduced frequency of occurrence for certain flooding events is suggested by the CSIROmk2 A2 and B2 model projections along with the HadCM3 A2. However by the end of the century all runs, with the exception of CSIRO B2, suggest a reduction in the return period of selected flood events. In the most extreme case (CGCM2 A2) it is suggested that the magnitude of a flooding event with a return period of 50 years under baseline conditions will occur once every 7.66 years by the end of the century.

Table 5.11 Changes in the frequency of selected flood recurrence intervals from the control period for each future time period for the Glenamong catchment

2020s	CGCM2-A2	CGCM2-B2	CSIRO-A2	CSIRO-B2	HADCM3-A2	HADCM3-B2
t2	1.89	2.81	1.67	2.31	1.72	1.71
t5	3.54	5.17	3.58	6.98	3.67	4
t10	5.51	7.56	6.77	15.21	6.7	7.83
t15	7.07	9.46	9.71	23.98	9.66	11.85
t20	8.46	11.06	12.67	32.87	12.79	15.78
t50	14.71	17.59	29.39	87.16	30.29	40.49
2050s	CGCM2-A2	CGCM2-B2	CSIRO-A2	CSIRO-B2	HADCM3-A2	HADCM3-B2
t2	1.6	2.08	2.03	1.43	2.13	1.64
t5	2.35	3.29	5.38	2.69	6.66	3.28
t10	3.14	4.46	11.26	4.89	15.25	5.64
t15	3.72	5.36	16.82	7.27	24.48	7.87
t20	4.21	6.11	22.52	9.73	34.93	9.91
t50	6.26	9.07	55.53	25.52	100.45	21.08
2080s	CGCM2-A2	CGCM2-B2	CSIRO-A2	CSIRO-B2	HADCM3-A2	HADCM3-B2
t2	2.32	2.27	1.45	1.7	1.39	1.58
t5	3.47	4.16	2.62	4.25	2.57	2.89
t10	4.47	5.98	4.62	8.98	4.25	4.32
t15	5.14	7.57	6.54	14.23	5.74	5.44
t20	5.67	8.93	8.53	19.71	7.2	6.35
t50	7.66	14.71	20.68	55.37	14.18	10.26

5.10.3 Maurmatta Catchment

Projected changes in the monthly flow regime for the Maurmatta catchment are outlined in Figure 5.16. No clear signal of change in monthly flows is exhibited for the 2020s with the majority of model runs for each month lying within the bounds of natural variability. Conversely by the 2050s there is clear evidence of a shift towards an increased seasonality in the flow regime. This finding is in-line with the anticipated occurrence of wetter winters and drier summers. Changes for the months of January, April and March are significant outside natural variability. The majority of model simulations exhibit decreases in monthly flows from March through to October. By the 2080s this increased seasonality is further amplified with significant increases in mean flow projected for the month of January, while significant decreases are suggested for June, August and September. The largest uncertainty bounds are associated with the month of May.

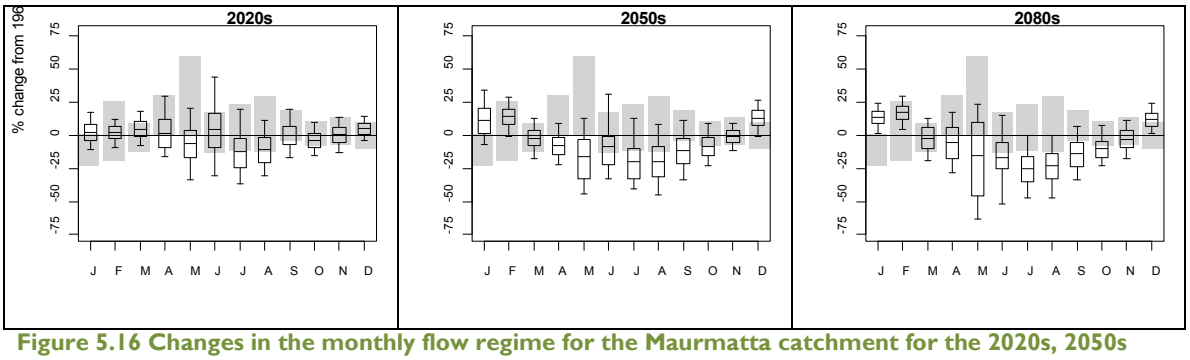

Figure 5.16 Changes in the monthly flow regime for the Maurmatta catchment for the 2020s, 2050s and 2080s relative to the control period 1961-90

From Figure 5.17 model simulations suggest that an increase in high flows is likely whilst a decrease in low flows is suggested for the majority of model runs. This underlying trend, of increases and decreases for Q05 and Q95 respectively, is anticipated to become more pronounced as the century progresses.

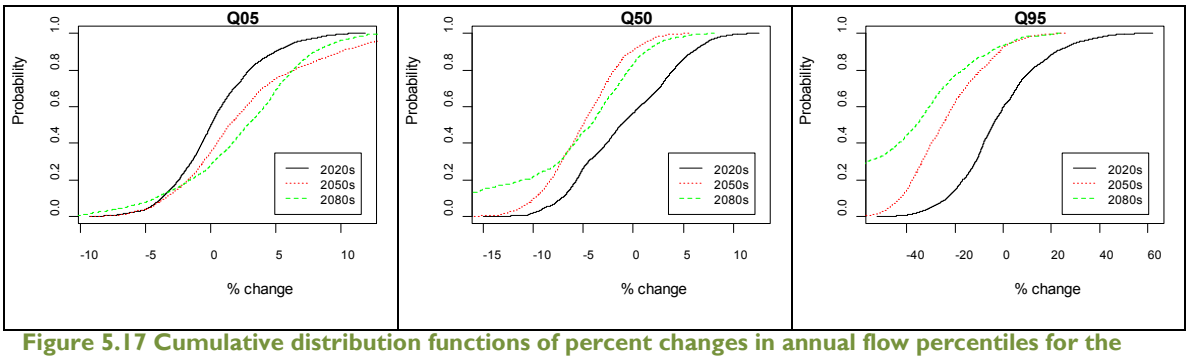

Figure 5.17 Cumulative distribution functions of percent changes in annual flow percentiles for the Maurmatta catchment

Projected changes in the frequency of low flow events for the Maurmatta catchment are illustrated in Figure 5.18. Model simulations suggest an increase in the frequency of low flow days for each future time horizon with increases of 7.27, 19.45 and 31.7 days projected for the 2020s, 2050s and 2080s respectively. On a seasonal basis the greatest increase in the number of Q95 days is projected to occur for the summer (18.47) over the 2080s horizon. Uncertainty ranges are also largest for this season, particularly over the 2080s, with model projections ranging from a reduction of almost nine days per year to an increase of up to 45 days. The spring also exhibits a notable increase in low flow days for the same horizon (8.95) with uncertainty bounds again spanning a sign change (-9.84 to +27.74).

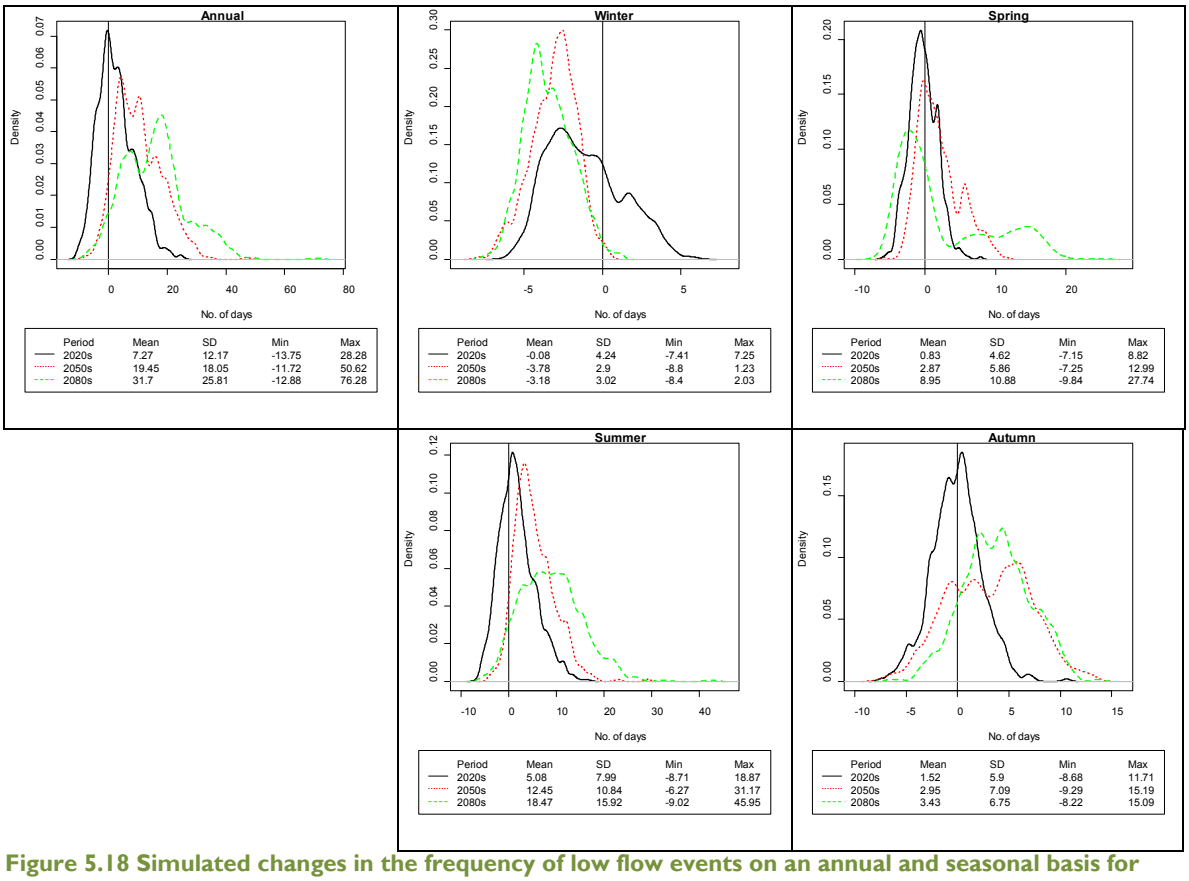

Figure 5.18 Simulated changes in the frequency of low flow events on an annual and seasonal basis for each future time period in the Maurmatta catchment

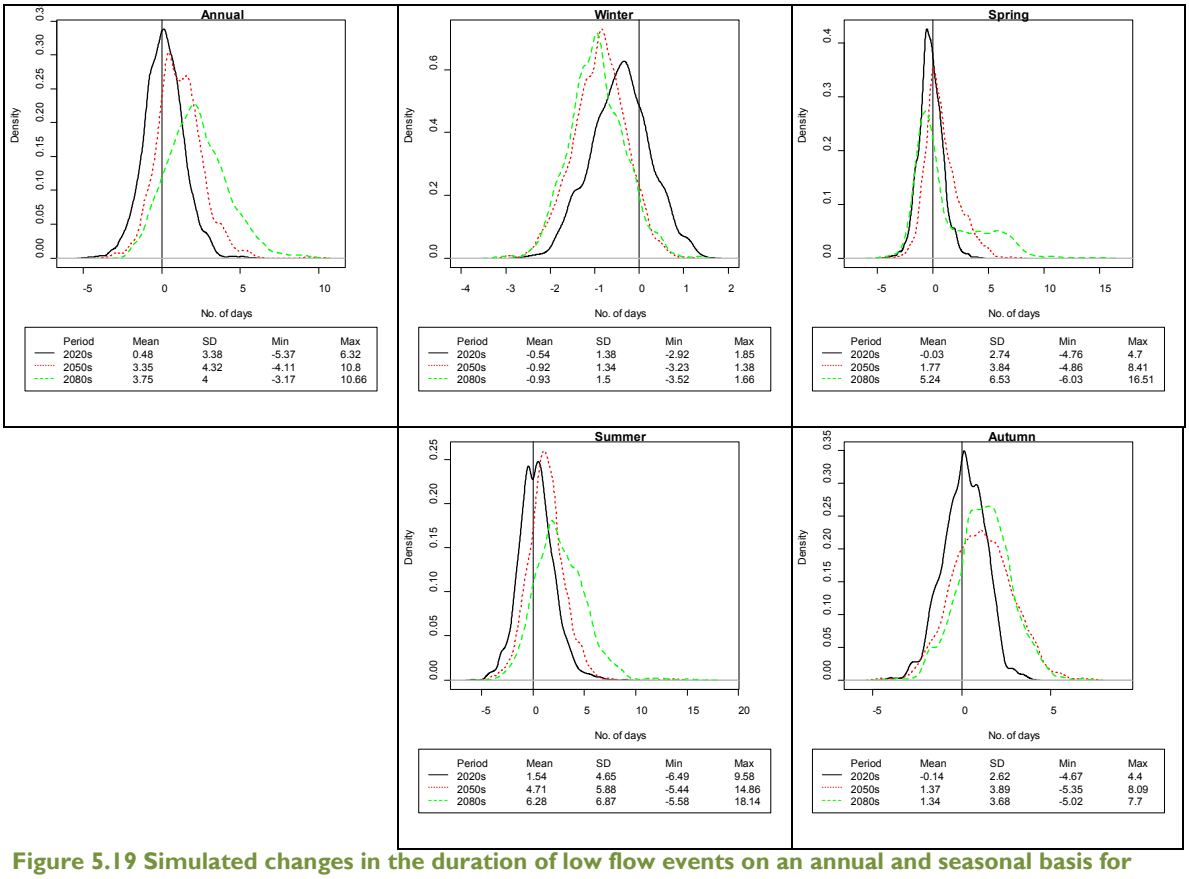

Figure 5.19 Simulated changes in the duration of low flow events on an annual and seasonal basis for each future time period in the Maurmatta catchment.

Figure 5.19 depicts the simulated changes in the duration of low flow events for the Maurmatta catchment. An average increase in the duration of low flow events of approximately three days is suggested by the end of the century. However model runs returned a maximum increase of almost 11 days. On a seasonal basis the greatest increases are associated with spring (+5.24) and summer (+ 6.28) for the 2080s.

5.10.4 Altahoney Catchment

Projected changes in the monthly mean flow regime for the Altahoney catchment are displayed in Figure 5.20. For the 2020s there is no clear indication of any changes in the flow regime outside the bounds of reference variability. The seasonality of the streamflow regime begins to become more pronounced by the 2050s with significant changes in catchment discharge returned for the months of December, May and September. By the 2080s the seasonality of the flow regime is projected to become heightened further. Increases in January and December are deemed to be significant when considered against baseline conditions whilst decreases in catchment discharge are significant for September. For the remaining months model simulations are not considered to be significant. Projections for the month of March display the widest uncertainty bounds with model runs ranging from -75% to +25%.

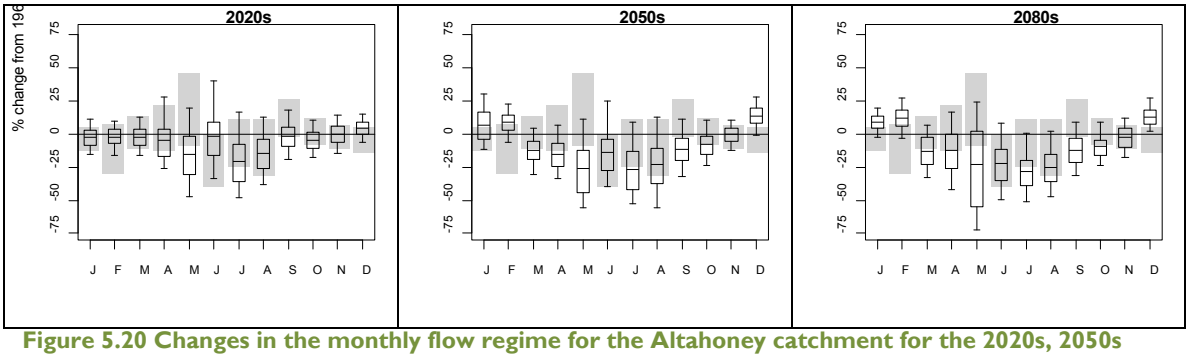

Figure 5.20 Changes in the monthly flow regime for the Altahoney catchment for the 2020s, 2050s and 2080s relative to the control period 1961-90.

Changes in the full range of flow conditions for the Altahoney over each future time horizon are examined using the following flow percentiles: Q05, Q50 and Q95. The cumulative distribution functions in Figure 5.21, constructed using the combined model simulations, depict the simulated changes for each percentile. Model projections suggest an increase in extreme high flows is likely with their occurrence becoming more frequent as the century progresses. A decrease in low flows is also suggested.

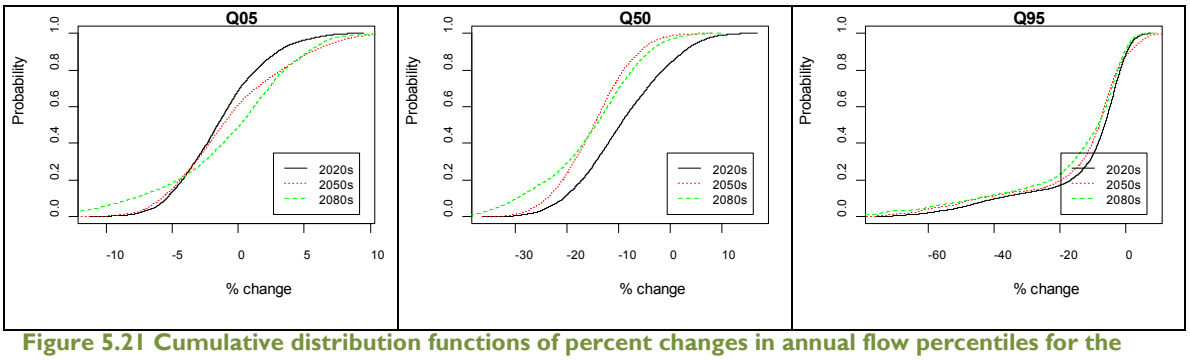

Figure 5.21 Cumulative distribution functions of percent changes in annual flow percentiles for the Altahoney catchment

Changes in the frequency of low flow events for the Altahoney catchment are presented in Figure 5.22. The results indicate an increase in the frequency of low flow events over each future period - with increases of 12.22, 11.23 and 28.17 days being returned for the 2020s, 2050s and 2080s respectively. On a seasonal basis the greatest increase in the number of low flow days is projected for the summer (14.77) over the 2080s horizon. The range in model projections are largest for this season, particularly the 2080s, with changes ranging from a reduction of almost sixteen days per year to an increase of up to 52 days. The spring also exhibits a notable increase in low flow days for the same horizon (+10.28) with uncertainty bounds again spanning a sign change (-10.55 to +31.12).

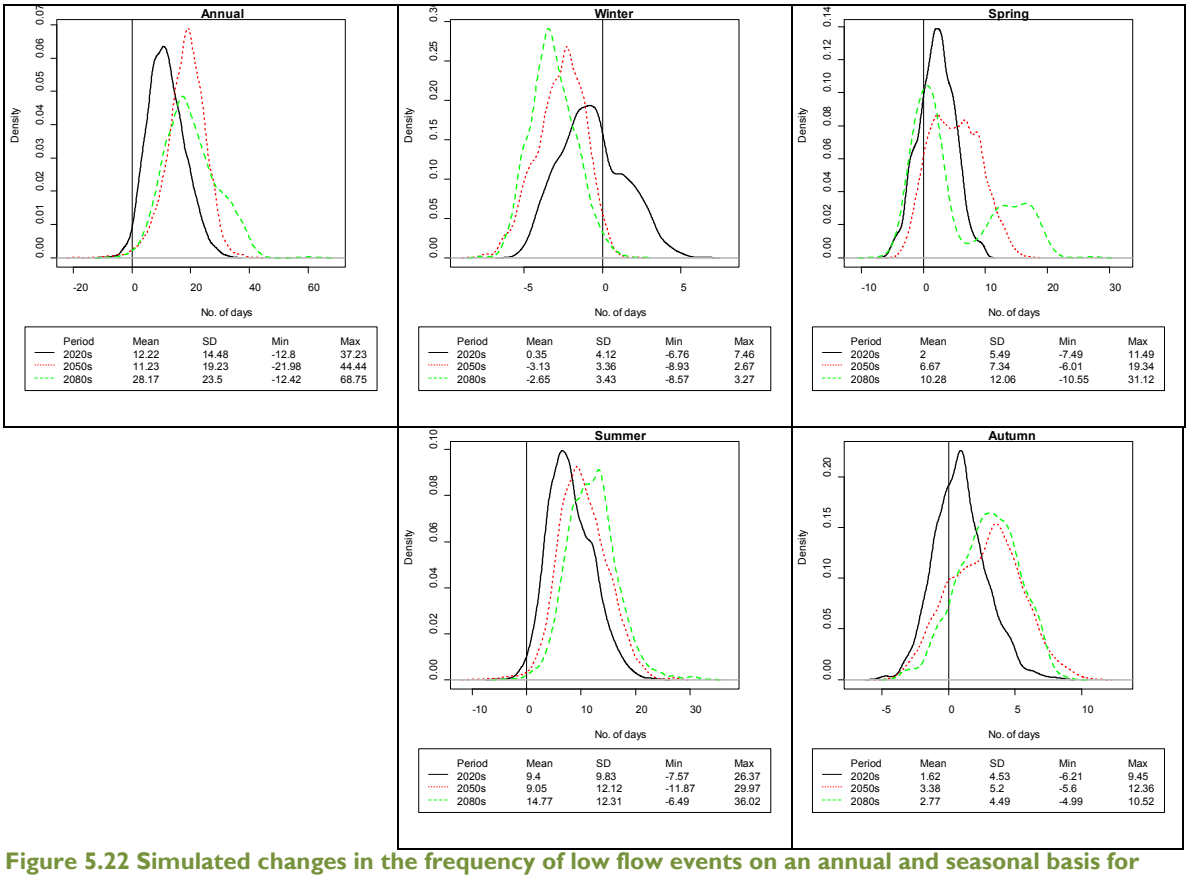

Figure 5.22 Simulated changes in the frequency of low flow events on an annual and seasonal basis for each future time period in the Altahoney catchment

Figure 5.23 depicts the simulated changes in the duration of low flow events for the Altahoney catchment. The duration of low flow events is calculated using the cumulative number of days for which average streamflow is below the Q95 threshold. On an annual basis an average increase in the duration of low flow events of approximately four days is suggested by the end of the century. The greatest increases in the average duration of Q95 flow conditions, on a seasonal basis, are shown for spring (+ 3.06) and summer (+ 5.42) over the 2080s. However the maximum increase returned by model simulations was much higher, over 14 days in both instances.

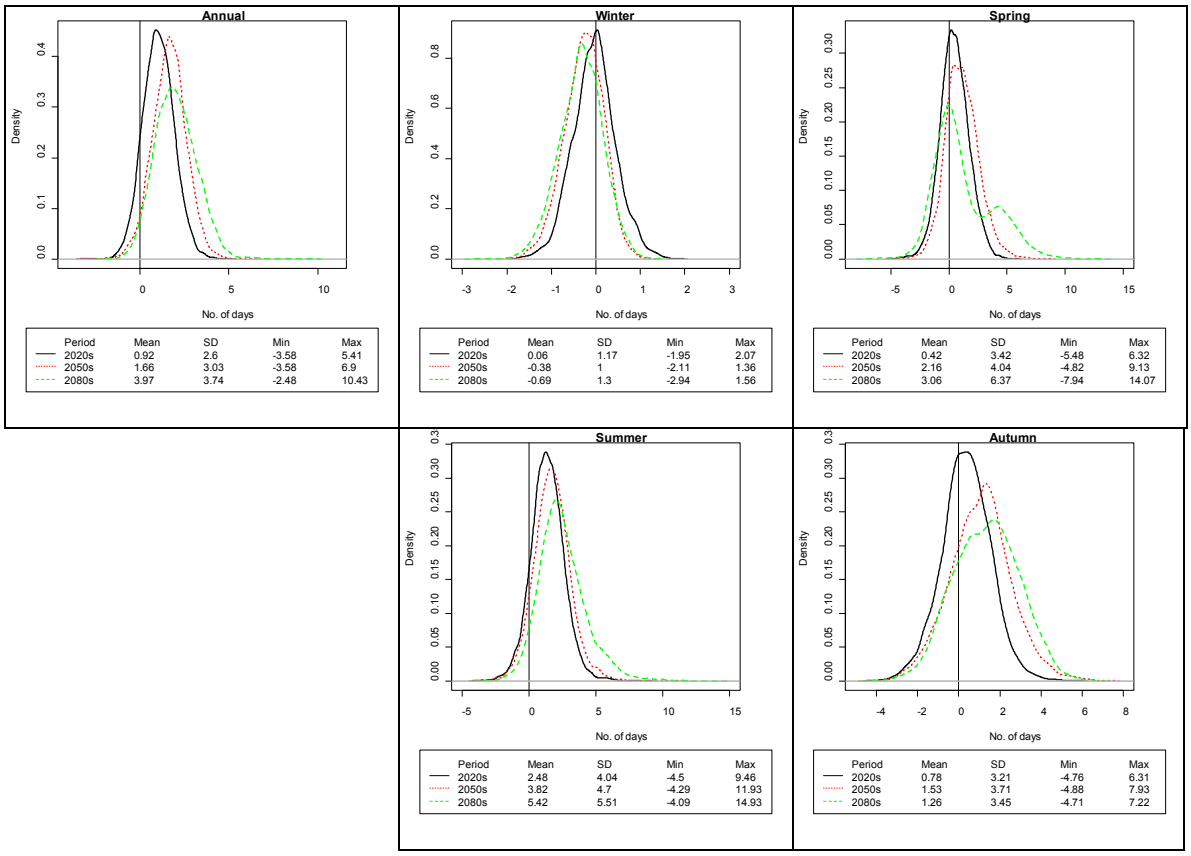

Figure 5.23 Simulated changes in the duration of low flow events on an annual and seasonal basis for each future time period in the Altahoney catchment

Table 5.13 displays the projected changes in the frequency of selected flood events for each future time period. For each future time period the greatest increases in frequency are derived from the CGCM2 GCM which projects a consistent decrease in the return period for all flood events over each time horizon. On the other hand a reduced frequency of occurrence of the selected flood events is suggest by the CSIRO A2 and B2 runs and Hadley A2 runs for the 2020s and 2050s. However, by the end of the century all runs with the exception of CSIRO model suggest and increase in the frequency of selected flood events. In the most extreme

case (HadCM3-B2) the current flood with a return period of 50 years is likely to occur once every 8.24 years by the 2080s.

Table 5.13 Changes in the frequency of selected flood recurrence intervals from the control period for each future time period for the Altahoney catchment.

2020s	CGCM2-A2	CGCM2-B2	CSIRO-A2	CSIRO-B2	HADCM3-A2	HADCM3-B2
t2	1.98	3.04	1.80	2.41	1.64	1.84
t5	3.79	5.80	4.73	7.72	3.53	4.55
t10	6.16	8.21	10.09	17.12	6.75	8.95
t15	7.93	10.14	15.62	25.72	10.43	13.42
t20	9.54	11.68	21.41	35.19	14.12	17.50
t50	16.53	16.63	56.96	88.44	37.51	41.52
2050s	**CGCM2-A2**	**CGCM2-B2**	**CSIRO-A2**	**CSIRO-B2**	**HADCM3-A2**	**HADCM3-B2**
t2	1.71	2.31	2.42	1.55	2.0	1.70
t5	2.74	3.66	8.15	3.22	6.67	3.34
t10	4.07	4.70	19.42	6.20	16.16	5.42
t15	5.06	5.50	31.59	9.02	27.92	7.22
t20	6.00	6.06	44.66	12.23	40.20	8.71
t50	10.036	7.82	129.92	31.90	122.97	15.92
2080s	**CGCM2-A2**	**CGCM2-B2**	**CSIRO-A2**	**CSIRO-B2**	**HADCM3-A2**	**HADCM3-B2**
t2	2.37	2.49	1.61	1.82	1.36	1.59
t5	3.59	4.20	3.51	4.47	2.68	2.76
t10	4.81	5.55	7.28	10.31	4.58	3.95
t15	5.58	6.59	11.55	15.75	6.39	4.84
t20	6.26	7.39	16.35	22.05	8.00	5.51
t50	8.68	9.82	52.14	61.60	15.68	8.24

5.10.5 Goulan Catchment

Figure 5.24 displays the projected changes in the mean monthly flow regime for the Goulan catchment. As the results for each month are within the bounds of reference variability model simulations indicate no clear change in monthly flows over the 2020s. By the 2050s the picture is a little clearer with some indication of a shift towards an increase in the seasonality of the streamflow regime. Changes for the months of March, July, September and October are significant outside reference variability. Over the 2080s horizon the exhibited pattern of increased seasonality remains largely the same as under the 2050s with decreases in flow now being significant for the months of March, July, August, September and October. As opposed to the other catchments considered none of the winter months display any significant increase in mean streamflow.

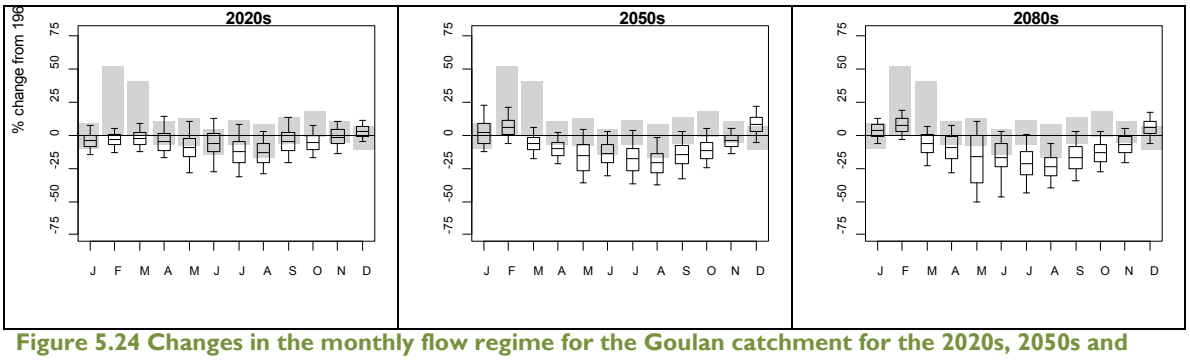

Figure 5.24 Changes in the monthly flow regime for the Goulan catchment for the 2020s, 2050s and 2080s relative to the control period 1961-90

Changes in the distribution of flow conditions for each future horizon were determined by analysing projected changes in the Q05, Q50 and Q95 flow percentiles. From Figure 5.25 model simulations suggest that an increase in high flows is likely, becoming more extreme by the end of the century. A decrease in low flows is also suggested similarly becoming more pronounced as the century progresses.

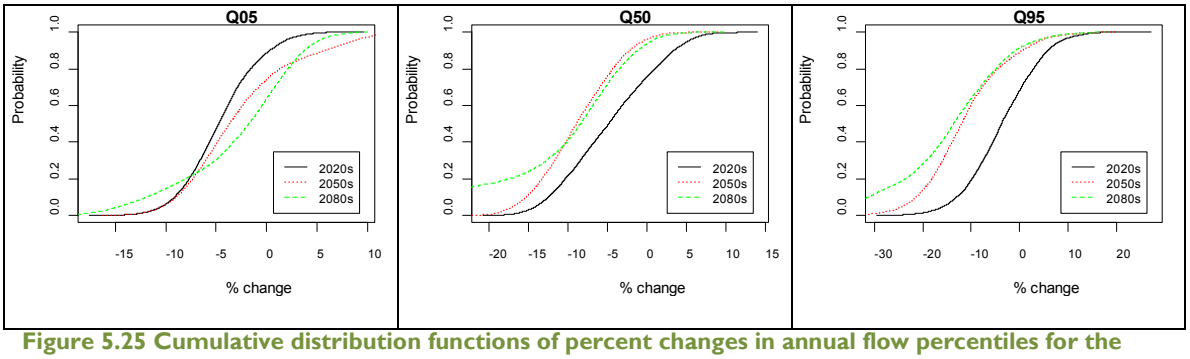

Figure 5.25 Cumulative distribution functions of percent changes in annual flow percentiles for the Goulan catchment

Changes in the frequency of low flow events for the Goulan catchment are displayed Figure 5.26. Projected changes in the number of days for which flows fall below this threshold, relative to the baseline period, are quantified for each future horizon. Model simulations suggest an increase in the frequency of low flow events for each horizon - with increases of 8.27, 12.32 and 37.88 days projected for the 2020s, 2050s and 2080s respectively. On a seasonal basis the greatest increase in the number of low flow days is projected to occur for the summer (19.7) over the 2080s. Uncertainty ranges are also largest for this season, particularly for the 2080s, with model simulations ranging from a reduction of almost 16 days per year to an increase of up to 56. Spring and autumn also exhibit a notable shift in the average occurrence of low flows with an increase of 11.58 and 8.42 respectively for the 2080s.

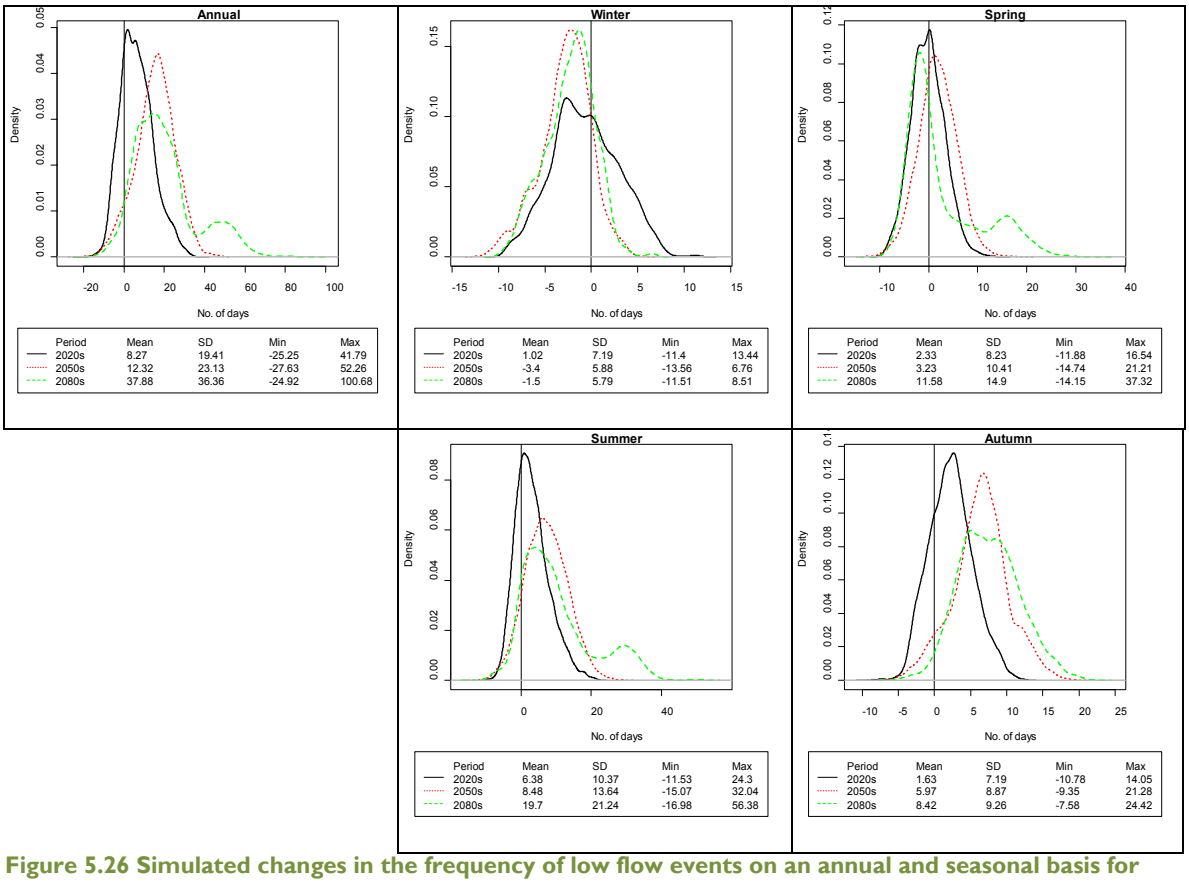

Figure 5.26 Simulated changes in the frequency of low flow events on an annual and seasonal basis for each future time period in the Goulan catchment.

Figure 5.27 depicts the simulated changes in the duration of low flow events. On an annual basis an increase in the duration of low flow events is evident for the each future horizon with increases of 2.38, 6.97 and 12.14 days for the 2020s, 2050s and 2080s respectively. The greatest increases in the duration of low flows are shown for spring and summer by the end of the century, with the latter showing an increase of over 20 days in the average duration of low flow conditions. Models simulations vary around this considerably with future model runs for this period ranging from -6.85 to +48.19.

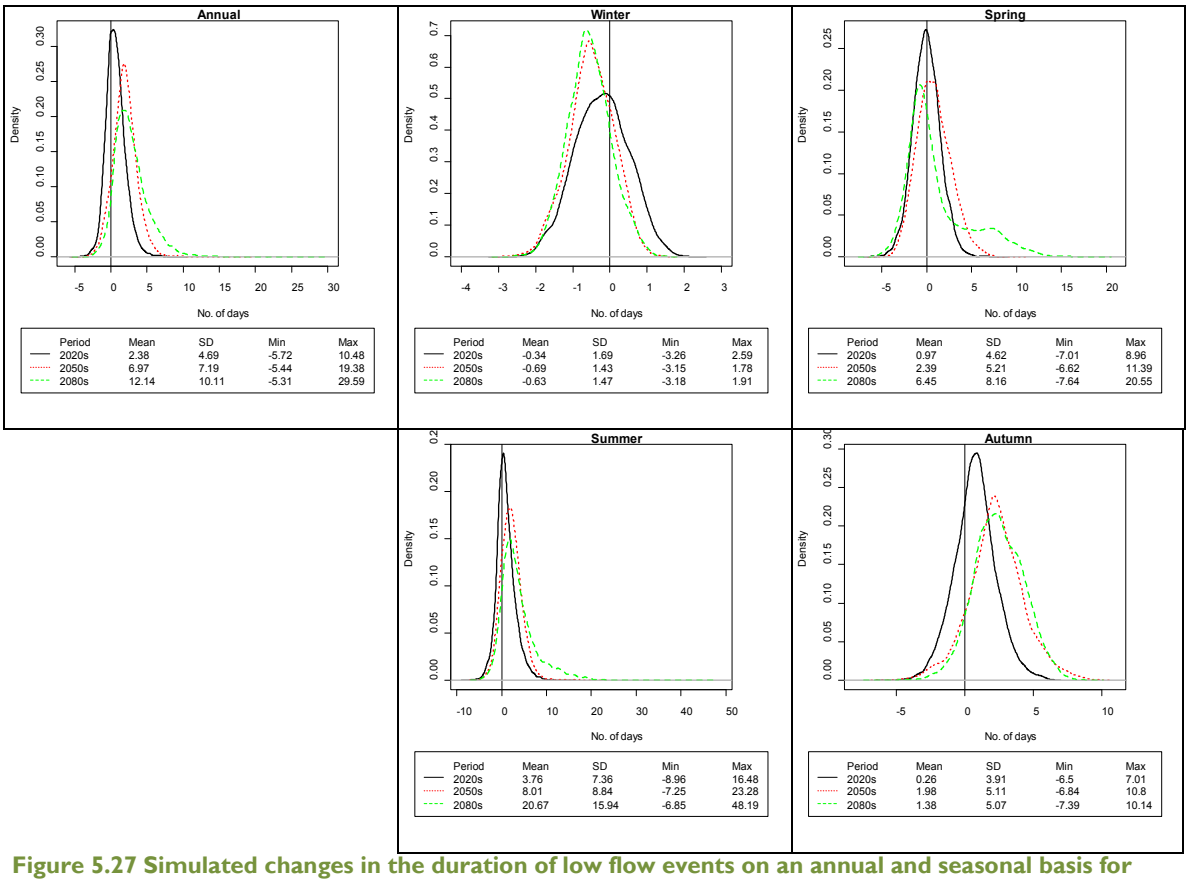

Figure 5.27 Simulated changes in the duration of low flow events on an annual and seasonal basis for each future time period in the Goulan catchment

Table 5.14 shows the projected changes in the frequency of selected flood events for each future time horizon. For each period the greatest in the frequency of flooding events of a given magnitude are derived from the CGCM2 GCM. Using the output from this model hydrological simulations suggest a consistent decrease in the return period for all flood events over each time horizon. Conversely a reduction in the frequency flooding events is suggested by the CSIRO A2 and B2 as well as the Hadley A2 for the 2020s and 2050s. However, by the end of the century all runs with the exception of CSIRO model suggest and increase in the frequency of selected flood events. In the most extreme case (HadCM3-B2) the current flood with a return period of 50 years is likely to occur once every 8.24 years by the 2080s.

Table 5.14 Changes in the frequency of selected flood recurrence intervals from the control period for each future time period

2020s	CGCM2-A2	CGCM2-B2	CSIRO-A2	CSIRO-B2	HADCM3-A2	HADCM3-B2
t2	2.71	3.07	1.67	2.51	1.82	1.78
t5	4.49	6.94	3.84	7.63	4.39	4.66
t10	7.91	11.56	7.37	18.73	9.20	10.65
t15	11.15	16.17	10.80	29.91	13.92	17.45
t20	13.99	20.14	13.70	42.71	19.29	25.71
t50	28.73	38.13	31.47	129.88	51.40	101.73
2050s	**CGCM2-A2**	**CGCM2-B2**	**CSIRO-A2**	**CSIRO-B2**	**HADCM3-A2**	**HADCM3-B2**
t2	1.62	2.11	2.05	1.46	2.36	1.72
t5	2.63	3.97	6.79	2.61	9.3	3.85
t10	3.77	6.16	18.68	4.96	24.35	7.26
t15	4.73	8.35	34.82	7.31	39.84	10.44
t20	5.51	10.25	51.96	10.05	57.79	13.77
t50	9.04	19.01	229.81	29.92	165.45	35.02
2080s	**CGCM2-A2**	**CGCM2-B2**	**CSIRO-A2**	**CSIRO-B2**	**HADCM3-A2**	**HADCM3-B2**
t2	2.33	2.48	1.45	1.68	1.40	1.61
t5	3.81	5.17	2.85	3.78	2.82	3.15
t10	5.17	8.49	5.49	7.94	5.36	5.02
t15	6.17	11.91	8.43	11.85	7.72	6.43
t20	6.93	14.93	11.16	16.11	10.30	7.74
t50	9.93	29.25	31.98	42.36	24.17	13.97

5.10.6 Srahrevagh Catchment

Projected changes in the monthly mean flow regime for the Srahrevagh catchment are displayed in Figure 5.29. For the 2020s there is no clear indication of any change in the flow regime outside the bounds of reference variability. The seasonality of the streamflow regime begins to become more pronounced by the 2050s with significant changes in catchment discharge returned for the months of September and December. By the 2080s the seasonality of the flow regime, it is suggested, will be enhanced further. Increases in December are deemed to be significant whilst decreases in streamflow are shown to be significant for August and September. For the remaining months model simulations are not considered to be significant.

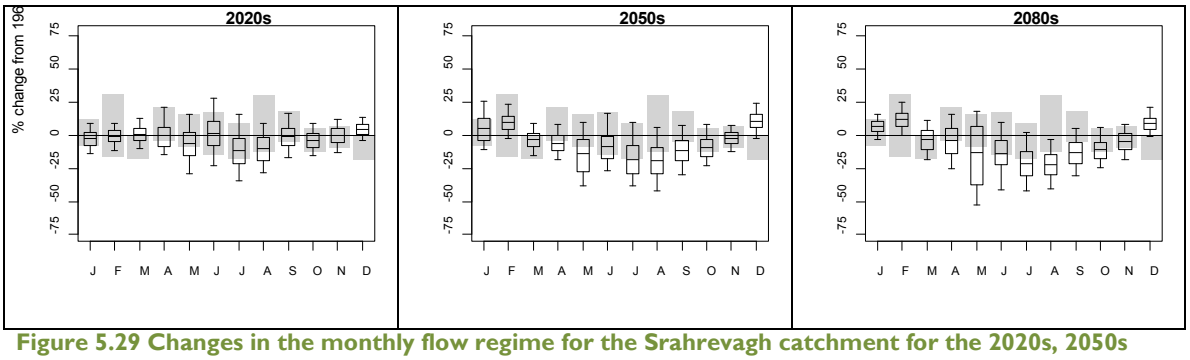

Figure 5.29 Changes in the monthly flow regime for the Srahrevagh catchment for the 2020s, 2050s and 2080s relative to the control period 1961-90.

Changes in the full range of flow conditions for the Srahrevagh over each future time horizon are examined using: Q05, Q50 and Q95. The cumulative distribution functions in Figure 5.30 display the model simulated changes for each percentile. Projections suggest a decrease in extreme low flows is likely with their occurrence becoming more frequent as the century progresses. Also noteworthy is the projected increase in Q05 flows.

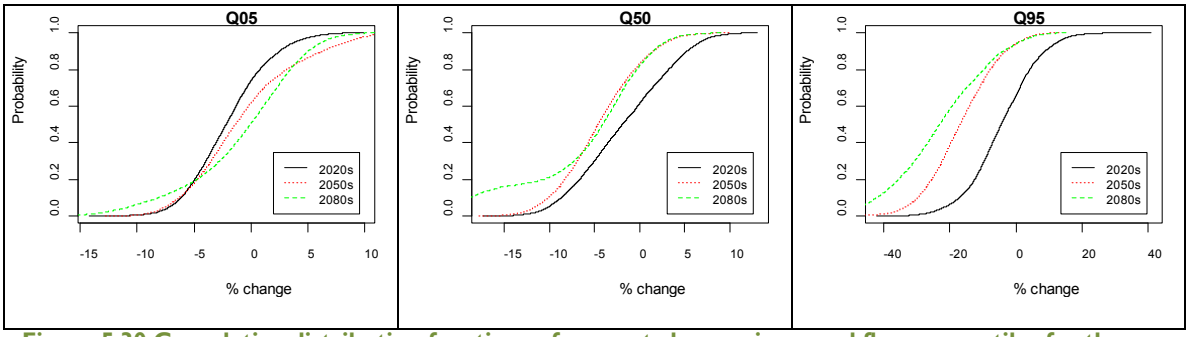

Figure 5.30 Cumulative distribution functions of percent changes in annual flow percentiles for the Srahrevagh catchment

Model returned changes in the frequency of Q95 flow events for the Srahrevagh catchment are displayed Figure 5.31. Model simulations suggest an increase in the frequency of low flow events for future period - with increases of 9.18, 19.95 and 29.27 days projected for the 2020s, 2050s and 2080s respectively. On a seasonal basis the greatest increase in the number of low flow days is projected to occur for the summer (18.95) over the 2080s. Uncertainty ranges are also largest for this season, particularly for the 2080s, with model simulations ranging from a reduction of almost 12 days per annum to an increase of up to 50. Spring and autumn also exhibit a notable shift in the average occurrence of low flows with an increase of 8.17 and 5.4 for the 2080s respectively.

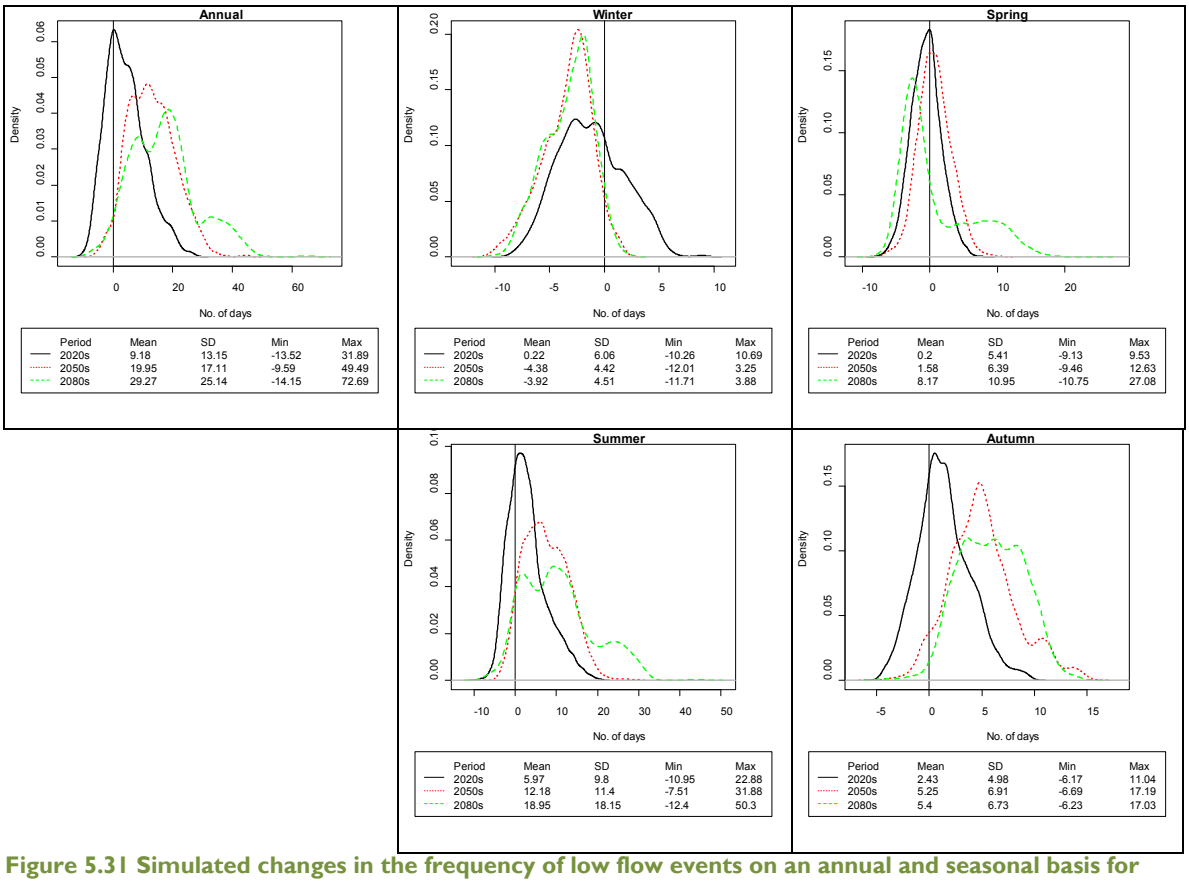

Figure 5.31 Simulated changes in the frequency of low flow events on an annual and seasonal basis for each future time period in the Srahrevagh catchment

Figure 5.32 depicts the simulated changes in the duration of low flow events. On an annual basis an increase in the duration of low flow events is evident for the each future horizon with increases of .59, 3.3 and 2.63 days for the 2020s, 2050s and 2080s respectively. The greatest increases in the duration of low flows conditions are returned for spring and summer over the 2080s, with the latter showing an increase of over 7 days.

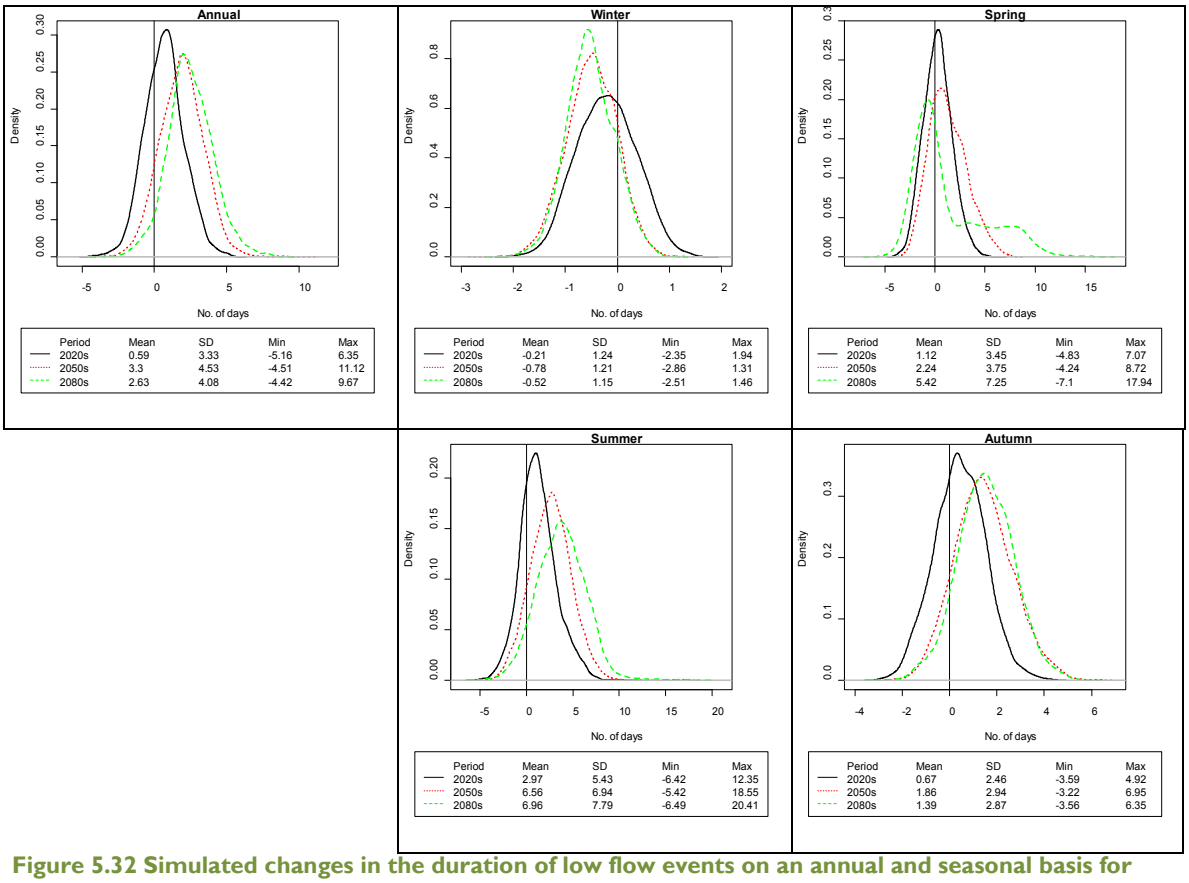

Figure 5.32 Simulated changes in the duration of low flow events on an annual and seasonal basis for each future time period in the Srahrevagh catchment.

Table 5.14 displays the projected changes in the frequency of selected flood events for each future time period. Model simulations which employed climate data from the CGCM2 GCM project a decrease in the return period for all flood events over each time horizon. A reduced frequency of occurrence for a number of flood events is suggest by the CSIRO A2 and B2 models as well as the Hadley A2 GCM for the 2020s and 2050s. However, by the end of the century all runs with the exception of CSIRO model suggest a decrease in the return period for all events of a given magnitude. In the most extreme case (CGCM2-A2) the current flood with a return period of 50 years is likely to occur once every 7.08 years by the 2080s.

Table 5.14 Changes in the frequency of selected flood recurrence intervals from the control period for each future time period

2020s	CGCM2-A2	CGCM2-B2	CSIRO-A2	CSIRO-B2	HADCM3-A2	HADCM3-B2
t2	1.98	2.91	1.71	2.42	1.71	1.71
t5	3.94	5.73	3.96	7.41	3.80	4.28
t10	6.73	8.17	7.34	16.53	7.31	9.19
t15	8.55	10.35	10.62	26.27	10.97	13.52
t20	10.22	12.35	13.83	35.41	14.23	18.87
t50	19.32	19.63	29.94	98.26	37.03	49.76
2050s	CGCM2-A2	CGCM2-B2	CSIRO-A2	CSIRO-B2	HADCM3-A2	HADCM3-B2
t2	1.62	2.16	2.13	1.49	2.14	1.67
t5	2.52	3.70	6.87	2.79	7.68	3.47
t10	3.66	5.01	16.10	5.07	19.56	6.13
t15	4.37	6.18	26.82	7.48	33.74	8.11
t20	5.00	7.26	38.66	9.76	47.41	10.29
t50	8.26	11.17	114.49	26.01	158.33	20.24
2050s	CGCM2-A2	CGCM2-B2	CSIRO-A2	CSIRO-B2	HADCM3-A2	HADCM3-B2
t2	2.21	2.33	1.48	1.72	1.39	1.53
t5	3.36	4.22	2.85	4.12	2.68	2.80
t10	4.48	5.87	5.10	8.51	4.67	4.30
t15	5.08	7.35	7.48	13.24	6.58	5.27
t20	5.57	8.71	9.97	17.71	8.18	6.24
t50	7.08	13.69	24.47	49.14	17.84	9.93

5.11 Implications for the Catchment

For any given catchment system changes in local climate conditions have the potential to fundamentally alter key aspects of their hydrological cycle including the generation of surface runoff, groundwater recharge, evapotranspiration rates and the dynamics of groundwater-surface water interactions. In the context of this study the impact of climate change on the streamflow regime of each catchment was assessed. A flow regime describes the average seasonal behaviour of flow and encompasses the timing, size and duration of flow events in a river system. Flow regimes influence the morphology of river channels, biodiversity and key processes which sustain the aquatic ecosystem. In this regard maintaining a 'natural' flow regime is essential to the ecological health and overall well being of a catchment system. Any alterations in climate therefore have potentially far-reaching implications not just for flow conditions but for other aspects of the catchment which are directly and indirectly linked to this. Outlined below are some of the key findings for the catchments included in this study

followed by a number of general conclusions which can be made regarding the impact climate change is likely to have on the Burrishoole system as a whole.
Due to the projected increase in winter precipitation average streamflow is expected to increase by up to 25% for the months of January and/or December for all catchments over the period 2069-2099. For the month of June reductions of up to 40% were returned for three of the selected catchments (Glendahurk, Maurmatta and Goulan). Accompanied by this is a suggested decrease in mean flow of between 15 – 40% for the months of September, October and August variously across all catchments. A reduction in the return period for flooding events is expected for each catchment, the most extreme of which are associated with the Glendahurk, Altahoney and Goulan with exhibited reductions in the return period of a 50 year event to between 7 and 9 years by the 2080s. Model simulations indicate an increase in extremely low summer flow for each catchment, an outcome which is commensurate with the projected decreases in summer precipitation. For all catchments, by the 2080s, model simulations suggest an increase in the number of extreme low flows days (≤Q95) of between 13 and 20%. Associated with this is an increase of between 4 and 7 days in the consecutive number of days for which flows are equal to or below the Q95 threshold for all catchments during the summer season. Model simulations suggest that the incidence of summer low flows will increase as the century progresses.

Given the similarity of their physical characteristics (e.g. soil type, land-use, etc.) model simulations for each catchment were shown to largely agree in terms of both the timing and magnitude of projected changes in their respective flow regimes. This aspect of the model results allows robust inferences to be made about the overall response of the Burrishoole system to changes in local climate conditions and the implications this may have for its aquatic environment as well as the overall management of the catchment itself.

A number of general conclusions can be made regarding key changes in the streamflow hydrology of the Burrishoole system under the conditions of future climate forcing.

- Model simulations suggest an amplification of the seasonal flow regime for all catchments (i.e. higher winter flows accompanied by lower summer flows) with this underlying trend becoming more pronounced as the century progresses.
- A shift in mean flow (Q50) conditions for a number of months was found with projected changes being deemed significant (i.e. outside the bounds of natural variability under baseline climate conditions) over the 2050s and to a greater extent

the 2080s. Simulated changes in mean monthly flows over the 2020s were found not to be significant with regards to reference variability.

- An increase in the incidence of extreme low flows (Q95), most notably during the summer and spring seasons, is projected. Associated with this is a suggested increase in the average number of consecutive days for which flows are equal to or below the Q95 threshold. Low flow events are anticipated to become more frequent through the latter half of the century.
- An increase in the occurrence of peak discharge events, characterized using the Q05 flow threshold, is projected. Associated with this is a reduction in the return period for flooding events. Model simulations suggest the frequency of extreme high flows will increase as the century progresses.

As noted by Krasovskaia and Gottschalk (2002) the characteristics of a catchments flow regime are dependent on the climate and physiographic features of the drainage area. Advancing this it can be said that the characteristics of any catchment play a central role in determining its capacity to exacerbate or mitigate changes in streamflow arising from alterations in local climate conditions. The response of the Burrishoole catchment to projected changes in the local precipitation regime, embodied by the principal findings from this study outlined above, can be linked to the physical attributes of the system itself.

The climate scenarios developed for the Burrishoole catchment suggest an increasing tendency towards a more distinct seasonal precipitation regime leading to wetter winters and drier summers with this trend likely to become more pronounced over the latter part of the century. In catchments whose hydrological regime is significantly influenced by groundwater flow increased winter receipts can be beneficial by recharging groundwater stores to a higher level and thus providing ample baseflow with which to sustain river levels during drier periods of the year. Essentially groundwater dominated catchments have the capacity to store the additional rainfall received during the winter for release during the drier summer months. The Burrishoole system however does not possess the storage properties required to moderate the influence of an increasingly seasonal rainfall regime. The catchment is underlain by relatively unproductive aquifers limiting its overall groundwater storage capacity. This feature of the Burrishoole system leaves it vulnerable to the anticipated changes in its precipitation regime, a fact underlined by the suggested increase in the occurrence of extreme low flows especially during the drier summer months.

The topography of each catchment, along with the dominance of blanket peat, promotes the rapid transmission of rainfall received over the drainage area to the stream network. This aspect of the Burrishoole's hydrological system impedes groundwater recharge and contributes to the 'flashy' nature of the flow response to precipitation events. In essence the Burrishoole system lacks the capacity to buffer or dampen the flood causing potential of heavy rainfall events suggesting it is sensitive to more intense precipitation events. This assertion is backed-up by the projected increase in the frequency of high flow and flooding events under changing climate conditions.

Of specific interest in this study are the impacts of a changing flow regime on the catchments capacity to sustain and nurture indigenous stocks of Atlantic salmon. As hydrological conditions are of fundamental importance to the well being of salmonid fish anticipated changes in different components of the natural flow regime, including mean and extreme conditions, have wide ranging implications for Atlantic salmon populations in the Burrishoole catchment.

It is known that each component of the natural flow regime (e.g. high, mean and low flows) play an important role in different aspects of the salmon's life cycle. Spates are required for fish migration while flooding events are beneficial for de-silting spawning gravels and contribute to the overall maintenance of the stream network. Low and medium flows control the amount of available habitat and have a significant influence on fish migration. As pointed out by Gilvear et al. (2002) hydrology determines not only the physical habitat in which salmon live but the organisms on which they feed, who themselves are also dependent on flow conditions. This alludes to the multiple direct and indirect relationships which exist between river flow and salmonid populations.

Outlined below are the potential impacts of climate induced alterations in different aspects of a flow regime for each life stage of the Atlantic salmon as presented by Walsh and Kilsby (2007).

Spawning and Egg Deposition

- An increase in flash flooding could lead to the wash out of eggs laid in gravels.
- A sudden decrease in flows levels could leave redds stranded out of water before fertilization or after preventing the emergence of fry.
- Higher flows may lead to increased sediment loads which could cause the siltation of redds.
- The reduced availability of spawning habitat caused by decreased or increased flows.

Alevins

- An increase in flow velocity could lead to the displacement of newly emerged salmon downstream.
- *Juvenile Salmon*
- Successive reduced flow years may have a detrimental effect on salmon stocks, taking years to recover.

Smolts, Migration and Returning Salmon

- Wetter Springs may induce earlier migration of smolts to sea which may reduce survival capacity in the marine environment.
- A reduction in the number of spates may hamper the upstream migration of returning fish.
- Rapid reductions in flow may lead to stranding of migratory salmonids.

5.12 Summary

To assess the potential impacts of climate change on the Burrishoole catchment system a conceptual rainfall-runoff model was employed to simulate streamflow under the forcing conditions of future climate using scenarios derived from grid-scale GCM output. To account for the uncertainty associated with local-scale estimates of future climate change the output from three GCMs (HadCM3, CSIROmk2 and CGCM2), each run under both the A2 and B2 SRES emission scenarios, were downscaled using two different regression-based methods. Flow conditions for each of the five selected sub-catchments which comprise part of the greater Burrishoole catchment system, along with the adjacent Glendahurk catchment, were modelled using the downscaled climate scenarios. To address the uncertainty associated with identifying optimum parameter values an ensemble of equally plausible parameter sets were used when modelling future conditions for each catchment. Model projections were considered over three future time horizons (2020s, 2050s and 2080s) relative to the standard baseline period (1961-1990). To determine whether simulated changes could be correctly attributed to an anthropogenically induced shift in local climate conditions the natural variability of the flow regime under 'current' and future climate was explicitly considered when interpreting results.

Given the similarity of each of the six selected catchments, in terms of their physiographic features, their response to changing climate conditions is taken to be representative of changes in the hydrology of the Burrishoole system as a whole. This is defensible given the correspondence shown between the model results for each individual catchment. Generally model simulations suggested an increasing tendency towards a more distinct seasonal

streamflow regime across the catchment with higher flows occurring in winter (DJF) and lower flows during the summer (JJA) and autumn (SON). This is commensurate with predicted changes in the catchments precipitation regime. Increased winter flows coupled with the fast response time of the Burrishoole system leave it vulnerable to more intense precipitation events. This manifests itself in a projected decrease in the return period for peak discharge and flooding events. Also suggested is an increase in summer and spring low flows. In general the results suggest a greater deviation from reference conditions, for both mean and extreme flows, as the century progresses with changes being more acute under the A2 emission scenario when compared to the less carbon intensive B2 scenario.

Any alterations in the prevailing flow conditions, or what can be taken as the 'natural' flow regime, have significant implications for the well-being of the Burrishoole catchments aquatic ecosystem including its capacity to sustain and nurture Atlantic salmon populations. All aspects of a river systems streamflow regime, including extreme flows, play an important role at each stage in the salmon's life cycle. However a more extreme flow regime, as is suggested by model projections, has the potential to significantly disrupt the habitat conditions required to sustain salmon populations and allow them to successfully complete different stages in their life cycle. In this regard understanding the implications of a climate induced shift in the flow regime is important when devising future management strategies and making policy decisions for the catchment.

The Burrishoole system remains relatively untouched by human activity and as such future management will present unique challenges as reducing the human impact (e.g. removing impoundments and modifications, greater control on pollution, reducing abstractions) on it will not play as great a role in mitigating the long term effects of climate change when compared with other catchments which have been subjected to significant human interference. Managing the catchment will essentially require adaptation to and mitigation of a shift in the 'natural' flow regime which will be difficult given the physical characteristics of the catchment itself. Future management strategies may look at altering land-use practices across the catchment or examine the possibilities for micro-managing different aspects of the stream channels themselves, including their morphology and riparian zones, with a view to sustaining optimal habitat conditions (e.g. spawning grounds) for Atlantic salmon populations.

5.13 Key Findings

- Projected changes in streamflow for each catchment were found to be relatively similar with no one catchment exhibiting deviations from the general trend in changing flow conditions found across the Burrishoole system. This is indicative of the relatively similar physical characteristics presented by each catchment.
- Given the dominant role runoff plays in shaping each catchments hydrology, projected changes in streamflow conditions are predominantly driven by, and are sensitive to, alterations in the local precipitation regime (i.e. wetter winters and drier summers).
- An increase in the seasonality of the flow regime (i.e. higher winter flows and lower summer flows) is projected for all catchments with this underlying trend becoming more pronounced as the century progresses.
- Changes in mean flows for each month over the 2020s were deemed to lie within the bounds of natural variability for the baseline period and thus could not be clearly attributed to the underlying climate change 'signal'. This is a finding common to all selected catchments.
- By the 2050s model simulations suggest a clear shift in mean flow conditions outside reference variability for some months. The most consistent changes across each catchment were found for to occur for the winter (DJF) and autumn (SON) months. Comparatively fewer significant changes for the spring (MAM) and summer (JJA) months were found.
- Over the 2080s mean monthly flows deviate further from baseline conditions and as such projected changes for a greater number of months were deemed to be significant with regards to baseline variability. Significant increases in mean flow for the months of January and December, accompanied by decreases for the months of June, October and August, are suggested for the majority of catchments.
- The incidence of extreme low flows, defined using the Q95 flow threshold, is anticipated to increase during the summer and spring seasons with this trend becoming more pronounced through the latter part of the century.
- A reduction in low flows is accompanied by an increase in the average number of consecutive days for which streamflow is equal to or less than the Q95 threshold. This was found to be most extreme for the spring and summer seasons over the 2080s.
- Model simulations indicate an increase in high flows (Q05) as the century progresses with deviations from reference conditions being most apparent over the latter half of the century.
- Although there is a degree of inter-model variability regarding the projected return period for flooding events it is generally evident that the occurrence of floods will

increase. This is a finding common to each catchment and is more extreme under the A2 emissions pathway.

- The absence of any significant storage capacity across the Burrishoole system suggests that it is unable to provide any natural means of flow regulation which could moderate the impact of an increasingly seasonal rainfall regime on flow conditions - thereby leaving the catchment vulnerable to changes in local climate. This is illustrated by the projected increase in low flows during the summer months when baseflow is required to sustain river levels.
- The 'flashy' nature of the streamflow response to precipitation events, a trait exhibited by all catchments, highlights the inability of each system to buffer or dampen the impact of heavy rainfall on peak discharge. This alludes to the sensitivity of the catchment to any intensification in its rainfall regime under future climate forcing, a point underlined by the projected increase in high flow and flooding events.
- Projected changes in the flow regime for the Burrishoole catchment have potentially significant implications for the catchments aquatic ecosystem including its capacity to sustain and nurture Atlantic salmon populations.
- Management of the catchment will require explicit consideration of the likely impacts climate change will have on its hydrological regime.

5.14 References

Arnell, N. (2003) 'Relative effects of multi-decadal climatic variability and changes in the mean and variability of climate due to global warming: future streamflows in Britain', Journal of Hydrology, 270, 195-213.

Arnell, N.W. and Reynard, N.S. (1996) 'The effect of climate change due to global warming on river flows in Great Britain', Journal of Hydrology, 183, 397-424.

Beck, M.B. (1987) 'Water quality modeling: a review of the analysis of uncertainty', Water Resources Research 23, 938-944.

Beven, K.J. (2006) 'A manifesto for the equifinality thesis', Journal of Hydrology, 320 (1–2), 18–36.

Beven, K.J. and Freer, J., (2001) 'Equifinality, data assimilation, and uncertainty estimation in mechanistic modeling of complex environmental systems using the GLUE methodology', Journal of Hydrology, 249, 11–29.

Beven, K. (1993) 'Prophecy, reality and uncertainty in distributed hydrological modelling', Advances in Water Resources, 16, 41-51.

Beven, K., Binley, A. (1992) 'The future of distributed models-model calibration and uncertainty prediction', Hydrological Processes, 6, 279-298.

Blazkova, S. and Beven, K.J. (2002) 'Flood frequency estimation by continuous simulation for a catchment treated as ungauged (with uncertainty)', Water Resources Research, 38(8), 1139.

Boé, J., Terray, L., Habets, F. and Martin, E. (2007) 'Statistical and dynamical downscaling of the Seine basin climate for hydro-meteorological studies', International Journal of Climatology, 27(12), 1643-1655.

Boer, G. B., Flato, G., and Ramsden, D. (2000) 'A transient climate change simulation with greenhouse gas and aerosol forcing: projected climate to the twenty-first century',Climate Dynamics, 16: 427–450.

Booij, M.J. (2005) 'Impact of climate change on river flooding assessed with different spatial model resolutions', Journal of Hydrology, 303, 176-198.

Butts, M.B., Payne, J.T., Kristensen, M., Madsen, H. (2004) 'An evaluation of the impact of model structure on hydrological modeling uncertainty for stream-flow simulation', Journal of Hydrology 298, 242-266.

Cameron, D., Beven, K., Naden, P. (2000) 'Flood frequency estimation by continuous simulation under climate change (with uncertainty)', Hydrology and Earth System Sciences, 4(3), 393-405.

Charlton, R. and Moore, S. (2003) The Impact of Climate Change on Water Resources in Ireland. In Sweeney, J. et al. "Climate Change, Scenarios and Impacts for Ireland", EPA Publication, 81-102.

Campolo, M., Andreussi, P. and Soldati, A. (1999) 'River flood forecasting with a neural network model', Water Resources Research. 35(4), 1191–1197.

Cunnane, C. and Regan, S. (1994) Hydrology and freshwater resources, in, McWilliams, B.E., (ed) Climate Change: Studies of the implications for Ireland. Department of the Environment, Stationery Office, Dublin, 89-108.

Déqué, M. (2007) 'Frequency of precipitation and temperature extremes over France in an anthropogenic scenario: Model results and statistical correction according to observed values', Global and Planetary Change, 57,16–26.

Diaz-Nieto, J. and Wilby, R.L. (2005) 'A comparison of statistical downscaling and climate change factor methods; impacts on low flows in the River Thames, United Kingdom', Climatic Change, 69(2-3), 245-268.

Duan, Q., Sorooshian, S., and Gupta, V. K. (1992) 'Effective and efficient global optimization for conceptual rainfall-runoff models', Water Resources Research, 28(4),1015-1031.

Fowler, H.J. and Kilsby, C.G. (2007) 'Using regional climate model data to simulate historical and future river flows in northwest England', Climatic Change, 80(3-4), 337-367.

Freer, J., Beven, K.J., Ambroise, B. (1996) 'Bayesian estimation of uncertainty in runoff prediction and the value of data: an application of the GLUE approach', Water Resources Research, 32(7), 2161–2173.

Friedland, K.D., MacLean, J.C., Hansen, L.P., Peyronnet, A.J., Karlsson, L., Reddin, D.G., Ó Maoiléidigh, N. and McCarthy, J.L. (2009) 'The recruitment of Altantic salmon in Europe', ICES Journal of Marine Science 66(2):289-304

Gardiner, M.J. and Radford, T. (1980) Ireland, General Soil Map. National Soil Survey, Dublin.

Gilvear, D.J., Heal, K.V. and Stephen, A. (2001) 'Hydrology and the ecological quality of Scottish river ecosystems', The Science of the Total Environment 294, 131-159.

GSI (2003) Geological Survey of Ireland, Draft National Aquifer Map.

Harlin, J. and Kung, C.S. (1992) 'Parameter uncertainty and simulation of design floods in Sweden', Journal of Hydrology, 137, 209-230.

Holden, J. and Burt, T.P. (2003) 'Hydrological Studies on Blanket Peat: The Significance of the Acrotelm-Catotelm Model', Journal of Ecology, 91(1), 86-102.

Hornberger, G.M., and Spear, R.C., (1981) 'An approach to the preliminary analysis or environmental systems', Journal of Environmental Management, 12, 7-18.

Hosking J.R.M and Wallis, J.R. (1997) Regional frequency analysis: an approach based on L-moments. Cambridge University Press, 224pp.

Hulme, M. and Jenkins, G. J. (1998) Climate Change Scenarios for the U.K.: Scientific Report, UKCIP Technical Report No. 1, Climatic Research Unit, Norwich, 80 pp

Krasovskaia I. and Gottschalk (2002) 'River Flow Regimes in a Changing Climate', Journal of Hydrological Sciences, 47(4), 597.

Landwehr, J.M., Matalas, N.C., and Wallis, J.R. (1979) 'Probability weighted moments compared with some traditional techniques for estimating Gumbel parameters and quantiles', Water Resources Research, 15, 1055-64.

Manley, R.E. (1993) HYSIM Reference Manual. R.E. Manley Consultancy, Cambridge. 63pp.

Marshall, L., Nolt, D. and Sharma, A. (2007) Towards dynamic catchment modelling: a Bayesian hierarchical mixtures of experts framework. Hydrological Processes, 21(7), 847-861.

Melching, C.S. (1995) Reliability Estimation. In: Singh, V.P. (Ed.) Computer Models of Watershed Hydrology, Water Resources Publications, Colorado.

Minns, A.W. and Hall, M.J. (1996) 'Artificial neural networks as rainfall runoff models', Hydrological Sciences, 41(3), 399–417.

Montanari, A. (2005) 'Large sample behaviours of the generalized likelihood uncertainty estimation (GLUE) in assessing the uncertainty of rainfall–runoff simulations', Water Resources Research, 41.

Montanari, A., (2007) 'What do we mean by 'uncertainty'? The need for a consistent wording about uncertainty assessment in hydrology. Hydrological Processes', 21, 841–845.

Murphy, C. and Charlton, R. (2008) Climate Change and Catchment Hydrology, in Sweeney, J. (ed.) Climate Change: Refining the Impacts. Environmental Protection Agency, Johnstown Castle, Wexford, Government Publications.

Murphy, C., Fealy, R., Charlton, R. and Sweeney, J.S. (2006) 'The reliability of an "off the shelf" conceptual rainfall-runoff model for use in climate impact assessment: uncertainty quantification using Latin Hypercube Sampling', Area, 38(1), 65-78.

Niel H, Paturel JE, and Servat E (2003) 'Study of parameter stability of a lumped hydrologic model in a context of climatic variability', Journal of Hydrology, 278, 213–230.

O'Sullivan, G. (ed.) (1994) CORINE Land Cover Project (Ireland). Project Report, December 1994. Ordnance Survey of Ireland and Ordnance Survey of Northern Ireland Belfast, Dublin.

Pilling, C.G. and Jones, J.A.A. (1999) 'High resolution climate change scenarios: implications for British runoff', Hydrological Processes, 13, 2877-2895.

Poole, W.R., (1994). A population study of the European Eel (Anguilla anguilla (L.)) in the Burrishoole System, Ireland, with special reference to growth and movement. PhD Thesis, Dublin University; 416pp.

Prudhomme, C and Davies, H. (2009) 'Assessing uncertainties in climate change impact analyses on the river flow regimes in the UK. Part 2: future climates', Climatic Change, 93(1-2), 197-222.

Prudhomme, C., Dorte, J. Svensson, C. (2003) 'Uncertainty and climate change impact on the flood regime of small UK catchments', Journal of Hydrology, 277, 1-23.

M.P. Rajurkar, M.P., Kothyari, U.C. and Chaube, U.C. (2004) 'Modeling of the daily rainfall-runoff relationship with artificial neural network', Journal of Hydrology, 285(1-4), 96-113.

Refsgaard, J.C., der Sluijs, J.P., Brown, J., and van der Keur, P. (2006) 'A framework for dealing with uncertainty due to model structure error', Advances in Water Resources, 29,1586–1597.

Robson, A. and Reed, D. (1999) Flood Estimation Handbook. 3. Statistical procedures for flood frequency estimation. Institute of Hydrology, Wallingford.

Sefton, C.E.M. and Boorman, D.B. (1997) 'A regional investigation into climate change impacts on UK streamflows', Journal of Hydrology, 195, 26-44.

Smith, G. (2005) Environmental Protection Agency Hydrological Digital Elevation Model (DEM). Information available at http://www.epa.ie/metadataxml/written/DTM.xml.

Sorooshian, S., Gupta, V. K. (1995) Model calibration. In: Computer Models of Watershed Hydrology, V. P. Singh, (Ed.), Water Resources Publications, 23–63.

Steele-Dunne, S., Lynch, P., McGrath, R., Semmler T., Wang, S., Hanafin, J., Nolan, P. (2008) 'The impacts of climate change on hydrology in Ireland', Journal of Hydrology 356, 28–45

Taylor, E. B. (1991) 'A review of local adaptation in Salmonidae, with particular reference to Pacific and Atlantic salmon', Aquaculture, 98: 185–207

Uhlenbrook, S., Seibert, J., Leibundgut, C. And Rodhe, A. (1999) 'Prediction uncertainty of conceptual rainfall runoff models caused by problems in identifying model parameters and structure', Hydrological Sciences Journal 44(5), 779-797.

Walsh, C.L. and Kilsby, C.G. (2007) 'Implications of climate change on flow regime affecting Atlantic salmon', Hydrol. Earth Syst. Sci., 11(3), 1127-1143.

Wilby, R.L. (2005) 'Uncertainty in water resource model parameters used for climate change impact assessment', Hydrological Processes, 19 (16) 3201-3219.

Wilby, R.L. and Harris, I. (2006) 'A Framework for assessing uncertainties in climate change impacts: Low flow scenarios for the River Thames, UK.', Water Resources Research, 42, W02419, doi:10.1029/2005WR004065

Winfield, I.J., James, B.J., and Fletcher, J.M. (2004) A Review of the Implications of Climate Change for Atlantic Salmon. Unpublished Report for the University of Newcastle upon Tyne. Centre for Ecology and Hydrology, Windermere, Ambleside, UK.

Wood, A., Leung, L.R., Sridhar, V., and Lettenmaier, D.P. (2004) 'Hydrologic implications of dynamical and statistical approaches to downscaling climate outputs', Climatic Change, 62,189–216.

Young, P.C., (1983). The validity and credibility of models for badly defined systems. In Beck, M.B. and Van Straten G. (eds) Uncertainty and Forecasting of Water Quality. Springer Verlag, New York, pp.69-98.

6 Modelling Climate Change Impacts on Key Water Quality Parameters in the Burrishoole Catchment

Eleanor Jennings, Rachel Erdil and David Taylor

6.1 Introduction

Projected changes in climate if realised are likley to affect a range of water quality parameters which in turn impact on fish growth and survival. These parameters include water temperature, water dissolved oxygen (DO) and dissolved organic carbon (DOC) concentrations. As reviewed in Chapter 2, increases in RWT can have a direct influence on fish survival through an increase in the number of days when temperatures exceed critical threshold values. In addition, although most salmonid spawning and juvenile growth stages occur in fluvial systems, changes in lake water temperature (LWT) may also affect survival rates. Inshore areas of Lough Feeagh, for example, provide nursery habitat for older age classes (Matthews et al., 1997). The lake is also the main feeding area for salmon during smoltification, the final months of the freshwater cycle before they migrate to sea. Recent research has also highlighted the positive impact of higher spring water temperature in the Burrishoole system on salmon survival during smoltification (McGinnity et al., 2009). When thermal stratification develops in lakes during warm calm weather, warmer upper waters are separated from cooler deeper waters by a thermocline, a water layer over which temperature drops rapidly (Imberger and Patterson, 1989; Wetzel, 2001). These lower waters can provide a refuge for salmonids during periods of high water temperature (Tanaka et al., 2000; Mathes et al., 2010).

In addition to these direct temperature impacts, and as reviewed in Section 2.3.1, fish are also particularly sensitive to low DO concentrations (Alabaster and Gough, 1986; Youngson et al., 2004; Greig et al., 2006). Temperature is one of the key drivers of changes in DO solubility. However, DO levels are also related to decomposition of organic carbon and to rates of primary production. In humic lakes such as Lough Feeagh, DOC supplying the microbial portion of the food-web, may be an equal or more important source of carbon than primary production (Prairie, 2007). Mineralisation of even a small portion of this carbon may fuel the upper trophic levels, including fish, via the bacterioplankton-protozoan link (Tranvik, 1992; Tulonen et al., 1992; Kankaala et al., 1996; Drakare et al., 2002; Prairie, 2007). Both the production and transport of DOC are strongly influenced by climate and the recent large-scale

increases in DOC levels have been linked, in part, to climate (e.g. Freeman et al., 2001; Evans et al., 2006; Worrall et al., 2006; Erlandsson et al., 2008) (for review see Jennings et al., 2010). More importantly these increases in the export of DOC from catchment soils represent a transfer of carbon from long-term terrestrial stores to more labile forms that can further contribute to atmospheric concentrations of CO_2 and, therefore, potentially contribute to further warming (Knorr et al., 2005; Davidson and Janssens, 2006). In this chapter the impacts of the projected changes in climate on river water temperature (RWT), LWT, DO solubility and DOC concentrations are explored using a range of modelling techniques.

6.2 River Water Temperature

6.2.1 Introduction

Alterations in RWT have been attributed to thermal effluent pollution, deforestation, and most recently, to global climate change (Sinokrot et al., 1995; Mohseni et al., 2003; Caissie, 2006). Increased air temperatures over the past century have caused RWTs in many river systems around the world to approach the lethal limit for coldwater-adapted fish (Eaton et al., 1995). For example, in an upland river in Scotland Langan et al. (2001) found that winter RWT maxima have increased by 2°C in the last 30 years, most likely due to rising seasonal air temperature. Similarly, in a study of Minnesota (USA) streams, Mohseni et al. (2003) used models to project that, with a doubling of atmospheric CO_2 concentrations and the corresponding effects on RWT, habitats for coldwater fish would decrease by 36%. Under future projected global warming, RWT will almost certainly rise further, altering fish habitat ranges, necessitating adaptive responses from fish and new management strategies, and possibly resulting in biodiversity loss (Schindler, 2001; Caissie, 2006).

6.2.2 Review of RWT models

A review of the literature on simple river water temperature modelling approaches based on air temperature was undertaken in order to inform the selection of an effective model for the Burrishoole catchment. A wide variety of models has have been developed to simulate RWT and, in turn, to project future RWT in attempts to better understand the impact of global climate change on aquatic ecosystems. Water temperature in a given river is dependent on physical characteristics of the watershed and surrounding atmosphere, in particular air temperature, solar radiation, relative humidity, wind speed, stream depth, and groundwater inflow (Sinokrot and Stefan, 1994; Mohseni and Stefan, 1999). Deterministic heat budget models, which take into account all of the influential parameters, have been constructed to estimate hourly and daily RWT within 0.2 and 1.0°C, respectively (Sinokrot and Stefan, 1993). While providing excellent predictive capabilities, heat budget models require a large amount of

meteorological data. This can pose a problem in climate change impacts studies because many meteorological parameters cannot be accurately projected for future time periods using Global Climate Models (GCMs) (Lau et al., 1996).

Conversely, linear and logistic regression based models and moving average methods have been developed to simulate RWT using air temperature as the dominant or sole predictor variable. These approaches have been favoured because of the ease of air temperature data acquisition, the reasonable approximation of RWT that they provide, and because air temperature is one of the most accurately projected climate variables using global climate models (GCMs) (Lau et al., 1996; Webb et al., 2003). In their physical interpretation of the heat budget for a river, Mohseni and Stefan (1999) illustrated that air temperature is a good predictor of RWT because the primary heat exchange in most river systems is at the water-atmosphere interface. Long term studies of trends in air and water temperatures have further supported this conclusion. Using 25 years of air and RWT data, Hari et al. (2006) found regionally coherent warming in Swiss rivers and streams at all altitudes which corresponded closely with rising regional air temperatures. Similarly, Webb (1987, 1992) found an almost 1:1 relationship between weekly and monthly mean RWT and air temperature for 36 streams in the UK. Following on from Webb's early work, Arnell (1998) stated in a review of stream research in the UK that the temperature of river water in Britain is largely determined by air temperature, except when cooler groundwater dominates inflows or in shady reaches of streams. Additional factors such as the time scale of analysis, other stream characteristics (e.g. wind sheltering), and regional climate can also affect the linearity of the air-river water temperature correlation (Erickson and Stefan, 2000). Some researchers have argued that because of these confounding factors, models based solely on air temperature data are over-generalisations of the complex thermal regime of rivers (Mohseni et al., 1998; Bogan et al., 2004).

In order to improve the fit of air-water temperature models to data from any catchment, it is important to understand the factors, such as catchment characteristics and hydrology, time scale, seasonality, and regional climate can affect the relationship. Air and water temperatures are most highly correlated when a river is well-mixed in the vertical and transverse directions of a cross-section and when the primary heat exchange occurs at the air-water interface (Erickson and Stefan, 2000). The complexity of the thermal regime of rivers, however, dictates that RWT is not solely controlled by the heat exchange at the air-water interface. Secondary factors such as catchment topography, river discharge and incoming water temperature, groundwater inputs, channel shading from surrounding vegetation, and heat exchange at the

streambed, have been shown to influence RWT and alter the linearity of air-water temperature relationships (Sinokrot and Stefan, 1993; Caissie et al., 2001; Gu and Li, 2002). Multiple regression analyses in other studies have suggested that the effects of secondary factors on the heat balance of many streams are small (explaining less than 5% of the variation in RWT) compared to the influence of air temperature (Mohseni et al., 1999; Erickson and Stefan, 2000; Webb et al., 2003; Hari et al., 2006). Bogan et al. (2004) determined that in streams with high flow rates and/or large catchments, RWT was primarily controlled by atmospheric heat exchange.

Groundwater and other subsurface water inflows to rivers provide a baseflow that exerts a stabilising influence on RWT, which reduces the influences of short-term variations in air temperature (Sinokrot et al., 1995). The temperature of groundwater is fairly constant and is related to mean annual air temperature (Todd, 1980). Rivers with small watersheds or rivers heavily influenced by groundwater and subsurface water inflows may have poor air-water temperature correlations because the short residence time of the water does not allow for river water equilibration with the atmosphere (Erickson and Stefan, 2000).

River shading by riparian vegetation reduces the total incident solar radiation on a river water surface, which can dramatically affect RWT. The effect of river shading depends on river width, season, and the percentage of the upstream (above the gauging station) river length covered by riparian vegetation. Unusually elevated RWT are observed when periods of decreased shading occur simultaneously with low flow episodes (Erickson and Stefan, 2000). Similarly, wind sheltering reduces the convective heat transfer between the water surface and atmosphere. This insulating factor makes RWT less responsive to changes in air temperature (Erickson and Stefan, 2000).

Least squares linear regression models

Three types of regression models (linear, multiple, and logistic regression) have been used to model the fluctuations in RWT, primarily as a function of air temperature (e.g. Crisp and Howson, 1982; Mohseni et al., 1998; Webb et al., 2003). Simple least squares linear regression models (Equation 6.1) are usually generated using weekly mean or monthly mean air temperature data since water temperature is not often autocorrelated within that time interval, and hence linear regression models remain valid (Crisp and Howson, 1982; Elliott, 1984; Erickson and Stefan, 2000).

$T_w(t) = A + B*T_a(t)$ **Equation 6.1**

Where,

T_a °C = air temperature

T_w °C = river water temperature for a given time slice (t)

A and B are y-intercept (dimensionless) and the slope of the regression line (°C), respectively.

In a study of changes in migratory trout (Salmo trutta) populations in relation to extrinsic factors, Elliott (1984) developed an air-water temperature model using bi-weekly mean RWT from a stream in the English Lake District and regional air temperature data. The model was created using data from the period November 1966–December 1969, when air and water temperatures were highly correlated ($r^2 = 0.97$, $p < 0.001$). The linear regression model (slope 0.80 $\pm$ 0.03 at 95% confidence level) was subsequently used to estimate bi-weekly mean RWT from January 1970–April 1983. Water temperatures over 1970–1983 were occasionally manually checked to validate the assumption that observed RWT closely followed the modelled trend (Elliott, 1984). Webb and Nobilis (1997) also used the least-squares linear regression approach to create an air-water temperature model for the Krems River in Austria using 90 years of monthly mean data (slope = 0.69, $r^2 = 0.97$, RMSE<0.8°C). The model was then used to predict monthly mean RWT for 1991–1993, with RMSE <0.8°C and projected RWT always within 2°C of observed RWT values (Webb and Nobilis, 1997).

In linear regression models, the chosen time scale (data averaged over sub-daily, daily, weekly, or monthly intervals) will directly affect the regression equation in the form of changing slope and intercept (Erickson and Stefan, 2000). Few studies have used simple linear regression models with mean daily data because increased scatter and lower sensitivity have been observed using data at this time step versus weekly mean or monthly mean data (Stefan and Preud'homme, 1993; Pilgrim et al., 1998). Issues of autocorrelation also arise in daily models (Erickson and Stefan, 2000). Catchment characteristics, such as groundwater inputs, can also directly alter the slope and intercept of the regression equation (Caissie, 2006). For example, regression models for primarily non-groundwater fed streams tend to have steeper slopes with intercepts closer to 0°C, while those for groundwater-dominated streams usually show shallower regression slopes with higher y-intercepts (Caissie, 2006).

Non-linearity at extreme temperatures

Many studies have shown that the relationship between air temperature and RWT tends to depart from linearity as air temperatures fall below 0°C (Figure 6.1) (e.g. Crisp and Howson, 1982; Webb and Nobilis, 1997; Mohseni et al., 1998; Webb et al., 2003; Morrill et al., 2005). This phenomenon has been attributed to the release of latent heat associated with ice formation, which buffers the thermal regimes of rivers and prevents RWT from falling much below 0°C (Erickson and Stefan, 2000; Webb et al., 2003). Erickson and Stefan (2000) observed the same behaviour in rivers in warmer climates (i.e. Oklahoma, USA) when air temperature rose above 25°C. That behaviour was attributed to increased evaporative cooling as a result of the increased moisture-holding capacity of the atmosphere (Erickson and Stefan, 2000). Using data from 584 rivers in the USA, Mohseni et al. (1998) illustrated that across both temperature extremes, the air-water temperature relationship adopts an S-shaped curve, which can be modelled with a non-linear logistic regression.

Some investigators have tackled the non-linearity problem by eliminating periods when air temperature was below or at the freezing point in their air-water temperature models (Morrill et al., 2005). Webb and Nobilis (1997), however, did not find any evidence in their study of an Austrian catchment that deriving separate equations for the air-water temperature relationship above and below 0°C air temperature resulted in improved RWT model projections. In the moderate maritime climate of south-west England, where air temperatures rarely extend beyond the thresholds of <0°C and >25°C, Webb et al. (2003) found that the rate of increase in RWT with air temperature declined as air temperatures approached and exceeded both 0°C and 20°C. Using the logistic regression developed by Mohseni et al. (1998), Webb et al. (2003) observed clear non-linearity at extreme temperatures with hourly and daily RWT values, but not with weekly mean values. Although air temperatures in the Burrishoole catchment do not typically extend beyond these thresholds, future air temperatures may more commonly fall below 0°C or exceed 25°C as a result of global climate change (Erickson and Stefan, 2000) and the nature of (e.g. linearity) air-water temperature response relationships may change (Mohseni and Stefan, 1999).

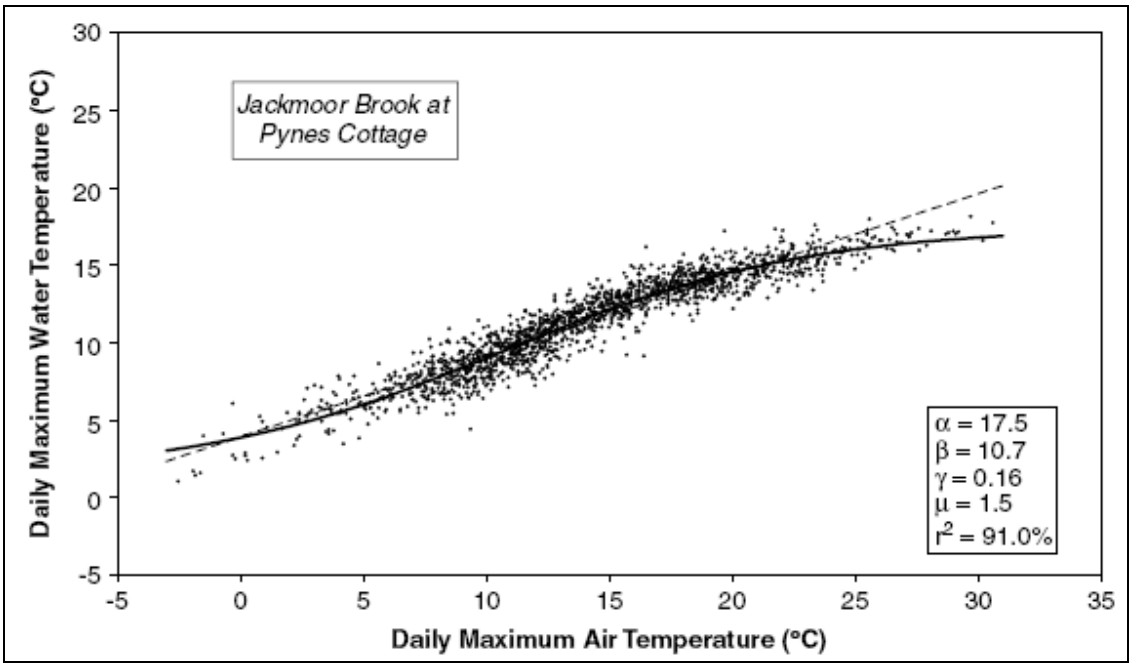

Figure 6.1: The relationship between daily maximum air and water temperature in Jackmoor Brook (UK). The solid line represents the non-linear logistic function fitted to the data. The parameters of the curve and the explained variance (r^2) are shown in the inset box. The dashed line represents a simple linear regression (from Webb et al. 2003).

Logistic regression models

Logistic regression models have been used to solve the problem of non-linearity in the air-water temperature relationship at extreme low (<0°C) and high (>25°C) air temperatures (Erickson and Stefan, 2000; Caissie et al., 2001; Webb et al., 2003; Morrill et al., 2005). The S-shaped logistic functions are constructed with hourly, daily, and weekly mean data. Linearity of the water-air temperature relationship tends to remain strong in monthly data, and hence simple linear regression models are preferred at that time step (Caissie, 2006). Most logistic regression models in the literature are based on the function developed by Mohseni et al. (1998) (Figure 6.2).

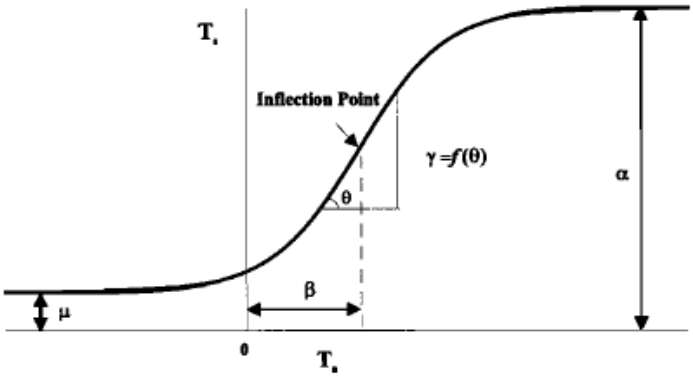

Figure 6.2: A schematic representation of the logistic function parameters (from Mohseni et al., 1998).

Exponential smoothing filter

In a study of the air-water temperature relationship in Swiss alpine lakes and rivers, Livingstone and Hari (2008) observed that both river and lake water temperatures reflected short-term fluctuations in regional air temperature, but with a slight lag and less high-frequency variability. This study was based on earlier work, which had demonstrated that the lake surface water temperature in at a large number of sites on the Swiss plateau responded coherently to regional climatic forcing, including air temperature, cloud cover, and wind speed (Livingstone and Lotter, 1998; Livingstone et al., 1999; Livingstone and Dokulil, 2001; Livingstone et al., 2005). A degree of inertia in the response of lake surface water temperatures to regional air temperatures had also previously been noted; the lake water temperature series had lower variance when compared with the air temperature series (Livingstone et al., 2005). Livingstone et al. (2005) approached the problem of inertia by applying an exponential smoothing filter, a low-pass filter developed by Kettle et al. (2004) for lakes in Greenland, to the daily mean Swiss regional air temperature series. The proportion of shared variance (r^2) between the air and lake water temperature time series increased from 70.6% to 88.3% with the smoothing of regional air temperatures (Livingstone et al., 2005). Livingstone and Hari (2008) reported similar results for RWT, where the correlation between RWT and regional AT was greatly improved by applying an exponential smoothing filter to the air temperature data set. For example, for their data the proportion of variance shared between the RWT and AT time series increased from 71.4% to 92.2% for data from 1997. A version of the exponential smoothing filter ((Kettle et al. 2004, Livingstone et al. 2005a, Livingstone and Padisak 2007) and applied to RWT by Livingstone and Hari (2008) is shown as Equation 6.2.

$$S_i = (1 - \alpha)\, S_{i-1} + \alpha T_i \qquad \textbf{Equation 6.2}$$

Where,

S_i is the smoothed mean daily air temperature on given day (i)

S_{i-1} is the smoothed mean daily air temperature on the previous day

T_i is the mean daily air temperature on day i, and,

α (alpha) is the smoothing coefficient.

In the exponential smoothing filter, the air temperature time series is smoothed by a coefficient alpha (α), which represents the influence of environmental factors (e.g. shading, wind sheltering) that cause the air-water temperature relationship to depart from linearity. Alpha varies from a value of 0 (maximum smoothing) to 1 (no smoothing). A value of 0 implies a maximum internal memory effect, whereas a value of 1 implies no memory effect and

maximum external forcing through air temperature (Livingstone and Hari, 2008). The equation has a physical basis as described by Newton's Law of Cooling (Livingstone et al., 2005). Additional manipulations to the air temperature data sets before applying the exponential filter, such as dividing the time series into individual months or detrending to remove seasonal effects, have been shown to further improve the correlation between regional air temperature and RWT (Livingstone and Hari, 2008). With seasonal detrending and application of the smoothing filter, Livingstone and Hari (2008) found that the variability in regional air temperature statistically explained over 90% of the variability in mean regional RWT from summer – autumn in their Swiss study catchments.

6.2.3 Data used for RWT Modelling

The RWT time series used to test possible models were the same as those described earlier in this report in Chapter 2; RWT data from the Black River and two of its tributaries (the Altahoney and Goulaun), the Glenamong River, the Glendahurk River and the Tarsaghaun River (see Figure 1.3). The RWT data for the Black and Glenamong Rivers were recorded at 2-minute intervals using a Quanta data logger from 2003/2004, depending on the site. In the Altahoney, Goulaun, and Tarsaghaun Rivers, RWT was logged at 30-minute intervals, and at 60-minute intervals in the Glendahurk River, using Stowaway TidbiTs (Onset Computer Corporation). Daily and monthly mean river water temperature values were calculated from these data. The RWT time series used for training the models were limited to segments of four or five years of data because of gaps in recorded data due to mechanical failure and maintenance. The fit between modelled and observed RWT data was determined using the Nash-Sutcliffe (NS) coefficient (Nash and Sutcliffe, 1970). The maximum perfect score for the NS coefficient is 1.0. Physically, the NS coefficient is 1 minus the ratio of the root mean square error (RMSE) to the variance of the observed data.

Linear regression models (daily and weekly time step), moving averages (3, 5, 7, and 9 day), and an exponential smoothing filter were run using daily mean air temperature (average of maximum and minimum temperatures for each day) from the Millrace Meteorological Station and tested against both a catchment mean RWT time series and individual RWT data from the sites. The best fit linear regression models were created using weekly mean RWT and air temperature data (average of seven daily mean values), then used to predict RWT on a daily time step using daily mean air temperature data. A summary of the results for the two sites which had the poorest (Altahoney) and strongest (Goulaun) correlation with smoothed air temperature is presented in Table 6.1. A 5-day moving average of daily mean air temperature was the most successful moving average model tested. However, the exponential smoothing

filter (Livingstone and Hari, 2008) consistently yielded the best fit of modelled RWT to observed RWT for all six sites as determined by the NS coefficient. The exponential smoothing filter (Livingstone and Hari, 2008) was selected for use in the current study.

Table 6.1: Nash-Sutcliffe coefficients for fit of modelled RWT data to observed RWT data for each model type tested in the Altahoney (worst fit) and Goulaun (best fit) Rivers.

	MODEL TYPE		
River	**Linear regression**	**5-day Moving average**	**Smoothing filter**
Altahoney	0.78	0.64	0.80
Goulaun	0.88	0.89	0.94

6.2.4 Use of the Exponential Smoothing Filter to Estimate River Water Temperature

The datasets used to provide alpha (α) values for estimating projected changes in RWT were: 1) mean daily air temperature (based on maximum and minimum air temperature) recorded at the Millrace Meteorological Station and 2) a catchment mean daily RWT time series calculated using the Black, Glenamong, Glendahurk and Tarsaghaun datasets. The data for the period 1/6/2004-31/5/2006 were used for optimisation of alpha values and the data for the period 1/6/2006-31/5/2008 were used for validation of the approach. A catchment mean RWT time series was used to improve the robustness of the estimates because of the relatively short observed RWT datasets available for the Burrishoole catchment. The use of a catchment mean RWT series was justified by the high degree of coherence in fluctuations in RWT in the Burrishoole catchment (see Chapter 2) (Livingstone and Lotter, 1998; Livingstone et al., 2005). The Altahoney and Goulaun time series were excluded from the catchment mean because, as described in Chapter 2, both sites showed RWT behaviour not representative of the overall trends or extremes in water temperature in the catchment.

Alpha was first optimised for each individual season according to the following definition of seasons: winter, December, January, February; spring, March, April, May; summer, June, July, August; and autumn, September, October, November (Figure 6.3). Coefficients of determination (r^2) between measured RWT and estimated RWT were assessed both before and after linear detrending (to remove within-season trends). Although the coefficients of determination were lower in spring and autumn for detrended data, similar optimum alpha values were indicated using both original and detrended data. For all seasons there was a relatively broad spread of alpha values that were equal to or close to the optimised value (Figure 6.3) For each season a set of future simulations were produced using alpha values which were at either end of the range within $\pm$ 5% of the maximum r^2 value for the

optimisation dataset: winter (DJF) 0.7 and 0.8; spring (MAM) 0.5 and 0.8; summer (JJA) 0.6 and 0.9; autumn (SON) 0.6and 0.8.

The exponential smoothing filter was then applied to projected mean daily air temperature calculated from the six minimum daily and six maximum daily air temperature time series for the HadCM3, CSIRO Mk2, and CGCM2 GCMs with the A2 and B2 emissions scenarios (Chapter 4). The A2 scenario describes a very heterogeneous world with a continuously increasing population (Nakicenovic et al., 2000). Economic development is primarily regionally oriented and per capita economic growth and technological change more fragmented and slower than in the other storylines. The B2 emissions scenario is based on a population growth rate that is lower than the A2 scenario, with intermediate levels of economic development. For each GCM-emission scenario combination, one hundred data sets of air temperature were run with two sets of seasonal alpha values to generate two hundred data sets of future projected catchment mean RWT. Twelve monthly mean RWT data sets (one high alpha and one low alpha time set for each GCM-emission scenario combination) were then generated to facilitate incorporation of projected RWT into fish growth models. Future climate simulations of monthly RWT are presented as boxplots of the 5%ile, 25%ile, 50%ile, 75%ile and 95%ile. The 25%ile and 75%ile ranges for the historical variability in river water temperature, calculated from smoothed Millrace air temperature over 1969-1999, are also included in all graphs to provide a common frame of reference. The differences between GCM-scenario combinations were examined using the Kolmogorov-Smirnov (KS) test which tests for differences in location and shape of the distribution.

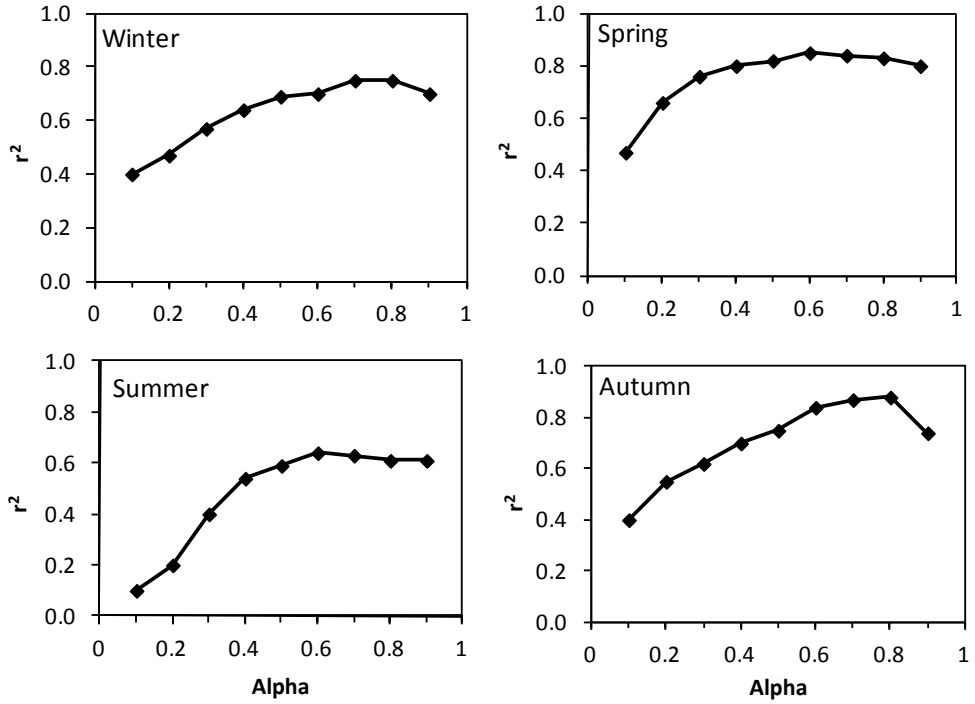

Figure 6.3: Coefficients of determination (r^2) for the relationship between smoothed air temperature calculated using a range of alpha (α) values, and measured river water temperature (RWT), for each season. Air temperature and RWT data used were mean daily values from 1/6/2004-31/5/2005.

6.2.5 Projected Changes in RWT for the Burrishoole Catchment

An increase in annual mean smoothed air temperature, and therefore estimated RWT, from the baseline period (1961-1990) was projected for all three time periods for both the A2 and B2 emissions scenarios using all three models (Tables 6.2, 6.3 and 6.4). With the exception of the time horizon 2040-2059 for the A2 model, the greatest increases were projected using air temperature data output from the CSIRO Mk2 model. The median annual mean RWT for 1961-1990 for both the A2 and B2 emission scenarios and this model were 9.8°C, while the values for 2010-2039 were both10.9°C, an increase of +1.1◦C. The annual mean smoothed air temperature and estimated RWT based on simulations using historical air temperature data from Newport for 1969-1999 (observed) was 10.1◦C. The increases in mean annual RWT for the subsequent time periods for this model and the A2 scenario were +1.4◦C (2050-2059) and +2.3◦C (2070-2099) (Table 6.2), while those for the B2 scenario were +1.6◦C (2050-2059) and +1.9◦C (2070-2099)(Table 6.3).

Projected increases in monthly RWT were higher for simulations based on the A2 scenario than those based on the B2 scenario (Tables 6.2 and 6.3; Figures 6.4 and 6.5). The currently observed seasonal pattern in river water temperature, with lower temperatures in the winter and highest temperatures in the late summer, was replicated in all future simulations. An increase in mean monthly RWT from the baseline (1961-1990) period was projected for all

three time periods for both the A2 and B2 emissions scenarios using the CSIRO Mk2 and the CGCM2models, while there were small decreases projected for some winter months for the more recent time horizon (2010-2039) based on air temperature projected using the HadCM3 model (Table 6.2 and 6.3). In general, the lowest increases were in summer months with higher increases in the autumn and winter. The increases for the A2 scenario based on output from the CSIRO Mk2 for the time period 2010 to 2039, for example, ranged from +0.4°C in May to +1.3°C in November (Table 6.2). For the B2 scenario, the corresponding increases ranged from +0.7°C in June to +1.4°C in January, September, and November.

Table 6.2: A2 scenario: river water temperature in °C for the observed period and for the 1961–1990 (1970s) period for the three GCM models together with the absolute change from this period for the 2010–2039 (2020s), 2040–2069 (2050s) and 2070–2099 (2080s) periods.

A2	AT	J	F	M	A	M	J	J	A	S	O	N	D	Year
Observed	**°C**	**5.8**	**5.9**	**6.8**	**8.9**	**11.1**	**13.4**	**15.2**	**15.0**	**13.3**	**11.3**	**8.0**	**6.7**	**10.1**
HadCM3	1970s	5.9	5.5	6.9	8.6	10.9	13.3	14.9	14.8	13.2	10.9	7.8	7.0	9.7
change	2020s	0.2	0.5	0.1	0.2	0.5	0.3	0.1	0.4	0.4	0.2	-0.2	-0.8	0.6
	2050s	0.9	1.1	0.2	0.7	0.7	0.5	0.9	0.9	1.7	0.9	0.7	-0.3	0.8
	2080s	1.5	1.7	1.5	1.4	1.5	1.4	1.8	2.0	2.2	2.6	1.4	0.5	1.9
CSIRO-MK2	1970s	5.4	5.5	6.6	8.5	11.0	13.4	14.9	14.8	13.2	10.9	7.7	6.4	9.8
change	2020s	0.8	0.5	1.1	1.2	0.4	0.6	0.6	0.6	0.9	1.1	1.3	1.2	1.1
	2050s	1.5	1.1	1.5	1.7	1.2	1.0	1.2	1.3	1.8	1.8	1.8	1.6	1.4
	2080s	2.7	2.2	2.6	2.6	1.9	1.5	2.1	2.2	2.8	2.7	3.1	2.9	2.3
CGCM2	1970s	5.5	5.4	6.9	8.6	11.1	13.5	14.9	14.9	13.2	10.9	7.5	6.4	9.9
change	2020s	0.8	0.6	0.8	0.9	0.9	0.8	0.8	0.9	0.8	0.7	0.7	0.9	0.8
	2050s	1.5	1.3	1.5	1.3	1.4	1.4	1.6	1.6	1.7	1.9	2.0	1.6	1.6
	2080s	1.6	1.6	1.7	1.9	2.0	2.0	2.1	2.1	2.5	2.4	2.4	2.3	2.0

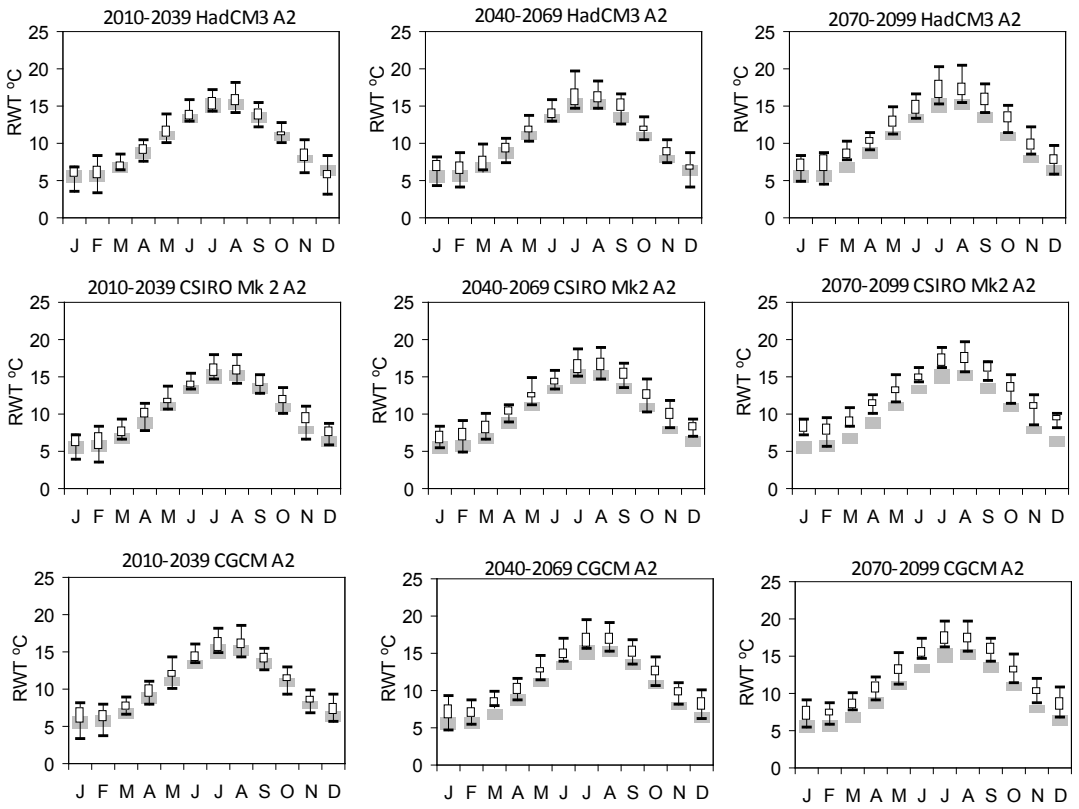

Figure 6.4: A2 scenario: boxplots of river water temperature (RWT) in °C for the three GCM models for the future time periods 2010–2039, 2040–2069 and 2070–2099. Shaded areas are the 25 percentile to 75 percentile range for model runs using historical meteorological data and are used to represent observed variability.

Table 6.3: B2 scenario: river water temperature in °C for the observed period and for the 1961–1990 (1970s) period for the three GCM models together with the absolute change from this period for the 2010–2039 (2020s), 2040–2069 (2050s) and 2070–2099 (2080s) periods.

B2	AT	J	F	M	A	M	J	J	A	S	O	N	D	Year
Observed	**°C**	**5.8**	**5.9**	**6.8**	**8.9**	**11.1**	**13.4**	**15.2**	**15.0**	**13.3**	**11.3**	**8.0**	**6.7**	**10.1**
HadCM3	1970s	5.9	5.6	6.9	8.6	11.0	13.4	14.9	14.8	13.2	10.9	7.8	7.0	9.7
Change	2020s	-0.3	0.7	0.1	0.5	0.4	0.2	0.2	0.5	0.9	0.6	0.8	-1.2	0.6
	2050s	0.3	0.3	0.1	0.6	0.8	0.4	0.6	0.7	0.8	0.9	1.2	0.0	0.8
	2080s	0.6	1.0	0.6	1.1	1.2	1.2	1.0	1.2	1.3	1.7	1.6	-0.1	1.3
CSIRO-MK2	1970s	5.5	5.7	6.8	8.6	10.9	13.4	14.9	14.9	13.3	11.0	7.7	6.5	9.8
Change	2020s	1.4	1.2	1.1	0.9	0.8	1.0	0.7	0.9	1.4	1.0	1.4	0.9	1.1
	2050s	1.7	1.4	1.6	1.6	1.6	1.3	1.1	1.4	1.9	1.6	2.4	1.6	1.6
	2080s	2.2	1.9	2.1	2.1	1.8	1.4	1.4	1.8	2.3	2.4	2.9	2.3	1.9
CGCM2	1970s	5.5	5.4	6.9	8.6	11.0	13.5	14.9	14.9	13.2	10.9	7.6	6.4	9.9
Change	2020s	1.0	1.0	0.8	0.8	0.5	0.7	0.9	0.8	0.8	0.9	0.9	1.0	0.8
	2050s	1.2	1.1	1.2	1.4	1.3	1.1	1.3	1.2	1.3	1.4	1.3	1.3	1.3
	2080s	1.1	1.4	1.3	1.7	1.4	1.3	1.4	1.7	2.2	2.4	2.3	2.0	1.7

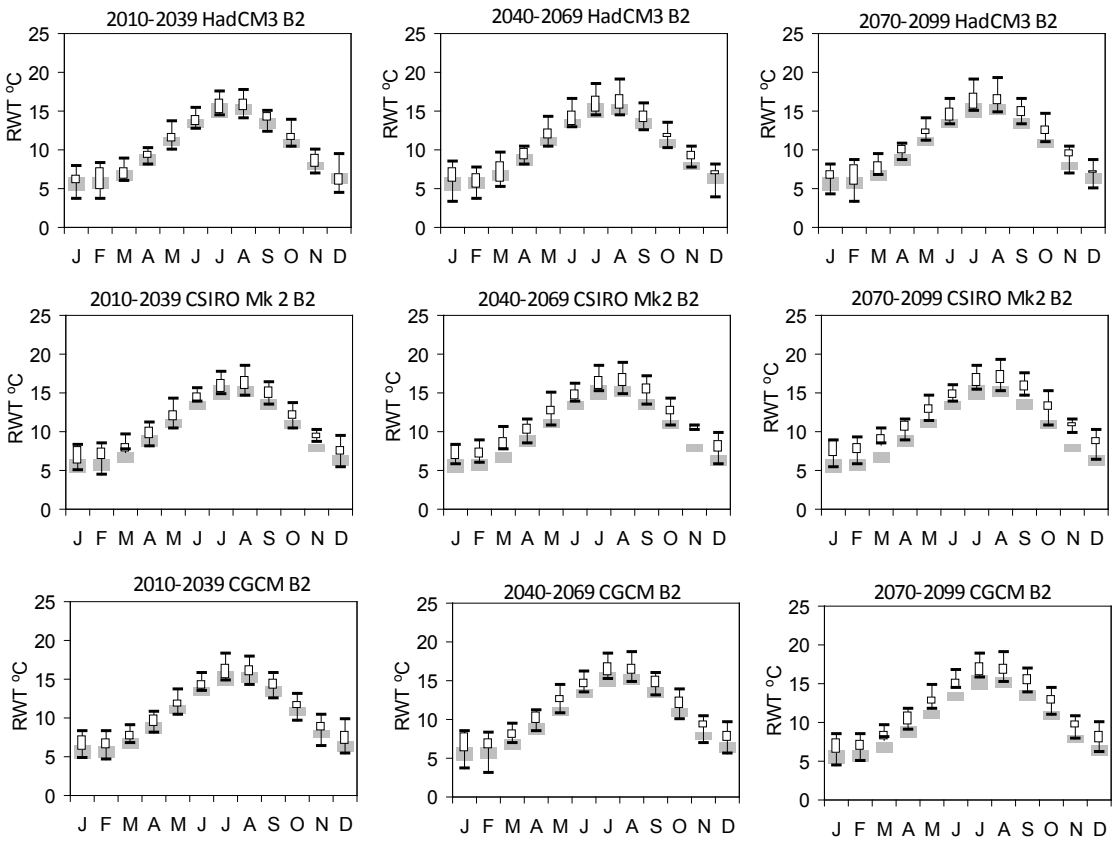

Figure 6.5: B2 scenario: boxplots of river water temperature (RWT) in °C based on the B2 scenario for the three GCM models for the future time periods 2010–2039, 2040–2069 and 2070–2099. Shaded areas are the 25 percentile to 75 percentile range for model runs using historical meteorological data and are used to represent observed variability.

The projected increases in annual RWT for the combined models for the A2 scenario were +0.8°C (2010-2039), +1.3°C (2040-2059) and +2.1°C (2070-2099) while those for the B2 scenario, which has a lower population growth rate, with intermediate levels of economic development, were +0.8°C (2010-2039), +1.2°C (2040-2059) and +1.6°C (2070-2099) (Table 6.4). For the future horizon 2070-2099 increases in monthly RWT were highest for months between August and November (ranging from +2.1°C in August to +2.6°C in October) and lowest for June (+1.6°C) (Figure 6.6). The greatest increases for the B2 emissions scenario were in October (+2.1°C) and November (+2.2°C), with lowest increases in January, March, June and July (+1.3°C).

Table 6.4: River water temperature (RWT, °C) for the observed period 1961-1990 (1970s) and the mean absolute change for the three GCM models combined and the A2 and b2 scenarios for the 2010–2039 (2020s), 2040–2069 (2050s) and 2070–2099 (2080s) time periods.

RWT		J	F	M	A	M	J	J	A	S	O	N	D	Year
Observed	**°C**	**5.8**	**5.9**	**6.8**	**8.9**	**11.1**	**13.4**	**15.2**	**15.0**	**13.3**	**11.3**	**8.0**	**6.7**	**10.1**
A2	1970s	5.6	5.5	6.8	8.6	11.0	13.4	14.9	14.8	13.2	10.9	7.7	6.6	9.8
change	2020s	0.6	0.5	0.7	0.8	0.6	0.6	0.5	0.6	0.7	0.7	0.6	0.4	0.8
	2050s	1.3	1.2	1.1	1.2	1.1	1.0	1.2	1.3	1.7	1.5	1.5	1.0	1.3
	2080s	1.9	1.8	1.9	2.0	1.8	1.6	2.0	2.1	2.5	2.6	2.3	1.9	2.1
B2	1970s	5.6	5.6	6.9	8.6	11.0	13.4	14.9	14.9	13.2	10.9	7.7	6.6	9.8
change	2020s	0.7	1.0	0.7	0.7	0.6	0.6	0.6	0.7	1.0	0.8	1.0	0.2	0.8
	2050s	1.1	0.9	1.0	1.2	1.2	0.9	1.0	1.1	1.3	1.3	1.6	1.0	1.2
	2080s	1.3	1.4	1.3	1.6	1.5	1.3	1.3	1.6	1.9	2.2	2.3	1.4	1.6

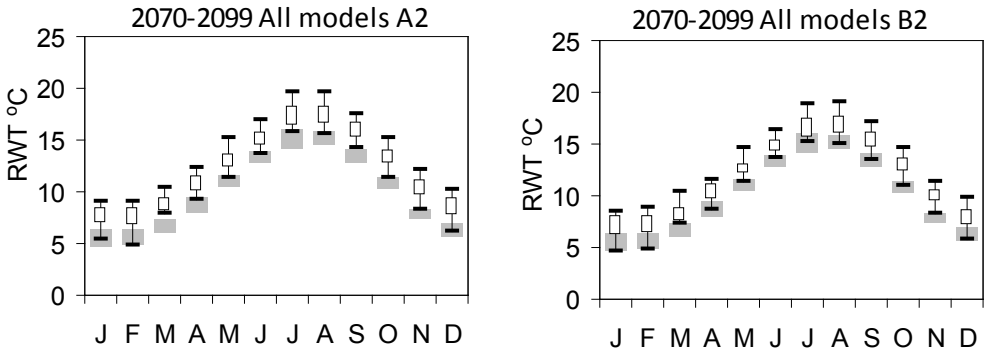

Figure 6.6: Boxplots of mean monthly RWT (°C) for the overall A2 and B2 scenarios (outputs from three GCM models combined = All models)) for the time period 2070-2099. Shaded areas are the 25 percentile to 75 percentile range for model runs using historical meteorological data and are used to represent observed variability.

6.3 Dissolved Organic Carbon

6.3.1 Dissolved Organic Carbon Model Description

The dissolved organic carbon (DOC) model which was used in this study was originally developed in response to user needs in the 1980s and 1990s (Naden, 1991; Naden and Watts, 1998). Based on experimental work at Leeds University in the 1980s, the release of water colour was modelled as a two stage process: peat decomposition produced soluble DOC compounds which were then washed out of the soil. The model was then further developed during an EU project, Climate Impacts on European Lakes (CLIME), which included Marine Institute, Newport, as partners (Naden et al., 2010). The model was dynamically coupled with the Generalized Watershed Loading Functions (GWLF) model hydrology in the visual modelling software package Vensim (Ventana Systems, Inc.). GWLF is a non point-source loading model developed by Haith and Tubbs (1981) to simulate monthly dissolved and total

nutrient loads in streamflow. The GWLF version that was used was created by New York City Department of Environmental Protection (Schneiderman et al., 2002; Schneiderman et al., 2010). The hydrology subroutine of GWLF is driven by daily temperature and precipitation data and water balances are calculated on a daily interval. Streamflow consists of surface (or rapid) runoff and fast and slow baseflow components. Rapid runoff is calculated using the SCS curve number method (Ogrosky and Mockus, 1964). In CLIME, land use classification for this method was based on European CORINE level 3 land cover classes and work included an evaluation of the ranges of runoff curve numbers used for these land use classes in European catchments. Other model improvements in CLIME included the development of an improved optimisation procedure for the GWLF hydrology model.

The DOC model is driven by daily values of soil temperature, soil moisture levels and runoff. It is assumed that the production of DOC is not limited by the availability of organic matter and so is independent of the total carbon store (Naden et al., 2010). The production of DOC compounds during peat decomposition in the model is dependent on both soil temperatures and soil moisture levels (Figure 6.7). Soil moisture is represented in the hydrological model as the unsaturated zone i.e. the soil moisture content between field capacity and wilting point, while soil temperature is estimated by a 10-day moving average of the air temperature above zero. Decomposition is assumed to cease when soil temperature is zero. The DOC which is produced by decomposition accumulates in the model in a soil store (Figure 6.7). Washout of this store is modelled as a function of the store of DOC available for export and the water flux in the different hydrological pathways. There are three hydrological pathways described within the GWLF hydrology model: surface runoff, rapid subsurface flow which is fed from percolation when the unsaturated zone is full, and slow subsurface flow which is fed via deep percolation and maintains river baseflows during dry periods. For each of the three pathways, the amount of DOC which is exported is calculated as a function of the total available DOC store, the water flux in the pathway and a rate constant.

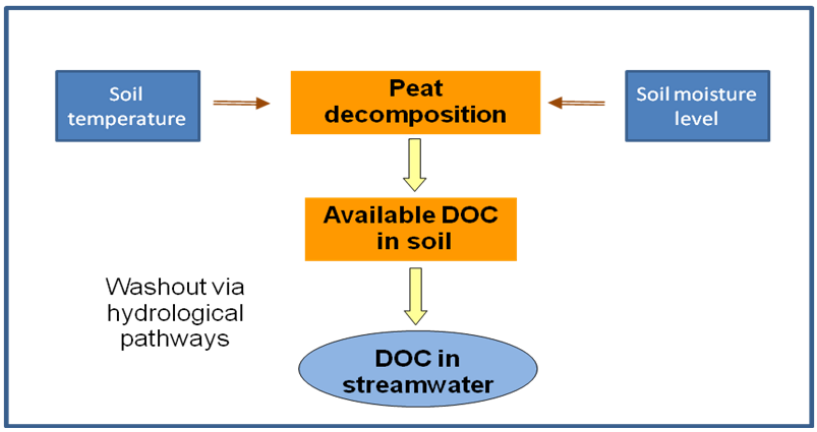

Figure 6.7: Diagram of dissolved organic carbon (DOC) model structure.

6.3.2 Model Validation and Application

Prior to running the future climate simulations, the hydrology model and DOC model were calibrated and validated for the site using observed data. A hydrology optimisation procedure was carried out which minimises the sum of the residuals between simulated and measured streamflow using two iterations of a ten step sequential optimisation (Schneiderman et al., 2010). The daily streamflow data from 2001 to 2003 were used to calibrate the hydrology model, while the data from 2004 to 2006 were used for model validation. The Nash-Sutcliffe (NS) coefficients for the calibration and validation periods for streamflow were 0.77 and 0.83 respectively. The best fit was obtained using data from a set of rain-gauges situated in the subcatchment. The fit with data from the meteorological station at Newport was poorer (NS = 0.42), possibly due to periods of localised precipitation that were not captured by the Newport station. Hydrology model constants obtained in the optimisation were used in all future climate simulations.

An in-situ instrument which measures chromophoric dissolved organic matter (CDOM) fluorescence in stream water, a proxy for DOC, was installed on the Glenamong River in 2003. The data were converted to DOC concentrations based on data collected in 2003-2006. DOC concentrations ranged from 4 to 18 mg DOC L^{-1} with a mean of 6.2 mg DOC L^{-1}. The availability of these high frequency data facilitated validation of the DOC model for this site.

In a previous application of the model, a single step optimisation was performed for the five DOC model parameters based on comparison of observed and modelled data (Naden et al. 2010). The optimised values for the activation energy (which controls the temperature dependence of decomposition) and the aerobic factor (which describes the relative rate of aerobic decomposition rates) for the Glenamong site were 4.9 kJ g C^{-1} and 0 respectively.

This value for the activation energy is at the lower end of the range of 4.8 to 14.8 kJ g C^{-1} quoted for decomposition measured as CO_2 efflux from Scottish peats (Chapman and Thurlow, 1998) and slightly below that indicated by similar measurements at a Galway site (Byrne et al., 2002). However, the value for the aerobic factor was not in agreement with literature on the impact of soil moisture on decomposition rates which indicates that decomposition is dependent on both temperature and soil moisture (Clark et al., 2005; Naden et al., 2010).

In the current application, the values for these two parameters were based on a study at a peat site in the UK and set at 4 and 9 respectively (Clark et al., 2005). To explore parameter uncertainty for the remaining three constants, 50,000 runs of the model were carried out using parameter sets which were independently and randomly selected from a uniform distribution of values between selected limits. Figure 6.8 shows the likelihood plots for each parameter for those runs with a NS efficiency value above 0.35; the higher the NS value, the better is the model fit (Figure 6.8). In contrast to a previous exploration of uncertainty in the model in which all five DOC parameters were included (Jennings et al., 2005), all three constants showed a relatively well-defined peak in the likelihood function. The parameter sets associated with the five best-fit model runs (NS > 0.45) were used in future climate simulations.

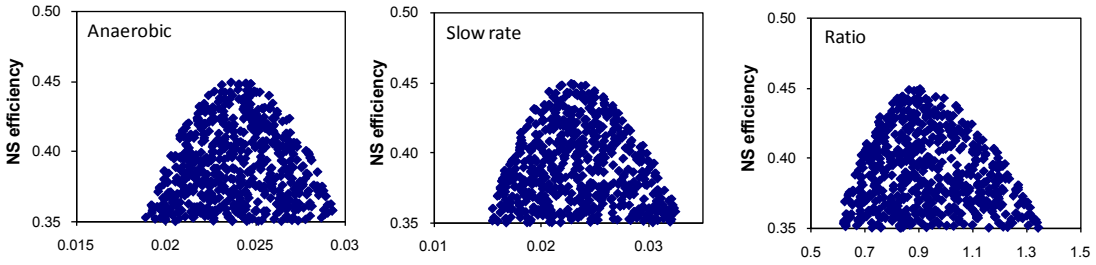

Figure 6.8: Dotty plots for a selected range of parameter values plotted against the Nash-Sutcliffe (NS) efficiency for model runs for three model parameters: 1. anaerobic decomposition (anaerobic), 2. the slow wash-out rate (slow rate) and 3. ratio between fast and slow wash-out (ratio).

For each GCM-scenario combination, one hundred data sets of air temperature and precipitation were used with each of the five selected DOC parameter sets. In addition, a single run was included using projected precipitation based on the GLM, again with each of the five DOC parameter datasets. For all simulations, PE was calculated within the GWLF hydrology model (using the Hargreaves-Samani equation (Hargreaves and Samani, 1982)), to retain the relationship between air temperature and PE in each individual simulation. The DOC model was also run using 100 synthetic datasets of air temperature and precipitation to provide an estimate of past variability at the site. These data were produced by block

resampling the historical air temperature data from the Newport station and the adjusted Newport precipitation dataset described in Chapter 4 and are referred to as the observed dataset. Mean monthly DOC concentration were output from each run. The 25%ile and 75%ile ranges for the historical variability are included in all graphs to provide a common frame of reference. Future climate simulations are presented as boxplots of the 5%ile, 25%ile, 50%ile, 75%ile and 95%ile values of mean monthly concentrations. The differences between GCM-scenario combinations was examined using the Kolmogorov-Smirnov (KS) test which tests for differences in location and shape of the distribution.

6.3.3 Projected Changes in DOC Concentration

An increase in mean annual DOC concentration from the baseline 1961-1990 period to the more immediate future period, 2010-2039, was projected for all model scenario combinations (Tables 6.5 and 6.6). The median annual value for the observed dataset was 6.5 mg DOC L^{-1}. The median values for 1961-1990 based on the output from the three GCMs were 6.9 mg DOC L^{-1}, 6.2 mg DOC L^{-1} and 7.1 mg DOC L^{-1} for the Had CM3, CSIRO Mk2 and CGCM22 models respectively. The relative increase projected for these median concentrations for 2010-2039 were +0.7 mg DOC L^{-1} for both the Had CM3 and CSIRO Mk 2 models and +1.2 mg DOC L^{-1} for the CGCM2 model. The increases for the simulations based on the B2 scenario for the same time horizon were +0.1 mg DOC L^{-1}, +0.9 mg L^{-1} and +0.6 mg L^{-1} for the Had CM3, CSIRO Mk2 and CGCM2 simulations. The overall increase from 1961-1990 to 2010-2039 based on all three GCM datasets combined for the A2 scenario was +0.9 mg DOC L^{-1} while that for the B2 scenario was +0.6 DOC mg L^{-1} (Table 6.7). Both increases were significant (Kolmogorov-Smirnov test on n=3000 randomly sampled values, $p<0.001$). The distributions for the A2 and the B2 scenarios for 2010-2039 were also significantly different from each other; however, there was no significant difference between simulations for the overall A2 and B2 datasets for 1961-1990. The increases in annual concentration for both the 2040-2069 and 2070-2099 time periods exceeded those for 2010-2039 for all model-scenario combinations (Table 6.5 and 6.6). The absolute increases for the A2 simulations from 1961-1990 to 2040-2069 were +1.0 mg DOC L^{-1} (Had CM3), +1.9 mg DOC L^{-1} (CSIRO Mk2) and +2.3 mg DOC L^{-1} (CGCM2). Those for 2070-2099 were +2.7 mg DOC L^{-1} (Had CM3), +2.3 mg DOC L^{-1} (CSIRO Mk2) and +4.8 mg DOC L^{-1} (CGCM2). The increases for the B2 scenario for the same time periods ranged from +1.0 mg DOC L^{-1} to +1.9 mg DOC L^{-1} (2040-2069) and from +1.1 mg DOC L^{-1} to +2.4 mg DOC L^{-1} (2070-2099).

Table 6.5: A2 scenario: dissolved organic carbon (DOC) concentration (mg L^{-1}) for the observed period and for the 1961–1990 (1970s) period for the three GCM models together with the absolute change from this period for the 2010–2039 (2020s) , 2040–2069 (2050s) and 2070–2099 (2080s).

A2	DOC	J	F	M	A	M	J	J	A	S	O	N	D	Year
Observed	**mg L^{-1}**	**6.5**	**5.9**	**5.6**	**5.5**	**5.5**	**5.5**	**5.8**	**6.4**	**7.4**	**8.4**	**8.5**	**7.5**	**6.5**
HadCM3	1970s	6.9	6.2	5.9	5.7	5.8	5.8	6.0	6.6	7.5	9.0	9.2	8.1	6.9
change	2020s	0.7	0.6	0.5	0.6	0.6	0.6	0.6	0.4	0.7	0.9	0.7	0.7	0.7
	2050s	1.3	1.0	0.9	1.0	0.9	0.9	1.0	0.8	0.7	0.9	1.4	1.4	1.0
	2080s	3.1	2.2	2.0	2.2	2.4	2.4	2.3	2.0	2.2	3.4	4.7	4.0	2.7
CSIRO-MK2	1970s	6.7	6.0	5.6	5.4	5.3	5.3	5.2	5.5	6.2	6.7	7.8	7.5	6.2
change	2020s	1.1	0.7	0.6	0.5	0.5	0.6	0.6	0.6	0.5	0.6	0.9	1.1	0.7
	2050s	2.5	2.0	1.7	1.6	1.6	1.6	1.7	1.6	1.4	1.8	2.6	2.7	1.9
	2080s	2.7	2.2	1.9	1.9	1.8	1.8	1.9	1.9	1.9	2.5	3.1	3.6	2.3
CGCM2	1970s	7.3	6.7	6.3	6.1	6.2	6.1	6.2	6.3	6.9	8.2	9.1	8.2	7.1
change	2020s	1.4	1.1	1.1	1.1	0.9	1.0	1.1	1.1	1.3	1.4	1.9	1.8	1.2
	2050s	2.6	2.1	2.0	2.0	1.8	2.0	1.9	2.1	2.3	2.4	3.2	3.4	2.3
	2080s	5.2	4.4	4.2	4.2	4.1	4.3	4.3	4.5	4.6	4.9	6.0	6.0	4.8

Table 6.6: B2 scenario: dissolved organic carbon (DOC) concentration (mg L-1) for the observed period and for the 1961–1990 (1970s) period for the three GCM models together with the absolute change from this period for the 2010–2039 (2020s) , 2040–2069 (2050s) and 2070–2099 (2080s).

B2	DOC	J	F	M	A	M	J	J	A	S	O	N	D	Year
Observed	**mg L^{-1}**	**6.5**	**5.9**	**5.6**	**5.5**	**5.5**	**5.5**	**5.8**	**6.4**	**7.4**	**8.4**	**8.5**	**7.5**	**6.5**
HadCM3	1970s	6.2	5.6	5.3	5.2	5.3	5.3	5.5	6.2	7.0	8.3	8.5	7.2	6.4
change	2020s	0.2	0.2	0.3	0.2	0.1	0.2	0.1	0.0	0.4	0.4	0.4	0.2	0.1
	2050s	1.1	0.9	0.8	0.9	0.9	0.9	0.9	0.4	0.9	1.1	1.7	1.5	1.0
	2080s	1.3	0.9	0.9	0.9	0.9	0.9	0.9	0.7	1.4	1.5	1.9	1.7	1.1
CSIRO-MK2	1970s	7.2	6.5	5.9	5.7	5.5	5.5	5.5	5.6	6.4	6.9	8.1	8.0	6.4
change	2020s	1.0	0.9	0.9	0.8	0.8	0.8	0.8	0.7	0.9	0.8	1.0	1.3	0.9
	2050s	1.3	0.7	0.6	0.7	0.9	0.9	1.0	1.1	1.2	1.3	1.5	1.8	1.1
	2080s	2.1	1.7	1.4	1.4	1.5	1.5	1.5	1.4	1.2	1.5	2.1	2.4	1.7
CGCM2	1970s	7.1	6.6	6.2	6.0	6.1	6.0	6.0	6.2	6.8	8.1	9.0	8.1	7.0
change	2020s	0.9	0.7	0.7	0.7	0.4	0.5	0.4	0.5	0.8	0.7	1.1	1.2	0.6
	2050s	2.3	1.9	1.7	1.7	1.5	1.7	1.6	1.8	2.0	2.3	2.7	2.9	1.9
	2080s	2.9	2.3	2.2	2.3	2.1	2.2	2.1	2.2	2.4	2.7	3.5	3.4	2.4

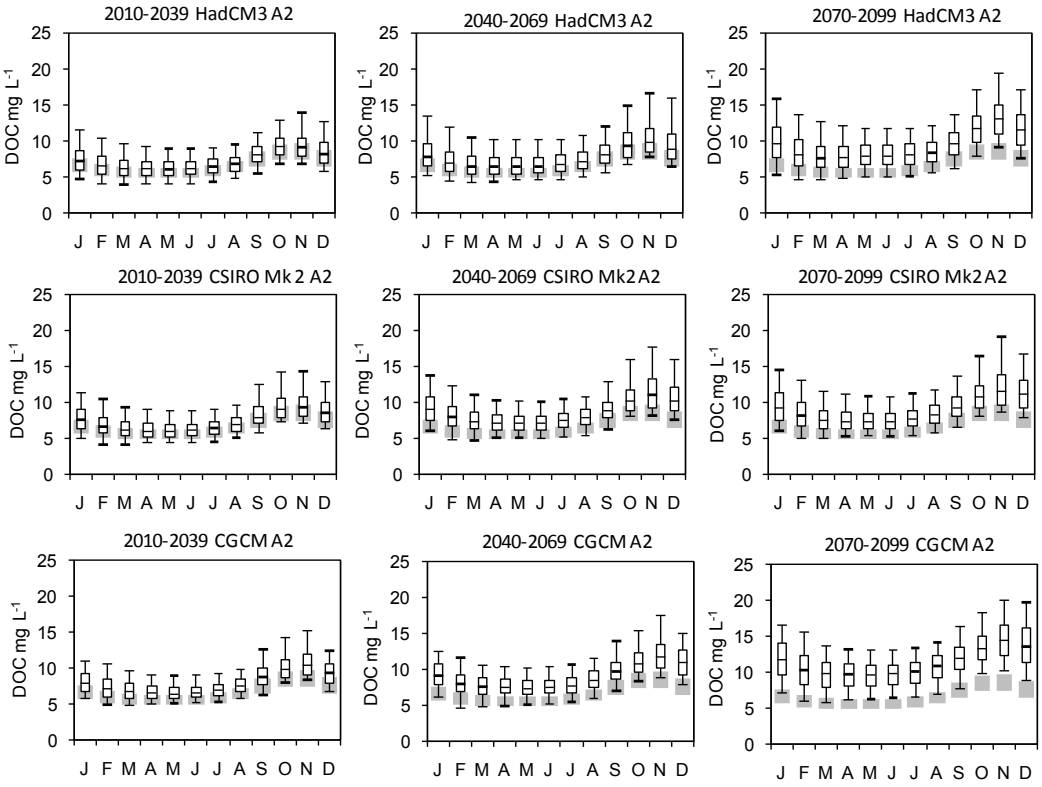

Figure 6.9: A2: boxplots of projected monthly DOC concentration (mg L^{-1}) for the 3 GCM models for 2010-2039, 2040-2069 and 2070-2099. Shaded areas are the 25 percentile to 75 percentile range for model runs using historical meteorological data and represent observed variability.

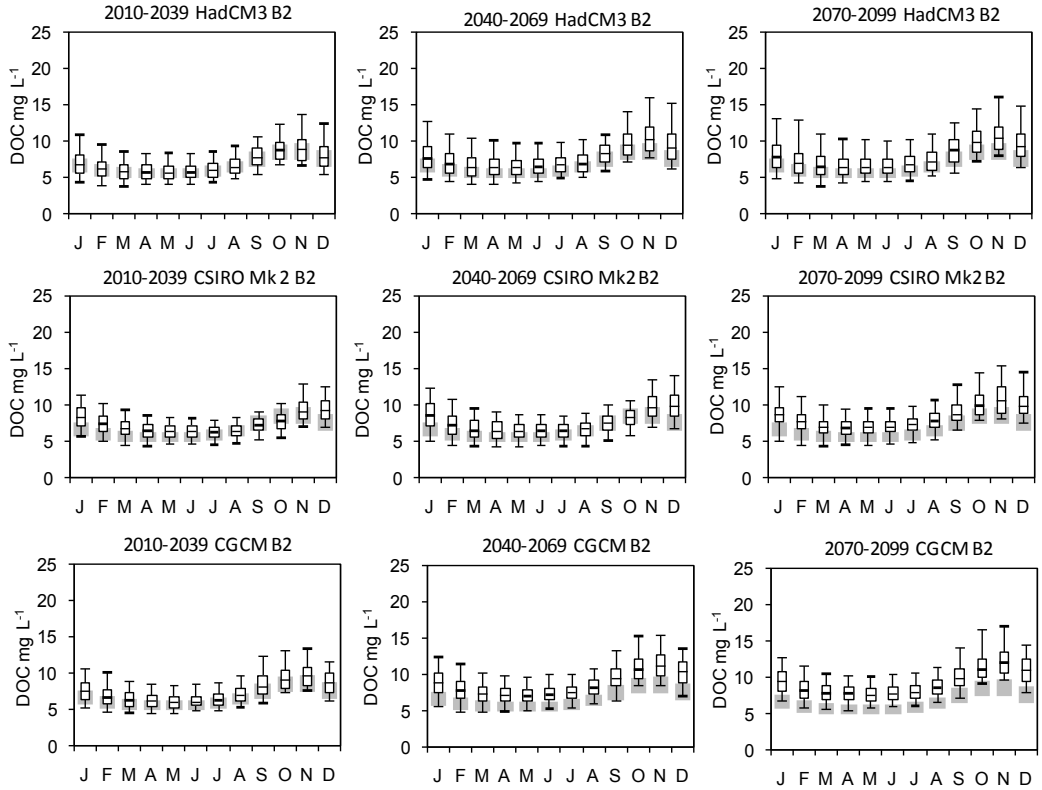

Figure 6.10: B2: boxplots of projected monthly DOC concentration (mg L^{-1}) for the 3 GCM models for 2010-2039, 2040-2069 and 2070-2099. Shaded areas are the 25 percentile to 75 percentile range for model runs using historical meteorological data and represent observed variability.

For both scenarios, the simulations based on the CGCM2 output produced the highest absolute increases for the overall time period, while the Had CM3 model produced the lowest. The increase from 1961-1990 to 2040-2069 based on all driving data and for all three models for the A2 scenario was 1.8 mg L^{-1} while that for the B2 scenario was 1.4 mg L^{-1} (Table 6.6). The overall increase from 1961-1990 to 2070-2099 for the A2 scenario was 2.4 mg L^{-1} while that for the B2 scenario was 1.8 mg L^{-1}. All were significantly different from the simulated annual means for 1961-1990. Significant increases in DOC concentrations were also indicated for all months for each of the three time periods (Figures 6.9, 6.10 and 6.11; Table 6.7). While these were generally of a similar magnitude to the increases in annual values, the increase for each model-scenario combination was always lower in the late summer and highest in November/December. This seasonal pattern in DOC concentrations was driven in the model by the seasonal patterns in temperature, soil moisture levels and flow and replicated the currently observed pattern. The data for the overall A2 simulations for 2071-2099 are used to illustrate the combined impact of these three driving variables (Figure 6.11). In the model, decomposition of peat soils is driven by temperature and by the depth of the soil unsaturated zone, a measure of soil moisture levels. The impact of low soil moisture levels is confined to the summer months, when evapotranspiration exceeds precipitation and the soil unsaturated zone deepens.

Soil temperatures, which are a function of air temperature in the model, are also at their highest during this period. These two factors result in a seasonal peak in the store of available DOC in the soil and were a major factor in the projected increases in stream concentrations. The median depth of the unsaturated zone in July in the observed dataset, for example, was 2.7 cm: the projected value for the A2 scenario was 5.1 cm (Figure 6.12). In addition, while the unsaturated zone had recharged by October in the observed dataset, soil moisture was depleted until November for 2071-2099. The store of DOC produced by these seasonal drivers was washed out by higher surface and sub-surface runoff in November and December (Figure 6.11). While there is no overall increase in annual streamflow in these simulations, there was a reduction in flow rates in the late summer and autumn. This reduction would also contribute to higher available soil carbon stores in the November/December period.

Table 6.7: Dissolved organic carbon (DOC) concentration (mg L^{-1}) for the observed period (1961–1990) and for a 1961–1990 (1970s) control period for the combined GCM models for the A2 and B2 scenarios together with the absolute change from this period for the 2010–2039 (2020s), 2040–2069 (2050s) and 2070–2099 (2080s).

DOC		J	F	M	A	M	J	J	A	S	O	N	D	Year
Observed	**mg L-1**	**6.5**	**5.9**	**5.6**	**5.5**	**5.5**	**5.5**	**5.8**	**6.4**	**7.4**	**8.4**	**8.5**	**7.5**	**6.5**
A2	1970s	6.9	6.3	5.9	5.7	5.7	5.7	5.7	6.1	6.8	7.9	8.6	7.9	6.6
change	2020s	1.1	0.8	0.7	0.8	0.7	0.8	0.8	0.7	0.9	1.0	1.2	1.2	0.9
	2050s	2.2	1.8	1.6	1.6	1.5	1.5	1.6	1.5	1.5	1.8	2.5	2.6	1.8
	2080s	3.6	2.0	1.7	1.9	1.9	1.9	1.9	1.8	1.9	2.5	3.6	3.6	2.4
B2	1970s	6.8	6.2	5.8	5.6	5.6	5.6	5.7	6.1	6.7	7.9	8.5	7.8	6.6
change	2020s	0.8	0.7	0.6	0.6	0.5	0.5	0.5	0.4	0.6	0.5	0.8	1.0	0.6
	2050s	1.7	1.2	1.1	1.2	1.1	1.2	1.2	1.0	1.3	1.4	2.0	2.1	1.4
	2080s	2.2	1.8	1.6	1.6	1.5	1.6	1.5	1.4	1.7	1.9	2.5	2.6	1.8

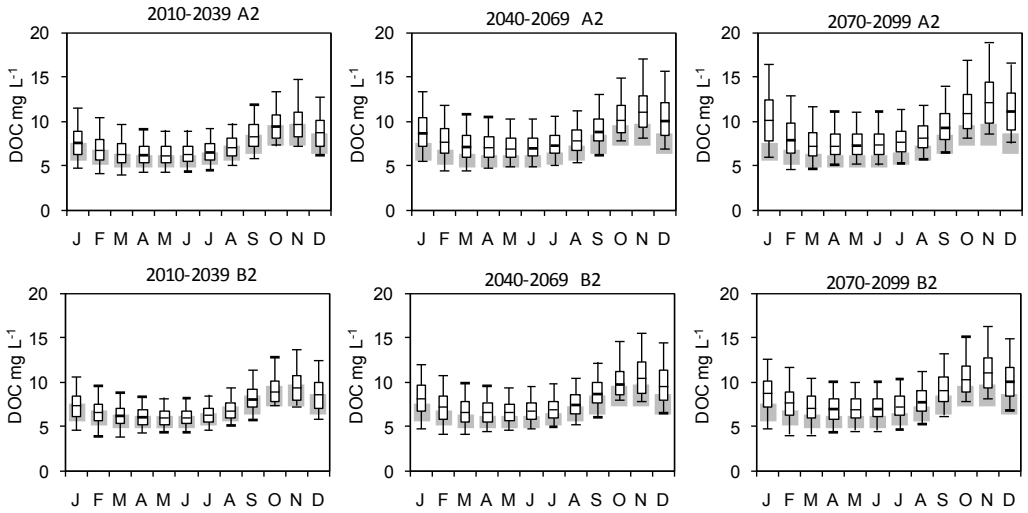

Figure 6.11: Boxplots of mean monthly DOC concentration (mg L^{-1}) for the A2 and B2 scenarios (three GCMs combined) for 2010–2039, 2040–2069 and 2070–2099. Shaded areas are the 25 to 75 percentile range for runs using historical meteorological data and represent observed variability.

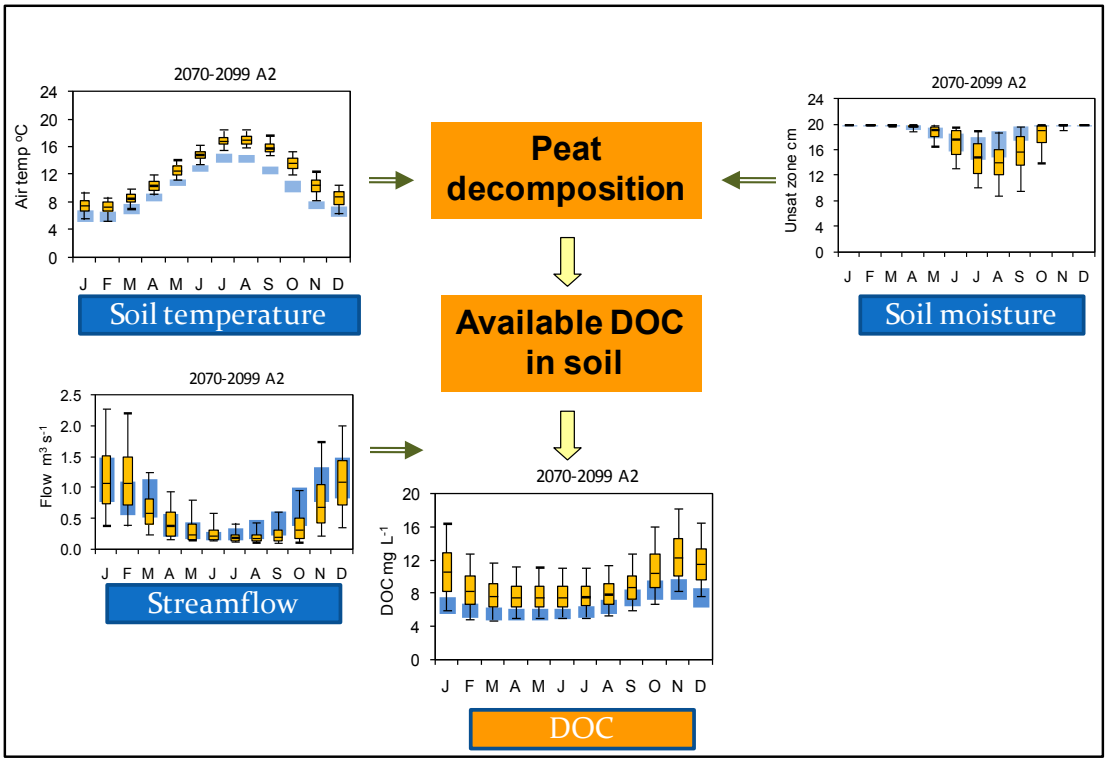

Figure 6.12: Diagram based on the DOC model structure with boxplots for projected air temperature (°C), unsaturated zone (soil moisture, cm), streamflow (m s^{-1}) and DOC (mg L^{-1}), combined models, A2 scenario, 2070-2099. Blue shaded areas are the 25 to 75 percentile range for runs using historical meteorological data and represent observed variability.

6.4 Estimation of the Effects of Projected Changes in RWT on Dissolved Oxygen Solubility

6.4.1 Introduction

Early approaches to modelling DO levels in water included the mass balance approach of the UK Royal Commission in 1912 and the Streeter and Phelps equation which simulated DO and biological oxygen demand (BOD) in rivers (Cox, 2003). These equations are still used in wastewater engineering and form the basis of simulating DO concentrations in most widely used water quality models (Cox, 2003) including the in-lake biological model CAEDYM (Hipsey, 2006). These approaches include the estimation of the DO concentration of water (in mg L^{-1}) using a physical equation based on the relationship of DO solubility to temperature (APHA, 1992). This equation calculates DO concentrations in the absence of the biological processes of photosynthesis and respiration. Deviations from this relationship would be expected during periods of high biological activity. The overall DO concentration in stream waters in process driven models (e.g., QUAL2K and CAEDYM) is described generally as follows:

$$DO_d = DO_{td}(elev) + DO_{photo} - DO_{respir} - DO_{decomp} \qquad \textbf{Equation 6.3}$$

Where,

DO_d = mean [DO] (mg L^{-1}) on day d

t = mean daily RWT

$DO_{td}(elev)$ = [DO] at t corrected for elevation

DO_{photo} = DO produced by primary producers

$DO_{respire}$ = DO respired by primary producers

DO_{decomp} = DO consumed during decomposition

Few data are available on phytoplankton productivity in streams in the Burrishoole catchment. However, available nutrient concentration data indicates that the system is oligotrophic and therefore primary productivity is likely to be low. In addition, data from the biological monitoring program for Lough Feeagh has indicated that water column primary production (i.e. phytoplankton biomass) is also low (with an annual maximum chlorophyll a <4 mg m^{-3}, de Eyto pers comm.). No data are available on in-stream benthic algae which would contribute to overall primary productivity, and to plant photosynthesis and respiration. Aerobic decomposition of DOC and particulate organic carbon would also make a significant contribution to oxygen consumption and overall DO levels in streams.

In the current project, the impact of the projected increases in RWT on DO solubility, together with elevation and aeration effects, was assessed (APHA, 1992) (Equation 5.4):

$DO = P_{wt} - p*0.625/(35-t)$ **Equation 6.4**

where,

DO = estimated dissolved oxygen concentration (mg DO L^{-1})

P_{wt} = partial pressure of water at t (hPa)

p = barometric pressure at site altitude (hPa)

t =water temperature (°C)

It should be noted that this describes only the physical portion of Equation 6.3. A more comprehensive assessment of future climate impacts on in-stream DO levels would require more detailed data on biological and chemical parameters and could form the basis of a future study.

6.4.2 Model Application

Application of the equation 6.4 to the RWT data for the Glenamong for the 2004-2006 period showed good agreement for DO concentrations in months between September and May (Figure 6.13). Negative deviations from this relationship occurred during summer months, the time of peak biological activity. The magnitude of this deviation, which represented the biological processes described in Equation 6.3 rather than the physical processes, ranged from 0.1 to 3.1 mg DO L^{-1}. The difference of 3.1 mg DO L^{-1} between the modelled and measured data occurred in June 2004; the measured DO concentration on that date was 6.8 mg DO L^{-1}. Equation 6.4 was applied to the future RWT datasets described in Section 6.2 giving 200 future simulations for each GCM model-emissions scenario combination. Mean monthly DO concentrations were calculated for each month and each year. A measure of historical variability was obtained by applying the equation to the smoothed air temperature for 1969-1999. The projected drop in DO concentration between the 1961 to 1990 period and the 2071 to 2099 period was also subtracted from measured daily values for May to September 2006 to place the estimated future impact of changes in RWT on DO solubility in the context of current biological activity.

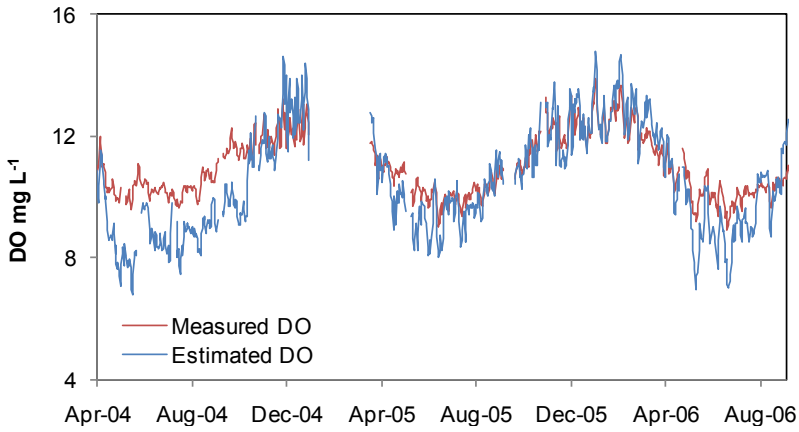

Figure 6.13: Measured (red) and estimated (blue) mean daily dissolved oxygen (DO) concentration (mg L^{-1}) in the Glenamong River, May 2004 to September 2006.

6.4.3 Impact of Projected Changes in RWT on In-Stream DO Levels

A decrease in mean annual DO concentration from the baseline 1961-1990 period to the 2010-2039 period was projected for all scenarios (Table 6.8 and 6.9). These decreases ranged from -0.1 to -0.3 mg DO L^{-1} for the simulations based on the B2 scenario. The median value for the B2 scenario for1961-1990 was 11.4 mg DO L^{-1} for the Had CM3, CSIRO Mk2 and CGCM2 models, while the median values for 2010-2039 were 11.2, 11.1 and 11.2 mg DO L^{-1}, respectively. The absolute changes for the same time period for the A2 scenario ranged from -0.1 to -0.2 mg DO L^{-1}. The A2 value for 1961-1990 was 11.4 mg DO L^{-1} for the Had CM3, CSIRO Mk2 and CGCM2 models, while the values for 2010-2039 were 11.3, 11.1 and 11.1 mg DO L^{-1} respectively.

The decreases in annual mean DO concentration for both the 2040-2069 and 2070-2099 time periods exceeded those for 2010-2039 for all model-scenario combinations (Table 6.8 and 6.9). The decreases for the A2 simulations were -0.2 (to 11.3 mg DO L^{-1}), -0.4 (to 11.0 mg DO L^{-1}) and -0.4 (to 11.0 mg DO L^{-1}) for 2040-2069 and -0.4 (to 10.9 mg DO L^{-1}), -0.6 (10.7 mg DO L^{-1}) and -0.5 (10.8 mg DO L^{-1}) for 2070-2099 for the Had CM3, CSIRO Mk2 and CGCM2 models respectively. The absolute change for the B2 simulations for the same time periods ranged from -0.2 mg DO L^{-1} to -0.4 mg DO L^{-1} (2040-2069) and from -0.3 to -0.6 mg DO L^{-1} (2070-2099). For both scenarios, the simulations based on the CSIRO Mk2 output produced the largest absolute decreases in DO concentration, reflecting the higher project RWT and air temperatures for this model, while the Had CM3 produced the lowest changes. For the 2070-2099 period, the simulations based on the A2 scenario indicated greater decreases in DO concentrations than the B2 scenario.

The currently observed seasonal pattern, with lower concentrations in summer and highest concentrations in winter, was replicated in all future simulations (Figure 6.14 and 6.15). The

relative decrease for each model-scenario combination was always lower in the late summer and highest in late autumn to mid-winter (November to January). This seasonal pattern in DO concentrations was driven by the seasonal patterns in projected RWT. However, while the overall decreases in DO concentrations were greater in winter months (Table 6.10), these would not be expected to impact on fish survival as catchment streams are well aerated during that period of the year. DO values during summer are the most biologically relevant as minimum concentrations generally occur in this period.

Decreases in DO concentration during summer are a function of both decreased solubility of DO due to higher temperatures, and net respiration from primary producers and decomposers. As the latter processes where not included in the current modelling exercise, the decrease in DO indicated by the overall A2 and B2 simulations for 2071-2099 were placed in the context of the measured summer values for the measured DO values for the Glenamong for June and July 2006 (Figure 6.16). Measured monthly average DO concentrations were 8.4 and 8.5 mg DO L^{-1}, while minimum measured daily values were 6.9 and 7.0 mg DO L^{-1} for June and July respectively. The difference between the mean DO concentration estimated for those months based on Equation 6.4, and therefore due to temperature driven changes in solubility alone, and measured monthly mean DO concentrations (representative of all factors) was -1.3 mg DO L^{-1} for both months. This difference would, therefore, be due to biological activity.

The additional projected decreases for the time period 2070-2099 -due to the impact of future changes in RWT on solubility for the A2 and B2 scenarios for 2070-2099 were -0.3 and -0.4 mg DO L^{-1} respectively, which would represent a further decrease of 4%-6% on the concentrations measured in June and July 2006 (Figure 6.13). Mean daily levels would therefore have remained above all critical values for salmonids described in Chapter 2. It should also be noted however that DO levels would be lowest during night-time, depending on rates of primary production. As described above, the lowest hourly DO concentrations in the Glenamong between 2004 and 2006 occurred at midnight on the 6th June (5.3 mg DO L^{-1}).An increase in projected RWT similar to that for the time period 2070-2099 would be expected to further reduce this to a concentration of 4.9 and 5.0 mg DO L^{-1} for the A2 and B2 scenarios respectively.

Table 6.8: A2 scenario: dissolved oxygen (DO) concentration (mg L-1) for 1961–1990 (1970s) for the three GCM models and absolute change from this period for the 2010–2039 (2020s), 2040–2069 (2050s) and 2070–2099 (2080s) periods.

A2	DO	J	F	M	A	M	J	J	A	S	O	N	D	Year
Observed	**mg L-1**	**12.5**	**12.5**	**12.2**	**11.6**	**11.0**	**10.5**	**10.1**	**10.1**	**10.5**	**11.0**	**11.9**	**12.3**	**11.3**
HadCM3	1970s	12.5	12.6	12.2	11.7	11.1	10.5	10.1	10.2	10.5	11.1	12.0	12.0	11.4
change	2020s	-0.1	-0.2	0.0	-0.1	-0.1	-0.1	0.0	-0.1	-0.1	-0.1	0.0	0.0	0.0
	2050s	-0.3	-0.3	-0.1	-0.2	-0.2	-0.1	-0.2	-0.2	-0.4	-0.2	-0.2	-0.2	-0.2
	2080s	-0.4	-0.5	-0.4	-0.4	-0.4	-0.3	-0.4	-0.4	-0.5	-0.6	-0.4	-0.4	-0.4
CSIROMk2	1970s	12.6	12.6	12.3	11.7	11.0	10.5	10.1	10.1	10.5	11.1	11.9	11.9	11.4
change	2020s	-0.3	-0.2	-0.3	-0.3	-0.1	-0.1	-0.1	-0.1	-0.2	-0.3	-0.4	-0.4	-0.2
	2050s	-0.5	-0.3	-0.4	-0.5	-0.3	-0.2	-0.2	-0.3	-0.4	-0.4	-0.5	-0.5	-0.4
	2080s	-0.8	-0.7	-0.7	-0.7	-0.4	-0.3	-0.4	-0.4	-0.6	-0.7	-0.9	-0.9	-0.6
CGCM2	1970s	12.6	12.6	12.2	11.7	11.0	10.4	10.1	10.1	10.5	11.1	12.0	12.0	11.4
change	2020s	-0.3	-0.2	-0.2	-0.2	-0.2	-0.2	-0.2	-0.2	-0.2	-0.2	-0.2	-0.2	-0.2
	2050s	-0.5	-0.4	-0.4	-0.4	-0.4	-0.3	-0.3	-0.3	-0.4	-0.5	-0.6	-0.6	-0.4
	2080s	-0.5	-0.5	-0.5	-0.5	-0.5	-0.4	-0.4	-0.4	-0.5	-0.6	-0.7	-0.7	-0.5

Table 6.9: B2 scenario: dissolved oxygen (DO) concentration (mg L-1) for 1961–1990 (1970s) for the three GCM models and absolute change from this period for the 2010–2039 (2020s), 2040–2069 (2050s) and 2070–2099 (2080s) periods.

B2	DO	J	F	M	A	M	J	J	A	S	O	N	D	Year
Observed	**mg L-1**	**12.5**	**12.5**	**12.2**	**11.6**	**11.0**	**10.5**	**10.1**	**10.1**	**10.5**	**11.0**	**11.9**	**12.3**	**11.3**
HadCM3	1970s	12.5	12.6	12.2	11.7	11.1	10.5	10.1	10.2	10.5	11.1	12.0	12.0	11.4
change	2020s	0.1	-0.2	0.0	-0.1	-0.1	-0.1	0.0	-0.1	-0.2	-0.1	-0.3	-0.3	-0.1
	2050s	-0.1	-0.1	0.0	-0.2	-0.2	-0.1	-0.1	-0.2	-0.2	-0.2	-0.3	-0.3	-0.2
	2080s	-0.2	-0.3	-0.2	-0.3	-0.3	-0.3	-0.2	-0.2	-0.3	-0.4	-0.5	-0.5	-0.3
CSIROMk2	1970s	12.6	12.6	12.3	11.7	11.0	10.5	10.1	10.1	10.5	11.1	11.9	11.9	11.4
change	2020s	-0.5	-0.5	-0.4	-0.3	-0.2	-0.2	-0.2	-0.2	-0.3	-0.3	-0.4	-0.4	-0.3
	2050s	-0.6	-0.5	-0.5	-0.5	-0.4	-0.3	-0.2	-0.3	-0.4	-0.4	-0.7	-0.7	-0.4
	2080s	-0.7	-0.6	-0.6	-0.6	-0.4	-0.3	-0.3	-0.4	-0.5	-0.6	-0.8	-0.8	-0.5
CGCM2	1970s	12.6	12.6	12.2	11.7	11.0	10.4	10.1	10.1	10.5	11.1	12.0	12.0	11.4
change	2020s	-0.3	-0.3	-0.2	-0.2	-0.1	-0.1	-0.2	-0.2	-0.2	-0.2	-0.2	-0.2	-0.2
	2050s	-0.3	-0.3	-0.3	-0.3	-0.3	-0.2	-0.3	-0.2	-0.3	-0.3	-0.4	-0.4	-0.3
	2080s	-0.3	-0.4	-0.4	-0.4	-0.3	-0.3	-0.3	-0.3	-0.5	-0.5	-0.6	-0.6	-0.4

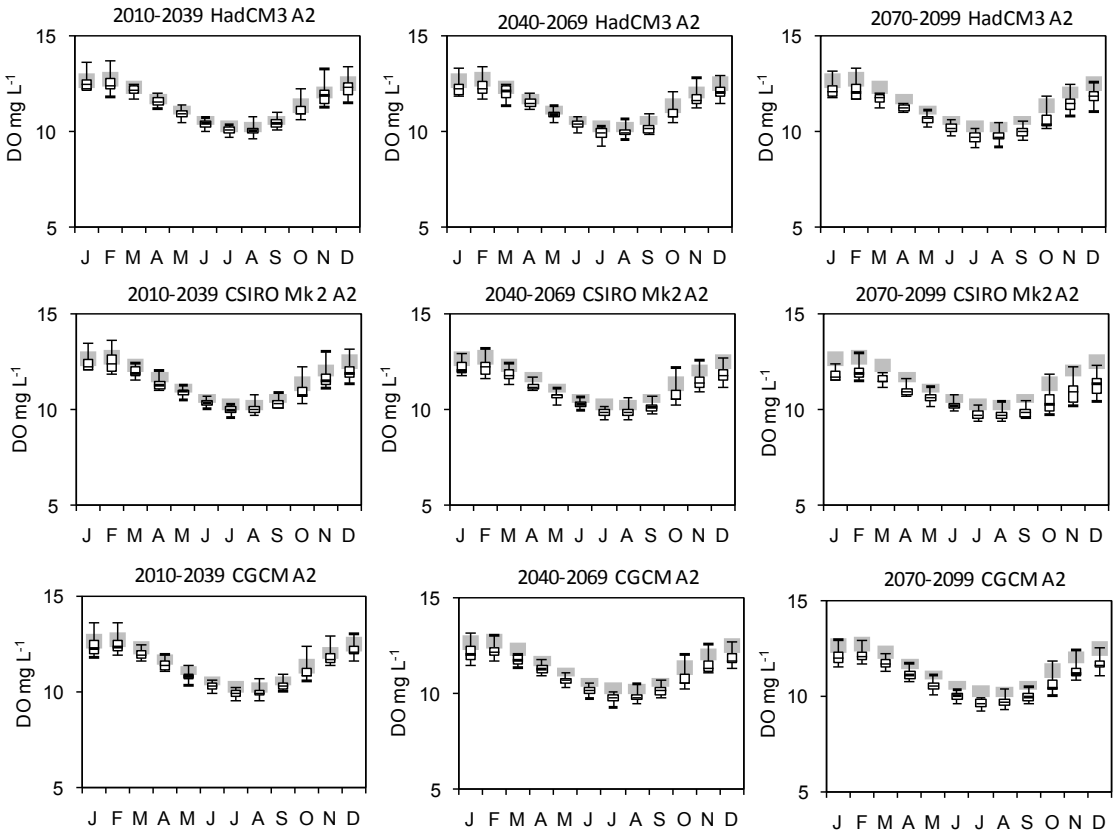

Figure 6.14: A2 scenario: boxplots of dissolved oxygen (DO) concentration (mg L^{-1}) for the three GCM models for three periods: 2010-2039, 2040-2069 and 2070-2099. Shaded areas are the 25 percentile to 75 percentile range for model runs using historical meteorological data and are used to represent observed variability.

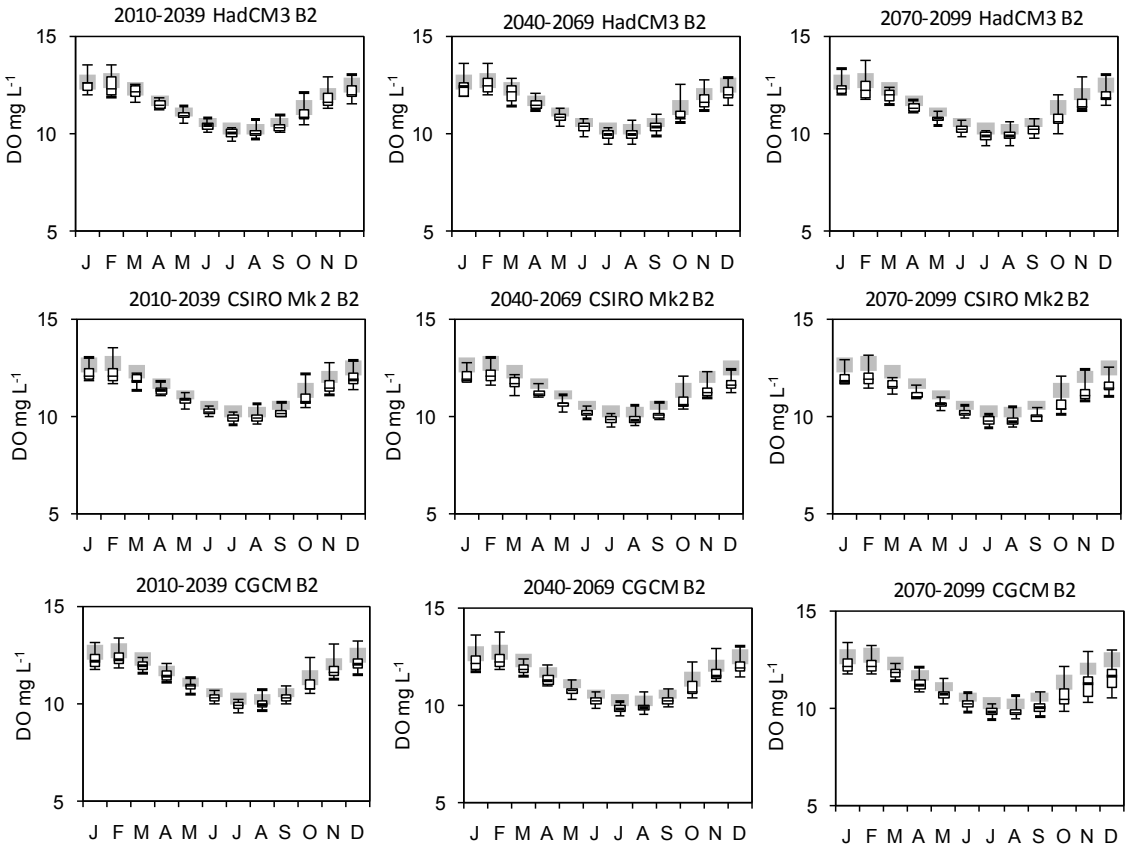

Figure 6.15: B2 scenario: boxplots of dissolved oxygen (DO) concentration (mg L^{-1}) for the three GCM models for three periods: 2010-2039, 2040-2069 and 2070-2099. Shaded areas are the 25 percentile to 75 percentile range for model runs using historical meteorological data and are used to represent observed variability.

Table 6.10: Deviation from the 1961–1990 period for the overall A2 and B2 scenario for the 2010-2039 (2020s), 2040-2069 (2050s) and 2070-2099 (2080s) (mg DO L^{-1}).

	DO mg L^{-1}	J	F	M	A	M	J	J	A	S	O	N	D
A2	2020s	-0.2	-0.2	-0.2	-0.2	-0.1	-0.1	-0.1	-0.1	-0.2	-0.2	-0.2	-0.2
	2050s	-0.4	-0.4	-0.3	-0.3	-0.3	-0.2	-0.2	-0.3	-0.4	-0.4	-0.4	-0.4
	2080s	-0.6	-0.6	-0.5	-0.5	-0.4	-0.3	-0.4	-0.4	-0.6	-0.6	-0.7	-0.7
B2	2020s	-0.2	-0.3	-0.2	-0.2	-0.1	-0.1	-0.1	-0.2	-0.2	-0.2	-0.3	-0.3
	2050s	-0.3	-0.3	-0.3	-0.3	-0.3	-0.2	-0.2	-0.2	-0.3	-0.3	-0.4	-0.4
	2080s	-0.4	-0.5	-0.4	-0.4	-0.3	-0.3	-0.3	-0.3	-0.4	-0.5	-0.6	-0.6

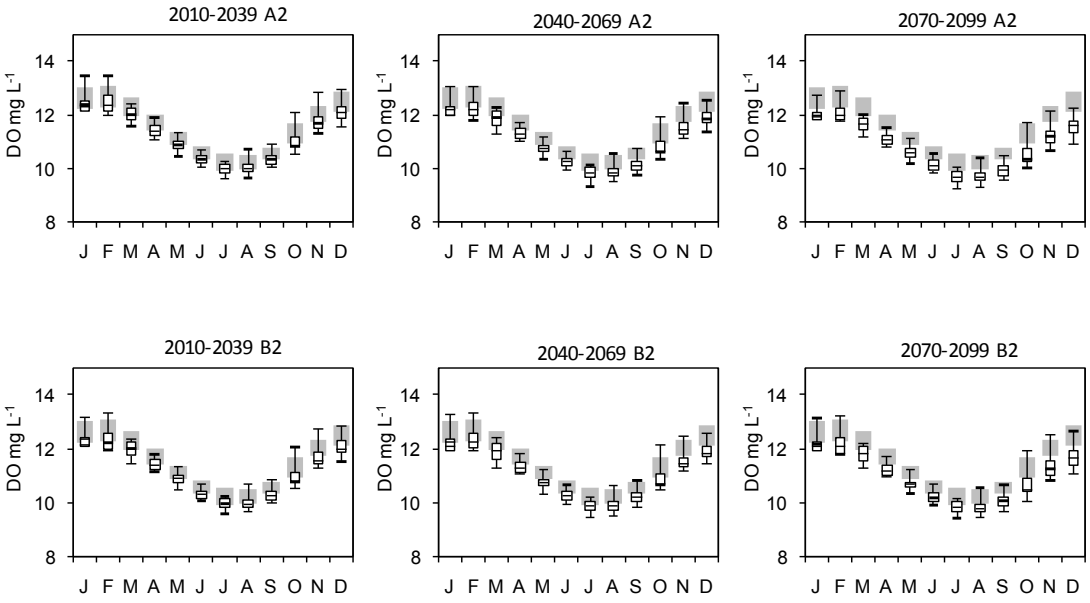

Figure 6.16: B2 scenario: boxplots of dissolved oxygen (DO) concentration (mg L-1) for the combined GCM models for both the A2 and B2 scenarios for three periods: 2010–2039, 2040–2069 and 2070–2099. Shaded areas are the 25 percentile to 75 percentile range for model runs using historical meteorological data and are used to represent observed variability.

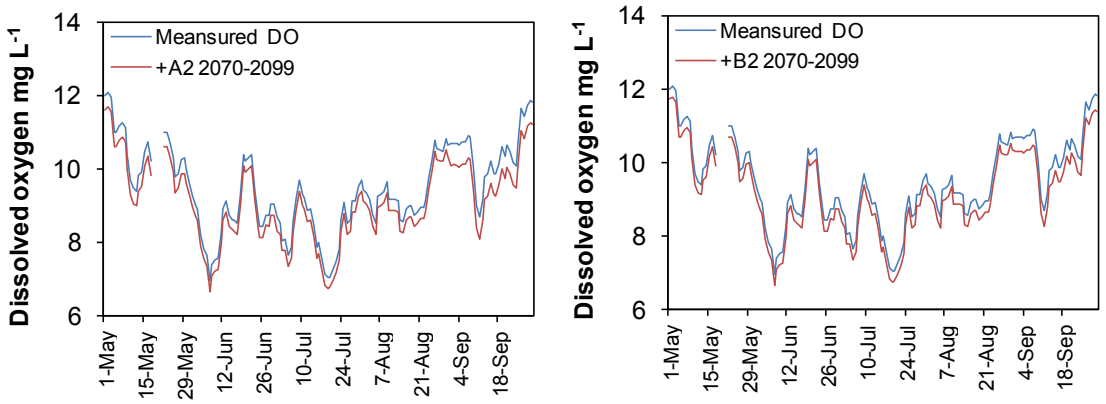

Figure 6.17: Measured dissolved oxygen (DO) concentration (mg DO L^{-1}), Glenamong River, May to September 2006 (blue lines): these measured data plus the projected decrease in DO concentrations due to the effect of projected river water temperature increase on DO concentrations, for both the A2 and B2 scenarios for 2070-2099 (red lines).

6.5 Lake Water Temperature

6.5.1 Lake Water Temperature Model (DYRESM)

DYRESM (Dynamic Reservoir Simulation Model) is a one-dimensional hydrodynamics model for predicting the vertical distribution of temperature, salinity and density in lakes. The model and software were available from the Centre for Water Research (CWR), University of Western Australia (Imberger & Patterson 1981). DYRESM provides a means of predicting seasonal and interannual variation in lakes and reservoirs, as well as investigating the sensitivity

to long-term changes in environmental factors or catchment properties (Imerito 2007). The model can be run at daily or subdaily time-steps. Model input data requirements are relatively extensive and include daily data for solar radiation, cloud cover, wind speed, vapour pressure, air temperature, and precipitation. Data are also required on lake bathymetry, inflow volume and inflow water temperature. DYRESM model outputs include water temperature and density. The results can be interpolated to give a high resolution two-dimensional output of the modelled water temperature at the deepest point in a lake over time. The model relies on parameterisations derived from detailed process studies (both from the field and in the laboratory) and is unique in that reliable projections are obtained without calibration (Imerito, 2007).

6.5.2 DYRESM Application and Validation

Data from the meteorological stations at Newport and Belmullet were used to validate DYRESM for Lough Feeagh. Relative humidity values were converted to vapour pressure (Imerito, 2007). A range of meteorological parameters, including solar radiation and wind speed data, were also available for some shorter periods from a monitoring buoy situated at the deepest point on the lake from 1996 to present. A comparison of wind speed data from these buoys with wind data from Belmullet showed that both datasets had similar values at low speeds. At higher wind speed, however, values measured at the two stations tended to be greater than those measured on the Feeagh buoy. Wind speed data from the Belmullet meteorological station were corrected based on the regression relationship between the the two datasets. Where measurements of streamflow were not available, simulated streamflow data were generated using the hydrology subroutine of the GWLF model (Schneiderman et al., 2002). Smoothed air temperature calculated as described in section 6.2 was used as a surrogate for stream water temperature. Data for surface water temperature (SWT) (0.5m) and deep water temperature (DWT) (40m) were output from the model simulations. The simulations for Feeagh were validated using a long-term record of water temperature, measured using a Negretti chart recorder, from a site situated close to the lake outflow for 1974 to 1990 which are representative of lake surface water temperature (Figure 6.18a) and data from the buoy thermistor chain (Figure 6.18b and 6.18c). The model fit when compared to the long-term daily SWT data was good with a NS coefficient of 0.98 (1974 to 1990). Projected air temperature, wind speed, precipitation, and solar radiation data were available as model input data for future climate simulations using DYRESM. The ratio of solar radiation to clear-sky solar radiation (relative shortwave radiation) was used as a substitute for cloud cover in net longwave radiation calculations (Allen et al., 1998).

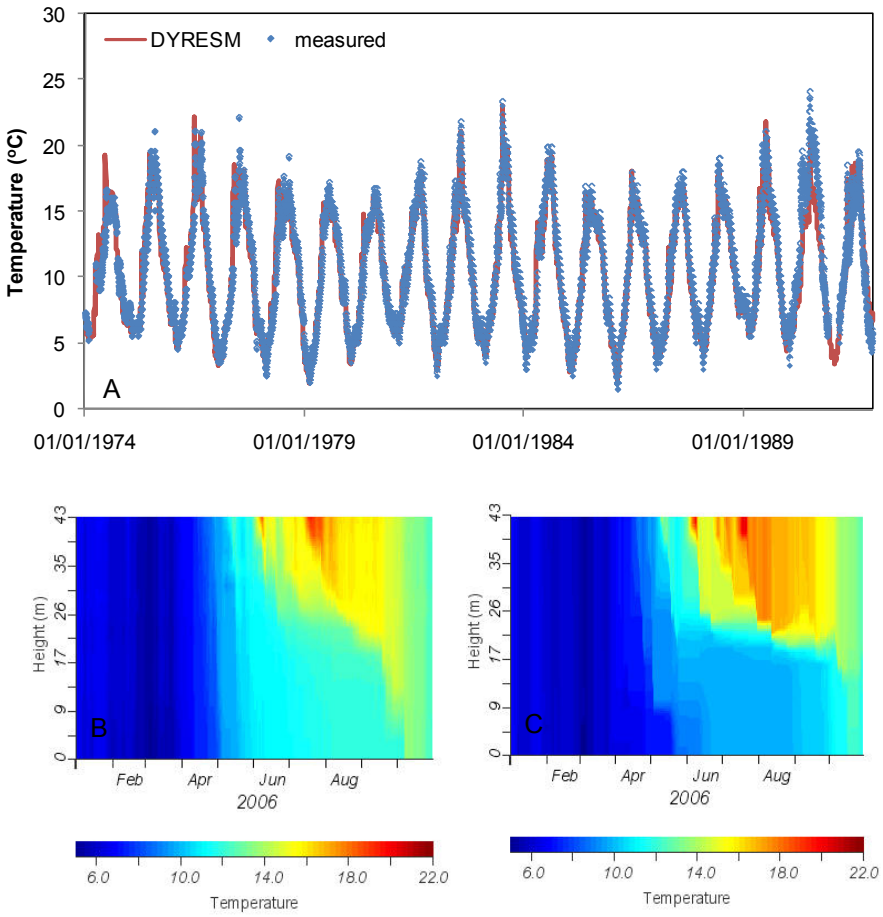

Figure 6.18: a) Measured and modelled surface water temperature (daily at midnight, °C), Lough Feeagh, 1974-1990; b) and c): interpolated plots of water temperature profiles for Lough Feeagh based on B. measured water temperature data (10 depths between the surface and 43m; daily averages based on data logged at two minute intervals) and C. DYRESM modelled water temperature, January to October 2006 (height (m) = m above lake bed).

Ten simulations were carried out for each model-emissions scenario combination. These included one dataset each with downscaled wind speed or precipitation data based on a GLM. DYRESM simulations using historical driving data from 1969-199 were used to provide a measure of historical variability. Mean monthly water temperatures were calculated for two depths: 0.5m and 40m. The 25%ile and 75%ile ranges for the historical variability are included in all graphs to provide a common frame of reference. Future climate simulations are presented as boxplots of the 5%ile, 25%ile, 50%ile, 75%ile and 95%ile values of mean monthly temperatures. The difference between the GCM-scenario combinations was examined using the Kolmogorov-Smirnov (KS) test which tests for differences in location and shape of the distribution.

6.5.3 Projected Changes in LWT

Mean annual surface water temperature in Lough Feeagh was projected to increase under both the A2 and B2 scenarios for all time periods (Tables 6.11). The median increase was greater

for each A2 scenario than for equivalent B2 scenario. The greatest increase in annual temperature was projected when the model was run using input data based on the CSIRO Mk2 model and the A2 emissions scenario: these were 1.0°C, 1.8°C and 2.5°C for the 2010-2039, 2040-2069 and 2070-2099 time periods respectively (Table 6.11). The increases for the CSIRO B2 simulations for these same time periods were 1.1°C, 1.7°C and 2.1°C. The lowest increases were for the CGCM2 GCM: for the A2 scenario these were 0.8°C, 1.5°C and 1.9°C while for the B2 scenarios they were 0.8°C, 1.3°C and 1.6°C. The overall increases for the A2 scenario were 0.6°C, 1.5°C and 2.1°C for the 2010-2039, 2040-2069 and 2070-2099 time periods respectively, while those for the B2 scenario were 0.8°C, 1.3 °C and 1.5°C.

The increases in mean annual surface water temperatures were also apparent in the monthly mean values (Figures 6.19 and 6.20, and Table 6.11). There was a tendency for greater projected increases in the autumn and winter months than for summer months for the simulations based on the CSIRO Mk2 and CGCM2 GCMs. In contrast, higher increases were indicated in summer for the Had CM3 model. The projected increases for the combined simulations (all three GCM models) based on the A2 scenario for the more immediate future (2010 to 2039) ranged from 0.4°C in June to 0.9°C in April. For the period 2040-2069, they ranged from 0.9°C in June to 1.6°C in September. The lowest monthly increases for the period 2070-2099 were again in June (1.8°C) while the highest were in August/September (2.3°C). The increases in mean monthly SWT for the B2 scenario were slightly higher for the 2010-2039 period than those for the overall A2 scenario (Figure 6.20). However, in contrast the increase for the 2070-2099 period was lower for the simulations based on the B2 emission scenario than the A2 scenario by c. 0.3 °C to 0.4°C in all months.

The most striking difference between the projections for DWT and SWT related to a difference in the seasonal pattern during months when the model lake was stratified (Figure 6.21, 6.22, 6.23 and 6.24 and Table 6.12). Simulated deep temperatures were similar to surface temperatures in those months during which the lake was fully mixed i.e. between December and April (Figures 6.22 and 6.23; Tables 6.13 and 6.14). In contrast, surface water temperatures were greater than DWT in periods when the lake was stratified in the simulations based on historical data and for all future climate simulations: these differences ranged up to 6.5°C. While significant increases were projected for DWT during the mixed period that were similar to those projected for SWT, there was no significant increase in DWT for any GCM-emission scenario combination during the months between May and October (Table 6.13 and 6.14). This lack of any increase in deep water temperature reflected model structure but also may have replicated a potential buffering of the water column below the thermoclime from the influence of changes in local weather.

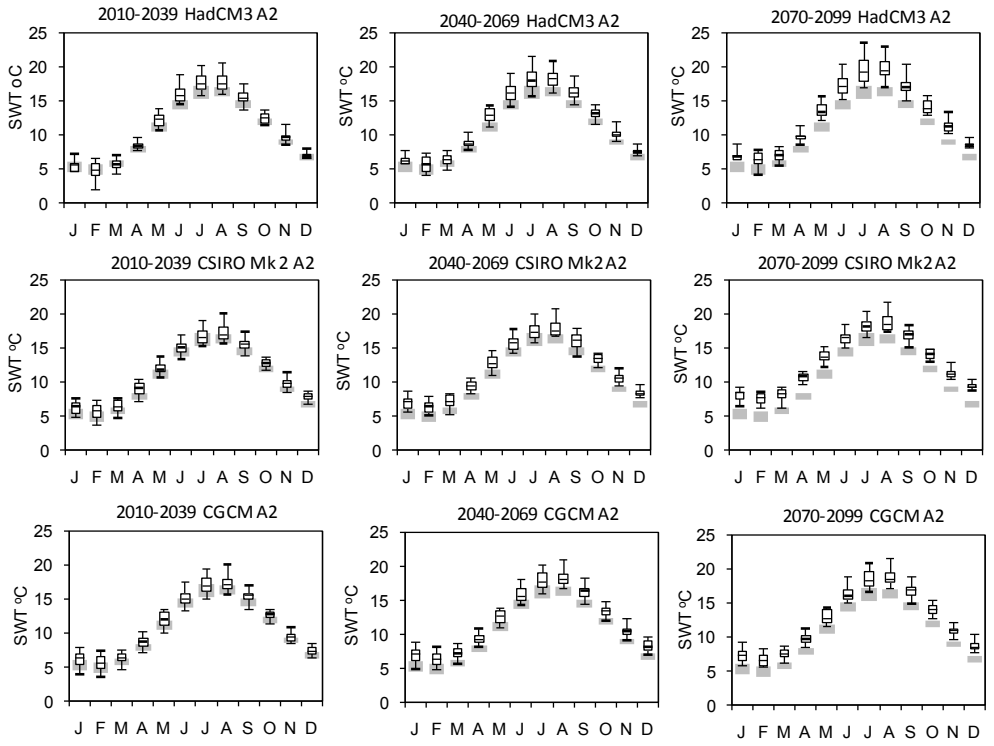

Figure 6.19: A2 scenario: boxplots of lake surface water temperature (SWT) °C for the three GCM models for the time periods 2010-2039, 2040-2069 and 2070-2099. Shaded areas are the 25 percentile to 75 percentile range for model runs using resampled historical meteorological data and represent observed variability.

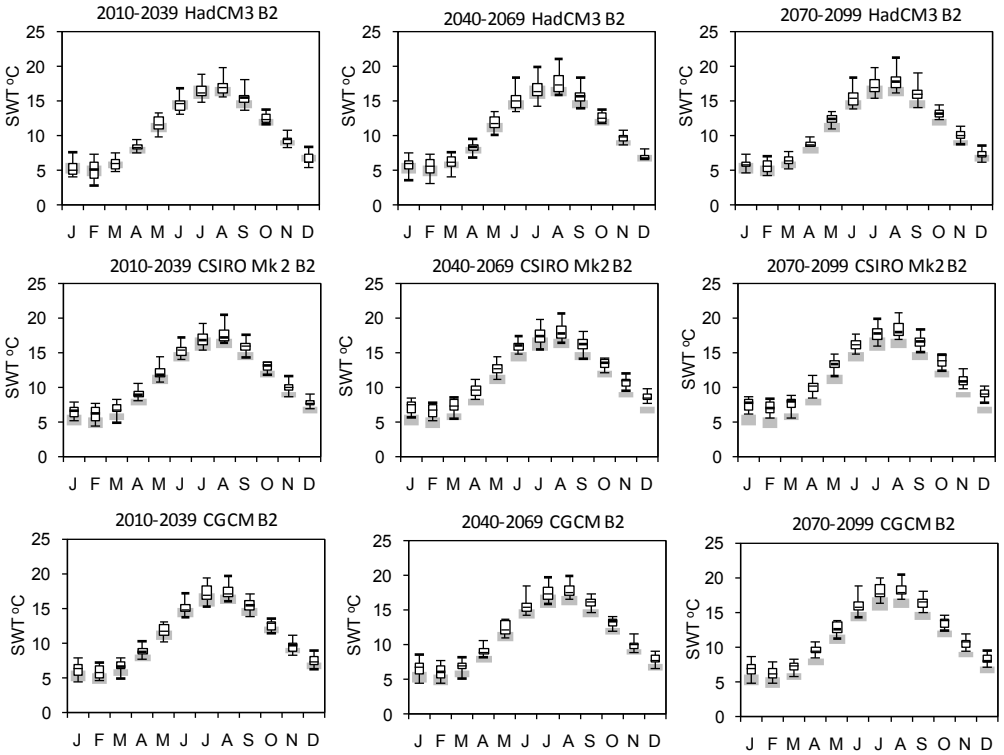

Figure 6.20: B2 scenario: boxplots of lake surface water temperature (SWT) °C for the three GCM models for the time periods 2010-2039, 2040-2069 and 2070-2099. Shaded areas are the 25 percentile to 75 percentile range for model runs using resampled historical meteorological data and represent observed variability.

Table 6.11: Lake surface water temperature (SWT) in °C (0.5 m) for the observed period and for the 1961–1990 (1970s) period for the three GCM models together with the absolute change from this period for the 2010–2039 (2020s), 2040–2069 (2050s) and 2070–2099 (2080s) periods for the A2 and B2 scenarios.

A2	SWT	J	F	M	A	M	J	J	A	S	O	N	D	Year
Observed	**°C**	**5.5**	**4.9**	**5.7**	**7.8**	**11.0**	**14.4**	**16.0**	**16.2**	**14.5**	**11.9**	**9.0**	**6.5**	**10.3**
HadCM3	1970s	4.5	4.3	5.0	6.8	9.7	12.8	14.7	15.2	13.9	11.3	8.2	6.2	9.4
change	2020s	0.1	-0.2	0.0	0.6	1.3	1.3	1.5	1.3	0.8	0.6	0.7	0.0	0.6
	2050s	0.7	0.7	0.7	0.8	1.9	1.7	1.9	2.0	1.6	1.3	1.1	0.3	1.2
	2080s	1.3	1.4	1.3	2.0	2.3	2.6	3.2	3.2	2.4	1.9	2.3	1.5	2.2
CSIRO-MK2	1970s	4.5	3.8	4.6	6.9	10.7	14.0	16.2	16.4	14.4	11.4	8.6	6.2	9.8
change	2020s	0.9	0.8	0.7	1.3	0.8	0.6	0.5	0.7	1.0	0.8	0.9	1.3	1.0
	2050s	1.6	1.5	1.5	1.7	1.7	1.4	1.3	1.3	1.6	1.5	1.6	1.8	1.6
	2080s	2.9	2.7	2.5	3.1	2.7	2.1	2.1	2.2	2.5	2.2	2.2	2.7	2.5
CGCM2	1970s	4.4	3.8	4.6	7.0	10.5	14.3	16.1	16.4	14.4	11.4	8.5	6.0	9.8
change	2020s	0.9	0.6	0.7	0.9	1.0	0.5	0.8	0.8	1.0	0.9	0.4	0.7	0.8
	2050s	1.6	1.4	1.5	1.4	1.7	1.1	1.7	1.8	1.9	1.6	1.5	1.7	1.5
	2080s	1.8	1.5	1.9	1.9	1.7	1.6	2.2	2.2	2.4	2.1	2.0	2.0	1.9
B2	**AT**	**J**	**F**	**M**	**A**	**M**	**J**	**J**	**A**	**S**	**O**	**N**	**D**	**Year**
Observed	**°C**	**5.5**	**4.9**	**5.7**	**7.8**	**11.0**	**14.4**	**16.0**	**16.2**	**14.5**	**11.9**	**9.0**	**6.5**	**10.4**
HadCM3	1970s	5.1	4.2	4.9	7.2	10.5	14.3	16.3	16.1	14.2	11.6	8.8	6.7	10.1
change	2020s	-0.5	0.2	0.3	0.5	0.6	0.2	0.2	0.7	0.9	0.3	0.4	-0.3	0.2
	2050s	0.4	0.7	0.5	0.6	0.7	0.5	0.3	1.0	1.1	0.6	0.8	0.2	0.6
	2080s	0.3	0.6	0.7	0.8	1.4	0.9	0.9	1.5	1.4	1.3	1.0	0.6	0.8
CSIRO-MK2	1970s	4.5	3.8	4.6	6.9	10.7	14.0	16.2	16.4	14.4	11.4	8.6	6.2	9.8
change	2020s	1.1	1.3	1.1	1.1	0.8	0.9	0.8	0.9	1.4	1.2	1.0	1.1	1.1
	2050s	2.0	1.8	1.6	1.8	1.7	1.6	1.3	1.5	1.7	1.6	2.0	1.9	1.7
	2080s	2.2	2.1	2.3	2.3	2.3	1.7	1.7	1.7	2.1	2.0	1.9	2.4	2.1
CGCM2	1970s	4.4	3.9	4.5	7.0	10.6	14.4	16.1	16.5	14.4	11.3	8.4	6.0	9.8
change	2020s	0.8	0.9	1.0	1.0	0.8	0.3	0.9	0.8	0.9	0.9	0.7	0.8	0.8
	2050s	1.2	1.1	1.2	1.1	1.1	0.9	1.3	1.3	1.6	1.4	1.1	1.2	1.3
	2080s	1.4	1.2	1.6	1.6	1.6	1.3	1.6	1.7	1.9	1.9	1.7	1.5	1.6

Table 6.12: Lake deep water temperature (DWT) in °C (40 m) for the observed period and for the 1961–1990 (1970s) period for the three GCM models together with the absolute change from this period for the 2010–2039 (2020s), 2040–2069 (2050s) and 2070–2099 (2080s) periods for the A2 and B2 scenarios.

A2	DWT	J	F	M	A	M	J	J	A	S	O	N	D	Year
Observed	**°C**	**5.5**	**4.9**	**5.7**	**7.1**	**8.2**	**9.2**	**9.6**	**9.7**	**9.8**	**10.9**	**8.7**	**6.5**	**7.4**
HadCM3	1970s	4.6	4.1	4.7	5.9	6.8	7.9	8.6	8.7	8.6	9.2	8.1	6.6	6.9
change	2020s	0.8	0.6	0.4	0.3	0.9	0.4	0.3	0.6	0.5	0.0	1.0	0.9	0.8
	2050s	1.5	1.2	1.3	0.7	1.0	1.0	0.6	0.5	0.6	1.3	1.8	1.5	1.1
	2080s	2.8	2.4	2.1	2.0	1.8	1.4	1.0	1.0	1.1	0.9	2.2	2.3	1.9
CSIRO-MK2	1970s	4.7	3.8	4.6	5.8	6.9	7.9	8.3	8.6	9.1	9.7	8.3	6.2	7.0
change	2020s	0.7	0.9	0.4	0.4	0.8	0.4	0.6	0.6	0.0	-0.4	0.7	1.3	0.6
	2050s	1.4	1.5	1.3	0.9	0.9	0.9	0.9	0.6	0.2	0.9	1.5	1.8	1.0
	2080s	2.8	2.7	2.2	2.1	1.8	1.4	1.3	1.1	0.7	0.4	1.9	2.6	1.7
CGCM2	1970s	4.6	4.1	4.7	5.9	6.8	7.9	8.6	8.7	8.6	9.2	8.1	6.6	6.9
change	2020s	0.7	0.4	0.5	0.7	1.1	0.8	1.0	1.0	1.0	0.4	0.5	0.1	0.9
	2050s	1.4	1.2	1.2	1.2	1.5	1.0	0.7	0.8	0.7	0.5	1.6	1.0	1.2
	2080s	1.7	1.4	1.5	1.4	2.0	1.7	1.2	1.2	1.1	0.8	2.0	1.4	1.6
B2	**AT**	**J**	**F**	**M**	**A**	**M**	**J**	**J**	**A**	**S**	**O**	**N**	**D**	**Year**
Observed	**°C**	**5.5**	**4.9**	**5.7**	**7.1**	**8.2**	**9.2**	**9.6**	**9.7**	**9.8**	**10.9**	**8.7**	**6.5**	**7.4**
HadCM3	1970s	5.2	4.3	4.9	6.0	7.3	8.6	8.8	8.8	8.7	9.2	8.5	6.7	7.3
change	2020s	-0.5	0.1	0.1	-0.1	-0.4	-0.5	-0.1	-0.1	-0.1	0.0	0.1	-0.6	-0.4
	2050s	0.4	0.5	0.2	0.5	0.6	0.1	0.4	0.3	0.3	0.2	0.6	0.0	0.4
	2080s	0.2	0.6	0.4	0.4	0.4	0.1	0.3	0.3	0.3	0.7	1.0	0.5	0.3
CSIRO-MK2	1970s	4.7	3.8	4.6	5.8	6.9	8.1	8.6	8.6	8.9	9.5	8.3	6.1	7.0
change	2020s	1.0	1.3	0.9	0.9	0.7	0.4	0.4	0.4	-0.1	0.1	1.1	1.0	0.7
	2050s	1.8	1.8	1.4	1.2	1.1	0.8	0.8	0.8	0.3	0.4	1.8	1.8	1.1
	2080s	2.1	2.1	1.9	1.6	1.5	0.8	0.6	0.6	0.2	0.0	1.7	2.5	1.3
CGCM2	1970s	4.5	3.9	4.5	6.0	7.3	8.3	8.7	9.1	8.9	9.1	8.2	6.0	7.0
change	2020s	0.7	0.9	1.0	0.9	0.9	0.7	0.6	0.1	0.2	0.4	0.6	0.7	0.6
	2050s	1.1	1.1	1.1	1.2	0.9	0.6	0.3	0.0	0.0	0.1	0.9	1.1	0.8
	2080s	1.3	1.2	1.3	1.4	1.3	0.9	0.8	0.4	0.4	0.6	1.2	1.4	1.0

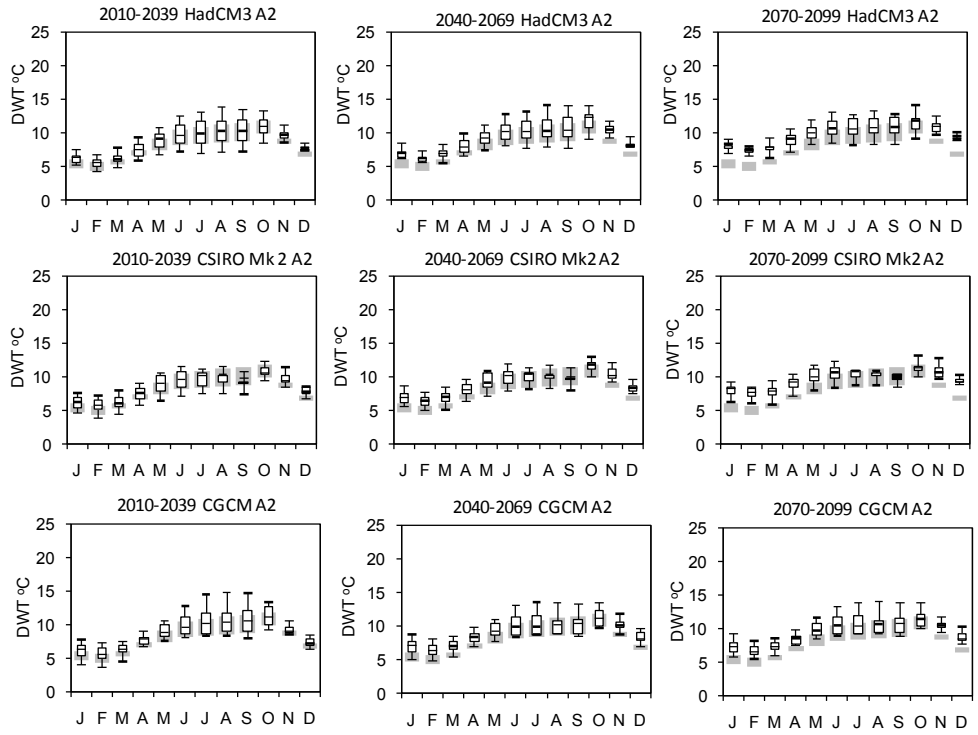

Figure 6.21 A2 scenario: boxplots of lake deep water temperature (DWT, °C) for the three GCM models for 2010-2039, 2040-2069 and 2070-2099. Shaded areas are the 25 percentile to 75 percentile range for runs using resampled historical meteorological data and represent observed variability.

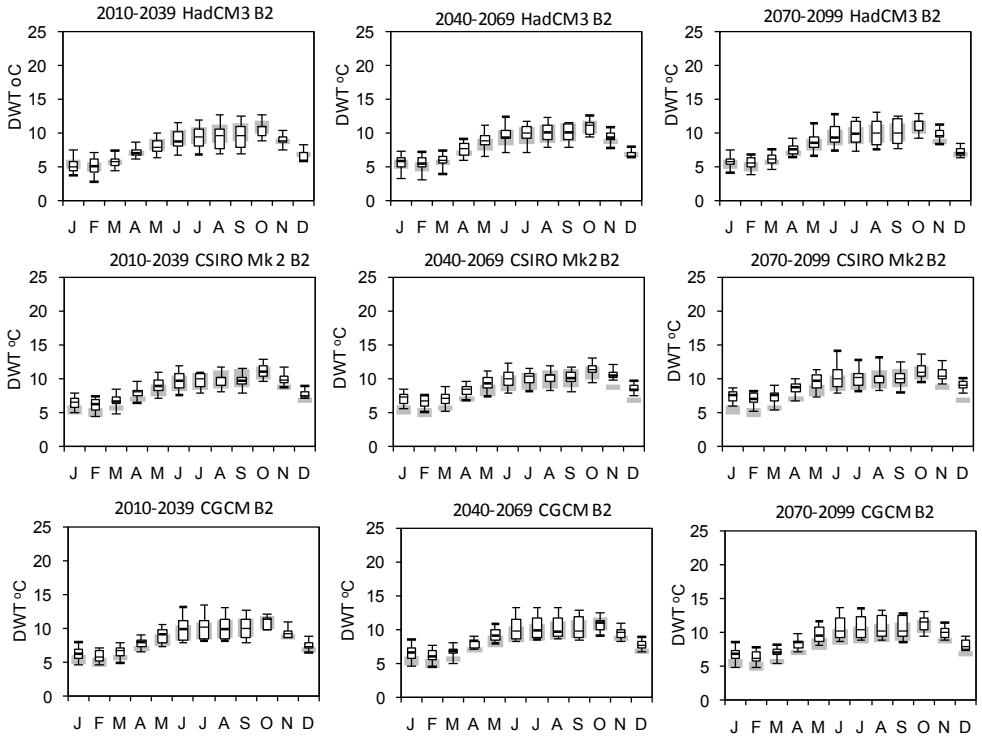

Figure 6.22: B2 scenario: boxplots of lake deep water temperature (DWT, °C) for the three GCM models for 2010-2039, 2040-2069 and 2070-2099. Shaded areas are the 25 percentile to 75 percentile range for runs using resampled historical meteorological data and represent observed variability.

Table 6.13: Overall A2 scenario: lake surface water temperature (SWT) (0.5 m) and deep water temperature (DWT) (40 m) in °C for the observed period and for the 1961–1990 (1970s) period for the combined GCM models together with the absolute change from this period for the 2010–2039 (2020s), 2040–2069 (2050s) and 2070–2099 (2080s) periods for the A2 scenario.c

A2		J	F	M	A	M	J	J	A	S	O	N	D	Year
SWT observed	**°C**	**5.5**	**4.9**	**5.7**	**7.8**	**11.0**	**14.4**	**16.0**	**16.2**	**14.5**	**11.9**	**9.0**	**6.5**	**10.3**
A2	1970s	4.4	3.8	4.6	6.9	10.6	14.2	16.2	16.4	14.3	11.4	8.5	6.1	9.8
change	2020s	0.7	0.6	0.5	0.9	0.7	0.4	0.5	0.7	0.9	0.7	0.6	0.6	0.6
	2050s	1.4	1.4	1.4	1.3	1.4	0.9	1.2	1.4	1.6	1.3	1.3	1.4	1.5
	2080s	2.0	2.0	2.0	2.1	2.0	1.8	2.2	2.3	2.3	2.0	2.2	2.0	2.1
DWT observed	**°C**	**5.5**	**4.9**	**5.7**	**7.1**	**8.2**	**9.2**	**9.6**	**9.7**	**9.8**	**10.9**	**8.7**	**6.5**	**8.0**
A2	1970s	4.5	3.9	4.6	5.8	7.0	8.1	8.6	8.8	8.7	9.5	8.3	6.1	7.0
change	2020s	0.7	0.7	0.4	0.5	0.5	0.2	0.1	0.2	0.3	-0.1	0.4	0.5	0.4
	2050s	1.4	1.4	1.2	0.8	0.8	0.4	0.3	0.2	0.4	0.4	1.3	1.2	0.8
	2080s	1.9	2.0	1.8	1.6	1.6	1.0	0.9	0.8	0.9	0.5	1.8	2.0	1.4

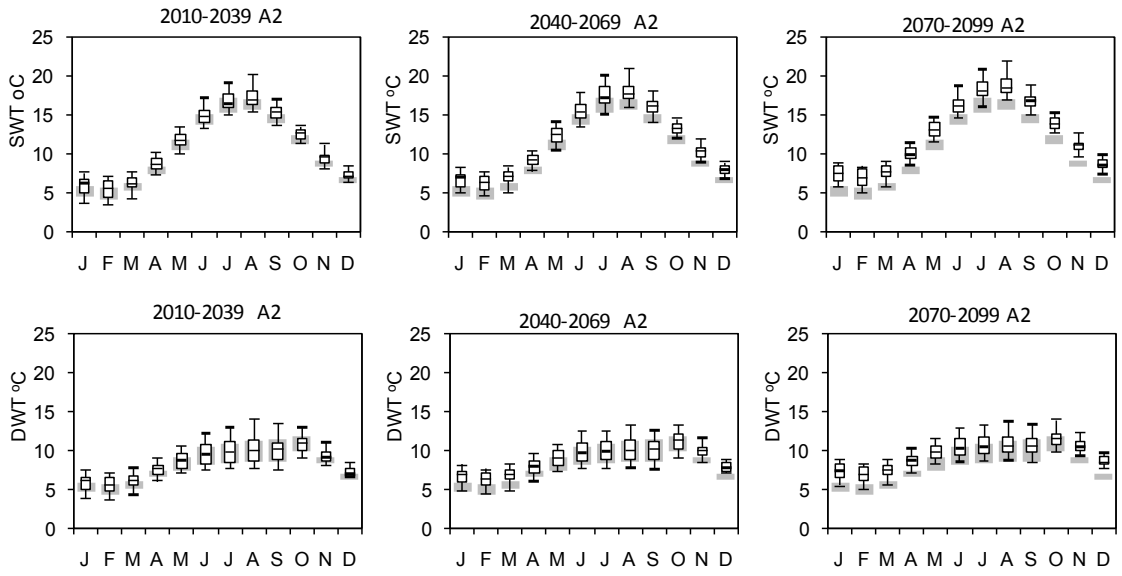

Figure 6.23: Boxplots of lake surface (SWT) and deep water temperature (DWT) (°C) based on the A2 scenario for the three GCM models combined for time periods 2010-2039, 2040-2069 and 2070-2099. Shaded areas are the 25 percentile to 75 percentile range for model runs using resampled historical meteorological data and are used to represent observed variability.

Table 6.14: Overall B2 scenario: lake surface water temperature (SWT) (0.5 m) and deep water temperature (DWT) (40 m) in °C for the observed period and for the 1961–1990 (1970s) period for the combined GCM models together with the absolute change from this period for the 2010–2039 (2020s), 2040–2069 (2050s) and 2070–2099 (2080s) periods for the A2 scenario

B2		J	F	M	A	M	J	J	A	S	O	N	D	Year
SWT observed	**°C**	**5.5**	**4.9**	**5.7**	**7.8**	**11.0**	**14.4**	**16.0**	**16.2**	**14.5**	**11.9**	**9.0**	**6.5**	**10.3**
B2	1970s	4.6	4.0	4.6	7.0	10.6	14.2	16.2	16.4	14.3	11.4	8.6	6.1	9.8
change	2020s	0.7	0.9	0.9	0.9	0.7	0.6	0.7	0.8	1.0	0.9	0.7	0.8	0.8
	2050s	1.4	1.1	1.2	1.1	1.1	1.1	1.1	1.4	1.5	1.2	1.2	1.2	1.3
	2080s	1.4	1.3	1.5	1.6	1.6	1.4	1.5	1.7	1.8	1.7	1.6	1.5	1.5
DWT observed	**°C**	**5.5**	**4.9**	**5.7**	**7.1**	**8.2**	**9.2**	**9.6**	**9.7**	**9.8**	**10.9**	**8.7**	**6.5**	**8.0**
B2	1970s	4.7	4.0	4.6	5.9	7.2	8.4	8.8	8.8	8.8	9.2	8.3	6.1	7.1
change	2020s	0.6	0.9	0.7	0.5	0.3	0.0	0.1	0.2	0.0	0.3	0.6	0.7	0.4
	2050s	1.3	1.2	1.0	0.9	0.8	0.4	0.4	0.3	0.3	0.4	1.1	1.1	0.7
	2080s	1.3	1.4	1.2	1.1	1.1	0.5	0.4	0.4	0.3	0.4	1.5	1.5	0.9

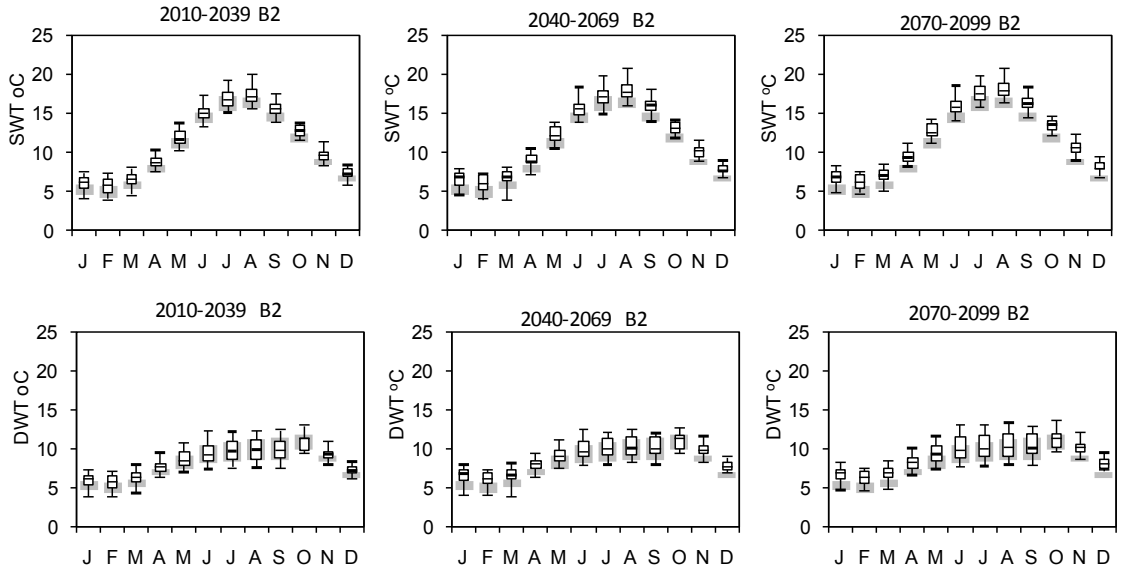

Figure 6.24: Boxplots of lake surface (SWT) and deep water temperature (DWT) (°C) based on the B2 scenario for the three GCM models combined for time periods 2010-2039, 2040-2069 and 2070-2099. Shaded areas are the 25 percentile to 75 percentile range for model runs using resampled historical meteorological data and are used to represent observed variability.

6.6 Summary

Projected changes in water quality parameters which were identified in this study and which could directly affect fish growth and survival include increase in RWT and lake SWT, together with decreases in DO and DOC concentrations. Increases in water temperature may have both potential positive and negative consequences for fish populations, biodiversity and ecosystem functioning in the Burrishoole catchment. Many of the rivers in Burrishoole are

important spawning grounds for Atlantic salmon and brown trout while Lough Feeagh is particularly important habitat during salmon smoltification. The lake also has a resident trout population and can hold up to 90% of the eel population (de Eyto pers. comm.).

The implications of the projected increases in river and lake water temperatures for fish populations are discussed in more detail in Chapter 7.

The decreases in DO levels simulated for catchment streams in Burrishoole relate solely to the physical impact of RWT on DO solubility. The greatest projected decreases were indicated for simulations based on the A2 scenario for the time period 2071-2099, the simulations with the highest RWT. However, despite the dominant influence of RWT on DO levels, these higher temperatures resulted in only a 4% to7% decrease in average daily values. It should be emphasised that increases in temperature will also influence rates of organic matter decomposition by bacteria and possibly rates of in-stream primary productivity. Primary production will also be affected by any change in solar radiation. Little in-stream data on primary production and decomposition is currently available for Burrishoole. Simulations of all in-stream processes would require this additional data, in particular data on benthic producers, but could form the basis of a further study at postgraduate level.

Increases in DOC concentrations were projected for all GCM model and emission scenarios from the 2010-2039 period onwards. The projected increases would have consequences for the ecology of Lough Feeagh and other lakes in peaty catchments. Lough Feeagh is an important fish habitat, especially for the freshwater stages of salmon and sea trout. Many highly coloured lakes like Feeagh exhibit net heterotrophy due to the central role of catchment DOC in fuelling the upper trophic levels via the bacterioplankton-protozoan link (e.g. Tranvik, 1992; Kankaala et al., 1996). The projected increases in DOC may, therefore, alter the food-web dynamics in the lake. However, reduced light intensity also lowers the reactive distance of fish and their ability for size-selective predation (Wissel et al., 2003). The hypolimnion can also easily become anoxic during periods of intense stratification as DOC is decomposed (Salonen et al., 1984). This anoxic zone can provide a refuge for prey species which are less sensitive to oxygen availability than fish (Wissel et al., 2003). In addition to these local impacts, the projected increases in DOC concentration may have implications for water treatment, as described earlier, and on the global carbon cycle should they impact on a regional scale. A positive feedback mechanism between decomposition in organic soils and climate change has been suggested, with changes in climate driving increases in the export of DOC which in turn

would increase atmospheric CO_2 concentrations and contribute to further global warming (Knorr et al., 2005; Davidson and Janssens, 2006).

High DOC concentrations will also impact on stream pH levels as many DOC compounds are organic acids (Clark et al., 2005; Evans, 2005). Although the assessment of local and regional weather on stream pH levels in Chapter 2 also highlighted the strong relationship between climatic factors and low pH events, modelling the impact of projected changes in climate on stream pH levels was beyond the scope and timeframe of the present study. The processes contributing to in-stream pH levels are complex and include those both within catchment soils and surface waters, together with impacts of regional scale pollution and local landuse changes (Eshleman et al., 1992; Foster et al., 2001; Cox, 2003; Clark et al., 2005; Evans, 2005). A review of the potential use of models which simulate in-stream pH undertaken during the project, including in particular the QUAL 2K model, highlighted difficulties in identifying one model which could potentially be used to simulate future impacts (Appendix III). A particular challenge would be modelling dynamic changes in stream pH levels at a sub-daily timestep. The assessment of in-stream pH levels in the most acidic stream in the Burrishoole catchment and presented in Chapter 2 illustrated the rapid temporal changes which can occur in stream pH levels. The difficulties in applying a single model has been addressed by some authors by combining regional scale models that simulate large-scale atmospheric impacts with empirical relationships which describe the relationship between flow and pH (e.g. Foster et al., 2001; Evans, 2005). This approach does not, however, include sub-daily in-stream processes which can also have a major impact on H^+ concentrations but which are included in more complex models such as QUAL 2K. Modelling of in-stream pH levels also requires reliable in-stream pH data together with flow and in-stream processes and on soils processes. While the recent upgrading of pH probes in the river monitoring stations at Burrishoole would facilitate any future modelling exercise, additional data on a range of in-stream processes would be required, for example primary productivity and respiration of both in-stream and benthic algae and decomposition rates of DOC. This work could form the basis of a future study on present and future climate impacts on the in-stream conditions for salmonid species. This could also be used to provide information on the impact of biological processes on DO levels and address potential impacts of biological changes on DO concentrations at a sub-daily interval.

6.7 Key Findings

- Projected changes in climate are likely to affect a range of water quality parameters, including water temperature, water DO concentrations and DOC concentrations, which may impact on fish growth and survival.
- The projected increases in annual RWT for the combined GCM models for the A2 scenario were +0.8◦C (2010-2039), +1.3◦C (2040-2059) and +2.1◦C (2070-2099). Those for the B2 scenario were +0.8◦C (2010-2039), +1.2◦C (2040-2059) and +1.6◦C (2070-2099). In general, increases were greatest in the autumn and early winter.
- Increases in DOC concentrations were also projected for all GCM model and emission scenario combinations from the 2010–2039 period onwards. The overall increase from 1961–1990 to 2070–2099 for the A2 scenario was 2.4 mg DOC L^{-1} while that for the B2 scenario was 1.8 mg DOC L^{-1}.
- In spite of the dominant influence of RWT on DO levels, projected changes in temperatures resulted in only an additional 4% to 7% decrease in average daily DO concentrations during summer months.
- The overall increases in lake SWT for the A2 scenario for the three time horizons 2010–2039, 2040–2069 and 2070–2099 were 0.6◦C, 1.5◦C and 2.1◦C respectively, while those for the B2 scenario were 0.8◦C, 1.3◦C and 1.5◦C for the same time periods.
- While DWT was projected to increase by a similar range to SWT during months when the lake was fully mixed, there was no significant increase in DWTs during months when the lake was stratified.

6.8 References

Alabaster, J. S. and Gough P. J. (1986) 'The dissolved oxygen and temperature requirements of Atlantic salmon, *Salmo salar L.*, in the Thames Estuary'. *Journal of Fish Biology* 29, 613–621.

Allen, R.G., Pereiira, L.S. Raes, D. and Smith, M. (1998) *Crop evapotransipation: guidelines for computing crop water requirements. FAO irrigation and drainage paper 56*. Food and Agriculture Organisation of the United Nations, Rome.

APHA (1992) '*Standard methods for the examination of water and wastewater'*, 18th ed. American Public Health Association, Washington, DC.

Arnell, N.W. (1998) 'Climate change and water resources in Britain', *Climate Change* 39, 83-110.

Bogan, T., Stefan, H.G., and Mohseni, O. (2004) 'Imprints of secondary heat sources on the stream temperature/equilibrium temperature relationship', *Water Resources Research* 40, doi: 10.1029/2003WR002733.

Byrne, K., Farrell, E.P. Papen, H. And Butterbach-Bahl, K. (2000) Carbon dioxide and methane fluxes in forested and virgin peatland in the west of Ireland. *Internationale Vereinigung für Theoreische und Angewandte Limnologie* 27, 1387-1390.

Caissie, D. (2006) 'The thermal regime of rivers: a review', *Freshwater Biology* 51, 1389-1406.

Caissie, D., El-Jabi, N., and Satish, M.G. (2001) 'Modelling of maximum daily water temperatures in a small stream using air temperatures', *Journal of Hydrology* 251, 14-28.

Chapman, S.J. and Thurlow, M. (1998) 'Peat respiration at low temperatures', *Soil Biology and Biochemistry* 30, 1013-1021.

Clark, J.M., Chapman, P.J., Adamson, J.K. and Lane, S.N. (2005) 'Influence of drought induced acidification on the mobility of dissolved organic carbon in a peat soil', *Global Change Biology* 11, 791-809.

Cox, B.A. (2003) 'A review of currently available in-stream water-quality models and their applicability for simulating dissolved oxygen in lowland rivers', *The Science of the Total Environment* 314-316, 335-377.

Crisp, D.T. and Howson, G. (1982) 'Effect of air temperature upon mean water temperature in streams in the north Pennines and English Lake District', *Freshwater Biology* 12, 359-367.

Cunjak, R.A., Caissie D., El-Jabi, N., Hardie, P., Conlon, J.H., Pollock, T.L., Gibson, D.J., and Komadina-Douthwright, S. (1993) 'The Catamaran Brook (New Brunswick) habitat research project: biological, physical and chemical conditions (1990-1992)', *Canadian Technical Report of Fisheries and Aquatic Sciences* 1914, 1-81.

Davidson, E.A. and Janssens, I.A. (2006) 'Temperature sensitivity of soil carbon decomposition and feedbacks to climate change', *Nature* 440, 165-173.

Drakare S, Blomqvist P, Bergström A-K, Jansson M (2002) 'Primary production and phytoplankton composition in relation to DOC input and bacterioplankton production in humic Lake Örträsket', *Freshwater Biology* 47, 41 – 52.

Eaton, J.G., McCormick, J.H., Stefan, H.G., and Hondzo, M. (1995) 'Extreme value analysis of a fish/temperature field database', *Ecological Engineering* 4, 289-305.

Elliott, J.M. (1984) 'Numerical changes and population regulation in young migratory trout *Salmo trutta* in a lake district stream, 1966-83', *The Journal of Animal Ecology* 53(1), 327-350.

Erickson, T.R. and Stefan, H.G. (2000) 'Linear air/water temperature correlations for streams during open water periods', *Journal of Hydrologic Engineering* 5(3), 317-321.

Erlandsson, M., Buffam, I., Fölster, J., Laudon, H., Temnerud, J., Weyhenmeyer1, G.A. and Bishop, K. (2008) '35 years of synchrony in the organic matter concentrations of Swedish rivers explained by variation in flow and sulphate', *Global Change Biology* doi:10.1111/j.1365-2486.2008.01551.x.

Eshleman, K.N., Wigington, P.J., Davies, T.D. and Tranter M. (1992) 'Modelling episodic acidification of surface waters: The state of science.' *Environmental Pollution* 77, 287-295.

Evans, C.D., Monteith D.T and Cooper D.M. (2005) 'Long-term increases in surface water dissolved organic carbon: observations, possible causes and environmental impacts', *Environmental Pollution* 137, 55-71.

Evans, C.D., Chapman, P.J., Clark, J.M., Monteith, D.T. and Cresser, M.S. (2006) 'Alternative explanations for rising dissolved organic carbon export from organic soils', *Global Change Biology* 12, 2044-2053.

Freeman, C., Evans, C.D., Monteith, D.T., Reynolds, B. and Fenner, N. (2001) 'Export of organic carbon from peat soils', *Nature,* 412, 785.

Foster, H.J., Reynolds, B., Lees, M.J. and Wheater, H.S., (2001) 'A hydrochemical modelling framework for combined assessment of spatial and temporal variability in stream chemistry: application to Plynlimon, Wales.' *Hydrology and Earth System Science* 5, 49-54.

Grieg, S., Sear, D., and Carling, P. (2007) 'A field-based assessment of oxygen supply to incubating Atlantic salmon (*Salmo salar*) embryos', *Hydrological Processes* 21, 3087-3100.

Graham, C.T. and Harrod, C. (2009) 'Implications of climate change for the fishes of the British Isles', *Journal of Fish Biology* 74, 1143-1205.

Gu, R.R. and Li, Y. (2002) 'River temperature sensitivity to hydraulic and meteorological parameters', *Journal of Environmental Management* 66, 43-56.

Haith, D. A. and Tubbs, L. J. (1981) 'Watershed Loading Functions for Nonpoint Sources. ASCE', *Journal of Environmental Engineering* 107(EE1):121-137.

Hari, R.E., Livingstone, D.M., Siber, R., Burkhardt-Holm, P. and Güttinger, H. (2006) 'Consequences of climatic change for water temperature and brown trout populations in Alpine rivers and streams', *Global Change Biology* 12, 10-26

Hargreaves, G.H. and Samani, Z.A. (1982) "Estimating potential evapotranspiration" *J. Irrig. and Drain. Engrg., ASCE*, 108, 223–230.

Hipsey, M.R., Romero, J.R., Antenucci, J.P. and Hamilton, D. (2006) 'Computational Aquatic Ecosystem Dynamics Model. v. 2.3 Science Manual. Centre for Water Research, the University of Western Australia (online)', http://www.cwr.uwa.edu.au/ services/models/legacy/model/dyresmcaedym/

Imberger, J. and Patterson, J.C. (1989) '*Physical limnology*' p 303-475 In Advances in applied mechanics, volume 27, Academic Press.

Jennings, E., Naden, P., Järvinen, M., Moore, K., Nic Aongusa, C., Tamm, T. and Järvet, A. (2005) *'Report on Testing of the DOC Model in 'Warm World' Mode. CLIME project deliverable 5.3'*, 88pp.

Jennings, E., Allott, N., Arvola, L., Jarvinen, M., Moore, K., Naden, P., Nic Aongusa, C., Noges, T. and Weyhermeyer, G. (2010) '*Impacts of climate on the flux of dissolved organic carbon from catchments'*, In D.G. George (ed.) The Impact of Climate Change on European Lakes. Springer.

Kankaala, P., Arvola, L., Tulonen, T. and Ojala, A. (1996) 'Carbon budget for the pelagic food web of the euphotic zone in a boreal lake (Lake Pääjärvi)', *Canadian Journal of Fisheries and Aquatic Sci*ences 53, 1663-1674.

Kettle, H., Thompson, R., Anderson, N.J., and Livingstone, D.M. (2004) 'Empirical modelling of summer lake surface temperatures in southwest Greenland', *Limnology and Oceanography* 49(1), 271-282.

Knorr, W., Prentice, I. C., House, J. I. and Holland, E. A. (2005) 'Long-term sensitivity of soil carbon to warming', *Nature* 433, 298-301.

Langan, S.J., Johnston, L., Donaghy, M.J., Youngson, A.F., Hay, D.W., and Soulsby, C. (2001) 'Variation in river water temperatures in an upland stream over a 30-year period', *Science of the Total Environment* 265, 195-207.

Lau, K.-M., Kim, J.H., and Sud, Y. (1996) 'Comparison of Hydrologic Processes in AMIP CGMs', *Bulletin of the American Meteorological Society* 77(10), 2209-2227.

Livingstone, D.M. and Dokulil, M.T. (2001) 'Eighty years of spatially coherent Austrian lake surface temperatures and their relationship to regional air temperature and the North Atlantic Oscillation', *Limnology and Oceanography* 46(5), 1220-1227.

Livingstone, D.M. and Hari, R.E. (2008) 'Coherence in the response of river and lake temperatures in Switzerland to short-term climatic fluctuations in summer', *Internationale Vereinigung für Theoreische und Angewandte Limnologie* 30(3), 449-454.

Livingstone, D.M. and Lotter, A.F. (1998) 'The relationship between air and water temperatures in lakes of the Swiss Plateau: a case study with palæolimnological implications', *Journal of Paleolimnology* 19, 181-198.

Livingstone, D.M., Lotter, A.F., and Kettle, H. (2005) 'Altitude-dependent differences in the primary physical response of mountain lakes to climatic forcing', *Limnology and Oceanography* 50(4), 1313-1325.

Livingstone, D.M., Lotter, A.F., and Walker, I.R. (1999) 'The decrease in summer surface water temperature with altitude in Swiss Alpine lakes: a comparison with air temperature lapse rates', *Arctic, Antarctic and Alpine Research* 31, 341-352.

Mathes, M.H., Hinch, S.G., Cooke, S.J., Crossin, G.T., Patterson, D.A., Lotto, A.G. and Farrell, A.P. (2010) 'Effect of water temperature, timing, physiological condition, and lake thermal refugia on migrating adult Weaver Creek sockeye salmon (*Oncorhynchus nerka*)', Can. J. Fish. Aquat. Sci. 67, 70–84.

Matthews, M.A.,Poole, W.R., Dillane, M.G and Whelen, K.F. (1997) Juvenile recruitment and smolt output of brown trout (*Salmo trutta L.*) and Atlantic salmon (Salmo salar L.) from a lacustrine system in western Ireland', *Fisheries Research* 31, 19-37.

McGinnity, P., Jennings, E., DeEyto, E., Allot, N., Samuelsson, P., Rogan G., Whelan, K., and Cross, T. (2009) 'Impact of naturally spawning captive-bred Atlantic salmon on wild populations: depressed recruitment and increased risk of climate-mediated extinction', *Proceedings of the Royal Society B – Biological Sciences* 276(1673), 3601-3610.

Mohseni, O. and Stefan, H.G. (1999) 'Stream temperature/air temperature relationship: a physical interpretation', *Journal of Hydrology* 218, 128-141.

Mohseni, O., Erickson, T.R., and Stefan, H.G. (1999) 'Sensitivity of stream temperatures in the United States to air temperatures projected under a global warming scenario', *Water Resources Research* 35(12), 3723-3733.

Mohseni, O., Stefan, H.G., and Eaton, J.G. (2003) 'Global warming and potential changes in fish habitat in U.S. streams', *Climatic Change* 59, 389-409.

Mohseni, O., Stefan, H.G., and Erickson, T.R. (1998) 'A nonlinear regression model for weekly stream temperatures', *Water Resources Research* 34(10), 2685-2693.

Monteith, D., Stoddard, J.L., Evans, C.D., de Wit, H.A., Forsius, M., Høgåsen, T., Winander, A., Skjelkvåle, B.L., Jeffries, D.S., Vuorenmaa, J., Keller, B., Kopácek, J. and Vesely, J., (2007) 'Dissolved organic carbon trends resulting from changes in atmospheric deposition chemistry', *Nature* 450, doi:10.1083/natare06316.

Morrill, J.C., Bales, R.C., and Conklin, M.H. (2005) 'Estimating stream temperature from air temperature: implications for future water quality', *Journal of Environmental Engineering* 131(1), 139-146.

Naden, P.S. (1991) '*Modelling water colour in upland catchments', Report to Yorkshire Water*, Institute of Hydrology, Wallingford, UK. 114pp.

Naden, P.S. and Watts, C.D. (1998) 'Development of the EPIC colour prediction model: Phase II. Report for Yorkshire Water, Institute of Hydrology, Wallingford, UK, 42pp.

Naden, P., Allott, N., Arvola, L., Jarvinen, M., Jennings, E., Moore, K., Nic Aongusa, C., Pierson, D. and Schneidermen, E. (2010) Modelling the effects of climate change on dissolved organic carbon. In D.G. George (Ed.) The Impact of Climate Change on European Lakes. Springer.

Nash, J.E. and Sutcliffe, J.V. (1970) 'River flow forecasting through conceptual models, I-A, Discussion of principles', *Journal of Hydrology* 10, 282-290.

Ogrosky, H.O. and Mockus, V. (1964) '*Hydrology of agricultural lands'*, In V. T. Chow (ed.). Handbook of Applied Hydrology. McGraw-Hill, New York.

Pilgrim, J.M., Fang, X., and Stefan, H.G. (1998) 'Stream temperature correlations with air temperatures in Minnesota: implications for climate warming', *Journal of the American Water Resources Association* 34(5), 1109-1121.

Prairie, Y. (2007) 'Carbocentric limnology: looking back, looking forward', *Canadian Journal of Fisheries and Aquatic Sciences* 65, 543-548.

Salonen, K., Arvola, L. and Rask, M. (1984) 'Autumnal and vernal circulation of small forest lakes in Southern Finland', *Verh. Internat. Verein. Limnol.* 22, 103-107.

Schindler, D.W. (2001) 'The cumulative effects of climate warming and other human stresses on Canadian freshwaters in the new millennium', *Canadian Journal of Fisheries and Aquatic Sciences* 58, 18-29.

Schneiderman, E., Järvinen, M., Jennings, E., May, L., Moore, K., Naden, P., Pierson, D.C. (2010) 'Modeling the effects of climate change on catchment hydrology with the GWLF model', In D.G. George (Ed.) T*he Impact of Climate Change on European Lakes*. Springer.

Schneiderman, E.M., Pierson, D.C., Lounsbury D.G. and Zion, M.S. 2002. 'Modeling the hydrochemistry of the Cannonsville Watershed with the Generalized Watershed Loading Functions GWLF.' *Journal of the American Water Resources Association* 38, 1323-1347.

Sinokrot, B.A. and Stefan, H.G. (1993) 'Stream temperature dynamics: measurements and modelling', *Water Resources Research* 29, 2299-2312.

Sinokrot, B.A. and Stefan, H.G. (1994) 'Stream water temperature sensitivity to weather and bed parameters', *Journal of Hydraulic Engineering* 120, 722-736.

Sinokrot, B.A., Stefan, H.G., McCormick, J.H. and Eaton, J.G. (1995) 'Modeling of climate change effects on stream temperatures and fish habitats below dams and near groundwater inputs', *Climatic Change* 30, 181-200.

Stefan, H.G. and Preud'homme, E.B. (1993) 'Stream temperature estimation from air temperature', *Water Resources Bulletin* 29, 27-45.

Tanaka, H., Takagi, Y. and Naito, Y. (2000) 'Behavioural thermoregulation of homing chum salmon.' *Journal of Experimental Biology* 203, 1825–1833.

Todd, D.K. (1980) '*Groundwater hydrology'*. New York, Wiley.

Tranvik, L.J. (1992) 'Allochthonous dissolved organic matter as an energy source for pelagic bacteria and the concept of the microbial loop.' *Hydrobiologia* 229: 107-114.

Tulonen, T., Salonen, K. and Arvola, L. (1992) 'Effect of different molecular weight fractions of dissolved organic matter on the growth of bacteria, algae and protozoa from a highly humic lake.' *Hydrobiologia* 229, 239-252.

Webb, B.W. and Nobilis, F. (1997) 'A long-term perspective on the nature of the air-water temperature relationship: a case study', *Hydrological Processes* 11, 137-147.

Webb, B.W., Clack, P.D., and Walling, D.E. (2003) 'Water-air temperature relationships in a Devon River system and the role of flow', *Hydrological Processes* 17, 3069-3084.

Wetzel RG (2001) *Limnology: Lake and River Ecosystems 3rd Edition'*, Academic Press San Diego CA USA.

Wissel, B., Boeing, W.J. and Ramcharan, C.W. (2003) 'Effects of water color on predation regimes and zooplankton assemblages in freshwater lakes.' *Limnology and Oceanography* 48, 1965-1976.

Worrall, F., Burt, T. and Adamson, J. (2005) 'Fluxes of dissolved carbon dioxide and inorganic carbon from an upland peat catchment: implications for soil respiration.' *Biogeochemistry* 73, 515-539.

Worrall, F., Burt, T. and Adamson, A. (2006) 'Long-term changes in hydrological pathways in an upland peat catchment—recovery from severe drought?' *Journal of Hydrology* 321, 5-20.

Youngson, A.F., Malcolm, I.A., Thorley, J.L., Bacon, P.J., Soulsby, C. (2004) 'Long-residence groundwater effects on incubating salmonid eggs: low hyporheic oxygen impairs embryo development and causes mortality'. *Canadian Journal of Fisheries and Aquatic Sciences* 61, 2278-2287.

7 Potential Impacts of Climate Change on Fish Populations in the Burrishoole

Ciar O'Toole, Russell Poole, Mary Dillane, Ger Rogan, Elvira de Eyto, Lee Hancox, Eleanor Jennings and Jonathan White

7.1 Introduction

The projected changes in climate and water-quality parameters described in this report which could directly affect fish growth and survival include increases in RWT and lake SWT, and changes in river flow related to changing rainfall patterns, decreases in DO and DOC concentrations and river flow related to changing rainfall patterns.

Temperature can influence growth and survival in a number of ways. The first section in this chapter uses a simple model to estimate what the growth rate of salmonids maybe under different water temperature scenarios using the projected climate change models. The second section looks at the other effects of temperature, such as lethal limits, and the projected changes in RWT and LWT for the Burrishoole.

7.2 Modelled Freshwater Fish Growth

7.2.1 Introduction

Temperature affects metabolic processes and growth in fishes as well as influencing the timing and duration of most life-history stages from fry emergence, parr size and smolt emigration (Connor et al., 2002). Fish are sensitive to temperature changes both through heat exchange in the gills and by heat transfer through the body wall (Elliott, 1981). Because of the allometric relationship between the volume and the surface area of a fish, small fish are more susceptible to fluctuations in water temperature than larger ones (Elliott, 1994).

Elliott et al. (1995) and Elliott and Hurley (1997) developed models linking temperature, specific growth rate for Atlantic salmon and brown trout parr and the initial mass of the fish. These parameters were estimated from laboratory experiments over a range of water temperatures. The parameters are upper, lower and optimal temperature for growth as well as growth rate at optimal temperature (Elliott and Hurley, 1997).

The Elliott et al. (1994 and 1995) models form triangular curves with temperatures at beginning, end and at maximum growth forming the triangles corners. The effect of a

temperature increase depends on whether the temperature is above or below the point for optimal growth. To the left of this point, an increase in temperature results in increased growth given adequate food intake, to the right, growth will decrease (Jonsson and Jonsson, 2009). A reason for the triangular shape may be that the scope for growth increases with temperature until constrained by oxygen content in the water (Brett, 1952, 1964).

A study by Davidson and Jansens (2006) used the growth models of Elliott et al. (1995) and Elliott and Hurley (1997) to predict size at age for some British populations of trout and salmon in conjunction with predicted temperatures for the UK by UKCIP (2002). The current study carried out similar analyses using Burrishoole catchment salmon and trout data and using downscaled future temperature projections for the catchment (Chapter 4).

7.3 Methods

7.3.1 River Temperature Data

The projected river water temperature (RWT) datasets used were based on the projected daily smothed air temperature (S AT) data output as described in Chapter 6 (section 6.2) of this report. RWT datasets from the Burrishoole Catchment include those from the Black River and two of its tributaries (the Altahoney and Gaulaun), the Glenamong River (Figure 1.3), the Glendahurk River and the Tarsaghaun River. RWT has been logged at these sites using ONSET TidbiTs since 2003/2004. There is generally a high level of coherence between the data sets. However, the logger in the Atlahoney is situated in a deeper pool which is shaded by a rock overhang. This logger records consistently lower RWT in summer. The Gaulaun site is downstream from a small lake and generally has a more smoothed temperature record. These two sites were omitted from the calculated catchment mean RWT, although the Altahoney data are interesting in terms of refuges for fish from higher temperatures in summer.

7.3.2 Simulated Freshwater Growth

The growth model of Elliott et al. (1995) and Elliott and Hurley (1997) were used to predict size at age for juvenile salmon and sea trout smolts in the Burrishoole catchment, based on monthly mean RWT 1961-2007, and future projected RWT from 2008-2100 (Rescale, 2010). The formula used is as follows:

$W_t = (W^b_o + bc\ (T\text{-}T_{LIM})_t/100(T_m - T_{LIM}))^{1/b}$ **Equation 7.2**

Where

t is the time in days;

W_0 is initial fish mass;

W_t is final fish mass (after t days at T°C);

T is water temperature (°C);

b is the exponent for the power transformation of mass that produces linear growth with time = 0.308 for trout and 0.310 for salmon.

c is growth rate of a 1g fish at the optimum temperature = 2.803 for trout and 3.503 for salmon.

T_M is optimum temperature for growth = 13.11°C for trout and 15.94 °C for salmon.

T_L is the lower temperature at which growth ceases = 3.56 for trout and 5.99°C for salmon.

T_U is the upper temperature at which growth ceases = 19.48°C for trout and 22.51°C for salmon.

T_{LIM} is T_L if $T \leq T_M$ or $T_{LIM} = T_U$ if $T > T_M$.

In the absence of information on emergence date or appropriate field length/weight measurements, a growth year of 1 April - 31 March and an initial fish mass of 0.25g for trout and 0.15g for salmon on the 1st May was assumed in all cases (based on estimates from Elliott et al., 1995) and Elliott and Hurley (1997). It was also assumed in the model that zero growth occured from 1st October to 1 April in the first year for both species on reccomendation of Elliott et al. (1995) and Elliott and Hurley (1997).

7.3.3 Model Calibration

To test the suitability of the Elliott salmon and trout models to salmon and trout in the Burrishoole, a calibration exercise was carried out on a random years data. Trout samples collected in Bunaveela were chosen for this because of a suitable sample size and variety in the age classes of fish sampled. Records of trout weight were used in accordance with the growth formula of Elliott et al. (1995) and Elliott and Hurley (1997), using an assumed weight at bith of 0.25g and hatching date of 1 April. These details were then used to forecast an estimate of Wtb (final mass raised to the mass exponent) and weight at catch given the same limiting growth variables and days. Mean weight of caught fish was 38.7g while the estimation of weigth, following growth time, limiting temperatures, growth rate and power transformation of

mass that produces linear growth with time, was 43.46g, within the 95% confidence limits of the weighed fish (33.01 to 44.39g) (Table 7.1).

7.3.4 Back Calculated Freshwater Growth

Back calculated lengths for both salmon and trout were calculated from fish scales using the methods described previously (Sections 3.5 & 3.6).

Table 7.1: Estimation of catch weight from modelled growth variables derived from observed catch weights given limiting temperatures and time between birth and capture.

Obs(Wbt)			E(Wbt)		
n	67	67	***n***	30	67
df	66	66	***df***	29	66
Obs(Wbt)	38.70	2.997	***E(Wbt)***	43.46	3.195
Obs s2t	564.09	0.22	***E s2***	0.00	0.00
Obs st	23.75	0.47	***E s***	0.00	0.00
± 95% cl	5.69	0.11	***± 95% cl***	0.00	0.00

7.4 Results

7.4.1 Salmon

Figures 7.1 to 7.3 show the projected weight of salmon in the Burrishoole catchment up to 2099. The three models (CGCM, CSIRO and HAD) and both scenarios (A2 and B2) all indicated increased growth for salmon in the coming century. Table 7.2 gives the critical temperatures for juvenile salmon growth and survival and which fall within the bounds of the predicted temperatures in this model. The model however, does not factor in winter time growth, therefore the effect of warmer winters, as predicted is not examined in this case. Extreme events, such as droughts or floods during critical phases of the juvenile salmons life cycle are also not considered in the model.

Table 7.2: Critical temps (Atlantic salmon juveniles) for different biological processes.

Parameter	Reference	Temperature °C
8 Feeding	Elliot (1991)	7-22.5
9 Seek shelter	Gardiner (1984)	<9
10 Egg mortality	Peterson et al. (1977)	<4
11 Hatching temp.	Crisp (1981)	2.4-12
12 Upper incipient lethal temp. (parr)	Elliot (1991)	27.8 ± 0.2
13 Upper critical range	Elliot (1994)	22-33
14 Lower critical range (parr)	Elliot (1994)	0-7
15 Move to cooler water (parr)	Gibson (1966)	22
16 Optimum growth (parr)	Dwyer and Piper (1987)	16
17 Smolt Run (range)	Byrne et al. (2003)	5.5-15.5

a)

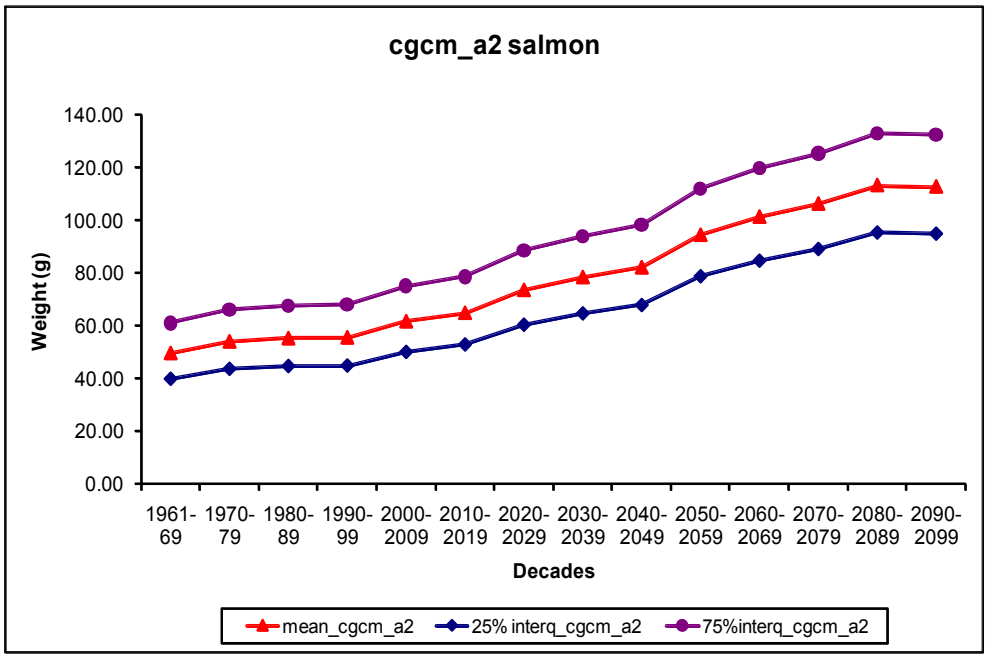

b)

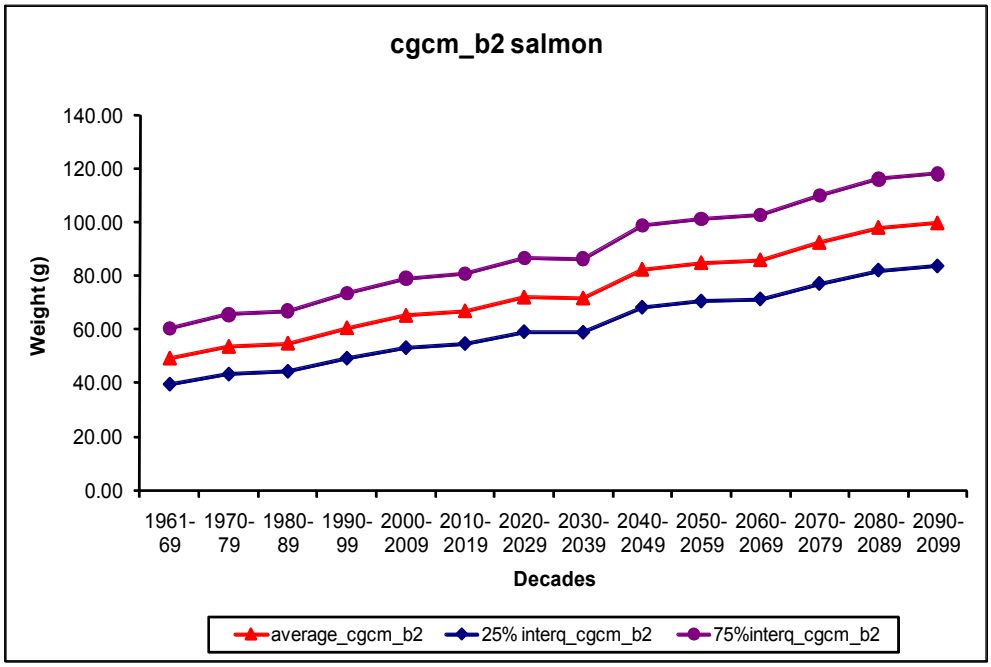

Figure7.1: Simulated growth in weight (g) for a two year old salmon smolt in the Burrishoole catchment using projected water temperatures from the CGCM model and Elliott and Hurley (1997) growth model for salmon. a) Shows projections using the CGCM A2 scenario and b) shows projections using the CGCM B2 scenario the red line indicates mean weight (g), the blue line indicates the 75% inter-quartile range and the purple line indicates the 25% inter-quartile range.

a)

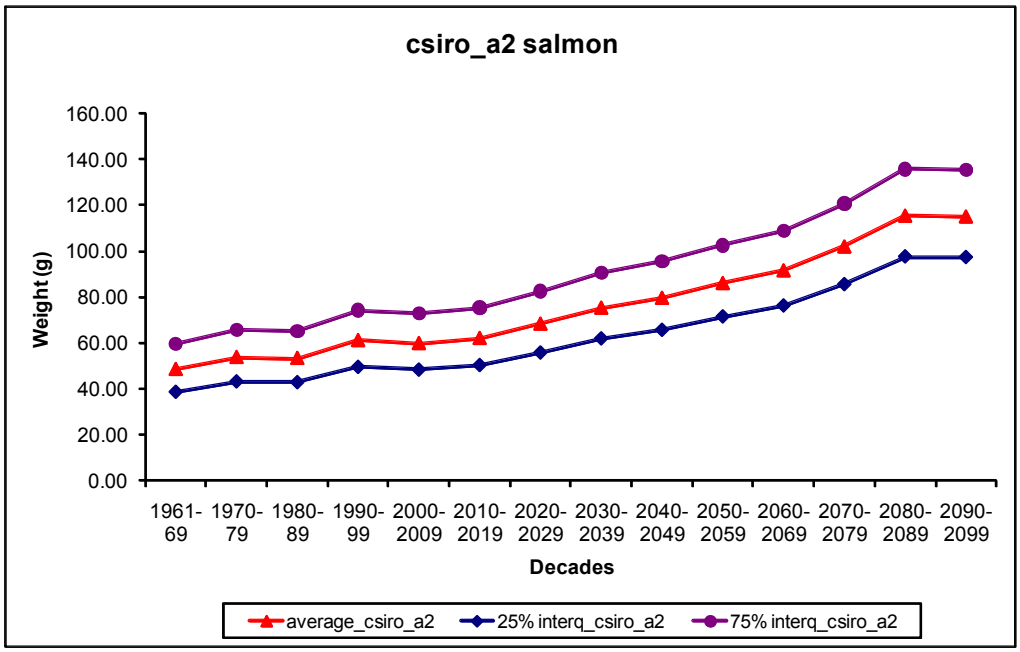

b)

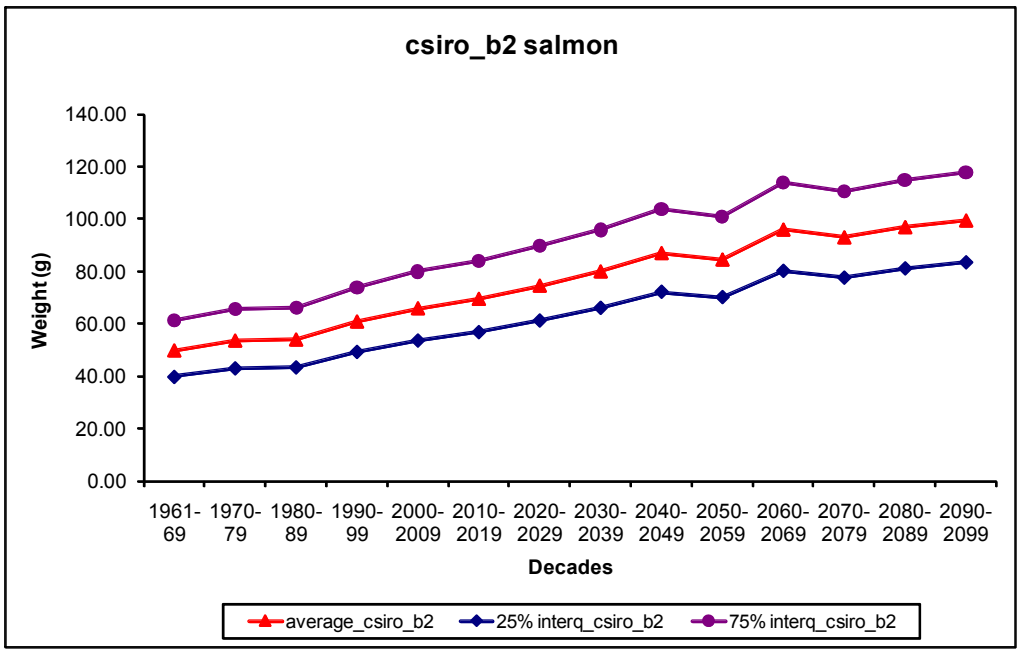

Figure 7.2: Simulated growth in weight for a two year old salmon smolt in the Burrishoole catchment using predicted water temperatures from the CSIRO model and Elliott and Hurley (1997) growth model for salmon. a) Shows projections using the CSIRO A2 scenario and b) shows projections using the CSIRO B2 scenario the red line indicates mean weight (g), the blue line indicates the 75% inter-quartile range and the purple line indicates the 25% inter-quartile range.

a)

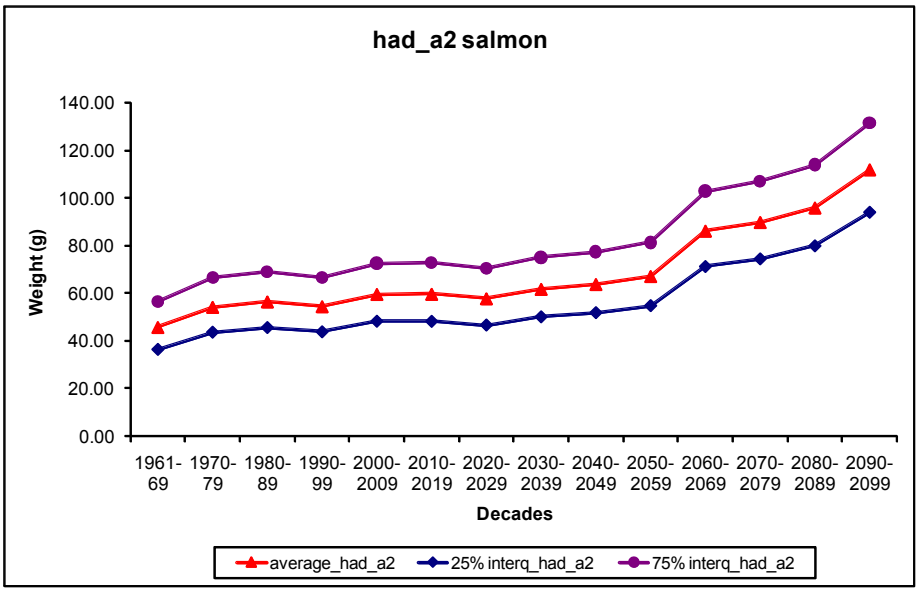

b)

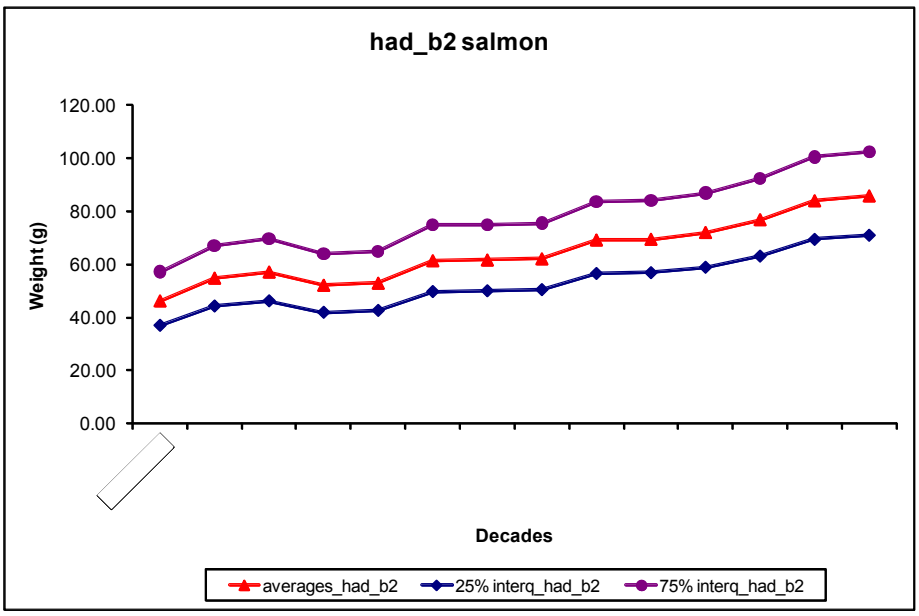

Figure 7.3: Simulated growth in weight for a two year old salmon smolt in the Burrishoole catchment using predicted water temperatures from the HAD model and Elliott and Hurley (1997) growth model for salmon. a) Shows projections using the HAD A2 scenario and b) shows projections using the HAD B2 scenario the red line indicates mean weight (g), the blue line indicates the 75% inter-quartile range and the purple line indicates the 25% inter-quartile range.

7.4.2 Trout

Figures 7.4 to 7.6 show the predicted weight of trout in the Burrishoole catchment up to 2099. The three models (CGCM, CSIRO and HAD) and both scenarios (A2 and B2) all indicate a levelling off in the growth rate for trout (weight, g) before the weight starts to decline in the coming century. Table 7.3 show the critical temperatures for juvenile trout growth and survival and which are exceeded by the predicted temperatures in this model. The results in Figures 7.4 to 7.6 vary in the timing and the severity in the decline of trout weight in the Burrishoole catchment, but all models and scenarios project a similar trend over the coming century.

The model however, does not factor in winter-time growth, therefore the effect of warmer winters, as indicated by the downscaled climate scenarios in Chapter 4, is not examined in this case. Extreme events, such as droughts or floods during critical phases of the juvenile trout life cycle were also not considered in the model.

Table 7.2: Critical temperatures for yellow trout Salmo trutta.

Parameter	Reference	Temperature (°C)
18 Feeding	Elliot (1991)	7-22.5
19 Seek shelter	Gardiner (1984)	<9
20 Hatching temp	Crisp (1981)	1.9-11.2
21 Egg mortality	Peterson et al. (1977)	<4
22 Upper incipient lethal temp.	Elliot (1994)	24.7
23 Upper Critical Range	Elliot (1994)	19-30
24 Lower Critical Range	Elliot (1994)	0-4
25 Smolt run range	Byrne et al. (2004)	5-13

a)

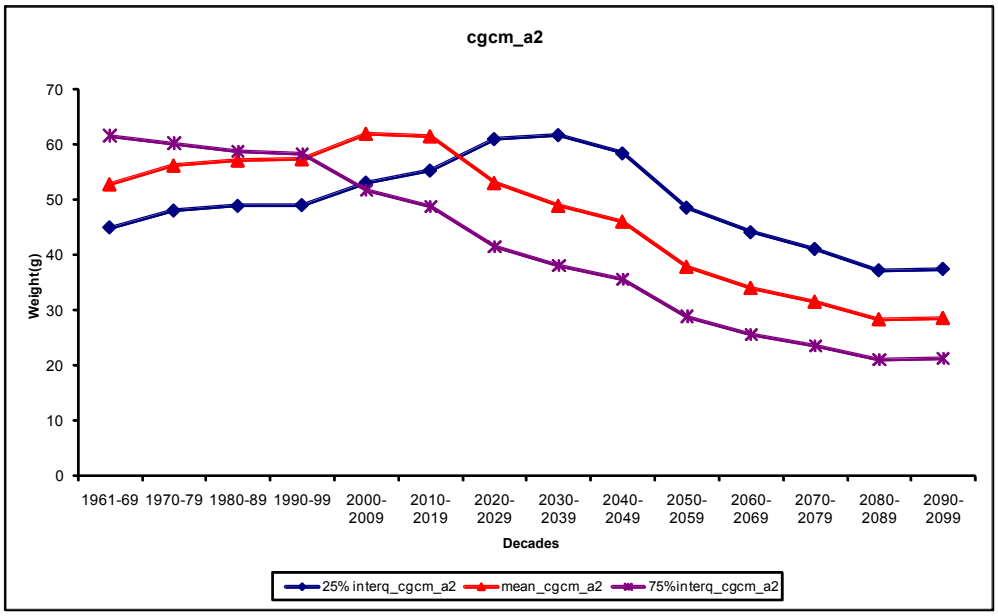

b)

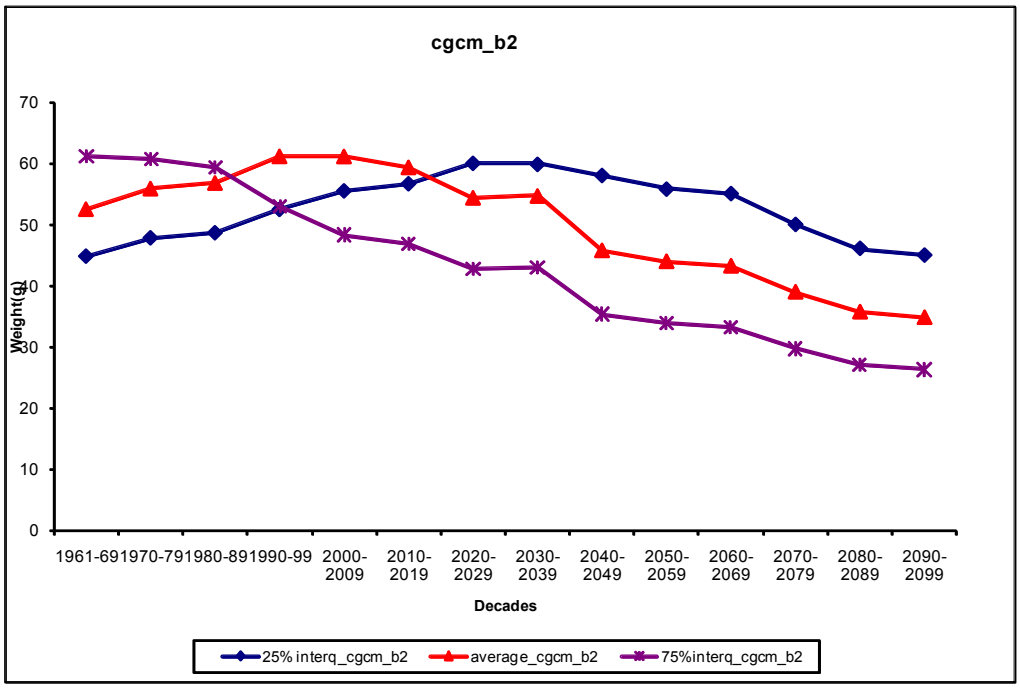

Figure 7.4: Simulated growth for in weight for a two year old trout in the Burrishoole catchment using predicted water temperatures from the CGCM model and Elliott et al. (1995) growth model for trout. a) Shows projections using the CGCM A2 scenario and b) shows projections using the CGCM B2 scenario. The red line indicates mean weight (g), the blue line indicates the 75% interquartile range and the purple line indicates the 25% interquartile range.

a)

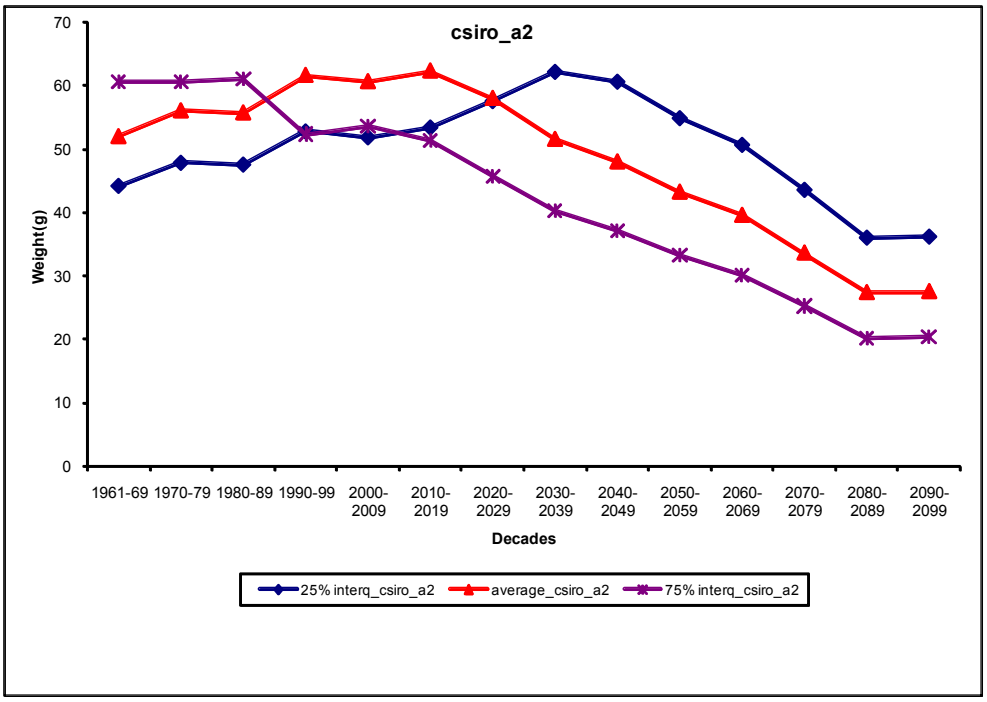

b)

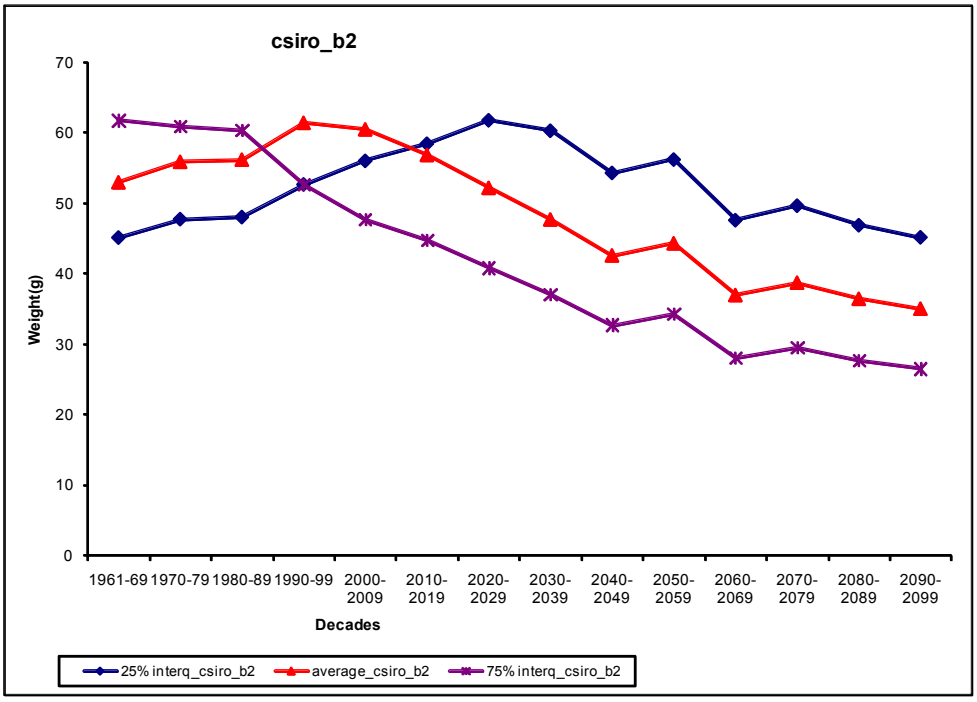

Figure 7.5 Simulated growth in weight for a two year old for trout in the Burrishoole catchment using predicted water temperatures from the CSIRO model and Elliott and Hurley (1997) growth model for trout. a) Shows projections using the CSIRO A2 scenario and b) shows projections using the CSIRO B2 scenario the red line indicates mean weight (g), the blue line indicates the 75% interquartile range and the purple line indicates the 25% interquartile range.

a)

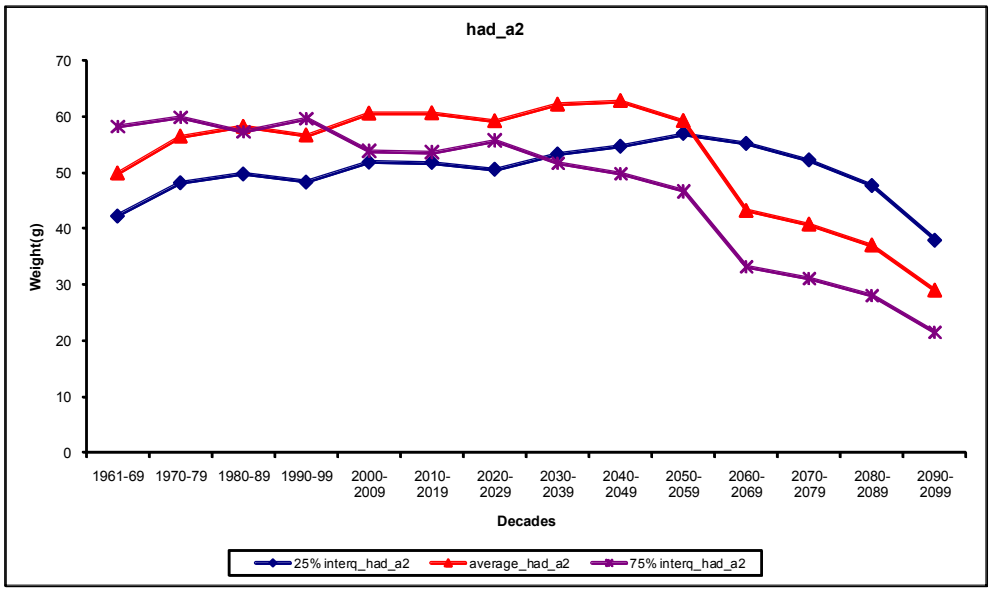

b)

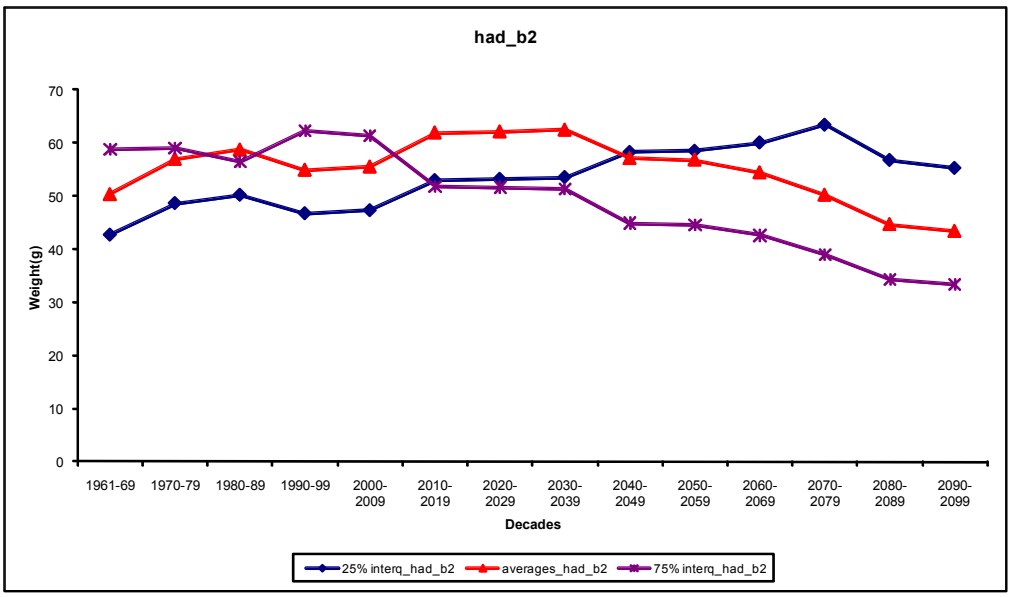

Figure 7.6: Simulations growth in weight for a two year old trout in the Burrishoole catchment using predicted water temperatures from the HAD model and Elliott and Hurley (1997) growth model for trout. a) Shows projections using the HAD A2 scenario and b) shows projections using the HAD B2 scenario the red line indicates mean weight (g), the blue line indicates the 75% interquartile range and the purple line indicates the 25% interquartile range.

7.5 Discussion

There is little potential for local adaptation in heat tolerance among populations within a species (Elliott, 1994). If the fish have no access to a suitable coldwater refuge, the population is extirpated if the water temperature exceeds the upper lethal temperature (Berman and Quinn, 1991). Within populations, thermal tolerance is influenced by the size, age and

physiological state of the fish (Jonsson and Jonsson, 2009). For example, the youngest life stages are most vulnerable to both lowest and highest temperatures (Brett, 1952), as well as to changes in temperature (Elliott, 1994). Salmonids have a low tolerance to high water temperatures due to the low solubility of oxygen in warm water; it is therefore difficult to differentiate between effects of high temperature and effects of low oxygen concentrations (Wootton, 1998).

Water temperature influences the movements of parr. For instance, during periods of very high temperature (above 23°C for S. salar), parr in rivers may seek cool water sources, although 0+ fish do not seem to exhibit the same behaviour, indicating that this behaviour may be linked to fish size and previous experience in the habitat (Breau et al, 2007). Therefore, the younger fish may be more exposed to high temperatures than older ones at the same time that they are more susceptible to high temperatures and rapid fluctuations in temperature (Jonsson and Jonsson, 2009).

In winter, *S. salar* prefer water temperatures below 10°C, and this preferred temperature increases from winter to spring, along with increases in natural food availability and endogenous seasonal increases in appetite and growth rates (Jonsson and Jonsson, 2009). During the wintertime, salmon and trout parr exhibit a negative relationship between tendency to seek shelter and water temperature (Valdimarsson et al., 1997). When the water temperature falls below 7-11°C, the parr become photo negative, leave their territories in riffles and find daytime concealment in pools or crevices in the river bottom substratum (Jonsson and Jonsson, 2009). Their behaviour changes in relation to light, with an increasing tendency to seek shade with increasing light intensities (Jonsson and Jonsson, 2009).

A possible reason why young salmonids leave riffles at lower temperatures may be due to the fact that their ability to retain their position is reduced at lower water temperatures (Rimmer et al., 1985, Graham et al., 1996). The ability to swim against strong currents decreases rapidly once water temperatures fall below 6-8°C and their metabolic rate decreases also. The ability to swim against the current also decreases over time during winter, possibly as a result of lower lipid reserves and decreased glycogenic reserves in muscles and the liver (Jonsson and Jonsson, 2009). Another reason for seeking shelter during daytime during periods of low water temperature may be to avoid endothermic predators as their activity is not slowed down during cold weather (Valdimarsson et al., 1997).

This study finds that salmon growth is set to increase in the Burrishoole catchment over the coming century, a finding supported by the work of Davidson and Hazelwood (2005) who predict that some British salmon stocks will also see increases in their growth rates in freshwater in the coming century due to increased river water temperatures. Unlike salmon, this study found that for trout growth, under all climate scenarios, it is predicted that there will be a levelling off in the growth rate (weight, g) before the weight gain starts to decline in the coming century. Davidson and Hazelwood (2005) also predict that trout growth in general will decline in coming years due to the influence of climate change. It is thought that this reduction may be due to the reduced "thermal tolerance" of trout as a species (Elliott, 1994). Trout have a narrower temperature range for which growth is positive (4-19°C) when compared to salmon (6-23°C) (see Tables 7-2 and 7-3). As well as the study by Davidson et al (2006), a similar prediction about salmon and trout growth with increased river water temperatures was made by Elliott (1994) and McCarthy and Houlihan (1997).

Some limitations of the model used in this study are linked to the assumptions made when running the model. Size and time of emergence are held constant in the model, even though time of emergence in the Burrishoole catchment is thought to be earlier in more recent years than historically and can be highly variable (Chapter 3). Previous studies have also shown the size and time of emergence for sea trout to be highly variable from year to year (Elliott, 1984, Elliott et al, 2000).

It is also assumed that no growth occurs between 1st October and 31st March in the first year. This may not hold true in a situation where warmer winters are predicted to become more common or in catchments like the Burrishoole where the number of faster growing 1+ smolts is thought to be increasing.

The values for the growth rates of both trout and salmon refer to hatchery reared fish on maximum rations, whereas we are attempting to model fish growth in a wild situation. It is suggested that future study should include a more specific model developed for the Burrishoole catchment using data collected from fish growing in the wild.

7.6 Potential Impacts of Climate Change on Fish Populations

The projected changes in climate and water-quality parameters described in this report which could directly affect fish growth and survival include increases in RWT and lake SWT, and

changes in river flow related to changing rainfall patterns, decreases in DO and DOC concentrations and river flow related to changing rainfall patterns.

7.6.1 Impacts of Projected Temperatures on Salmonids

Increases in water temperature may potentially have both positive and negative consequences for salmonid populations and ecosystem functioning in the Burrishoole catchment. Direct temperature impacts would include changes in the number of times when threshold values are exceeded and to the impacts of upward trends in mean temperatures on physiology and phenology. The projected monthly mean RWTs and lake SWTs in Burrishoole remained within the ideal range for salmonid fish habitats (7°C to 20°C). However, the number of days when RWT exceeded 22°C – for example, the threshold when salmon parr cease feeding and seek refuge (Elliot, 1991; Cunjak et al., 1993) – increased in all four time-horizons for both scenarios (Figure 7.7; Table 7.4). There was also a slight increase in the number of days when RWT exceeded 26oC (the ultimate lethal threshold for trout parr) in the two later time-horizons: 2040–2069 and 2070–2099. It is notable, however, that the number of days when lake SWT was projected to exceed the 22°C threshold was much lower than that indicated for RWT, and was confined to simulations based on the HadCM3 model (Figure 7.7a and b; Table 7.4).

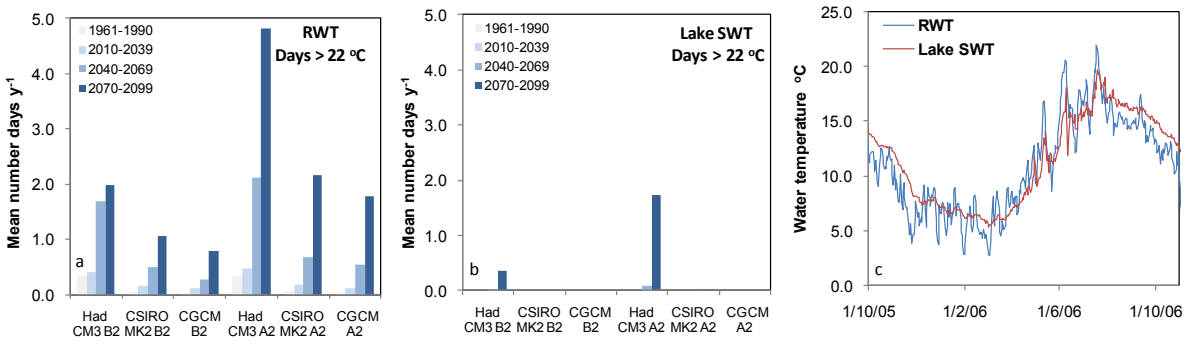

Figure 7.7: Number of days over 22oC (upper threshold for S. salar parr to cease feeding and to seek refuge) for a (left) RWT, b (centre) SWT and c (right) RWT and lake SWT.

This difference in the occurrence of extreme temperatures between the lake and catchment rivers reflects the more buffered nature of lake SWT, as illustrated using measured data from Lough Feeagh and one of the catchment RWT monitoring sites for 2005/2006 (Figure 7.8c). The lower projected increase in deeper waters in the lake during summer months also highlights the potential for these deep lake waters below the thermocline to provide a refuge for fish species if surface waters should exceed critical thresholds (Tanaka et al., 2000; Mathes et al., 2010).

Table 7.3: Average number of days/year when projected river water temperature was above critical temperature thresholds for A2 and B2 scenarios.

°C	Threshold	Period	A2	B2
22	26 Seek refugia (salmon parr)	1961–1990	0.15	0.13
		2010–2039	0.26	0.23
	27 Upper range feeding (salmon parr)	2040–2069	1.11	0.82
		2070–2099	2.91	1.27
26	Ultimate lethal level (trout parr)	1961–1990	0.00	0.00
		2010–2039	0.00	0.00
		2040–2069	0.01	0.02
		2070–2099	0.05	0.02
30	Ultimate lethal level (salmon parr)	1961–1990	0.00	0.00
		2010–2039	0.00	0.00
		2040–2069	0.00	0.00
		2070–2099	0.02	0.00

The temperature thresholds presented in Table 7.4 are all at the extreme high end of the temperature range and more likely to occur in summer. However, the season with the greatest projected increase in both RWT and lake SWT in Burrishoole was winter. A recent study based on data from the Burrishoole system has shown that higher water temperatures during the first and second winters, when salmonid eggs were incubating in gravel beds and when fish were in the parr life stage, respectively, have had negative impacts on salmon freshwater survival (McGinnity et al., 2009). A dearth of such long time-series datasets for key taxonomic groups, including fish, and a shortage of studies on ecological responses to combined pressures, were identified as major knowledge gaps in research supporting the EU Water Framework Directive (Directive 2000/60/EC) by Heiskanen and Solimini (2005). Adult Atlantic salmon in the Burrishoole river system typically spawn in late November, December and early January. Historical estimates of egg deposition in the catchment included eggs from both wild salmon and those from adults from an experimental captive breeding and smolt release (ranching) programme established between 1960 and 1964. Returning ranched adults, surplus to the requirements of the breeding programme, were allowed to ascend the river system until 1997 and could therefore interbreed with wild fish (Thompson et al., 1998). The numbers of ranched fish entering the river has since been curtailed to prevent such interbreeding.

Analyses of these data indicated that 76% of the variability in freshwater survival was explained by five climate-related factors and the proportion of eggs contributed by ranched fish. The proportion of eggs from ranched fish had a negative impact on survival (McGinnity et al., 2009). Higher water temperatures in the first winter when eggs were incubating in gravel beds and

during the second winter when fish were in the parr stage also had negative impacts on survival. The impact of higher winter water temperatures was, however, significantly greater when there was a larger cohort of ranched fish in the total population, suggesting that the progeny of ranched fish are more sensitive to projected temperature increases. Poor survival during the first winter was attributed to the fact that warmer water surrounding incubating eggs may lead to earlier hatching, before sufficient food supplies are available. A locally adapted population of salmon may be expected to match the energy demands of a typical winter by producing eggs with sufficient energy reserves while egg size in captive-bred populations evolves in a benign hatchery environment where there is no penalty for producing small eggs (Heath et al., 2003). Similarly, in the case of parr, elevated temperatures are known to increase fish metabolism, so juvenile fish may deplete their energy reserves before an adequate spring food supply becomes available (Metcalfe et al., 1992). The study also found, however, that high spring temperature just before smolts migrated to sea had a positive impact on survival (McGinnity et al., 2009).

Future changes in water temperature were simulated for Lough Feeagh in that study using output for two time-horizons: a control period of 1961–1990 and the late 21st century, 2071–2100. Future egg-to-smolt survival was then estimated with low and high populations of ranched fish. The results indicated no reduction in survival when the proportion of eggs from ranched fish was low. Poor outcomes and considerably lower survival were predicted when the proportion of eggs from ranched fish was high. During the current project, McGinnity et al.'s (2009) model was used to assess egg-to-smolt survival using the lake SWT data presented in Section 6. Projected survival rates were produced for the four time-horizons with both low and high populations of ranched fish. These new projections gave information on projected changes over the intermediate time-horizons (2010–2039 and 2040–2069) in addition to the control period (1961–1990) and the late 21st century (2070–2099). Estimates of survival were also produced using historical data, again for populations with low and high numbers of ranched fish. These historical estimates (grey boxes in Figure 7.8) indicated a potential 29% reduction in survival when numbers of ranched fish were consistently high. The addition of future climate data resulted in further projected reductions in survival, but only for the population with a high proportion of ranched fish. For the A2 scenario median survival rates for the population with high levels of ranched fish decreased by 7%, 30% and 44% for the 2020s, 2050s and 2080s respectively (Table 7.5). The reductions for the B2 scenario were 18%, 32% and 26%.

Many fish species have shown the ability to adapt to changing temperatures when exposed gradually to increases (Graham and Harrod, 2009). These results presented here support the conclusions of McGinnity et al. (2009) that wild salmon populations may be able to adapt to projected increases in temperatures. However, it also supports the suggestion that cultured fish capable of breeding in the wild should not be deliberately introduced into natural salmon rivers, and that measures must also be found to reduce the numbers of escaped farm salmon in nature, if wild salmon populations are to adapt successfully to climate change. Further development of fish growth models will help to clarify responses for species and populations and inform catchment management strategies.

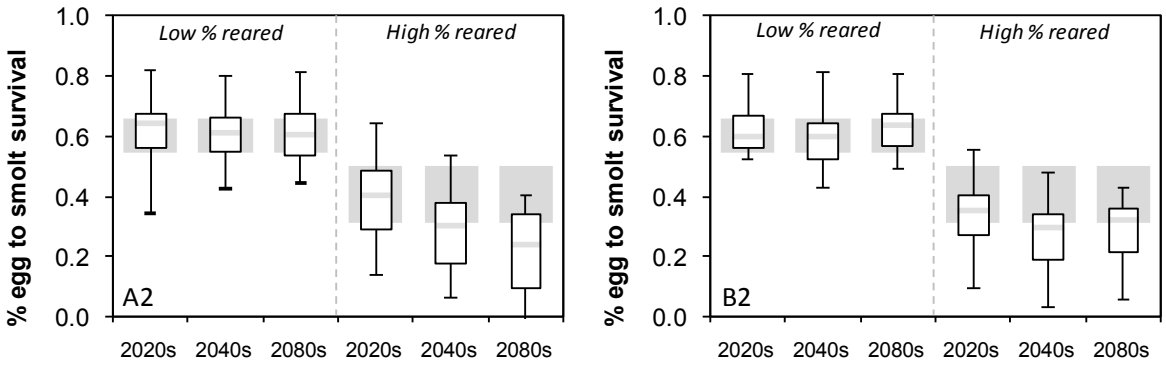

Figure 7.8: Boxplots of projected impacts of changes in water temperature and precipitation on salmon egg to smolt survival in the Burrishoole catchment for populations with low and high proportions of ranched fish. The grey boxes are estimates of egg-to-smolt survival produced using historical data (25th and 75th percentiles).

Table 7.4: Projected salmon egg to smolt survival for the observed period (1961–1990) together with the absolute % change from this period for the 2010–2039, 2040–2069 and 2070–2099 for both the A2 scenario and the B2 scenario.

	Low	% change	High	% change
Observed	0.61		0.43	
2010–2039 A2	0.03	6	-0.03	-7
2010–2039 B2	-0.01	-2	-0.08	-18
2040–2069 A2	0.00	1	-0.13	-30
2040–2069 B2	-0.01	-1	-0.14	-32
2070–2099 A2	0.00	0	-0.19	-44
2070–2099 B2	0.03	5	-0.11	-26

7.6.2 Impacts of Climate-Related Change in Flow Rates on Fish Populations

Migration, particularly in freshwater fish, has often been regarded as an adaptive strategy to increase growth and survival which may contribute to increased abundance (Northcote, 1978). Salmonids migrate downstream to sea as smolts in springtime. Adult salmon return to

freshwater to spawn as early as December/January as multi-sea winter salmon and right through the summer months and into the autumn as one sea winter grilse. The projected changes in hydrology for the Burrishoole catchment include higher winter flows and lower summer flows (Section 5). Droughts leading to low water levels can result in delayed downstream migration of smolts and also present difficulty for adults to return to freshwater from the sea. Low summer flows in combination with high temperatures can be serious and lead to mortality, particularly where adult salmonids returning from the sea get delayed for extended periods and are unable to migrate upstream into freshwater (e.g. Solomon and Sambrook, 2004; Graham and Harrod, 2009). It is likely that the impact of the projected changes in water flow will be more profound in the smaller spatey catchments than in the larger catchments, although prolonged droughts experienced in recent years can result in significant delays to both downstream smolt migrations and upstream returns of adults.

7.6.3 Water-Level Changes and Juvenile Fish

Droughts that lead to unusually low water levels can have impacts on different life stages of fish at different times of the year. Winter droughts may have an impact on accessibility to spawning beds for adult salmonids and after spawning can lead to isolation and the drying of redds and nursery habitat, leading to higher mortalities of eggs and fry. Summer droughts can also lead to mortalities because parts of the stream beds are left dry. These droughts often affect only one life stage and do not usually feed through to have a marked impact on the overall population. Extreme and repeated drought may, however, affect the population density of future spawning adults. Elliott (1994) demonstrated the effect of summer drought on trout survival in a stream in the UK and concluded that higher mortality was most probably due to a marked reduction in the wetted area of stream available to trout and subsequent retarded growth of fish. Where significant pool area and/or lakes exist in a catchment, the impact of summer drought on juveniles might be lower.

The impact of high flows in winter is less clear. Extreme high flows during winter can have a devastating impact on salmonids' survival with the scouring of spawning beds and the possible mortality of adults, eggs and fry. The increase in the frequency and volume of winter floods that is projected under the climate change scenarios therefore could have serious consequences for the viability of some stocks. High autumn and winter precipitation can, in contrast, also have a positive impact on survival of fry (Jonsson et al., 2005; Crozier et al., 2008; McGinnity et al., 2009). Jonsson et al. (2005) attributed this effect to an enlargement of the aquatic habitat in streams and an improvement in the production of food organisms for emerging fry. High autumn flows have also been found to be strongly positively correlated with

juvenile survival in Chinook salmon but only in populations in cooler, narrower streams (Crozier et al., 2008).

7.6.4 Combined Impacts of Temperature and Water Level on Smolts

In Irish waters, salmon are obligate migrators; if they smoltify but are not able to migrate they die; trout appear more flexible. There is a short window of opportunity for downstream migration of smolts – mostly in April and May – which is dependent on environmental factors, such as water temperature and water level (Byrne et al., 2003; Byrne et al., 2004). Trout are not believed to be obligate migrators. Trout populations can be made up of anadromous and resident cohorts and it is believed that if a sea trout smolt does not get to migrate, it can revert and migrate as an older fish. The term smoltification describes two different phenomena: transformation and migration. Light and temperature are both involved in the process of smoltification: the increase in day-length in the spring (photoperiod) acts as the synchroniser of an endogenous rhythm, the environmental factor that most influences the onset of parr-to-smolt transformation (Byrne et al., 2004, Jonsson and Jonsson, 2009). Temperature can affect both the transformation and the migration of smolts. A number of studies have shown that salmonids do not commence migration until a threshold temperature has been reached (Solomon, 1978), but it has been shown that temperatures above a certain threshold tend to cause a premature decrease in euryhalinity, or a detransformation in salmonids (Zaugg, 1982). There is a lack of published information in this regard relating to sea trout.

Rainfall tends to have an indirect impact on the migration process through changes in water levels; low water levels tend to inhibit or at least deter smolt migration, simply by impeding the successful passage of smolts to the sea. The effect of a spring drought in 1980 on the descent of smolts in the Burrishoole fishery is a case in point (Cross and Piggins, 1982). In that year, a prolonged dry period with low water levels from early April delayed the whole smolt run into June (Figure 7.9). A similar phenomenon occurred in 2010 with the smolt run being delayed by a spring drought.

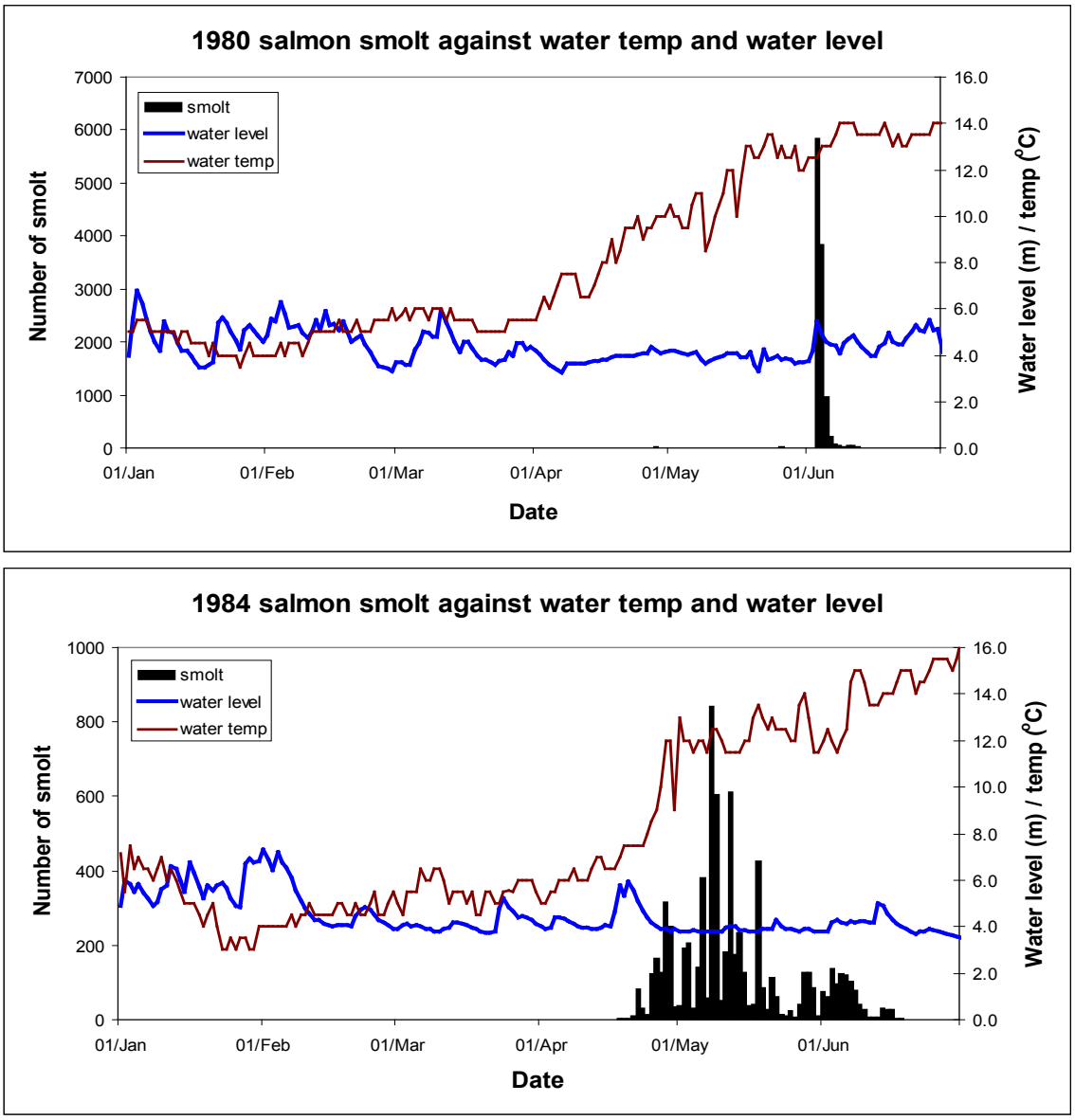

Figure 7.9: Examples of salmon smolt migration timing plotted along with water temperature (oC) and water level (m) for 1980 (delayed by drought – top) and 1984 (not delayed – bottom). (*Note different Y-axis).

Previous work carried out in the Burrishoole catchment looked at cumulative sea trout smolt migrations in the system from 1975 to 1990 (Whelan et al., 1993). These were compared with the corresponding freshwater temperatures and rainfall levels. Sea temperatures for the past 15 years were also plotted and their patterns noted. The sea trout smolt migration did not usually commence until freshwater temperature reached a threshold level of 9°C. Rainfall levels affected the timing of the downstream migration indirectly, through its impact on water levels. Recruitment was adversely affected by the occurrence of temperatures of 13°C or higher before sea trout smolt migration had taken place. No evidence was found to suggest that warm springs resulted in higher recruitment of sea trout smolts in the Burrishoole catchment.

Anadromous salmonids smolt and migrate to sea during spring. Byrne et al. (2003; 2004) divided factors controlling the smolt run into regulating and controlling factors. Regulating factors operate before (affecting the physiological smoltification process) and controlling factors operate during the smolt run (such as those controlling speed of downstream migration). The primary regulating factors of the smolt run are photoperiod and temperature. Day length is a timer, and increasing and decreasing photoperiods are major predictive, proximate factors which indicate the season (Wootton, 1998). Temperature affects the rate of development, and low-water temperature can limit the response of salmon parr to increased day length (McCormick et al., 2002).

Water temperature is largely responsible for annual variation. To smolt successfully, fish require a certain amount of heat, which can be measured in degree days (number of days x mean temperature [°C]). Zydlewski et al. (2005) showed that the temperature experienced over time determines the behavioural and physiological changes associated with the smoltification process as well as the onset and ending of the smolt run in salmon. The main controlling factors of smolt migrations are water temperature, water flow and changes to both these factors. Some studies indicate a pervasive effect of temperature and temperature increases for the initiation of a seaward migration in salmonids (Jonsson and Ruud-Hansen, 1985, Jutila et al., 2005). Smolt migration seems not to be triggered by either a specific water temperature or a specific number of degree days but is controlled by a combination of the actual temperature and temperature increase in the water during spring (Byrne et al., 2004).

7.6.5 Impacts of Climate-Related Change in Dissolved Oxygen and Dissolved Organic Carbon on Fish Populations

Despite the dominant influence of RWT on DO levels, projected increases in RWT resulted in only a 4% to 7% decrease in average daily DO concentrations. However, these increases in water temperature will also influence rates of organic matter decomposition by bacteria and possibly rates of in-stream primary productivity. The projected changes in the concentration of DOC in streams could also impact on rates of decomposition rates and therefore oxygen consumption during summer. Increases in DOC concentrations were projected for all GCM model and emission scenarios from the 2010–2039 period onwards. However, the greatest increases in DOC levels occurred during autumn, a period when catchment streams are generally well oxygenated. The projected increases would, however, have consequences for the ecology of Lough Feeagh and other lakes in peaty catchments. Many highly coloured lakes like Feeagh exhibit net heterotrophy due to the central role of catchment DOC in fuelling the upper trophic levels via the bacterioplankton-protozoan link (e.g. Tranvik, 1992; Kankaala et

al., 1996). The projected increases in DOC may, therefore, alter the food-web dynamics in the lake. Reduced light intensity also lowers the reactive distance of fish and their ability for size-selective predation (Wissel et al., 2003). The hypolimnion can also easily become anoxic during periods of intense stratification as DOC is decomposed (Salonen et al., 1984). This oxygen-depleted zone can then provide a refuge for prey species less sensitive to oxygen availability than fish (Wissel et al., 2003). In addition to these local impacts, the projected increases in DOC concentration may have implications for water treatment in peat catchments (Jennings et al., 2006; Naden et al., 2010) and on the global carbon cycle should they have an impact on a regional scale. A positive feedback mechanism between decomposition in organic soils and climate change has been suggested, with changes in climate driving increases in the export of DOC which in turn would increase atmospheric CO_2 concentrations and contribute to further global warming (Knorr et al., 2005; Davidson and Janssens, 2006).

High DOC concentrations can also affect stream pH levels as many DOC compounds are organic acids (Clark et al., 2005; Evans et al., 2005). The processes contributing to in-stream pH levels are complex however and include processes occurring in catchment soils and surface waters, together with impacts of regional-scale pollution and local land-use changes (Cox, 2003; Clark et al., 2005; Evans et al., 2005). The assessment of in-stream pH levels in the Burrishoole system in Section 3 highlighted both the rapid temporal changes which can occur in pH levels during high-flow events and the potential influence of regional pollution sources.

7.7 Summary

The projected changes in climate and water-quality parameters described in this report which could directly affect fish growth and survival include increases in RWT and lake SWT, and changes in river flow related to changing rainfall patterns, decreases in DO and DOC concentrations and river flow related to changing rainfall patterns.

Increases in water temperature may have both potential positive and negative consequences for salmonid populations and ecosystem functioning in the Burrishoole catchment. Direct temperature impacts would include changes in the number of times when threshold values are exceeded and to the impacts of upward trends in mean temperatures on physiology and phenology. The projected monthly mean RWTs and lake SWTs in Burrishoole remained within the ideal range for salmonid fish habitats (7°C to 20°C). However, the number of days when RWT exceeded 22°C, for example, the threshold when salmon parr cease feeding and seek refuge, increased in all four time-horizons for both scenarios. There was also an increase in the number of days when RWT exceeded 26°C (the ultimate lethal threshold for trout parr) in the

two later time-horizons: 2040–2069 and 2070–2099. It is notable, however, that the number of days when lake SWT was projected to exceed the 22◦C threshold was much lower than that indicated for RWT reflecting the more buffered nature of lake SWT, and these higher lake temperatures were confined to simulations based on the HadCM3 model.

Other changes due to temperature would include changes in hatching time, fry survival and growth rate, which may also have a knock-on effect on salmon and sea trout smolt size and age. There are indications that 76% of the variability in freshwater survival could be explained by five climate-related factors and the proportion of eggs contributed by ranched fish. The proportion of eggs from ranched fish had a negative impact on survival. Higher water temperatures in the first winter when eggs were incubating in gravel beds and during the second winter when fish were in the parr stage also had negative impacts on survival. The impact of higher winter water temperatures was, however, significantly greater when there was a larger cohort of ranched fish in the total population, suggesting that the progeny of ranched fish are more sensitive to projected temperature increases. Poor survival during the first winter was attributed to the fact that warmer water surrounding incubating eggs may lead to earlier hatching, before sufficient food supplies are available. Future egg-to-smolt survival was estimated with low and high populations of ranched fish. The results indicated no reduction in survival when the proportion of eggs from ranched fish was low. Poor outcomes and considerably lower survival were predicted when the proportion of eggs from ranched fish was high.

This study found that salmon growth is set to increase in the Burrishoole catchment over the coming century, similar to predictions that some British salmon stocks will also see increases in their growth rates in freshwater in the coming century due to increased river water temperatures. Unlike salmon, this study found that for trout growth, under all climate scenarios, it is predicted that there will be a levelling off in the growth rate (weight, g) before the weight gain starts to decline in the coming century.

Migration, particularly in freshwater fish, has often been regarded as an adaptive strategy to increase growth and survival which may contribute to increased abundance. Salmonids migrate downstream to sea as smolts in springtime. Adult salmon return to freshwater to spawn as early as December/January as multi-sea winter salmon and right through the summer months and into the autumn as one sea winter grilse. The projected changes in hydrology for the Burrishoole catchment include higher winter flows and lower summer flows. Droughts leading to low water levels can result in delayed downstream migration of smolts and also present

difficulty for adults to return to freshwater from the sea. Low summer flows in combination with high temperatures can be serious and lead to mortality, particularly where adult salmonids returning from the sea get delayed for extended periods and are unable to migrate upstream into freshwater. It is likely that the impact of the projected changes in water flow will be more profound in the smaller spatey catchments than in the larger catchments, although prolonged droughts experienced in recent years can result in significant delays to both downstream smolt migrations and upstream returns of adults.

Droughts that lead to unusually low water levels can have impacts on different life stages of fish at different times of the year. Winter droughts may have an impact on accessibility to spawning beds for adult salmonids and after spawning can lead to isolation and the drying of redds and nursery habitat, leading to higher mortalities of eggs and fry. Summer droughts can also lead to mortalities because parts of the stream beds are left dry. These droughts often affect only one life stage and do not usually feed through to have a marked impact on the overall population. Extreme and repeated drought may, however, affect the population density of future spawning adults. Where significant pool area and/or lakes exist in a catchment, the impact of summer drought on juveniles might be lower.

The impact of high flows in winter is less clear. Extreme high flows during winter can have a devastating impact on salmonids' survival with the scouring of spawning beds and the possible mortality of adults, eggs and fry. The increase in the frequency and volume of winter floods that is projected under the climate change scenarios therefore could have serious consequences for the viability of some stocks.

In Irish waters, salmon are obligate migrators; if they smoltify but are not able to migrate they die; trout appear more flexible. There is a short window of opportunity for downstream migration of smolts – mostly in April and May – which is dependent on environmental factors, such as water temperature and water level. Light and temperature are both involved in the process of smoltification: the increase in day-length in the spring (photoperiod) acts as the synchroniser of an endogenous rhythm, the environmental factor that most influences the onset of parr-to-smolt transformation. Temperature can affect both the transformation and the migration of smolts and therefore projected increases in temperature may have consequences for smoltification and migration timing.

Rainfall tends to have an indirect impact on the migration process through changes in water levels; low water levels tend to inhibit or at least deter smolt migration, simply by impeding the

successful passage of smolts to the sea such as observed in 1980 and 2010. These delays may result in poor marine survival of the delayed salmon smolts. The projected changes in flow rates for Burrishoole include an increase in the incidence of extreme low flows during summer and spring, with this trend becoming more pronounced through the latter part of the century. Such an increase is likely to have negative consequences for salmonids in Burrishoole similar to those reported for 1980.

Despite the dominant influence of RWT on DO levels, projected increases in RWT resulted in only a 4% to 7% decrease in average daily DO concentrations. However, these increases in water temperature will also influence rates of organic matter decomposition by bacteria and possibly rates of in-stream primary productivity. The projected changes in the concentration of DOC in streams could also impact on rates of decomposition rates and therefore oxygen consumption during summer. Increases in DOC concentrations were projected for all GCM model and emission scenarios from the 2010–2039 period onwards. However, the greatest increases in DOC levels occurred during autumn, a period when catchment streams are generally well oxygenated. The projected increases would, however, have consequences for the ecology of Lough Feeagh and other lakes in peaty catchments, possibly altering the food-web dynamics in the lake. In addition to these local impacts, the projected increases in DOC concentration may have implications for water treatment in peat catchments and on the global carbon cycle should they have an impact on a regional scale.

High DOC concentrations can also affect stream pH levels as many DOC compounds are organic acids. The processes contributing to in-stream pH levels are complex however and include processes occurring in catchment soils and surface waters, together with impacts of regional-scale pollution and local land-use changes. The assessment of in-stream pH levels in the Burrishoole system in Section 3 highlighted both the rapid temporal changes which can occur in pH levels during high-flow events and the potential influence of regional pollution sources.

7.8 Key Findings

- Salmon growth is projected to increase in the Burrishoole catchment over the coming century, a finding supported by the work of Davidson and Hazelwood (2005) who suggest that some British salmon stocks will also see increases in their growth rates in freshwater in the coming century due to increased river water temperatures.

- Unlike salmon, this study found that for trout growth, under all climate scenarios, it is projected that there will be a levelling off in the growth rate (weight, g) before the weight gain starts to decline in the coming century.
- The projected changes in climate and water-quality parameters described in this report which could directly affect fish growth and survival include increases in RWT and lake SWT, and changes in river flow related to changing rainfall patterns, decreases in DO and DOC concentrations and river flow related to changing rainfall patterns.
- Droughts leading to low water levels can result in delayed downstream migration of smolts and also present difficulty for adults to return to freshwater from the sea. Low summer flows in combination with high temperatures can be serious and lead to mortality, particularly where adult salmonids returning from the sea get delayed for extended periods and are unable to migrate upstream into freshwater.
- Winter droughts may have an impact on accessibility to spawning beds for adult salmonids and after spawning can lead to isolation and the drying of redds and nursery habitat, leading to higher mortalities of eggs and fry. Summer droughts can also lead to mortalities because parts of the stream beds are left dry.
- Extreme high flows during winter can have a significant negative impact on salmonids' survival with the scouring of spawning beds and the possible mortality of adults, eggs and fry. The increase in the frequency and volume of winter floods that is projected under the climate change scenarios therefore could have serious consequences for the viability of some stocks.
- Projected changes to rainfall patterns will impact on water flow regimes in rivers, which will affect the timing of migrations into and out of freshwater and may reduce the survival of various life history stages of salmonids.
- Projected changes in lake water temperature may also affect survival rates, particularly where inshore areas of lakes provide nursery habitat for older age classes.
- Thermal stratification, where warmer upper lake waters are separated from cooler deeper waters by a thermocline, may provide a refuge for salmonids during periods of high water temperature. The lack of any projected increase in DWTs in the lake in summer months also highlights the potential for waters below the thermocline to provide a refuge for fish species if surface water temperatures should exceed critical thresholds.
- Monthly mean projected RWTs and lake SWTs remained within the ideal range for salmonid fish habitats (7°C to 20°C). However, the number of days when RWT exceeded 22◦C, for example, the threshold when salmon parr cease feeding and seek refuge, increased in all four time periods for both scenarios.

- The season with the greatest increase in RWT and lake SWT was winter. Higher water temperatures during the first and second winters when eggs were incubating in gravel beds and when fish were in the parr life-stage, respectively, has previously been found to have negative impacts on survival for Atlantic salmon at Burrishoole. This impact was greater when the population had a high proportion of ranched (cultured origin) fish.
- Estimates of future survival were produced based on this model for the three future time-horizons. There were reductions in survival for all three time periods, but only for the population with a high proportion of ranched fish, suggesting that the wild population will be able to adapt to increasing winter temperatures.
- The changes observed in these stocks of migratory fish are thought to be due to a number of complex and sometimes interrelated factors, of which weather patterns and climate change may play an important role.
- The changes to fish populations in the catchment already observed and the possible responses to climate change, while specific to Burrishoole, may be taken as indicative to many similar peaty spate river systems. Fish populations in lowland systems with slower water-level changes and different water chemistry may respond differently to those in more upland catchments.

7.9 References

Berman, C. H. and Quinn, T. P. (1991) 'Behavioural thermoregulation and homing in spring Chinook salmon, *Oncorhynchus tshawytscha* (Walbaum), in the Yakima River', Journal of Fish Biology 39, 301.312. doi: 10.1111/j.1095-8649.1991.tb04364.x

Breau, C., Cunjak, R. A. *and* Bremset, G. *(*2007) 'Age-specific aggregation of wild juvenile Atlantic salmon *Salmo salar* at cool water sources during high temperature events', *Journal of Fish Biology,* 71, 1179–1191.

Brett, J. R. *(*1952) 'Temperature tolerance in young Pacific salmon genus *Oncorhynchus', Journal of the Fisheries Research Board of Canada* 9, 265–323.

Brett, *J. R. (1964)* 'The respiratory metabolism and swimming performance of young sockeye salmon', *Journal of the Fisheries Research Board of Canada* 21, 1183–1226.

Byrne, C.J., Poole, R., Rogan, G., Dillane, M. and Whelan, K.F. (2003) 'Temporal and environmental influences on the variation in Atlantic salmon smolt migration in the Burrishoole system 1970–2000', Journal of Fish Biology, 63, 1552–1564.

Byrne, C.J., Poole, R., Dillane, M., Rogan, G. and Whelan, K.F. (2004) 'Temporal and environmental influences on the variation in sea trout (*Salmo trutta L.*) smolt migration in the Burrishoole system in the west of Ireland from 1971 to 2000', Fisheries Research, 66, 85–94.

Caissie, D. (2006) 'The thermal regime of rivers: a review', Freshwater Biology, 51, 1389–1406.

Clark, J.M., Chapman, P.J., Adamson, J.K. and Lane, S.N. (2005) 'Influence of drought induced acidification on the mobility of dissolved organic carbon in a peat soil', Global Change Biology, 11, 791–809.

Connor, W. P., Burge, H. L., Waitt, R. and Bjornn, T. C. (2002) 'Juvenile life history of wild fall Chinook salmon in the Snake and Clearwater Rivers', *North American Journal of Fisheries Management* 22, 703–712.

Cox, B.A. (2003) 'A review of currently available in-stream water-quality models and their applicability for simulating dissolved oxygen in lowland rivers', Science of the Total Environment, 314–16, 335–377.

Cross, T.F. and Piggins, D.J. (1982) The effect of abnormal climate conditions on the smolt run of 1980 and subsequent returns of Atlantic salmon and sea trout. ICES CM:M26:8.

Crozier, L.G., Zabel, R.W. and Hamlet, A.F. (2008) 'Predicting differential effects of climate change at the population level with life-cycle models of spring Chinook salmon', Global Change Biology, 14, 236–249.

Cunjak, R.A., Caissie D., El-Jabi, N., Hardie, P., Conlon, J.H., Pollock, T.L., Gibson, D.J. and Komadina-Douthwright, S. (1993) 'The Catamaran Brook (New Brunswick) habitat research project: biological, physical and chemical conditions (1990–1992)', Canadian Technical Report of Fisheries and Aquatic Sciences 1914, 1–81.

Davidson, I.C. and Hazelwood, M.S. (2005) Effect of Climate Change on Salmon Fisheries, Science Report. W2-047/SR. Bristol. Environment Agency, pp.47

Davidson, E.A. and Janssens, I.A. (2006) 'Temperature sensitivity of soil carbon decomposition and feedbacks to climate change', Nature, 440, 165–173.

Elliott, J.M. (1981) 'Some aspects of thermal stress on freshwater teleosts'. In A.D. Pickering (ed.) Stress and Fish. London, Academic Press.

Elliott, J.M. (1991) 'Tolerance and resistance to thermal stress in juvenile Atlantic salmon, *Salmo salar*', Freshwater Biology, 25, 61–70.

Elliott, J. M. (1994) Quantitative Ecology and the Brown Trout. Oxford Series in Ecology and Evolution. Oxford: Oxford University Press.

Elliott, J. M., Hurley, M. A. and Fryer, R. J. (1995) 'A new, improved growth model for brown trout, *Salmo trutta* L', Functional Ecology 9, 290.298.

Elliott, J. M. and Hurley, M. A. (1997) 'A functional model for maximum growth of Atlantic salmon parr, *Salmo salar*, from two populations in Northwest England', Functional Ecology 11, 592.603.

Elliott J.M and Hurley, M.A. (2000) 'Daily energy intake and growth of piscivorous brown trout', Freshwater Biology, 22, 237–245.

Evans, C.D., Monteith D.T. and Cooper D.M. (2005) 'Long-term increases in surface water dissolved organic carbon: observations, possible causes and environmental impacts', Environmental Pollution, 137, 55–71.

Graham, W. D., Thorpe, J. E. and Metcalfe, N. B. (1996) 'Seasonal current holding performance of juvenile Atlantic salmon in relation to temperature and smolting', Canadian Journal of Fisheries and Aquatic Sciences 53, 80-86.

Graham, C.T. and Harrod, C. (2009) 'Implications of climate change for the fishes of the British Isles', Journal of Fish Biology, 74, 1143–1205.

Heath D.D., Moya-Larano J. and Fox C.W. (2003) 'Rapid evolution of egg size in captive salmon', Science, 299, 1738–1740.

Heiskanen, A.-S. and Solimini, A.G. (Eds) (2005) Relationships between Pressures, Chemical Status and Biological Quality Elements. Analysis of the Current Knowledge Gaps for the Implementation of the Water Framework Directive. Report to the EU. JRC # EUR 21497 EN.

Helsel, D. R. and Hirsch, R. M. (2002) Statistical Methods in Water Resources, USGS Techniques of Water Resources Investigations, Book 4, Chapter A3, 510 p.

Jennings, E., Nic Aongusa, C., Allott, C., Naden, P., O'Hea, B., Pierson, D. and Schneiderman, E. (2006) Future climate change and water colour in Irish peatland catchments: results from the CLIME project. Proceedings of the National Hydrology Seminar 2006: Water Resources in Ireland and Climate Change, Tullamore.

Jonsson, B. and Jonsson, N. (2009) 'A review of the likely effects of climate change on anadromous Atlantic salmon *Salmo salar* and brown trout *Salmo trutta* , with particular reference to water temperature and flow', Journal of Fish Biology, 75, 2381–2447.

Jonsson, N., Jonsson, B. and Hansen, L.P. (2005) 'Does climate during embryonic development influence parr growth and age of seaward migration in Atlantic salmon (*Salmo salar*)?' Canadian Journal of Fisheries and Aquatic Sciences, 62, 2502–2508.

Jonsson, B. and Ruud-Hansen, J. (1985) 'Water temperature as the primary influence on timing of seaward migration of Atlantic salmon (Salmo salar) smolts', Canadian Journal of Aquatic Science, 42, 593–595.

Jutila, E., Jokikokko, E. and Julkunen, M. (2005) 'The smolt run postsmolt survival of Atlantic salmon, *Salmo salar* L., in relation to early summer water temperatures in the northern Baltic Sea', *Ecology of Freshwater Fish* 14**,** 69–78. doi: 10.1111/j.1600-0633.2005.00079.x

Kankaala, P., Arvola, L., Tulonen, T. and Ojala, A. (1996) 'Carbon budget for the pelagic food web of the euphotic zone in a boreal lake (Lake Pääjärvi)', Canadian Journal of Fisheries and Aquatic Sciences, 53, 1663–1674.

Knorr, W., Prentice, I. C., House, J. I. and Holland, E. A. (2005) 'Long-term sensitivity of soil carbon to warming', Nature, 433, 298–301.

Livingstone, D.M. and Hari, R.E. (2008) 'Coherence in the response of river and lake temperatures in Switzerland to short-term climatic fluctuations in summer', Internationale Vereinigung für Theoreische und Angewandte Limnologie, 30, 449–454.

Livingstone, D.M., Lotter, A.F. and Kettle, H. (2005) 'Altitude-dependent differences in the primary physical response of mountain lakes to climatic forcing', Limnology and Oceanography, 50, 1313–1325.

Mathes, M.H., Hinch, S.G., Cooke, S.J., Crossin, G.T., Patterson, D.A., Lotto, A.G. and Farrell, A.P. (2010) 'Effect of water temperature, timing, physiological condition, and lake thermal refugia on migrating adult Weaver Creek sockeye salmon (Oncorhynchus nerka)', Canadian Journal of Fisheries and Aquatic Sciences, 67, 70–84.

McCarthy, I. D. and Houlihan, D. F. (1997) The effect of temperature on protein synthesisin fish: the possible consequences for wild Atlantic salmon (*Salmo salar* L.) stocks in Europe as a result of global warming. In Global Warming: Implications for Freshwater and Marine Fish (Wood, C. M. and McDonald, G., eds), pp. 51.77. Cambridge: Cambridge University Press.

McCormick, S.D., Shrimpton, J.M., Bjornsson, B.T. and Moriyama, S. (2002) 'Effects of an advanced temperature cycle on smolt development and endrocrinology indicate that temperature is not a zeitgeber for smelting in Atlantic salmon', Journal of Experimental Biology, 205, 3553–3560.

McGinnity, P., Jennings, E., DeEyto, E., Allot, N., Samuelsson, P., Rogan G., Whelan, K. and Cross, T. (2009) 'Impact of naturally spawning captive-bred Atlantic salmon on wild populations: depressed recruitment and increased risk of climate-mediated extinction', Proceedings of the Royal Society B – Biological Sciences, 276, 3601–3610.

Metcalfe, N.B, and Thorpe, J. E. (1992) 'Anorexia and Defended Energy Levels in Over-Wintering Juvenile Salmon', Journal of Animal Ecology. 61: 175-181.

Mohseni, O., Erickson, T.R., and Stefan, H.G. (1999) 'Sensitivity of stream temperatures in the United States to air temperatures projected under a global warming scenario', Water Resources Research 35(12), 3723-3733.

Naden, P., Allott, N., Arvola, L., Jarvinen, M., Jennings, E., Moore, K., Nic Aongusa, C., Pierson, D. and Schneidermen, E. (2010) Modelling the effects of climate change on dissolved organic carbon. In D.G. George (ed.) The Impact of Climate Change on European Lakes. Springer.

Rimmer, D. M., Saunders, R. L. and Paim, U. (1985) 'Effects of temperature and season on the photobehavior of Atlantic salmon (Salmo salar)', Canadian Journal of Zoology 68, 1098.1103.

Salonen, K., Arvola, L. and Rask, M. (1984) 'Autumnal and vernal circulation of small forest lakes in Southern Finland', Verh. Internat. Verein. Limnol., 22, 103–107.

Skilbrei, O.T. (1991) 'Importance of threshold length and photoperiod for the development of bimodal lengthfrequency distribution in Atlantic salmon (*Salmo salar*)', Canadian Journal of Fisheries and Aquatic Sciences, 48, 2163–2172.

Solomon, D. J. (1978) 'Some observations on salmon smolt migrations in a chalkstream', *Journal of Fish Biology* 12**,** 571–574. doi: 10.1111/j.1095-8649.1978.tb04203.x

Solomon, D.J. and Sambrook H.T. (2004) 'Effects of hot dry summers on the loss of Atlantic salmon, *Salmo salar*, from estuaries in South West England', Fisheries Management and Ecology, 11, 353–363.

Tanaka, H., Takagi, Y. and Naito, Y. (2000) 'Behavioural thermoregulation of homing chum salmon', Journal of Experimental Biology, 203, 1825–1833.

Thompson, C., Poole, R., Matthews, M. and Ferguson, A. (1998) 'Comparison, using minisatellite DNA profiling, of secondary male contribution in the fertilisation of wild and ranched Atlantic salmon (*Salmo salar*) ova', Canadian Journal of Fisheries and Aquatic Science, 55, 2011–2018.

Tranvik, L.J. (1992) 'Allochthonous dissolved organic matter as an energy source for pelagic bacteria and the concept of the microbial loop', Hydrobiologia, 229, 107–114.

Valdimarsson, S. K., Metcalfe, N. B., Thorpe, J. E. and Hundtingford, F. A. (1997) 'Seasonal changes in sheltering: effect of light and temperature on diel activity in juvenile salmon', Animal Behaviour 54, 1405.1412.

Whelan, K.F., Galvin, P.T., Poole, W.R. and Cooke, D.J. (1993) 'Environmental factors influencing the migration and survival of sea trout (*Salmo trutta* L.) smolts', ICES CM 1993/M:48.

Wissel, B., Boeing, W.J. and Ramcharan, C.W. (2003) 'Effects of water color on predation regimes and zooplankton assemblages in freshwater lakes', Limnology and Oceanography, 48, 1965–1976.

Wootton, R.J. (1998) Ecology of Teleost Fishes. 2nd edition. Dordrecht, Kuwar Academic Publishers.

Zaugg, W.S. (1982) 'Relationships between smolt indices and migration in controlled and natural environments'. In E.L. Brannon, E.O. Salo (eds.) Proceedings of the Salmon and Trout Migratory Behaviour Symposium. University of Washington. Seattle, Washington, pp.173–183.

Zydlewski, G.B., Haro, A. and McCormick, S.D. (2005) 'Evidence for cumulative temperature as an initiating and terminating factor in downstream migratory behavior of Atlantic salmon (*Salmo salar*) smolts', Canadian Journal of Fisheries and Aquatic Sciences, 62, 68–7.

8. APPENDIX I: QUALITY CONTROL PROCEDURES

8.1 Precipitation

The technical procedures used to quality control precipitation data are described below. The procedures were carried out in Microsoft Excel using filters and subtotals. The table below shows the overview of the steps involved in QC of the rain data, and after that is the detailed description of the procedures involved.

Table 8.1 Procedure for quality control of rain data

Step No.	Procedure
1	All individual files copied to centralised folder
2	All individual file data for each location put into 1 file for all years
3	QC column added
4	Extra tips at start & end of each record examined and edited as appropriate, and code & notes added to QC column
5	Gaps & odd readings identified
6	Missing data recorded as 0 is removed and code & notes added to QC column
7	Maintenance dates identified and code & notes added to QC column
8	Partial data identified and code & notes added to QC column
9	Other QC of gaps / odd readings - check against weather, water levels etc. and code & notes added to QC column
10	Final dataset with all years and QC columns saved

Files were copied from raw data storage into one central folder on local drive. All files were re-named and were in the same format, e.g. "sitename dd-mm-yyyy.xls". Each file was opened and on second sheet checked how many tips were recorded for first and last days. Made sure this agreed with data on 1st sheet. If not Sheet 1 amended. Ensured first and last tip events were not counted as these are initiation events and not true 0.2mm tips. Checked the times of tips to make sure they were not <1 sec apart. If so reading was removed them as they were probably a result of the bucket being knocked while download was in progress.

Data (including any comments / red numbers) was copied into template rain file on correct year worksheet. Missing dates were inserted. For each worksheet, selected "mm Rain" column, copied and "pasted special" > "values". This removed the formulae that were copied from the original files and pasted the values only, so that Excel would not recalculate the values when cells were moved. Data was sorted by date. Dates with two entries were identified, these are download dates. QC code and comments identifying these download dates was added. The 2 entries were added together for each download date and 1 of the duplicate entries was removed (i.e. deleted duplicate row). Examined notebooks and records and identified any special events, missing data, equipment changes etc and added QC as needed. Removed any 0s that did not relate to dry days but to missing data. It rains most days in Furnace, a string of days with 0mm rainfall is considered suspect. Subtotals were used to calculate monthly, seasonal and yearly totals. Note: DO NOT subtotal seasons to get annual sums or averages as seasons cross over years.

Filters were used to count the number of days with missing / removed data for each month, season and year, i.e. to get missing monthly values went to daily tab, counted number of missing days – including date collection started on. Then each number was put into comments column of months tab for correct month (Table 8.2). This was done for each month and year.

Table 8.2 Example of total monthly rainfall data which has been quality controlled

Year	Season No.	Month	mm Rain	QC Code	Comments
2005	13	Apr-05	136.0		
2005	13	May-05	156.4		
2005	14	Jun-05	94.0		
2005	14	Jul-05	25.8	QC3	data missing for 17 days

All rain data from the start of data collection until approximately August 2009 was QC-ed as part of the RESCALE project. Template files have been created and are available for future update to Marine Institute staff.

8.2 Water Level

The technical procedures to quality control water level data are described below. The procedures were carried out in Microsoft Excel using filters and subtotals. The table below shows the overview of the steps involved in QC of the rain data, and after that is the detailed description of the procedures involved

Table 8.3 Procedure for quality control of water level data

Step No.	Procedure
1	All individual files copied to centralised water level folder
2	All individual file data for each location put into 1 file for all years
3	QC column added
4	Gaps & odd readings identified
5	Missing data recorded as 0 removed and code & notes added to QC column
6	Maintenance dates identified and code & notes added to QC column
7	Partial data identified and code & notes added to QC column
8	Jumps in data due to calibration identified, data altered and code & notes added to QC column
9	Other QC of gaps / odd readings - checking against weather, other water levels etc and code & notes added to QC column
10	Final dataset with all years and QC columns saved

Files were copied from raw data storage into one central folder on local drive. All files were re-named and were in the same format, e.g. "sitename dd-mm-yyyy.xls. Each file was opened and data (including any comments / red numbers) copied into correct year worksheet in template water level file. Missing times and/or dates were inserted.

Template saved as "sitename_yearfrom-yearto.xls". Each date has 96 entries as readings are taken every 15 minutes. Dates with an extra reading were identified, these were download dates. QC code and comment were added to download times and the extra reading was removed.

Examined notebooks and records and identified any special events, missing data, equipment changes etc and added QC and comments as needed. Removed any 0s that did not relate to droughts but to missing data. When downloading sometimes the water level recorder will be calibrated to a new level. Ensured the water level for the preceding period was altered by whatever was calibration was performed i.e. + or – some value less than 1. Data was changed and noted in the QC and comments columns. To convert water level to flow a rating curve equation was used. The same QC codes and comments were used for flow as water level.

All water level and flow data from the start of data collection until approximately August 2009 was QC-ed as part of the RESCALE project. Template files have been created and are available for future update to Marine Institute staff.

8.3 Temperature Tidbits

The technical procedures to quality control temperature tidbit data are described below. The procedures were carried out in Microsoft Excel using filters and subtotals. The table below shows the overview of the steps involved in QC of the rain data, and after that is the detailed description of the procedures involved

Files were copied from raw data storage into one central folder on local drive. All files were re-named and were in the same format, e.g. "sitename dd-mm-yyyy.xls. Each file was opened and data (including any comments / red numbers) copied into correct year worksheet in template water temperature file. Missing times and/or dates were inserted. Template saved as "sitename_yearfrom-yearto.xls". Each date will have 48 entries as tidbits log a reading every 30 minutes. Dates with extra readings and time changes were identified, these are download dates. QC code and comment were added to download times and the extra reading was removed.

Table 8.4 Procedure for quality control of water level data

Step No.	Procedure
1	All individual files copied to centralised folder
2	All individual file data for each location put into 1 file for all years
3	QC column added
4	Spurious readings at start of record removed
5	Gaps & odd readings identified and removed as appropriate and code & notes added to QC column
6	Missing data recorded as 0 removed and code & notes added to QC column
7	Maintenance dates identified and code & notes added to QC column
8	Other QC of gaps / odd readings - checking against weather data, other tidbits and code & notes added to QC column
9	Final dataset with all years and QC columns saved

Examined notebooks and records and identified any special events, missing data, equipment changes etc and added QC and comments as needed. Removed any 0s that relate to missing data and added QC codes and comments as appropriate.

All temperature tidbit data from the start of data collection until approximately August 2009 was QC-ed as part of the RESCALE project. Template files have been created and are available for future update to Marine Institute staff.

8.4 Automatic River Monitoring Systems

The technical procedures to quality control Automatic River Monitoring System (ARMS) data are described below. The procedures were carried out in Microsoft Excel using filters and subtotals. ARMS data is logged every 2 minutes as well as hourly and daily averages. QC should be done on the highest resolution data, e.g. 2 minutely. This is due to possible spurious and erroneous readings that occur during cleaning/maintenance etc. Equipment must be removed from the water during cleaning so often a spike in the data is found. This is not a true reading but when the logger calculates the hourly and daily average the reading is included and an abnormal average is obtained. The same can happen when there is a fault in the equipment which causes it to give the error code reading of 999.99. This value will be counted in the hourly and daily average that the logger calculates. Therefore it is important to do all QC on the raw high-resolution files.

Table 8.5 Procedure for quality control of ARMS data

Step No.	Procedure
1	Relevant ARMS template file is opened
2	Template file saved as "'river name"_ARMS_"year".xls'
3	Template file has 5 worksheets each with 90-day blocks
4	Raw data copied into relevant worksheet
5	Data checked for missing times
6	Missing times inserted using "missingTime" macro
7	Missing data noted in QC Code and Comments columns
8	Cleaning and maintenance dates noted in QC Code and Comments columns
9	Any other issues such as malfunctions, calibrations, equipment changes, upgrades, floods, loss of equipment etc noted in QC Code and Comments columns
10	High / low values due to cleaning noted in QC & comments column

All ARMS data from the start of data collection until December 2008 were QC-ed as part of the RESCALE project. Template files have been created and are available for future update to Marine Institute staff.

The ARMS data-files produced contain readings from all parameters measured: temperature, dissolved oxygen, pH, conductivity, depth and turbidity. The QC procedure outlined above is not sufficient for in-depth analysis of the data however it is an excellent starting point, with all issues clearly marked and searchable in the QC and Comments columns. For study of particular parameters further QC of the data is required. Each parameter has issues relating specifically to itself, e.g. dissolved oxygen meters are known to suffer from torn membranes, pH meters are subject to drift and certain calibration procedures are needed for turbidity. One such parameter, pH was studied in detail and the extra QC procedures needed are outlined below.

After the general QC as above was done the following procedure was followed for QC of the pH data. A similar procedure can be followed for any of the other parameters in the ARMS data file. Yet further QC of the pH data was undertaken due to equipment fault and drift and is detailed in Chapter 2.

Table 8.6 Procedure for in-depth quality control of pH data

Step No.	Procedure
1	Date, day, time, pH, QC Code and Comments columns copied from ARMS file into new pH file
2	Data graphed in HYDRAS program for visual inspection
3	Very high / low / noisy data noted
4	Dates and times of odd data checked for maintenance, cleaning or other recorded issues
5	Spurious and erroneous data with recorded reason removed from pH data column to adjacent column and QC Code and comments added
6	Spurious and erroneous data with no recorded reason checked against other parameters
7	Spurious and erroneous data moved to adjacent column as appropriate and QC Code and Comments added and minute data file saved
8	Data anti-logged, averaged and re-logged to get average daily pH
9	Daily pH and QC Codes and Comments saved in new file

9 APPENDIX II: QUALITY CONTROL ISSUES WITH DISSOLVED OXYGEN (DO) DATA

Dissolved oxygen was measured at 2-minute intervals in the Glenamong, Black, and Srahrevagh Rivers over the periods 2003 – 2007, 2004 – 2008, and 2004 – 2006 respectively, using ARMS data recorders. All data were subjected to basic quality control assessment as described in Appendix I whereby spurious data points associated with equipment calibration, maintenance, and malfunction were removed, shifts in magnitude of readings were corrected, and gaps in the data record were identified. Large portions of the datasets were not useable due to noise, gaps in the record, and possible drift, which could not be accurately corrected because of the variability in the data (Figure 9.1).

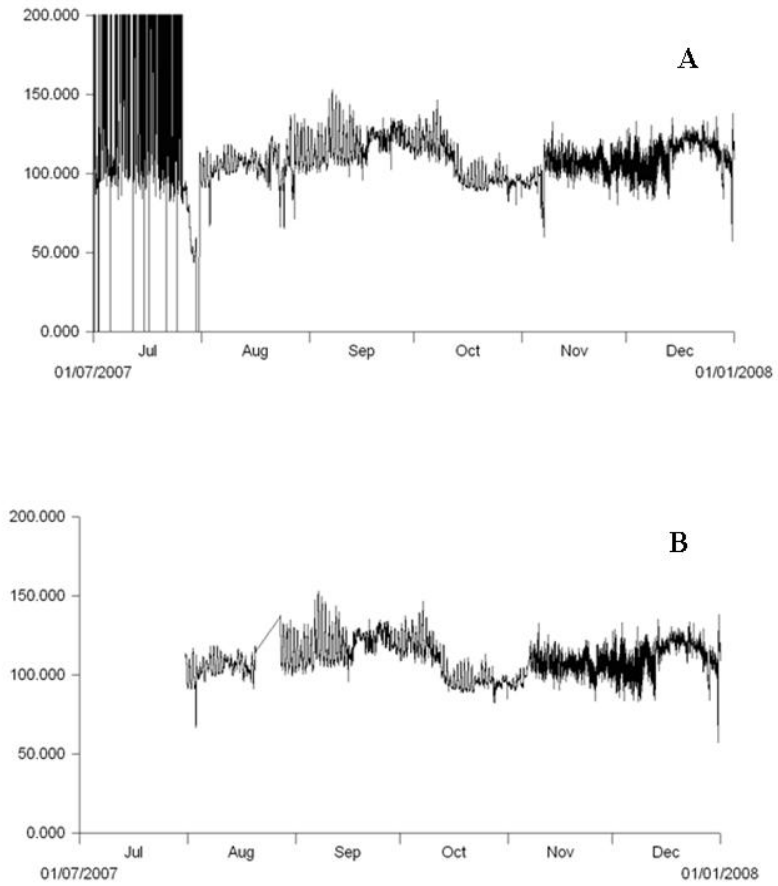

Figure 9.1 Raw (A) and quality control corrected (B) high frequency dissolved oxygen data from the Black River over the period July 2007 – January 2008. A) illustrates the level of noise and spurious data points present in the raw DO datasets for the Black, Glenamong, and Srahrevagh Rivers. B) shows the types of gaps left after correction of the data, plus the level of variability and noise still present in the data.

The Glenamong River was selected for further study because the DO record at that site was the most complete and showed the least unexplained noise of the three stream sites. In

addition, the Glenamong River was the only site where concurrent high frequency mea7surements of DOC levels (using CDOM fluorescence) were available. Dissolved oxygen levels were measured in the Glenamong from August 2003 to May 2008. Between 2003 and 2007, data were missing for 141 days, or 8.6% of the total record. Much of the Glenamong DO dataset was unsuitable for data analysis: the 2003 record was only 5 months long, data were missing in the 2004 record from January to April and extreme noise was observed in the autumn months, the 2005 record was littered with gaps and noisy periods, and periods affected by instrumental drift were evident in both the 2007 and 2008 records (Figure 9.2). From 2003 to 2008, dissolved oxygen measurements in the Glenamong River were made using traditional Clark cell membrane-covered probe. As these traditional probes are susceptible to a range of problems, it is expected that the noise and drift in DO values observed throughout the record resulted from their use. The older probes were replaced by Hydrollab Datasonde 5 chemiluminescent probes in 2009.

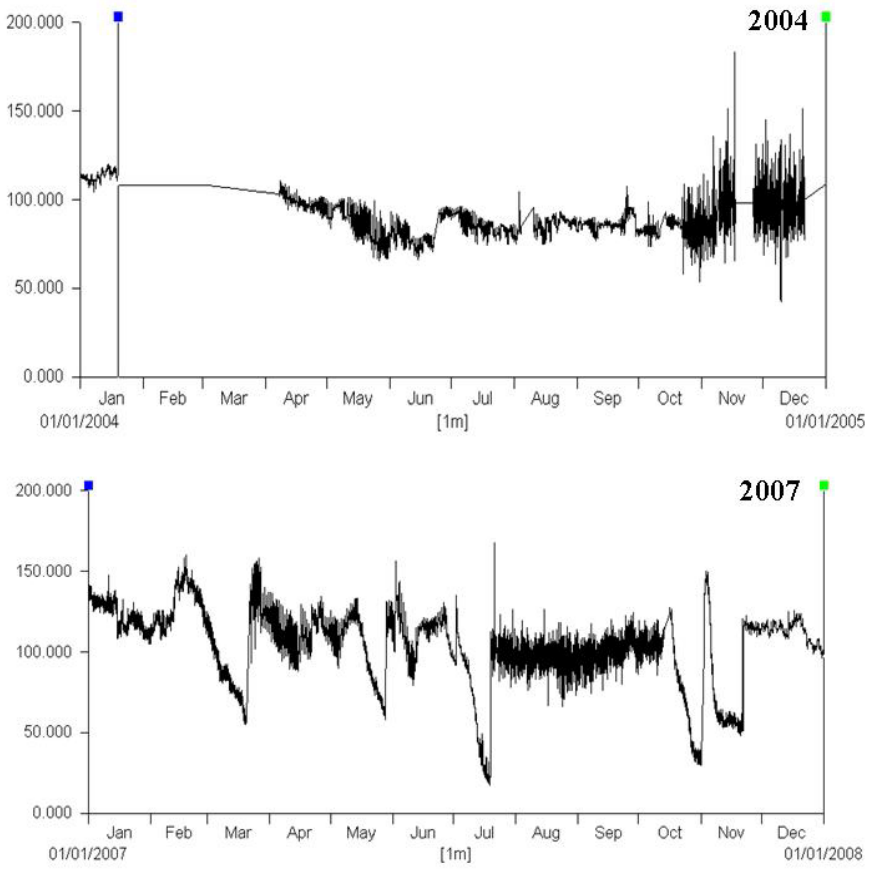

Figure 9.2 High frequency dissolved oxygen data from the Glenamong River in 2004 and 2007 illustrating problems with gaps in the data record and periods of unexplained instrumental drift, respectively.

Dissolved oxygen data from the Glenamong River for September 2005 to November 2006 were selected for data analysis because the period offered a relatively continuous set of daily

mean data for DO, RWT, and flow. The data for this entire period were corrected according to standard quality control protocols as described previously (Appendix I) and DO data from 1 January to 20 February 2006 were drift corrected in using the HYDRAS program (Figure 9.3).

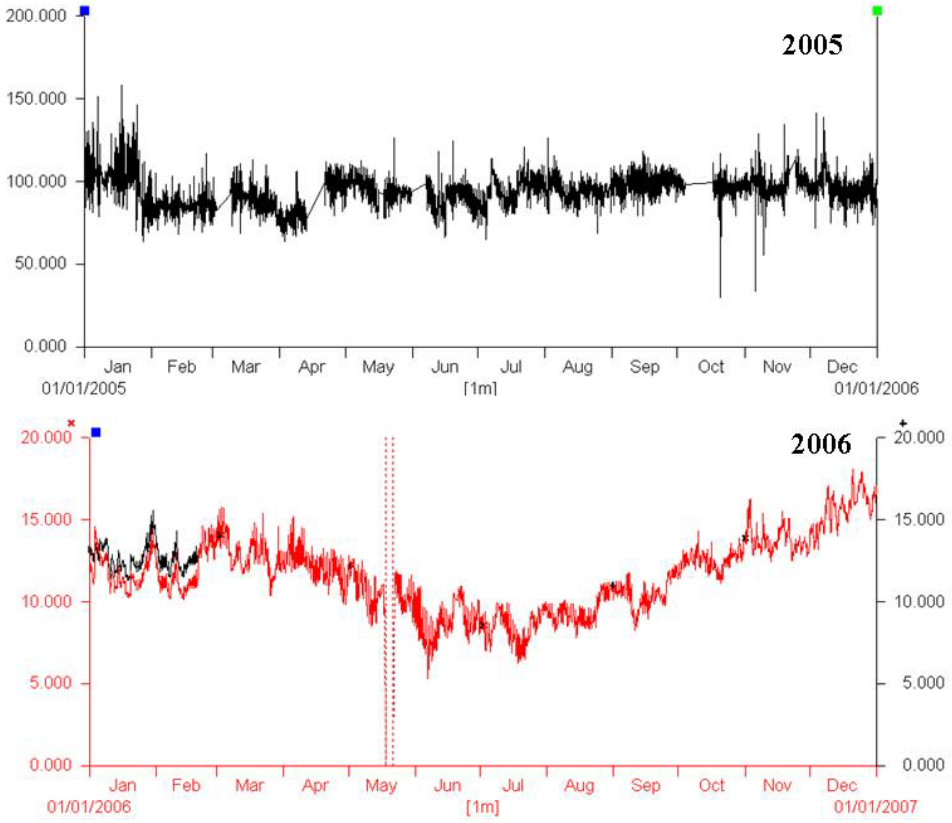

Figure 9.3 Corrected high frequency DO data from the Glenamong River in 2005 and 2006. Straight lines in the 2005 record show gaps in the data set. The black segment of the 2006 record shows the period that underwent drift correction in HYDRAS.

10 APPENDIX III: REVIEW OF THE QUAL2K MODEL

10.1 Introduction

A vast array of models have been developed and used to assess water quality in catchments, to investigate the impact of development (e.g. deforestation) and pollution events (e.g. sewage discharges) on water quality, and to project impacts of climate change on aquatic ecosystems (Abbott et al., 1986; Brown and Barnwell, 1987; Whitehead et al., 1997; Cox, 2003; Chapra et al., 2008). While some models have been applied in a wide range of study sitesmany water quality models are developed for a specific environment or catchment, and hence are not applicable to other situations. The latter is particularly true for European modelling studies (Cox, 2003). Many other models, such as the catchment models SIMCAT and TOMCAT, which are used extensively by the UK Environment Agency, are not widely documented in scientific literature because they are used primarily by government bodies or private consultancy for regulation and management (Jamieson and Fedra, 1996; Cox, 2003). The suitability of a model for a particular study site depends on the purpose for which the model was developed, the water quality variables to be simulated, data availability, whether input data are discrete observed measurements or statistical distributions (deterministic vs. stochastic), and if temporal variability needs to be included (dynamic vs. steady-state).

The US EPA's QUAL2K model, and its predecessor QUAL2E (Brown and Barnwell, 1987), have been widely used to simulate nutrient dynamics, algal production, pH, and dissolved oxygen in both small river systems and large catchments (Park and Lee, 2002; Chapra et al., 2008; Fang et al., 2008). QUAL2K provides a simple but comprehensive way to simulate nutrient dynamics; it is relatively easy to use and understand because of the extensive documentation of model code and theoretical background; it does not require large inputs of hydrological or sediment data; it includes automatic uncertainty analysis; and it is available free of charge from the US EPA (Cox, 2003). The aim of this section is to undertake a preliminary review the QUAL2K model and assess whether it would be suitable for future use in teh Burrishoole catchment.

10.2 QUAL2K Model Description and Data Requirements

QUAL2K (Q2K) is a one-dimensional, steady-state model of in-stream flow and water quality (Chapra et al., 2008). Water flow and the advection and dispersion of solutes are represented in only one direction (usually downstream in a river model), so the river channel is assumed to be mixed completely both vertically and horizontally. To simplify the amount of hydrological

input data required, Q2K assumes that the river channel has a trapezoidal cross-section. Having steady-state hydraulics, Q2K also assumes non-uniform steady flow in the river, and hence cannot be used to model variable flow conditions. Q2K employs a diurnal heat budget and diurnal water quality kinetics. The stream heat budget and water temperature are simulated in the model as a function of meteorology (e.g. solar radiation and cloud cover). All water quality variables are also modelled on a daily time scale (Chapra et al., 2008). A basic list of model inputs is shown in Table 10.1.

Table 10.1 Model inputs required to run QUAL2K (Chapra et al., 2008; Fang et al., 2008)

Data type	Required model inputs
Geographic data	River identification data GPS points for reach boundaries
Hydraulic data	Hydraulic coefficients for the model based on velocity, water depth, and flow Basic river geometry
Inputs and outputs	Type and location of point sources (e.g. wastewater treatment plants) and abstractions (e.g. canals) Type and location of diffuse sources (e.g. groundwater)
In-stream processes	Rate constants for dissolved oxygen consumption, BOD, sediment oxygen demand (SOD), among others Values from the literature or user's manual are often used
Observeddata for calibration	Measured data for all water quality parameters to be simulated (e.g. flow, temperature, DO, TP, pH)

The QUAL2K model conceptualises a catchment system by dividing the main river channel and its tributaries into a series of river reaches within each branch (or 'segment') of the river (Figure 10.1) (Chapra et al., 2008). Although the hydraulic properties within each reach are assumed to be the same, different hydrochemical conditions (e.g. pollutant inputs) can be simulated in neighbouring reaches. Each reach is also divided into a series of equally-spaced sub-reaches. The sub-reach (or 'element') is the main computational unit of the model. QUAL2K can be used to simulate up to fifteen water quality parameters, including water temperature, biological oxygen demand (BOD), Chlorophyll-a, phosphorus (organic and dissolved), nitrogen (organic, ammonium, nitrite, nitrate), dissolved oxygen (DO), and pH along a stream reach and several tributaries. Model output is calculated separately for each branch of the river. A solute mass balance is calculated for each parameter in each river reach

using finite difference solutions to the one dimensional advective-dispersive mass transport equations (Figure 10.1). The main assumptions in the solute mass-balance are that solutes are completely mixed over the cross-section, advective transport is with mean flow, and dispersive transport is proportional to the concentration gradient (Chapra et al., 2008).

Most water quality parameters in the Q2K model are simulated using first-order decay equations, but DO, BOD, nitrate, and phosphate are represented in more detail. The dissolved oxygen concentration in the modelled stream reach is a function of algal productivity, nitrogen and phosphorus availability, and BOD processes, but is also influenced by atmospheric re-aeration and sediment oxygen demand, which are simulated internally. Slowly and rapidly oxidising forms of carbonaceous BOD (CBOD) are used to represent total carbon in the Q2K model. The primary internal source of CBOD is detrital phytoplankton carbon, which is generated through the death of phytoplankton and benthic algae, and zooplankton predation. Q2K also simulates attached bottom algae through growth (by photosynthesis), respiration, and settling onto the sediments of the river bed. Both alkalinity and total inorganic carbon are simulated in the Q2K model, and then are used to simulate pH of river water (Chapra et al., 2008).

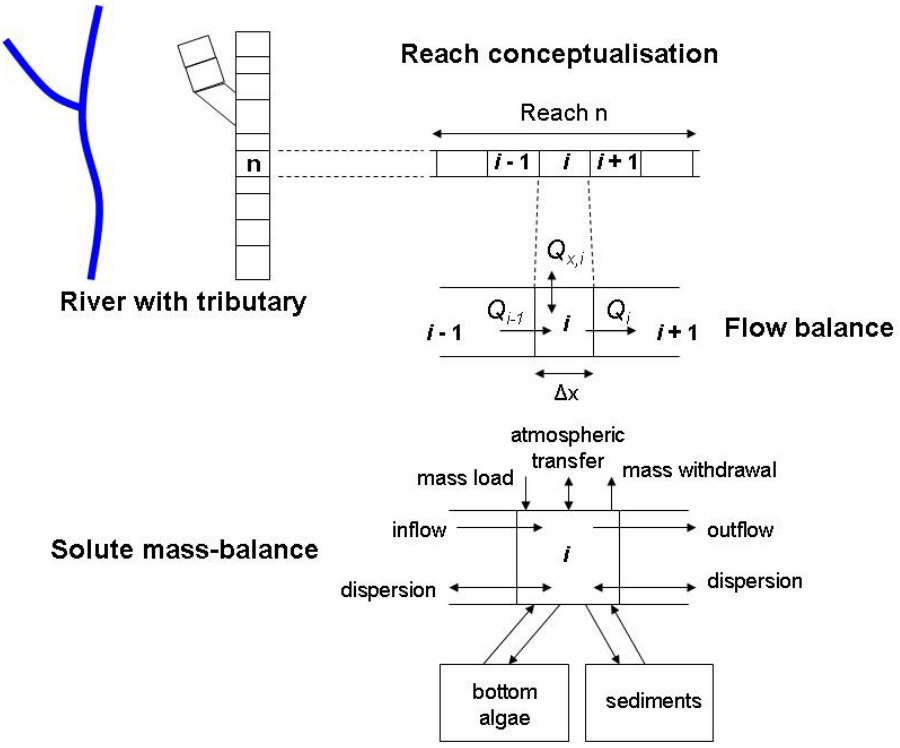

Figure 10.1 Schematic overview of the QUAL2K river model. In the steady-state flow balance Qi-1 is the inflow to sub-reach i from the upstream element i – 1; Qi is the outflow into the downstream element i + 1; and Qx,i is the net sum of all external inflows (discharges minus withdrawals) due to point and nonpoint sources. This figure was adapted from Cox (2003) and Chapra et al. (2008).

10.3 Previous Applications of the QUAL2K Model

The QUAL2K model and its predecessor QUAL2E have been widely applied to lowland rivers in North America and Asia to assess water quality and inform catchment management strategies, usually at heavily impacted sites (e.g. Park and Lee, 2002; Azzellino et al., 2006; Fang et al., 2008). Q2K was most commonly used to simulate the impact of point and non-point source pollution on BOD, DO, and nutrient content of river waters, and to assess management strategies through hypothetical scenarios altering river inputs. Fang et al. (2008) employed the Q2K model to assess the spatial distribution in BOD downstream along the Qiantang River, a tributary of the Yangzi River and a major waterway in China. The Qiantang River and a main tributary of the river were divided into 25 reaches marked by changes in hydraulic flow or water quality and in-stream reaction coefficients (e.g. BOD, SOD) were determined through laboratory experiments and using values published in the literature. The model was calibrated for low-flow conditions since the most critical pollution incidents in the Qiantang River occurred during periods of low flow. Fang et al. (2008) observed that BOD and DO simulated with the Q2K model agreed well with observed data for the main river channel, but that modelled BOD did not match measured data for the tributary because of the prevalence of illegal discharge causing extremely high levels of BOD. The Q2K model was also used to test the impact of two management scenarios, where inputs of waste discharges to the river and the BOD limit of discharged water were decreased, on water quality in the Qiantang River (Fang et al., 2008).

Park and Lee (2002) applied the Q2K model to the Nakdong River, one of four major lowland river systems in Korea. The main river channel and numerous tributaries were divided into 54 reaches and calibrated for average spring/fall conditions in Korea where the river systems are almost at steady-state. Hydraulic parameters of the river, such as velocity, cross-sectional area and depth, were calculated from flow using Manning's equation. Park and Lee (2002) found that the Q2K model was a good predictor of total phosphorus, chlorophyll-a, BOD, DO, and total nitrogen. The researchers concluded that the QUAL2K model was a much better simulator of in-stream BOD and DO than its predecessor QUAL2E because it took into account the contribution of algal death to BOD.

10.4 Potential for Application of QUAL2K Model for Burrishoole

The QUAL2K model has many benefits; it only requires partial hydraulic and sediment data, it can simulate bottom algae and its contribution to BOD, and it can be used to model snapshots

of different hydrochemical conditions throughout a catchment (Park and Lee, 2002; Cox, 2003; Fang et al., 2008). Conversely, Q2K is a steady-state model, so it cannot be used to model water quality in rivers where flow is variable and cannot simulate temporal variability in a river. Although the model user manual states that Q2K can simulate seasonal and diurnal effects, some studies have highlighted that Q2K is not a true dynamic model, and hence does not account for true variable diurnal effects (Cox, 2003). Q2K is also a deterministic model with no stochastic component, so it cannot project flow or concentrations of key solutes as percentiles. Similarly, a danger with deterministic models is that calibrating the model with limited data may result in poor simulations because identical environmental and catchment conditions are required for the validation and future prediction scenarios (Fang et al., 2008).

QUAL2K is not however suitable for simulating water quality where sites are prone to highly variable flow; in addition the model is limited by steady-state hydraulics. The Q2K model could be used to simulate "snapshots" of future climate conditions on a range of environments. Q2K has been shown to be an excellent predictor of in-stream BOD, DO, nutrients, and pH (Park and Lee, 2002; Cox, 2003), so providing that periods were selected where river flow is approximately at steady-state, the model may provide an interesting way to simulate the dynamic biological and chemical processes in the rivers of the Burrishoole catchment at, for example, a diurnal timescale.

10.5 References

Abbott, M.B., Bathurst, J.C., Cunge, J.A., O'Connell, P.E., and Rasmussen, J. (1986) 'An introduction to the European hydrological system – Systeme Hydrologique Europeen, 'SHE'. Structure of a physically-based, distributed modelling system', Journal of Hydrology 87, 61-77.

Brown, L.C. and Barnwell, T.O. (2007) The enhanced stream water quality models QUAL2E and QUAL2E-UNCAS: documentation and user manual (EPA/600/3-87/007). Washington, D.C., US Environmental Protection Agency.

Chapra, S., Pelletier, G., and Tao, H. (2008) QUAL2K: A Modeling Framework for Simulating River and Stream Water Quality, Version 2.11: Documentation and Users Manual. Medford, MA, USA, Tufts University Civil and Environmental Engineering Department.

Cox, B.A. (2003) 'A review of currently available in-stream water-quality models and their applicability for simulating dissolved oxygen in lowland rivers', The Science of the Total Environment 314-316, 335-377.

Fang, X. and Stefan, H.G. (1996) 'Dynamics of heat exchange between sediment and water in a lake', Water Resources Research 32(6), 1719-1727.

Fang, X., Zhang, J., Chen, Y., and Xu, X. (2008) 'QUAL2K Model Used in the Water Quality Assessment of Qiantang River, China', Water Environment Research 80(11), 2125-2133.

Jamieson, D.G. and Fedra, K. (1996) 'The 'WaterWare' decision-support system for river-basin planning. 2: Planning capability', Journal of Hydrology 177, 177-198.

Park, S.S. and Lee, Y.S. (2002) 'A water quality modeling study of the Nakdong River, Korea', Ecological Modelling 152, 65-75.

Whitehead, P.G., Williams, R.J., and Lewis, D.R. (1997) 'Quality simulation along river systems (QUASAR): model theory and development', Science of the Total Environment 194-195, 447-456

11 Appendix IV: Supporting Information on Salmon Growth

Table 11.1 Bonferroni pairwise differences for year 2 annual growth

Years	1968	1977	1982	1984	1994	1997	2003	2004	2005	2006	2007	2008
1968		0.05	0.05	0.05		0.05					0.05	-
1977	0.05		-	-	-	-	-	-	-	-	-	-
1982	0.05	-		-	-	-	-	-	-	-	-	-
1984	0.05	-	-		-	0.05	-	-	-	-	0.05	-
1994	-	-	-	-		-	-	-	-	-	-	-
1997	0.05	-	-	0.05	-		-	0.05	-	0.05	-	-
2003	-	-	-	-	-	-		-	-	-	-	-
2004	-	-	-	-	-	0.05	-		-	-	-	-
2005	-	-	-	-	-	-	-	-		-	-	-
2006	-	-	-	-	-	0.05	-	-	-		-	-
2007	0.05	-	-	0.05	-	-	-	-	-	-		-
2008	-	-	-	-	-	-	-	-	-	-	-	

Table 11.2: Bonferroni pairwise comparison analysis of seasons

Summer	1968	1977	1982	1984	1994	1997	2003	2004	2005	2006	2007	2008
1968		-	-	-	-	-	-	-	-	-	-	-
1977	-		-	-	-	-	-	-	-	-	-	-
1982	-	-		-	-	-	-	-	-	-	-	-
1984	-	-	-		-	-	-	-	-	-	-	-
1994	-	-	-	-		-	-	-	-	-	-	-
1997	-	-	-	-	-		-	-	-	0.05	0.05	-
2003	-	-	-	-	-	-		-	-	-	-	-
2004	-	-	-	-	-	-	-		-	-	-	-
2005	-	-	-	-	-	-	-	-		-	-	-
2006	-	-	-	-	-	0.05	-	-	-		-	-
2007	-	-	-	-	-	0.05	-	-	-	-		-
2008	-	-	-	-	-	-	-	-	-	-	-	
Winter	**1968**	**1977**	**1982**	**1984**	**1994**	**1997**	**2003**	**2004**	**2005**	**2006**	**2007**	**2008**
1968		-	-	-	-	-	-	-	-	-	-	-
1977	-		-	-	-	-	-	-	-	-	-	0.05
1982	-	-		-	-	-	-	-	-	-	-	0.05
1984	-	-	-		-	-	-	-	-	-	-	0.05
1994	-	-	-	-		-	-	-	-	-	-	0.05
1997	-	-	-	-	-		-	-	-	-	-	0.05
2003	-	-	-	-	-	-		-	-	-	-	0.05
2004	-	-	-	-	-	-	-		-	-	-	0.05
2005	-	-	-	-	-	-	-	-		-	-	0.05
2006	-	-	-	-	-	-	-	-	-		-	0.05
2007	-	-	-	-	-	-	-	-	-	-		0.05
2008	-	0.05	0.05	0.05	0.05	0.05	0.05	0.05	0.05	0.05	0.05	

Summer 2	1968	1977	1982	1984	1994	1997	2003	2004	2005	2006	2007	2008
1968		-	0.05	0.05	-	-	-	-	-	-	-	-
1977	-		-	-	-	-	-	-	-	-	-	-
1982	0.05	-		-	-	-	-	-	-	-	-	-
1984	0.05	-	-		-	-	-	-	-	-	-	-
1994	-	-	-	-		-	-	-	-	-	-	-
1997	-	-	-	-	-		-	0.05	0.05	-	-	-
2003	-	-	-	-	-	-		-	-	-	-	-
2004	-	-	-	-	-	0.05	-		-	-	-	-
2005	-	-	-	-	-	0.05	-	-		-	-	-
2006	-	-	-	-	-	-	-	-	-		-	-
2007	-	-	-	-	-	-	-	-	-	-		-
2008	-	-	-	-	-	-	-	-	-	-	-	
Winter 2	1968	1977	1982	1984	1994	1997	2003	2004	2005	2006	2007	2008
1968		-	-	-	-	-	-	-	-	-	-	-
1977	-		-	-	-	-	-	-	-	0.05	-	0.05
1982	-	-		-	-	-	-	-	-	0.05	-	0.05
1984	0.05	-	-		0.05	0.05	0.05	0.05	0.05	0.05	0.05	0.05
1994	-	-	-	0.05		-	-	-	0.05	-	-	0.05
1997	-	-	-	0.05	-		-	-	0.05	-	-	0.05
2003	-	-	-	0.05	-	-		-	-	-	-	0.05
2004	-	-	-	0.05	-	-	-		0.05	-	-	0.05
2005	0.05	-	-	0.05	0.05	0.05	-	0.05		0.05	0.05	0.05
2006	-	0.05	0.05	0.05	-	-	-	-	0.05		-	0.05
2007	-	-	-	0.05	-	-	-	-	0.05	-		0.05
2008	-	0.05	0.05	0.05	0.05	0.05	0.05	0.05	0.05	0.05	0.05	

a)

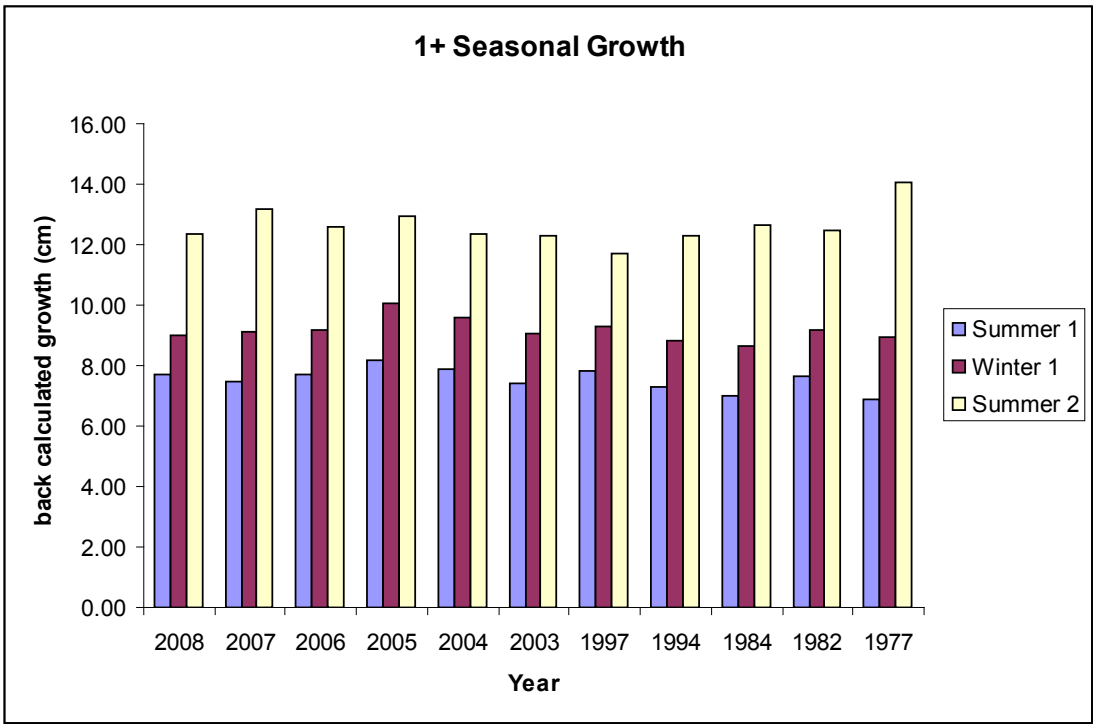
1+ Seasonal Growth
back calculated growth (cm)
16.00
14.00
12.00
10.00
8.00
6.00
4.00
2.00
0.00
2008
2007
2006
2005
2004
2003
1997
1994
1984
1982
1977
Year
Summer 1
Winter 1
Summer 2

b)

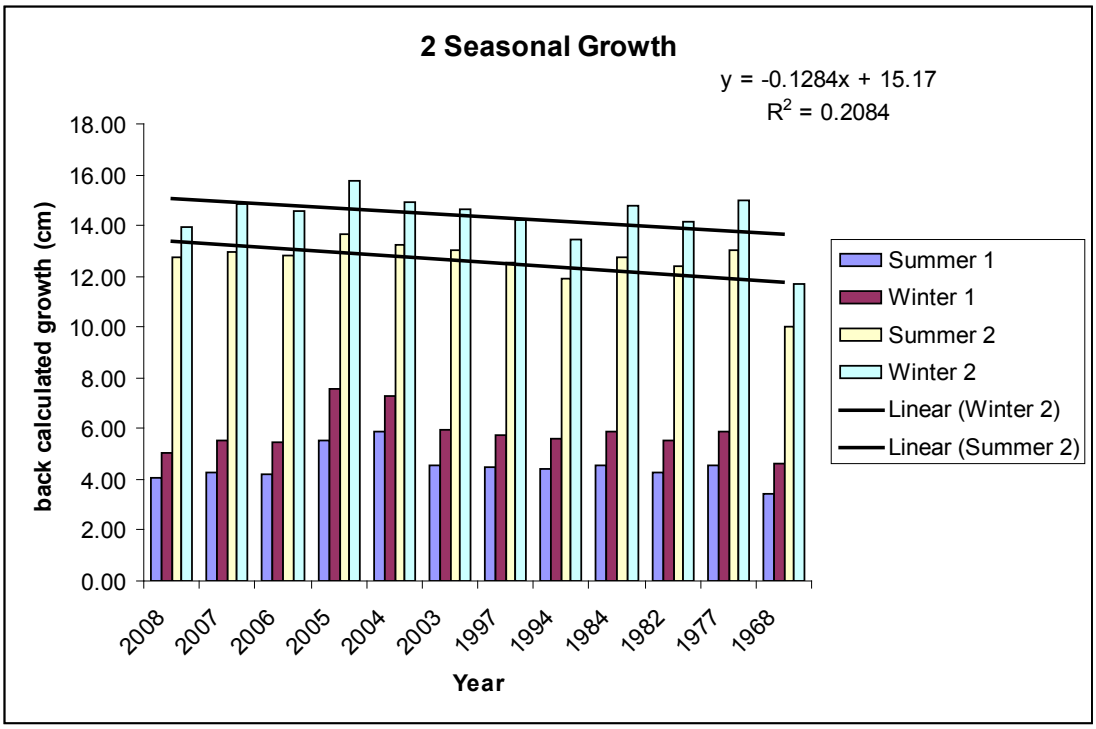
2 Seasonal Growth
y = -0.1284x + 15.17
R2 = 0.2084
back calculated growth (cm)
18.00
16.00
14.00
12.00
10.00
8.00
6.00
4.00
2.00
0.00
2008
2007
2006
2005
2004
2003
1997
1994
1984
1982
1977
1968
Year
Summer 1
Winter 1
Summer 2
Winter 2
Linear (Winter 2)
Linear (Summer 2)

c)

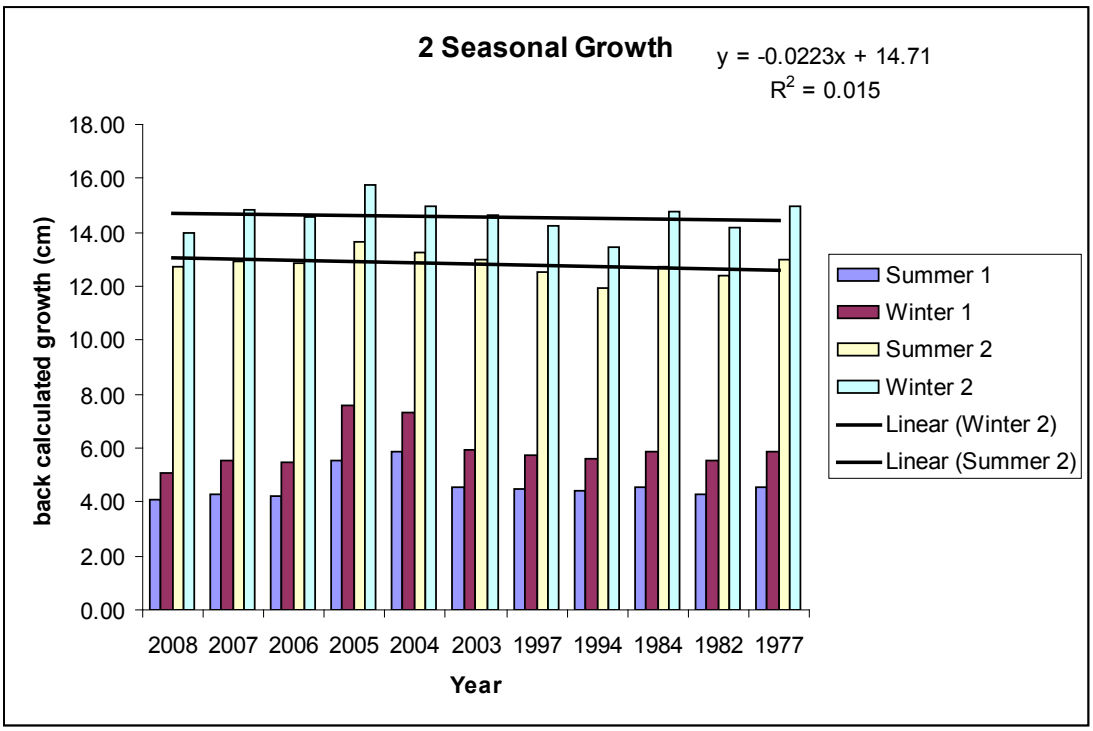

d)

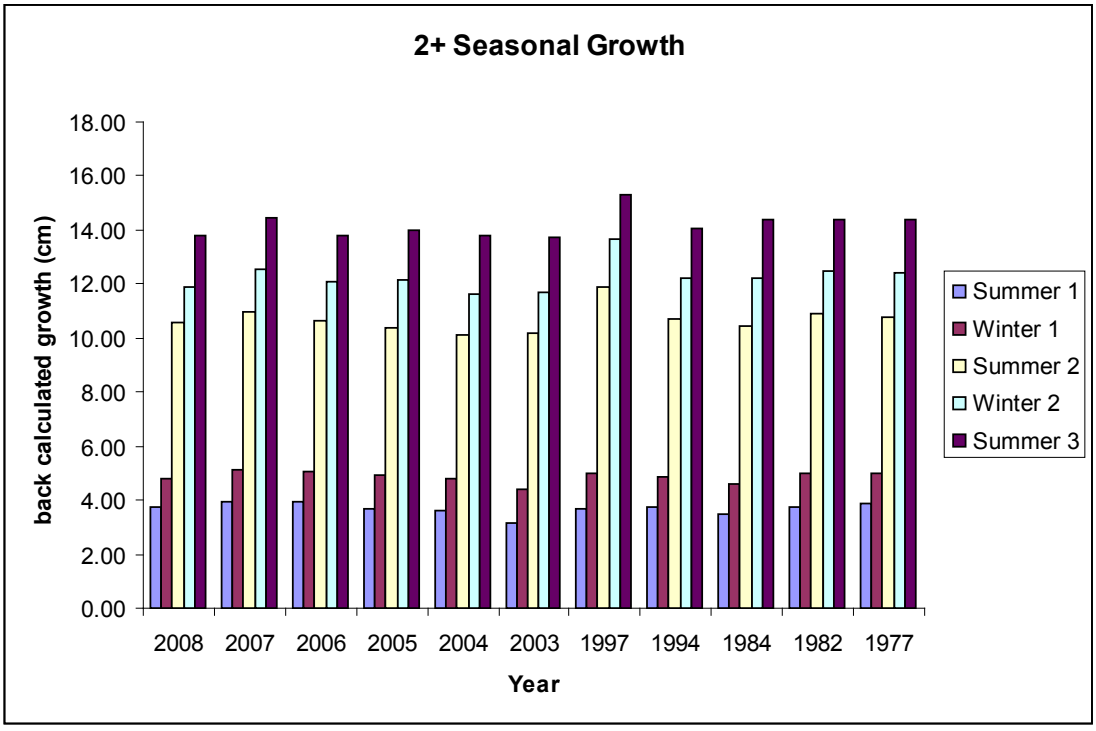

Figure 11.1: Seasonal growth in salmon, excluding 1968 (with the exception of b), for comparison.

a)

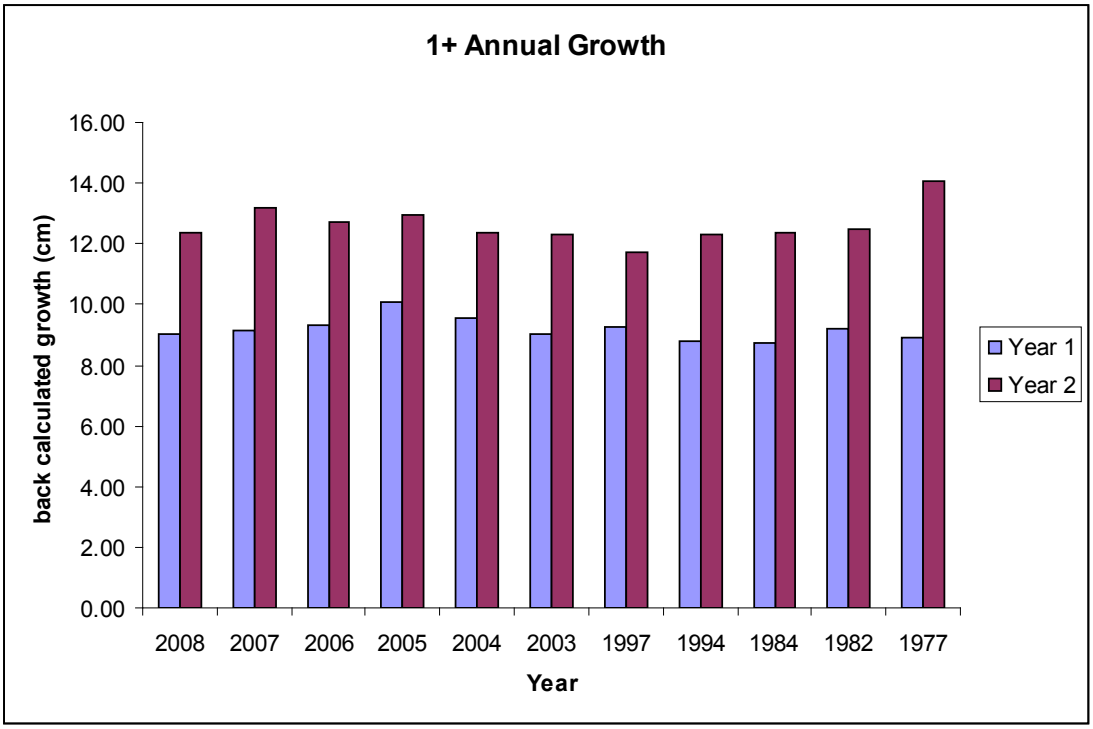
1+ Annual Growth
back calculated growth (cm)
16.00
14.00
12.00
10.00
8.00
6.00
4.00
2.00
0.00
2008 2007 2006 2005 2004 2003 1997 1994 1984 1982 1977
Year
Year 1
Year 2

b)

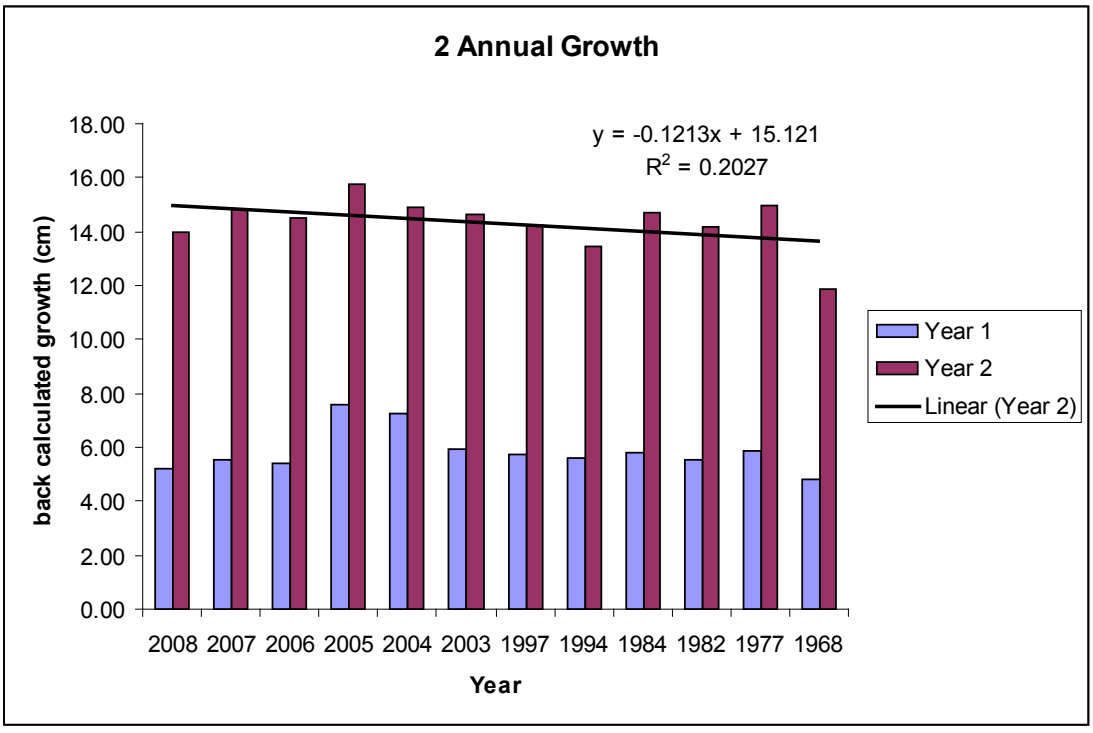
2 Annual Growth
y = -0.1213x + 15.121
R2 = 0.2027
back calculated growth (cm)
18.00
16.00
14.00
12.00
10.00
8.00
6.00
4.00
2.00
0.00
2008 2007 2006 2005 2004 2003 1997 1994 1984 1982 1977 1968
Year
Year 1
Year 2
Linear (Year 2)

c)

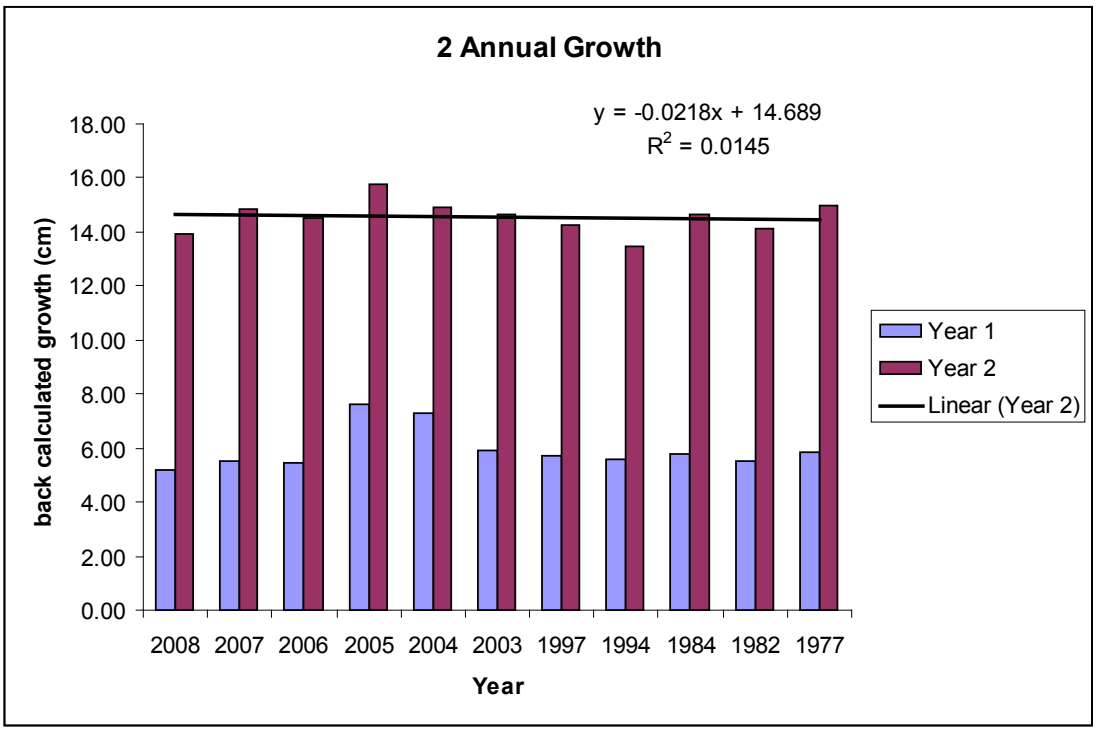

d)

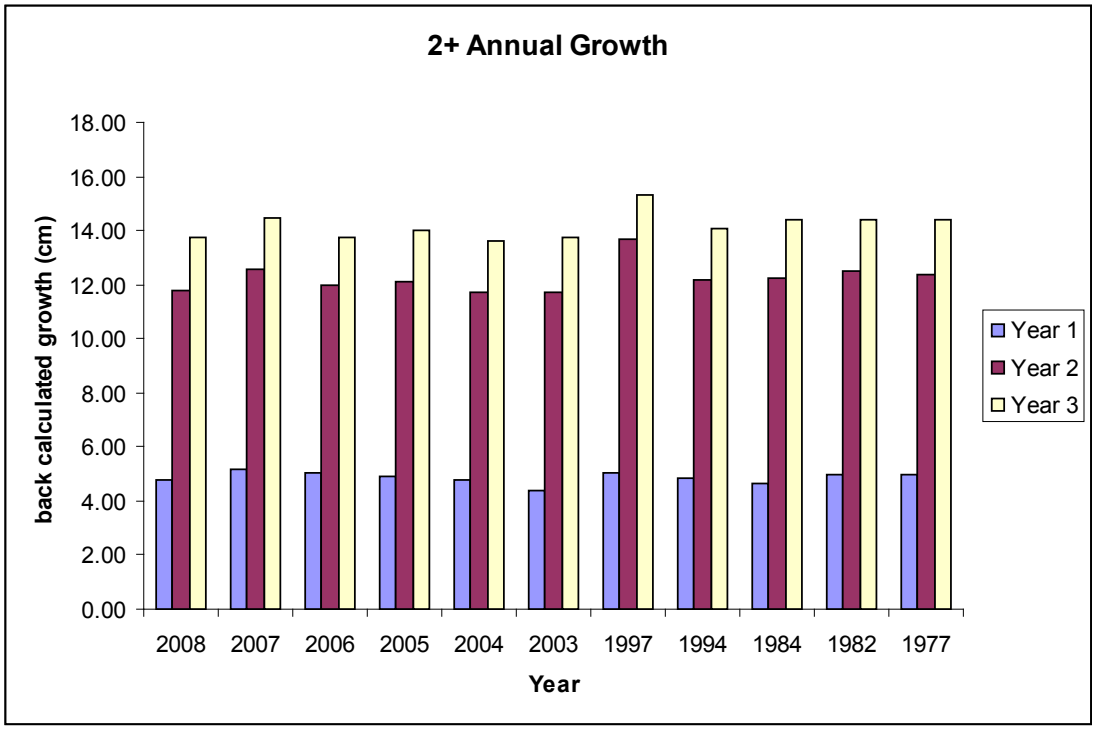

Figure 11.2: Annual growth in salmon, excluding 1968 (with the exception of b), for comparison.

Table 11.3: Bonferroni pairwise comparisons for circuli counts

Summer	1968	1977	1982	1984	1994	1997	2003	2004	2005	2006	2007	2008
1968		-	-	-	-	-	-	-	-	-	-	-
1977	-		-	-	-	-	-	-	-	-	-	-
1982	-	-		-	-	-	-	-	-	-	0.05	-
1984	-	-	-		-	-	-	-	0.05	0.05	0.05	0.05
1994	-	-	-	-		-	-	-	-	-	-	-
1997	-	-	-	-	-		-	-	0.05	0.05	0.05	0.05
2003	-	-	-	-	-	-		-	-	-	-	-
2004	-	-	-	-	-	-	-		-	-	0.05	-
2005	-	-	-	0.05	-	0.05	-	-		-	-	-
2006	-	-	-	0.05	-	0.05	-	-	-		-	-
2007	-	-	0.05	0.05	-	0.05	-	0.05	-	-		-
2008	-	-	-	0.05	-	0.05	-	-	-	-	-	
Winter	1968	1977	1982	1984	1994	1997	2003	2004	2005	2006	2007	2008
1968		-	-	-	-	-	-	-	-	-	-	-
1977	-		-	-	-	-	-	-	-	-	0.05	-
1982	-	-		-	-	-	-	-	-	-	0.05	-
1984	-	-	-		-	-	-	0.05	0.05	0.05	0.05	-
1994	-	-	-	-		-	-	-	0.05	-	0.05	-
1997	-	-	-	-	-		-	-	0.05	-	-	-
2003	-	-	-	-	-	-		-	-	-	-	-
2004	-	-	-	0.05	-	-	-		-	-	-	-
2005	-	-	-	0.05	0.05	0.05	-	-		-	-	-
2006	-	-	-	0.05	-	-	-	-	-		0.05	-
2007	-	0.05	0.05	0.05	0.05	-	-	-	-	0.05		0.05
2008	-	-	-	-	-	-	-	-	-	-	0.05	

Summer 2	1968	1977	1982	1984	1994	1997	2003	2004	2005	2006	2007	2008
1968		-	-	-	-	-	-	-	-	-	-	-
1977	-		-	-	-	-	-	-	-	-	-	0.05
1982	-	-		-	-	-	-	-	-	-	-	-
1984	-	-	-		-	-	-	-	-	-	-	0.05
1994	-	-	-	-		-	-	-	-	-	-	-
1997	-	-	-	-	-		-	-	-	-	-	-
2003	-	-	-	-	-	-		-	-	-	-	-
2004	-	-	-	-	-	-	-		-	-	-	-
2005	-	-	-	-	-	-	-	-		-	-	-
2006	-	-	-	-	-	-	-	-	-		-	-
2007	-	-	-	-	-	-	-	-	-	-		-
2008	-	0.05	-	0.05	-	-	-	-	-	-	-	
Winter 2	1968	1977	1982	1984	1994	1997	2003	2004	2005	2006	2007	2008
1968		-	-	-	-	-	-	-	-	-	0.05	-
1977	-		-	-	-	-	-	-	0.05	-	0.05	-
1982	-	-		-	-	-	-	-	0.05	-	0.05	-
1984	-	-	-		-	-	-	-	0.05	-	0.05	-
1994	-	-	-	-		-	-	-	0.05	-	0.05	-
1997	-	-	-	-	-		-	-	0.05	-	0.05	-
2003	-	-	-	-	-	-		-	0.05	-	-	-
2004	-	-	-	-	-	-	-		0.05	-	0.05	-
2005	-	0.05	0.05	0.05	0.05	0.05	0.05	0.05		0.05	-	0.05
2006	-	-	-	-	-	-	-	-	0.05		0.05	-
2007	0.05	0.05	0.05	0.05	0.05	0.05	-	0.05	-	0.05		0.05
2008	-	-	-	-	-	-	-	-	0.05	-	0.05	

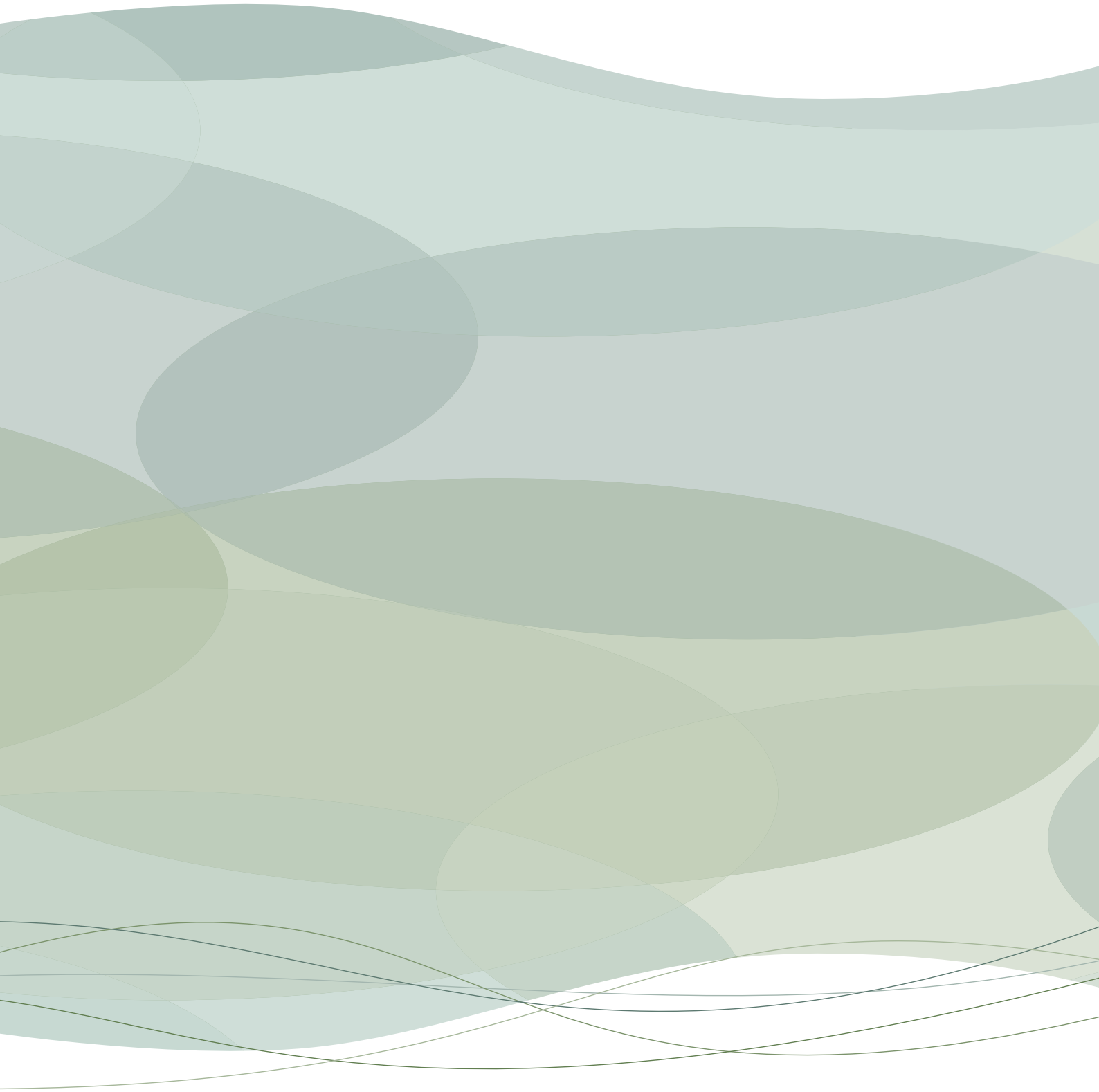

www.marine.ie

Headquarters
Marine Institute
Rinville
Oranmore
Co. Galway
Tel: +353 91 730 400
Fax: +353 91 730 470
Email:
institute.mail@marine.ie

Marine Institute Regional Offices & Labratories
Marine Institute
80 Harcourt Street
Dublin 2
Tel: +353 1 476 6500
Fax: +353 1 478 4988

Marine Institute
Furnace
Newport
Co. Mayo
Tel: +353 98 42300
Fax: +353 98 42340